

**2021-2022 Basic and
Clinical Science
Course, Section 12:
Retina and Vitreous**





AMERICAN ACADEMY
OF OPHTHALMOLOGY®
Protecting Sight. Empowering Lives.

12 | Retina and Vitreous

Last major revision 2018-2019

2021-2022
BCSC
Basic and Clinical
Science Course™

*Funded in part by the Educational Trust
Fund/Retina Research Foundation*



Published after collaborative
review with the European Board
of Ophthalmology subcommittee

The American Academy of Ophthalmology is accredited by the Accreditation Council for Continuing Medical Education (ACCME) to provide continuing medical education for physicians.

The American Academy of Ophthalmology designates this enduring material for a maximum of 15 AMA PRA Category 1 Credits™. Physicians should claim only the credit commensurate with the extent of their participation in the activity.

Originally released June 2018; reviewed for currency August 2020; CME expiration date: June 1, 2022. AMA PRA Category 1 Credits™ may be claimed only once between June 1, 2018, and the expiration date.

BCSC® volumes are designed to increase the physician's ophthalmic knowledge through study and review. Users of this activity are encouraged to read the text and then answer the study questions provided at the back of the book.

To claim AMA PRA Category 1 Credits™ upon completion of this activity, learners must demonstrate appropriate knowledge and participation in the activity by taking the posttest for Section 12 and achieving a score of 80% or higher. For further details, please see the instructions for requesting CME credit at the back of the book.

The Academy provides this material for educational purposes only. It is not intended to represent the only or best method or procedure in every case, nor to replace a physician's own judgment or give specific advice for case management. Including all indications, contraindications, side effects, and alternative agents for each drug or treatment is beyond the scope of this material. All information and recommendations should be verified, prior to use, with current information included in the manufacturers' package inserts or other independent sources, and considered in light of the patient's condition and history. Reference to certain drugs, instruments, and other products in this course is made for illustrative purposes only and is not intended to constitute an endorsement of such. Some material may include information on applications that are not considered community standard, that reflect indications not included in approved FDA labeling, or that are approved for use only in restricted research settings. **The FDA has stated that it is the responsibility of the physician to determine the FDA status of each drug or device he or she wishes to use, and to use them with appropriate, informed patient consent in compliance with applicable law.** The Academy specifically disclaims any and all liability for injury or other damages of any kind, from negligence or otherwise, for any and all claims that may arise from the use of any recommendations or other information contained herein.

All trademarks, trade names, logos, brand names, and service marks of the American Academy of Ophthalmology (AAO), whether registered or unregistered, are the property of AAO and are protected by US and international trademark laws. These trademarks include, but are not limited to, AAO; AAOE; AMERICAN ACADEMY OF OPHTHALMOLOGY; BASIC AND CLINICAL SCIENCE COURSE; BCSC; EYENET; EYEWIKI; FOCAL POINTS; FOCUS DESIGN (logo on cover); IRIS; IRIS REGISTRY; ISRS; OKAP; ONE NETWORK; OPHTHALMOLOGY; OPHTHALMOLOGY GLAUCOMA; OPHTHALMOLOGY RETINA; OPHTHALMOLOGY SCIENCE; OPHTHALMOLOGY WORLD NEWS; PREFERRED PRACTICE PATTERN; PROTECTING SIGHT. EMPOWERING LIVES.; THE OPHTHALMIC NEWS AND EDUCATION NETWORK.

Cover image: From BCSC Section 8, *External Disease and Cornea*. Fluorescein brightly stains the base of the herpes simplex virus epithelial dendritic lesions in a cornea after LASIK. (Courtesy of Arie L. Marcovich, MD, PhD.)



Copyright © 2021 American Academy of Ophthalmology. All rights reserved. No part of this publication may be reproduced without written permission.

Printed in China.

Basic and Clinical Science Course



Christopher J. Rapuano, MD, Philadelphia, Pennsylvania
Senior Secretary for Clinical Education



J. Timothy Stout, MD, PhD, MBA, Houston, Texas
Secretary for Lifelong Learning and Assessment



Colin A. McCannel, MD, Los Angeles, California
BCSC Course Chair

Section 12

Faculty for the Major Revision



Colin A. McCannel, MD
Chair
Los Angeles, California



Brian C. Leonard, MD
Ottawa, Canada



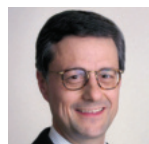
Audina M. Berrocal, MD
Miami, Florida



Richard B. Rosen, MD
New York, New York



Graham E. Holder, PhD
London, United Kingdom



Richard F. Spaide, MD
New York, New York



Stephen J. Kim, MD
Nashville, Tennessee



Jennifer K. Sun, MD, MPH
Boston, Massachusetts

The Academy wishes to acknowledge the *American Society of Retina Specialists* (ASRS), the *Macula Society*, and the *Retina Society* for recommending faculty members to the BCSC Section 12 committee.

The Academy also wishes to acknowledge the following committees for review of this edition:

Committee on Aging: Amy C. Shefler, MD, Houston, Texas

Vision Rehabilitation Committee: William M. McLaughlin Jr, DO, Allentown, Pennsylvania

Practicing Ophthalmologists Advisory Committee for Education: David J. Browning, MD, PhD, *Primary Reviewer*, Charlotte, North Carolina; Edward K. Isbey III, MD, *Chair*, Asheville, North Carolina; Alice Bashinsky, MD, Asheville, North Carolina; Bradley D. Fouraker, MD, Tampa, Florida; Steven J. Grosser, MD, Golden Valley, Minnesota; Stephen R. Klapper, MD, Carmel, Indiana; James A. Savage, MD, Memphis, Tennessee; Michelle S. Ying, MD, Ladson, South Carolina

The Academy also wishes to acknowledge the following committee for assistance in developing study questions and answers for this BCSC Section:

Self-Assessment Committee: Stephen R. Russell, MD, Iowa City, Iowa; Paul B. Griggs, MD, Seattle, Washington; Rachel M. Huckfeldt, MD, Boston, Massachusetts; Ravi S. J. Singh, MD, Shawnee Mission, Kansas

In addition, the Academy wishes to recognize the important contributions of Michael B. Gorin, MD, PhD, in the development of Chapter 13.



European Board of Ophthalmology: Catherine Creuzot-Garcher, MD, PhD, *EBO Chair*, Dijon, France; Peter J. Ringens, MD, PhD, *EBO Liaison*, Maastricht, Netherlands; Anat Loewenstein, MD, Tel Aviv-Yafo, Israel; Pascale G. Massin, MD, Paris, France; Edoardo Midena, MD, Padua, Italy; Ramin Tadayoni, MD, PhD, Paris, France; Sebastian Wolf, MD, PhD, Bern, Switzerland

Financial Disclosures

Academy staff members who contributed to the development of this product state that within the 12 months prior to their contributions to this CME activity and for the duration of development, they have had no financial interest in or other relationship with any entity discussed in this course that produces, markets, resells, or distributes ophthalmic health care goods or services consumed by or used in patients, or with any competing commercial product or service.

The authors and reviewers state that within the 12 months prior to their contributions to this CME activity and for the duration of development, they have had the following financial relationships:*

Dr Berrocal: Alcon (C), Allergan (C), Bausch + Lomb (C), Bayer HealthCare Pharmaceuticals (L), DORC Dutch Ophthalmic Research Center (International)/Dutch Ophthalmic USA (L), Visunex Medical Systems (C)

Dr Browning: Aerpio Therapeutics (S), Alcon (S), Alimera Sciences (C), Genentech (S), Novartis Pharmaceuticals (S), Ohr Pharmaceutical (S), Pfizer (S), Regeneron Pharmaceuticals (S), ZEISS (O)

Dr Creuzot-Garcher: Allergan (C, L), Bausch + Lomb (C, L), Bayer (C, L), Novartis Pharmaceuticals (C, L, S), Roche (C), Théa (C, S)

Dr Fouraker: Addition Technology (C, L), Alcon (C, L), KeraVision (C, L), OASIS Medical (C, L)

Dr Gorin: University of Pittsburgh (P); University of California, Los Angeles (P)

Dr Grosser: Injectsense (O), Ivantis (O)

Dr Holder: Isarna Therapeutics (C), Roche (C), Servier Laboratories (C)

Dr Huckfeldt: Applied Genetic Technologies Corporation (S), Spark Therapeutics (S)

Dr Isbey: Alcon (S), Allscripts (C), Bausch + Lomb (S), Medflow (C), Oculos Clinical Research (S)

Dr Klapper: AdOM Advanced Optical Technologies (O)

Dr Leonard: Abbott Medical Optics (S), Alcon (S), Allergan (S), Annidis (O), Bausch + Lomb (S), Bayer HealthCare Pharmaceuticals (S), Johnson & Johnson Vision (S), Novartis Pharmaceuticals (S), Ophthalmic Direct (S), Shire (S)

Dr Loewenstein: Alcon (C), Allergan (C, L), Bayer (C, L), ForSight Labs (C), Notal Vision (C), Novartis Pharmaceuticals (C, L)

Dr Massin: Allergan (C, L), Bayer (C), Novartis Pharmaceuticals (C, L)

Dr McCannel: DORC Dutch Ophthalmic Research Center (International)/Dutch Ophthalmic USA (C, L), Genentech (S), Insight Instruments (C), Santen Pharmaceutical (C)

Dr Rosen: Allergan (S), Boehringer Ingelheim (C), cellVIEW (C), Clarity Medical Systems (C), Genentech (S), Glauco-Health (C), Guardion Health Sciences (C), Nano Retina (C), Ocata Therapeutics (C), OD-OS (C), Opticology (O), Optovue (C, P), Regeneron Pharmaceuticals (C)

Dr Russell: Acucela (S), IDx (O), Spark Therapeutics (C, S), University of Iowa (P)

Dr Shefler: Allergan (C), Aura Biosciences (S), Genentech (S), Regeneron Pharmaceuticals (S)

Dr Spaide: Bausch + Lomb (C), Genentech (C), Topcon Medical Systems (C, P)

Dr Sun: Adaptive Sensory Technology (S), Allergan (C), Bayer HealthCare Pharmaceuticals (L), Boston Micromachines Corporation (S), Eleven Biotherapeutics (C), Genentech (S), KalVista Pharmaceuticals (S), Merck & Co. (C), Novartis Pharmaceuticals (C), Optovue (S), Regeneron Pharmaceuticals (C)

Dr Tadayoni: Alcon (C, L, S), Alimera Sciences (C, L), Allergan (C, L, S), Bausch + Lomb (C, L), Bayer HealthCare Pharmaceuticals (C, L), Genentech (C), Novartis Pharmaceuticals (C, L, S), ThromboGenics (C), ZEISS (C, L)

Dr Wolf: Alcon (C), Allergan (C), Bayer HealthCare Pharmaceuticals (C, L, S), Heidelberg Engineering (C, S), Novartis Pharmaceuticals (C, S), Optos (S), Roche (C)

The other authors and reviewers state that within the 12 months prior to their contributions to this CME activity and for the duration of development, they have had no financial interest in or other relationship with any entity discussed in this course that produces, markets, resells, or distributes ophthalmic health care goods or services consumed by or used in patients, or with any competing commercial product or service.

* C = consultant fee, paid advisory boards, or fees for attending a meeting; E = employed by or received a W2 from a commercial company; L = lecture fees or honoraria, travel fees or reimbursements when speaking at the invitation of a commercial company; O = equity ownership/stock options in publicly or privately traded firms, excluding mutual funds; P = patents and/or royalties for intellectual property; S = grant support or other financial support to the investigator from all sources, including research support from government agencies, foundations, device manufacturers, and/or pharmaceutical companies

Recent Past Faculty

Neal H. Atebara, MD

Emmett Cunningham Jr, MD, PhD, MPH

David Sarraf, MD

In addition, the Academy gratefully acknowledges the contributions of numerous past faculty and advisory committee members who have played an important role in the development of previous editions of the Basic and Clinical Science Course.

American Academy of Ophthalmology Staff

Dale E. Fajardo, EdD, MBA, *Vice President, Education*

Beth Wilson, *Director, Continuing Professional Development*

Denise Evenson, *Director, Brand & Creative*

Ann McGuire, *Acquisitions and Development Manager*

Stephanie Tanaka, *Publications Manager*

Susan Malloy, *Acquisitions Editor and Program Manager*

Jasmine Chen, *Manager of E-Learning*

Lana Ip, *Senior Designer*

Beth Collins, *Medical Editor*

Eric Gerdes, *Interactive Designer*

Lynda Hanwella, *Publications Specialist*

American Academy of Ophthalmology
655 Beach Street
Box 7424
San Francisco, CA 94120-7424

Contents

Introduction to the BCSC	xvii
Objectives	1
Introduction	3

PART I Fundamentals and Diagnostic Approaches **5**

1 Basic Anatomy	7
The Vitreous	7
Neurosensory Retina	9
Retinal Topography	9
Retinal Layers and Neurosensory Elements	10
Retinal Vasculature and Oxygen Supply	16
Retinal Pigment Epithelium	17
Bruch Membrane	19
Choroid	19
Sclera	20
2 Diagnostic Approach to Retinal Disease	21
Ophthalmoscopy	21
Imaging Technologies	22
Fundus Camera Imaging	22
Scanning Laser Ophthalmoscopy	24
Optical Coherence Tomography	25
Optical Coherence Tomography Angiography	28
Fundus Autofluorescence	29
Adaptive Optics Imaging	33
Retinal Angiographic Techniques	33
Ultrasonography	39
3 Retinal Physiology and Psychophysics	41
Electrophysiologic Testing	41
Electroretinography	42
Full-Field (Ganzfeld) ERG	42
Multifocal ERG	45
Pattern ERG	45
Clinical Considerations	46
Electro-oculography	50
Visual Evoked Cortical Potentials	52
Psychophysical Testing	53

Color Vision	54
Contrast Sensitivity	56
Dark Adaptometry	57
PART II Disorders of the Retina and Vitreous	59
4 Age-Related Macular Degeneration and Other Causes of Choroidal Neovascularization	61
Age-Related Macular Degeneration	61
Genetics and AMD	62
Nonneovascular AMD	63
Neovascular AMD	71
Other Causes of Choroidal Neovascularization	86
Ocular Histoplasmosis Syndrome	86
Angioid Streaks	87
Pathologic Myopia	89
Idiopathic CNV and Miscellaneous Causes of CNV	89
5 Retinal Vascular Disease: Diabetic Retinopathy	91
Terminology and Classification	91
Diabetes Terminology	91
Diabetic Retinopathy Terminology	91
Epidemiology of Diabetic Retinopathy	92
Pathogenesis of Diabetic Retinopathy	93
Recommended Diabetes Mellitus–Related Ophthalmic Examinations	93
Systemic Medical Management of Diabetic Retinopathy	96
Abnormalities Associated With Vision Loss From Diabetic Retinopathy	98
Nonproliferative Diabetic Retinopathy	99
Treatment of Nonproliferative Diabetic Retinopathy	101
Proliferative Diabetic Retinopathy	102
Management of Proliferative Diabetic Retinopathy and Its Complications	103
Diabetic Macular Edema	108
Classification of Diabetic Macular Edema	109
Treatment of Diabetic Macular Edema	110
Cataract Surgery in Patients With Diabetes Mellitus	116
6 Retinal Vascular Diseases Associated With Cardiovascular Disease	121
Systemic Arterial Hypertension	121
Hypertensive Retinopathy	121
Hypertensive Choroidopathy	123
Hypertensive Optic Neuropathy	123

Retinal Vein Occlusion	125
Branch Retinal Vein Occlusion	126
Central Retinal Vein Occlusion	130
Pharmacologic Management of Retinal Vein Occlusion	135
Ocular Ischemic Syndrome and Retinopathy of Carotid	
Occlusive Disease	138
Symptoms and Signs of Ocular Ischemic Syndrome	138
Etiology and Course of Ocular Ischemic Syndrome	139
Treatment of Ocular Ischemic Syndrome	140
Arterial Occlusive Disease	140
Capillary Retinal Arteriole Obstruction (Cotton-Wool Spots)	140
Branch Retinal Artery Occlusion	141
Cilioretinal Artery Occlusion	143
Paracentral Acute Middle Maculopathy	143
Central Retinal Artery Occlusion	143
Ophthalmic Artery Occlusion.	146
Arterial Macroaneurysms	147
7 Other Retinal Vascular Diseases	149
Sickle Cell Retinopathy	149
Nonproliferative Sickle Cell Retinopathy	149
Proliferative Sickle Cell Retinopathy	150
Other Ocular Abnormalities in Sickle Cell Hemoglobinopathies	154
Management of Sickle Cell Retinopathy	154
Vasculitis	155
Cystoid Macular Edema	156
Etiologies of CME	157
Incidence of CME	157
Treatment of CME	159
Coats Disease	159
Macular Telangiectasia	161
Macular Telangiectasia Type 1	161
Macular Telangiectasia Type 2	161
Macular Telangiectasia Type 3	164
Phakomatoses	165
Von Hippel-Lindau Disease	165
Wyburn-Mason Syndrome	168
Retinal Cavernous Hemangioma	168
Radiation Retinopathy.	170
Valsalva Retinopathy	171
Purtscher Retinopathy and Purtscherlike Retinopathy	171
Terson Syndrome	173

8 Retinopathy of Prematurity	175
Introduction	175
Epidemiology	175
Terminology and Classification	175
Pathophysiology of ROP	180
Natural Course	181
Associated Conditions and Late Sequelae	181
Screening Recommendations	182
Screening Criteria	182
Screening Intervals	183
Fundus Photographic Screening of ROP	184
Prevention and Risk Factors	184
Treatment	185
Laser and Cryoablation Surgery	185
Anti-VEGF Drugs	186
Vitrectomy and Scleral Buckling Surgery	187
9 Choroidal Disease	189
Central Serous Chorioretinopathy	189
Demographics	189
Imaging	191
Differential Diagnosis	193
Treatment	194
Choroidal Perfusion Abnormalities	194
Arteritic Disease	195
Nonarteritic Disease	195
Choriocapillaris Blood Flow Abnormalities	198
Increased Venous Pressure	198
Age-Related Choroidal Atrophy	200
Choroidal Folds	200
Choroidal Hemangiomas	202
Uveal Effusion Syndrome	203
Bilateral Diffuse Uveal Melanocytic Proliferation	204
10 Myopia and Pathologic Myopia	207
Prevention	207
The Retina	208
Bruch Membrane	210
Choroidal Neovascularization	211
The Choroid in Pathologic Myopia	212
The Sclera	216
The Optic Nerve	217

11 Focal and Diffuse Choroidal and Retinal Inflammation	219
Noninfectious Retinal and Choroidal Inflammation	219
White Dot Syndromes	219
Chorioretinal Autoimmune Conditions	229
Sympathetic Ophthalmia	233
Uveitis Masquerade: Intraocular Lymphoma	233
Infectious Retinal and Choroidal Inflammation	235
Cytomegalovirus Retinitis	235
Non-CMV Necrotizing Herpetic Retinitis	236
Endogenous Bacterial Endophthalmitis	237
Fungal Endophthalmitis	239
Tuberculosis	240
Syphilitic Chorioretinitis	241
Cat-Scratch Disease	242
Toxoplasmic Retinochoroiditis	243
Toxocariasis	244
Lyme Disease	245
Diffuse Unilateral Subacute Neuroretinitis	246
West Nile Virus Chorioretinitis	246
Zika Virus Chorioretinitis	247
Ebola Virus Panuveitis	247
Chikungunya Virus Retinitis	247
12 Congenital and Stationary Retinal Disease	249
Color Vision (Cone System) Abnormalities	249
Congenital Color Deficiency	249
Night Vision (Rod System) Abnormalities	251
Congenital Night-Blinding Disorders With Normal Fundi	251
Congenital Night-Blinding Disorders With Fundus Abnormality	252
13 Hereditary Retinal and Choroidal Dystrophies	255
Classification	255
General Diagnostic Considerations	258
General Genetic Considerations	259
General Management Considerations	259
Diffuse Dystrophies	261
Diffuse Photoreceptor Dystrophies	261
Choroidal Dystrophies	267
Macular Dystrophies	269
Stargardt Disease	269
Best Disease or Best Vitelliform Dystrophy	271
Adult-Onset Vitelliform Lesions	272
Early-Onset “Drusenoid” Macular Dystrophies	273
Pattern Dystrophies	276
Atypical and “Occult” Macular Dystrophies	277
Inner Retinal Dystrophies	278
X-Linked Retinoschisis	278

14 Retinal Degenerations Associated With Systemic Disease	281
Retinal Degeneration With Systemic Involvement	281
Infantile-Onset to Early Childhood-Onset Syndromes	281
Bardet-Biedl Syndrome	281
Hearing Loss and Pigmentary Retinopathy: Usher Syndrome	284
Neuromuscular Disorders	285
Other Organ System Disorders	285
Paraneoplastic and Autoimmune Retinopathies	286
Metabolic Diseases	288
Albinism	288
Central Nervous System Metabolic Abnormalities	288
Amino Acid Disorders	293
Mitochondrial Disorders	293
15 Systemic Drug-Induced Retinal Toxicity	295
Drugs Causing Abnormalities of the Retinal Pigment Epithelium/	
Photoreceptor Complex	295
Chloroquine Derivatives	295
Phenothiazines	297
Miscellaneous Medications	298
Drugs Causing Occlusive Retinopathy or Microvasculopathy	300
Drugs Causing Ganglion Cell and Optic Nerve Toxicity	301
Drugs Causing Macular Edema	301
Drugs Causing Crystalline Retinopathy	302
Drugs Causing Abnormalities in Color Vision and	
Electroretinography	304
Miscellaneous Drugs Causing Ocular Toxicities	305
16 Retinal Detachment and Predisposing Lesions	307
Posterior Vitreous Detachment	307
Examination and Management of Posterior Vitreous Detachment	309
Lesions That Predispose Eyes to Retinal Detachment	309
Lattice Degeneration	309
Vitreoretinal Tufts	311
Meridional Folds, Enclosed Ora Bays, and Peripheral Retinal	
Excavations	312
Lesions That Do Not Predispose Eyes to Retinal Detachment	313
Paving-Stone Degeneration	313
Retinal Pigment Epithelial Hyperplasia	313
Retinal Pigment Epithelial Hypertrophy	314
Peripheral Cystoid Degeneration	314
Retinal Breaks	314
Traumatic Breaks	315
Trauma in Young Eyes	316

Prophylactic Treatment of Retinal Breaks	317
Symptomatic Retinal Breaks	318
Asymptomatic Retinal Breaks	318
Lattice Degeneration	319
Aphakia and Pseudophakia	319
Fellow Eye in Patients With Retinal Detachment	319
Subclinical Retinal Detachment	319
Retinal Detachment	320
Rhegmatogenous Retinal Detachment	320
Tractional Retinal Detachment	325
Exudative Retinal Detachment	325
Differential Diagnosis of Retinal Detachment	326
Retinoschisis	326
Differentiation of Retinoschisis From Rhegmatogenous Retinal Detachment	327
Macular Lesions Associated With Retinal Detachment	328
Optic Pit Maculopathy	328
Macular Holes in High Myopia	330
17 Diseases of the Vitreous and Vitreoretinal Interface	331
Posterior Vitreous Detachment	331
Epiretinal Membranes	332
Vitreomacular Traction Diseases	336
Idiopathic Macular Holes	337
Developmental Abnormalities	340
Tunica Vasculosa Lentis	340
Prepapillary Vascular Loops	341
Persistent Fetal Vasculature	341
Hereditary Hyaloideoretinopathies With Optically Empty Vitreous:	
Wagner and Stickler Syndromes	342
Familial Exudative Vitreoretinopathy	343
Vitreous Opacities	344
Vitreous Degeneration and Detachment Associated Opacities (“Floaters”)	344
Asteroid Hyalosis	346
Vitreous Hemorrhage	347
Pigment Granules	348
Cholesterolosis	348
Amyloidosis	348
Vitreous Abnormalities Secondary to Surgery	349
18 Posterior Segment Manifestations of Trauma	351
Evaluation of the Patient After Ocular Trauma	351
Blunt Trauma Without Break in Eye Wall	353
Commotio Retinae	353
Choroidal Rupture	354
Posttraumatic Macular Hole	355

Vitreous Hemorrhage	357
Traumatic Chorioretinal Disruption (Retinal Sclopeteria).	357
Open-Globe Injuries	358
Scleral Rupture	358
Lacerating and Penetrating Injuries	358
Perforating Injuries	358
Surgical Management	359
Intraocular Foreign Bodies	360
Posttraumatic Endophthalmitis	362
Prognostication of Globe Injuries	363
Sympathetic Ophthalmia	364
Avulsion of the Optic Nerve Head.	365
Abusive Head Trauma	365
Photic Damage	367
Solar Retinopathy	367
Phototoxicity From Ophthalmic Instrumentation	368
Occupational Light Toxicity	369
Handheld Laser-Pointer Injury	369
PART III Selected Therapeutic Topics	371
19 Laser Therapy for Posterior Segment Diseases	373
Basic Principles of Photocoagulation	373
Choice of Laser Wavelength	373
Practical Aspects of Laser Photocoagulation	375
Complications of Photocoagulation	378
Transpupillary Thermotherapy	380
Photodynamic Therapy	380
Complications of Photodynamic Therapy.	380
20 Vitreoretinal Surgery and Intravitreal Injections	381
Pars Plana Vitrectomy	381
Vitrectomy for Selected Macular Diseases	382
Macular Epiretinal Membranes	382
Vitreomacular Traction Diseases	382
Submacular Hemorrhage.	385
Vitrectomy for Vitreous Opacities.	386
Vitrectomy for Complications of Diabetic Retinopathy.	386
Vitreous Hemorrhage	386
Diabetic Tractional Retinal Detachment	387
Diabetic Macular Edema	388
Vitrectomy for Posterior Segment Complications of Anterior	
Segment Surgery	388
Postoperative Endophthalmitis	388
Retained Lens Fragments After Phacoemulsification	391
Posteriorly Dislocated Intraocular Lenses.	393
Cystoid Macular Edema	393

Suprachoroidal Hemorrhage	394
Needle Penetration of the Globe.	395
Rhegmatogenous Retinal Detachment Surgery	396
Techniques for Surgical Repair of Retinal Detachments	397
Outcomes Following Retinal Reattachment Surgery	401
Complications of Pars Plana Vitrectomy	402
Intravitreal Injections	403
 Basic Texts.	405
Related Academy Materials	407
Requesting Continuing Medical Education Credit.	409
Study Questions	411
Answer Sheet for Section 12 Study Questions.	421
Answers.	423
Index	431

Introduction to the BCSC

The Basic and Clinical Science Course (BCSC) is designed to meet the needs of residents and practitioners for a comprehensive yet concise curriculum of the field of ophthalmology. The BCSC has developed from its original brief outline format, which relied heavily on outside readings, to a more convenient and educationally useful self-contained text. The Academy updates and revises the course annually, with the goals of integrating the basic science and clinical practice of ophthalmology and of keeping ophthalmologists current with new developments in the various subspecialties.

The BCSC incorporates the effort and expertise of more than 100 ophthalmologists, organized into 13 Section faculties, working with Academy editorial staff. In addition, the course continues to benefit from many lasting contributions made by the faculties of previous editions. Members of the Academy Practicing Ophthalmologists Advisory Committee for Education, Committee on Aging, and Vision Rehabilitation Committee review every volume before major revisions. Members of the European Board of Ophthalmology, organized into Section faculties, also review each volume before major revisions, focusing primarily on differences between American and European ophthalmology practice.

Organization of the Course

The Basic and Clinical Science Course comprises 13 volumes, incorporating fundamental ophthalmic knowledge, subspecialty areas, and special topics:

- 1 Update on General Medicine
- 2 Fundamentals and Principles of Ophthalmology
- 3 Clinical Optics
- 4 Ophthalmic Pathology and Intraocular Tumors
- 5 Neuro-Ophthalmology
- 6 Pediatric Ophthalmology and Strabismus
- 7 Oculofacial Plastic and Orbital Surgery
- 8 External Disease and Cornea
- 9 Uveitis and Ocular Inflammation
- 10 Glaucoma
- 11 Lens and Cataract
- 12 Retina and Vitreous
- 13 Refractive Surgery

References

Readers who wish to explore specific topics in greater detail may consult the references cited within each chapter and listed in the Basic Texts section at the back of the book. These references are intended to be selective rather than exhaustive, chosen by the BCSC faculty as being important, current, and readily available to residents and practitioners.

Multimedia

This edition of Section 12, *Retina and Vitreous*, includes videos related to topics covered in the book and interactive content, or “activities,” developed by members of the BCSC faculty. The videos and activities are available to readers of the print and electronic versions of Section 12 (www.aao.org/bcscvideo_section12 and www.aao.org/bcscactivity_section12). Mobile-device users can scan the QR codes below (a QR-code reader may need to be installed on the device) to access the videos and activities.



Videos



Activities

Self-Assessment and CME Credit

Each volume of the BCSC is designed as an independent study activity for ophthalmology residents and practitioners. The learning objectives for this volume are given on page 1. The text, illustrations, and references provide the information necessary to achieve the objectives; the study questions allow readers to test their understanding of the material and their mastery of the objectives. Physicians who wish to claim CME credit for this educational activity may do so by following the instructions given at the end of the book.*

Conclusion

The Basic and Clinical Science Course has expanded greatly over the years, with the addition of much new text, numerous illustrations, and video content. Recent editions have sought to place greater emphasis on clinical applicability while maintaining a solid foundation in basic science. As with any educational program, it reflects the experience of its authors. As its faculties change and medicine progresses, new viewpoints emerge on controversial subjects and techniques. Not all alternate approaches can be included in this series; as with any educational endeavor, the learner should seek additional sources, including Academy Preferred Practice Pattern Guidelines.

The BCSC faculty and staff continually strive to improve the educational usefulness of the course; you, the reader, can contribute to this ongoing process. If you have any suggestions or questions about the series, please do not hesitate to contact the faculty or the editors.

The authors, editors, and reviewers hope that your study of the BCSC will be of lasting value and that each Section will serve as a practical resource for quality patient care.

*This activity meets the Self-Assessment CME requirements defined by the American Board of Ophthalmology (ABO). Please be advised that the ABO is not an accrediting body for purposes of any CME program. ABO does not sponsor this or any outside activity, and ABO does not endorse any particular CME activity. Complete information regarding the ABO Self-Assessment CME Maintenance of Certification requirements is available at <https://abop.org/maintain-certification/cme-self-assessment/>.

Objectives

Upon completion of BCSC Section 12, *Retina and Vitreous*, the learner should be able to

- understand the basic structure and function of the retina and its relationship to the pigment epithelium, choroid, and vitreous
 - select appropriate methods of examination, based on an understanding of the relative benefits and disadvantages of different examination techniques
 - identify vitreoretinal diseases by their clinical appearance and features of supportive diagnostic testing
 - select appropriate ancillary studies to help establish the diagnosis of different vitreoretinal disorders and follow them over time
 - explain how to incorporate data from major prospective clinical trials in the management of vitreoretinal disorders
 - describe the impact of ocular conditions on the retina, such as in severe myopia
 - list the retinal manifestations of inherited diseases, as well as the likely course of these diseases over time
 - identify retinal toxicities of medications
 - describe the appropriateness and timing of prophylactic interventions
 - explain the urgency of intervention for different vitreoretinal conditions
 - describe the impact of trauma on the eye and vision, to better counsel patients about visual outcomes
 - explain the appropriateness and timing of surgical intervention for vitreoretinal diseases to patients
-

Introduction

The retina is the delicate neuroepithelium that lines the posterior segment of the eye, adhering firmly to the optic nerve head posteriorly and to the ora serrata anteriorly. Divided into central and extra-areal periphery, this layer of modified sensory cilia serves important aspects of visual function, including:

- detail discrimination
- color perception
- vision in dim illumination
- peripheral vision

The vitreous, which is the transparent structure that fills the posterior segment eye cavity, plays an important role in many diseases of the posterior segment. Understanding its structure and the changes it may undergo as a result of aging is key to understanding many vitreoretinal disorders.

BCSC Section 12, Retina and Vitreous, is arranged into 3 parts. Part I, Fundamentals and Diagnostic Approaches, covers retinal anatomy, imaging, and functional evaluation in 3 chapters. Chapter 1 provides an overview of the anatomy of the posterior segment. Chapter 2 discusses examination techniques, including dilated slit-lamp biomicroscopy in combination with precorneal non-contact or contact lenses, as well as indirect ophthalmoscopy, which is often aided by scleral indentation to facilitate viewing the anterior retina.

Documenting clinical findings, either by description or by illustration, remains an essential element of a complete posterior segment examination. In addition, ancillary testing, such as fundus photography, autofluorescence, fluorescein angiography, indocyanine green angiography, optical coherence tomography (OCT), scanning laser ophthalmoscopy, microperimetry, and electrophysiology, may provide additional diagnostic information or help detect changes over time. The various incarnations of OCT (time-domain, spectral-domain, and swept-source) deserve special mention; OCT has become perhaps the most commonly ordered ancillary ophthalmic test and is revolutionizing our understanding of many vitreoretinal conditions.

Chapter 3 reviews electrophysiologic tests and their significance in diagnosis and follow-up of retinal disease. Ultrasonography, or echography, employing both A- and B-scan techniques, is useful for examining patients with opaque media, can aid in the diagnosis of retinal or choroidal lesions, and can be used to monitor a lesion's size.

Depending on their location, developmental or acquired alterations in the posterior segment may or may not be symptomatic. Many vitreoretinal diseases, such as diabetic retinopathy or age-related macular degeneration, may be asymptomatic until the disease

4 • Retina and Vitreous

progresses to a more advanced stage. Vitreoretinal disease symptoms, when they occur, may include the following:

- transient or persistent reduction in visual acuity
- dyschromatopsias (alterations in color vision or perception)
- delayed photostress recovery (delayed adaptation to reduced lighting)
- photophobia
- metamorphopsia (wavy or distorted vision)
- floaters
- photopsia (flashes)
- scotomas (blind spots/areas)
- loss of visual field
- nyctalopia (night blindness)

Part II, Disorders of the Retina and Vitreous, which includes Chapters 4 through 18, discusses specific diseases of and trauma to the posterior segment. Appropriate diagnostic techniques are indicated throughout these discussions. By necessity, the illustrative findings associated with the described vitreoretinal disorders are presented as highlights—using schematics as well as the different imaging technologies—rather than as a comprehensive collection. Narratives describing the management of, and therapy for, the retinal disorders covered in Part II are complemented by descriptions of the important clinical trials that have helped establish appropriate evidence-based practices. Because of the increasing prevalence of myopia and its vitreoretinal complications, this edition features a new chapter dedicated to this topic (Chapter 10: Myopia and Pathologic Myopia). In Part III, Selected Therapeutic Topics, Chapters 19 and 20 offer more detailed information on the 3 most important posterior segment treatment approaches: vitreoretinal surgery, laser surgery, and intravitreal injection of effective pharmacologic agents, especially anti-vascular endothelial growth factor treatments. The emergence of each of these treatment approaches has been associated with dramatic improvements in the outcomes retina specialists can accomplish in terms of preserving or restoring patients' vision.

Increasingly, when treating patients with vitreoretinal disorders, clinicians base treatment decisions on evidence from clinical trials. Readers should familiarize themselves with those topics important for interpreting the scientific literature, such as study design, levels of evidence, results interpretation, and clinical practice applications of trial results (see BCSC Section 1, *Update on General Medicine*, Chapter 1).

This book is not meant as a thorough review of the field but rather serves as what a group of experts considers the most important highlights of the specialty. Thus, readers interested in more comprehensive information can obtain additional detail from the selected references as well as from references that appear at the end of the book on the Basic Texts page. Lastly, this edition includes a new feature: activities that will supplement the recently introduced videos in better illustrating specific topics; these features may be accessed through the print and electronic forms of this volume.



PART I

Fundamentals and Diagnostic Approaches

Basic Anatomy

The Vitreous

The vitreous is a transparent gel composed principally of water, collagen, and hyaluronic acid; it occupies 80% of the volume of the eye. The vitreous body is divided into 2 main topographic areas: the central, or core, and the peripheral, or cortical, vitreous. The vitreous gel is made up of collagen fibrils separated by hydrated hyaluronic acid molecules, which act as fillers and separators between adjacent collagen fibrils.

The anterior surface of the vitreous body is called the anterior cortical gel, made up of a condensation of collagenous fibers that attach to the posterior lens capsule, forming the ligament of Wieger (Fig 1-1). The retro-lental indentation of the anterior vitreous is called the patellar fossa. The potential space between the peripheral posterior lens and the anterior cortical gel bordered by the Wieger ligament is called the Berger space. In the vitreous base, the collagen fibers are particularly dense; they are firmly attached to the anterior retina and posterior pars plana, creating a ringlike area that extends approximately 2 mm anterior and 3–4 mm posterior to the ora serrata. The vitreous is not only attached at its base; it is also firmly attached to the lens capsule, retinal vessels, optic nerve, and macula. The densely packed collagen fibrils in the cortical vitreous form the cortical gel. Posteriorly, fibers course in a direction roughly parallel to the inner surface of the retina, forming the preretinal tract. The vitreous attaches to the retinal surface, specifically the internal limiting membrane, via the adhesion molecules fibronectin and laminin. There is no basement membrane between the vitreous base and lens, an area called the annular gap, which is a ringlike zone important for diffusion between the aqueous and vitreous compartments. The space known as the premacular bursa, or the precortical vitreous pocket (see Fig 1-1), which is anterior to the posterior attachment of the vitreous to the macula, is believed to decrease the tractional forces generated during ocular motion by the inertial movement of the vitreous relative to the macula. The vitreous inserts on the edges of the optic nerve head, creating a funnel-shaped void of vitreous. This void is the opening of the Cloquet canal and is referred to as the area of Martegiani. The anatomy of the vitreous is difficult to delineate *in vivo*; however, the vitreous appears to contain interconnected cisterns and canals, most notably the ciliobursal canal that connects the ciliary body and macula. The vitreous also contains hyalocytes, which arise from bone marrow-derived stem cells. Oxygen is derived from diffusion from choroidal and retinal circulation. Hyalocytes consume most of this, limiting the amount of oxygen that reaches the lens and

8 • Retina and Vitreous

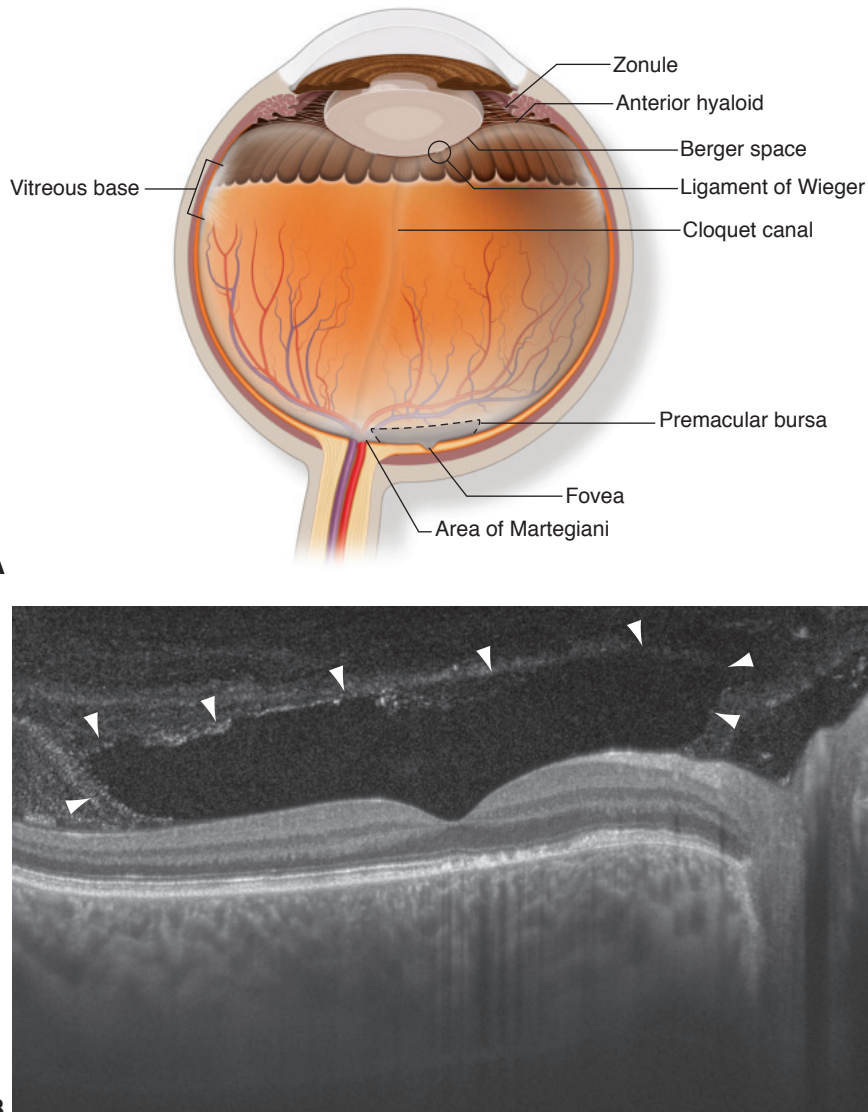


Figure 1-1 Cross section of vitreous anatomy. **A**, Cross section diagram of the eye with emphasis on the anatomical features of the vitreous. The vitreous is most firmly attached to the retina at the vitreous base, and it also has adhesions at the optic nerve, along vessels, at the fovea, and to the posterior lens capsule. A prominent area of liquefaction of the premacular vitreous gel is called the premacular bursa, or precortical vitreous pocket. **B**, Swept-source optical coherence tomography (SS-OCT) image of posterior vitreous and macula region demonstrates the signal void in the vitreous cavity in front of the macula that represents the premacular bursa (arrowheads). Note also the very thick macular choroid and photoreceptor disruption in the central macula, extending nasally. (Part A illustration by Mark M. Miller; part B courtesy of Srinivas Sadda, MD.)

anterior segment. The vitreous has high ascorbate levels, which protects against oxidative damage (eg, to the lens).

Neurosensory Retina

Retinal Topography

The central area of the retina, or macula, measures approximately 5.5 mm in diameter and is centered between the optic nerve head and the temporal vascular arcades. On histologic examination, this area features 2 or more layers of ganglion cells, accounting for half of all the ganglion cells in the retina. Oxygenated carotenoids, in particular lutein and zeaxanthin, accumulate within the central macula and contribute to its yellow color.

The central 1.5 mm of the macula, which is called the *fovea* (or *fovea centralis*), is specialized for high spatial acuity and color vision. The fovea has a margin, a downward slope, and a floor known as the *foveola*, a 0.35-mm-diameter region where cones are slender, elongated, and densely packed. At the very center of the foveola is a small depression, 150–200 μm in diameter, known as the *umbo*. Within the fovea is a region devoid of retinal vessels known as the *foveal avascular zone* (FAZ). The geometric center of the FAZ is often taken to be the center of the macula and thus the point of fixation; it is an important landmark in fluorescein angiography. Surrounding the fovea is the *parafovea*, a ring 0.5 mm in width where the ganglion cell layer, inner nuclear layer, and outer plexiform layer (also known as *Henle fiber layer*) are thickest. Surrounding this zone is the *perifovea*, a ring approximately 1.5 mm wide (Table 1-1). Thus, the umbo forms the center of the macula, and the periphery of the perifovea forms its margin, which is sometimes referred to as the *area centralis* (Fig 1-2).

The retina outside the macula, sometimes referred to as the extra-areal periphery, is commonly divided into a few concentric regions, starting with the *near periphery*, a 1.5-mm ring peripheral to the temporal major vascular arcades. The *equatorial retina*

Figure 1-2 Anatomical macula, also called *area centralis* or *posterior pole*. The anatomical fovea and foveola are contained within the center of the anatomical macula. Letters indicate borders of: a = umbo; b = foveola; c = fovea; c to d = parafoveal macula; d to e = perifoveal macula; e = macula. (Courtesy of Hermann D. Schubert, MD.)

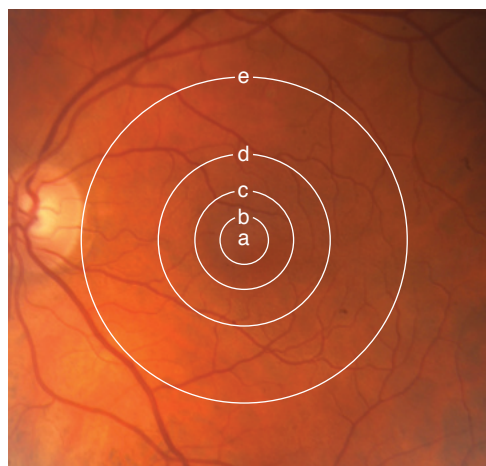


Table 1-1 Anatomical Terminology of the Macula (Area Centralis)

Term	Synonym	Histologic Definition	Clinical Observation and Size
Macula	Posterior pole Area centralis	Contains 2 or more ganglion cell layers	Area between vascular arcades 5.5 mm in diameter centered ~4.0 mm temporal and 0.8 mm inferior to the center of the optic nerve head
Perifovea		From the outermost limit of the parafovea to the outer limit of the macula	Ring 1.5 mm in width surrounding the parafovea
Parafovea		Margin, where the ganglion cell layer, inner nuclear layer, and Henle fiber layer are thickest (ie, the retina is thickest)	Ring 0.5 mm in width surrounding the fovea
Fovea	Fovea centralis	A depression in the inner retina; has a margin, slope, and floor, the photoreceptor layer of which is entirely cones	A concave central retinal depression seen on slit-lamp examination 1.5 mm in diameter (about 1 disc diameter, or 5°)
Foveola		The floor of the fovea features cones only, arranged in the shape of a cake, where the inner nuclear layer and ganglion cell layer are laterally displaced	0.35 mm in diameter, usually smaller than the foveal avascular zone
Umbo	Fixation Light reflex	Small (150–200 µm) center of the floor of the foveola; features elongated cones	Observed point corresponding to the normal light reflex but not solely responsible for this light reflex

is the retina around the equator, and the region anterior to the equatorial retina is called the *peripheral retina*. In the far periphery, the border between the retina and the pars plana is called the *ora serrata*. The posterior border of the vitreous base is typically located between the ora serrata and the equator of the eye. This region is where most retinal tears occur. Jetties of retinal tissue, called *dentate processes*, extend anteriorly into the pars plana. These processes are more prominent nasally. *Ora bays* are posterior extensions of the pars plana toward the retina. On occasion, dentate processes may wrap around a portion of an ora bay to form an enclosed ora bay. A *meridional fold* is a radially oriented, prominent thickening of retinal tissue that extends into the pars plana. When aligned with a ciliary process, such folds are known as a *meridional complex* (Fig 1-3).

Retinal Layers and Neurosensory Elements

The layers of the retina can be seen in cross-sectional histologic preparations, and most layers can be identified with spectral-domain optical coherence tomography (SD-OCT)

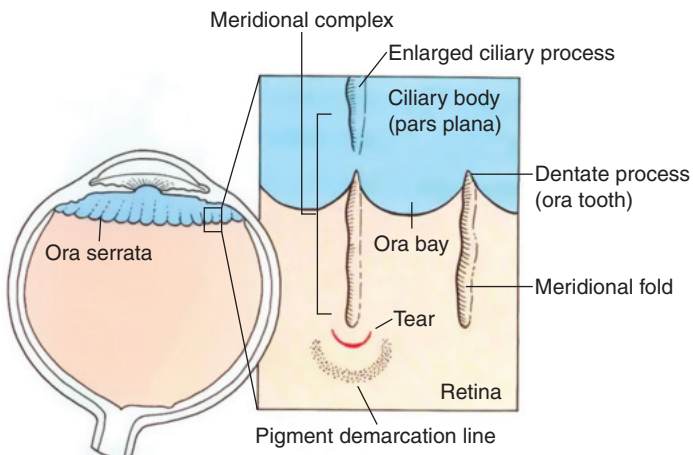


Figure 1-3 Schematic of the ora serrata, showing an ora bay and dentate process. Meridional folds are pleats of redundant retina. Tears may occur at the posterior end of such folds. (Used with permission from Federman JL, Gouras P, Schubert H, et al. Retina and vitreous. In: Podos SM, Yanoff M, eds. Textbook of Ophthalmology. Vol 9. London: Mosby; 1988.)

(see Activity 2-1). The layers of the retina as seen on histologic section, in order from the inner to outer retina, are listed here (Fig 1-4):

- internal limiting membrane (ILM)
- nerve fiber layer (NFL; the axons of the ganglion cell layer)
- ganglion cell layer (GCL)
- inner plexiform layer (IPL)
- inner nuclear layer (INL)
- middle limiting membrane (MLM)
- outer plexiform layer (OPL)
- Henle fiber layer (HFL)
- outer nuclear layer (ONL; the nuclei of the photoreceptors)
- external limiting membrane (ELM)
- rod and cone inner segments (IS)
- rod and cone outer segments (OS)

To reach the photoreceptors, light must travel through the full thickness of the retina. The density and distribution of photoreceptors vary with their topographic location. In the fovea, densely packed cones are predominantly red- and green-sensitive, with a density exceeding 140,000 cones/mm². The foveola has no rods; the fovea contains only photoreceptors, rods and cones, and processes of Müller cells. The number of cone photoreceptors decreases rapidly in areas farther away from the center, even though 90% of cones overall reside outside the foveal region. The rods have their greatest density in a zone lying approximately 4 mm from the foveal center, or 12° from fixation, where they reach a peak density of about 160,000 rods/mm². The density of rods also decreases toward the

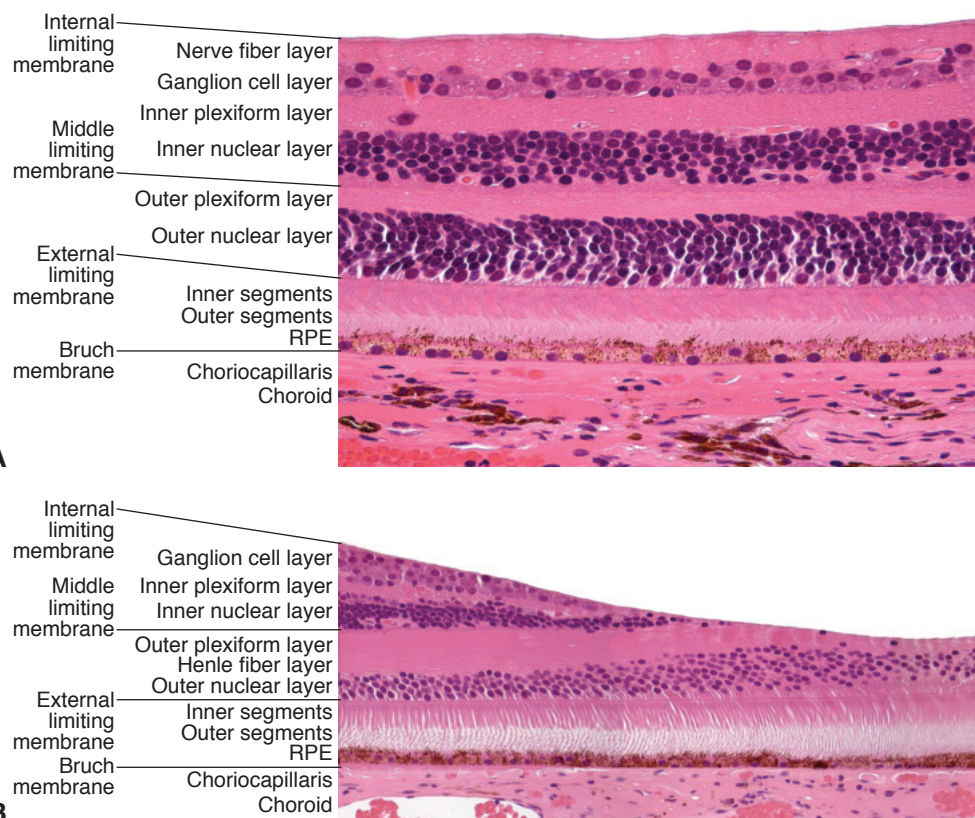


Figure 1-4 Cross-sectional photomicrographs of peripheral macular and foveal retina (H&E stain). **A**, Cross section of the retina and choroid, showing the layers of the retina (labeled). **B**, In the fovea, the inner cellular layers are laterally displaced, and there is an increased density of pigment in the retinal pigment epithelium (RPE). Note that on the right edge of the image, the inner cellular layers are laterally displaced. This allows the incident light to fall directly on to the photoreceptors, avoiding the inner retinal layers, thereby reducing the potential for scattering of light. An additional characteristic of the foveal region is that there is increased density of pigment in the RPE. (Courtesy of Ralph Eagle, MD.)

periphery. A small area of high rod concentration ($176,000$ rods/ mm^2) has been found in the superior macula. The arrangement of rods and cones can be visualized with noninvasive adaptive optics imaging (Fig 1-5).

The light-sensitive molecules in rods and cones are derived from vitamin A and are contained in the disc membranes of the photoreceptor outer segments. The discs are attached to a cilium, which is rooted through neurotubules in the ellipsoid and myoid of the inner segment. The ellipsoid, which is adjacent to the cilium, contains mitochondria and is responsible for the cone shape. The myoid, which is closer to the photoreceptor nucleus, contains endoplasmic reticulum. The mitochondria, cilia, and inner discs together form the *inner-outer segment junction*, which provides evidence of the origin of the photoreceptor as a modified sensory cilium prone to the full range of ciliopathies. Rod outer segments may contain up to 1000 discs stacked like coins. These discs are renewed in and

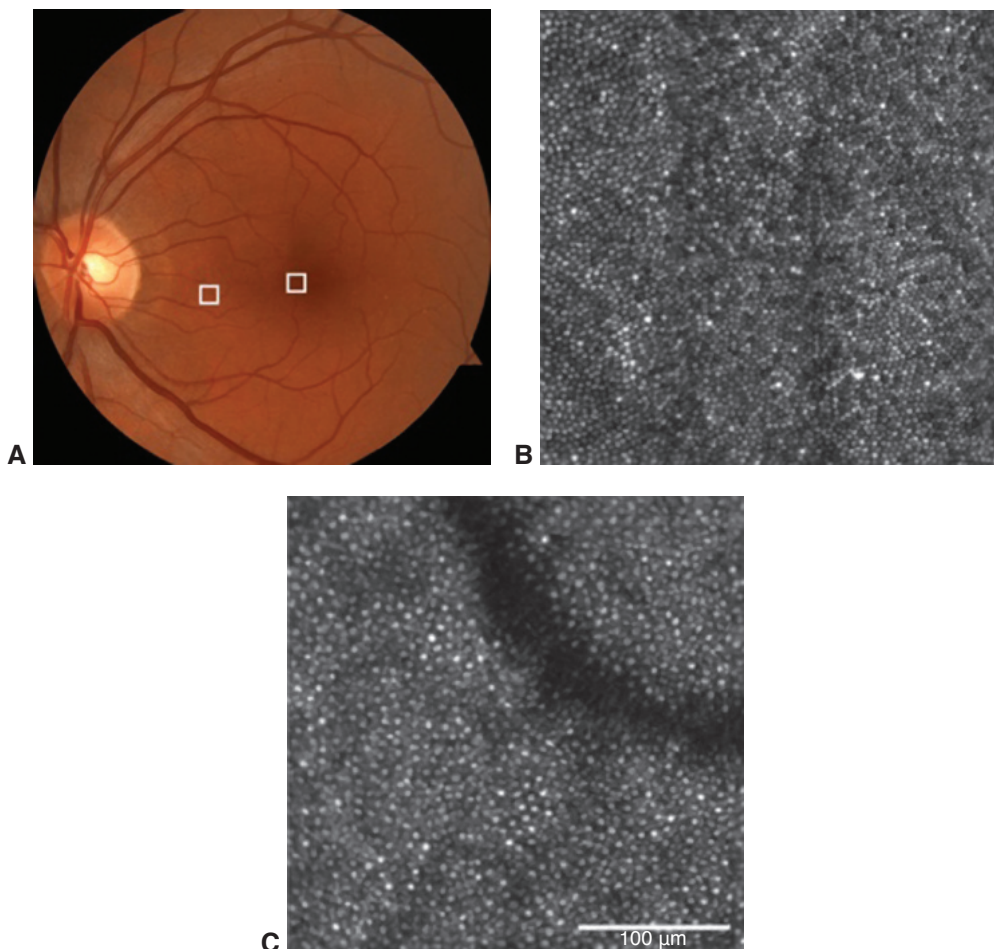


Figure 1-5 Comparison of a conventional fundus photograph (**A**) and confocal adaptive optics scanning laser ophthalmoscope (AOSLO) images of a healthy left-eye macula. The white box on the fundus photo that is closer to the fovea is 0.5° from fixation and represents a 300×300 -micron area of macula. The corresponding AOSLO image of the retina within that white box (**B**) shows cones that are smaller and very tightly packed; no rods are visible. The white box on the fundus photo that is closer to the optic nerve is 7° from fixation and also represents a 300×300 -micron area of macula. The corresponding AOSLO image (**C**) shows cones that are larger and less densely packed; intervening rods are starting to become visible. (Courtesy of Mina M. Chung, MD, and Hongxin Song, MD, PhD.)

shed from the outer retina and are phagocytosed by the retinal pigment epithelium (RPE) for processing and recycling of components (Fig 1-6).

Cone photoreceptors have a 1-to-1 synapse with a type of bipolar cell known as a *midget bipolar cell*. Other types of bipolar cells also synapse with each cone. Conversely, more than 1 rod—and sometimes more than 100 rods—converge on each bipolar cell. Bipolar cells, the first neurons of the visual pathway, synapse with ganglion cells, the second neurons of the visual pathway in the IPL. The ganglion cells summate responses from

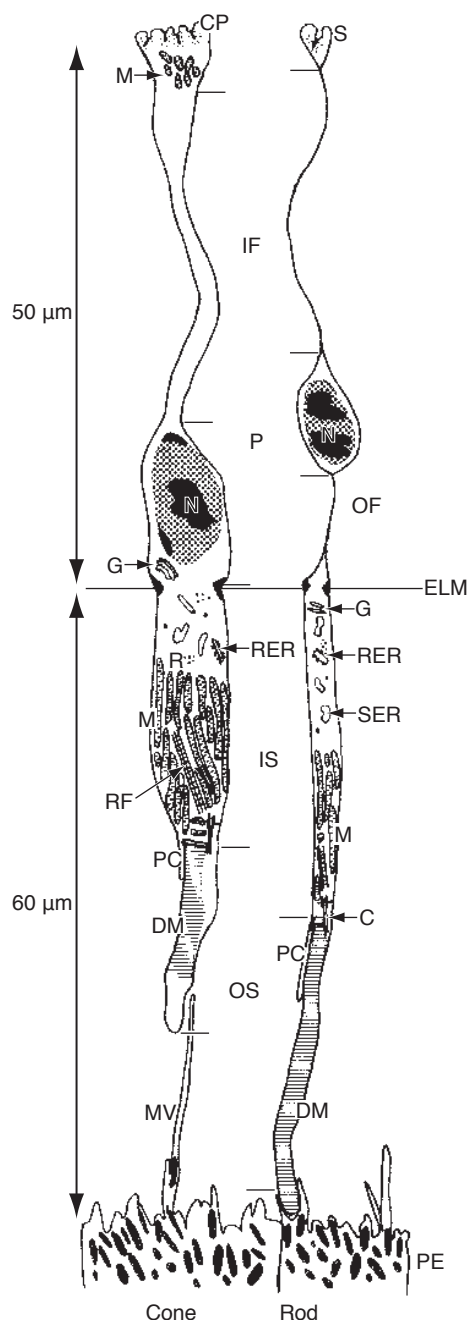


Figure 1-6 Schematic of a cone cell (left) and a rod cell (right) in the peripheral retina. C = cilium; CP = cone cell pedicle; DM = membranous discs; ELM = external limiting membrane; G = Golgi apparatus; IF = inner fiber; IS = inner segment; M = mitochondria; MV = microvilli of pigment epithelial cells; N = nucleus; OF = outer fiber; OS = outer segment; P = perikaryon; PC = processus calycoides; PE = pigment epithelium; R = free ribosomes; RER = rough endoplasmic reticulum; RF = rootlet fiber; S = rod cell spherule; SER = smooth endoplasmic reticulum. (Used with permission from Krebs W, Krebs I. Primate Retina and Choroid. Atlas of Fine Structure in Man and Monkey. New York: Springer Verlag; 1991.)

bipolar and amacrine cells and develop action potentials that are conducted to the dorsolateral geniculate nucleus and the third neuron in the brain. Amacrine cells on the inside of the INL help process signals by responding to specific alterations in retinal stimuli, such as sudden changes in light intensity or the presence of certain sizes of stimuli. The outside of the INL is composed of horizontal cells. In the NFL, axons of the GCL course along the inner portion of the retina to form the optic nerve, a brain tract. The ILM, which is formed by the footplates of Müller cells, is attached to the posterior cortical gel of the vitreous (Fig 1-7).

Two additional intraretinal “membranes” identified by histologists, the ELM and MLM, are actually junctional systems, not true membranes. At the outer extent of the Müller cells, zonular attachments between photoreceptors and Müller cells create the ELM, a structure visible with both light microscopy and OCT. Thus, the Müller cells whose nuclei reside in the INL course through almost the entire thickness of the retina. The inner third of the OPL has a linear density in which synaptic and desmosomal connections occur between the photoreceptor inner fibers and the processes of the bipolar cells. This

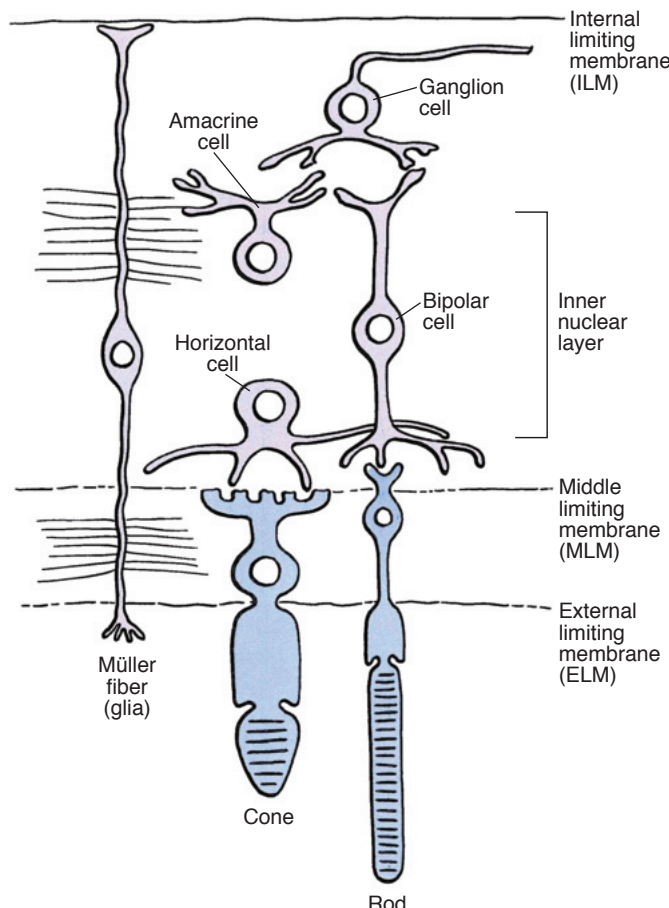


Figure 1-7 Schematic of the neuronal connections in the retina and participating cells. (*Illustration by Mark Miller.*)

linear density, which is also apparent with OCT, is the junctional system that has been called the MLM.

Retinal Vasculature and Oxygen Supply

The vascular supply of the retina comes from the retinal circulation for the inner retina, and indirectly from the choroidal circulation for the avascular outer retina. The central retinal artery (a branch of the ophthalmic artery) enters the eye and divides into 4 branches, each supplying blood to a quadrant of the retina. These branches are located in the inner retina. Occasionally, a cilioretinal artery, derived from the ciliary circulation, will supply a portion of the inner retina (Fig 1-8). On a tissue level, the retina is supplied by up to 4 layers of vessels: the *radial peripapillary capillary network* located in the nerve fiber layer and around the optic nerve head, the *superficial vascular plexus* in the retinal ganglion cell layer, and the *deep capillary plexus* with 2 capillary beds, one on either side of the INL. Although the superficial layer of the deep capillary plexus is sometimes referred to as the intermediate capillary plexus, typically both layers are collectively referred to as the deep capillary plexus. With the advent of OCT angiography, which is able to visualize these distinct capillary layers, interest in this anatomy has grown. The retinal vasculature, including its capillaries, retains the blood–brain barrier with tight junctions between capillary endothelial cells. Blood from the capillaries is collected by the retinal venous system; it eventually leaves the eye through the central retinal vein by way of branch retinal veins.

The outer retinal layers, beginning with the outer plexiform layer, derive their oxygen supply from the choroidal circulation. The exact boundary between the retinal vascular



Figure 1-8 A central retinal artery occlusion in a young patient with a previously unknown patent foramen ovale. Presumably, an embolus from the systemic circulation passed through the patent foramen ovale and lodged in the central retinal artery, occluding its blood flow. Fortunately, a cilioretinal artery supplied part of the eye's retina. Note the retinal ischemic whitening in the distribution of the central retinal artery but preservation of the normal retinal transparency in the zone supplied by the cilioretinal artery. (Used with permission from Ho IV, Spaide RF. Central retinal artery occlusion associated with a patent foramen ovale. *Retina*. 2007;27(2):259–260.)

supply and the diffusion from the choriocapillaris varies according to the topographic location, retinal thickness, and amount of light present. See also the section Choroid later in this chapter, as well as Part I, Anatomy, of BCSC Section 2, *Fundamentals and Principles of Ophthalmology*.

Retinal Pigment Epithelium

The RPE is a monolayer of pigmented cells derived from the outer layer of the optic cup. This layer is continuous with the pigment epithelium of the ciliary body and iris. RPE cells are hexagonal, cuboidal cells approximately 16 µm in diameter. In the macula, however, the cells are taller and denser than in the periphery. The lateral surfaces of adjacent cells are closely apposed and joined by tight junctional complexes (zonulae occludentes) near the apices, forming apical girdles and the outer blood–ocular barrier. Each RPE cell has an apex and base; the apical portion envelops the outer segments of the photoreceptor cells with villous processes (Fig 1-9). The basal surface of the cells shows a rich infolding of the plasma membrane. The basement membrane does not follow these infoldings. The typical RPE cell has several melanosomes, each designed to absorb light. Melanosomes are spheroidal; their melanin is distributed on protein fibers.

The RPE contributes to retinal function in several ways; it

- absorbs light
- phagocytoses rod and cone outer segments
- participates in retinal and polyunsaturated fatty acid metabolism
- forms the outer blood–ocular barrier
- maintains the subretinal space
- heals and forms scar tissue
- regenerates and recycles visual pigment

RPE cells serve a phagocytic function, continually ingesting the disc membranes shed by the outer segments of the photoreceptor cells. Over the course of a lifetime, each RPE cell is thought to phagocytose billions of outer segments. This process of shedding, phagocytosis, and photoreceptor renewal follows a daily (circadian) rhythm. Rods shed discs at dawn, and cones shed them at dusk. The ingested outer segments are digested gradually, broken down by enzymes from *lysosomes*.

Visual pigments contain 11-*cis*-retinaldehyde that is converted to 11-*trans*-retinaldehyde in the outer segments of the retina. Most of regeneration of the 11-*cis* to the 11-*trans* configuration occurs in the RPE and requires a highly efficient transfer of metabolites from the outer segments to the RPE cells and back. The interdigititation of the RPE and outer segments help facilitate the regeneration by increasing the surface area of contact and allowing for close proximity. The visual pigments' biochemical cycle is discussed in more detail in BCSC Section 2, *Fundamentals and Principles of Ophthalmology*.

A variety of pathologic changes—caused by such factors as genetic defects, drugs, dietary insufficiency (of vitamin A), or senescence—can impair the process of phagocytosis and renewal. Physical separation of the retina from the RPE, which occurs when subretinal fluid (ie, retinal detachment) or blood is present, also disrupts the important exchange of metabolites.

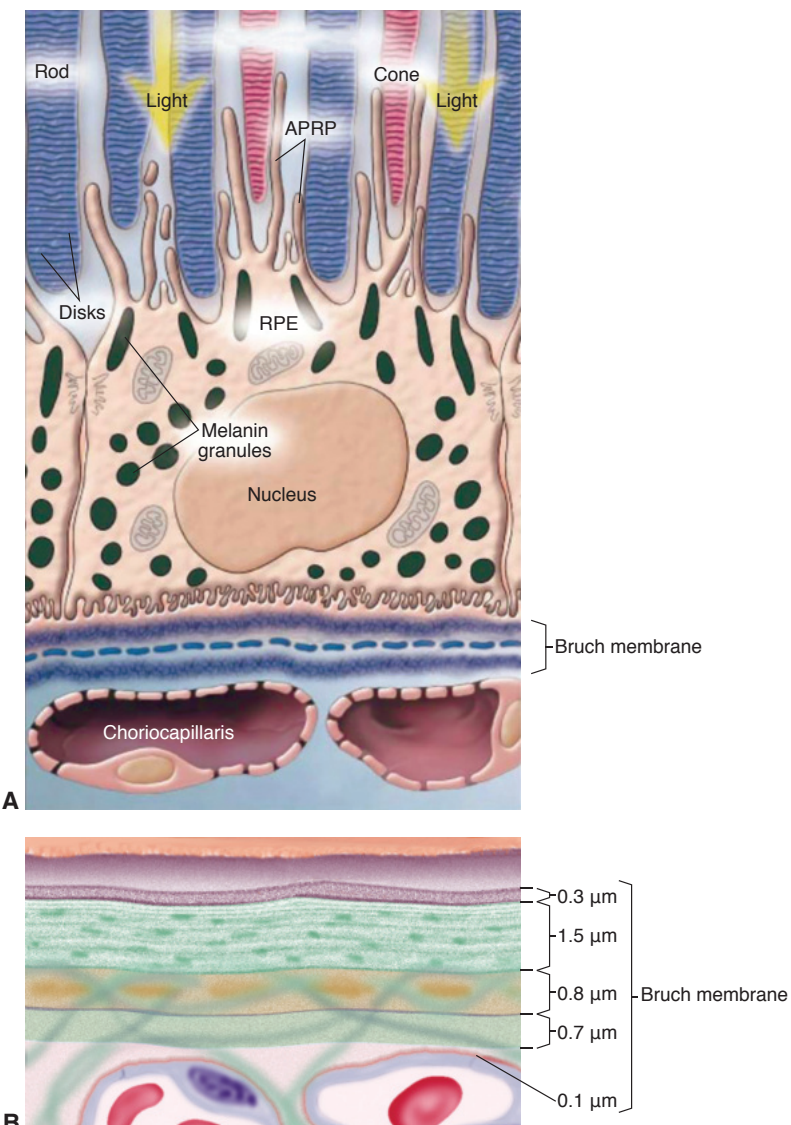


Figure 1-9 Illustrations of the Bruch membrane. **A**, The RPE and its relationship to the photoreceptors and Bruch membrane. Note the interdigitations and villi from the RPE that make contact with the outer segments of both rods and cones. **B**, The folded plasmalemma of the RPE rests on its smooth basement membrane ($0.3\text{ }\mu\text{m}$ thick) bordering the inner collagenous layer ($1.5\text{ }\mu\text{m}$ thick). The outer collagenous layer ($0.7\text{ }\mu\text{m}$ thick) borders the elastic layer ($0.8\text{ }\mu\text{m}$ thick) and is continuous with intercapillary bridges and the subcapillary fibrous tissue. (Part A courtesy of the University of Rochester; part B by Daniel Casper, MD, PhD.)

The RPE functions as a barrier to prevent diffusion of metabolites between the choroid and the subretinal space. Because of this, the environment of the photoreceptors is largely regulated by the selective transport properties of the RPE. The RPE has a high capacity for water transport, so in a healthy eye, fluid does not accumulate in the subretinal space. This RPE-mediated dehydration of the subretinal space also modulates the

bonding properties of the interphotoreceptor matrix, which acts as a bridge between the RPE and photoreceptors and helps bond the neurosensory retina to the RPE. With deterioration or loss of the RPE, there is corresponding atrophy of the overlying photoreceptors and underlying choriocapillaris.

Bruch Membrane

The basal portion of the RPE is attached to Bruch membrane, which has 5 layers. Starting with the innermost, these layers (see Fig 1-9) are the

- basement membrane of the RPE
- inner collagenous zone
- middle layer of elastic fibers
- outer collagenous zone
- basement membrane of the endothelium of the choriocapillaris

Degeneration of Bruch membrane over time is associated with buildup of lipids and oxidatively damaged materials as well as calcification. In some disease states, such as pseudoxanthoma elasticum, extensive Bruch membrane calcification leads to fractures, for example, angiod streaks. In age-related macular degeneration, areas of calcification with microscopic breaks have also been found.

Choroid

Blood enters the choroid through the posterior ciliary arteries (Fig 1-10). The outer layer of large-caliber choroidal vessels, known as the Haller layer, is relatively thick. The choroidal vessels in this layer divide into smaller-diameter vessels and precapillary arterioles in a layer known as the Sattler layer. These vessels distribute the blood throughout the choroid, reducing arterial pressure to the relatively low pressure found in the choriocapillaris. The choroid has a maximal thickness posteriorly. On histologic examination, it is 0.22 mm thick in the central macular region, becoming progressively thinner anteriorly; at the ora serrata, it is 0.1 mm thick. Subfoveal choroidal thickness measured *in vivo* among healthy volunteers with a mean age of 50 years by SD-OCT is approximately 287 μ m. However, thickness changes with age and disease states of the eye. The presence of thin choroid (leptochoroid) and thick choroid (pachychoroid) is associated with ocular disease.

In the posterior pole, the choriocapillaris forms a plexus of capillaries, even though the capillaries themselves are not arranged strictly into lobules. The capillary arrangement becomes more irregular toward the periphery, where the capillaries are arranged more radially. Interspersed between the vessels of the choroid are loose connective tissue, fibroblasts, and melanocytes.

After passing through the choriocapillaris, the blood is collected in venules, which coalesce into collecting channels, or ampullae, of the vortex veins. Most eyes have 4 or 5 vortex veins, which exit the eye at or posterior to the equator. The vortex veins drain into the superior and inferior ophthalmic veins.

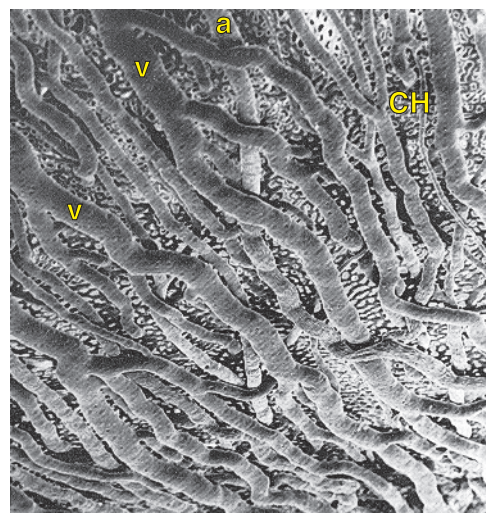


Figure 1-10 Scanning electron micrograph of the choroid. Vascular cast of the choroid from the posterior pole of a 62-year-old man, demonstrating arteries (a), veins (v), and the choriocapillaris (CH). (70 \times) (Courtesy of A. Fryczkowski, MD.)

The choroid supplies the metabolic needs of the retina, which has one of the highest metabolic rates per gram of tissue in the body. In some estimates, the choroidal circulation supplies 90% of the oxygen consumed by the retina, primarily by the photoreceptors. The choroid also has the highest blood flow of any tissue, and the venous blood exiting the choroid still has a very high oxygen tension. The RPE cells, which are anatomically closely associated with the choriocapillaris, are exposed to the highest oxygen tensions of any perfused tissue, increasing the risk of oxidative damage. The rapid flow in the choroid also acts as a heat sink, removing thermal energy obtained by light absorption.

Sclera

The sclera is composed of collagen and a few elastic fibers embedded in a matrix of proteoglycans. It terminates at the histologists' limbus. The sclera does not have uniform thickness; it is thinnest immediately behind the muscle insertion, whereas it is thicker just posterior to the limbus.

The sclera is normally permeable to the passage of molecules in both directions. Up to 40% of the aqueous leaves the eye via uveoscleral outflow, making the sclera an important path of fluid movement. Scleral permeability allows drugs to be delivered to the eye by means of injection into the sub-Tenon space. The sclera is a hydrophilic tissue and is therefore only variably permeable to hydrophobic or amphiphilic substances or medications. This characteristic is an important consideration for periocular injection of pharmacologic agents.

Hogan MJ, Alvarado JA, Weddell JE. *Histology of the Human Eye*. Philadelphia: Saunders; 1971:chaps 5, 8, 9, 11.

Polyak SL. *The Retina*. Chicago: University of Chicago Press; 1941.

Worst JGF, Los LI. *Cisternal Anatomy of the Vitreous*. Amsterdam: Kugler; 1995.

Mrejen S, Spaide RF. Optical coherence tomography: imaging of the choroid and beyond. *Surv Ophthalmol*. 2013;58(5):387–429.

CHAPTER 2

Diagnostic Approach to Retinal Disease



This chapter includes related videos, which can be accessed by scanning the QR codes provided in the text or going to www.aao.org/bcscvideo_section12.



This chapter includes a related activity, which can be accessed by scanning the QR code provided in the text or going to www.aao.org/bcscactivity_section12.

Testing for retinal disease is directed by the clinical examination of the patient, which starts with obtaining a thorough patient history, including family history, and a careful review of systems. The patient should undergo a detailed ophthalmic examination, including visual acuity measurement and testing for a relative afferent pupillary defect. In addition, in-office Amsler grid testing can provide evidence of macular disease, if present.

This chapter explores some of the imaging modalities used to evaluate retinal disease. Each modality supplies a limited set of information; no particular modality supplies all of the information about every disease. In order to understand the layers of the fundus and their disease manifestations, it is necessary to employ multimodal imaging, mastering many forms of ocular imaging and rapidly integrating the information gleaned into a more complete whole.

Ophthalmoscopy

The direct ophthalmoscope provides an upright, monocular, high-magnification ($15\times$) image of the retina. The instrument's lack of stereopsis, small field of view ($5^\circ\text{--}8^\circ$), and poor view of the retinal periphery limit its use. Therefore, indirect ophthalmoscopy has largely supplanted direct ophthalmoscopy. In indirect ophthalmoscopy, illumination is directed into the eye through an aspheric lens; this lens helps form a flat inverted aerial image between the lens and the observer. The magnification is calculated by dividing the dioptric power of the examination lens into -60 . For example, a 20 D lens would have a magnification of -3 ; the negative sign indicates an inverted image. The binocular indirect ophthalmoscope has a unitary magnification. Through the use of prisms, it reduces the distance between the pupils in the instrument, and, using a mirror, it reduces the distance from the light source to the optical axis, so that all 3 fit into the entrance pupil of the eye (see Chapter 8 in BCSC Section 3, *Clinical Optics*). Binocular indirect ophthalmoscopes

allow for stereopsis, have a field of view that depends on the dioptric power of the condensing lens (higher powers deliver wider angles of view, but at a lesser magnification), and, with ocular steering, can visualize the entire fundus as compared with direct ophthalmoscopes. If the patient's pupil can be dilated widely, the ora serrata may be seen without any additional instrumentation. If the pupil cannot be widely dilated or the clinician needs to see peripheral retinal details in profile, scleral depression must be performed.

The disadvantages of binocular indirect ophthalmoscopy include low magnification and the inverted image. A binocular indirect ophthalmoscope offers no additional magnification of the aerial image. Indirect ophthalmoscopy can also be performed with a slit lamp by using a non-contact lens, for example, a 60 D or 78 D lens. With a 60 D lens, the magnification afforded by the lens is 1; however, the slit lamp typically has a magnification of 10 \times or 16 \times . The slit beam can be used to directly or indirectly illuminate the posterior portion of the vitreous as well as retinal structures. The field of view provided by the lenses is good; a little less than 70° with a 60 D lens and more than 80° with the 78 D lens. Ocular steering can be used to evaluate a large area of the fundus. Higher dioptric lenses can help visualize wide areas of the retina even if the pupil does not dilate. These lenses may have a field of view of 100° or more. With noncontact indirect biomicroscopy, the power and capabilities of a slit lamp with a wide field of view may be employed without having to contact the eye; subsequent ocular imaging can proceed without a problem because no contact is made with the cornea. The main disadvantage is that the image created is inverted.

A direct-contact lens provides 1 of the highest resolution methods to view the fundus. Although these lenses provide no significant magnification, they obviate the refractive power, and potentially any astigmatism, of the cornea. The 3-mirror lens is commonly used in this method. The central portion is used to directly visualize the posterior pole and has a field of view of a little more than 20°. The 3 mirrors can be used to evaluate the midperiphery and far periphery of the retina as well as the angle. The advantages of direct-contact biomicroscopy include high resolution and a noninverted image. The disadvantages include having a limited field of view through any 1 component of the lens, needing to rotate the lens on the patient's eye while performing the examination, and needing to manipulate the cornea or use a viscous coupling fluid, either of which may hinder subsequent ocular imaging. Indirect-contact lenses provide the largest field of view of any lens used for ophthalmoscopy, often more than 150°. They can be used with ocular steering to easily visualize the ora serrata.

Lenses are chosen at the discretion of the examining clinician, according to what is needed for the specific examination. For example, an opacified posterior capsule with a small posterior capsulotomy may inhibit good visualization of the retinal periphery with a 3-mirror lens, but pose no significant problem for a wide-field indirect-contact lens.

Imaging Technologies

Fundus Camera Imaging

The fundus camera uses a variation of indirect ophthalmoscopy in which the objective lens is used to deliver a cone of light through the entrance pupil, subsequently forming

a flat inverted aerial image within the body of the camera, using light reflected from the eye. This image is transferred and projected on to an image sensor through a system of relay lenses. Fundus cameras use flash illumination to obtain high-quality images of the eye. Color fundus photography provides photographic records of the state of a patient's fundus for the patient's medical records; these images may also be used in research and for teaching. Because a large amount of information can be extracted from a simple color fundus photograph (Fig 2-1), this mode of imaging has been the cornerstone of many large epidemiologic and treatment studies. The color rendition is the best of any imaging system in terms of color accuracy, noise, and resolution. With the use of filters, the fundus camera can also be used to obtain fluorescein and indocyanine green angiography, in addition to autofluorescence. Imaging from fundus cameras may suffer from cloudy media in which light scattering obscures fundus details and reduces image contrast. A capacitor must be charged to power the flash unit; therefore, fundus cameras are typically only able to record images at a speed of approximately once per second.

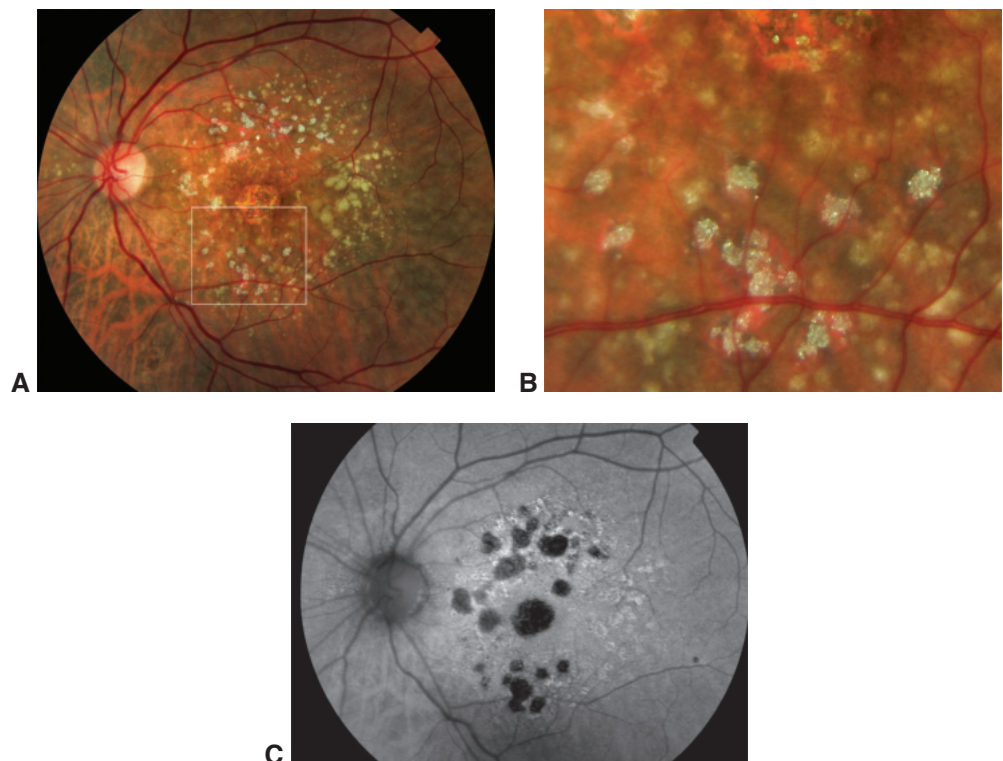


Figure 2-1 Multimodal imaging of refractile drusen and associated atrophy. **A**, Color fundus photograph of geographic atrophy with refractile drusen. **B**, Enlarging the section within the white square from **A** shows a remarkable amount of information, even the diamond-like particles that seem to correspond to hydroxyapatite spherules seen in histologic sections of drusen. **C**, Fundus autofluorescence (AF) image shows attenuated autofluorescence in areas of geographic atrophy also shown in the color photograph; it also reveals an absence of autofluorescence colocalizing in the locations of the refractile drusen. (Courtesy of Richard F. Spaide, MD.)

Scanning Laser Ophthalmoscopy

The confocal scanning laser ophthalmoscope (SLO) generates retinal images by scanning an illuminated spot on the retina in a raster pattern. It uses a Maxwellian view system to build the retinal image. Because the system is confocal, the scattered light can be rejected by the crystalline lens, as can the fluorescence, allowing for the use of shorter wavelengths in autofluorescence imaging. A photodiode is used to detect the light received from the eye. Because photodiodes are cheaper than high-resolution 2-dimensional sensors, some of the increased costs of the scanning mechanism are offset.

A variety of wavelengths can be used as dictated by need and the availability of a laser system. Infrared imaging can be used to evaluate the fundus; in some circumstances, it provides more comprehensive information than that revealed by color photography. For example, some types of pseudodrusen (subretinal drusenoid deposits) are not as prominent in color fundus photographs, but are easy to view in infrared images. Choroidal nevi reflect infrared light, consequently appearing bright in infrared imaging. The infrared image can be used to perform ocular tracking.

The chief factor that determines the resolution of SLOs is the size of the illuminated spot on the retina, which in turn is determined by the wavelength used, the numerical aperture of the illuminating system, any aberrations in the optical system, and scattering. SLOs scan the fundus with a dense pattern of spots. The resolution depends on the number of spots per unit area; a metric that is sometimes called the “digital resolution.” The digital resolution is invariably higher than the true optical resolution because the spots overlap.

In angiography, the dye is injected and then imaging begins. Some systems are able to obtain high-speed (eg, 15 frames per second) imaging of the dye’s passage through the eye. If the excitation laser and the barrier filter are put into place, no fluorescein dye is used, and the gain is turned up, an autofluorescent image of the fundus can be obtained. This method uses a blue-green wavelength that is absorbed by macular pigment. The field of view of a scanning laser imaging system is determined by its mechanical scanning system as well as the optics used to image the eye. The posterior pole can be imaged using various scan parameters. With wider-angle lens attachments, up to 55°, and in some cases 110°, can be visualized.

A second approach to scanning laser ophthalmoscopy uses an ellipsoidal mirror. Rays emanating from one focus point on an ellipse will converge on the second focus point. If ellipse is rotated along an axis, an ellipsoidal surface can be generated. If this surface is then made into a mirror, rays passing through one point will converge on the second point. If one point is placed at the entrance pupil of the eye, light rays emanating from a large solid angle will converge on the second focus point of the ellipsoidal mirror to form an image. Commercial systems that use this principle are able to obtain images approximately 200° wide. With ocular steering, nearly all of the retina can be imaged. In this method, 2 lasers are used to obtain a pseudocolor-scaled image: a red laser and a green laser. Angiography can be performed with the use of the appropriate excitation lasers. The number of points imaged is large, and these systems do not record video-rate angiography. The systems that employ an ellipsoidal mirror have limited confocality; a green laser needs to be used in order obtain autofluorescent images.

Optical Coherence Tomography

Optical coherence tomography (OCT) is a noninvasive, noncontact imaging modality that produces micrometer-resolution images of tissue. Low-coherence light is directed into tissue and into a reference arm. An interferometer combines the light returning from the tissue with the light from the reference arm, producing an interferogram. The benefit of using low-coherence light is that its spectral makeup changes rapidly with time; thus, light produced at a particular instant will not interfere well with light produced at other times. This means the exact position from which the interfering light came can be determined by the resolution dictated by the coherence length of the light source, which is typically 5–7 μm. In any given A-scan, time-domain OCT is used to interrogate each point in the tissue sequentially. In more modern techniques, for example either spectral-domain (SD) or swept-source (SS) OCT, a more efficient approach is taken. In SD-OCT, a broad-spectrum light source is used, and the resulting interferogram produced varies with the reflectivity of the tissue. SS-OCT uses a more complicated light source that sequentially scans through successive wavelengths of light across a spectral range (see Optical Coherence Tomography Technologies: A Comparison of SD-OCT and SS-OCT).

OPTICAL COHERENCE TOMOGRAPHY TECHNOLOGIES: A COMPARISON OF SD-OCT AND SS-OCT

In SD-OCT, a broad-spectrum light source is used, and the resulting interferogram varies with the reflectivity of the tissue, which depends on how far that reflecting surface is from the same distance in the reference arm; this imaging focal point is known as the zero-delay line. Thus, in SD-OCT the interferogram has frequency encoding of depth; a Fourier transform can be used to calculate the amount of reflectivity and its depth in the tissue. However, the ability of SD-OCT to detect the interferogram decreases at higher frequencies; deeper structures can be visualized, but not as effectively. A variation on this technique, enhanced depth imaging (EDI) OCT, places the zero-delay line at the deepest part of the tissue being evaluated. Deeper structures may be better visualized, but at the expense of seeing the more superficial structures. In conventional SD-OCT, the peak sensitivity is placed in the vitreous, making it possible to visualize a structure with very low reflectivity. The choroid is not visualized well with this approach. EDI-OCT is able to image the choroid, but the vitreous is not visualized well. Therefore, the clinician must choose the most appropriate imaging modality according to the situation in order to obtain an optimal image from the desired level.

In swept-source (SS) OCT, a light source sequentially scans through successive wavelengths of light across a spectral range. Over time, each sweep of light builds an interferogram. The light sources currently available are based on microelectromechanical systems, which are small and

(Continued on next page)

(continued)

fast. The disadvantages to using physical methods to obtain a swept laser output include phase jitter and mode hopping. Coming to market in the near future is a new light source, called an akinetic laser, which uses electronic means to sweep wavelengths, thereby avoiding the mechanical method of selecting wavelengths. The akinetic laser reduces phase jitter and is able to select narrow regions of light wavelengths; with these abilities, systems may soon be able to scan the entire depth of the eye, from cornea to choroid, in 1 scan.

SS-OCT systems display little change in sensitivity with increasing depth. Therefore, it is not necessary to choose whether to highlight the vitreous or choroid in an image, because both can be imaged well simultaneously. With improvements in spectrometers, SD-OCT systems might have lower amounts of sensitivity fall-off with increased depth and thus may remain competitive in the marketplace. SS-OCT is generally done at somewhat longer wavelengths because of the availability of light sources. The longer wavelengths help visualize deeper structures, with a slight trade-off in decreased lateral resolution (remember, the smallest spot size is related to wavelength).

Finally, SD-OCT systems use a line-charge coupled device to detect the interferogram after it has passed through a diffraction grating. The detector's sensitivity and response time are the major determinants of the device's scan speed. In SS-OCT, the detector is the relatively simple and high-speed photodiode, and the scan speeds can be quite fast. However, because safety standards limit the amount of light used in the eye, higher-speed imaging often comes at the expense of decreased signal-to-noise ratio. Faster scan speeds are good for area coverage and reduced imaging time, but they are a disadvantage in terms of noise.

Both SD-OCT and SS-OCT create an A-scan through tissue. B-scans consist of a collection of many A-scans conducted through a plane of tissue. A volume scan consists of an assembly of numerous B-scans; this volume scan is stored in computer memory as a block of data in which each memory location stores a value that corresponds to a specific small volume of tissue. The *voxels* (a portmanteau of volume and pixels) in the volume of data may be represented in many ways; 1 simple way is to make planar slices producing an image called a C-scan. C-scans are difficult to interpret because in a curved structure, many planes of tissue can be crossed. Another, more advanced method is to segment the data according to tissue planes; a thickness of voxels presented this way is called an *en face scan*. The tissue thicknesses can be measured in an en face scan; the retinal nerve fiber layer is commonly measured. Maps of the thickness of the retina or a specific retinal layer can also be produced. Actual correlation between OCT scans and histology of the retina has not yet been thoroughly explored, and the correlation of the identity of structures seen in OCT has changed numerous times. The International Nomenclature of OCT Panel has proposed nomenclature terminology, but these assignments are likely to change over time (Activity 2-1).



ACTIVITY 2-1 Optical coherence tomography (OCT) nomenclature terminology, based on the International Nomenclature for OCT Panel for Normal OCT Terminology.



From Staurenghi G, Sadda S, Chakravarthy U, Spaide RF; International Nomenclature for Optical Coherence Tomography (IN•OCT) Panel. Proposed lexicon for anatomic landmarks in normal posterior segment spectral-domain optical coherence tomography: the IN•OCT consensus. Ophthalmology. 2014;121(8):1572–1578.

Access all Section 12 activities at www.aao.org/bcscactivity_section12.

Some OCT scanners offer eye movement tracking. With the addition of this feature, ocular motion can be detected and corrected in the final image, improving the quality of the resulting scan. Tracking methods rely on recognizing fundus features and registering the scan pattern with the fundus image. This capability expands the utility of OCT; with it, scans interrupted by patient blinks still produce usable images. In addition, it is possible to perform repeated scans of the same fundus location over time, enabling assessment of disease progression (Fig 2-2).

In addition to B-scans and en face imaging, volume rendering shows the 3-dimensional character of the tissue. Compared to ordinary B-scans, volume rendering is computationally intensive. It is used in radiology, but is not yet widely used in ophthalmology (Fig 2-3).

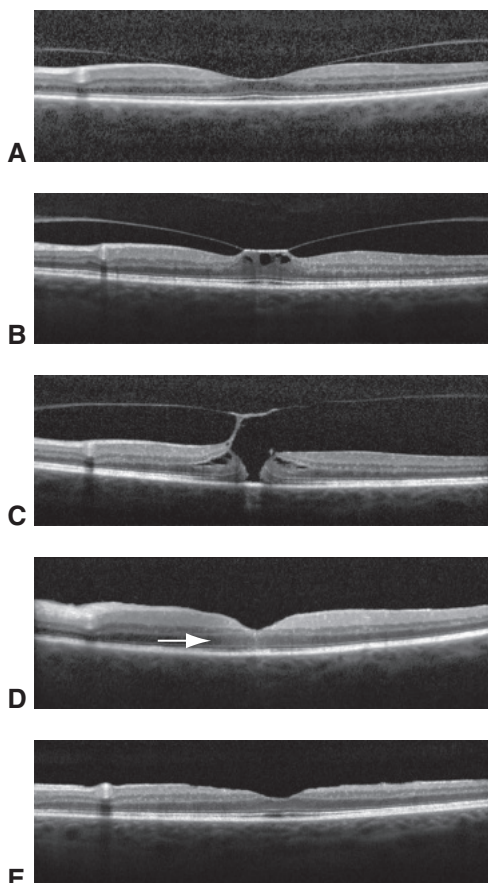


Figure 2-2 Evolution of a macular hole, visualized with optical coherence tomography (OCT). **A**, OCT image of a patient with a perifoveal posterior vitreous detachment and no obvious traction on the macula. **B**, After 1 year, the patient experienced visual distortion; the image shows obvious traction with foveal tractional cavitations. **C**, Image taken 2 months later; note the full-thickness macular hole. **D**, Image taken 1 month after macular hole surgery; the hole is closed. Note the subtle area of increased reflectivity in the center. **E**, Image taken 3 months later shows the fovea with a nearly normal contour and laminar structure. (Courtesy of Richard F. Spaide, MD.)

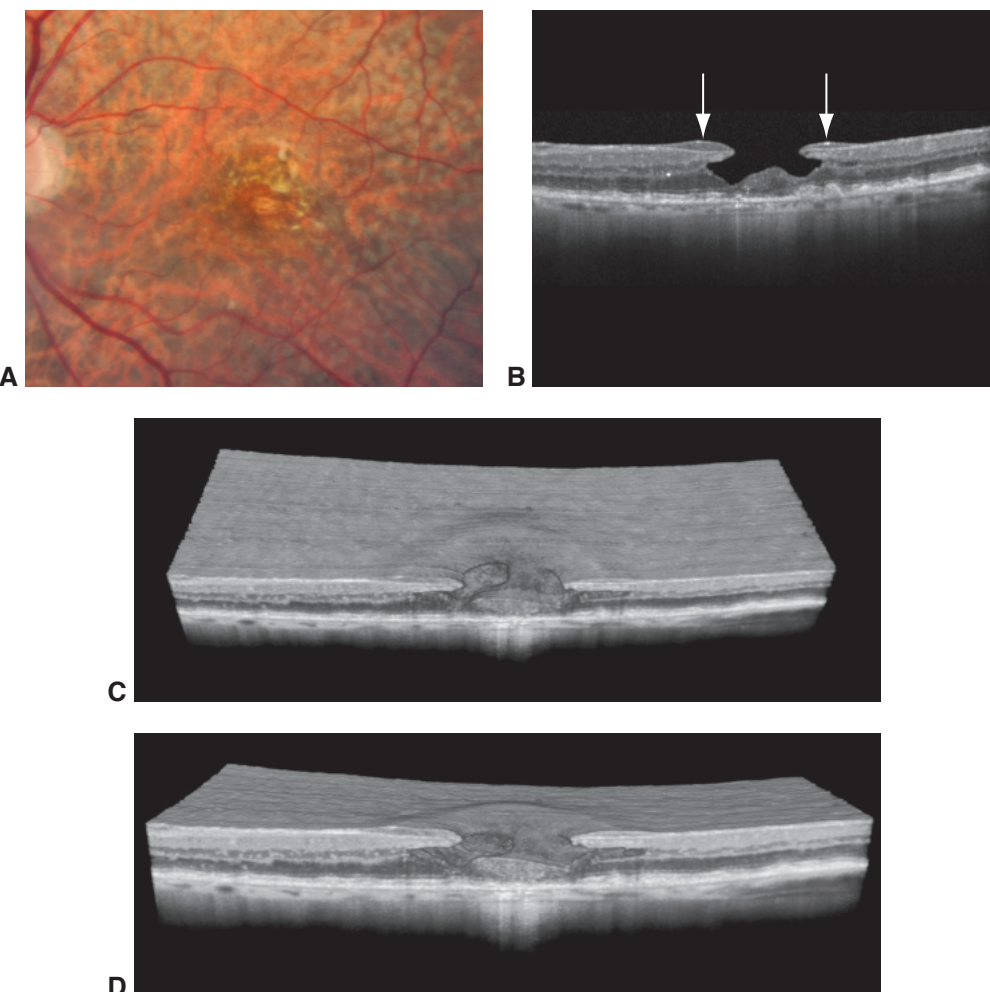


Figure 2-3 Imaging of a lamellar macular hole. **A**, Fundus photograph of a patient with prominent drusen and distorted vision. **B**, A B-scan section of the OCT imaging shows a lamellar hole with an unusually thick epiretinal membrane, which is sometimes seen in association with lamellar macular holes. **C** and **D**, Two different views from volume-rendered imaging of the lamellar macular hole taken in sections, showing the thick epiretinal membrane, as well as the absence of induced distortion of the retina. Note the cavities within the undermined retina and the attachment of the proliferation to the central foveal tissue. (*Courtesy of Richard F. Spaide, MD.*)

Optical Coherence Tomography Angiography

In a series of images taken at a sufficient interval, a moving object will appear at different positions on the successive images. When these images are compared pixel by pixel, nonmoving regions will show no change, while moving objects will produce areas that show high variance. If the color black is assigned to areas of low variance (ie, areas that do not move), and the color white is assigned to areas with high variance, then the resulting image will highlight movement; this is called motion contrast. The retina has no moving parts, except for the flow of blood. If the images are high resolution, successive retinal

images can show the movement of blood through the retina. Images taken with OCT are not only high resolution but also depth-resolved. Therefore, data obtained from tissue can be compared with successive data. The result is a 3-dimensional visualization of movement within the retina, corresponding to blood flow in its various layers.

Unlike fluorescein angiography, which can only visualize the superficial capillary plexus, optical coherence tomography angiography (OCTA) can image all capillary layers, including the superficial plexus, the radial peripapillary capillary network, and the deep vascular plexus. This provides huge opportunities to advance our understanding of retinal diseases. En face OCT is another way to visualize flow information. En face imaging of flow in the retina is a useful technique because the resulting image of the retina is arranged in layers, as is its blood supply. In this method, a slab of the flow information corresponding to the expected position of a layer of vessels is selected. Next, the brightest pixel in each column of voxels is selected and displayed, which is called a maximal intensity projection. This projection creates a flat image from the data, which exists in 3 dimensions.

OCTA can visualize the retinal vasculature at a higher resolution than any other current imaging modality (Fig 2-4). However, OCTA is prone to artifacts; understanding how these artifacts are created is key to understanding and interpreting the images produced. Motion results in bright areas in the image, but this motion does not necessarily come from blood flow. For example, if the patient's eye moves during the examination, portions of the resulting image will contain motion artifacts. Multiple automatic scans with eye tracking and software repair can suppress most motion artifacts. Another type of defect, called a projection artifact, is created when light passes through a blood vessel and strikes a deeper reflective structure; over time, the light that reflects from that structure will change, mimicking the overlying blood vessel. The image created will have what appears to be 2 levels of the same vessel: the first at its actual location and the second at the level of the reflecting structure. Several mathematical approaches can remove projection artifacts. A third potential issue in OCTA is the appearance of dark areas on the image. Dark areas visualized in the fundus can be the result of a lack of blood flow, or at least blood flow too slow to be detected in successive scans at the interval time used. However, frequently it is too difficult to ascertain whether there is a true lack of flow, so the dark areas on the images are called signal voids.

Finally, segmentation works well on normal retinas, but the more diseased a retina is, the less accurate the segmentation becomes. If the layer has not been segmented properly, it becomes much more difficult to visualize the flow in any given layer. This difficulty has led to the creation of alternate methods of showing flow data, such as volume rendering (Fig 2-5).

Fundus Autofluorescence

Fundus autofluorescence (AF) is a rapid, noncontact, noninvasive way to visualize fluorophores in the fundus. In this method, excitation light is introduced to the eye; fluorescence from intrinsic fluorophores is detected by using a barrier filter to exclude that excitation light from the image. The creation of fluorophores starts with visual pigment, which contains many conjugated double bonds. The visual pigment's absorption of light energy may also lead to the creation of reactive molecular species that can cross-react to other

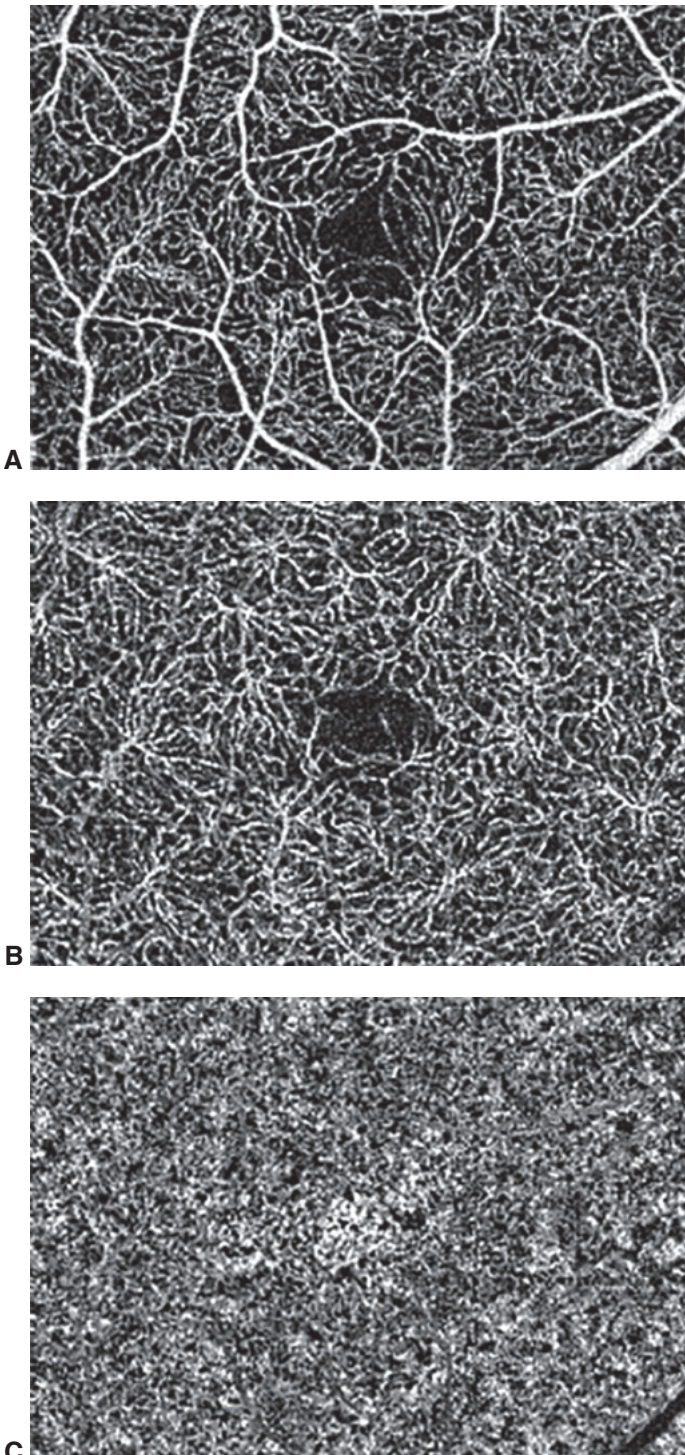


Figure 2-4 OCT angiography with projection artifact removal. **A**, Image showing a superficial vascular plexus with fractal branching. **B**, Image showing a deep vascular plexus. Its vessels are small and do not show the same branching characteristic as the superficial vascular plexus. **C**, Image of the choriocapillaris with dark areas; these low-signal areas are called signal voids. (Courtesy of Richard F. Spaide, MD.)

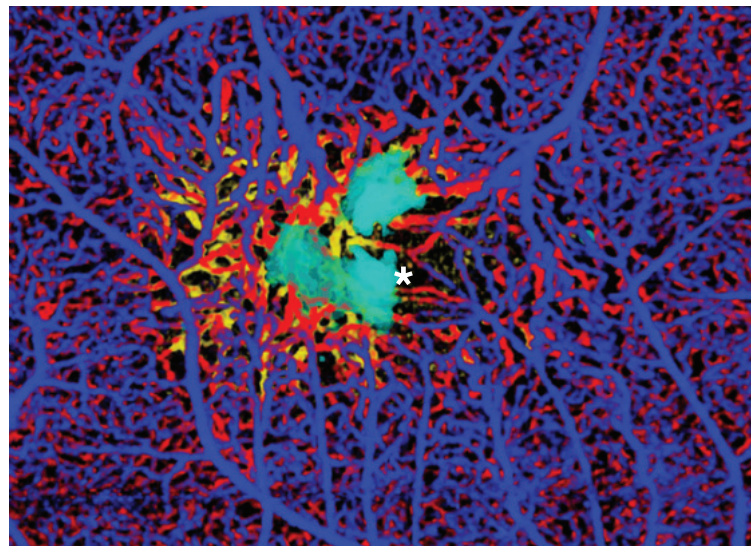


Figure 2-5 Volume-rendered image of type 2 macular telangiectasia. The vessels at the level of the inner plexus are blue, those at the level of the deep plexus are red, and the vessels deep within the deep plexus, at the outer nuclear layer or below, are yellow. Note the tractional displacement of the vessels that leads to a near obliteration of the foveal avascular zone (*asterisk*). The foveal cavitations are shown in cyan. (Courtesy of Richard F. Spaide, MD.)

molecules; 1 such molecule is the bis-retinoid A2E, a component derived from 2 molecules of vitamin A aldehyde and 1 molecule of ethanolamine. A2E appears to accumulate in Stargardt disease, in which a defective adenosine triphosphate-binding cassette protein (encoded by *ABCA4*) prevents proper transport of vitamin A derivatives across disc membranes in photoreceptors. This causes abnormal accumulation of 11-*trans*-retinal and several downstream reaction byproducts that are difficult for retinal pigment epithelium (RPE) cells to process. These products then accumulate in lysosomes as lipofuscin. Similar bis-retinoids accumulate within the lysosomes of RPE cells as a normal part of the aging process; they are not necessarily harmful. If the RPE cell dies, the contained lipofuscin disperses, resulting in a loss of autofluorescence, so that these areas appear dark on autofluorescence images. If there is a tear in the RPE, which is usually seen patients with choroidal neovascularization (CNV), the scrolled RPE is hyperautofluorescent because of reduplication, while the bared area shows no autofluorescence signal (Fig 2-6). This mechanism of autofluorescence loss is used to monitor the absence of RPE cells in a variety of diseases.

There are 2 main types of systems used to image autofluorescence. A fundus camera uses special filters that are tuned to detect autofluorescence from lipofuscin without being swamped by autofluorescence from the crystalline lens, which may be derived, in part, from tryptophan and by nonenzymatic glycosylation of lens proteins. These cameras use wavelengths in the green end of the spectrum, and the recorded autofluorescence begins closer to the orange wavelengths. The excitation wavelengths are not absorbed by macular pigment. Commercial SLOs initially used blue excitation light intended to excite fluorescein, but these wavelengths were absorbed by macular pigment. Later, using a green laser for excitation was introduced; green light is not absorbed by macular pigment. By

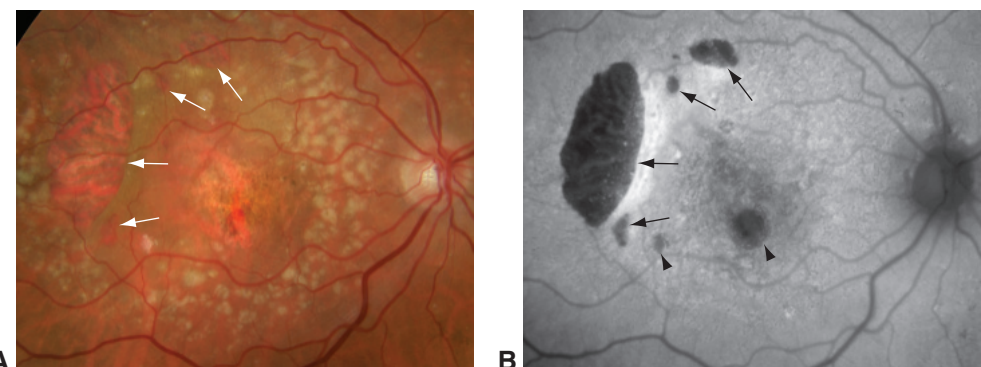


Figure 2-6 Tears in the retinal pigment epithelium (RPE). **A**, Fundus photograph of a patient with choroidal neovascularization (CNV) who was given an intravitreal injection of an anti-vascular endothelial growth factor agent and developed what appeared to be 4 RPE tears (arrows). **B**, Fundus AF reveals the absence of autofluorescence and an increased signal where the RPE appears to be scrolled, thus confirming the CNRPE tear (arrows). Small areas of atrophy are also revealed by the autofluorescence (arrowheads). (Courtesy of Richard F Spaide, MD.)

comparing the ratio of green light autofluorescence in 2 registered fundus images, it is possible to make a 2-dimensional map of macular pigment density.

Although lipofuscin in the RPE is the main source of autofluorescence from the fundus, accumulation of fluorophore in the subretinal space is another important signal source for the evaluation of some diseases, such as central serous chorioretinopathy. After the disease is present for a few months, the detachment becomes lighter and slightly more yellow in color, and the detachment also becomes hyperautofluorescent. This hyperautofluorescence is easier to detect with a fundus camera than with an SLO system for 2 main reasons. First, SLO systems are confocal; if the plane of focus is at the level of the RPE, the top of the detachment may not be in the confocal range. Second, the wavelengths used for fundus camera autofluorescence are more closely tuned to the fluorescence wavelengths emitted by fluorophores in the retina. Upon OCT imaging, an accumulation of material was found on the back surface of the retina in eyes with central serous chorioretinopathy with hyperautofluorescent detachments. It is thought that the photoreceptor outer segments are typically phagocytized and processed by the RPE, but if the retina has been physically elevated by fluid, the photoreceptors become separated from the RPE, thus impeding phagocytosis. This mechanism of disease pathophysiology may also be seen in vitelliform deposits in vitelliform macular dystrophy, adult vitelliform lesions, the yellow material that builds up under chronic retinal detachments caused by optic pit maculopathy, and pockets of retained subretinal fluid after detachment surgery.

Near-infrared fundus autofluorescence (NIA) imaging using 787-nm excitation and greater than 800-nm emission reveals fluorescence that was previously attributed to melanin from the RPE and the deeper layers of the choroid. However, lipofuscin can also fluoresce in the wavelengths mentioned, and it appears that during lipofuscin processing, melanosomes are fused with lysosomes to produce melanolysosomes. The melanin may

bind to some of the free radicals in lipofuscin, but in any case, molecular cross-linking occurs. The resulting melanolipofuscin also fluoresces in the selected ranges. Thus, it may be possible to detect differing molecular species with autofluorescence. In addition, in time-resolved fluorescence imaging, different molecules can fluoresce at the same wavelengths but at measurably different times after excitation. Using time-resolved imaging with a phasor approach allows *in vivo* identification of various molecular species, as well as measurement of the reduction–oxidation reaction state. Studies are being conducted on hyperspectral autofluorescence in which differing wavelengths of fluorescence are measured in order to try to understand more about the formation of component molecules.

Schmitz-Valckenberg S, Holz FG, Bird AC, Spaide RF. Fundus autofluorescence imaging: review and perspectives. *Retina*. 2008;28(3):385–409.

Adaptive Optics Imaging

Adaptive optics imaging is a collection of techniques that compensates for wavefront alterations in real time. These techniques, which were developed for use in astronomical telescopes, can help compensate for changes induced by variations in tear film and ocular currents, among other causes. The photoreceptors in the retina can act as waveguides; if light is within the acceptance angle of the waveguide they augment the reflection produced. This augmentation provides an opportunity to visualize individual photoreceptors in the retina. These photoreceptors are stimulated with a laser, allowing imaging information to be obtained about specific types of photoreceptors. However, this type of imaging is extremely time consuming, and it requires expensive custom-built instruments to obtain satisfactory results. Significant adoption of adaptive optics imaging in eye clinics has been prevented by the time required, the complexity of the instrumentation, and the limited ability to image all patients (eg, patients with media opacities or intraocular lenses cannot be imaged).

Retinal Angiographic Techniques

Fluorescein angiography

Fluorescein dye ranges from yellow to orange-red in color, depending on its concentration. Its peak excitation is 465–490 nm and its peak emission is 520–530 nm in physiologic environments. Fluorescein is approximately 80% protein-bound in circulation; the blood–retina barrier prevents it from diffusing into retinal tissue. However, leakage can show in areas with new vessel growth, which lack a blood–ocular barrier, or regions with blood–ocular barrier defects induced by inflammation or ischemia. Fluorescein readily leaks from the choriocapillaris, staining the surrounding tissue. This rapid leakage, as well as the light absorption and scattering by the pigment in the RPE and choroid, prevents widespread use of fluorescein in choroidal imaging.

Typically, 2–3 mL of a 25% sterile solution or 5 mL of a 10% sterile solution is injected in the antecubital vein. The dye is typically visible within 12 to 14 seconds, rapidly filling the arterial system (Fig 2-7). It is possible to detect dye in the choroidal circulation before

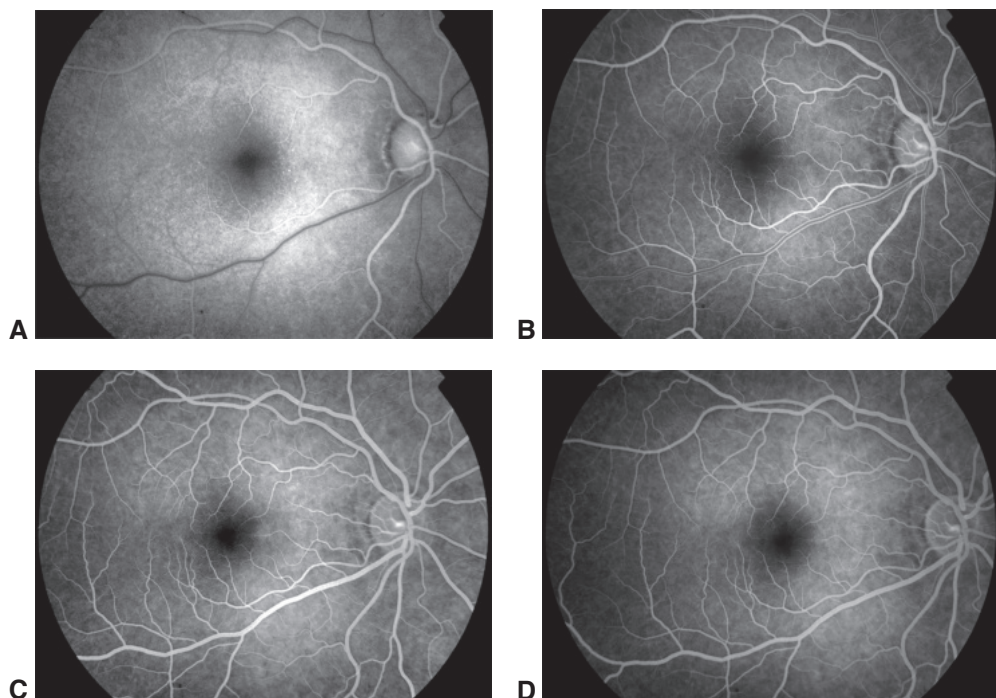


Figure 2-7 Fluorescein angiogram of a healthy eye. **A**, The choroid fills approximately a half-second before the retina. The image shows the dye front beginning to enter the retinal arteries. **B**, The laminar filling after dye injection. **C**, The arteriovenous-filling stage. **D**, After time, the fluorescence decreases as the dye is removed from the blood stream. (*Courtesy of Richard F. Spaide, MD.*)

the retinal arteries fill; in the eyes of young, healthy patients, the arteries fill in 1 or 2 seconds, and dye begins to appear in a laminar filling pattern in the retinal veins. The choroid may not fill uniformly. Any areas in the choroid that do not fill by the time the retinal circulation reaches the laminar flow stage are considered signs of abnormal choroidal filling. Once dye reaches the choriocapillaris, it leaks and stains Bruch membrane and the stroma, and details in the choroid are lost. If the dye injection was rapid, the bolus of dye will enter and leave the ocular circulation only to return a few seconds later; this is called the recirculation phase. During the fluorescein angiogram, the fovea appears darker than the surrounding areas because of the presence of macular pigment; the RPE cells under the macula are slightly taller and contain more melanin than peripheral RPE cells, and there are no retinal vessels. Over several minutes, the dye is removed from circulation and the intensity of the fluorescence decreases.

Abnormalities observed with FA can be grouped into 3 categories, each associated with one of the following types of fluorescence:

- autofluorescence
- hypofluorescence
- hyperfluorescence

Autofluorescence is fluorescence that appears with the excitation and barrier filters in place before the fluorescein dye is injected; it is caused by endogenously fluorescent constituents of tissue such as accumulation of outer segments, lipofuscin, or optic nerve head drusen. *Hypofluorescence* occurs when normal fluorescence is reduced or absent; it is present in 2 major patterns:

1. vascular filling defects
2. blocked fluorescence

Vascular filling defects are defects in which retinal or choroidal vessels fail to fill because of an intravascular obstruction that results in nonperfusion of an artery, vein, or capillary. These defects appear as either a delay in or complete absence of filling of the involved vessels. *Blocked fluorescence* occurs when the stimulation or visualization of the fluorescein is obstructed by fibrous tissue, pigment, or blood that blocks normal retinal or choroidal fluorescence in the area. The depth of a lesion can be easily determined by relating the level of the blocked fluorescence to details of the retinal circulation. For example, if lesions block the choroidal circulation, but retinal vessels are present on top of this blocking defect, then the lesions are located above the choroid and below the retinal vessels.

Hyperfluorescence occurs when the fluorescence is abnormally excessive, typically extending beyond the borders of recognized structures; this manifests in a few major patterns:

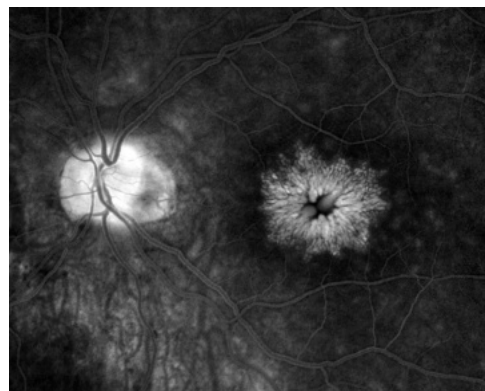
- leakage
- staining
- pooling
- transmission, or window, defect
- autofluorescence

Leakage, which is a gradual, marked increase in fluorescence over the course of the study, results from the seepage of fluorescein molecules across the blood–retina barrier. When the outer blood–retina barrier is compromised, the dye traverses across the pigment epithelium into the subretinal space or neurosensory retina. When the inner blood–retina barrier is compromised, the dye leaks through vascular walls into the retinal parenchyma, fibrotic tissue, and cystoid spaces. Dye can also leak through the posterior blood–retina barrier (the RPE) and accumulate in the subretinal space, fibrotic tissue, or directly into the retina, if the external limiting membrane of the retina is compromised.

Staining refers to a pattern of hyperfluorescence in which the fluorescence increases in intensity through transit views, and persists in late views, but in which the borders remain intact throughout the study. Staining results from fluorescein entry into a solid tissue or material that retains the fluorescein, such as a scar, drusen, optic nerve tissue, or sclera.

Pooling refers to the accumulation of fluorescein in a fluid-filled space in the retina or choroid (Fig 2-8). As fluorescein leaks into the space, the margins of the space trap the fluorescein and appear distinct, for example, as seen in an RPE detachment in central serous chorioretinopathy.

Figure 2-8 Fluorescein angiogram of an eye with post-surgical cystoid macular edema. The fluorescein dye pools in the petaloid cystoid spaces within the central macula, and there is late staining of the optic nerve head. (Courtesy of Richard F. Spaide, MD.)



A *transmission defect*, or *window defect*, refers to a view of the normal choroidal fluorescence through a defect in the pigment of the RPE. In a transmission defect, hyperfluorescence occurs early, corresponding to filling of the choroidal circulation, and reaches its greatest intensity with the peak of choroidal filling. The fluorescence does not increase in intensity or shape and usually fades in the late phases as the choroidal fluorescence becomes diluted by blood that does not contain fluorescein. The fluorescein remains in the choroid and does not enter the retina.

Multiple defects may be present in a diseased eye. For example, in an elderly patient with CNV, the choroid will often show segmental filling delays; there will be hyperfluorescence in the fovea because of the proliferation of vessels that leak; and there will be late leakage from CNV (Fig 2-9).

Fluorescein angiography has traditionally been imaged with a fundus camera or an SLO that had a field of view up to about 50°. There are also wide-angle scanning laser systems that are able to image most of the fundus, including the periphery (Fig 2-10).

Adverse effects of fluorescein angiography All patients injected with fluorescein experience a temporary yellowing of the skin and conjunctiva that lasts 6–12 hours. The most common adverse effects include nausea and vomiting (in approximately 5% of injections) and the development of hives (also in approximately 5% of injections). The nausea will pass in a few seconds without treatment. Hives, unless very mild, are usually treated with diphenhydramine. More serious adverse effects such as hypotension, shock, laryngeal spasm, or even death have occurred, but only in rare instances. Prior urticarial reactions increase a patient's risk of having a similar reaction after subsequent injections; however, premedicating the individual with antihistamines, corticosteroids, or both appears to decrease the risk. Extravasation of the dye into the skin during injection can be painful, requiring application of ice-cold compresses to the affected area for 5–10 minutes. Close follow-up of the patient over hours or days until the edema, pain, and redness resolve is advised. Although teratogenic effects have *not* been identified, many ophthalmologists avoid using FA in pregnant women in the first trimester unless absolutely necessary. In lactating women, fluorescein is transmitted to breast milk.

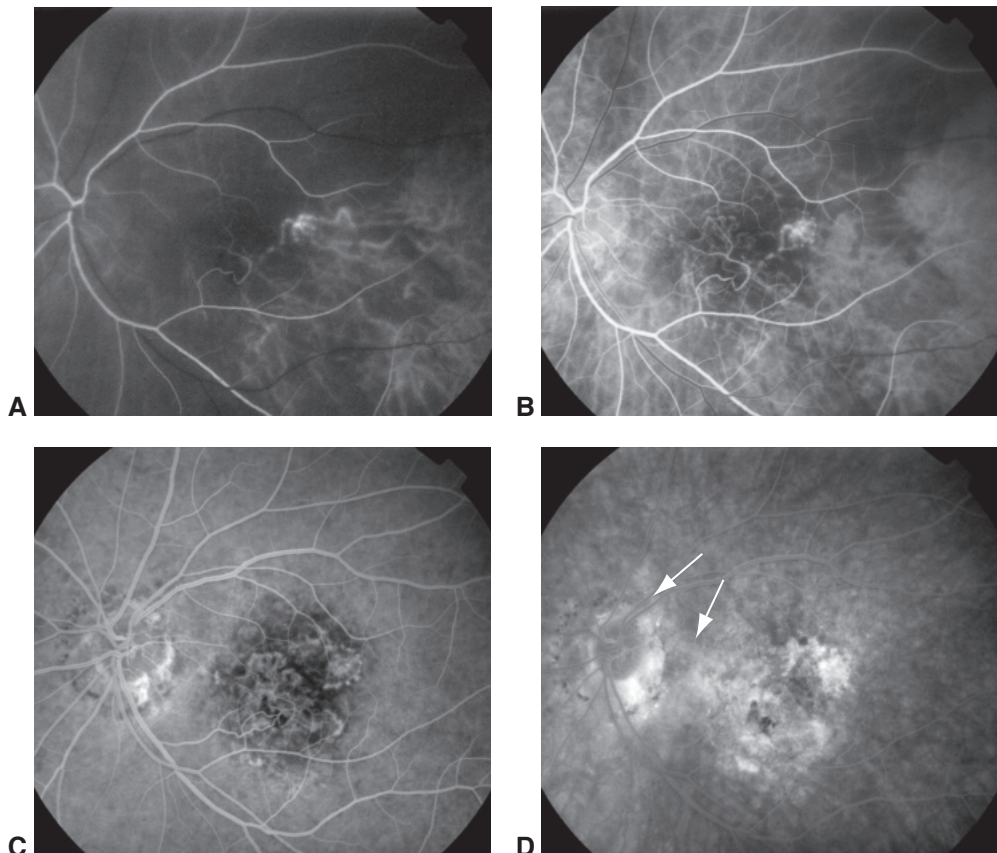


Figure 2-9 Fluorescein angiography of an eye with CNV. **A**, The choroid displays delayed filling. By the time dye reaches the central retinal artery, only a few choroidal vessels contain dye. **B**, In the early laminar-filling stage, a large portion of the choroid still shows poor filling. **C**, In the arteriovenous stage, the choriocapillaris appears uniformly filled. The clearly defined network of choroidal neovascular vessels is revealed in the central macula. **D**, The late-phase angiogram reveals leakage around the vessels with the earliest filling, an image consistent with classic CNV. There is also late staining and mild leakage from a poorly defined region (arrows), which is consistent with occult CNV. (Courtesy of Richard F. Spaide, MD.)

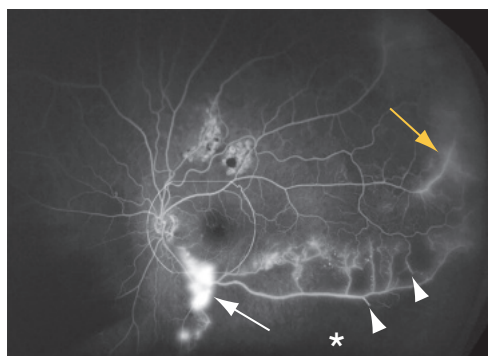


Figure 2-10 Wide-angle fluorescein angiogram image of an eye with retinal vasculitis shows numerous occlusions that do not occur at a vascular crossing (arrowheads) and are associated with a large area of nonperfusion (asterisk). Adjacent to that area of nonperfusion is retinal neovascularization (arrow) showing profuse leakage. The white outline delineates the area imaged with a 45° fundus camera. There is leakage from peripheral vessels (yellow arrow) and from some vessels bordering regions of absent perfusion. (Courtesy of Richard F. Spaide, MD.)

Berkow JW, Flower RW, Orth DH, Kelley JS. *Fluorescein and Indocyanine Green Angiography: Technique and Interpretation*. 2nd ed. Ophthalmology Monograph 5. San Francisco: American Academy of Ophthalmology; 1997.

Kwiterovich KA, Maguire MG, Murphy RP, et al. Frequency of adverse systemic reactions after fluorescein angiography. Results of a prospective study. *Ophthalmology*. 1991;98(7):1139–1142.

Indocyanine green angiography

Indocyanine green (ICG) is a water-soluble, tricarbocyanine dye that is almost completely protein-bound (98%) after intravenous injection. Because the dye is protein-bound, diffusion through the small fenestrations of the choriocapillaris is limited. The intravascular retention of ICG, coupled with low permeability, makes ICG angiography ideal for imaging choroidal vessels. ICG is metabolized in the liver and excreted into the bile. Both the excitation (790–805 nm) and emission peak (825–835 nm) are in the near-infrared range. Because its fluorescence efficacy is low, practical ICG angiography can only be performed with digital sensors.

ICG angiography is used to image polypoidal choroidal vasculopathy, which is a common form of choroidal neovascularization (Fig 2-11), and to provide important information about the pathophysiology of type 3 neovascularization (also known as retinal angiomatous proliferation). With the use of ICG angiography, it was discovered that patients with drusen could have asymptomatic choroidal neovascularization. ICG angiography may also be used to help diagnose inflammatory diseases such as birdshot chorioretinopathy, multifocal choroiditis, and panuveitis. Eyes with central serous chorioretinopathy show multifocal areas of choroidal vascular hyperpermeability when visualized with ICG angiography. However, the use of ICG angiography to diagnose uveitis or

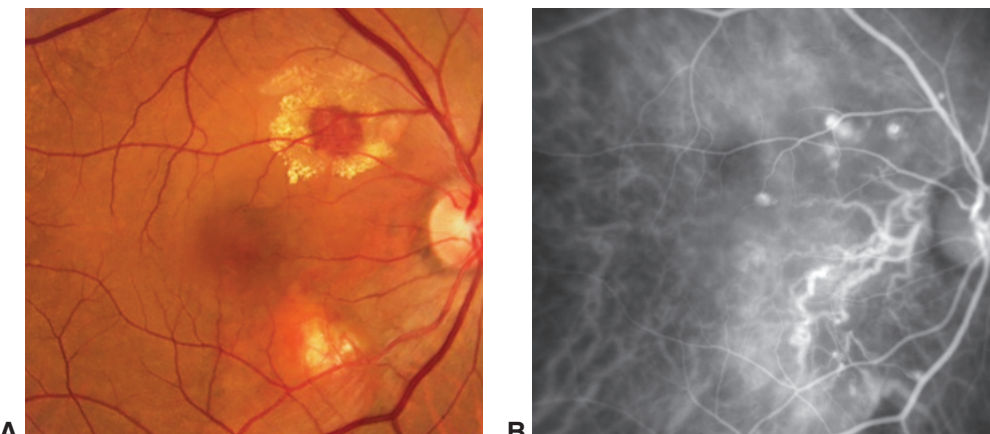


Figure 2-11 Polypoidal choroidal vasculopathy. **A**, Fundus photograph shows an area of lipid exudation surrounding a hemorrhage, large orange-colored vessels, and an area of decreased pigmentation inferotemporal to the optic nerve. **B**, The indocyanine green angiographic image clearly shows the sub-RPE vessels affected by polypoidal choroidal vasculopathy. (Courtesy of Richard F. Spaide, MD.)

central serous chorioretinopathy has been mostly supplanted by the use of a combination of autofluorescence imaging with enhanced depth imaging (EDI) OCT.

Adverse effects of indocyanine green angiography Mild adverse events occur in fewer than 1% of patients. ICG is dissolved in a 5% sodium iodide (an additive used in table salt) solution. There is no reason to suspect that a shellfish allergy should preclude the use of ICG. However, angiographic facilities should have emergency plans and establish protocols to manage complications associated with either fluorescein or ICG administration, including anaphylaxis. ICG may persist in the blood longer in patients with liver disease.

Ultrasonography

Contact B-scan ultrasonography is the most common form of ultrasonography used in the clinic. In contact B-scan ultrasonography, a 10-MHz probe is placed on the patient's eyelid. A piezoelectric crystal is used to send and receive sound waves for each A-scan. The ultrasound beam is about 1 mm wide at the level of the retina, which severely limits the lateral resolution. The axial resolution, which is the resolution along the axis of the ultrasound beam, is very different in the eye versus as measured with flat surfaces. This difference is due to the interaction of the eye's curved surfaces with the lateral summation of the signal. Contact B-scan ultrasonography is used to evaluate tumor thickness, detect foreign bodies, assess choroidal or retinal detachments, and analyze the vitreous. Drusen of the optic nerve head can be detected by observing small areas of bright reflection in the nerve that cause shadows. Careful ultrasonography is able to detect retinal tears. Ultrasonography also has the ability to image the eye during saccades, because the imaging doesn't have to occur through the pupil. Information gained during dynamic examinations is helpful when examining the vitreous and in differentiating retinoschisis from true detachment. Contact B-scan ultrasonography can produce images through opaque media (Figs 2-12 and 2-13; Videos 2-1 and 2-2).

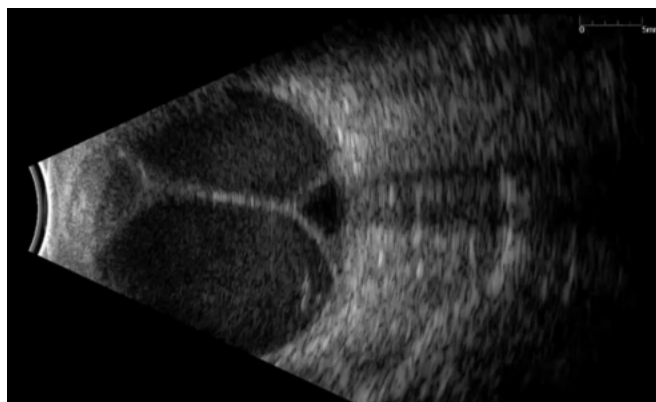


Figure 2-12 Contact B-scan ultrasonography shows massive choroidal effusions (kissing chorioidals) containing liquefied blood. The corresponding video (Video 2-1) shows the swirling of the blood within the chorioidals with eye movement. The dynamic evaluation of the ocular contents during ultrasonography is a powerful tool. (*Courtesy of Yale Fisher, MD, and www.ophthalmicedge.org.*)

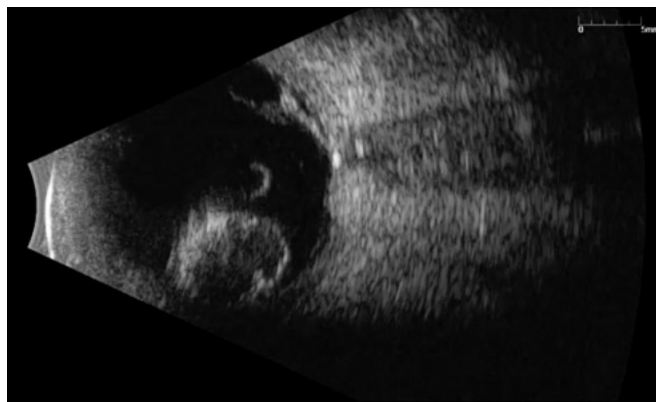


Figure 2-13 Dislocated cataractous lens in the vitreous cavity. Inferior equatorial B-scan view demonstrates strongly reflective ovoid lesion with moderately reflective internal signals consistent with a dislocated lens. The corresponding video (Video 2-2) shows the vitreous and lens and their interactions during eye movement. (*Courtesy of Yale Fisher, MD, and www.opthalmicedge.org.*)

Ultrasound biomicroscopy uses higher frequencies and thus offers higher resolution images, but at the cost of decreased tissue penetration depth. The probe, typically 50 MHz, is contained inside a soft, water-filled bag that is placed against the patient's eye. Ultrasound biomicroscopy is used to evaluate the anterior chamber and ciliary body; it can also be used to visualize the vitreous insertion anteriorly. Typical uses in a retinal practice include the evaluation of tumors, iris cysts, foreign bodies, anterior suprachoroidal effusions, cyclodialysis clefts, intraocular lens placement, and hyphemas.



VIDEO 2-1 Contact B-scan ultrasonography showing massive choroidal effusions.

Courtesy of Yale Fisher, MD, and www.opthalmicedge.org.

Access all Section 12 videos at www.aao.org/bcscvideo_section12.



VIDEO 2-2 Dislocated cataractous lens in the vitreous cavity.

Courtesy of Yale Fisher, MD, and www.opthalmicedge.org.



Coleman DJ, Silverman RH, Lizzi FL, et al. *Ultrasonography of the Eye and Orbit*. 2nd ed. Philadelphia: Lippincott Williams & Wilkins; 2006.

DiBernardo CW, Greenberg EF. *Ophthalmic Ultrasound: A Diagnostic Atlas*. 2nd ed. New York: Thieme; 2006.

Fisher Y. *Ultrasound*. www.opthalmicedge.org. Accessed September 4, 2020.

CHAPTER 3

Retinal Physiology and Psychophysics

Electrophysiologic Testing

Most electrophysiologic tests use evoked potential techniques in which a controlled stimulus is used to evoke an electrophysiologic response. Different techniques can be used to assess the function of the majority of the visual system, extending from the retinal pigment epithelium (RPE) to the primary visual cortex. Dysfunction discovered at one level usually signals abnormalities in another; for example, an abnormal cortical response to a pattern visual stimulus could reflect an uncorrected refractive error, maculopathy, optic neuropathy, primary dysfunction of the posterior visual pathways, or other conditions.

Electrophysiologic testing provides objective measures of visual system function, which are interpreted in conjunction with structural imaging data; normal structure should not be assumed to mean normal function. In addition, in order to accurately interpret the data obtained during electrophysiologic testing, the clinician needs to know the origin of the signals to be able to relate the findings from a particular patient's test to the underlying pathophysiology. Although this chapter does not provide instructions for a comprehensive diagnostic review, the principles of localization in the examples included here may be applicable to other disorders. In addition to diagnostic uses, electrophysiologic data are used in objective monitoring, either of disease progression or the efficacy of treatment, or as both an outcome measure and an index of safety in the evaluation of novel therapeutic interventions.

A thorough patient history and careful ophthalmic examination helps the clinician determine the most appropriate tests to employ; those tests should then be performed using standardized protocols. The International Society for Clinical Electrophysiology of Vision (ISCEV) publishes minimum standards for performing the routine tests, thus enabling meaningful interlaboratory comparison and literature searches. Many laboratories, particularly those with a strong research interest, use more complex test protocols but also always include the standard responses. The International Federation for Clinical Neurophysiology has also published guidelines for visual system testing, which incorporate suggested test protocols based on patient symptoms.

Fishman GA, Birch DG, Holder GE, Brigell MG. *Electrophysiologic Testing in Disorders of the Retina, Optic Nerve, and Visual Pathway*. 2nd ed. Ophthalmology Monograph 2. San Francisco: American Academy of Ophthalmology; 2001.

Holder GE, Celesia GG, Miyake Y, Tobimatsu S, Weleber RG; International Federation of Clinical Neurophysiology. International Federation of Clinical Neurophysiology: recommendations for visual system testing. *Clin Neurophysiol*. 2010;121(9):1393–1409. International Society for Clinical Electrophysiology of Vision. *Standards, guidelines, and extended protocols*. www.iscev.org/standards/index.html. Accessed September 4, 2020.

Electroretinography

The clinical electroretinogram (ERG) measures a massed electrical response from the retina, usually evoked by a brief flash of light. ERGs are usually recorded using active electrodes that contact the bulbar conjunctiva, with reference electrodes at the outer canthi. The active electrodes can be contact lens electrodes, although gold foil electrodes, H-K loop electrodes, and DTL fiber electrodes are also commonly used. The 3 main types of electroretinogram—the full-field (Ganzfeld) electroretinogram (ERG), the multifocal ERG (mfERG), and the pattern ERG (PERG)—are discussed in the following sections.

Full-Field (Ganzfeld) ERG

In full-field ERG, a Ganzfeld bowl uniformly illuminates the entire retina with a full-field luminance stimulus; the Ganzfeld also provides a uniform background for photopic adaptation and photopic ERG recording. Regular calibration of flash strength is required for clinical accuracy. Figure 3-1 shows typical ERG responses, but normal values vary with recording techniques, and each laboratory must establish its own normative data. Even with standardization, variations in the type of electrode and specific equipment will affect the test results.

Most laboratories dark-adapt the patient while the pupils are dilating, position the corneal electrodes under dim red light, and then commence stimulation using an interstimulus interval sufficient to allow the retina to recover between flashes (from 2 seconds for low intensities up to 20 seconds for high intensities). Many laboratories record responses to a series of increasing stimulus strengths. The patient is then light-adapted (using standardized background intensity and adaptation time), and photopic testing is performed, in which the stimuli are delivered under rod-suppressing background illumination.

The ISCEV standard full-field ERG consists of 6 different responses (see Fig 3-1). Nomenclature is based on the flash strength as measured in cd s/m² (candela-seconds per square meter) and the adaptive state of the eye (ie, dark-adapted [DA] or light-adapted [LA]). Older terms are given in parentheses in the following list. Measurement of the ERG focuses on the size and timing of the major components, as indicated in Figure 3-1.

1. DA 0.01 (*rod-specific*): In this response, a b-wave arises in the on-bipolar cells (BPCs) (inner nuclear layer) of the rod system. A reduction in this response identifies dysfunction within the rod system, but, as it arises at an inner retinal level, this response cannot differentiate between dysfunction at the level of the photoreceptor and inner retinal dysfunction. It therefore acts as a measure of rod system sensitivity.

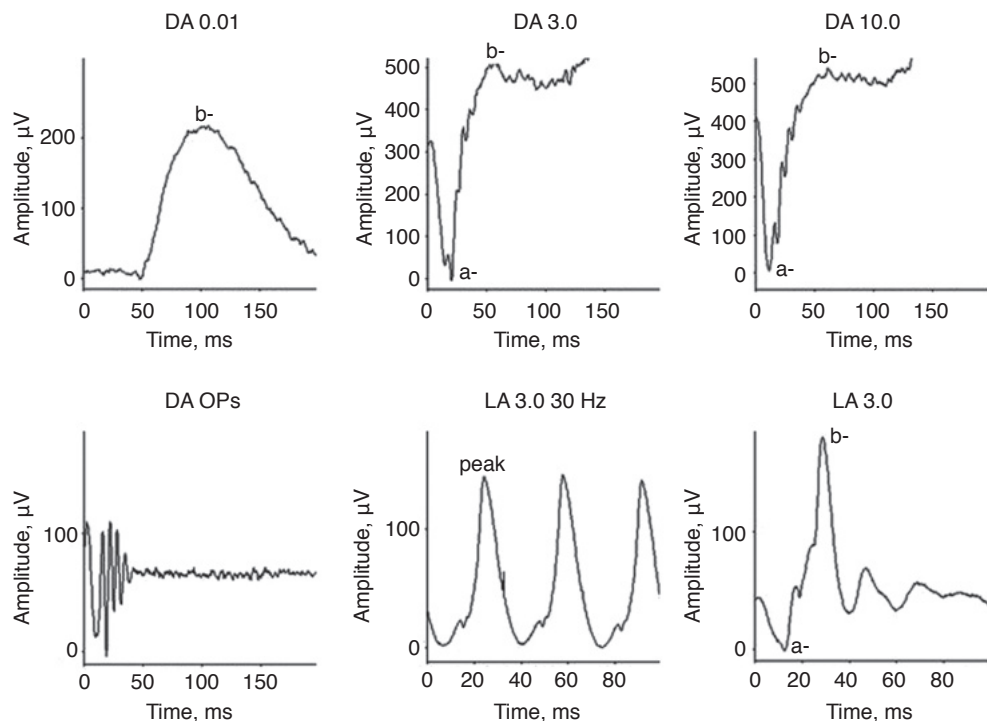


Figure 3-1 Basic electroretinogram (ERG) responses as defined by the International Society for Clinical Electrophysiology of Vision. The amplitude and peak times are typical, but normal values must be established for each laboratory using local techniques. a = a-wave; b = b-wave; DA = dark-adapted; LA = light-adapted; OPs = oscillatory potentials; numbers following abbreviations denote stimulus intensity (in candela-seconds per square meter). (Courtesy of Graham E. Holder, PhD.)

2. *DA 3.0 (mixed rod-cone):* This response consists of an a-wave and a b-wave. The a-wave at this flash strength usually has 2 peaks between approximately 15 and 21 milliseconds (ms), either of which may be prominent. Because only approximately the first 8 ms of the DA a-wave reflects photoreceptor hyperpolarization, the ISCEV standard now includes additional brighter flash testing for better diagnostic specificity.
3. *DA 10.0/30.0:* At either of these flash strengths, the a-wave has an easily measurable peak, and most of the a-wave reflects photoreceptor function. This response can therefore localize dysfunction either to a photoreceptor or inner-retinal level. Thus, a reduced DA 0.01 response accompanied by marked reduction in the a-wave of the DA 10.0/30.0 response indicates photoreceptor dysfunction; however, if the a-wave amplitude is normal or near-normal and the b-wave amplitude is lower than the a-wave (known as a negative or electronegative ERG waveform), then dysfunction occurs post-phototransduction, at an inner-retinal level.
4. *Oscillatory potentials:* These small oscillations on the ascending limb of the b-wave probably arise largely in the amacrine cells and can be made more visible by filtering.

They are reduced in retinal ischemic states and in most cases of congenital stationary night blindness but overall have limited diagnostic value.

5. *LA 3.0 (photopic single-flash)*: This ERG is obtained by stimulating with a flash superimposed upon a rod-suppressing background. The a-wave relates to function in the cone photoreceptors and off-BPCs. The b-wave arises as a synchronized component in on- and off-BPCs. This response thus enables some localization of cone-system dysfunction.
6. *LA 3.0 30 Hz (photopic flicker)*: The temporal resolution of the rod system is poor, and this response arises in the cone system. It is the more sensitive measure of cone-system dysfunction but allows no anatomical specificity. Both timing and amplitude are important parameters; delay in the flicker ERG response is a sensitive measure of generalized retinal cone system dysfunction, whereas reduced amplitude but normal peak time usually indicates restricted loss of function.

A number of factors influence the size and timing of a normal ERG response, including pupil size; pupil diameter should always be measured. ERG amplitude declines with age, and age-related controls are needed. Newborns have small ERGs with simplified waveforms. The responses mature rapidly, reaching adult values in the first year of life. The ERG is relatively insensitive to refractive error; highly myopic eyes have lower amplitude ERGs but without the peak-time delay usually associated with inherited retinal degeneration.

As a biological signal, ERGs have inherent noise. If amplitudes remain within the reference range (“normal range”) a reduction over time of more than 25% is usually considered significant. For peak-time measures, a change greater than 3 ms is regarded as significant for cone-derived response a- or b-waves and brighter-flash dark-adapted a-waves, and a change greater than 6 ms is significant for dark-adapted b-waves.

In general, ERG peak-time shift suggests generalized dysfunction, whereas simple amplitude reduction suggests restricted loss of function such as may occur in a partial retinal detachment (loss of function in the detached area of retina but normal function in the attached retina), branch vascular occlusion, regional uveitic damage, or restricted (“sector”) forms of retinitis pigmentosa (RP). Timing is often best assessed using the 30-Hz flicker ERG peak time. Generalized inflammatory disease, such as posterior uveitis, may be associated with delay but preservation of amplitude. Indeed, marked 30 Hz flicker delay with a high amplitude almost always indicates an inflammatory etiology.

Figure 3-2 presents examples of ERG patterns found in association with specific disorders. The full-field ERG is a mass response from the whole retina, and dysfunction confined to the macula is therefore accompanied by normal full-field ERG responses. Even though the central macula is cone-dense, the majority of retinal cones lie outside the macula; thus, the macula contributes little to a full-field ERG. Because abnormal photopic ERG responses indicate cone dysfunction outside the macula, ERG testing therefore helps the clinician distinguish between a macular dystrophy phenotype (normal ERG response) and a cone or cone-rod dystrophy phenotype (abnormal ERG response), which may have more serious visual implications for the patient. For example, *ABCA4* retinopathy (eg, Stargardt disease; fundus flavimaculatus) can, in some patients, be associated with severe

generalized cone and rod system dysfunction. If the full-field ERGs of the patient are normal at presentation, the dysfunction is confined to the macula and has prognostic value: 80% of such patients will still have normal full-field ERG responses at 10-year follow up.

Fujinami K, Lois N, Davidson AE, et al. A longitudinal study of Stargardt disease: clinical and electrophysiologic assessment, progression, and genotype correlations. *Am J Ophthalmol.* 2013; 155(6): 1075–1088.

Multifocal ERG

The multifocal ERG (mfERG) can produce a topographic ERG map of central retinal cone-system function, which can help the clinician diagnose macular dysfunction and assess the extent of central retinal involvement in generalized retinal disease (Fig 3-3). The stimulus consists of multiple hexagons, smaller in the center than the periphery to reflect cone photoreceptor density, each of which flashes with a pseudorandom sequence. Cross-correlation techniques are used to calculate the small ERGs corresponding to each hexagon. Overall stimulus field size is usually approximately 50°. For patients with stable and accurate fixation (essential for obtaining technically satisfactory and clinically meaningful results), mfERG can objectively determine the spatial distribution of macular dysfunction. The mfERG is less sensitive than the pattern ERG for disorders such as cystoid macular edema, in which primary photoreceptor dysfunction is not the main pathophysiological feature; mfERG and PERG can provide complementary information. Clinicians have increasingly used mfERG in the diagnosis of hydroxychloroquine toxicity (Fig 3-4). There may be relative sparing of the response to the central foveal hexagon with involvement of the responses to the ring of surrounding hexagons; a ring analysis may be beneficial. However, it should be noted that recently it has been demonstrated that Asian patients may show an extra-macular pattern of damage, which would not be detected by mfERG.

Marmor MF, Kellner U, Lai TY, Melles RB, Mieler WF; American Academy of Ophthalmology. Recommendations on screening for chloroquine and hydroxychloroquine retinopathy (2016 revision). *Ophthalmology.* 2016;123(6):1386–1394.

Pattern ERG

The pattern ERG (PERG) is the retinal response to an isoluminant alternating checkerboard stimulus presented to the macula. The stimulus is thus primarily alternating contrast. The responses are small, and signal averaging is needed. However, when technical factors are considered, PERG reliability is similar to full-field ERG. There are 2 main components, P50 and N95, with most subjects showing an earlier negative component, N35. N95 arises in the retinal ganglion cells (RGCs) and thus acts as a direct measure of central RGC function. The P50 component depends upon macular photoreceptor function, even though approximately 70% of it arises in the RGCs; the amplitude of P50 is clinically useful as an objective index of macular function. The image must be in focus on the macula, and PERGs are recorded with electrodes that spare the optics of the eye; contact lens electrodes are not suitable. Because the PERG is evoked by a stimulus similar to that used in recording the visual evoked potential (VEP) (discussed later in this chapter), knowledge

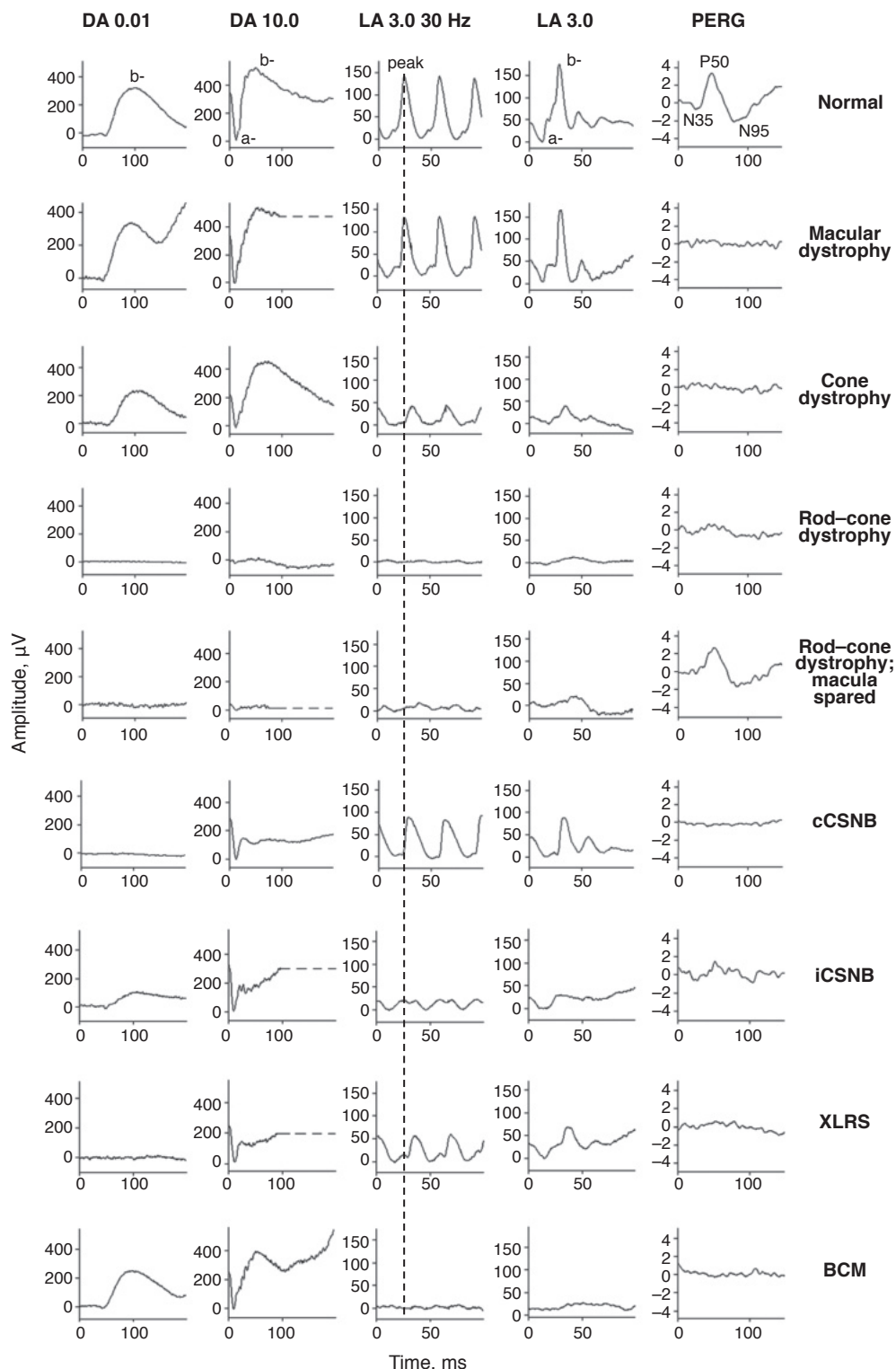
of the PERG helps the clinician provide a more accurate interpretation of abnormal VEP findings. PERG is also useful in diagnosing primary ganglion cell disease such as dominantly inherited optic atrophy or Leber hereditary optic neuropathy.

Holder GE. Pattern electroretinography (PERG) and an integrated approach to visual pathway diagnosis. *Prog Retin Eye Res.* 2001;20(4):531–561.

Clinical Considerations

The ERG provides objective retinal functional data and is therefore important in the diagnosis, management, and follow-up of retinal disease. Symptomatic indications include night blindness, in which the potentially blinding rod–cone dystrophies must be distinguished from the relatively benign congenital stationary night blindness (CSNB). The dystrophies are associated with markedly abnormal a-waves in the dark-adapted bright-flash ERGs; CSNB is usually associated with a normal a-wave and a “negative” ERG waveform (see Fig 3-2). Other symptomatic indications include photophobia, which indicates generalized cone dysfunction (as in cone dystrophy), and photopsia or shimmering, which can sometimes signal the development of autoimmune retinopathy, possibly paraneoplastic. The ERG is increasingly used in the assessment and monitoring of inflammatory

Figure 3-2 *Opposite:* ERG findings in various disorders, with typical **Normal** waveforms shown at the top. The timing of the 30 Hz flicker ERG is shown by the vertical *dashed line*. For all responses, the flash occurs at time 0 ms. **Macular dystrophy,** Full-field ERG responses are all normal, but the pattern ERG (PERG) is undetectable. **Cone dystrophy,** DA 0.10 (rod-specific) and DA 10.0 ERG responses are normal; photopic flicker and single-flash ERGs are reduced and delayed; the PERG response is subnormal, indicating macular involvement. **Rod-cone dystrophy,** Retinitis pigmentosa (RP) with macular involvement; all ERG responses are markedly subnormal, with rod ERGs more affected than cone ERGs, severe reduction of the DA 10.0 a-wave, indicating photoreceptor disease, and delayed 30-Hz and single-flash cone ERGs, indicating generalized cone system dysfunction. Abnormal PERG response shows macular involvement. **Rod-cone dystrophy (RP); macula spared,** Full-field ERGs show an abnormal rod–cone response pattern similar to that shown directly above, but a normal PERG response shows macular sparing. **cCSNB,** “Complete” congenital stationary night blindness. Findings show loss of on-pathway function at a postreceptoral level. DA 0.01 response is undetectable; DA 10.0 response is profoundly electronegative, with the normal a-wave reflecting normal photoreceptor function and the marked relative b-wave reduction showing inner retinal disease; 30-Hz flicker ERG shows only minor changes in waveform and mild delay; LA 3.0 ERG shows changes diagnostic of loss of cone on-pathway function but sparing of the off-pathway. The a-wave commences normally but then shows a broadened trough. The b-wave rises sharply, with loss of the photopic oscillatory potentials, and marked reduction in the b:a ratio. The PERG response is markedly subnormal. **iCSNB,** “Incomplete” CSNB. DA 0.01 response is subnormal but detectable; DA 10.0 response is markedly electronegative; 30-Hz flicker ERG response is markedly subnormal, showing delay and a characteristic triphasic waveform; LA 3.0 single-flash photopic ERG shows a subnormal a-wave and a markedly subnormal b-wave, reflecting involvement of both on- and off-cone pathways; the PERG response is subnormal. **XLRS,** X-linked retinoschisis. DA 0.01 response is severely reduced; DA 10.0 response is profoundly electronegative; 30-Hz flicker ERG shows delay; LA 3.0 ERG shows delay and marked reduction in the b:a ratio; the PERG response is markedly subnormal. **BCM,** Blue-cone (S-cone) monochromatism. DA 0.01 and DA 10.0 ERG responses are normal; 30-Hz flicker ERG is virtually undetectable; LA 3.0 response shows only a small b-wave at approximately 50 ms consistent with an S-cone origin; PERG is undetectable. (Courtesy of Graham E. Holder, PhD.)



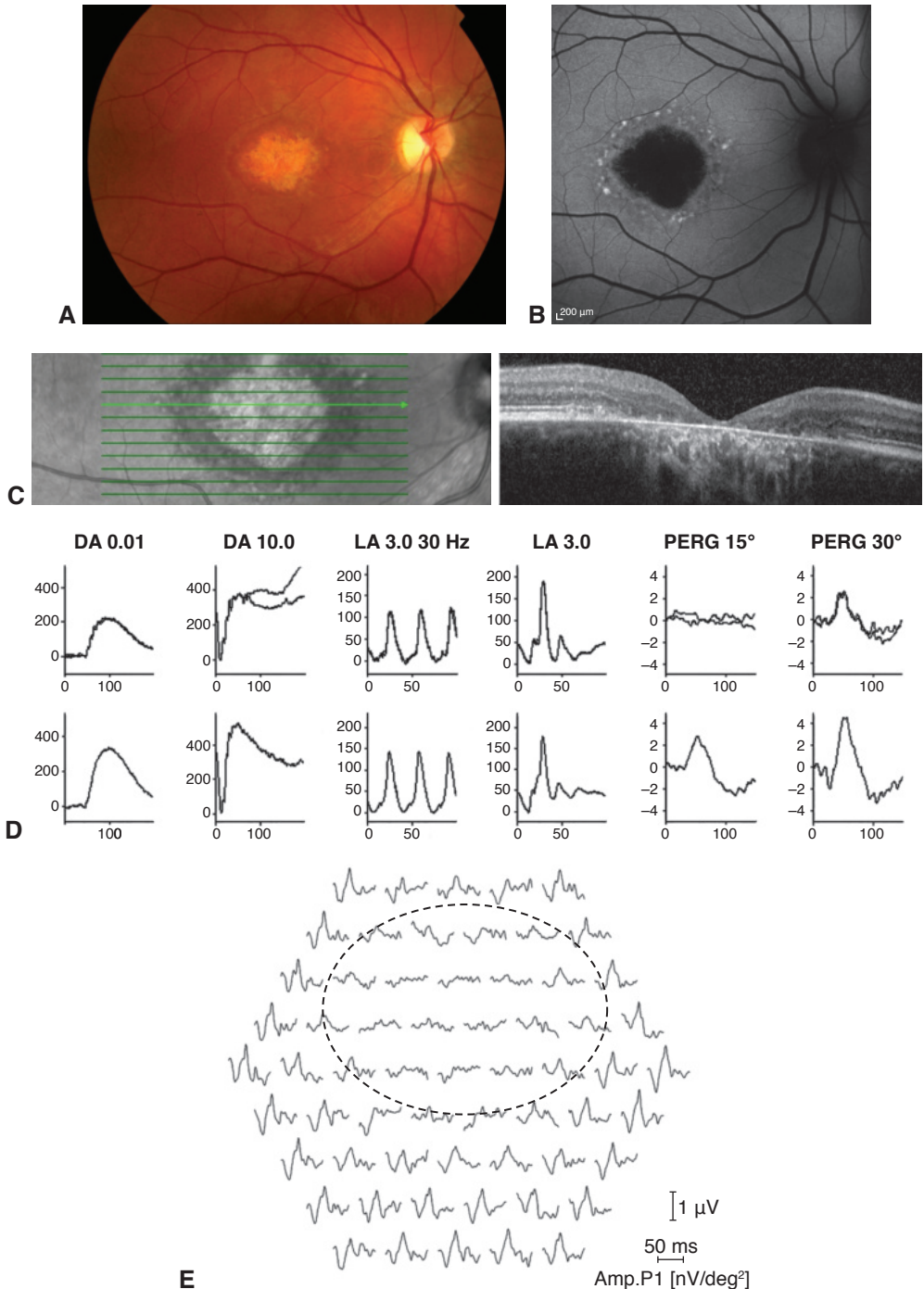


Figure 3-3 Multifocal (mfERG), full-field, and pattern ERG (PERG) recordings from a patient with *ABCA4* retinopathy (Stargardt disease; fundus flavimaculatus) demonstrate the importance of fixation in mfERG recording and interpretation. **A**, Fundus photography, **B**, fundus autofluorescence imaging, and **C**, near-infrared imaging and SD-OCT show macular atrophy centralized on the fovea. **D**, ERG responses are normal (see Fig 3-1 for terminology; x-axis = μV ; y-axis = ms); PERG response to a 15° field is undetectable, but PERG response to a 30° field is present but subnormal. **E**, mfERG shows an area of dysfunction that is localized, but apparently not around the fovea, which simply reflects the eccentric fixation often present in a patient with a central scotoma. (Courtesy of Graham E. Holder, PhD.)

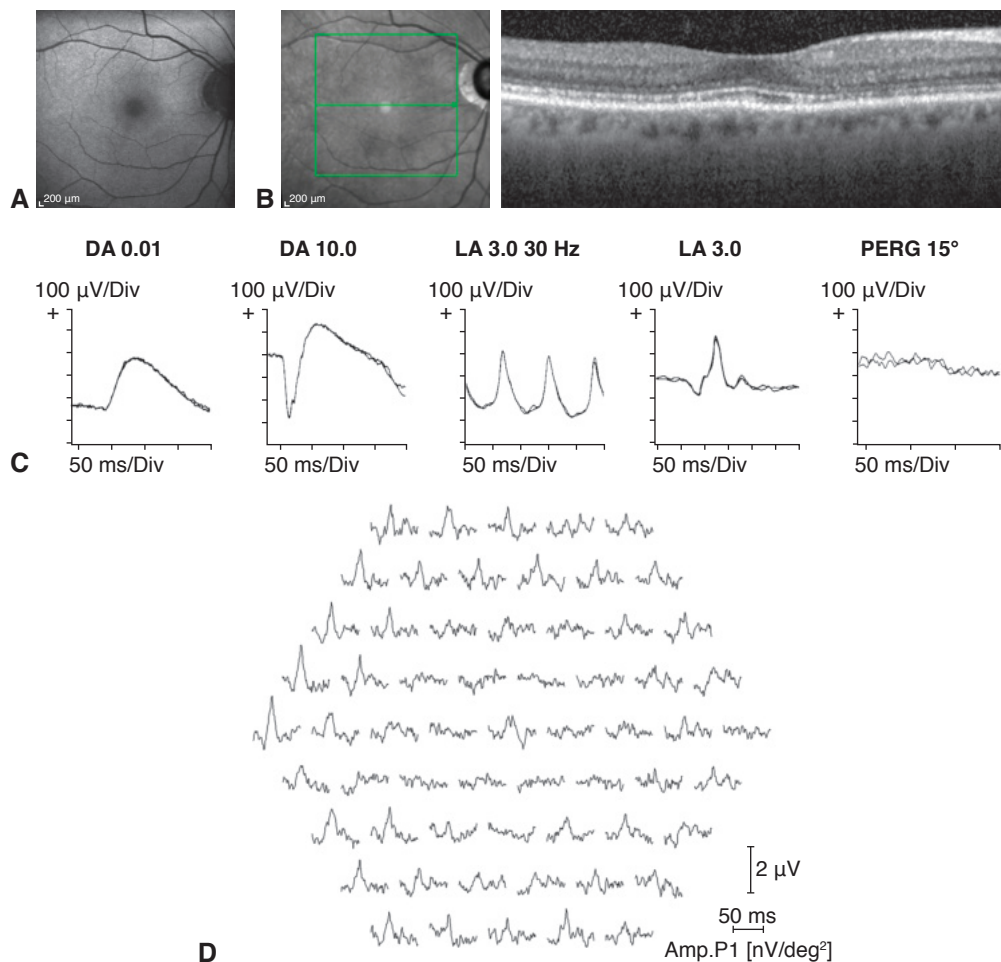


Figure 3-4 mfERG, full-field, and PERG recordings in a patient with hydroxychloroquine toxicity. **A**, Fundus autofluorescence imaging. **B**, Near-infrared imaging and spectral domain-optical coherence tomography (SD-OCT). The changes shown on OCT are less marked, particularly temporal to the fovea, than may have been predicted by the degree of functional loss. **C**, ERG responses are normal (see Fig 3-1 for terminology); PERG response to a 15° field is barely detectable. **D**, mfERG response shows marked abnormality with some sparing of the response to the central foveal hexagon but loss of parafoveal responses. (Courtesy of Graham E. Holder, PhD.)

disorders such as birdshot chorioretinopathy; objective functional data allow clinicians to make management decisions with more confidence. The ERG facilitates an objective assessment of disease severity, aiding in decisions on when and how to treat; following treatment, it provides a valuable measure of treatment efficacy that is more sensitive than conventional clinical parameters.

ERGs must always be taken in a clinical context, and to enable accurate ERG diagnosis, a careful clinical history should include previous drug and/or surgical treatment as well as a family history. Results are diagnostic (pathognomonic) only for 3 relatively rare inherited disorders: bradyopsia (mutation in *RGS9* or *R9AP*), enhanced S-cone syndrome (*NR2E3*), and “cone dystrophy with supernormal rod ERG” (*KCNV2*).

The ERG can be useful in assessing patients with vascular disease. In patients with central retinal artery occlusion (CRAO), the ERG is characteristically negative, reflecting the dual blood supply to the retina; the photoreceptors are supplied via choroidal circulation, but the central retinal artery supplies the inner nuclear layer. Thus, the b-wave amplitude is reduced but the a-wave is relatively preserved. In eyes with central retinal vein occlusion (CRVO), a negative ERG or delay in the 30-Hz flicker response suggests significant ischemia.

The ERG can also be helpful in determining the carrier state of individuals with X-linked disease. For example, carriers of X-linked RP usually have abnormal ERG findings that reflect lyonization, even with a healthy-appearing fundus. However, in choroideremia, carriers usually exhibit a normal ERG response despite an abnormal fundus appearance (also resulting from lyonization).

Electroretinography is suitable for use with children of all ages, providing objective functional data for patients who may not be able to describe their symptoms. In addition, the ERG may reveal retinal abnormalities prior to the development of fundus abnormalities. For young subjects, sedation, general anesthesia, or eyelid electrodes may be used. The latter are usually well tolerated and require neither sedation nor anesthesia. Interpretation of pediatric ERGs involves special considerations. Adult ERG values are not reached until 6–9 months of age, and, if general anesthesia is used, the effect of the anesthetic on the ERG must be considered.

- Johnson MA, Marcus S, Elman MJ, McPhee TJ. Neovascularization in central retinal vein occlusion: electroretinographic findings. *Arch Ophthalmol*. 1988;106(3):348–352.
Vincent A, Robson AG, Holder GE. Pathognomonic (diagnostic) ERGs. A review and update. *Retina*. 2013;33(1):5–12.

Electro-oculography

The electro-oculogram (EOG) assesses the health of the RPE and its interaction with the photoreceptors by measuring the corneo-retinal standing potential during dark adaptation (DA) and light adaptation (LA). The standing potential, which reflects the voltage differential across the RPE, is positive at the cornea (Fig 3-5). Estimates of trans-RPE potential range from 1 to 10 mV.

For an EOG test, the patient makes fixed 30° lateral eye movements for approximately 10 seconds each minute during 15 minutes of DA, and again during a 12-minute period of LA (Fig 3-6). The amplitude of the signal recorded between electrodes positioned at medial and lateral canthi reaches a minimum after approximately 12 minutes of DA—the dark trough—and a maximum at approximately 8 minutes of LA—the light peak. The ratio between the amplitude of the light peak to the dark trough is expressed as a percentage (the *Arden index or ratio*). A normal light rise will be greater than 170% and requires normally functioning photoreceptors in contact with a normally functioning RPE. The light peak reflects progressive depolarization of the RPE basal membrane via mechanisms that are not fully understood; however, the protein bestrophin is implicated in the final opening of chloride channels.

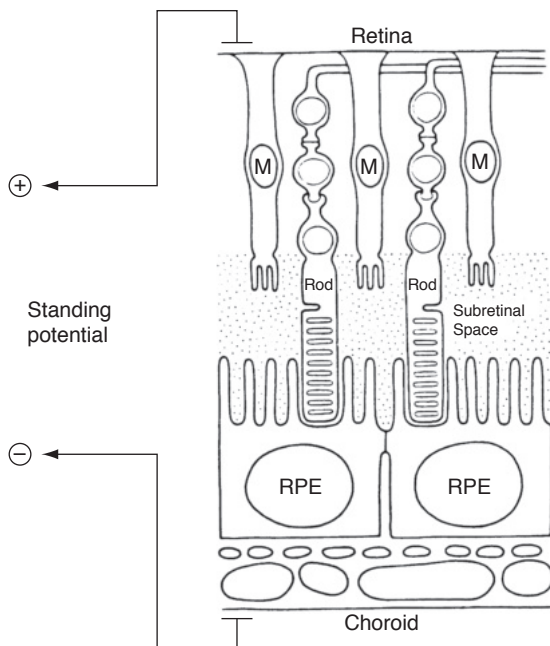


Figure 3-5 Electrical circuit of the standing potential. The retinal pigment epithelium (RPE) cells generate a voltage from apex to base due to the different ionic permeability characteristics on each surface and the presence of impermeable tight junctions between the cells. Changes in the voltage across the apical or basal RPE membrane are reflected in the standing potential and are measurable clinically as the c-wave on ERG or with electro-oculography. M = Müller cells. (Modified with permission from Steinberg RH. Monitoring communications between photoreceptors and pigment epithelial cells: effects of "mild" systemic hypoxia. Friedenwald Lecture. Invest Ophthalmol Vis Sci. 1987;28(12):1888–1904.)

Any disorder of rod photoreceptor function will affect an EOG, and the light rise is typically severely reduced in an EOG of any widespread photoreceptor degeneration, including RP. However, the EOG is principally used in clinical practice in the diagnosis of bestrophin mutations (see Chapter 13) and AZOOR (acute zonal occult outer retinopathy). In patients with Best disease, a dominantly inherited disorder caused by mutations in *BEST1*, a severely reduced or absent EOG light rise is accompanied by a normal ERG response. Severe loss of the EOG light rise is also seen in patients with autosomal recessive bestrophinopathy (ARB). ARB is a recessively inherited progressive retinal dystrophy and, unlike Best disease, requires biallelic mutation. Affected patients have abnormal ERG responses, but not sufficiently abnormal to explain the degree of EOG response abnormality. Also unlike Best disease, ARB carriers do not show an EOG response abnormality. The EOG findings in patients with adult vitelliform macular dystrophy may be mildly subnormal, but they are not as reduced as much as in Best disease.

Arden GB, Constable PA. The electro-oculogram. *Prog Retin Eye Res.* 2006;25(2):207–248.

Burgess R, Millar ID, Leroy BP, et al. Biallelic mutation of *BEST1* causes a distinct retinopathy in humans. *Am J Hum Genet.* 2008;82(1):19–31.

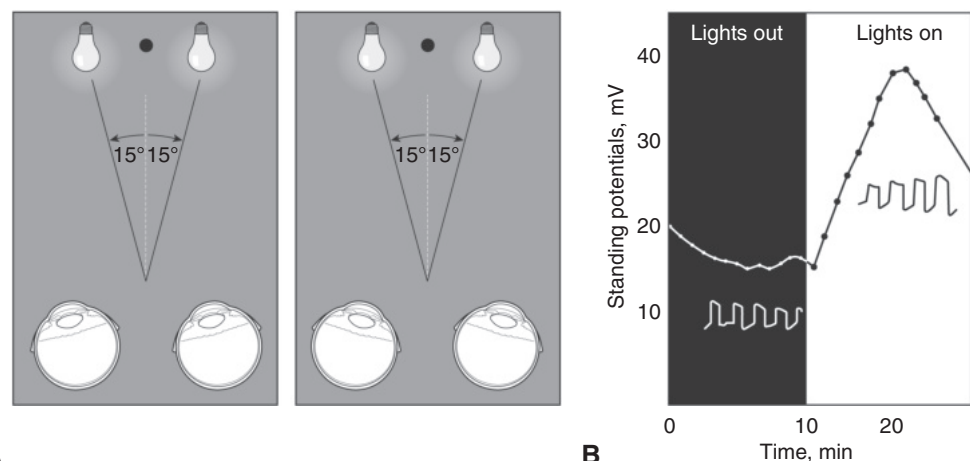


Figure 3-6 The clinical electro-oculogram (EOG). **A**, After electrodes are fixed to an area near the medial and lateral canthi, the subject is asked to look back and forth between 2 fixation targets (dimly lit lights), which are separated by a distance that results in a 30° horizontal eye movement. As each eye moves, the voltage between skin electrodes varies in proportion to the size of the standing potential of the eye (the voltage differential across the RPE). **B**, Plot of the amplitude of the oscillations. As the eyes turn toward the positive electrodes, an increased potential is measured; thus, the slow back-and-forth motions result in the relatively square-looking voltage curve. During testing, the standing potential diminishes to a minimum in the dark (the *dark trough*) and then rises to a maximum after the light is turned on (the *light peak*). In clinical practice, the EOG result is usually reported as the ratio between the light peak and the dark trough expressed as a percentage, the Arden index or ratio. (*Illustrations by Mark Miller.*)

Visual Evoked Cortical Potentials

Visual evoked potential (VEP; also, VECP or VER, for *visual evoked cortical potential* or *response*) testing measures electrical signals produced in the brain in response to stimulation of the retina by either light flashes or patterned stimuli (usually a black-and-white checkerboard that reverses its pattern on a TV monitor). The signals are recorded via electrodes placed on the occipital scalp. The VEP is extracted from the larger background electroencephalogram by averaging the responses to multiple reversals or flashes. Pattern-reversal VEPs (the black-and-white squares interchange without change in luminance) have a similar waveform across a population and a remarkably consistent timing; amplitudes show greater variability. Flash VEPs are far more variable across a population but can be useful when comparing eyes or hemispheric responses in the same patient; hemispheric comparison requires multiple recording channels. A normal pattern-reversal VEP (Fig 3-7) contains a major positive component at approximately 100 ms, P100. Measurement is usually taken of P100 amplitude and peak time (sometimes called *latency*).

In adults, VEPs are often used to demonstrate optic nerve conduction delay, particularly in patients with suspected multiple sclerosis; patients with demyelinating optic neuritis almost invariably show VEP delay even when visual acuity recovers (see Fig 3-7). However, there can be subclinical delay in patients without any history or signs of optic neuropathy. Most optic nerve diseases show VEP delay, but an abnormality can be confined to amplitude (interocular asymmetry), for example, in patients with nonarteritic anterior ischemic optic neuropathy. VEPs are crucial in patients with medically unexplained vision

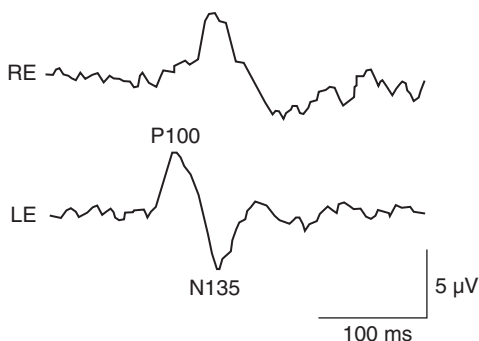


Figure 3-7 Pattern-reversal visual evoked potential from a patient with a 4-month history of right eye (RE) optic neuritis and recovery of right visual acuity to 20/20. Left eye (LE) response is normal; RE P100 component shows profound delay with preservation of amplitude and waveform. (*Courtesy of Graham E. Holder, PhD.*)

loss when the vision loss is suspected to be nonorganic. VEPs can objectively demonstrate normal function in the presence of symptoms that suggest otherwise. It is important to note that a delayed VEP is not diagnostic of optic nerve disease. Macular dysfunction can cause similarly abnormal findings, and assessment of macular function with mfERG or PERG enables improved VEP interpretation.

VEPs are indispensable in examining children, particularly those who are preverbal, who have apparent vision loss, or who present in infancy with roving eye movements or unexplained nystagmus. VEPs are used in conjunction with ERGs to discover any retinal or post-retinal dysfunction. However, caution must be exercised in any patient with nystagmus because that eye movement disorder can itself induce abnormal responses.

Pattern-appearance stimulation, in which the stimulus appears from a uniformly gray background and then disappears, maintaining isoluminance throughout, can also be used to elicit VEPs. VEPs recorded in this manner are particularly useful in demonstrating the intracranial misrouting associated with ocular or oculocutaneous albinism (requiring multiple recording channels) because they are less affected by nystagmus than reversal VEPs. Flash stimulation is effective for babies and infants who cannot maintain adequate fixation on a pattern stimulus. If the check size and contrast levels are varied, pattern-appearance VEPs can also be used to objectively assess visual system resolution, providing a surrogate measure of visual acuity.

Psychophysical Testing

Although electrophysiologic testing objectively assesses cell layers and cell types in the visual pathway, it does not always provide localized responses and may not be sensitive to small areas of localized dysfunction. Psychophysical tests can be highly sensitive, but they are subjective and are not level-specific; perception represents an integration of information provided by different parts of the visual pathway. Psychophysical tests relevant to retinal disease include testing of

- visual acuity
- visual field
- color vision
- contrast sensitivity
- dark adaptation

Color vision, contrast sensitivity, and dark adaptation testing are discussed in this chapter. See BCSC Section 3, *Clinical Optics*, for discussion of visual acuity and contrast sensitivity; Section 5, *Neuro-Ophthalmology*, for further discussion of contrast sensitivity; and BCSC Section 10, *Glaucoma*, for a discussion of visual field testing.

Dingcai C. Color vision and night vision. In: Ryan SJ, Schachat AP, Wilkinson CP, Hinton DR, Sadda SR, Wiedemann P, eds. *Retina*. 5th ed. Philadelphia: Elsevier/Saunders; 2013:285–299.

Color Vision

A healthy human retina has 3 cone types, each containing a different outer segment visual pigment: short-wavelength sensitive (S cone; formerly, *blue*), medium-wavelength sensitive (M cone; formerly, *green*), and long-wavelength sensitive (L cone; formerly, *red*) cones. The integrative cells in the retina and higher visual centers are organized primarily to recognize *contrasts* between light or colors, and the receptive fields of color-sensitive cells typically have regions that compare the intensity of red versus green or blue versus yellow.

The classification and the testing of dysfunctional color vision are based upon this contrast-recognition physiology. Red-green color deficiency, which is common in males through X-linked inheritance (6%–8% incidence), is traditionally separated into protan and deutan types, referring to absent or defective long-wavelength-sensitive or medium-wavelength-sensitive pigment, respectively. These distinctions have value in terms of patients' perception, even though individuals with normal color vision often have a duplication of pigment genes, and individuals with color-vision deficiency may not have single or simple gene defects. Blue-yellow color deficiency is rarely inherited and can be an important early marker for acquired disease. Inherited color vision defects are described in Chapter 12.

Testing of color vision

The most accurate instrument for classifying congenital red-green color defects is the *anomaloscope*, but it is not widely used. The patient views a split screen and is asked to match the yellow appearance of one half by mixing varying proportions of red and green light in the other half. Individuals with red-green color deficiency use abnormal proportions of red and green to make the match.

The most common tests of color vision use colored tablets or diagrams. These tests must be performed in appropriate lighting, usually illumination that mimics sunlight. Pseudoisochromatic plates, such as the *Ishihara* plates (which assess color discrimination along protan [red] and deutan [green] axes only) and *Hardy-Rand-Rittler* plates (which also assess the tritan [blue] axis), present colored numbers or figures against a background of colored dots (Fig 3-8). The colors of both figure and background are selected from hues that are difficult for a color-deficient person to distinguish. Individuals with defective color vision see either no pattern at all or an alternative pattern based on brightness rather than hue. These tests are quick to perform and sensitive for screening color vision, but they are not effective in classifying the deficiency.



Figure 3-8 Pseudoisochromatic plates. (Courtesy of Carl Regillo, MD.)

Panel tests, including the Farnsworth-Munsell 100 and the Farnsworth Panel D-15 hue tests, are more accurate in classifying color deficiency. The *Farnsworth-Munsell 100-hue test* is very sensitive because the difference in hues between adjacent tablets approximates the minimum that a typical observer can distinguish (1–4 nm). The spectrum is divided into 4 parts of 25 colored tablets each, and the patient is asked to discriminate between subtle shades of similar colors. However, the test is tiring and time-consuming.

Consisting of only 15 colored tablets, the *Farnsworth Panel D-15 test* (Fig 3-9) is quicker and more convenient for routine clinical use. The hues are more saturated, and they cover the spectrum so that patients will confuse colors for which they have deficient perception (such as red and green). The patient is asked to arrange the tablets in sequence, and errors can be quickly plotted to define the color deficiency. The D-15 test may miss mildly affected individuals, but it is still deemed useful because of its speed.



Figure 3-9 Panel D-15 test. (Courtesy of Luneau Ophtalmologie.)

The relative insensitivity may also be an asset in judging the practical significance of mild degrees of color deficiency. For example, individuals who fail the Ishihara plates but pass the D-15 test will probably not have color discrimination problems under most circumstances and in most occupations. Desaturated versions of the D-15 test, such as the L'Anthony D-15, which recognize more subtle degrees of color deficiency, are perhaps more clinically useful.

Individuals with major congenital color deficiencies typically show a distinct protan or deutan pattern on the D-15 scoring graph, whereas those with acquired optic nerve or retinal disease show an irregular pattern of errors. Tritan axis errors (blue-yellow confusion), which usually signify acquired disease, are readily detected using the D-15 test. Enlarged versions (PV-16 tests) are available for testing patients with reduced visual acuity.

Neitz M, Green DG, Neitz J. Visual acuity, color vision, and adaptation. In: Albert DM, Miller JW, Azar DT, Blodi BA, eds. *Albert & Jakobiec's Principles and Practice of Ophthalmology*. 3rd ed. Philadelphia: Saunders; 2008:chap 123.

Contrast Sensitivity

Contrast sensitivity (CS) is a very important concept to understand. The loss of CS often results in visual difficulties and dysfunction out of proportion to the patient's measured visual acuity. For example, patients with nonexudative macular degeneration or diabetic macular edema may have good measured visual acuity of 20/30 or better but report experiencing difficulty when performing routine visual tasks such as reading the newspaper or navigating stairways. Because a conventional Snellen visual acuity is based on high-contrast, achromatic, square-wave stimuli, it does not measure the patient's ability to perceive the subtleties of light. However, the visual system codes much of what is seen based on *contrast* rather than spatial resolution, with subtleties of light and dark providing most of the richness of visual perception. For example, when dusk, fog, or smoke reduce contrast, it becomes very difficult for anyone to resolve ordinary objects. Similarly, when patients become unable to perceive contrast under ordinary conditions, for example as a result of many retinal diseases or from media opacities, visual function is adversely impacted.

Testing of contrast sensitivity

Several clinical tests of CS are available. Most relate CS to *spatial frequency*, which refers to the size of the light–dark cycles. Individuals are typically most sensitive to contrast for objects that have a spatial frequency between 2 and 5 cycles per degree (Fig 3-10), but this sensitivity can change in patients with disease. Some tests use letters or optotypes of varying dimness and size to provide a more clinical context.

The *Pelli-Robson test* measures contrast sensitivity using a single, large letter size (20/60 optotype), with contrast varying across groups of letters. Patients read the letters, starting with the highest contrast, and continue until they are unable to read 2 or 3 letters in a single group. The subject is assigned a score based on the contrast of the last group in which 2 or 3 letters were correctly read. The Pelli-Robson score is a logarithmic measure

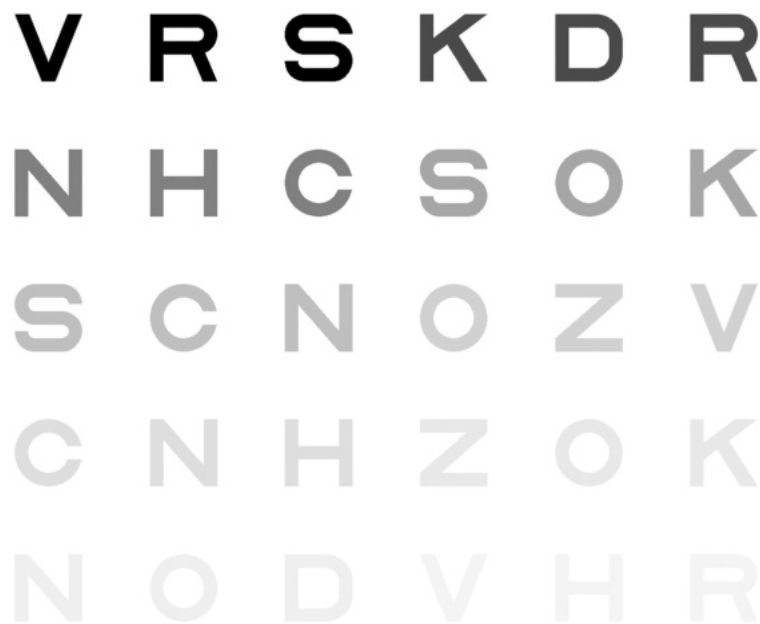


Figure 3-10 The top 5 of 8 lines of a standard Pelli-Robson contrast sensitivity chart. The top left 3-letter block has a log contrast value of 0.05; there is a log contrast change of 0.15 with each 3-letter block. In the full 8-line chart, the lowest contrast letters have a log value of 2.3; 2.0 represents normal contrast sensitivity. (Used with permission from Pelli DG, Robson JG, Wilkins AJ. The design of a new letter chart for measuring contrast sensitivity. *Clin Vision Sci.* 1988;2(3):187–199.)

of the subject's contrast sensitivity. Thus, a score of 2 means that the subject could read at least 2 of the 3 letters with a contrast of 1% (contrast sensitivity = 100%, or $\log_{10} 2$). That is, a score of 2.0 indicates normal contrast sensitivity of 100%. A Pelli-Robson contrast sensitivity score of less than 1.5 is consistent with visual impairment, and a score of less than 1.0 represents visual disability (see Fig 3-10).

Contrast sensitivity testing is discussed further in BCSC Section 3, *Clinical Optics*, and Section 5, *Neuro-Ophthalmology*.

Owsley C. Contrast sensitivity. *Ophthalmol Clin North Am.* 2003;16(2):171–177.

Rubin GS. Visual acuity and contrast sensitivity. In: Ryan SJ, Schachat AP, Wilkinson CP, Hinton DR, Sadda SR, Wiedemann P, eds. *Retina*. 5th ed. Philadelphia: Elsevier/Saunders; 2013:300–306.

Dark Adaptometry

The sensitivity of the human eye extends over a range of 10–11 \log_{10} units. Cones and rods adapt to different levels of background light through neural mechanisms and through the bleaching and regeneration of visual pigments. Clinical dark adaptometry primarily measures the absolute thresholds of cone and rod sensitivity.

Dark adaptation can be measured and quantified with the *Goldmann-Weekers (G-W) adaptometer*; however, it is neither widely available or used. Although newer instruments

have been introduced, they have yet to gain widespread acceptance, and the majority of the research literature is devoted to the G-W.

Dark adaptometry is useful in assessing patients with night blindness. Although it is a subjective test, dark adaptometry can complement the ERG; as a *focal test* (relevant when interpreting results from patients with local rather than generalized retinal dysfunction), it can be a more sensitive indicator of pathology than the ERG, especially early in the disease process. Dark adaptometry can also demonstrate the degree of cone adaptation in the evaluation of cone dysfunction syndromes.



PART II

Disorders of the Retina and Vitreous

CHAPTER 4

Age-Related Macular Degeneration and Other Causes of Choroidal Neovascularization



This chapter includes a related activity, which can be accessed by scanning the QR code provided in the text or going to www.aao.org/bcscactivity_section12.

This chapter reviews age-related macular degeneration and other conditions that cause choroidal neovascularization.

Age-Related Macular Degeneration

Age-related macular degeneration (AMD) is the leading cause of blindness in the developed world in people over 50 years. It is estimated that among North Americans, 11 million (85%–90% of all AMD patients) currently have “dry” (nonneovascular, or non-exudative) AMD and 1.5 million people (10%–15% of all AMD patients) have “wet” (neovascular) AMD. An estimated 71,000 new cases of neovascular AMD develop each year in North America.

Normal aging results in a spectrum of changes in the macula, many clinically undetected, that affect the outer retina, retinal pigment epithelium (RPE), Bruch membrane, and choriocapillaris:

- Photoreceptors are reduced in density and distribution.
- Ultrastructural changes in the pigment epithelium include loss of melanin granules, formation of lipofuscin granules, and accumulation of residual bodies.
- Basal laminar/linear deposits accumulate; these deposits consist of granular, lipid-rich material and widely spaced collagen fibers collecting between the plasma membrane of the RPE cell and the inner collagenous layer of Bruch membrane on either side of the basement membrane of the RPE (Fig 4-1; discussed later in the chapter).
- Progressive involutional changes occur in the choriocapillaris.

All of these changes represent aging and may not be part of AMD. Abnormalities associated with AMD that are not necessarily part of normal aging may be classified as non-neovascular or neovascular.

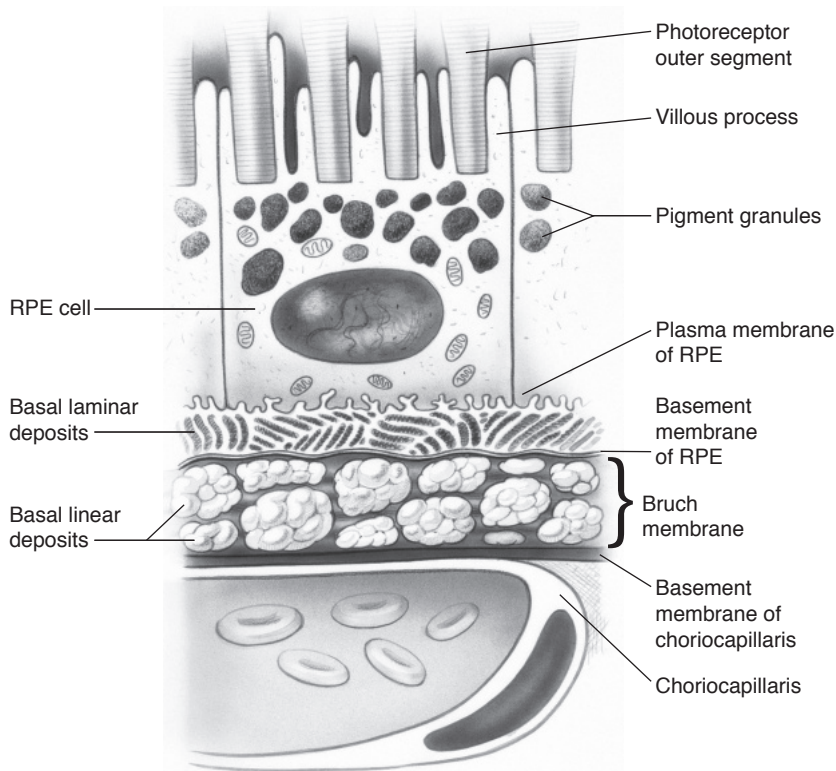


Figure 4-1 Schematic illustration of basal laminar deposits and basal linear deposits that result in a thickened inner collagenous layer of Bruch membrane. RPE = retinal pigment epithelium. (Illustration by Christine Gralapp.)

Population-based studies have demonstrated that of the risk factors for AMD, age is the first and foremost; in resource-rich countries, 10% of people over the age of 65 years and 25% over the age of 75 years have AMD. Additional risk factors include female sex, hypertension, hypercholesterolemia, cardiovascular disease, higher waist-to-hip ratio in men, positive family history, cigarette smoking, elevated levels of C-reactive protein and other inflammatory markers, hyperopia, and light iris color. Of modifiable risk factors, cigarette smoking has been consistently demonstrated to be most significant. Racial origin is another important risk factor. The 10-year longitudinal Multi-Ethnic Study of Atherosclerosis (MESA) found that the prevalence of AMD was highest in Whites (5.4%) and lowest in African Americans (2.4%); prevalence was intermediate in Hispanics (4.2%) and Asians (4.6%).

Klein R, Klein BE, Knudtson MD, et al. Prevalence of age-related macular degeneration in 4 racial/ethnic groups in the multi-ethnic study of atherosclerosis. *Ophthalmology*. 2006;113(3):373–380.

Genetics and AMD

The etiology of AMD remains poorly understood. Development of the disorder involves interplay between genetic predisposition and other risk factors. A recent genome-wide

association study of 43,000 people identified 52 genetic variants, both common and rare, located on the 34 loci associated with AMD. These genes harbor mutations that affect various biochemical pathways, including the complement cascade, lipid transport and metabolism (eg, *APOE*), modulation of the extracellular collagen matrix (eg, *COL8A1*, *COL10A1*, *TIMP3*), clearance of all-*trans*-retinaldehyde from photoreceptors (*ABCA4*), and angiogenesis (eg, *MMP9*, *VEGFA*). The alternate complement pathway includes the highest number of known AMD risk alleles, including *CFH*, *CFI*, *C2/CFB*, *C3*, and *C7*.

The 2 major susceptibility genes for AMD are *CFH* (1q31), which codes for complement factor H, and *ARMS2* (10q26), for which the gene product and function are poorly understood. *ARMS2/HTRA1* and *MMP20* are associated with choroidal neovascularization (CNV) lesion size. The *CFH* Y402H mutation confers a 4.6-fold increased risk for AMD when heterozygous and a 7.4-fold increased risk when homozygous. The *ARMS2* A69S mutation confers a 2.7-fold increased risk for AMD when heterozygous and an 8.2-fold increased risk when homozygous. When both genes are homozygous for the aforementioned mutations in an individual, the risk for AMD is increased to 50-fold.

Genetic testing is available for AMD and usually includes testing for many of the known risk alleles. However, the interpretation and usefulness of the results remain controversial, because unhealthy lifestyles increase AMD risk regardless of the AMD risk genotype. The risk models used either are poorly validated or add little information to the risks that can already be estimated from clinical findings and assessment of the patient's risk factors (eg, smoking history, family history). The American Academy of Ophthalmology's official recommendation is to defer genetic testing for complex disorders such as AMD until replicable studies have confirmed the value of such testing for prognostication or response to therapy. Pharmacogenomic testing is also possible; it aims to predict the optimal pharmacologic or nutritional-supplement interventions for a given patient. Evidence to support this approach is only beginning to emerge, and validation studies are lacking. However, this is a fast-moving area of research, and progression to useful testing is likely.

AAO Retina/Vitreous PPP Panel, Hoskins Center for Quality Eye Care. Preferred Practice Pattern® Guidelines. Age-Related Macular Degeneration. San Francisco: American Academy of Ophthalmology; 2015. Available at: www.aoa.org/ppp

Frisch LG, Igl W, Bailey JN, et al. A large genome-wide association study of age-related macular degeneration highlights contributions of rare and common variants. *Nat Genet*. 2016;48(2):134–143.

Nonneovascular AMD

The defining lesion of the nonneovascular form of AMD is the druse. Other indicators are abnormalities of the RPE, including hyperpigmentation and atrophy.

Drusen

Clinically, drusen are small, round, yellow lesions located along the basal surface of the RPE, mostly in the postequatorial retina (Fig 4-2). Histologically, this material corresponds to the abnormal thickening of the inner aspect of Bruch membrane shown in Figure 4-1.

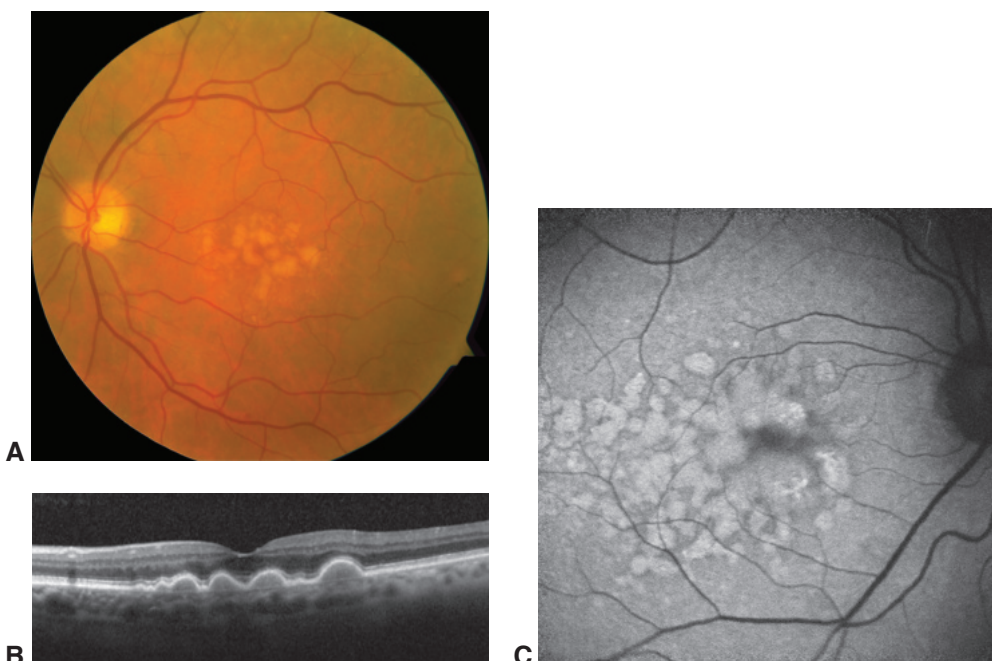


Figure 4-2 Drusen. **A**, Color fundus photograph shows soft, confluent, large drusen in a patient with nonneovascular (dry) age-related macular degeneration (AMD). **B**, Corresponding spectral-domain optical coherence tomography (SD-OCT) image of the soft drusen. **C**, Auto-fluorescence image of an eye with areas of confluent drusen. (Courtesy of David Sarraf, MD.)

Ultrastructurally, basal *laminar* deposits (granular, lipid-rich material and widely spaced collagen fibers between the plasma membrane and basement membrane of the RPE cell) and basal *linear* deposits (phospholipid vesicles and electron-dense granules *within* the inner collagenous zone of Bruch membrane) are present (see Fig 4-1).

The thickened inner aspect of Bruch membrane, along with the RPE, may separate from the rest of Bruch membrane, resulting in pigment epithelial detachment (PED). When small, such a detachment may be identified as a large or soft druse, and when larger, it may be recognized as a drusenoid PED.

Because drusen variably affect the overlying photoreceptors, there may be associated mild to moderate vision loss, decreased contrast sensitivity and color vision, and impairment of dark adaptation. Increasing size, number, and confluence of the drusen confer increasing risk of progression to CNV or geographic atrophy (GA), which the Age-Related Eye Disease Study (AREDS) referred to as stage 4 or the advanced stage of AMD. Drusen are categorized by size as small (usually $<63\text{ }\mu\text{m}$ diameter), intermediate (usually $63\text{--}124\text{ }\mu\text{m}$), or large (usually $\geq125\text{ }\mu\text{m}$). *Drusenoid PEDs* are confluent large drusen that coalesce into a PED ($>350\text{ }\mu\text{m}$ diameter). In AREDS, the risk of progression to stage 4 AMD over a 5-year period for patients with early AMD (many small drusen or few intermediate drusen, stage 2) was 1.3%. In contrast, the risk for patients with many intermediate drusen or even a single large druse (stage 3) was 18%.

Drusen can be further distinguished by their boundaries: hard (discrete and well demarcated), soft (amorphous and poorly demarcated; see Fig 4-2A, B), or confluent (contiguous drusen without clear boundaries; see Fig 4-2C). Hard drusen are well-defined focal areas of lipidization or hyalinization of the RPE–Bruch membrane complex. Soft drusen are associated with the presence of diffuse thickening of the inner aspects of Bruch membrane, that is, basal linear deposits. An eye with soft, and perhaps confluent, drusen is more likely to progress to atrophy or CNV than an eye with only hard drusen.

Reticular pseudodrusen or *subretinal drusenoid deposits* are similar in appearance to drusen; they can be recognized by their reticular-like network, seen best on fundus autofluorescence (Fig 4-3) and infrared imaging. These lesions are typically smaller than soft drusen, are located on the apical surface of the RPE, and commonly distribute in the superior macular region. Although they share some proteins with drusen (eg, apolipoprotein E, complement factor H, and vitronectin), they contain different lipids and do not contain shed disk remnants. Their presence has been associated with progressive atrophy of the photoreceptor layer, GA, and a greater risk of CNV.

Drusen occurring in patients younger than 50 years are discussed in the section “Early-onset ‘drusenoid’ macular dystrophies” in Chapter 13.

Fluorescein angiography of drusen Drusen appearance on fluorescein angiography (FA) can vary. Typically, small hard drusen hyperfluoresce early in FA studies because of a window defect, whereas larger soft and confluent drusen and drusenoid PEDs slowly and homogeneously stain late because of pooling of the fluorescein dye in the sub-PED compartment.

Optical coherence tomography of drusen Spectral-domain optical coherence tomography (SD-OCT) imaging of small and large drusen typically reveals sub-RPE nodular elevations or even small RPE detachments with a notable absence of intraretinal and subretinal

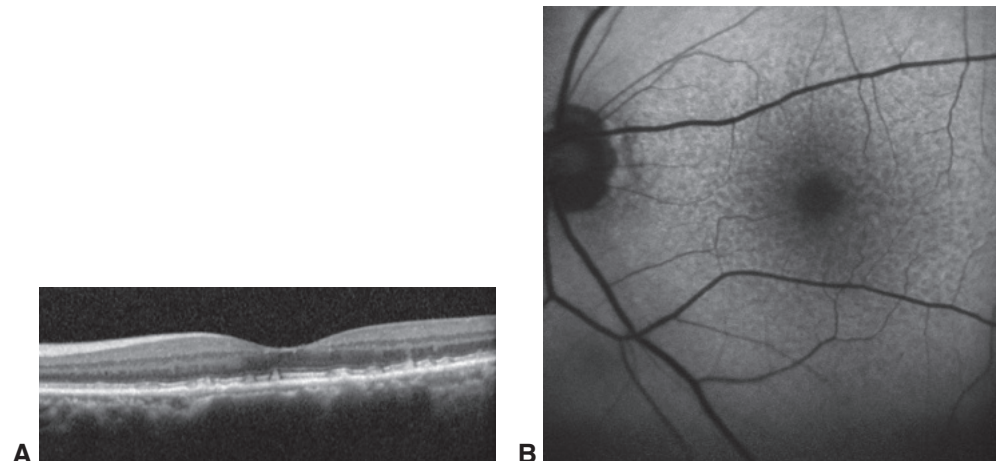


Figure 4-3 Reticular pseudodrusen. **A**, SD-OCT image demonstrates the location of reticular pseudodrusen above the RPE. **B**, Corresponding autofluorescence image shows the reticular network of these pseudodrusen. (Courtesy of David Sarraf, MD.)

fluid (see Fig 4-2). Reticular pseudodrusen are identified above the RPE and beneath the inner segment ellipsoid layer and are graded according to their degree of elevation (see Fig 4-3).

Enhanced depth imaging (EDI) OCT provides more details of choroidal architecture and a clearer definition of the choroidal-scleral interface, which is helpful in characterizing AMD. Choroidal thickness is often reduced in AMD.

Abnormalities of the retinal pigment epithelium

Characteristic RPE abnormalities seen in patients with nonneovascular AMD include focal hyperpigmentation, focal atrophy, and geographic atrophy. Focal RPE hyperpigmentation appears as increased pigmentation at the level of the outer retina. These areas typically produce blockage of fluorescence on FA, and appear as hyperreflective outer retinal foci on SD-OCT. The incidence of focal hyperpigmentations increases with age; their presence is associated with a greater risk of progression to the more advanced forms of AMD.

Focal atrophy appears as noncontiguous areas of pigment mottling or frank depigmentation. If such lesions are contiguous and have a diameter greater than 175 µm, they are described as *geographic atrophy* (GA) of the RPE. In areas of GA, absence or depigmentation of the RPE unmasks the choroidal vessels, making them visible. The overlying outer retina typically appears thin, and the underlying choriocapillaris is attenuated or atrophied. On FA, GA appears as well-circumscribed round to oval window defects; SD-OCT reveals the progressive loss of RPE, the overlying inner segment ellipsoid, and the photoreceptor layers. Areas of GA are densely hypoautofluorescent, making fundus autofluorescence a useful, noninvasive technique for monitoring disease progression (Fig 4-4).

Geographic atrophy often spares the fovea until late in the course of the disease. It may first present as 1 or more noncontiguous patches of atrophy around the fovea. These patches enlarge and coalesce, leaving the affected individual with dense paracentral scotomas, which can limit tasks such as reading. The rate of disease progression has been estimated at 1.79 mm²/year, but this may vary from individual to individual. Patients with GA may demonstrate good visual acuity (VA) until late in the disease, when the fovea becomes involved and VA declines due to central blindness, forcing the patient to use eccentric fixation on noncentral retina to read and perform other visual tasks.

Although not all eyes with drusen or drusenoid PED will develop atrophy, the incidence of atrophy appears to increase with age. Twelve to 20% of patients with GA experience severe vision loss, and 10% of patients with AMD and a VA of 20/200 or less have GA. Decreased contrast sensitivity and reduction in microperimetry sensitivity values reflect the presence of pseudodrusen prior to progression to GA.

Other abnormalities Chronic nonneovascular AMD can lead to progressive RPE atrophy and GA. As drusen resorb over time, atrophy of the RPE often remains. Dystrophic lipidization and calcification (“refractile” or “calcific” drusen) may occur, resulting in the development of refractile or crystalline lesions in the macula. Furthermore, pigment or pigment-laden cells (either RPE cells or macrophages that have ingested the pigment)

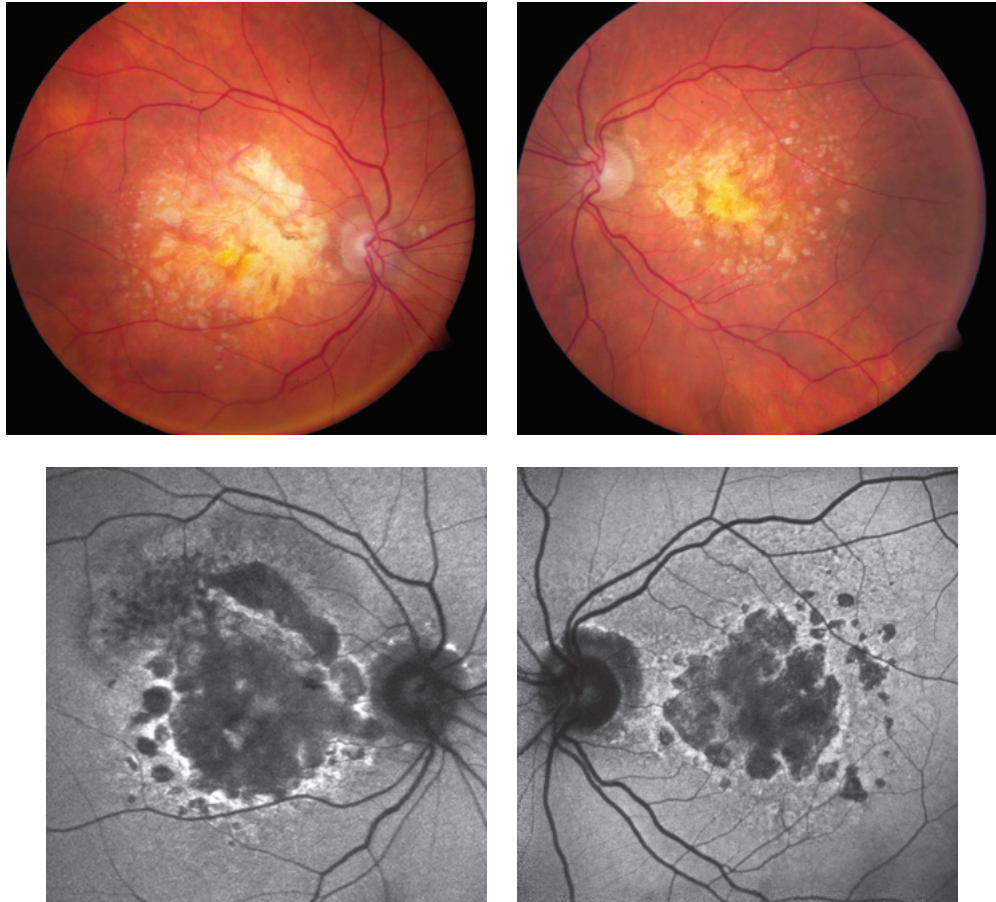


Figure 4-4 Geographic atrophy (GA). *Top*, Color fundus photographs of right (*left panel*) and left (*right panel*) eyes, demonstrating advanced GA. *Bottom*, Corresponding autofluorescent images of GA in the same patient with atrophic AMD. The areas of RPE atrophy are hypofluorescent (dark gray or black), the areas of "sick" RPE are hyperautofluorescent (brighter than background), and the areas of healthy RPE are gray. (*Courtesy of David Sarraf, MD.*)

may migrate to the photoreceptor level, resulting in focal clumps or a reticulated pattern of hyperpigmentation.

Differential diagnosis of nonneovascular AMD

Disorders that include RPE abnormalities may be misinterpreted as nonneovascular AMD. Central serous chorioretinopathy (CSC; discussed in Chapter 9) may produce RPE changes similar to those in AMD. In patients with CSC, EDI-OCT reveals a thickened choroid in the affected and fellow eyes, as opposed to the normal or thin choroid in eyes with AMD. Pattern dystrophies of the RPE present as areas of reticular or butterfly-shaped hyperpigmentation of the macula, which are often symmetrical in each eye. Patients with adult-onset vitelliform maculopathy may present with yellow subretinal lesions beneath

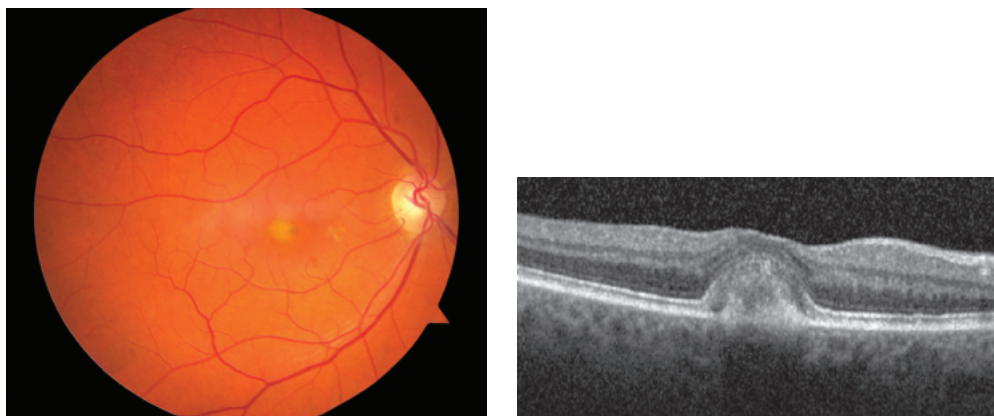


Figure 4-5 Color fundus photograph (*left*) and corresponding SD-OCT image (*right*) of adult-onset vitelliform maculopathy. The foveal region has a yellowish discoloration resembling an egg yolk. OCT demonstrates that the lesion is elevated. (*Courtesy of David Sarraf, MD.*)

the outer retina. On SD-OCT this condition appears as a hyperreflective, dome-shaped central lesion (Fig 4-5). FA shows early blocked fluorescence with a surrounding zone of hyperfluorescence. Late staining of the vitelliform material may occur and may help distinguish these cases from AMD. These features may occur in younger individuals (younger than 50 years). On the other hand, these changes may also be present in older individuals who have the more typical drusen and RPE abnormalities associated with AMD.

The retinal signs of *drug toxicity*, such as concentric macular atrophy caused by hydroxychloroquine toxicity, may resemble progressive geographic atrophy of AMD. Central RPE mottling associated with deferoxamine, pentosan polysulfate sodium, or cisplatin may also resemble nonneovascular AMD. A history of specific drug ingestion and lack of large drusen may help differentiate these abnormalities from AMD (see Chapter 15).

Management of nonneovascular AMD

Education and follow-up Eyes with soft drusen and RPE hyperpigmentation are at increased risk of developing GA and CNV. Because of this risk, patients with nonneovascular AMD should be educated about the symptoms of advanced AMD and instructed to contact an ophthalmologist promptly should these symptoms occur; ophthalmology office staff should respond to patient concerns without delay. If reduced VA or reduced vision function (eg, difficulty reading despite good measured visual acuity) is noted, a low vision evaluation should be considered after treatable pathology has been ruled out. Periodic examinations are advised to monitor for concurrent, treatable eye disease (eg, cataract, glaucoma) and to reevaluate low-vision needs. To learn about the American Academy of Ophthalmology's Initiative in Vision Rehabilitation and obtain a patient handout, visit the Low Vision and Vision Rehabilitation page on the ONE Network at www.aao.org/low-vision-and-vision-rehab.

Amsler grid testing Patients can use the Amsler grid at home to monitor for exudative macular degeneration; the test card contains white grid lines on a black background and a central dot for fixation. Each eye is tested *individually* with reading glasses and at reading

distance to check for any new metamorphopsia, scotoma, or other significant changes in central vision. Any changes noted by the patient should be evaluated promptly. Recent online or smart-phone application versions of the Amsler grid offer greater convenience for both patients and clinicians; the test results are instantly uploaded to alert the treating ophthalmologist of any acute visual changes.

Hyperacuity testing Vernier acuity measures a patient's ability to detect deviations in alignment of visual objects, for example 2 line segments. *Hyperacuity* is what helps the viewer discern minute deviations, down to even a single point on a line. Hyperacuity is extremely sensitive to any geometric shift in the outer retinal morphology, producing a perception of distortion. Preferential hyperacuity perimetry (PHP), which has been studied extensively, can detect recent-onset CNV in intermediate AMD patients with high sensitivity (82%), and high specificity (88%). One of those studies, the HOME study, which was a phase 3 randomized clinical trial with 1520 participants, demonstrated the efficacy and potential benefit of PHP in earlier CNV detection.

Shape-discrimination hyperacuity (SDH) employs a similar principle but instead tests for discrimination of shapes, such as the ability to discern a perfect circle from a distorted contour. A handheld SDH test, which is currently in trials, can be implemented as a smart-phone application for frequent, regular home monitoring.

Chew EY, Clemons TE, Harrington M, et al; AREDS2-HOME Study Research Group.

Effectiveness of different monitoring modalities in the detection of neovascular age-related macular degeneration: the Home Study, Report Number 3. *Retina*. 2016;36(8):1542–1547.

Keane PA, de Salvo G, Sim DA, Goverdhan S, Agrawal R, Tufail A. Strategies for improving early detection and diagnosis of neovascular age-related macular degeneration. *Clin Ophthalmol*. 2015;9:355–366.

Micronutrients Ophthalmologists should counsel patients about various epidemiologic studies that have demonstrated positive associations between the intake of certain micronutrients and a decreased risk of AMD, although only some micronutrients have been studied.

AREDS (Age-Related Eye Disease Study) first established the benefit of vitamin and zinc supplementation in reducing the risk of vision loss in nonexudative AMD. In the study, after supplementation with the antioxidant vitamins C (500 mg) and E (400 IU), beta carotene (15 mg), and the micronutrient zinc (80 mg zinc oxide and 2 mg cupric oxide to prevent zinc-induced anemia), patients with intermediate or advanced AMD showed a 25% risk reduction for progression to more-advanced stages of AMD and a 19% risk reduction in rates of moderate vision loss (≥ 3 lines of visual acuity) at 5 years. The study defined intermediate (stage 3) AMD as the presence of at least 1 large druse (≥ 125 μm), extensive intermediate drusen (63–124 μm diameter), or nonsubfoveal GA; advanced (stage 4) AMD was defined as vision loss due to neovascular AMD or subfoveal GA in only 1 eye. At 10 years, 44% of placebo recipients compared with 34% of the supplement recipients had advanced AMD (a 23% risk reduction). Among participants with no AMD or with only early-stage AMD (a few small drusen), there was no measurable benefit. There was no increased mortality among patients taking the formula recommended by AREDS.

AREDS developed a simplified 4-point grading scale for classifying the severity of AMD and predicting the disease course based on the following findings:

- presence of 1 or more large ($\geq 125\text{-}\mu\text{m}$ diameter) drusen (1 point)
- presence of any pigment abnormalities (1 point)
- for patients with no large drusen, presence of bilateral intermediate ($63\text{--}124\text{ }\mu\text{m}$) drusen (1 point)
- presence of neovascular AMD (2 points)

Risk factors were totaled across both eyes to reach a number between 0 and 4 that was used to estimate patients' 5- and 10-year risk of developing advanced AMD in 1 eye (Table 4-1).

A follow-up study, AREDS2, tested whether replacing beta carotene with xanthophylls (lutein and zeaxanthin) and adding omega-3 long-chain polyunsaturated fatty acids (LCPUFAs: docosahexaenoic acid [DHA] and eicosapentaenoic acid [EPA]) would further help reduce AMD progression in a large prospective trial. The response of the 4000 participants in the study confirmed the overall risk reduction found in the original AREDS study and concluded that lutein and zeaxanthin had similar effects to beta carotene, but without its increased risk for lung cancer in current and former smokers (reported in other studies). It also confirmed that 80 mg of zinc is an appropriate dose for AMD prophylaxis. The addition of LCPUFAs did not decrease the rate of progression to advanced AMD. The study's final recommendation was to modify the original AREDS supplement, replacing beta carotene with lutein and zeaxanthin, and not to add LCPUFAs (Table 4-2). Currently, patients with stage 3 or 4 AMD are advised to take the AREDS2 supplement.

Table 4-1 Five- and 10-Year Risks^a of Advanced AMD in 1 Eye

Number of Risk Factor Points	5-Year Risk, %	10-Year Risk, %
0	0.5	1
1	3	7
2	12	22
3	25	50
4	50	67

AMD=age-related macular degeneration.

^a Risks are based on the number of Age-Related Eye Disease Study (AREDS) risk factors (see text).

Table 4-2 AREDS2 Recommendations for Nutritional Supplementation^a

Nutrient	Daily Dose
Vitamin C	500 mg
Vitamin E	400 IU
Lutein	10 mg
Zeaxanthin	2 mg
Zinc	80 mg

AREDS2=Age-Related Eye Disease Study 2.

^a Recommendations for nutritional supplementation are based on the AREDS2 study (see text).

Age-Related Eye Disease Study 2 Research Group. Lutein + zeaxanthin and omega-3 fatty acids for age-related macular degeneration: the Age-Related Eye Disease Study 2 (AREDS2) randomized clinical trial. *JAMA*. 2013;309(19):2005–2015.

Ferris FL, Davis MD, Clemons TE, et al; Age-Related Eye Disease Study (AREDS) Research Group. A simplified severity scale for age-related macular degeneration: AREDS report no. 18. *Arch Ophthalmol*. 2005;123(11):1570–1574.

Lifestyle changes With increasing evidence that environment and health habits influence the development and progression of AMD, patients should be counseled to alter behaviors that put them at risk. Of particular importance are smoking cessation, obesity reduction, and blood pressure control. Cataract surgery has not been linked consistently to the progression of AMD, nor is there strong evidence linking UV (UV-A or UV-B) light exposure to the progression of AMD. It should be noted, however, that there are no adverse effects from wearing UV-protective glasses.

Disproven treatment approaches for nonneovascular AMD

Macular laser photocoagulation has been shown to stimulate drusen resolution or reduction, but there is no associated change in the natural course of vision loss or CNV development. No role was demonstrated for rheopheresis (filtering blood to alter its viscosity) in treatment of nonneovascular AMD. Lampalizumab (also known as *anti-factor D*), which selectively inhibits activation of the alternative complement pathway, has been studied in large phase-3 studies of patients with GA and was not found to be effective in preventing progression of the disease.

Neovascular AMD

The presence of CNV is the defining characteristic of the neovascular form of AMD. Degenerative changes in Bruch membrane (eg, the accumulation of drusen and progressive thickening of the membrane that characterize nonneovascular AMD) provide a proangiogenic environment that can stimulate neovascularization to develop in the choriocapillaris and perforate the membrane. These new vessels, which are accompanied by fibroblasts, may leak and bleed, disrupting the normal architecture of the RPE–photoreceptor complex with a degenerate fibrovascular complex that ultimately produces a hypertrophic fibrotic disciform scar.

Signs and symptoms of neovascular AMD

Patients with neovascular AMD describe a sudden onset of decreased vision, metamorphopsia, and/or paracentral scotomas. Amsler grid self-testing by patients is highly effective for early detection of neovascular AMD. Clinical signs of CNV may include subretinal or intraretinal fluid (eg, CME), exudate and/or blood, a pigment ring or gray-green membrane, irregular elevation of the RPE or a PED, an RPE tear, and/or a sea-fan pattern of subretinal vessels.

Anatomical classification of CNV

Currently, CNV is classified according to its level of origin. In type 1 neovascularization, new vessels originating from the choriocapillaris grow through a defect in Bruch membrane into the sub-RPE space (Fig 4-6). Fluid leakage and bleeding can produce a

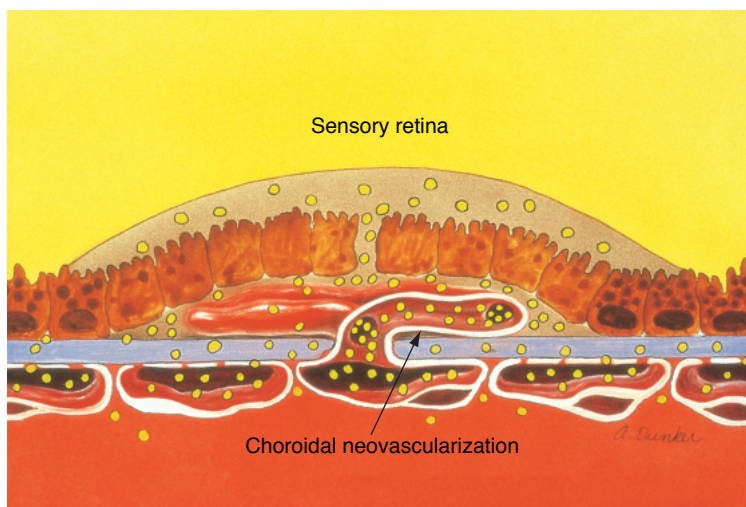


Figure 4-6 Schematic illustration of type 1 choroidal neovascularization (CNV) originating from the choriocapillaris, breaking through Bruch membrane, and proliferating in the sub-retinal pigment epithelial space. (Used with permission from Bressler NM, Bressler SB, Fine SL. Age-related macular degeneration. Surv Ophthalmol. 1988;32(6):375–413.)

vascularized serous or fibrovascular PED. These fibrovascular PEDs typically have an irregular surface contour. In type 2 neovascularization, the CNV originates between the RPE and the neurosensory retina. On examination, it typically appears as a lacy or gray-green lesion; in AMD, this finding is less common than type 1 neovascularization. In type 3 neovascularization, the neovascularization develops from the deep capillary plexus of the retina and grows downward toward the RPE. Because of their intraretinal origin, these lesions were originally termed *retinal angiomatous proliferations* (RAPS). On examination, they often appear as a small area of red discoloration, associated with retinal exudate or a bleb of subretinal fluid.

Left untreated, these neovascular membranes typically evolve into a hypertrophic, fibrotic scar that is disciform in appearance. The overlying retina suffers a loss of normal outer retinal architecture, which can lead to severe, permanent central vision loss.

Fluorescein angiography of CNV FA patterns of CNV may be classified as classic, occult, or some combination of both. Classic CNV refers to a bright, lacy, and well-defined hyperfluorescent lesion that appears in the early phase and progressively leaks by the late phases (Fig 4-7). Occult CNV refers to more diffuse hyperfluorescence that takes 1 of 2 forms: (1) PED, either fibrovascular PED or vascularized serous PED, or (2) late leakage from an undetermined source.

Fibrovascular PED is an irregular elevation of the RPE with progressive, stippled leakage on FA. Alternatively, the PED may pool dye rapidly in a homogenous ground-glass pattern that is consistent with a serous PED but has a notch, or hot spot, due to a vascular component, hence the term *vascularized serous PED* (Fig 4-8).

Late leakage from an undetermined source describes fluorescence at the level of the RPE that is poorly defined in the early phases of FA, but better appreciated in the late phases.

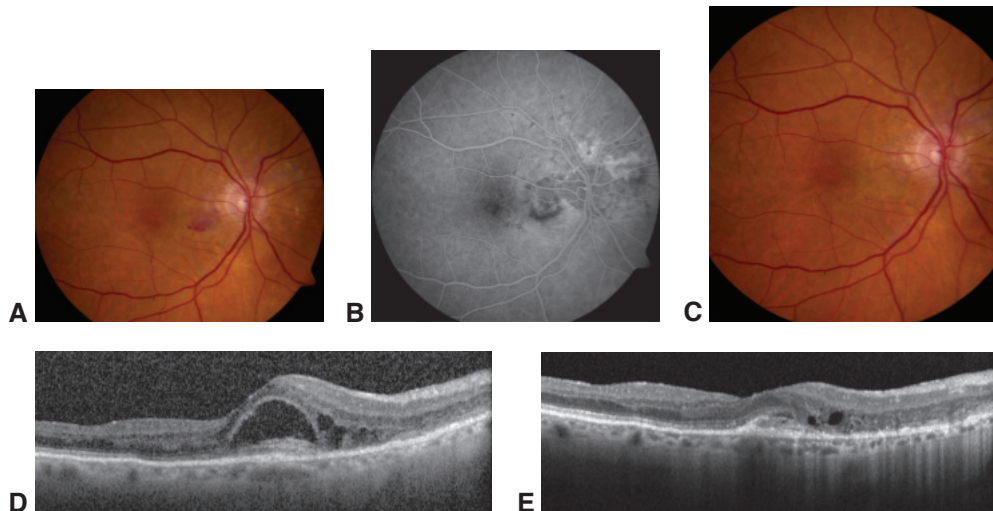


Figure 4-7 Color fundus photograph (**A**) and fluorescein angiography (FA) image (**B**) of classic extrafoveal CNV. Color fundus photograph (**C**) shows regression of CNV and resolution of hemorrhage after intravitreal bevacizumab therapy. SD-OCT images before (**D**) and after (**E**) bevacizumab therapy for type 2 neovascularization. Note resolution of subretinal fluid and contraction of type 2 neovascular membrane. (Courtesy of David Sarraf, MD.)

The angiographic appearance of occult CNV is consistent with type 1 neovascularization, whereas the appearance of classic CNV is more often related to type 2 neovascularization; however, this is not a hard-and-fast rule.

Type 3 neovascularization, or RAPs, may appear as a spot of retinal hemorrhage in the macula. It produces a focal hot spot on FA and indocyanine green (ICG) angiography with late CME or pooling into a PED.

Thick blood, pigment, scar tissue, or a PED may block fluorescence during angiography and obscure an underlying CNV. ICG angiography, with its longer wavelength fluorescence in the infrared spectrum, may be able to penetrate deeper through heme or pigment to reveal a hot spot that identifies CNV. Because it has 90% protein-binding, it can also differentiate between scar tissue or serous RPE fluid to reveal an active vascular lesion.

SD-OCT of CNV SD-OCT is noninvasive and is the most practical visualization technique for the diagnosis and classification of CNV as well as for monitoring the response to treatment. SD-OCT reveals the elevation of the RPE and PEDs produced by type 1 CNV. Serous PEDs appear as sharply elevated, dome-shaped lesions with hollow internal reflectivity and typically no associated subretinal or intraretinal fluid. Fibrovascular PEDs may or may not be sharply elevated and typically demonstrate lacy or polyp-like hyperreflective lesions on the undersurface of the RPE, with or without signs of contraction (Fig 4-9; Activity 4-1). Chronic fibrovascular PEDs often have a multilayered appearance due to sub-RPE cholesterol crystal precipitation in an aqueous environment; this appearance has been termed the “onion” sign. The fibrotic “bridge arch-shaped” serous PED can develop following anti-vascular endothelial growth factor (anti-VEGF) treatment and is associated with poor visual outcome.

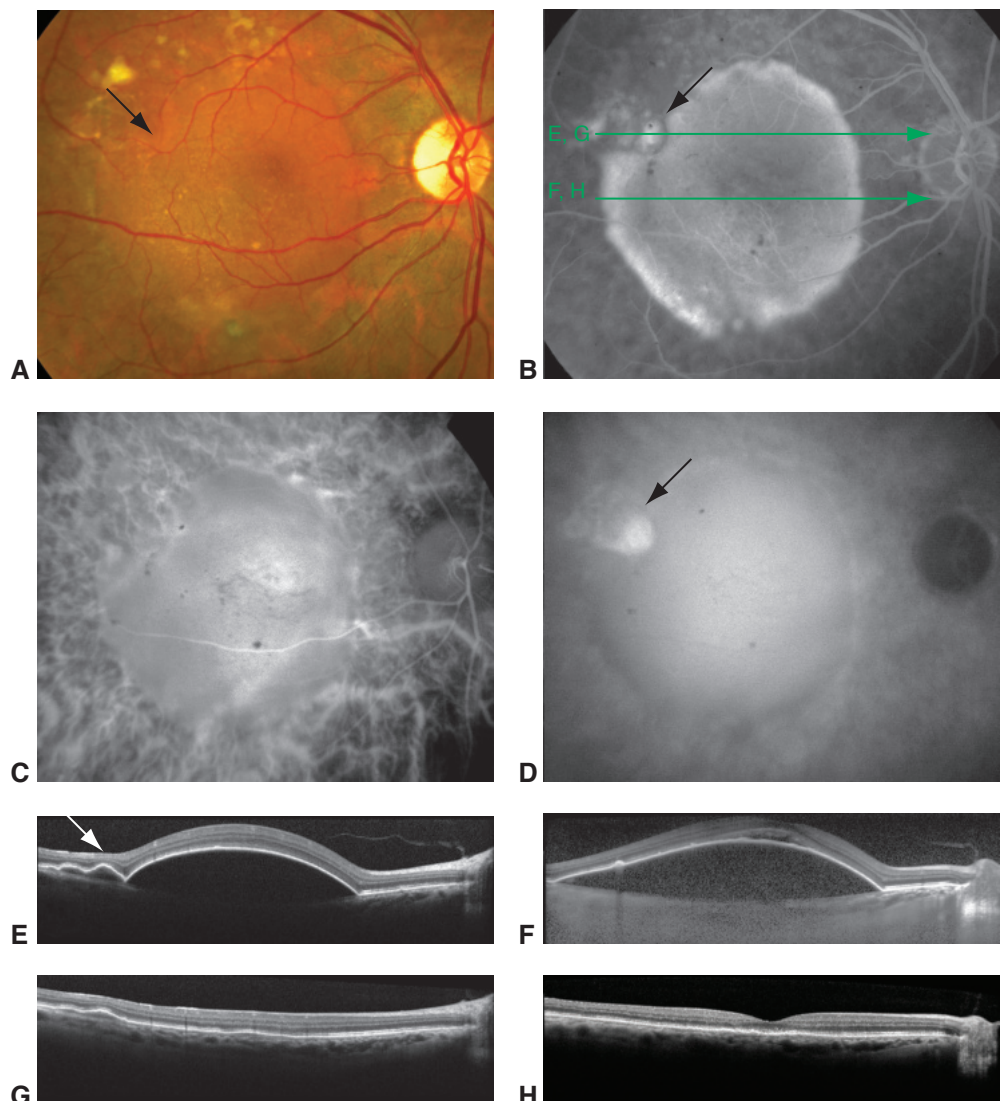


Figure 4-8 Vascularized serous pigment epithelial detachment (PED). **A**, Color fundus photograph of a vascularized serous PED with a notch (arrow) that corresponds to a hot spot on FA (black arrow in **B**). Green letters and arrows in **B** indicate the SD-OCT scan locations for parts **E** through **H**. Indocyanine green (ICG) angiography images early (**C**) and late (**D**) show pooling of the serous PED and hyperfluorescence of the hot spot (arrow in **D**). **E, F**, SD-OCT images of the large serous PED. Note the irregular portion of the PED (arrow in **E**), which corresponds to the hot spot and harbors the type 1 neovascular membrane. **G, H**, SD-OCT images show that the PED has resolved after therapy with anti–vascular endothelial growth factor (VEGF). (Used with permission from Mrejen S, Sarraf D, Mukkamala SK, Freund KB. Multimodal imaging of pigment epithelial detachment: a guide to evaluation. *Retina*. 2013;33(9):1735–1762.)



ACTIVITY 4-1 OCT Activity: OCT of subfoveal pigment epithelial detachment.

Courtesy of Colin A. McCannel, MD.

Access all Section 12 activities at www.aao.org/bcscactivity_section12.



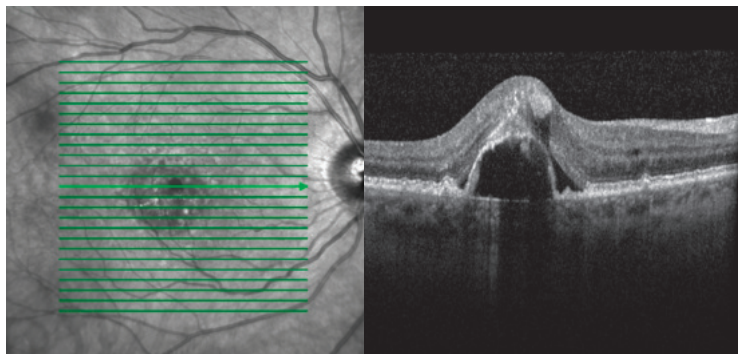


Figure 4-9 OCT image of a 61-year-old female patient who reported progressive decreased vision and onset of waviness of straight lines in the right eye. OCT shows a subfoveal pigment epithelial detachment with associated subretinal fluid, intraretinal fluid, and intrarectal hyperreflective material. There is also an area of hyperreflective material on the underside of the RPE, likely representing a neovascular complex (see slices 13 and 14 in Activity 4-1). Scrolling through the macula in Activity 4-1 reveals the extent of the lesion, as well as RPE irregularities that resemble small pigment epithelial detachments (drusen). (Courtesy of Colin A. McCannel, MD.)

Subretinal hyperreflective material (SHRM), which is hyperreflective on SD-OCT, is found between the retina and RPE in eyes with CNV. SHRM has an adverse effect on visual acuity, and results in scarring if it persists. Complex fibrovascular scarring may be visualized in the sub-PED compartment, with or without associated subretinal and/or intraretinal fluid.

Type 2 CNV appears as a hyperreflective band or plaque in the subneurosensory space, with associated subretinal and/or intraretinal fluid. Type 3 CNV presents on SD-OCT as hyperreflective foci emanating from the deep capillary plexus of the retina, with or without associated CME and PED. Recognition of these patterns may be helpful for differential diagnosis and predicting treatment outcomes.

Mrejen S, Sarraf D, Mukkamala SK, Freund KB. Multimodal imaging of pigment epithelial detachment: a guide to evaluation. *Retina*. 2013;33(9):1735–1762.

OCT Angiography of CNV OCT angiography (OCTA) reveals the structural details of CNV. The fine details of the vascular architecture of each CNV type can be easily visualized, free of the blur caused by fluorescein leakage in fluorescein angiography (Figs 4-10, 4-11, and 4-12).

Polypoidal choroidal vasculopathy Polypoidal choroidal vasculopathy (PCV), initially called *posterior uveal bleeding syndrome*, is a variant of CNV (type 1) and presents with multiple, recurrent serosanguineous RPE detachments. A network of polyps is associated with feeder vessels that adhere to the RPE monolayer of the fibrovascular PED in a “string-of-pearls” configuration. Although PCV was first discovered in hypertensive middle-aged women of African American or Asian ancestry, it has since been identified in women and men of all races. In Asians, however, 20%–50% of cases of neovascular AMD are PCV type, whereas in Whites the PCV type is responsible for <5% of cases of CNV. The associated serosanguineous detachments are often peripapillary and multifocal but may be peripheral, and there may be associated nodular, orange, subretinal lesions. Vitreous hemorrhage occurs more frequently in association with PCV than in non-PCV AMD. Soft drusen, typical

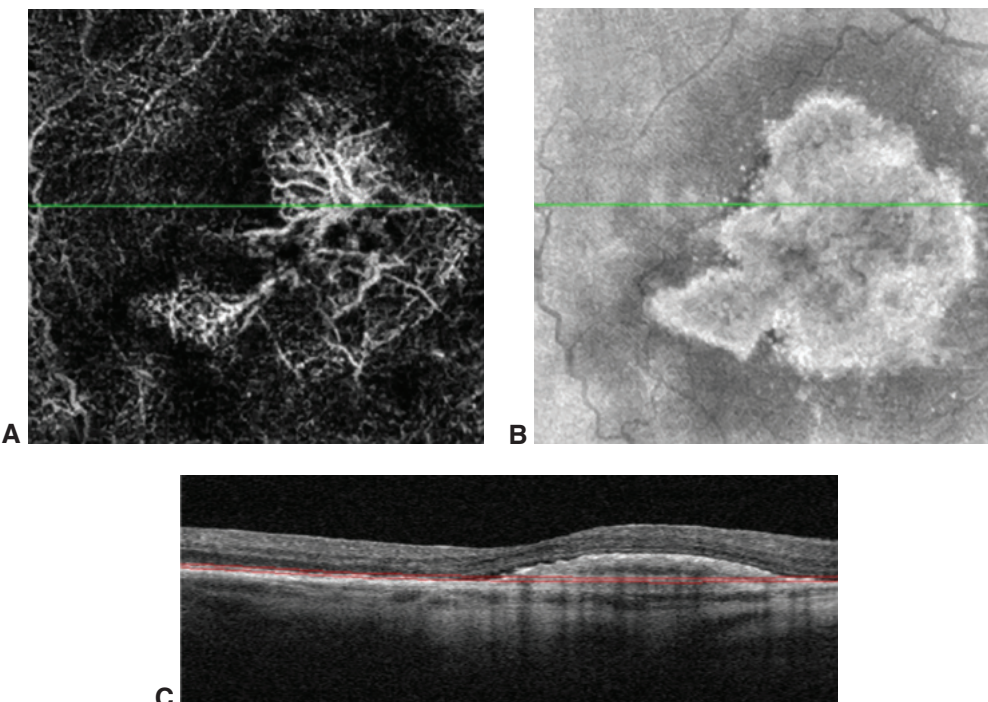


Figure 4-10 Type 1 CNV. **A**, OCT angiogram (OCTA) of type 1 CNV located beneath the RPE. The lesion has a “sea fan” configuration, with large feeder vessels and large caliper vessels. **B**, En face OCT structural image highlights the hyperreflective dome over the vessels. **C**, Cross-sectional B-scan OCT shows the distortion of the retinal profile caused by the CNV. (Courtesy of Richard B. Rosen, MD.)

in AMD, may or may not be present. A thickened or so-called *pachychoroid* is often present on EDI-OCT. Natural history and visual acuity outcomes of PCV may be better than those of CNV associated with AMD, except in cases with severe subretinal hemorrhage (Fig 4-13; see also Chapter 2, Fig 2-11 in this volume). ICG angiography, SD-OCT, and OCTA are useful for identifying the polyps. PCV is less responsive to anti-VEGF therapy than other types of CNV. The EVEREST Studies demonstrated that photodynamic therapy with verteporfin, with or without ranibizumab, results in better treatment response than ranibizumab alone.

Koh A, Lee WK, Chen LJ, et al. EVEREST study: efficacy and safety of verteporfin photodynamic therapy in combination with ranibizumab or alone versus ranibizumab monotherapy in patients with symptomatic macular polypoidal choroidal vasculopathy. *Retina*. 2012;32(8):1453–1464.

Differential diagnosis of neovascular AMD

There are many conditions associated with disruption of the Bruch membrane complex and secondary CNV that can mimic the CNV of AMD (see the section Other Causes of Choroidal Neovascularization later in this chapter).

Central serous chorioretinopathy can easily be confused with AMD. Subretinal fluid may be seen in both conditions; however, eyes with CSC typically do not have associated

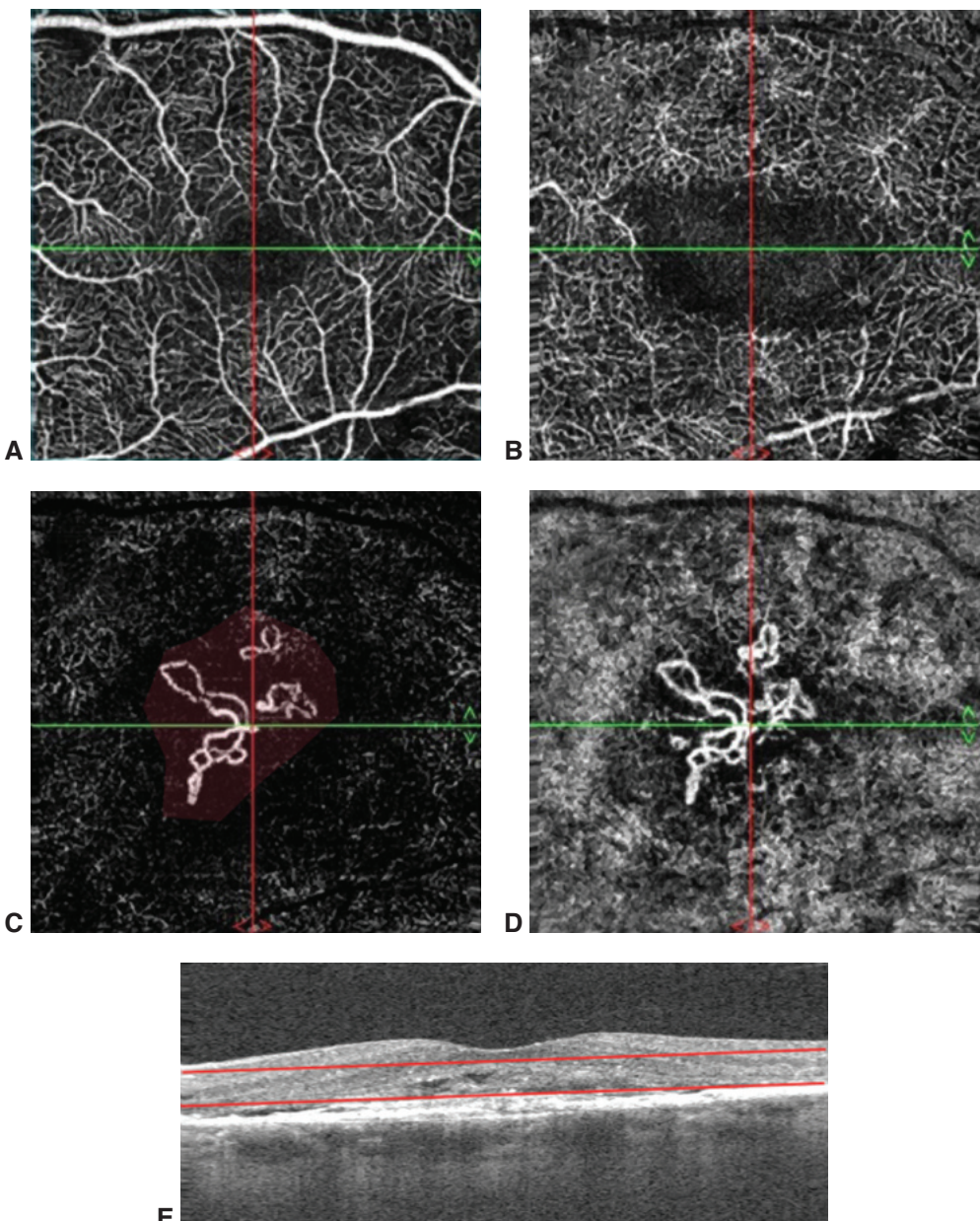


Figure 4-11 OCTA series of progressively deeper en face slices (**A–D**) of a type 2 CNV located above the RPE in the avascular zone of the retina. **A**, Superficial slab shows the superficial capillary plexus level and large retinal vessels. **B**, Deep capillary plexus level with an expanded foveal avascular zone (FAZ) caused by elevation of the underlying CNV. **C**, Avascular zone of the retina with CNV. **D**, Chorocapillaris level with CNV extending upward in the retina. **E**, Cross-sectional B-scan OCT shows disturbance in the RPE subretinal fluid and fibrosis. (Courtesy of Bruno Lumbroso.)

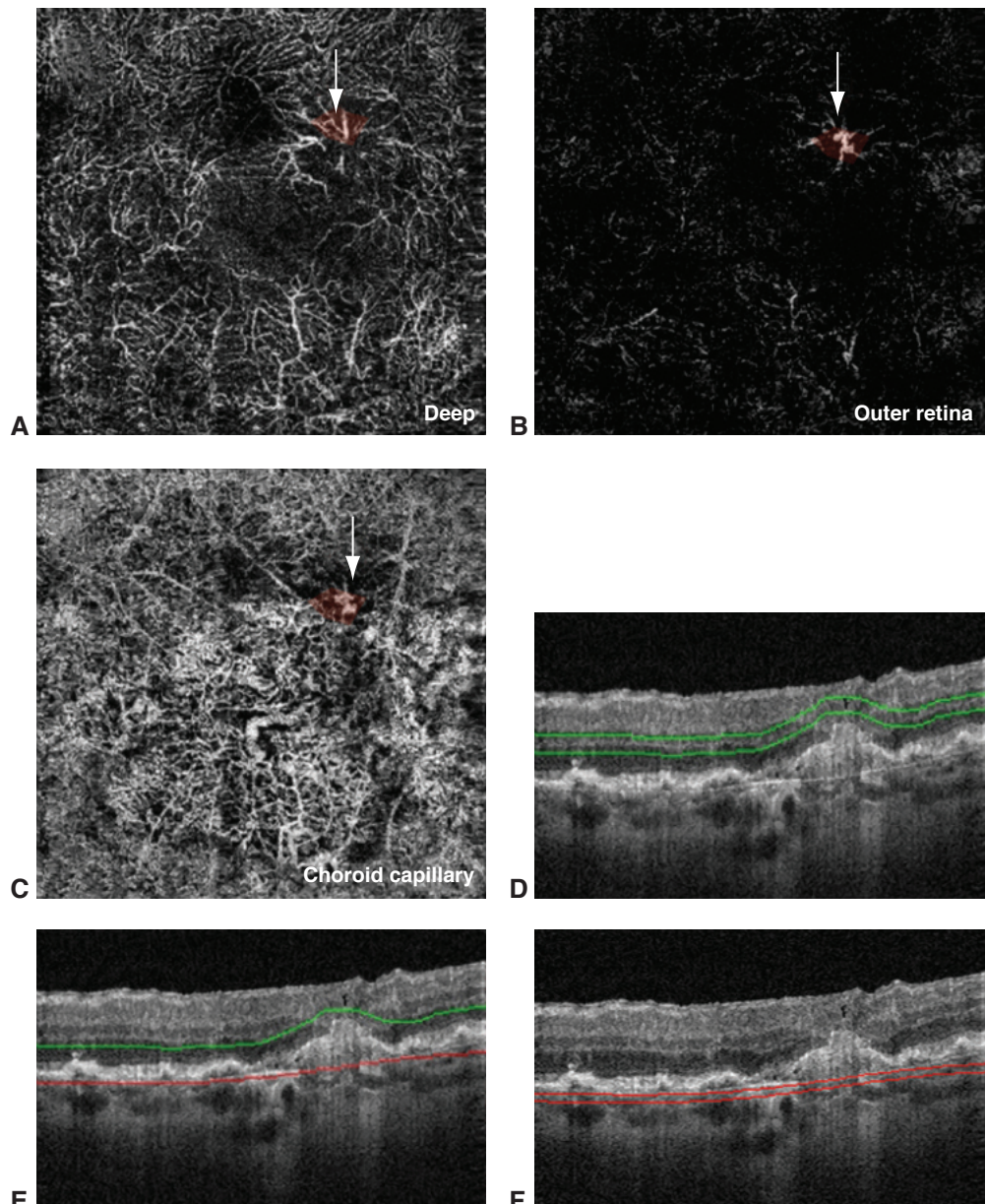


Figure 4-12 OCTA of type 3 CNV (retinal angiomatous proliferation lesion). **A**, Deep capillary plexus level reveals dilated blood vessels wider than surrounding capillaries near the edge of FAZ. **B**, Avascular zone level shows isolated CNV. **C**, Choriocapillaris level demonstrates interconnection of dilated deep capillary plexus vessels and choroidal vessels. **D**, Cross-sectional B-scan OCT shows segmentation of part **A**. **E**, Cross-sectional B-scan OCT shows segmentation of part **B**. **F**, Cross-sectional B-scan OCT shows segmentation of part **C**. (Courtesy of Richard B. Rosen, MD.)

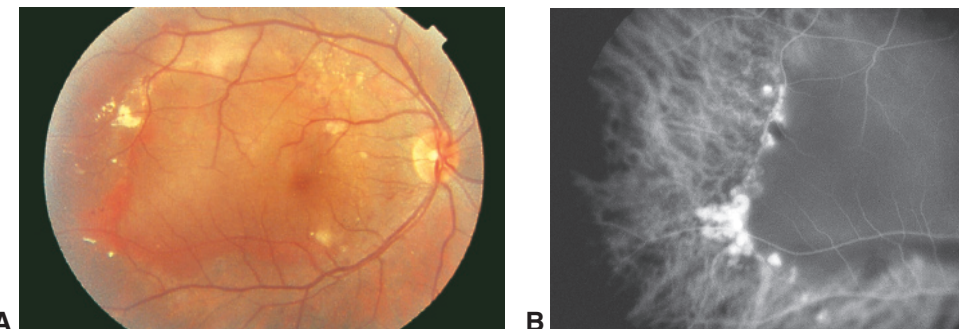


Figure 4-13 Polypoidal choroidal vasculopathy. **A**, Fundus photograph shows a large RPE detachment with multiple yellow-orange nodular lesions temporally. **B**, ICG angiogram demonstrates the characteristic polypoidal lesions temporally. (*Courtesy of Lawrence A. Yannuzzi, MD.*)

subretinal hemorrhage unless secondary CNV has developed. The choroidal layer, which is best visualized using EDI-OCT, is typically thick in eyes with CSC compared to the typical thin choroidal layer in eyes with AMD. CSC is further characterized by geographic patches of RPE pigment mottling that may extend to the inferior periphery in a drainage or drippage-like gravitational configuration often referred to as “guttering.” These lesions can be visualized with fluorescein angiography or autofluorescence imaging.

Management of neovascular AMD

If neovascular AMD is suspected clinically, OCT and FA studies should be obtained to help establish the diagnosis as well as for monitoring response to therapy.

Laser photocoagulation (“thermal laser”) Thermal laser treatment is now used only in very rare instances due to poor outcomes from high recurrence rates, as revealed in the Macular Photocoagulation Study Trials. Lesions sufficiently peripheral to the foveal center that present minimal risk of iatrogenic foveal laser damage and lower rate of recurrence may still benefit from laser photocoagulation treatment.

Photodynamic therapy (“cold laser”) PDT was introduced in 2000 as a less-destructive phototherapy for treating CNV. Treatment involves intravenous administration of the photosensitizing drug verteporfin followed by the application of light of a specific wavelength. The light incites a localized photochemical reaction in the targeted area, resulting in CNV thrombosis. Although PDT slows progression, it does not prevent significant vision loss in most eyes with CNV and has been shown to upregulate VEGF in the treatment area. Use of PDT for the management of exudative AMD is now rare, except for the most recalcitrant cases or for eyes with PCV.

Antiangiogenic therapies Angiogenesis is the formation of new blood vessels that sprout from existing vessels via a complex cascade of events. The first events in that cascade are vasodilation of existing vessels and increased vascular permeability. Next comes degradation of the surrounding extracellular matrix, facilitating migration and proliferation of endothelial cells. As endothelial cells join to create lumen, new capillaries develop and

then mature, remodeling into stable vascular networks. This cascade requires a balanced interplay of growth-promoting and growth-inhibiting angiogenic factors to proceed. Activators of angiogenesis include vascular endothelial growth factor (VEGF), fibroblast growth factor (FGF), transforming growth factor α (TGF- α) and TGF- β , angiopoietin-1, and angiopoietin-2. Inhibitors of angiogenesis include thrombospondin, angiostatin, endostatin, and pigment epithelium-derived factor (PEDF).

Most antiangiogenesis research has focused on the inhibition of VEGF, which increases in pigment epithelial cells in the early stages of AMD. High concentrations of VEGF in excised CNV and vitreous samples from patients with AMD have further suggested a causal role for VEGF in the initiation of neovascularization. VEGF is a homodimeric glycoprotein that has a heparin-binding growth factor specificity for vascular endothelial cells. It induces vascular permeability, angiogenesis, and lymphangiogenesis, and it acts as a survival factor for endothelial cells by preventing apoptosis. There are at least 4 major VEGF isoforms; VEGF₁₆₅ is thought to be the most dominant in AMD.

Pegaptanib In 2004, the US Food and Drug Administration (FDA) approved the first intravitreal anti-VEGF therapy, pegaptanib, an RNA oligonucleotide ligand (or aptamer) that binds human VEGF₁₆₅. Studies showed that it slowed vision loss, but it has since been supplanted by more effective agents.

Ranibizumab Ranibizumab is a recombinant humanized antibody fragment (Fab) that binds VEGF. Ranibizumab binds to and inhibits all active isoforms of VEGF-A as well as their active degradation products. Two studies, MARINA (Minimally Classic/Occult Trial of the Anti-VEGF Antibody Ranibizumab in the Treatment of Neovascular AMD) and ANCHOR (Anti-VEGF Antibody for the Treatment of Predominantly Classic Choroidal Neovascularization in AMD), demonstrated a loss of fewer than 15 ETDRS in 95% of ranibizumab-treated patients at 12 months compared with 62% of sham-treated patients and 64% of PDT-treated patients. In addition, 30%–40% of ranibizumab-treated patients experienced visual acuity improvement of 15 letters or more compared with 5% or less in the control participants (Fig 4-14, Table 4-3). Approximately 90% of ranibizumab-treated eyes lost fewer than 15 ETDRS letters at 24 months.

Visual acuity improvements in participants of the PIER (Phase 3b, Multicenter, Randomized, Double-Masked, Sham Injection-Controlled Study of the Efficacy and Safety of Ranibizumab in Subjects With Subfoveal Choroidal Neovascularization With or Without Classic Choroidal Neovascularization Secondary to AMD) and EXCITE (Efficacy and Safety of Ranibizumab in Patients With Subfoveal Choroidal Neovascularization Secondary to AMD) studies were similar to the improvements seen in the MARINA and ANCHOR studies over the first 3 months; however, treatment effects declined in participants undergoing quarterly (every 3 months) ranibizumab dosing as opposed to monthly dosing. These results suggest that quarterly treatment is suboptimal. However, accepted anti-VEGF treatment methods that deviate from the FDA-approved monthly injections include “as needed” and “treat and extend.” On the as-needed regimen, regular treatment is administered until the macula appears dry clinically and on OCT; after that, treatment is only resumed when signs of recurrent exudation appear. The treat-and-extend regimen also involves administration of regular monthly treatment until the macula is dry; after

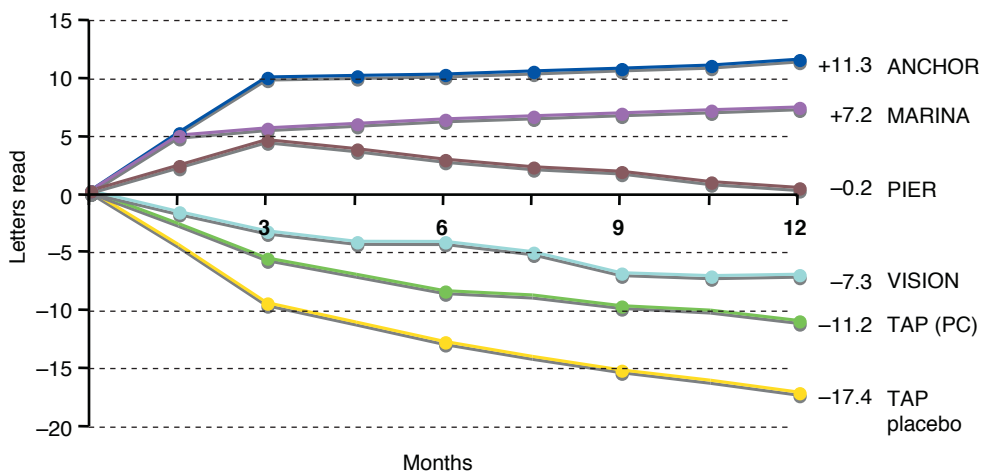


Figure 4-14 Graph illustrates the mean change in visual acuity (number of letters read) from several phase 3 clinical trials. Comparison of data between different trials should be interpreted with caution; the potentially different study inclusion criteria and baseline characteristics of eyes for different studies may affect the stated visual acuity gains. ANCHOR = Anti-VEGF Antibody for the Treatment of Predominantly Classic Choroidal Neovascularization in AMD; MARINA = Minimally Classic/Occult Trial of the Anti-VEGF Antibody Ranibizumab in the Treatment of Neovascular AMD; PC = predominantly classic; PIER = Phase 3b, Multi-center, Randomized, Double-Masked, Sham Injection-Controlled Study of the Efficacy and Safety of Ranibizumab in Subjects With Subfoveal Choroidal Neovascularization With or Without Classic Choroidal Neovascularization Secondary to AMD; TAP = Treatment of AMD with Photodynamic Therapy; VISION = VEGF Inhibition Study in Ocular Neovascularization. (Courtesy of Peter K. Kaiser, MD.)

that, treatment continues at progressively increasing intervals. This more cautious second approach continues to treat inactive CNV (albeit at longer intervals between injections) to avoid sudden recurrence of exudation (see Fig 4-14).

Several clinical trials have evaluated as-needed approaches to anti-VEGF therapy: PrONTO (Prospective Optical Coherence Tomography Imaging of Patients With Neovascular AMD Treated With Intraocular Ranibizumab), SAILOR (Study to Evaluate Ranibizumab in Subjects With Choroidal Neovascularization Secondary to AMD), SUSTAIN (Study of Ranibizumab in Patients with Subfoveal Choroidal Neovascularization Secondary to AMD), and HORIZON (Open-Label Extension Trial of Ranibizumab for Choroidal Neovascularization Secondary to AMD). In each of these studies, participants were administered 3 monthly injections, followed by various as-needed treatment regimens based on clinical and OCT-guided criteria. All of the studies had vision and OCT outcomes comparable to or reduced from those obtained with MARINA and ANCHOR. The HORIZON study was a continuation trial of patients enrolled in prior ranibizumab AMD trials. Eyes that had gained 10.2 letters on the ETDRS (Early Treatment Diabetic Retinopathy Study) eye chart during ANCHOR or MARINA after 2 years of monthly injections declined in visual acuity, ending with only a mean 2.0-letter gain compared with baseline (ie, they lost nearly 8 letters once the regimen was switched from monthly injections to an as-needed protocol). Experts believed the reason participants

Table 4-3 Selected Clinical Trials, Treatments, and Outcomes

Clinical Trial	Treatment	Outcome
ANCHOR	Ranibizumab monthly vs photodynamic therapy as needed on quarterly basis	Increase of 11.3 letters in ranibizumab monthly group vs decrease of 9.5 letters in verteporfin group ($P = <0.001$ at 2 years)
MARINA	Ranibizumab monthly vs sham treatment	Increase of 7.2 letters ranibizumab monthly group vs loss of 10.4 letters in the sham group ($P = <0.001$ at 2 years)
VIEW 1	Ranibizumab monthly vs aflibercept monthly and bimonthly	Increase of 8.1 letters in ranibizumab monthly group (94.4% lost fewer than 15 letters) Increase of 10.9 letters in aflibercept monthly group (95.1% lost fewer than 15 letters) Increase of 7.9 letters in aflibercept bimonthly group (95.1% lost fewer than 15 letters) Aflibercept deemed noninferior to ranibizumab
VIEW 2	Ranibizumab monthly vs aflibercept monthly and bimonthly	Increase of 9.4 letters in ranibizumab monthly group (94.4% lost fewer than 15 letters) Increase of 7.6 letters in aflibercept monthly group (95.6% lost fewer than 15 letters) Increase of 8.9 letters in aflibercept bimonthly group (95.6% lost fewer than 15 letters) Aflibercept deemed noninferior to ranibizumab

Data from Rofagha S, Bhisitkul RB, Boyer DS, Sadda SR, Zhang K; SEVEN-UP Study Group. Seven-year outcomes in ranibizumab-treated patients in ANCHOR, MARINA, and HORIZON: a multicenter cohort study (SEVEN-UP). *Ophthalmology*. 2013;120(11):2292–2299.

in the HORIZON study experienced a decline in visual acuity was because the study did not offer any re-treatment guidelines for investigators, resulting in a mean of 3.6 ranibizumab injections in the 12 months of the extension trial. HARBOR (A Study of Ranibizumab Administered Monthly or on an As-Needed Basis in Patients With Subfoveal Neovascular AMD) compared higher-dose (2.0 mg) with standard-dose (0.5 mg) ranibizumab therapy and failed to find any difference in visual acuity or anatomical outcomes between the 2 dosages.

Eyes with fibrovascular PEDs may be at increased risk for the development of an RPE tear following anti-VEGF therapy, especially for PEDs greater than 600 µm in height. The mechanism for the tear is believed to be contraction of the underlying type 1 CNV, resulting from the anti-VEGF drug action.

Brown DM, Kaiser PK, Michels M, et al; ANCHOR Study Group. Ranibizumab versus verteporfin for neovascular age-related macular degeneration. *N Engl J Med*. 2006;355(14):1432–1444.

Aflibercept Aflibercept (also known as *VEGF Trap*) is a soluble protein that acts as a VEGF receptor decoy; it combines the ligand-binding elements of the extracellular domains of VEGFR1 and VEGFR2 fused to the constant region (Fc) of immunoglobulin G (IgG).

Aflibercept binds both VEGF and placental-like growth factor and fully penetrates all retinal layers.

In the studies VIEW 1 and VIEW 2 (VEGF Trap-Eye: Investigation of Efficacy and Safety in Wet AMD 1 and 2), patients received aflibercept in monthly or every-second-month regimens, while a comparison group received monthly ranibizumab treatment. All aflibercept treatment regimens demonstrated noninferiority to ranibizumab monthly treatment. Patients receiving monthly aflibercept, 2 mg, gained 10.9 letters of visual acuity on average, whereas those receiving monthly ranibizumab, 0.5 mg, had a mean 8.1-letter gain ($P < .01$). Other aflibercept-dosed groups in the 2 studies had results similar to those from the patients receiving ranibizumab, and after 3 monthly doses, aflibercept administered every 2 months showed similar efficacy to ranibizumab administered monthly (see Fig 4-14, Table 4-3).

Mean letter increase at 96 weeks was 7.6 letters in the group treated every 8 weeks with 2 mg of aflibercept, compared with 7.9 letters in the monthly ranibizumab group; 3-line VA increases were seen in 30%–33% for each arm of the study. OCT-measured anatomical response was maintained through 2 years with no significant difference in central retinal thickness among the 4 groups. Safety profiles were similar for both aflibercept and ranibizumab.

Heier JS, Brown DM, Chong V, et al; VIEW 1 and VIEW 2 Study Groups. Intravitreal aflibercept (VEGF trap-eye) in wet age-related macular degeneration. *Ophthalmology*. 2012;119(12):2537–2548.

Bevacizumab In 2004, the FDA approved bevacizumab, which is a full-length monoclonal antibody against VEGF, for the treatment of metastatic colorectal cancer. It has also been used “off-label” for the treatment of AMD via intravitreal and intravenous administration. Although bevacizumab and ranibizumab are manufactured by the same pharmaceutical company, there are important differences between the drugs: bevacizumab is larger, with 2 antigen-binding domains, contrasted with the smaller ranibizumab with a single domain. In addition, bevacizumab costs substantially less, impacting its availability to some patients. Because full-length antibodies are not cleared as rapidly as fragment antibodies, intravitreal injections of bevacizumab have a longer systemic half-life than intravitreal injections of ranibizumab (~21 days for bevacizumab vs 2.2 hours for ranibizumab).

Bevacizumab’s similar efficacy compared with ranibizumab and its 40-fold lower wholesale cost has prompted several comparative efficacy studies. Table 4-4 summarizes the major studies comparing bevacizumab to ranibizumab efficacy in the management of neovascular AMD.

CATT (Comparison of Age-Related Macular Degeneration Treatments Trials) was the first and largest multicenter, randomized clinical trial to compare the relative safety and efficacy of ranibizumab with bevacizumab for the treatment of neovascular AMD. Funded by the US National Eye Institute, it studied 1208 patients. Results showed that bevacizumab was noninferior to ranibizumab therapy in monthly or as-needed delivery schedules over 2 years. Mean letters gained from baseline were 8.8 letters in the ranibizumab-monthly group, 7.8 letters in the bevacizumab-monthly group, 6.7 letters in the ranibizumab as-needed group, and 5.0 letters in the bevacizumab as-needed group. Systemic adverse events were significantly greater in the bevacizumab (39.9%) than in the ranibizumab (31.7%) group, but death and arteriothrombotic events were not statistically different between the 2 drugs. At 5 years, vision gains in the first 2 years were not

Table 4-4 Clinical Trials Comparing Bevacizumab to Ranibizumab

Study Abbreviation	Study Name	Location	Patients Enrolled	Treatment Regimen	Major Outcome
BRAMD	Comparing the Effectiveness of Bevacizumab to Ranibizumab in Patients with Exudative Age-Related Macular Degeneration	The Netherlands	327	Fixed interval dosing	Bevacizumab noninferior to ranibizumab with regard to visual acuity outcomes
CATT	Comparison of Age-Related Macular Degeneration Treatments Trials	United States	1208	As needed, fixed interval dosing	Bevacizumab noninferior to ranibizumab with regard to visual acuity outcomes
GEFAL	Groupe d'Evaluation Français Avastin vs Lucentis	France	501	As needed	No significant difference in outcomes between drugs
IWAN	Randomised Controlled Trial of Alternative Treatments to Inhibit VEGF in Age-Related Choroidal Neovascularisation	United Kingdom	610	As needed, fixed interval dosing	No statistically significant differences in visual or anatomical outcomes between drugs
LUCAS	Lucentis Compared to Avastin Study	Norway	432	Treat and extend	No significant differences in outcomes between drugs
MANTA	A Randomized Observer and Subject Masked Trial Comparing the Visual Outcome After Treatment With Ranibizumab or Bevacizumab in Patients With Neovascular Age-Related Macular Degeneration Multicenter Anti-VEGF Trial in Austria	Austria	321	As needed	Groups had similar visual acuity and anatomical outcomes

Data from CATT Research Group, Martin DF, Maguire MG, et al. Ranibizumab and bevacizumab for neovascular age-related macular degeneration. *N Engl J Med.* 2011;364(20):1897–1908; and from CATT Research Group, Martin DF, Maguire MG, et al. Ranibizumab and bevacizumab for treatment of neovascular age-related macular degeneration: two-year results. *Ophthalmology.* 2012;119(7):1388–1398.

sustained, but 50% of eyes maintained 20/40 or better visual acuity. Geographic atrophy development or increase appeared to be stimulated by anti-VEGF therapy, with evidence that progression was related to persistence or absence of subretinal fluid.

Clusters of severe vision loss due to endophthalmitis following bevacizumab injection related to a few instances of substandard and erroneous compounding practices have raised concerns about the off-label use of this drug in the United States. In response, legislative changes have led to improved regulation and increased monitoring of compounding pharmacies.

Treatment effect modifiers Vitreoretinal interface status may significantly modify the response to therapy with anti-VEGF agents. Hyaloidal separation appears to facilitate penetration of drug, so that fewer injections need to be administered, however, visual acuity is not affected. Eyes with epiretinal membrane may require more injections due to anatomic disturbance, reduced penetration, or associated inflammation.

Complications of intravitreal anti-angiogenic therapy Intravitreal injections are typically well tolerated. Minor complications such as subconjunctival hemorrhage and local irritation are common. In rare instances, serious ocular complications can occur, including inflammation, persistent ocular hypertension, retinal detachment, vitreous hemorrhage, and endophthalmitis. The rate of endophthalmitis is approximately 1 in 2000 or lower (see also Chapter 20 of this volume). Systemic administration of bevacizumab for cancer treatment has been shown to increase the risk of hypertension; thromboembolic events, especially myocardial infarctions and cerebral vascular accidents; gastrointestinal perforations; and bleeding. There is conflicting evidence whether intravitreal injections of any of these agents increase the rate of these complications.

Solomon SD, Lindsley K, Vedula SS, Krzystolik MG, Hawkins BS. Anti-vascular endothelial growth factor for neovascular age-related macular degeneration. *Cochrane Database Syst Rev*. 2014;(8):CD005139.

Combination treatment Combinations of therapies have been explored to address the complex interaction between inflammation, angiogenesis, and fibrosis that are thought to play a role in the limited success of the single agents currently available. Trials exploring the use of combination therapies (eg, RADICAL [Reduced Fluence Visudyne-Anti-VEGF-Dexamethasone in Combination for AMD Lesions] and DENALI [Safety and Efficacy of Verteporfin PDT Administered in Conjunction With Ranibizumab Versus Ranibizumab Monotherapy in Patients With Subfoveal CNV Secondary to AMD]) found that adding PDT to ranibizumab reduced re-treatment rates compared with ranibizumab monotherapy. However, visual outcomes were inferior to monotherapy. Combination strategy appeared beneficial in some cases of PCV recalcitrant to anti-VEGF therapy. Adding radiation to ranibizumab therapy may also reduce the injection burden, but again, visual outcomes were inferior to monotherapy.

Surgical treatments In cases of thick submacular hemorrhage, intravitreal or subretinal tissue plasminogen activator injection with pneumatic displacement may be helpful in some patients. Submacular surgery, involving the removal of the CNV from beneath the fovea, and macular translocation surgery, in which the fovea is moved over to an area of

healthier RPE, are complex surgical techniques that were developed prior to anti-VEGF agents and have largely been abandoned today.

Low vision therapies Despite the success of intravitreal anti-VEGF pharmacotherapy, a significant number of patients with AMD will ultimately progress to bilateral central blindness, for which few therapeutic options exist. The implantable miniature telescope can provide magnification up to factor of 2.7; its use improved visual acuity by 2 lines in the pivotal FDA trials. However, corneal decompensation due to endothelial cell loss is projected to bring the corneal transplant rate to 5% at 5 years after the implantation surgery.

Low vision rehabilitation Vision loss of any degree can have a profound effect on a patient's daily activities, especially reading and driving. Severe vision loss and central blindness resulting from AMD can be devastating. In addition, central scotomas may be complicated by visual release hallucinations (Charles Bonnet syndrome), which can overlay blank areas with small geometric figures or faces or any other image. Although primary efforts are focused on rescue therapies, consideration should be given to low vision rehabilitation strategies. Low vision rehabilitation and the use of optical and nonoptical devices can maintain the patient's functional status and sustain quality of life (see BCSC Section 3, *Clinical Optics*). Even patients who have undergone successful anti-VEGF therapy may retain visual acuity that has been reduced to the 20/50–20/70 range and can benefit from low vision strategies such as magnification (eg, high-plus lenses, video magnifiers), optimal lighting, and contrast enhancement techniques. Training on the use of eccentric fixation outside the area of scotoma that is produced by the disciform scar or area of atrophy may also be helpful. To foster such rehabilitation, clinicians should consider referring patients for low vision evaluation at local low vision centers or to state services for the blind, available in most US states.

The American Academy of Ophthalmology's Initiative in Vision Rehabilitation page on the ONE Network (www.aao.org/low-vision-and-vision-rehab) provides resources for low vision management, including patient handouts and information about additional vision rehabilitation opportunities beyond those provided by the ophthalmologist.

Other Causes of Choroidal Neovascularization

A number of other conditions may produce non-AMD macular degenerative changes with central vision loss caused by CNV, atrophy, or scarring. CNV management, while historically focused on laser therapies or PDT, has evolved to incorporate intravitreal anti-VEGF agents using treatment protocols similar to those used for neovascular AMD, with similar visual acuity gains.

Ocular Histoplasmosis Syndrome

Histoplasma capsulatum fungus is endemic to the Mississippi and Ohio River valleys. Humans become infected by inhaling the yeast form of this fungus, which then disseminates throughout the bloodstream. Although the systemic infection eventually subsides, the individual may be left with chorioretinal scars that produce visual symptoms years later.

Ocular histoplasmosis syndrome (OHS) is also referred to as *presumed ocular histoplasmosis syndrome (POHS)* because the causality has never been definitively confirmed. OHS is most prevalent among the population with the greatest percentage of positive skin reactors; over 90% of patients with the characteristic OHS fundus appearance react positively to histoplasmin skin testing. In 1 community with endemic histoplasmosis (where 60% of the total population reacted positively to histoplasmin skin testing), the characteristic peripheral lesions of OHS occurred in 2.6% of the total population surveyed and in 4.4% of the positive skin test responders. Only 1 individual with peripheral lesions showed disciform macular disease. The organism has been identified histologically in the choroid of 5 patients with OHS. Nevertheless, other etiologies besides *H capsulatum* may produce a similar phenotype (see also the section “Multifocal choroiditis” in Chapter 11).

Clinically, OHS presents with small, atrophic, “punched-out” chorioretinal scars in the midperiphery and posterior pole (“histo spots”), linear peripheral atrophic tracks, and juxtapapillary chorioretinal scarring with or without CNV in the macula (Fig 4-15). Lesions are bilateral in more than 60% of infected individuals, and characteristically, there is an absence of vitreous inflammation. Most patients with OHS are asymptomatic until the development of CNV, which may cause vision loss, metamorphopsia, and paracentral scotomas. FA and OCT findings are useful for guiding diagnosis and monitoring response to therapy. Other diseases with features similar to OHS include multifocal choroiditis and panuveitis; see also BCSC Section 9, *Uveitis and Ocular Inflammation*.

Management of ocular histoplasmosis syndrome

There is no specific medical management necessary for OHS. When CNV develops, anti-VEGF therapy is helpful.

Nielsen JS, Fick TA, Saggau DD, Barnes CH. Intravitreal anti-vascular endothelial growth factor therapy for choroidal neovascularization secondary to ocular histoplasmosis syndrome. *Retina*. 2012;32(3):468–472.

Angioid Streaks

Irregular dark red or brown lines radiating from a ring of peripapillary atrophy surrounding the optic nerve head are referred to as *angioid streaks* because their appearance mimics the appearance of blood vessels. On FA, characteristic window defects with late staining are noted resulting from dehiscences or cracks in the thickened and calcified Bruch membrane (Fig 4-16).

The systemic disease most commonly associated with angioid streaks is *pseudoxanthoma elasticum* (PXE), or Grönblad-Strandberg syndrome, a predominantly autosomal recessive disorder inherited through mutation in the *ABCC6* gene located on band 16p13.1. Additional fundus findings associated with PXE include optic nerve head drusen, peripheral round atrophic scars with a “comet” sign, and a mottled RPE appearance referred to as *peau d'orange* (“skin of an orange”). *Paget disease* of bone, *beta thalassemia*, *sickle cell anemia* (SS), and *Ehlers-Danlos syndrome* may also be associated with angioid streaks. If the ophthalmologist establishes a new diagnosis of angioid streaks, and the patient is not known to have any of the aforementioned conditions, the patient should be referred for work-up and management of the possible underlying systemic disease.

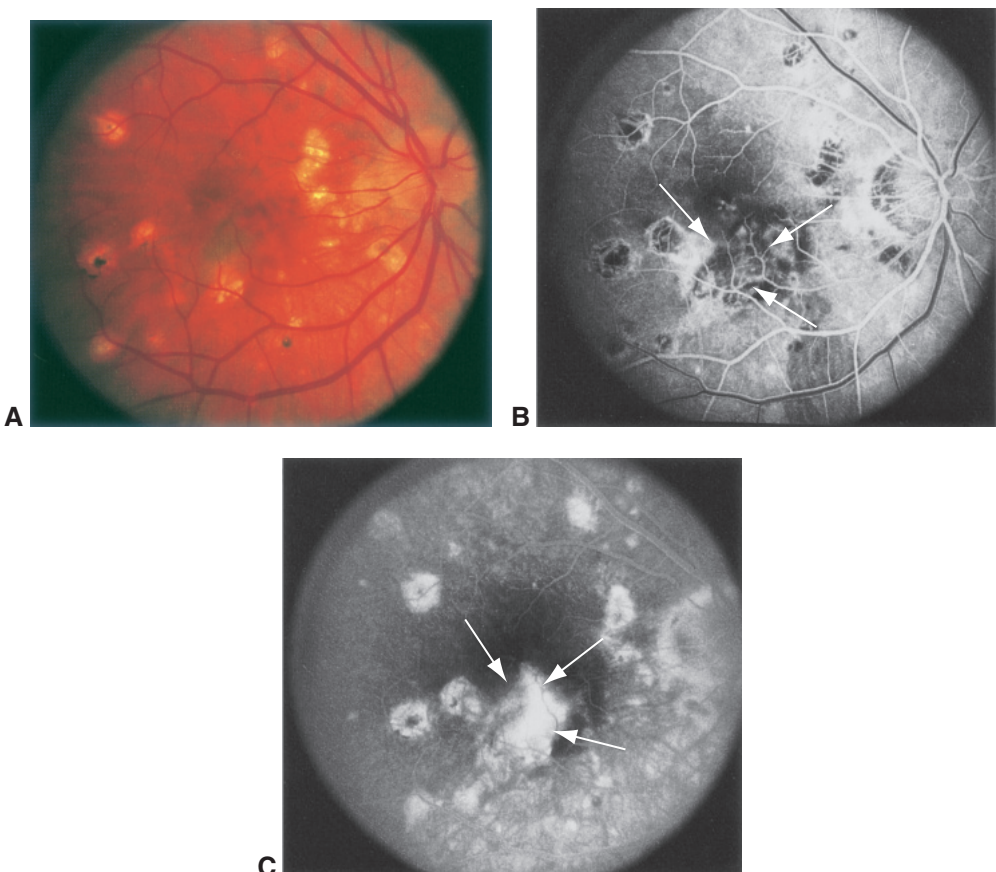


Figure 4-15 Ocular histoplasmosis syndrome with CNV. **A**, Fundus photograph shows peripapillary atrophy and numerous atrophic scars. **B**, Transit frame of the angiographic study reveals blocked fluorescence from blood and pigment as well as hyperfluorescence resulting from the CNV (arrows) and choroidal transmission in areas of atrophy. **C**, Leakage from the choroidal neovascular membrane (arrows) late in the study, as well as staining of the sclera beneath atrophic scars.

Angioid streaks usually are asymptomatic unless they are subfoveal. Visual disturbances may develop due to submacular hemorrhage resulting from trauma, but these disturbances may resolve spontaneously if there is no CNV. The most significant visual complication is the development of CNV.

Safety glasses are an advisable precaution for patients with angioid streaks because they can be highly susceptible to choroidal rupture following even minor blunt injury. Medical consultation is indicated to evaluate for systemic manifestations of PXE including “plucked chicken” skin appearance, calcific arteriosclerosis of coronary arteries, and gastrointestinal and cerebrovascular bleeding.

When CNV develops, treatment with anti-VEGF agents has supplanted the use of laser treatment or PDT, as noted previously.



Figure 4-16 Color montages of fundus photographs from a patient with pseudoxanthoma elasticum showing, in both eyes, angioid streaks radiating from the optic nerve head, a “peau d’orange” appearance of the fundus temporal to the macula, optic nerve head drusen, mid-peripheral comet lesions, and, in the left eye, an old, inactive CNV. (Courtesy of Stephen J. Kim, MD.)

Chang LK, Spaide RF, Brue C, Freund KB, Klancnik JM Jr, Slakter JS. Bevacizumab treatment for subfoveal choroidal neovascularization from causes other than age-related macular degeneration. *Arch Ophthalmol.* 2008;126(7):941–945.

Heier JS, Brown D, Ciulla T, et al. Ranibizumab for choroidal neovascularization secondary to causes other than age-related macular degeneration: a phase I clinical trial. *Ophthalmology.* 2011;118(1):111–118.

Pathologic Myopia

CNV may develop in 5%–10% of eyes with an axial length greater than 26.5 mm, with or without lacquer cracks or widespread chorioretinal degeneration (Fig 4-17). Treatment with laser therapy is often complicated when the laser scar expands through the foveal center over time (so-called *atrophy creep*). Although PDT has been shown to be beneficial, the mainstay of treatment is now intravitreal anti-VEGF therapy due to the excellent visual and anatomical outcomes. Several studies have demonstrated sustained regression of myopic CNV after anti-VEGF treatment, with stabilization or improvement of visual acuity after only 1 or 2 injections. For a more detailed discussion of myopia and pathologic myopia, please see Chapter 10 in this volume.

Wang E, Chen Y. Intravitreal anti-vascular endothelial growth factor for choroidal neovascularization secondary to pathologic myopia: systematic review and meta-analysis. *Retina.* 2013;33(7):1375–1392.

Idiopathic CNV and Miscellaneous Causes of CNV

CNV may complicate any one of the disorders known to damage Bruch membrane, including inflammatory chorioretinopathies, choroidal neoplasms, traumatic choroidal rupture, optic nerve head abnormalities, and others (Table 4-5). It may also develop in

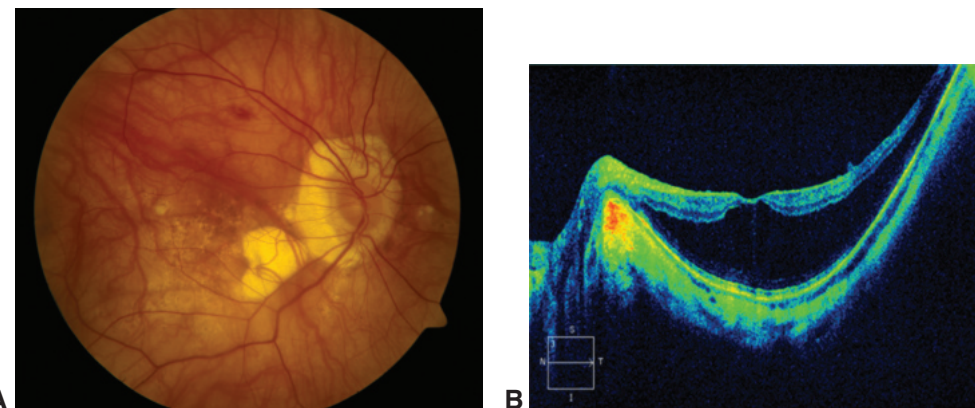


Figure 4-17 Pathologic myopia. **A**, Color fundus photograph of the right eye demonstrates myopic macular degeneration with pigment mottling and lacquer cracks centrally and geographic atrophy in the inferonasal macula. Extensive peripapillary atrophy of the RPE is also present. The small, round hemorrhage in the superior macula is not associated with CNV membrane. **B**, SD-OCT image of a patient's left eye with pathologic myopia shows a high-grade posterior staphyloma associated with myopic macular schisis. (Courtesy of David Sarraf, MD.)

eyes with no apparent risk factors or predisposing lesions (eg, idiopathic CNV). As in other forms of CNV, anti-VEGF therapies have become the treatment of choice.

Heier JS, Brown D, Ciulla T, et al. Ranibizumab for choroidal neovascularization secondary to causes other than age-related macular degeneration: a phase I clinical trial. *Ophthalmology*. 2011;118(1):111–118.

Kang HM, Koh HJ. Intravitreal anti-vascular endothelial growth factor therapy versus photodynamic therapy for idiopathic choroidal neovascularization. *Am J Ophthalmol*. 2013; 155(4):713–719.

Table 4-5 Conditions Associated with Choroidal Neovascularization

Degenerative	Tumor
Age-related macular degeneration	Choroidal nevus
Myopic degeneration	Choroidal hemangioma
Angioid streaks	Metastatic choroidal tumors
Heredodegenerative	Hamartoma of the RPE
Vitelliform maculopathy	Traumatic
Fundus flavimaculatus	Choroidal rupture
Optic nerve head drusen	Intense photocoagulation
Inflammatory	Idiopathic
Ocular histoplasmosis syndrome	
Multifocal choroiditis	
Serpiginous-like choroiditis (also called <i>multifocal serpiginoid choroiditis</i>)	
Toxoplasmosis	
Toxocariasis	
Rubella	
Vogt-Koyanagi-Harada syndrome	
Behçet disease	
Sympathetic ophthalmia	

RPE=retinal pigment epithelium.

CHAPTER 5

Retinal Vascular Disease: Diabetic Retinopathy



This chapter includes a related activity, which can be accessed by scanning the QR code provided in the text or going to www.aao.org/bcscactivity_section12.

Diabetic retinopathy is a leading cause of vision loss worldwide among patients aged 25–74 years, especially in developed countries such as the United States. This chapter provides a foundation for the evaluation and treatment of diabetic retinopathy.

Terminology and Classification

Diabetes Terminology

The terminology used for types of diabetes mellitus has evolved over the years. The American Diabetes Association (ADA) classifies diabetes mellitus as *type 1 diabetes mellitus*, formerly known as *insulin-dependent diabetes mellitus* (IDDM), and *type 2 diabetes mellitus*, formerly known as *non-insulin-dependent diabetes mellitus* (NIDDM). Type 1 diabetes mellitus results from the destruction of pancreatic β -cells, which usually leads to absolute insulin deficiency. This process can be either idiopathic or immune-mediated. Type 2 diabetes mellitus is characterized by insulin resistance that may or may not be accompanied by insulin deficiency. The ADA also recognizes other forms of diabetes mellitus, including a genetically mediated form secondary to endocrinopathy and drug- or chemical-induced diabetes mellitus.

Diabetic Retinopathy Terminology

Diabetic retinopathy is classified according to a severity scale based upon its clinical features. In *nonproliferative diabetic retinopathy* (NPDR), intraretinal vascular changes are present but there is no development of extraretinal fibrovascular tissue; NPDR is staged across a spectrum of severity as mild, moderate, or severe. Although NPDR has been referred to as *background diabetic retinopathy*, this term is no longer recommended. The most advanced level of diabetic retinopathy, which can develop after an eye has progressed through the sequential stages of NPDR, is *proliferative diabetic retinopathy*.

(PDR). PDR is defined by the presence of retinal neovascularization resulting from diabetes-induced ischemia and is clinically staged as either early PDR or PDR with high-risk characteristics. *Diabetic macular edema* (DME), or swelling of the central retina, results from abnormal vascular permeability and can develop in patients with any severity level of diabetic retinopathy. DME is classified as *center-involved* (or *central-involved*) DME if the central 1 mm-diameter retinal subfield is thickened on optical coherence tomography (OCT); it is classified as *non-center-involved DME* if retinal thickening occurs only outside the central retinal subfield. *Clinically significant diabetic macular edema* (CSME) is an older definition for macular edema that meets certain severity criteria for size and location.

In the BCSC, study results are reported using the terminology of the particular study being described, even though such usage may not conform to current terminology.

Epidemiology of Diabetic Retinopathy

Diabetes mellitus is a growing global epidemic that is expected to affect 642 million individuals by the year 2040, leading to an associated increased prevalence of diabetic retinopathy worldwide. One-third of the global population of individuals with diabetes mellitus is estimated to have diabetic retinopathy; of that group, one-third is likely to have vision-threatening diabetic retinopathy.

An important epidemiologic finding of the Wisconsin Epidemiologic Study of Diabetic Retinopathy (WESDR) was the direct association of an increased prevalence of diabetic retinopathy with longer duration of diabetes mellitus in patients with both type 1 and type 2 diabetes mellitus. In the WESDR cohort, after 20 years of diabetes mellitus, nearly 99% of patients with type 1 and 60% with type 2 disease demonstrated some degree of diabetic retinopathy. Proliferative diabetic retinopathy was found in 50% of type 1 patients who had 20 years' duration of disease and in 25% of type 2 patients who had 25 years' duration of disease. Furthermore, 3.6% of younger-onset patients (aged <30 years at diagnosis) and 1.6% of older-onset patients (aged 30 years or older at diagnosis) were found to have a visual acuity of 20/200 or worse. Such vision loss was attributable to diabetic retinopathy in 86% of the younger-onset patients and in 33% of the older-onset group.

WESDR epidemiologic data were based largely on White populations of northern European descent and therefore are not entirely applicable to other racial groups. According to the United States Centers for Disease Control and Prevention, in 2011, the age-adjusted percentage of adults with diagnosed diabetes mellitus who reported visual impairment was 20.7% for Black participants, 17.1% for White participants, and 15.6% for Hispanic participants. Recent studies have suggested that rates of diabetic retinopathy progression and vision loss are lower in the modern era due to improvements in systemic control and treatment advances.

Centers for Disease Control and Prevention. *Diabetes Report Card 2017*. Atlanta, GA:

Centers for Disease Control and Prevention, US Dept of Health and Human Services; 2018.

- Available at www.cdc.gov/diabetes/pdfs/library/diabetesreportcard2017-508.pdf. Accessed September 4, 2020.
- International Diabetes Federation website. Diabetes: Facts and figures. Available at www.idf.org/aboutdiabetes/what-is-diabetes. Accessed September 4, 2020.
- Klein R, Lee KE, Knudtson MD, Gangnon RE, Klein BE. Changes in visual impairment prevalence by period of diagnosis of diabetes: the Wisconsin Epidemiologic Study of Diabetic Retinopathy. *Ophthalmology*. 2009;116(10):1937–1942.
- Yau JW, Rogers SL, Kawasaki R, et al; Meta-Analysis for Eye Disease (META-EYE) Study Group. Global prevalence and major risk factors of diabetic retinopathy. *Diabetes Care*. 2012;35(3):556–564.

Pathogenesis of Diabetic Retinopathy

Although the primary cause of diabetic microvascular disease remains poorly understood, exposure to hyperglycemia over an extended period results in biochemical and molecular pathway changes, including increases in inflammatory oxidative stress, advanced glycation end products, and protein kinase C pathways that ultimately cause endothelial damage and pericyte loss. Numerous hematologic abnormalities are also associated with the onset and progression of retinopathy, including increased platelet adhesion, increased erythrocyte aggregation, and defective fibrinolysis. However, the precise role of each of these abnormalities in the pathogenesis of retinopathy—individually or in combination—is not well defined.

Over time, retinal capillary changes such as basement membrane thickening and selective loss of pericytes lead to capillary occlusion and retinal nonperfusion. High-resolution imaging of the retinal vasculature, now available through OCT angiography (OCTA) and adaptive optics scanning laser ophthalmoscopy, often reveals areas of vascular remodeling even in eyes with clinically mild diabetic retinopathy. Vascular abnormalities occur in both the superficial and deeper retinal capillary plexuses. These changes worsen with increasing levels of diabetic retinopathy severity (Fig 5-1). In addition, endothelial barrier decompensation leads to serum leakage and retinal edema. In late stages of the disease, retinal neovascularization develops in response to increases in intraocular vascular endothelial growth factor (VEGF), which is produced by ischemic retinal tissue.

Antonetti DA, Klein R, Gardner TW. Diabetic retinopathy. *N Engl J Med*. 2012;366(13):1227–1239.

Recommended Diabetes Mellitus–Related Ophthalmic Examinations

In the first 5 years following diagnosis of type 1 diabetes mellitus, retinopathy is rare. In contrast, at the time of their initial diagnosis of type 2 diabetes mellitus, a larger percentage of patients already have established retinopathy and require concomitant ophthalmic examination. Because pregnancy is associated with diabetic retinopathy progression, women with diabetes mellitus who become pregnant may require more frequent retinal

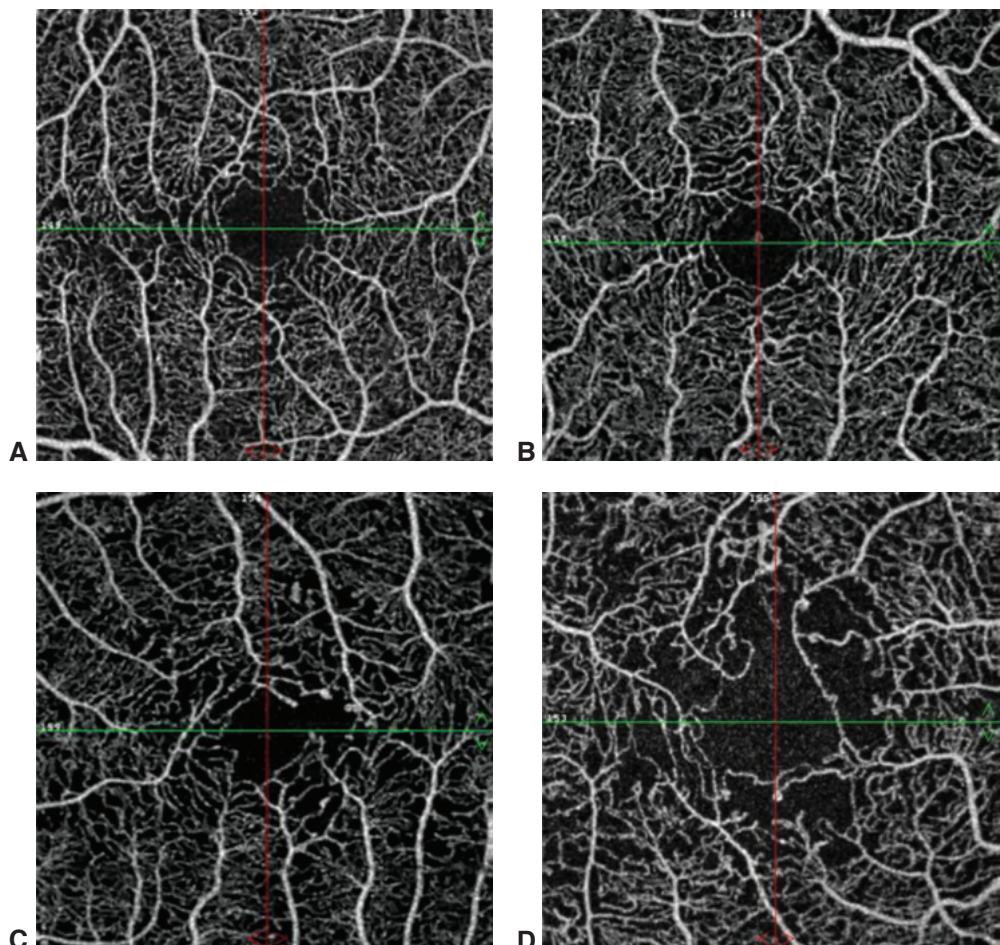


Figure 5-1 Optical coherence tomography angiography (OCTA) images demonstrate macular capillary nonperfusion and vascular tortuosity in diabetic eyes. The foveal avascular zone diameters in these images increase with worsening diabetic retinopathy severity level. **A**, Nondiabetic eye. **B**, Mild nonproliferative diabetic retinopathy (NPDR). **C**, Moderate NPDR. **D**, Proliferative diabetic retinopathy (PDR). (Courtesy of Jennifer K. Sun, MD, MPH.)

evaluations. An eye examination is recommended in the first trimester and thereafter at the discretion of the ophthalmologist for all pregnant patients with diabetic retinopathy (Table 5-1). Vision loss may occur from DME or from the complications of PDR. Although some regression of retinopathy may occur after delivery, photocoagulation treatment is generally recommended if high-risk PDR develops during or just before pregnancy. The frequency of follow-up visits depends on the severity of the retinopathy, history of blood glucose levels, and blood pressure control, as well as the threat to visual function from potentially missed opportunities to treat (Table 5-2).

American Academy of Ophthalmology Retina/Vitreous Panel. Preferred Practice® Pattern Guidelines. *Diabetic Retinopathy*. San Francisco: American Academy of Ophthalmology; 2016. Available at www.aao.org/ppp

Table 5-1 Recommended Eye Examination Schedule for Patients With Diabetes Mellitus

Diabetes Type	Recommended Time of First Eye Examination	Routine Minimum Follow-up Interval
Type 1	5 years after diagnosis	Annually
Type 2	Upon diagnosis	Annually
Type 1 or 2 and Pregnancy	Soon after conception and early in first trimester	No retinopathy to mild or moderate NPDR: every 3–12 months Severe NPDR or worse: every 1–3 months

NPDR=nonproliferative diabetic retinopathy.

Modified from American Academy of Ophthalmology Retina/Vitreous Panel. Preferred Practice Pattern® Guidelines. *Diabetic Retinopathy*. San Francisco: American Academy of Ophthalmology; 2016. Available at www.aao.org/ppp.

Table 5-2 Recommended Eye Examination Schedule Based on Diabetic Retinopathy Severity

Diabetic Retinopathy Severity	Presence of Macular Edema	Suggested Follow-up Interval (months)
Normal or minimal NPDR	No	12
Mild NPDR	No	12
	Non-CI DME	4–6
	CI DME ^a	1
Moderate NPDR	No	6–12
	Non-CI DME	3–6
	CI DME ^a	1
Severe NPDR ^b	No	4
	Non-CI DME	2–4
	CI DME ^a	1
Non-high-risk PDR ^c	No	4
	Non-CI DME	2–4
	CI DME ^a	1
High-risk PDR ^c	No	4
	Non-CI DME	4
	CI DME ^a	1
Inactive/involuted PDR	No	6–12
	Non-CI DME	4
	CI DME ^a	1

CI DME=center-involved diabetic macular edema; non-CI DME=non–center-involved diabetic macular edema; NPDR=nonproliferative diabetic retinopathy; PDR=proliferative diabetic retinopathy.

^aConsider intravitreal anti–vascular endothelial growth factor injection.

^bConsider panretinal scatter laser surgery.

^cConsider panretinal scatter laser surgery or intravitreal anti–vascular growth factor injection.

Modified from American Academy of Ophthalmology Retina/Vitreous Panel. Preferred Practice Pattern Guidelines. *Diabetic Retinopathy*. San Francisco: American Academy of Ophthalmology; 2016. Available at www.aao.org/ppp.

Systemic Medical Management of Diabetic Retinopathy

Good glycemic control is by far the most important factor in the medical management of diabetic retinopathy, as demonstrated by both the Diabetes Control and Complications Trial (DCCT; Clinical Trial 5-1) and the United Kingdom Prospective Diabetes Study (UKPDS; Clinical Trial 5-2). In these studies, intensive glycemic control was associated with a reduced risk of a new onset of retinopathy and with reduced progression of existing retinopathy in people with diabetes mellitus (type 1 in the DCCT and type 2 in the UKPDS). In addition, the DCCT demonstrated that intensive glycemic control (compared with conventional treatment) was associated with reductions in progression to severe NPDR and PDR, incidence of DME, and need for panretinal and focal photocoagulation. Even small changes in sustained hemoglobin A_{1c} (HbA_{1c}) levels were found to have a large impact on diabetic retinopathy progression. Indeed, when compared to standard glycemic control, intensive glycemic control was associated with decreases in retinopathy onset, progression of retinopathy, and need for ocular surgery over at least 2 subsequent decades, even after the DCCT study ended and the HbA_{1c} levels between

CLINICAL TRIAL 5-1

Diabetes Control and Complications Trial (DCCT)

Study questions:

1. Primary prevention study: Will intensive control of blood glucose level slow development and subsequent progression of diabetic retinopathy (neuropathy and nephropathy)?
2. Secondary intervention study: Will intensive control of blood glucose level slow progression of diabetic retinopathy (neuropathy and nephropathy)?

Enrollment:

1. 726 patients with type 1 diabetes mellitus (1–5 years' duration) and no diabetic retinopathy.
2. 715 patients with type 1 diabetes mellitus (1–15 years' duration) and mild to moderate diabetic retinopathy.

Study groups: Intensive control of blood glucose level (multiple daily insulin injections or insulin pump) vs conventional management.

Outcome variables: Development of diabetic retinopathy or progression of retinopathy by 3 steps using a modified Airlie House classification scale; neuropathy, nephropathy (albuminuria, microalbuminuria), and cardiovascular outcomes were also assessed.

Results: In the primary prevention cohort, intensive control reduced the risk of developing retinopathy by 76%, and in the secondary intervention cohort, it slowed progression of retinopathy by 54%. In the 2 cohorts combined, intensive control reduced the risk of clinical neuropathy by 60% and albuminuria (nephropathy) by 54%.

CLINICAL TRIAL 5-2

United Kingdom Prospective Diabetes Study (UKPDS)

Study questions:

1. Will intensive control of blood glucose level, in patients with type 2 diabetes mellitus, reduce the risk of microvascular complications of diabetes, including the risk of retinopathy progression?
2. Will intensive control of blood pressure, in patients with type 2 diabetes mellitus and elevated blood pressure, reduce the risk of microvascular complications of diabetes, including the risk of retinopathy progression?

Enrollment:

1. 4209 patients with newly diagnosed type 2 diabetes mellitus.
2. 1148 patients with hypertension and newly diagnosed type 2 diabetes mellitus.

Randomization:

1. Patients were randomly assigned to a conventional policy starting with diet (1138 patients) or to an intensive policy starting with a sulfonylurea—chlorpropamide (788 patients), glibenclamide (615 patients), or glipizide (170 patients) treatment—or treatment with insulin (1156 patients). If overweight and in the intensive group, patients were assigned to start treatment with metformin (342 patients).
2. Patients were randomly assigned to tight control of blood pressure (400 with angiotensin-converting enzyme [ACE] inhibitor and 398 with beta blockers) or to less tight control (390 patients).

Outcome variables: Development of any of 3 aggregate adverse outcomes and specific retinopathy-related outcomes (worsening of retinopathy on a modified Airlie House scale, retinal photocoagulation, vitreous hemorrhage, and worsening of visual acuity).

Results:

1. Intensive control of blood glucose level slowed progression of retinopathy and reduced the risk of other microvascular complications of diabetes mellitus. Sulfonylureas did not increase the risk of cardiovascular disease.
2. Intensive control of blood pressure slowed progression of retinopathy and reduced the risk of other microvascular and macrovascular complications of diabetes mellitus. No clinically or statistically significant difference was found in the comparison of blood pressure lowering with ACE inhibitors versus beta blockers.

the original randomization groups converged. This “metabolic memory” phenomenon implies sustained benefit from early intensive glycemic control. Based on the DCCT and UKPDS results, most patients with diabetes are now recommended to achieve an HbA_{1c} level of <7.0%. The Action to Control Cardiovascular Risk in Diabetes (ACCORD) trial and its follow-up (ACCORDION) study demonstrated a benefit for further reduction in HbA_{1c} levels down to <6.0% for slowed diabetic retinopathy progression in patients with type 2 diabetes mellitus; however, this intensive regimen is not generally recommended because it was also associated with greater mortality rate.

Hypertension, when poorly controlled over many years, is associated with a higher risk of progression of diabetic retinopathy and DME. The UKPDS showed that control of hypertension was also beneficial in reducing progression of retinopathy and vision loss. *Severe carotid artery occlusive disease* may result in advanced PDR as part of ocular ischemic syndrome. *Advanced diabetic nephropathy* and *anemia* may also exacerbate diabetic retinopathy. Abnormally high *lipid levels* are associated with greater risk of vision loss from DME-associated hard exudates.

- Aiello LP, Sun W, Das A, Gangaputra S, et al; DCCT/EDIC Research Group. Intensive diabetes therapy and ocular surgery in type 1 diabetes. *N Engl J Med.* 2015;372(18):1722–1733.
- Chew EY, Ambrosius WT, Davis MD, et al; ACCORD Study Group; ACCORD Eye Study Group. Effects of medical therapies on retinopathy progression in type 2 diabetes. *N Engl J Med.* 2010;363(3):233–244.
- Chew EY, Mills JL, Metzger BE, et al. Metabolic control and progression of retinopathy: The Diabetes in Early Pregnancy Study. National Institute of Child Health and Human Development Diabetes in Early Pregnancy Study. *Diabetes Care.* 1995;18(5):631–637.
- Diabetes Control and Complications Trial Research Group. Progression of retinopathy with intensive versus conventional treatment in the Diabetes Control and Complications Trial. *Ophthalmology.* 1995;102(4):647–661.
- Nathan DM, Genuth S, Lachin J, et al; Diabetes Control and Complications Trial Research Group. The effect of intensive treatment of diabetes on the development and progression of long-term complications in insulin-dependent diabetes mellitus. *N Engl J Med.* 1993; 329(14):977–986.
- UK Prospective Diabetes Study Group. Intensive blood-glucose control with sulphonylureas or insulin compared with conventional treatment and risk of complications in patients with type 2 diabetes (UKPDS 33). *Lancet.* 1998;352(9131):837–853.
- UK Prospective Diabetes Study Group. Tight blood pressure control and risk of macrovascular and microvascular complications in type 2 diabetes: UKPDS 38. *BMJ.* 1998;317(7160):703–713.

Abnormalities Associated With Vision Loss From Diabetic Retinopathy

Vision loss in patients with diabetic retinopathy is commonly associated with the following abnormalities:

- capillary leakage (DME)
- capillary occlusion (macular ischemia)
- sequelae from retinal ischemia (retinal neovascularization, vitreous hemorrhage, tractional retinal detachment, neovascular glaucoma)

Nonproliferative Diabetic Retinopathy

Retinal microvascular changes that occur in NPDR are limited to the retina and do not extend beyond the internal limiting membrane (ILM). Characteristic findings in NPDR include intraretinal hemorrhages, microaneurysms, cotton-wool spots, intraretinal microvascular abnormalities (IRMAs), and dilation and beading of retinal veins. The NPDR severity level (mild, moderate, severe) is graded based on the extent and severity of these findings as compared to standard photographs from the Early Treatment Diabetic Retinopathy Study (ETDRS). Rates of progression to more advanced disease are higher with increased baseline ETDRS retinopathy severity levels.

To help clinicians identify those patients at greatest risk of progression to PDR and high-risk PDR, the ETDRS investigators developed the 4:2:1 rule, which is largely based on results from the ETDRS Report Number 9 (Clinical Trial 5-3). A case of severe NPDR was defined as having any 1 of the following features:

- severe intraretinal hemorrhages and microaneurysms in 4 quadrants (Fig 5-2)
- definite venous beading in 2 or more quadrants (Fig 5-3)
- moderate IRMA in 1 or more quadrants (Fig 5-4)

CLINICAL TRIAL 5-3

Early Treatment Diabetic Retinopathy Study (ETDRS)

Study questions:

1. Is photocoagulation effective for treating DME?
2. Is photocoagulation effective for treating diabetic retinopathy?
3. Is aspirin effective for preventing progression of diabetic retinopathy?

Eligibility: Mild nonproliferative diabetic retinopathy through early proliferative diabetic retinopathy, with visual acuity 20/200 or better in each eye.

Randomization: 3711 participants: 1 eye randomly assigned to photocoagulation (scatter and/or focal) and 1 eye assigned to no photocoagulation; patients randomly assigned to 650 mg/day aspirin or placebo.

Outcome variables: Visual acuity less than 5/200 for at least 4 months; visual acuity worsening by doubling of initial visual angle (eg, 20/40 to 20/80); retinopathy progression.

Macular edema results:

1. Focal photocoagulation for DME decreased risk of moderate vision loss (doubling of initial visual angle).
2. Focal photocoagulation for DME increased chance of moderate vision gain (halving of initial visual angle).
3. Focal photocoagulation for DME reduced retinal thickening.

(Continued on next page)

(continued)

Early scatter photocoagulation results:

1. Early scatter photocoagulation resulted in a small reduction in the risk of severe vision loss (<5/200 for at least 4 months).
2. Early scatter photocoagulation is not indicated for eyes with mild to moderate diabetic retinopathy.
3. Early scatter photocoagulation may be most effective in patients with type 2 diabetes mellitus.

Aspirin use results:

1. Aspirin use did not alter progression of diabetic retinopathy.
2. Aspirin use did not increase risk of vitreous hemorrhage.
3. Aspirin use did not affect visual acuity.
4. Aspirin use reduced risk of cardiovascular morbidity and mortality.

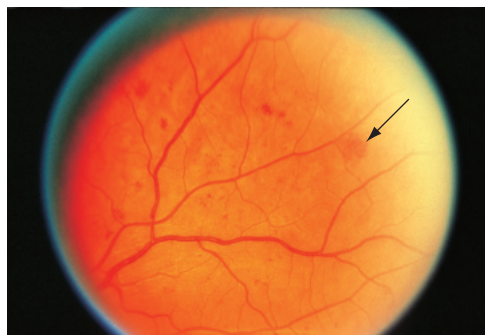
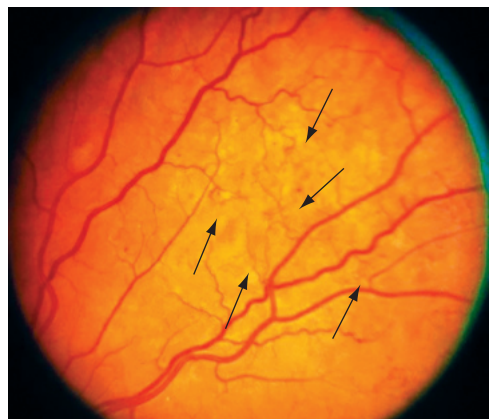
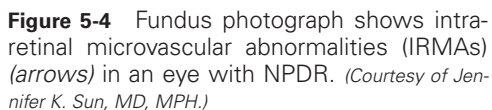


Figure 5-2 Fundus photograph shows diffuse intraretinal hemorrhages (arrow) and microaneurysms in an eye with NPDR. (Standard photograph 2A, courtesy of the Early Treatment Diabetic Study [ETDRS].)



Figure 5-3 Fundus photograph shows venous beading in an eye with NPDR (arrows). (Standard photograph 6B, courtesy of the ETDRS.)



In the ETDRS, patients with severe NPDR were found to have a 15% and 60% chance of progression to high-risk PDR within 1 and 3 years, respectively. Very severe NPDR, which was defined as having 2 or more of the features in the preceding list, increased the chance of progression to high-risk PDR within 1 year to 45%.

The ETDRS scale for classification of diabetic retinopathy severity level has been considered the gold-standard method for several decades. To employ it, clinicians need to acquire and interpret standardized photographic fields that cover approximately 90° of the posterior retina. With ultra-wide-field imaging, over 80% of the retina can now be visualized in a single 200° image. Peripheral diabetic retinopathy lesions are often present outside of the standard ETDRS fields; these suggest greater diabetic retinopathy severity in nearly 10% of eyes. Preliminary studies suggest that predominantly peripheral diabetic retinopathy lesions may be associated with greater risk of subsequent diabetic retinopathy progression. This association is being evaluated in the ongoing Diabetic Retinopathy Clinical Research Network (DRCR.net) Protocol AA.

Retinal capillary nonperfusion is a common finding in diabetic retinopathy, especially in more advanced levels of severity. Closure of retinal arterioles may result in larger areas of nonperfusion and progressive ischemia. The foveal avascular zone may appear increasingly irregular on fluorescein angiography (FA) or OCTA and enlarged as the innermost capillaries become nonperfused. Peripheral nonperfusion is frequently seen on ultra-wide-field FA, even in eyes with mild NPDR.

Patients with NPDR can lose visual function through 2 mechanisms: (1) increased intraretinal vascular permeability, resulting in macular edema (see the section Diabetic Macular Edema, later in this chapter), and (2) variable degrees of intraretinal capillary closure, resulting in macular ischemia.

Early Treatment Diabetic Retinopathy Study Research Group. Early photocoagulation for diabetic retinopathy. ETDRS report number 9. *Ophthalmology*. 1991;98(5 Suppl): 766–785.

Early Treatment Diabetic Retinopathy Study Research Group. Grading diabetic retinopathy from stereoscopic color fundus photographs—an extension of the modified Airlie House classification. ETDRS report number 10. *Ophthalmology*. 1991;98(5 Suppl): 786–806.

Silva PS, Cavallerano JD, Haddad NM, et al. Peripheral lesions identified on ultrawide field imaging predict increased risk of diabetic retinopathy progression over 4 years. *Ophthalmology*. 2015;122(5):949–956.

Treatment of Nonproliferative Diabetic Retinopathy

Aside from systemic control of blood glucose, lipids, and hypertension, there is no clear treatment mandate for eyes with NPDR without DME. Early treatment with panretinal photocoagulation should be considered for patients with severe NPDR or worse, especially if the patient has type 2 diabetes or is likely to be nonadherent to recommendations for follow-up or systemic control. In addition, anti-VEGF therapy given for DME has been shown to substantially improve diabetic retinopathy severity in eyes at all severity levels of NPDR. After 2 years of continuous, monthly treatment with an anti-VEGF drug, nearly

40% of eyes will improve by 2 or more levels on the ETDRS diabetic retinopathy severity scale. Although ranibizumab is FDA-approved for use in diabetic retinopathy, including NPDR without DME, large-scale randomized controlled trials to evaluate the efficacy and safety of anti-VEGF treatments in eyes with moderate to severe NPDR without DME are currently ongoing.

Intravitreal steroid therapy for DME has also been shown to improve diabetic retinopathy severity level. The ACCORD and Fenofibrate Intervention and Event Lowering in Diabetes (FIELD) studies demonstrated reductions in diabetic retinopathy progression after fenofibrate treatment in patients with type 2 diabetes through mechanisms that are likely independent of fenofibrate's effects on blood lipid levels. Finally, it has been hypothesized that creation of a posterior vitreous detachment might improve outcomes in diabetic eyes at risk of developing PDR because the vitreous scaffolding that enables extraretinal neovascular proliferation is removed. However, currently there is no role for surgery in the management of NPDR.

ACCORD Study Group; ACCORD Eye Study Group, Chew EY, Ambrosius WT, Davis MD, et al. Effects of medical therapies on retinopathy progression in type 2 diabetes. *N Engl J Med.* 2010;363(3):233–244.

Bressler SB, Qin H, Melia M, et al; Diabetic Retinopathy Clinical Research Network.

Exploratory analysis of the effect of intravitreal ranibizumab or triamcinolone on worsening of diabetic retinopathy in a randomized clinical trial. *JAMA Ophthalmol.* 2013;131(8):1033–1040.

Ferris F. Early photocoagulation in patients with either type I or type II diabetes. *Trans Am Ophthalmol Soc.* 1996;94:505–537.

Ip MS, Domalpally A, Sun JK, Ehrlich JS. Long-term effects of therapy with ranibizumab on diabetic retinopathy severity and baseline risk factors for worsening retinopathy. *Ophthalmology.* 2015;122(2):367–374.

Proliferative Diabetic Retinopathy

As retinopathy progresses, capillary damage and nonperfusion increase. Worsening retinal ischemia leads to release of vasoproliferative factors and the subsequent development of retinal neovascularization. VEGF is 1 of the major proangiogenic factors isolated from the vitreous of patients with PDR. This factor can stimulate neovascularization of the retina, optic nerve head, or anterior segment.

Extraretinal fibrovascular proliferation, which defines PDR, progresses through 3 stages:

1. Fine new vessels with minimal fibrous tissue cross and extend beyond the ILM, often using the posterior hyaloid as a scaffold.
2. The new vessels increase in size and extent, developing an increased fibrous component.
3. The new vessels regress, leaving residual fibrovascular tissue that may be tethered within the posterior hyaloid.

Neovascular proliferation is categorized by its location: either on or within a disc diameter of the disc (NVD, neovascularization of the disc) or elsewhere (NVE, neovascularization elsewhere).

Patients may receive treatment at any stage of PDR; however, treatment is usually considered mandatory once an eye has developed high-risk characteristics. PDR with high-risk characteristics is defined as having any of the following findings:

- any NVD with vitreous or preretinal hemorrhage
- extent of NVD *greater than or equal to* one-fourth disc area, with or without vitreous or preretinal hemorrhage (\geq ETDRS standard photograph 10A) (Fig 5-5)
- extent of NVE *greater than or equal to* one-half disc area, with vitreous or preretinal hemorrhage (Fig 5-6)

Treatment may be deferred in eyes that have not developed high-risk characteristics or in eyes that have peripheral neovascularization outside the 7 standard ETDRS fields without accompanying hemorrhage; these cases can be watched closely until the PDR worsens. However, eyes at especially high risk for diabetic retinopathy progression due to patient nonadherence or poor systemic control should be treated promptly.

Management of Proliferative Diabetic Retinopathy and Its Complications

The goal of management of PDR is to control ischemia and reduce ocular VEGF levels so that neovascularization can involute or regress. This management can be accomplished with intravitreal administration of anti-VEGF drugs or with ablation of ischemic retina via laser photocoagulation. Because of the contraction of fibrovascular tissue, treatment may be followed by increased vitreoretinal traction, recurring vitreous hemorrhage, tractional retinal detachment, and/or combined tractional and rhegmatogenous retinal detachment. Complications from PDR or its treatment—vitreous hemorrhage and tractional retinal detachment—can be addressed with vitreoretinal surgical interventions, when appropriate.

Nonsurgical management of proliferative diabetic retinopathy

Anti-VEGF and steroid drugs Multiple studies, including phase 3 trials of anti-VEGF drugs for the treatment of DME, have demonstrated that intravitreal administration (see the

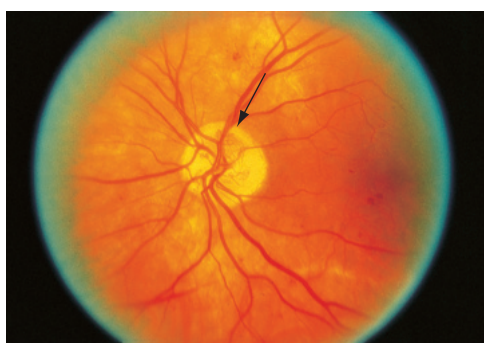


Figure 5-5 Fundus photograph of a left eye demonstrates neovascularization of the disc (NVD, arrow) with a small amount of vitreous hemorrhage. Even without vitreous hemorrhage, this degree of NVD is the lower limit of moderate NVD and is considered high-risk PDR. (Standard photograph 10A, courtesy of the Diabetic Retinopathy Study [DRS].)

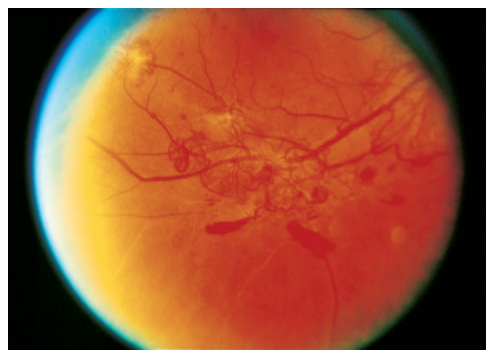


Figure 5-6 Fundus photograph of a right eye shows cotton-wool spots and moderate neovascularization elsewhere (NVE) with preretinal hemorrhage. (Standard photograph 7, courtesy of the DRS.)

section Intravitreal Injections in Chapter 20 of this volume for a discussion of the injection procedure) of anti-VEGF drugs is highly effective at regressing retinal neovascularization in eyes with PDR. Anti-VEGF therapy leads to regression of diabetic neovascular complexes in both newly diagnosed cases and chronic, refractory disease. Potential complications from the use of anti-VEGF drugs in the management of PDR include tractional retinal detachments, retinal tears, and combined tractional and rhegmatogenous retinal detachments that are related to the induced rapid contracture of the fibrovascular tissue.

Because of its effectiveness in regressing intraocular neovascularization and its generally favorable safety profile, anti-VEGF therapy is a reasonable first-line treatment alternative to panretinal photocoagulation (PRP) for many eyes with PDR. The DRCR.net Protocol S study randomized eyes with active PDR to treatment with either standard-care prompt PRP or intravitreal ranibizumab and deferred PRP. At 2 years, visual outcomes were equivalent between the PRP and anti-VEGF treated groups. However, ranibizumab treatment was associated with multiple benefits over PRP, including better average vision over the 2 years, reductions in peripheral visual field loss, reduced rates of vitrectomy surgery, and fewer cases of DME onset. Ranibizumab was well tolerated; no substantial differences in rates of major cardiovascular adverse events were found between the treatment groups. Longer-term follow-up through the full 5-year study duration will determine whether anti-VEGF treatment burden decreases over time and whether the anti-VEGF effect endures after treatments are halted. (For more on DRCR.net studies, see the sidebar Selected Diabetic Retinopathy Clinical Research Network Studies at the end of this chapter.)

Although ranibizumab is effective for PDR treatment and offers some advantages over PRP, whether to use anti-VEGF versus PRP should be based on individual patient circumstances. Patients receiving anti-VEGF need to be able to adhere to near monthly follow-up visits throughout the first 1–2 years of treatment. For patients who have a high likelihood of nonadherence due to medical instability or other limitations, treatment with PRP is the most appropriate option.

Anti-VEGF drugs also cause involution of anterior segment neovascularization and have been successfully used to treat neovascular glaucoma. In addition, when administered preoperatively, these drugs may be helpful as an adjunct to vitrectomy to manage complications of PDR.

Although steroid agents are not used for primary treatment of PDR, they do reduce PDR-related outcomes in diabetic eyes. Combined rates of vitreous hemorrhage, need for PRP, and development of neovascularization, as viewed on fundus photographs or during a clinical examination, are reduced in eyes receiving intravitreal steroid therapy for non-PDR indications, such as DME.

Surgical management of proliferative diabetic retinopathy

Laser surgery Over the past 4 decades, until the recent advent of anti-VEGF therapy, the mainstay of treatment for PDR was thermal laser photocoagulation in a panretinal pattern to induce regression of neovascularization. Treatment indications are still largely based on findings from the Diabetic Retinopathy Study (DRS) (Clinical Trial 5-4). For patients with high-risk PDR, PRP treatment in eyes not already receiving anti-VEGF therapy is almost always recommended. PRP destroys ischemic retina, which produces growth factors, such as VEGF, that promote disease progression. PRP also increases oxygen tension in the eye via 2 mechanisms: (1) decreasing oxygen consumption overall as a result of the purposeful

CLINICAL TRIAL 5-4

Diabetic Retinopathy Study (DRS)

Study question: Is photocoagulation (argon or xenon arc) effective for treating diabetic retinopathy?

Eligibility: PDR or bilateral severe NPDR, with visual acuity 20/100 or better in each eye.

Randomization: 1742 participants: 1 eye randomly assigned to photocoagulation (argon or xenon arc) and 1 eye assigned to no photocoagulation.

Outcome variable: Severe vision loss (SVL), ie, visual acuity less than 5/200 for at least 4 months, at 5 years.

Results: At 5 years of follow-up, eyes treated with PRP had a reduction of 50% or more in rates of SVL compared with untreated control eyes. Thus, photocoagulation (argon or xenon) reduces risk of SVL compared with no treatment. Treated eyes with high-risk PDR achieved the greatest benefit (Fig 5-7). Complications of argon laser PRP in the DRS were generally mild but included a decrease in visual acuity by 1 or more lines in 11% and visual field loss in 5%.

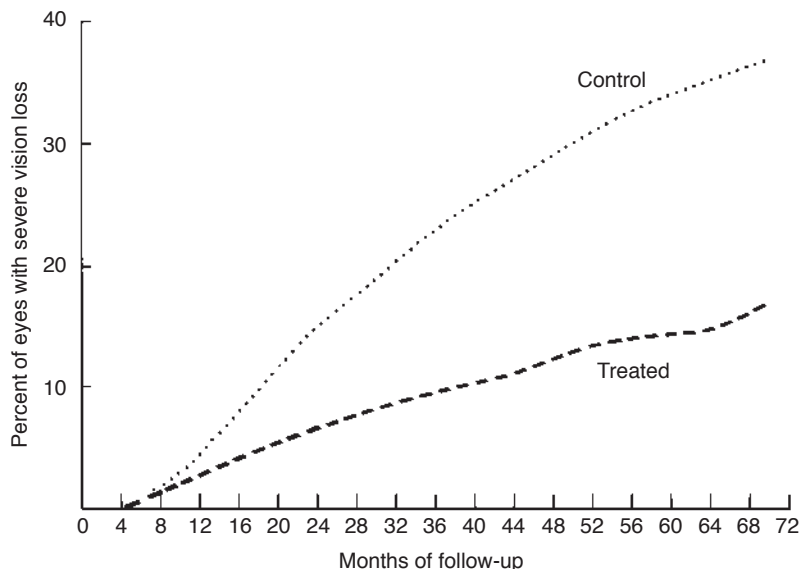


Figure 5-7 Comparison of treated versus control groups in the Diabetic Retinopathy Study shows cumulative percentage of eyes that experienced severe vision loss during the period of follow-up for argon laser and xenon arc treatment groups combined. (From Diabetic Retinopathy Study Research Group (DRS). Photocoagulation treatment of proliferative diabetic retinopathy. Clinical application of DRS findings. DRS report number 8. Ophthalmology. 1981;88(7):583–600.)

retinal destruction, and (2) increasing the diffusion of oxygen from the choroid in the areas of the photocoagulation scars. Collectively, these changes result in the regression of existing neovascular tissue and prevent progressive neovascularization.

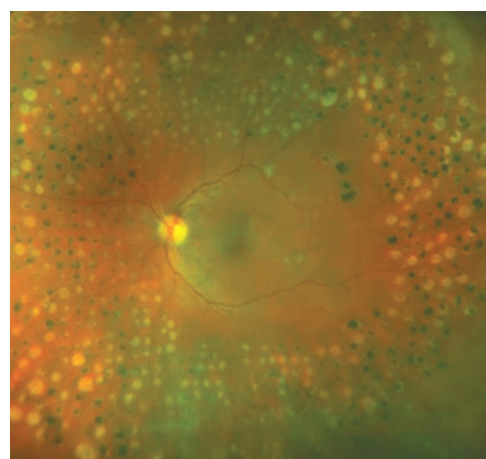
Treatment may be accomplished in a single session or over multiple sessions. The DRCR.net found no long-term vision benefit of multiple-session over single-session laser administration. After the initial PRP, additional therapy can be applied incrementally in an attempt to achieve complete regression of persistent or recurrent neovascularization. Some clinicians combine anti-VEGF therapy with PRP with the rationale that initial anti-VEGF therapy will regress neovascularization quickly, whereas the effect of the PRP will endure over subsequent years, without the need for long-term intravitreal injections.

Full PRP, as used in the DRS (see Clinical Trial 5-4) and ETDRS (see Clinical Trial 5-3), included 1200 or more 500- μm burns using argon green or blue-green lasers, separated from each other by one-half burn width (Fig 5-8). The use of automated pattern scan laser systems has been increasing in recent years; however, uncontrolled studies have suggested that pattern scan laser treatments may not be equivalent in their treatment effect on a burn-for-burn comparison; the burn-count target for equivalent treatment effect with pattern scan laser treatment may need to be higher.

Adverse effects of scatter PRP include choroidal detachment as well as decreases in night vision, color vision, contrast sensitivity, peripheral vision, and, in rare cases, pupillary dilation. Some patients may experience a transient loss of 1 or 2 lines of visual acuity or increased glare following treatment. Other transient adverse effects include loss of accommodation, loss of corneal sensitivity, and photopsias. Macular edema may also be precipitated or worsened by PRP. Sparing the horizontal meridians, that is, the path of the long ciliary vessels and nerves, protects accommodation pupillary function and corneal innervation. Heavy treatment, when necessary, should be performed in areas of the retina where vision loss is less noticed by patients or in areas that are associated with lower rates of morbidity. Great care must be taken to avoid foveal photocoagulation, especially when using image-inverting lenses.

Aiello LP, Avery RL, Arrigg PG, et al. Vascular endothelial growth factor in ocular fluid of patients with diabetic retinopathy and other retinal disorders. *N Engl J Med.* 1994;331(22):1480–1487.

Figure 5-8 Fundus photograph shows an eye that has undergone panretinal photocoagulation (PRP) treatment. Laser scars are characterized by either chorioretinal and retinal pigment epithelium (RPE) atrophy or RPE hyperpigmentation. (Courtesy of Jennifer K. Sun, MD, MPH.)



- Chew EY, Ferris FL III, Csaky KG, et al. The long-term effects of laser photocoagulation treatment in patients with diabetic retinopathy: the early treatment diabetic retinopathy follow-up study. *Ophthalmology*. 2003; 110(9):1683–1689.
- Diabetic Retinopathy Study Research Group. Photocoagulation treatment of proliferative diabetic retinopathy. Clinical application of Diabetic Retinopathy Study (DRS) findings, DRS report number 8. *Ophthalmology*. 1981;88(7):583–600.
- Gross JG, Glassman AR, Jampol LM, et al; Writing Committee for the Diabetic Retinopathy Clinical Research Network. Panretinal photocoagulation vs intravitreous ranibizumab for proliferative diabetic retinopathy: a randomized clinical trial. *JAMA*. 2015;314(20): 2137–2146.
- Silva PS, Cavallerano JD, Sun JK, et al. Proliferative diabetic retinopathy. In: Schachat AP, Wilkinson CP, Hinton DR, Sadda SR, Wiedemann P, eds. *Ryan's Retina*. 6th ed. Philadelphia: Elsevier/Saunders; 2018:1091–1121.

Management of neovascularization of the iris or anterior chamber angle

Small, isolated tufts of neovascularization at the pupillary border are relatively common in eyes of patients with diabetes mellitus. Treatment can be withheld in eyes with these tufts in favor of careful monitoring, with relatively short intervals between slit-lamp and gonioscopic examinations. Treatment should be considered for eyes that have contiguous neovascularization of the pupil and iris collarette, with or without inclusion of the anterior chamber angle, and if wide-field FA reveals widespread nonperfusion or peripheral neovascularization. Treatment usually consists of PRP; intravitreal injection of anti-VEGF drugs can be used as a temporizing measure to reduce neovascularization until definitive PRP is administered.

Vitrectomy surgery for complications of diabetic retinopathy

Indications for pars plana vitrectomy in patients with PDR are

- nonclearing vitreous hemorrhage
- significant recurring vitreous hemorrhage, despite use of maximal PRP
- dense premacular subhyaloid hemorrhage
- tractional retinal detachment involving or threatening the macula
- combined tractional and rhegmatogenous retinal detachment
- red blood cell-induced (erythroclastic) glaucoma and “ghost cell” glaucoma
- anterior segment neovascularization with media opacities preventing PRP

Vitreous hemorrhage

The Diabetic Retinopathy Vitrectomy Study (DRVS) was an early prospective, randomized clinical trial that investigated the role of vitrectomy in the management of eyes with severe PDR. Benefits of early (1–6 months after onset of vitreous hemorrhage) versus late (1 year after onset) vitrectomy were evaluated. Eyes of patients with type 1 diabetes mellitus and severe vitreous hemorrhage clearly demonstrated a benefit from earlier vitrectomy, whereas eyes of patients with type 2 or mixed diabetes did not.

If PRP has not been performed previously, earlier intervention is usually recommended. Patients with previous, well-placed, complete PRP who have vitreous hemorrhage secondary to PDR may be observed for a longer period prior to initiating intervention. Frequent echography (ultrasound) studies are necessary to monitor for retinal detachment in

patients with dense, nonclearing vitreous hemorrhages. If a retinal detachment is discovered, the timing for the vitrectomy depends upon the characteristics of the detachment. Patients with bilateral severe vitreous hemorrhage should undergo vitrectomy in 1 eye as soon as possible for vision rehabilitation. Recent advances in vitreoretinal surgery, including smaller-gauge instrumentation facilitating faster operating times and fewer complications, have led to earlier intervention for nonclearing vitreous hemorrhage.

Recchia FM, Scott IU, Brown GC, Brown MM, Ho AC, Ip MS. Small-gauge pars plana vitrectomy: a report by the American Academy of Ophthalmology. *Ophthalmology*. 2010; 117(9):1851–1857.

Simunovic MP, Maberley DA. Anti-vascular endothelial growth factor therapy for proliferative diabetic retinopathy: a systematic review and meta-analysis. *Retina*. 2015;35(10): 1931–1942.

Tractional retinal detachment

Complications from PDR may be exacerbated by vitreous attachment to and traction on fibrovascular proliferative tissue, often causing secondary tractional retinal detachments. Partial posterior vitreous detachment frequently develops in eyes with fibrovascular proliferation, resulting in traction on the new vessels and vitreous or preretinal hemorrhage. Tractional complications such as vitreous hemorrhage, retinal schisis, retinal detachment, or macular heterotopia may ensue, as well as progressive fibrovascular proliferation. Contraction of the fibrovascular proliferation and vitreous may result in retinal breaks and subsequent combined tractional and rhegmatogenous retinal detachment. The presence of chronic retinal detachment in eyes with PDR contributes to retinal ischemia and may account for the increased risk of anterior segment neovascularization in such eyes.

Tractional retinal detachment that does not involve the macula may remain stable for many years. When the macula becomes involved or is threatened, prompt vitrectomy is generally recommended. Combined tractional and rhegmatogenous retinal detachment may progress rapidly; urgent surgery should be considered for these patients.

A more extensive discussion of the surgical management of tractional retinal detachments secondary to PDR appears in the section Vitrectomy for Complications of Diabetic Retinopathy in Chapter 20 of this volume.

Diabetic Macular Edema

DME results from a hyperglycemia-induced breakdown of the blood–retina barrier, which leads to fluid extravasation from retinal vessels into the surrounding neural retina (Fig 5-9). A diagnosis of DME is made when retinal thickening that involves the macula is present. DME may be associated with hard exudates, which are precipitates of plasma lipoproteins. Central subfield–involved DME that affects the fovea is a common cause of vision loss in diabetic patients. In contrast, non–center-involved DME is unlikely to affect vision unless it progresses to center involvement. Although DME is increasingly common among eyes with more advanced diabetic retinopathy, DME can be present in any severity level of diabetic retinopathy. Even eyes with mild NPDR can have substantial vision loss from highly thickened retinas.

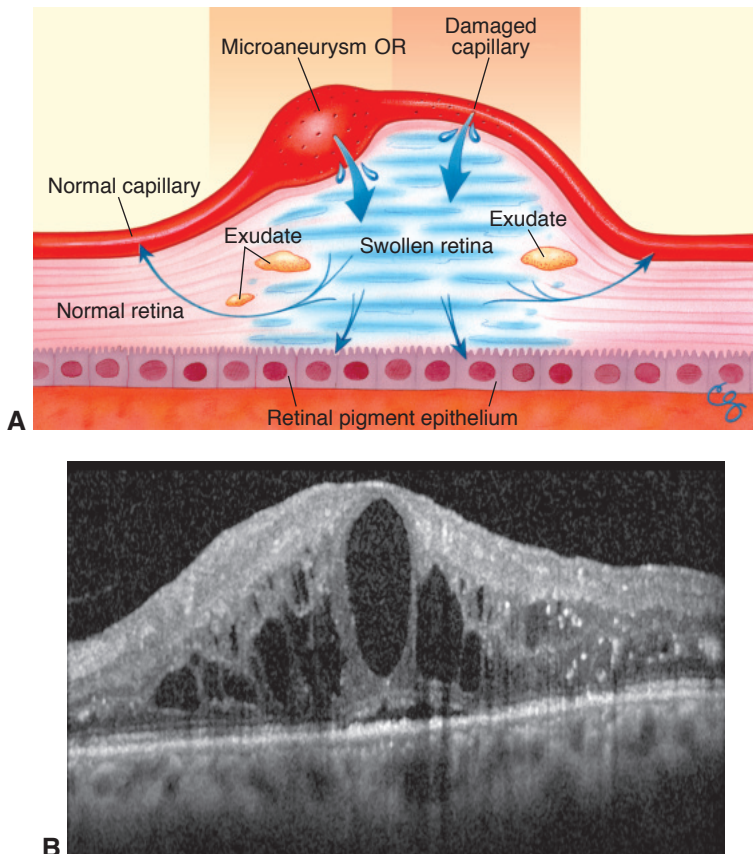


Figure 5-9 Diabetic macular edema (DME). **A**, Artist's rendering of the mechanism of DME, demonstrating development of retinal thickening from a breakdown of the blood–retina barrier. **B**, Spectral-domain OCT (SD-OCT) scan of DME. Whereas there are extensive cystic changes in the outer plexiform and outer nuclear layers, the external limiting membrane line appears intact across the extent of the scan, with the exception of shadowing artifacts from more superficial hyperreflective lesions. Note the foveal detachment. (Part A from Ginsburg LH, Aiello LM. *Diabetic retinopathy: classification, progression, and management*. Focal Points: Clinical Modules for Ophthalmologists. San Francisco: American Academy of Ophthalmology; 1993, module 7. Illustration by Christine Gralapp. Part B courtesy of Colin A. McCannel, MD.)

FA is useful in demonstrating the breakdown of the blood–retina barrier by showing local areas of retinal capillary leakage. However, leakage shown on the angiogram may occur in the absence of macular retinal thickening and is thus not considered macular edema. Examination with OCT or slit-lamp biomicroscopy are the most appropriate methods to evaluate eyes for the presence or absence of macular thickening.

Classification of Diabetic Macular Edema

Current algorithms for pharmacologic intervention in DME use a simple, OCT-based definition to classify DME as *center-involved* or *non-center-involved*. In *center-involved* DME, the central retinal subfield appears thickened on OCT scans. DME that does not affect the central subfield is termed *non-center-involved* (Fig 5-10; Activity 5-1).

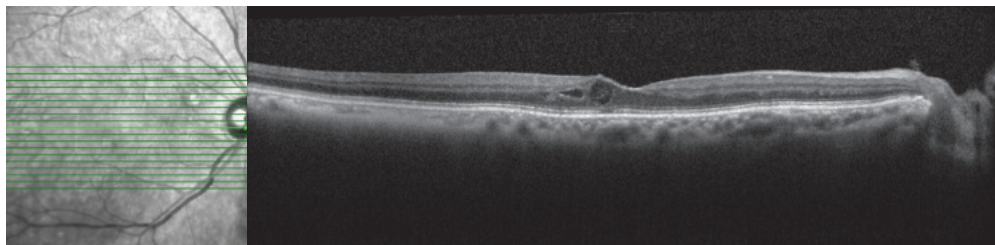


Figure 5-10 OCT volume scan of an eye with DME from a 75-year-old Hispanic male patient with a long history of poorly controlled type 2 diabetes mellitus (A_{1C} levels typically in the 9–9.6 range). The right eye is affected with moderate NPDR. The patient has undergone previous treatment with bevacizumab and afibbercept, but there is persistent center-involved DME. The cystic changes involving the temporal and inferior foveal region are most noticeable in slices 10 through 7 in Activity 5-1. (Courtesy of Colin A. McCannel, MD.)



ACTIVITY 5-1 OCT Activity: OCT of diabetic macular edema.

Courtesy of Colin A. McCannel, MD.

Access all Section 12 activities at www.aao.org/bcscactivity_section12.



The ETDRS was the first prospective, randomized clinical trial of photocoagulation in diabetic patients with less than high-risk PDR in order to establish standard treatment paradigms for managing DME (see Clinical Trial 5-3). It defined *clinically significant diabetic macular edema* (CSME) as the indication for focal laser photocoagulation treatment in the following settings:

- retinal thickening located at or within 500 μm of the center of the macula
- hard exudates at or within 500 μm of the center if associated with thickening of adjacent retina
- a zone of thickening larger than 1 disc area, if located within 1 disc diameter of the center of the macula

CSME is an older term that predates diagnoses made with OCT technology. Now that anti-VEGF treatment has supplanted macular laser photocoagulation as the first-line therapy for DME, the CSME diagnosis, which is made clinically, is much less frequently used.

Regardless of whether it is center-involved or non-center-involved, DME may manifest as focal or diffuse retinal thickening. *Focal macular edema* is characterized by areas of local fluorescein leakage from specific capillary lesions, such as microaneurysms (Fig 5-11A). *Diffuse macular edema* is characterized by extensive retinal capillary leakage and widespread breakdown of the blood–retina barrier, often accumulating in a cystoid configuration in the perifoveal macula (cystoid macular edema) (Fig 5-11B). Studies have not demonstrated any difference in treatment response corresponding to the pattern of macular edema, whether focal, diffuse, or a combination of these.

Treatment of Diabetic Macular Edema

In parallel with medical management and optimizing the health habits of the patient, ocular therapies should be considered to maximize visual function and prevent progressive vision loss. These therapies include ocular pharmacologic management and laser photocoagulation treatment. Treatment is typically indicated when the macular edema is center-involved and affects visual acuity. For patients with DME who are asymptomatic

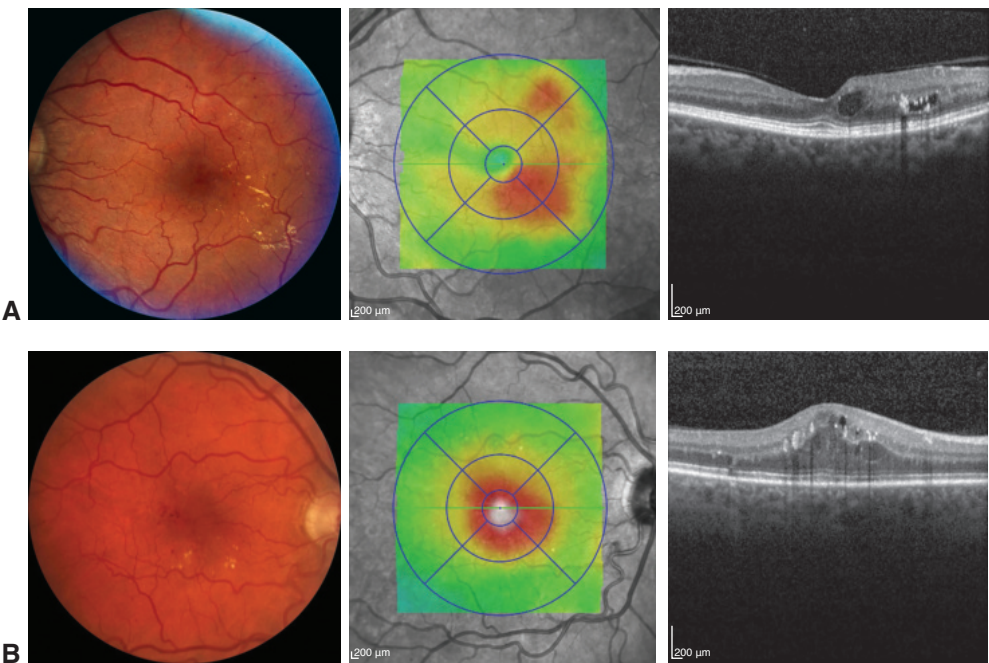


Figure 5-11 Imaging of eyes with DME on fundus photography and OCT. **A**, Eye with non-center-involved DME. **B**, Eye with center-involved DME. (Courtesy of Jennifer K. Sun, MD, MPH.)

or have normal visual acuity, the decision-making process for treatment is more complex. Factors that should be considered include the proximity of exudates or thickening to the fovea, the status and course of the fellow eye, any anticipated cataract surgery, the presence of high-risk PDR, treatment risks, and any systemic conditions or medications (such as thiazolidinediones) that might exacerbate or cause DME. It is preferable to initiate DME treatment before performing scatter photocoagulation and prior to cataract surgery to reduce the risk of DME resulting from these interventions.

Ocular pharmacologic management of diabetic macular edema

As mentioned, anti-VEGF drugs are now the first-line therapy for most eyes with center-involved DME, especially those with vision impairment caused by the DME. Corticosteroids are also useful as alternative agents for eyes that are not candidates for anti-VEGF therapy or that were incompletely responsive to previous anti-VEGF treatment.

Anti-VEGF drugs Currently available anti-VEGF drugs include aflibercept, bevacizumab, pegaptanib, and ranibizumab. Clinical trials have demonstrated that all of these medications are beneficial for eyes with DME. The DRCR.net Protocol I was the first phase 3 trial to demonstrate that intravitreal anti-VEGF therapy provides superior visual acuity outcomes as compared to laser treatment for center-involved DME. This study revealed that intravitreal ranibizumab combined with prompt or deferred (≥ 24 weeks) focal or grid-pattern laser treatment was more effective at both 1- and 2-year follow-up in increasing visual acuity than was focal/grid laser treatment alone or in combination with triamcinolone acetonide injections for the treatment of center-involved DME. After 1 year of treatment, eyes in the ranibizumab-treated groups gained on average 8–9 letters of visual acuity versus those in the laser monotherapy group, which gained an average of only 3 letters. Through

5 total years of follow-up, despite the number of injections given progressively decreasing, eyes in the ranibizumab treatment groups maintained the vision gains accrued in the first year of therapy (Fig 5-12). Results from this study also suggest that adding focal- or grid-pattern laser treatment at the initiation of intravitreal ranibizumab for DME is no better, and is possibly worse, for vision outcomes than deferring laser treatment for 24 weeks or more. Two additional parallel phase 3 trials, RISE and RIDE (identical study designs, both titled Ranibizumab Injection in Subjects With CSME With Center Involvement Secondary to Diabetes Mellitus) indicated that ranibizumab rapidly and sustainably improves vision, reduces the risk of further vision loss, and improves macular edema in patients with DME, with low rates of complications. At 36 months, the pooled data of these studies showed that the proportion of patients who gained 15 or more letters of visual acuity from baseline in the 0.3 mg and 0.5 mg ranibizumab-treated groups were 41% and 44%, respectively.

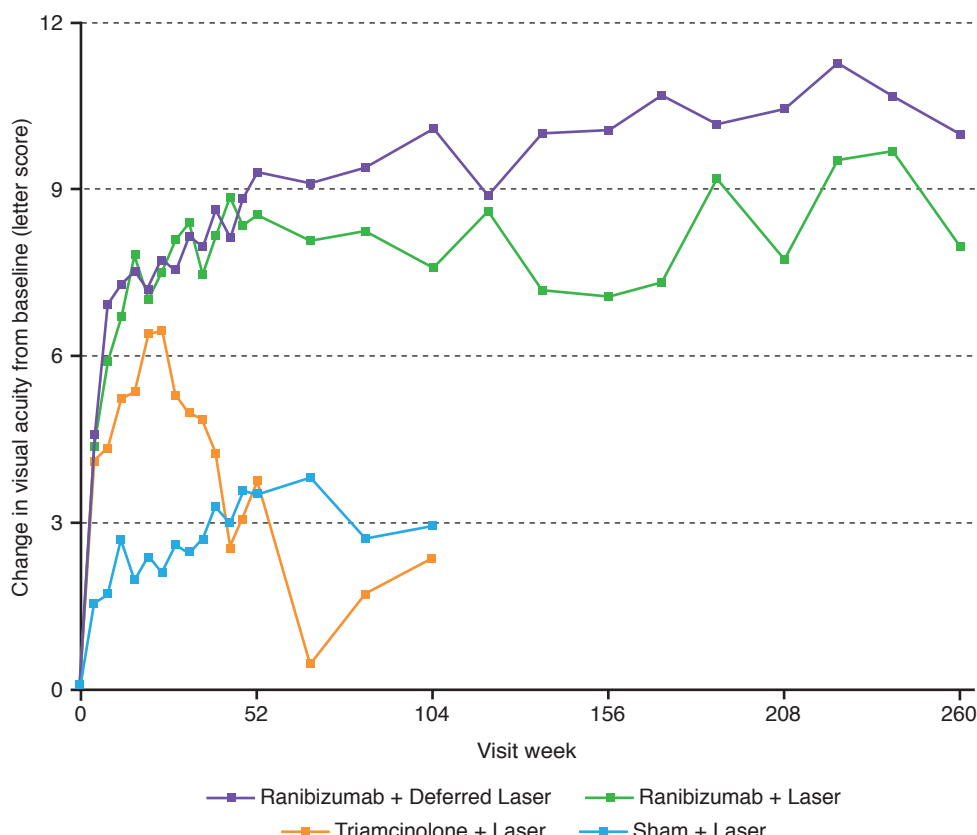


Figure 5-12 Results of the Diabetic Retinopathy Clinical Research Network (DRCR.net) Protocol I through 3 years demonstrating the superior visual acuity outcomes of treatment with ranibizumab, with either prompt or deferred laser treatment, compared with laser alone or in combination with triamcinolone through 2 years. Starting in the third year, only patients originally assigned to the ranibizumab groups were followed up. Results from years 3–5 suggest that treatment with ranibizumab plus prompt laser therapy is no better and is possibly worse than ranibizumab with deferred laser treatment. (From Diabetic Retinopathy Clinical Research Network, Elman MJ, Qin H, Aiello LP, et al. Intravitreal ranibizumab for diabetic macular edema with prompt versus deferred laser treatment: three-year randomized trial results. Ophthalmology. 2012;119(11):2312–2318.)

Phase 3 trials have also demonstrated excellent efficacy of aflibercept treatment for DME. After an initial phase of 5 monthly injections, after 148 weeks, groups undergoing therapy with aflibercept, both monthly and every 2 months, had substantial visual acuity gains compared with laser photocoagulation in both the VIVID (Intravitreal Aflibercept Injection in Vision Impairment Due to DME) and VISTA (Study of Intravitreal Aflibercept Injection in Patients With Diabetic Macular Edema) trials.

Although all of the available anti-VEGF agents are effective in the treatment of DME, results from the DRCR.net Protocol T study, which compared the effectiveness of aflibercept, bevacizumab, and ranibizumab for the treatment of DME, demonstrated the superiority of aflibercept over bevacizumab in improving ETDRS visual acuity gains after both 1 and 2 years of treatment. Aflibercept was also superior to ranibizumab at 1 year follow-up, but statistically similar at 2 years. The differences between the agents were due primarily to the effects of these agents in eyes with worse ($\leq 20/50$) baseline vision. In eyes with milder visual impairment (20/32 to 20/40), visual results were equivalent at both 1 and 2 years for all 3 treatment groups. At 2 years, rates of 10 or more letter visual acuity improvement in the aflibercept, bevacizumab, and ranibizumab groups were 50%, 41%, and 46%, respectively. In contrast, in eyes with worse visual impairment, 2-year rates of 10 or more letter improvement for the aflibercept, bevacizumab, and ranibizumab groups were 76%, 66%, and 71%, respectively. Rates of substantial vision loss were low in all 3 treatment groups.

In general, anti-VEGF agents are well tolerated. Associated adverse events are most commonly due to the intravitreal injection procedure rather than the medication. Serious intraocular events such as endophthalmitis are rare, with a prevalence of approximately 1 in 1000 injections. Systemic thromboembolic events are known to be associated with systemic anti-VEGF administration, but have not been shown to be more common among patients who receive intraocular anti-VEGF treatment. Combined rates of nonfatal myocardial infarction, nonfatal stroke, and vascular death were higher in the Protocol T patients treated with ranibizumab than the patients treated with the other 2 agents, but extensive analyses of adverse events across other studies have not demonstrated consistent differences in intraocular or systemic safety between the anti-VEGF agents.

Corticosteroids Use of intravitreal triamcinolone acetonide in patients with refractory DME has been reported to have beneficial effects in a number of small studies. However, at 2 years into the DRCR.net Protocol B trial, treatment with focal- or grid-pattern photocoagulation was found to be more effective, with fewer adverse effects, than treatment with 1-mg or 4-mg doses of preservative-free intravitreal triamcinolone. DRCR.net Protocol I also showed that at 2 years, treatment with intravitreal triamcinolone acetonide in combination with laser therapy was inferior to treatment with ranibizumab with or without laser therapy, as well as to laser treatment alone.

However, results from steroid-treated eyes that were pseudophakic at baseline, which therefore did not develop cataracts as a result of steroid treatment, were similar to those from anti-VEGF treated eyes and superior to the laser-treated group. Thus, steroid treatment may be a reasonable alternative to anti-VEGF in eyes with DME that have already undergone cataract surgery. Studies of 2 types of sustained-release steroid implants, made of dexamethasone and fluocinolone acetonide, respectively, have also demonstrated improved rates of 3 or more lines visual acuity gain with these agents. Nonetheless, because

of the higher rates of cataract and glaucoma development in steroid-treated eyes, corticosteroids are usually considered second-line agents for the treatment of DME. They can be a useful alternative for eyes that are not candidates for anti-VEGF therapy or that have been refractory despite previous anti-VEGF treatment. The DRCR.net Protocol U study, which evaluated eyes with persistent center-involved DME and visual impairment despite at least 6 prior injections of anti-VEGF agents, demonstrated that combination therapy with continued anti-VEGF treatment and a dexamethasone implant did not provide superior vision gains when compared to continued anti-VEGF treatment alone. However, eyes in the combination group did show greater improvements in retinal thickening over the 6-month study period.

- Boyer DS, Yoon YH, Belfort R Jr, et al; Ozurdex MEAD Study Group. Three-year, randomized, sham-controlled trial of dexamethasone intravitreal implant in patients with diabetic macular edema. *Ophthalmology*. 2014;121(10):1904–1914.
- Campochiaro PA, Brown DM, Pearson A, et al; FAME Study Group. Long-term benefit of sustained-delivery fluocinolone acetonide vitreous inserts for diabetic macular edema. *Ophthalmology*. 2011;118(4):626–635.
- Elman MJ, Aiello LP, Beck RW, et al; Diabetic Retinopathy Clinical Research Network. Randomized trial evaluating ranibizumab plus prompt or deferred laser or triamcinolone plus prompt laser for diabetic macular edema. *Ophthalmology*. 2010;117(6):1064–1077.
- Elman MJ, Ayala A, Bressler NM, et al; Diabetic Retinopathy Clinical Research Network. Intravitreal ranibizumab for diabetic macular edema with prompt versus deferred laser treatment: 5-year randomized trial results. *Ophthalmology*. 2015;122(2):375–381.
- Wells JA, Glassman AR, Ayala AR, et al; Diabetic Retinopathy Clinical Research Network. Afibercept, bevacizumab, or ranibizumab for diabetic macular edema. *N Engl J Med*. 2015;372(13):1193–1203.

Surgical management of diabetic macular edema

Focal- or grid-pattern macular laser photocoagulation still has an important role as an adjunctive treatment in eyes that are resistant to anti-VEGF agents; it is also appropriate as occasional first-line treatment in eyes with DME from clearly focal leakage that can be easily targeted by the laser. In addition, laser therapy may be a useful first-line treatment for patients who are not good candidates for anti-VEGF therapy because they are medically unstable or who are unable to adhere to near monthly treatment, especially in the first year. Pars plana vitrectomy is often effective in improving retinal thickening in eyes with DME, but is not always successful at improving vision. Further, definitive studies are needed to clearly define the role of vitrectomy in DME treatment.

Laser treatment of DME Although anti-VEGF therapy has largely supplanted laser photocoagulation for most cases of DME, laser treatment remains a well-proven treatment modality with minimal associated adverse events. In the ETDRS, macular focal- or grid-pattern laser photocoagulation treatment of CSME versus observation reduced the risk of moderate vision loss, increased the chance of vision improvement, and was associated with only minor visual field loss. Eyes with less than CSME showed no treatment benefit over the control group at 2 years. In current clinical practice, treatment of eyes with DME can usually be delayed until progression of edema threatens the center of the macula.

Potential adverse effects of macular laser therapy include paracentral scotomas, transient increases of edema and/or decreases in vision, laser scar expansion, subretinal fibrosis, choroidal neovascularization, and inadvertent foveal burns. However, if the laser

treatment is carefully and appropriately applied, most of these complications should be avoided. Clinical features associated with poorer visual acuity outcomes after photocoagulation treatment for DME include the following:

- macular ischemia (extensive perifoveal capillary nonperfusion)
- hard exudates in the fovea

Fluorescein angiography, along with an OCT thickness map, can be used to guide laser treatment for DME. The laser parameters typically used include spot sizes of 50–100 µm and burn durations of 0.1 second or less. For focal leakage, direct laser treatment using green or yellow wavelengths is applied to all leaking microaneurysms between 500 µm and 3000 µm from the center of the macula. For diffuse leakage or zones of capillary nonperfusion in the macula, a light-intensity grid pattern can be applied. Burns are typically separated by 1 burn width, and a green- or yellow-wavelength laser is used. Treatment should include areas of diffuse leakage more than 500 µm from the center of the macula and 500 µm from the temporal margin of the optic nerve head.

Laser sessions are typically repeated as often as every 16 weeks until retinal thickening has resolved or all of the leaking microaneurysms have been adequately treated. Some studies have suggested that micropulse, or sub-threshold intensity burns, may be as effective as standard macular laser treatment while reducing damage to the retinal pigment epithelium and outer retinal layers. Treatment of peripheral nonperfusion as visualized on ultra-wide-field FA with scatter photocoagulation does not improve visual acuity or retinal thickening in eyes with DME.

Early Treatment Diabetic Retinopathy Study Research Group. Treatment techniques and clinical guidelines for photocoagulation of diabetic macular edema. ETDRS report number 2. *Ophthalmology*. 1987;94(7):761–774.

Pars plana vitrectomy for DME Pars plana vitrectomy may be useful for treating DME. If there is evidence of posterior hyaloidal traction or an associated epiretinal membrane leading to mechanical traction, creation of a posterior vitreous detachment and possible ILM or epiretinal membrane peeling can be effective in reducing retinal thickening. Although the use of vitrectomy as first-line therapy for treatment of eyes with DME without vitreomacular traction is uncommon in the United States, it is more widely prevalent internationally. Vitrectomy generally improves retinal thickening in eyes with DME. However, multiple studies have demonstrated inconsistent effects of vitrectomy on visual acuity in eyes with DME, despite consistent improvements in edema. Eyes can experience either substantial vision gain or vision loss after vitrectomy. The DRCR.net Protocol D, which was a prospective observational case series, confirmed that after vitrectomy, retinal thickening was reduced in most eyes; however, median visual acuity remained unchanged over the 6-month follow-up period. As mentioned, the exact role of vitrectomy in the treatment of DME remains to be determined through future, large-scale definitive studies.

Haller JA, Qin H, Apte RS, et al; Diabetic Retinopathy Clinical Research Network Writing Committee. Vitrectomy outcomes in eyes with diabetic macular edema and vitreomacular traction. *Ophthalmology*. 2010;117(6):1087–1093.

Jackson TL, Nicod E, Angelis A, Grimaccia F, Pringle E, Kanavos P. Pars plana vitrectomy for diabetic macular edema: a systematic review, meta-analysis, and synthesis of safety literature. *Retina*. 2017; 37(5):886–895.

Cataract Surgery in Patients With Diabetes Mellitus

Patients with diabetes mellitus who undergo cataract surgery usually have excellent visual outcomes postoperatively. However, various studies suggest that both eyes with diabetic retinopathy and DME may worsen in severity after cataract surgery. In DRCR.net Protocol P, patients with NPDR but no history of DME were found to have a substantial risk of postoperative DME after cataract surgery. In Protocol Q, which enrolled patients with preexisting DME, only a small percentage of eyes had substantial visual acuity loss or definitive progression in central retinal thickening. Therefore, in clinical practice, it is common for patients with center-involved DME who are about to undergo cataract surgery to receive an anti-VEGF drug injection preoperatively or steroid injection perioperatively. In addition, control of systemic factors should be optimized as much as possible prior to surgery.

Patients with severe NPDR or PDR should be considered for scatter photocoagulation before undergoing cataract removal, if the ocular media are sufficiently clear to allow for treatment. If the density of the cataract precludes adequate evaluation of the retina or treatment, prompt postoperative retinal evaluation and treatment are recommended. In general, all patients with preexisting diabetic retinopathy should be reevaluated after cataract surgery.

Cataract surgeons should be mindful of the need for future regular retinal evaluations and the possibility of future surgical interventions. They should perform an adequate capsulorrhesis to avoid anterior capsular phimosis, and avoid the use of silicone lenses in diabetic eyes, because those lenses may fog with condensation during subsequent vitrectomies. BCSC Section 11, *Lens and Cataract*, briefly discusses the considerations the cataract surgeon must take into account in patients with diabetes mellitus.

Baker CW, Almukhtar T, Bressler NM, et al; Diabetic Retinopathy Clinical Research Network

Authors/Writing Committee. Macular edema after cataract surgery in eyes without pre-operative central-involved diabetic macular edema. *JAMA Ophthalmol*. 2013;131(7):870–879.

Bressler SB, Baker CW, Almukhtar T, et al; Diabetic Retinopathy Clinical Research Network

Authors/Writing Committee. Pilot study of individuals with diabetic macular edema undergoing cataract surgery. *JAMA Ophthalmol*. 2014;132(2):224–226.

SELECTED DIABETIC RETINOPATHY CLINICAL RESEARCH NETWORK STUDIES

The Diabetic Retinopathy Clinical Research Network (DRCR.net) was developed to conduct multicenter clinical research initiatives in diabetic eye disease that involve community practices as well as academic centers. Since its inception in 2002, the DRCR.net has conducted many of the studies that have established current standard-care practices for diabetic retinopathy and DME (Table 5-3).

Table 5-3 Diabetic Retinopathy Clinical Research Network (DRCR.net) Studies

Protocol	Study Name	End Date	Study Conclusions
A	A Pilot Study of Laser Photocoagulation for Diabetic Macular Edema	01/31/2008	In eyes with DME, an MMG photocoagulation technique was less effective at reducing OCT-measured retinal thickening over 12 months than the standard focal photocoagulation technique modified from the ETDRS.
B	A Randomized Trial Comparing Intravitreal Triamcinolone Acetonide and Laser Photocoagulation for Diabetic Macular Edema	10/03/2008	Over 2 years, focal/grid photocoagulation for center-involved DME was more effective and had fewer adverse effects than 1-mg or 4-mg doses of preservative-free intravitreal triamcinolone.
C	Temporal Variation in Optical Coherence Tomography Measurements of Retinal Thickening in Diabetic Macular Edema	05/20/2005	Although retinal thickening decreases slightly over the day on average, most eyes with DME have little meaningful change in OCT CST or visual acuity between the hours of 8 AM and 4 PM. A change in CST >11% is likely to be real.
D	Evaluation of Vitrectomy for Diabetic Macular Edema	02/26/2009	Vitrectomy reduces retinal thickening in most eyes with DME and vitreomacular traction. Although visual acuity outcomes improved by 10 or more letters in 38% of eyes, 22% lost 10 or more letters after vitrectomy.
E	A Pilot Study of Peribulbar Triamcinolone Acetonide for Diabetic Macular Edema	11/01/2007	In cases of DME where the patient has good visual acuity, peribulbar triamcinolone, with or without focal photocoagulation, is unlikely to be of substantial benefit.
F	An Observational Study of the Development of Diabetic Macular Edema Following Scatter Laser Photocoagulation	01/31/2008	Clinically meaningful differences in OCT thickness or visual acuity are not substantially different when PRP is applied in 1 sitting compared with 4 sittings.
G	Subclinical Diabetic Macular Edema Study	04/22/2009	Approximately one-quarter to one-half of eyes diagnosed with subclinical DME will progress to more definite thickening or be judged to need treatment for DME within 2 years. Because CST is greater in men than in women, studies involving comparisons of retinal thickness to expected norms should consider different mean values for men and women.
H	A Phase 2 Evaluation of Anti-VEGF Therapy for Diabetic Macular Edema: Bevacizumab (Avastin)	02/29/2008	Intravitreal bevacizumab can reduce DME in some eyes, but this preliminary study was not designed to definitively determine whether the treatment was beneficial.

(Continued)

Table 5-3 (*continued*)

Protocol	Study Name	End Date	Study Conclusions
I	Intravitreal Ranibizumab or Triamcinolone Acetonide in Combination with Laser Photocoagulation for Diabetic Macular Edema	12/31/2013	At 2 years, intravitreal ranibizumab with prompt or deferred (≥ 24 weeks) focal/grid laser photocoagulation is more effective in increasing visual acuity compared with focal/grid laser treatment alone or intravitreal triamcinolone with laser photocoagulation for the treatment of center-involved DME. Focal/grid laser treatment at the initiation of intravitreal ranibizumab is no better, and possibly worse, for vision outcomes than deferring laser treatment for 24 weeks or more in eyes with center-involved DME with vision impairment.
J	Intravitreal Ranibizumab or Triamcinolone Acetonide as Adjunctive Treatment to Panretinal Photocoagulation for Proliferative Diabetic Retinopathy	07/07/2010	The addition of 1 intravitreal triamcinolone injection or 2 intravitreal ranibizumab injections in eyes receiving focal/grid laser photocoagulation for DME and PRP is associated with better visual acuity outcomes and decreased macular edema by 14 weeks. Eyes that demonstrate a definite reduction in, but not complete resolution of, central DME at 16 weeks after focal/grid laser photocoagulation have a 23%–63% likelihood of continuing to improve without additional treatment.
K	The Course of Response to Focal Photocoagulation for Diabetic Macular Edema	06/19/2008	Across nationwide sites using a variety of autorefractors, visual acuity tended to be worse and more variable with autorefraction than manual refraction, suggesting that autorefraction is not a good substitute for manual refraction for clinical trials with improved visual acuity outcomes as a primary endpoint.
L	Evaluation of Visual Acuity Measurements in Eyes with Diabetic Macular Edema	11/06/2010	Use of a personalized intervention at ophthalmology visits, including HbA _{1c} measurement and counseling about the importance of glycemic control in reducing diabetic complications, was not effective in improving HbA _{1c} levels.
M	Effect of Diabetes Education During Retinal Ophthalmology Visits on Diabetes Control	12/31/2014	

Protocol	Study Name	End Date	Study Conclusions
N	An Evaluation of Intravitreal Ranibizumab for Vitreous Hemorrhage Due to Proliferative Diabetic Retinopathy	12/21/2012	Intravitreous ranibizumab versus saline did result in significantly different rates of vitrectomy by 16 weeks in eyes with vitreous hemorrhage from PDR. However, ranibizumab treatment resulted in improved short-term secondary outcomes including visual acuity improvement, increased panretinal photocoagulation completion rates, and reductions in recurrent vitreous hemorrhage.
O	Comparison of Time-Domain OCT and Spectral-Domain OCT Retinal Thickness Measurement in Diabetic Macular Edema	01/31/2013	This study of eyes with no to minimal nonproliferative diabetic retinopathy developed conversion equations to transform CST values obtained on a spectral-domain OCT to a time-domain OCT scale for group comparisons. In addition, values were established for machine and gender-specific thresholds to determine DME presence in diabetic eyes.
P	A Pilot Study in Individuals with Center-Involved DME Undergoing Cataract Surgery	11/12/2010	This small, observational study of eyes with DME undergoing cataract surgery revealed only a small percentage of eyes experienced substantial visual acuity loss or definitive worsening of DME after surgery.
Q	An Observational Study in Individuals with Diabetic Retinopathy without Center-Involved DME Undergoing Cataract Surgery	05/19/2011	A history of DME treatment and presence of non-center-involved DME are risk factors for development of center-involved DME after cataract surgery in eyes with diabetic retinopathy and no center-involved DME prior to surgery.
R	A Phase II Evaluation of Topical NSAIDs in Eyes with Non Central Involved DME	12/18/2013	At 1-year follow-up in eyes with non-center-involved DME, this study did not identify a difference between the effect of topical nepafenac 0.1% and placebo drops on OCT parameters or visual acuity.
S	Prompt Panretinal Photocoagulation versus Intravitreal Ranibizumab with Deferred Panretinal Photocoagulation for Proliferative Diabetic Retinopathy	—	Ranibizumab injections are an effective alternative to panretinal photocoagulation in treating PDR. At 2 years, visual acuity outcomes were noninferior to ranibizumab, while average visual acuity over the 2-year period was better and there was less peripheral field loss, reduced rates of DME onset, and fewer eyes that underwent vitrectomy.

(Continued)

Table 5-3 (*continued*)

Protocol	Study Name	End Date	Study Conclusions
T	A Comparative Effectiveness Study of Intravitreal Afibercept, Bevacizumab and Ranibizumab for Diabetic Macular Edema	10/18/2018	The 2-year clinical trial compared 3 drugs used to treat DME and found that gains in vision were greater for participants receiving the drug afibercept than for those receiving bevacizumab, but only among participants starting treatment with 20/50 or worse visual acuity. At 1 year, afibercept had superior gains to ranibizumab in this vision subgroup; however, a difference could not be identified at 2 years. The 3 drugs yielded similar gains in vision for patients with 20/32 or 20/40 visual acuity at the start of treatment.
U	Short-term Evaluation of Combination Corticosteroid + Anti-VEGF Treatment for Persistent Central-Involved Diabetic Macular Edema Following Anti-VEGFT Therapy	6/01/2017	In eyes with persistent DME and visual impairment despite previous anti-VEGF therapy, the dexamethasone + ranibizumab group experienced greater reduction of DME but no greater improvement in vision than the sham + ranibizumab group over 6 months.

CST = central subfield thickness; DME = diabetic macular edema; ETDRS = Early Treatment Diabetic Retinopathy Study; HbA_{1c} = hemoglobin A_{1c}; MMG = modified macular grid; OCT = optical coherence tomography; PDR = proliferative diabetic retinopathy.

Data from Diabetic Retinopathy Clinical Research Network (DRCR.net) website; accessed September 4, 2020. <https://public.jaeb.org/drcrnet>

CHAPTER 6

Retinal Vascular Diseases Associated With Cardiovascular Disease



This chapter includes related activities, which can be accessed by scanning the QR codes provided in the text or going to www.aao.org/bcscactivity_section12.

This chapter discusses retinal vascular diseases that are associated in some way with cardiovascular disease. When evaluating patients, it is important to consider the additional risk factors linked to many of these conditions.

Systemic Arterial Hypertension

Elevated blood pressure (BP) is defined as 120–129 mm Hg systolic *and* <80 mm Hg diastolic. Stage 1 hypertension is defined as 130–139 mm Hg systolic *or* 80–89 mm Hg diastolic. Stage 2 hypertension is defined as ≥140 mm Hg systolic *or* ≥90 mm Hg diastolic. According to estimates from the CDC and the WHO, more than 100 million people in the United States and more than 1 billion people worldwide have elevated BP.

Together with the heart, the kidneys, and the brain, the eye is a major target organ of systemic hypertension. Ocular effects of hypertension can be observed in the retina, choroid, and optic nerve. Retinal changes can be described and classified using ophthalmoscopy and angiography. An ophthalmologist's recognition of posterior segment vascular changes may even prompt the initial diagnosis of hypertension and alert the patient to the potential complications associated with this condition. BCSC Section 1, *Update on General Medicine*, discusses hypertension in more detail.

Kim SK, Mieler WF, Jakobiec F. Hypertension and its ocular manifestations. In: Albert DM, Miller JW, Azar DT, Blodi BA, eds. *Albert & Jakobiec's Principles and Practice of Ophthalmology*. 3rd ed. Philadelphia: Saunders; 2008:4367–4384.

Hypertensive Retinopathy

Hypertension affects arterioles and capillaries, the anatomic loci of both autoregulation and nonperfusion. An acute hypertensive episode may produce focal intraretinal

periarteriolar transudates (FIPTs) at the precapillary level. The presence of cotton-wool spots (also referred to as *soft exudates*) indicates ischemia of the retinal nerve fiber layer (Fig 6-1). Uncontrolled systemic hypertension leads to nonperfusion at various retinal levels as well as neuronal loss and associated scotomas. Other, more chronic, hypertensive retinal lesions include microaneurysms, intraretinal microvascular abnormalities (IRMAs), blot hemorrhages, lipid exudates (also referred to as *hard exudates*), venous beading, and neovascularization. The relationship between hypertensive vascular changes and arteriosclerotic vascular disease is complex, with wide variation related to the duration and severity of the hypertension, the presence of diabetic retinopathy, the severity of any dyslipidemia, patient age, and the patient's history of smoking. Hence, it is difficult to classify which retinal vascular changes have been caused strictly by hypertension; the often-cited focal arteriolar narrowing and arterial venous nicking have been shown to have little predictive value for actual hypertension severity. Nonetheless, one historical classification of mostly arteriosclerotic retinopathy is the Modified Scheie Classification of Hypertensive Retinopathy:

- Grade 0 No changes
- Grade 1 Barely detectable arterial narrowing
- Grade 2 Obvious arterial narrowing with focal irregularities
- Grade 3 Grade 2 plus retinal hemorrhages and/or exudates
- Grade 4 Grade 3 plus optic nerve head swelling

Hypertension may be complicated by branch retinal artery occlusion (BRAO), branch retinal vein occlusion (BRVO), central retinal vein occlusion (CRVO), or retinal arterial macroaneurysms (all discussed later in this chapter). In addition, the coexistence of hypertension and diabetes mellitus results in more severe retinopathy because precapillary and capillary insults act in combination.

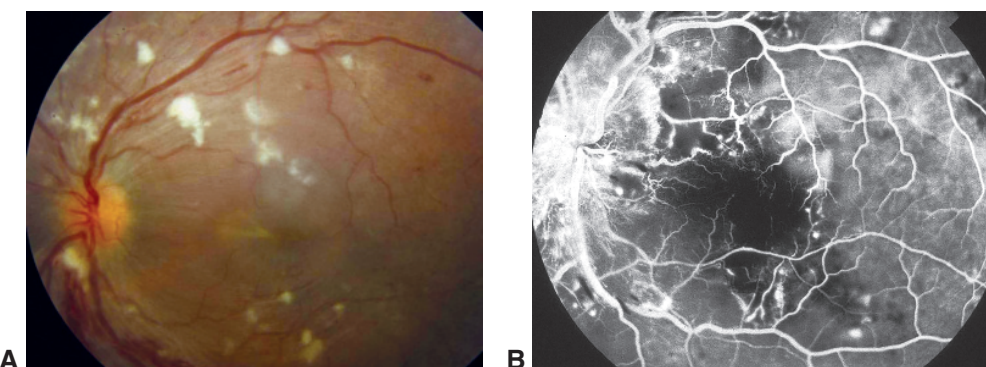


Figure 6-1 Severe hypertensive retinopathy. **A**, Fundus photograph from a 25-year-old man with renal hypertension shows large superficial and white cotton-wool spots contrasting with small, tan, and deep focal intraretinal periarteriolar transudates (FIPTs). **B**, Angiography image shows areas of nonperfusion corresponding to the cotton-wool spots and punctate hyperfluorescence corresponding to the FIPTs. (Courtesy of Hermann D. Schubert, MD.)

- Cheung CYL, Wong TY. Hypertension. In: Schachat AP, Wilkinson CP, Hinton DR, Sadda SR, Wiedemann P, eds. *Ryan's Retina*. 6th ed. Philadelphia: Elsevier/Saunders; 2018: chap 52.
- Wong TY, Mitchell P. The eye in hypertension. *Lancet*. 2007;369(9559):425–435.

Hypertensive Choroidopathy

Hypertensive choroidopathy typically occurs in young patients who have experienced an episode of acute, severe hypertension often associated with preeclampsia, eclampsia, pheochromocytoma, or renal hypertension (see Chapter 9 for more on choroidal disease). Lobular nonperfusion of the choriocapillaris may occur, initially resulting in tan, lobule-sized patches that, in time, become hyperpigmented and surrounded by margins of hypopigmentation—lesions known as *Elschnig spots* (Fig 6-2). Linear configurations of similar-appearing hyperpigmentations known as *Siegrist streaks* follow the meridional course of choroidal arteries. Fluorescein angiography shows focal choroidal hypoperfusion in the early phases and multiple subretinal areas of leakage in the late phases (Fig 6-3). Focal retinal pigment epithelium (RPE) detachments may occur, and, in severe cases, extensive bilateral exudative retinal detachments may develop.

Hypertensive Optic Neuropathy

Patients with optic neuropathy secondary to severe hypertension may exhibit linear peri-papillary flame-shaped hemorrhages, blurring of the optic nerve head margins, florid optic nerve head edema with secondary retinal venous stasis, and macular exudates (Fig 6-4). The



Figure 6-2 Fundus photograph shows Elschnig spots. (Courtesy of Harry W. Flynn, Jr, MD.)

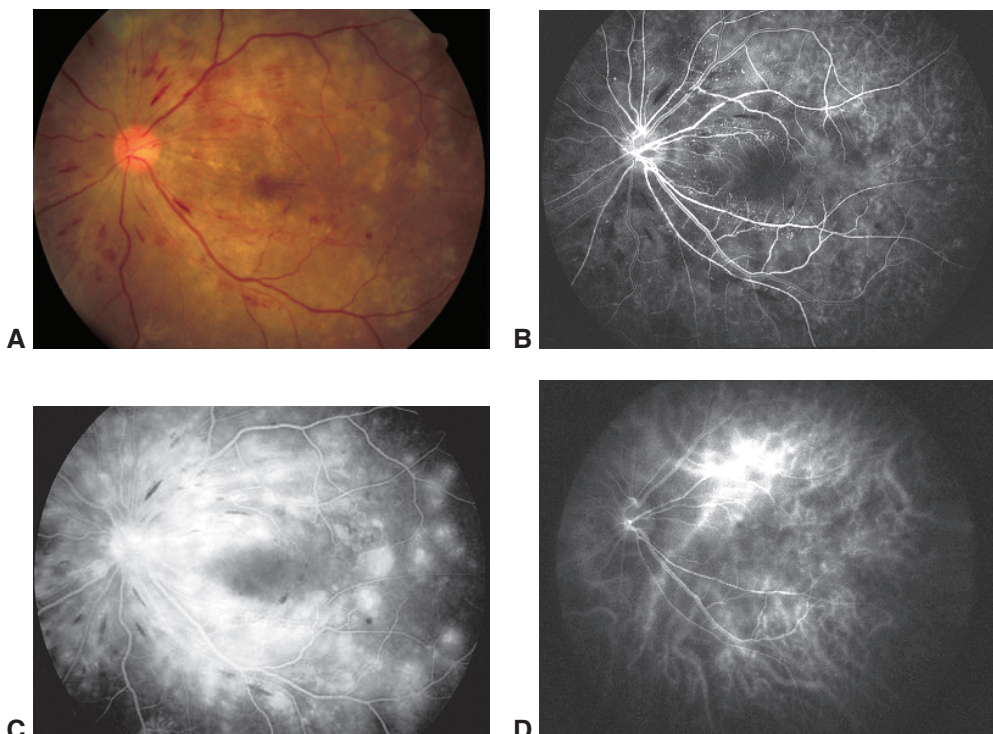


Figure 6-3 Malignant hypertension. **A**, Color fundus photograph of hypertensive retinopathy with shallow detachment of the macula, striae of the internal limiting membrane, splinter hemorrhages in the radial peripapillary net, hyperemia of the optic nerve, and a few lipid exudates in the macula. Multiple tan patches at the level of the retinal pigment epithelium (RPE) and inner choroid are due to hypertensive choroidopathy. **B**, Early fluorescein angiography image reveals retinal capillary nonperfusion, microaneurysms, and choroidal filling defects. **C**, Late angiography image shows intense vascular leakage as well as leakage from patches of hypertensive choroidopathy. **D**, Early indocyanine green (ICG) angiography image shows a "moth-eaten" appearance of the choriocapillaris. (Courtesy of Richard Spaide, MD.)

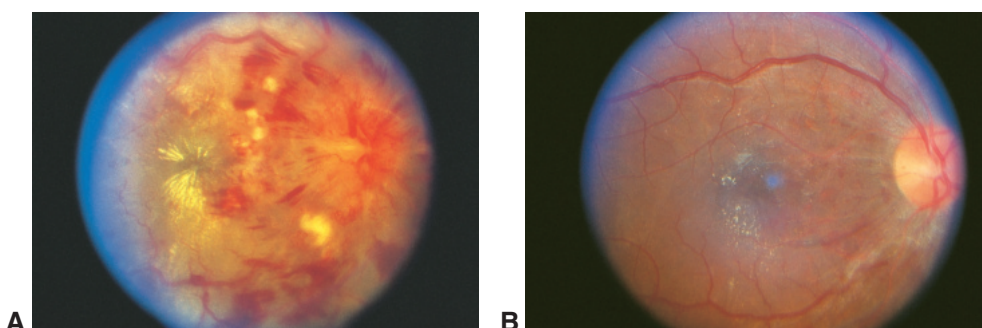


Figure 6-4 Severe hypertensive retinopathy with improvement. **A**, Fundus photograph of a 25-year-old patient with severe hypertension (210/140 mm Hg) and visual acuity loss to the 2/200 level. Note the optic nerve head edema, macular exudates, intraretinal hemorrhage with nerve fiber layer (NFL) infarct, and venous congestion. **B**, Fundus photograph of the same patient 10 weeks later, after treatment of hypertension and normalization of blood pressure. The optic nerve head is now normal, and minimal residual macular exudates are present. Visual acuity has returned to 20/50. (Courtesy of Harry W. Flynn, Jr, MD.)

differential diagnosis for patients with this clinical appearance includes CRVO, anterior ischemic optic neuropathy, diabetic papillopathy, radiation papillopathy, neuroretinitis, and retrobulbar tumor.

Retinal Vein Occlusion

Retinal vein occlusion (RVO) is most commonly associated with advancing age and hypertension; however, it also has less common or rare associations. A patient with RVO should be medically evaluated, and, in the absence of cardiovascular disease, a search for other causative or predisposing systemic conditions should be considered, especially among patients younger than 50 years old.

All patients with RVO should undergo a comprehensive ocular examination. Glaucoma, in both open- and narrow-angle forms, is a major risk factor for RVO. In the Eye Disease Case-Control Study (EDCC), a history of glaucoma was found to increase a patient's risk of CRVO by a factor of 5.3, and of BRVO by a factor of 2.5. Elevated retinal venous pressure and reduced blood flow are thought to be among the few avoidable factors associated with both branch and central retinal vein occlusion. Retinal venous pressure may increase in the supine position (ie, when sleeping), and blood pressure medications can reduce perfusion pressure and blood flow; therefore, it has been suggested that patients should avoid taking their blood pressure medications at bedtime.

Intraretinal hemorrhages and dilated tortuous retinal vasculature are classic findings in the affected retina, and in severe cases, cotton-wool spots may be present (Fig 6-5). In acute disease, the level of visual acuity impairment depends on the severity of the macular ischemia or edema and the presence of intraretinal hemorrhages affecting the fovea. Macular edema is best assessed with spectral-domain optical coherence tomography (SD-OCT), while ischemia is best detected using fluorescein angiography or OCT angiography. Without treatment, increasing amounts of ischemic retina confer increasing risk for neovascularization. In patients with BRVO, neovascularization most commonly occurs in the healthy retina at the border of the affected, ischemic retina or, less commonly, at the optic nerve head, and, in rare instances, in the anterior segment. In patients with CRVO, neovascularization occurs most commonly in the anterior segment, manifesting as iris or angle neovascularization, but can also occur in the retina or at the optic nerve head. Because anterior segment neovascularization is found in both branch and central retinal vein occlusions, periodic, undilated examinations of the iris and gonioscopy of the iridocorneal angle are recommended for all patients with RVO.

Improvement or spontaneous resolution can occur in patients with RVO. Improvement is usually associated with the development of adequate collateral blood flow. In BRVO, capillaries extending across the median raphe dilate, helping to compensate for the compromised venous drainage. In CRVO, small vessels that normally connect the retinal circulation to the choroidal circulation near the optic nerve head expand, resulting in the undulating appearance of optociliary shunt vessels. These mechanisms redirect venous drainage to the choroid, vortex veins, and superior and inferior ophthalmic veins in the orbit, bypassing the occluded central retinal vein. Chronic, untreated venous occlusive disease commonly leads to development of retinal microvascular changes characterized by microaneurysms, telangiectasias, and macular edema (Fig 6-6).

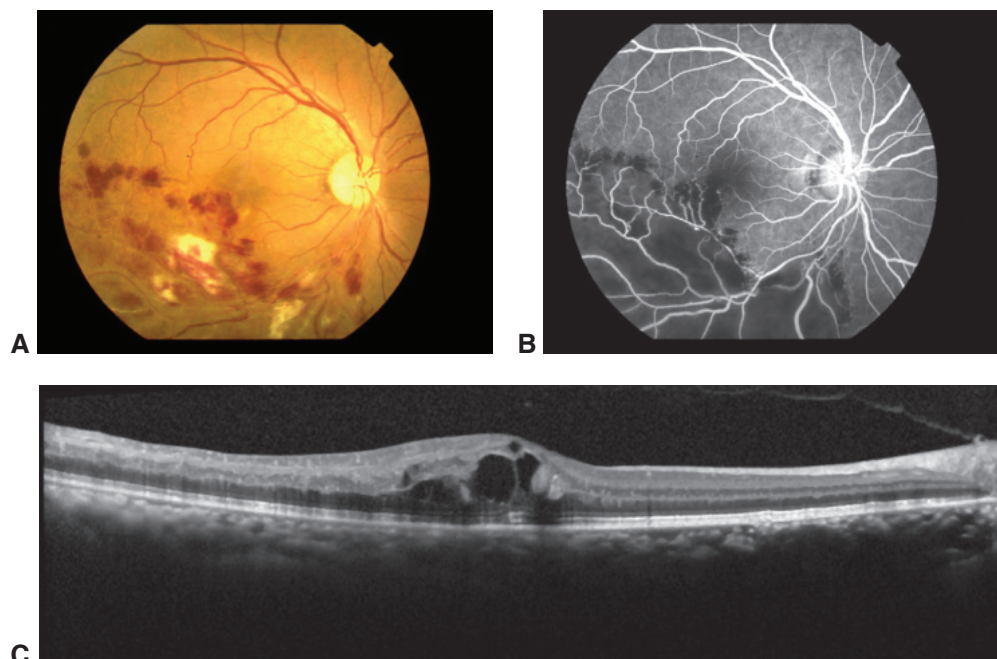


Figure 6-5 Branch retinal vein occlusion (BRVO) with ischemia. **A**, Fundus photograph shows inferotemporal BRVO. **B**, Fluorescein angiography image corresponding to **A** reveals pronounced retinal capillary nonperfusion in the distribution of the retina drained by the obstructed vein. **C**, Spectral-domain optical coherence tomography (SD-OCT) image of the same eye reveals cystoid macular edema (CME). (Courtesy of Neal H. Atebara, MD.)

Anti-vascular endothelial growth factor (VEGF) drugs are mainstay of RVO treatment because of their excellent efficacy and safety profiles. Best visual acuity outcomes are achieved by administering anti-VEGF treatment immediately upon diagnosis of RVO-related macular edema. Anti-VEGF treatment also suppresses neovascular complications of RVO. Intraocular steroid treatments and macular or scatter panretinal photocoagulation are also employed to manage vision loss from, and complications of, RVO.

Specific considerations for branch and central retinal vein occlusion are discussed in the following sections.

Goldman DR, Shah CP, Morley MG, Heier JS. Venous occlusive disease of the retina. In: Yanoff M, Duker JS, eds. *Ophthalmology*. 4th ed. Philadelphia: Elsevier/Saunders; 2014: 526–534.

Hayreh SS. Retinal vein occlusion. *Indian J Ophthalmol*. 1994;42(3):109–132.

Branch Retinal Vein Occlusion

In BRVO, obstruction of the vein occurs most commonly at an arteriovenous crossing, where thickening of the arterial wall compresses the adjacent vein within a common adventitial sheath. When the occlusion does not occur at an arteriovenous crossing, the possibility of an underlying retinochoroiditis or retinal vasculitis should be considered. The quadrant most commonly affected is the superotemporal (63%); a clinical finding of nasal

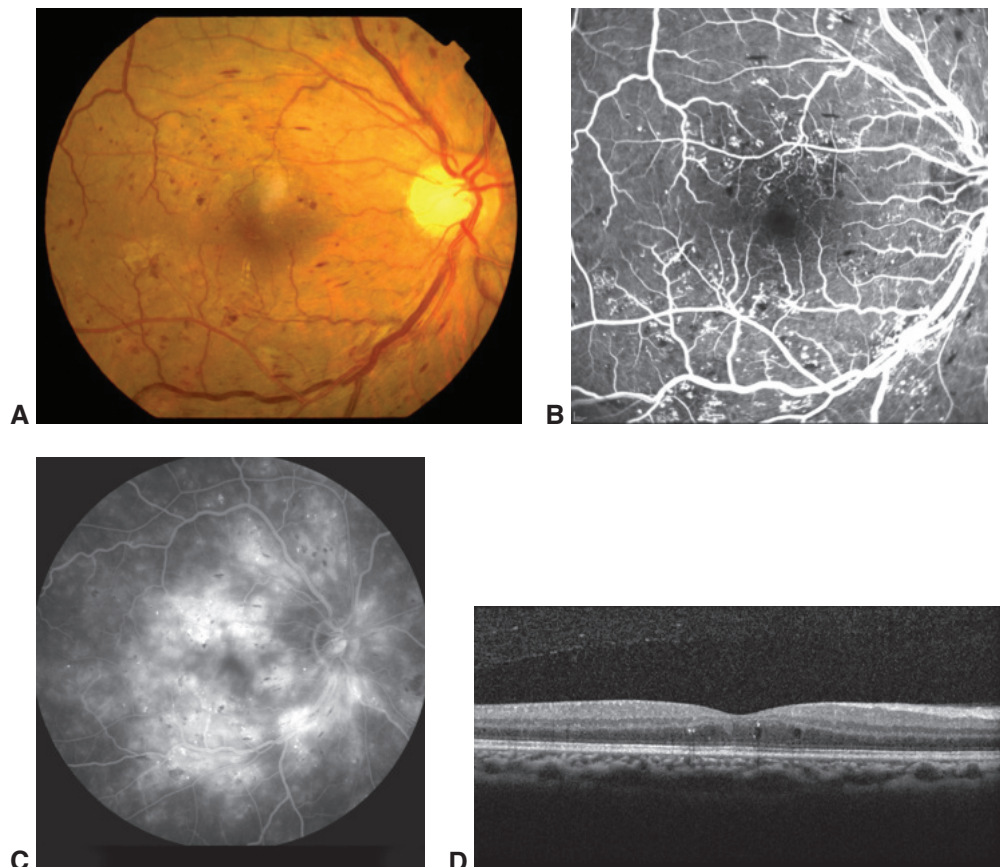


Figure 6-6 Chronic changes from nonischemic central retinal vein occlusion (CRVO) in a 30-year-old woman with a history of diabetes mellitus and blurry vision for 2 months. Visual acuity is 20/25. **A**, Color fundus photograph of a mild nonischemic, or perfused, CRVO. Dilated retinal veins and retinal hemorrhages are present, as are scant macular exudates inferior to fovea. **B**, Fluorescein angiography image taken 22 seconds after injection reveals capillary telangiectasias and microaneurysms throughout the posterior pole. **C**, Late angiogram taken at 9 minutes reveals diffuse retinovascular leakage and microaneurysms. **D**, OCT scan reveals mild cystic changes and microaneurysms but minimal retinal thickening and normal foveal contour. (Courtesy of Neal H. Atebara, MD.)

vascular occlusion is rare. The artery serving the area of venous occlusion may become narrowed and sheathed over time.

Risk factors for the development of BRVO

The mean age of patients at the time of occurrence is in the seventh decade. The EDCC and other studies have identified the following risk factors for the development of BRVO:

- increasing age
- history of systemic arterial hypertension
- history of smoking
- history of glaucoma
- hypercoagulable conditions

Other studies have disputed the role of smoking or glaucoma as risk factors for BRVO. Diabetes mellitus was not a major independent risk factor in the EDCC, although 10%–12% of patients with RVO have the disease.

Prognosis for patients with BRVO

In acute disease, the presence or absence of macular or foveal involvement determines the visual prognosis. Prior to the availability of pharmacologic intervention, the Branch Vein Occlusion Study (BVOS) found that the incidence of neovascularization from the retina or optic nerve was 36% in eyes with extensive retinal ischemia; extensive ischemia was defined as an area of at least 5 disc diameters in size. Vitreous hemorrhage developed in 60%–90% of such eyes if laser photocoagulation was not performed.

Over the long term, permanent vision loss may be related to macular ischemia, cystoid macular edema (CME), lipid residues (hard exudates) in the fovea, pigmentary macular disturbances, subretinal fibrosis, and epiretinal membrane formation. Less common causes of vision loss include vitreous hemorrhage, tractional retinal detachment, and rhegmatogenous retinal detachment (RRD). RRD typically develops following a break in retina adjacent to, or underlying retinal neovascularization induced by vitreous traction.

Treatment of BRVO

Pharmacologic management Pharmacologic management is currently the mainstay of RVO management. See the section Pharmacologic Management of Retinal Vein Occlusion for a discussion of this topic.

Surgical management of BRVO

MACULAR LASER SURGERY Laser grid photocoagulation may be applied to areas of macular edema caused by the obstructed vein (Fig 6-7). The BVOS found that laser-treated eyes with intact foveal vasculature, macular edema, and visual acuity in the 20/40–20/200 range were more likely to gain 2 lines of visual acuity (65%) than untreated eyes (37%). At 3-year follow-up, treated eyes were more likely to have 20/40 or better visual acuity than untreated eyes (60% vs 34%, respectively), with a mean visual acuity improvement of 1.3 ETDRS (Early Treatment of Diabetic Retinopathy Study) lines versus 0.2 line, respectively. In the BVOS, laser treatment of macular edema was delayed for at least 3 months to permit the maximum spontaneous resolution of intraretinal blood and the edema. While this practice may still be appropriate for macular laser therapy, treatment with pharmacologic agents should commence immediately upon diagnosis of BRVO.

SCATTER PHOTOCOAGULATION The BVOS showed that scatter photocoagulation to the area of retinal capillary nonperfusion is effective in causing regression of the new vessels in eyes with retinal, optic nerve head, or iris neovascularization (Fig 6-8); it also reduced the risk of vitreous hemorrhage from 60% to 30%. Although the BVOS showed that patients with large areas of nonperfusion (see Fig 6-5) were found to be at significant risk of developing neovascularization, the study concluded that ischemia alone was not an indication for treatment, provided that follow-up could be maintained.

Clinically, it is important to distinguish neovascularization of the optic nerve head or retina from collateral vessels, which have a larger caliber and do not leak when viewed

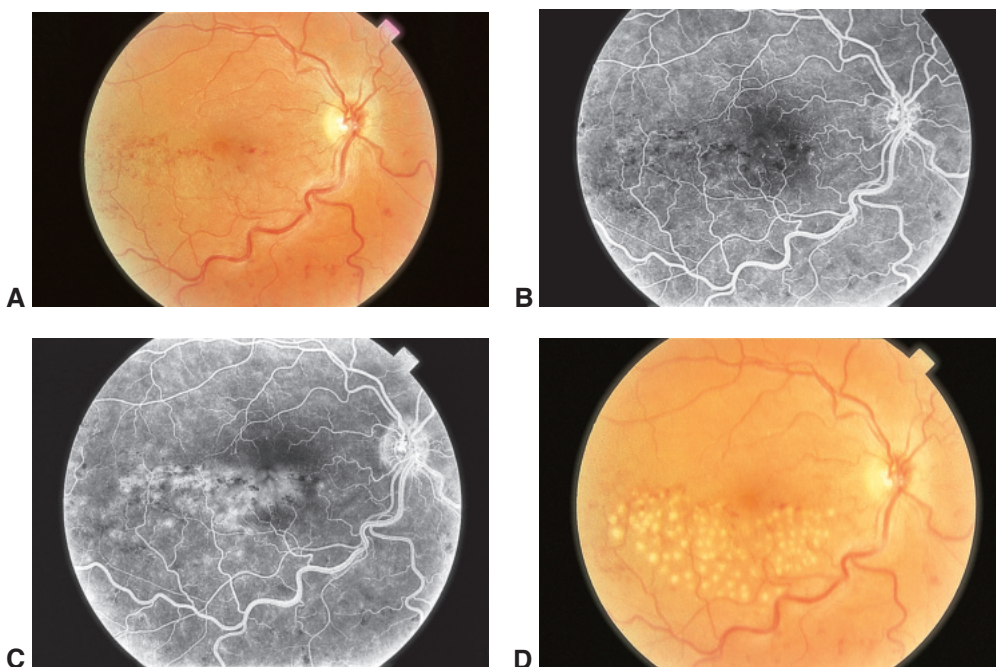


Figure 6-7 BRVO. **A**, Fundus photograph of inferotemporal BRVO. Corresponding fluorescein angiography images show, at 49 seconds after injection (**B**), telangiectatic vessels in the distribution of the inferotemporal vein, and at 393 seconds after injection (**C**), intraretinal leakage of dye from the capillaries in macular distribution of the vein occlusion (white). **D**, Fundus photograph after treatment shows a grid of macular photoocoagulation lesions in the affected area but sparing the foveal region. (Courtesy of Gary C. Brown, MD.)

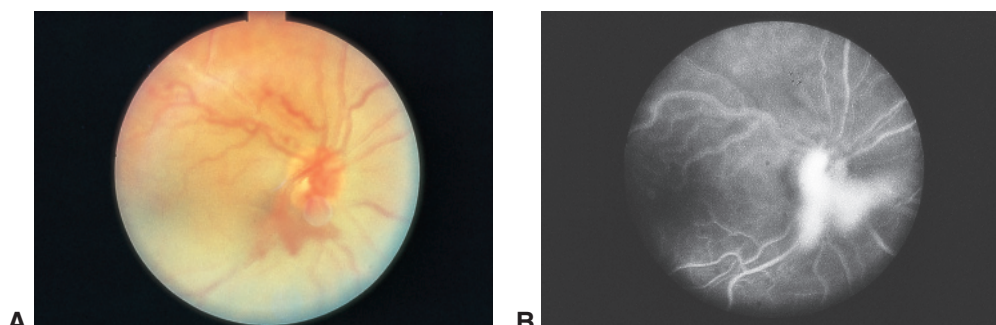


Figure 6-8 BRVO with neovascularization. **A**, Neovascularization of the optic nerve head occurring secondary to a superotemporal BRVO. **B**, Corresponding fluorescein angiography image taken 18 seconds after injection reveals marked hyperfluorescence of the new vessels originating on the optic nerve head. (Courtesy of Gary C. Brown, MD.)

with fluorescein angiography. Neovascularization of the iris occurs in approximately 2% of eyes with BRVO. In these cases, scatter laser photocoagulation in the distribution of the occluded vein should be considered to prevent the development of neovascular glaucoma.

Fuller JJ, Mason JO III. Retinal vein occlusions: update on diagnostic and therapeutic advances. *Focal Points: Clinical Modules for Ophthalmologists*. San Francisco: American Academy of Ophthalmology; 2007, module 5.

PARS PLANA VITRECTOMY Vitrectomy may be indicated for eyes that develop vitreous hemorrhage or retinal detachment (also see Chapters 16 and 20 in this volume).

Central Retinal Vein Occlusion

In CRVO, vision loss is most commonly sudden, with severity ranging along a continuum from mild (nonischemic) to severe (ischemic). Less commonly, patients may experience premonitory symptoms of transient obscuration of vision before overt retinal manifestations appear. CRVOs are considered intermediate, or indeterminate, if they are neither clearly ischemic nor nonischemic; however, more than 80% of intermediate eyes progressed to ischemic disease in the Central Vein Occlusion Study (CVOS).

Nonischemic (mild) CRVO, sometimes referred to as *partial, perfused, or venous stasis retinopathy*, is characterized by visual acuity of 20/200 or better, mild or no afferent pupillary defect, and mild visual field changes. Ophthalmoscopy shows mild dilation and tortuosity of all branches of the central retinal vein as well as dot- and flame-shaped hemorrhages in all quadrants of the retina (Fig 6-9). Macular edema with decreased visual acuity and mild optic nerve head swelling may be present (Activity 6-1; Fig 6-10). Fluorescein angiography usually demonstrates prolongation of the retinal circulation time with breakdown of capillary permeability but minimal areas of nonperfusion. Anterior segment neovascularization is rare in mild CRVO. Chronic nonischemic changes from CRVO include telangiectasias, microaneurysms, and macular pigmentary changes (see Fig 6-6).



ACTIVITY 6-1 OCT Activity: Macular OCT of CRVO eye with severe CME and foveal detachment.

Courtesy of Colin A. McCannel, MD.

Access all Section 12 activities at www.aao.org/bcscactivity_section12.



Ischemic (severe) CRVO, also known as *complete, nonperfused, or hemorrhagic retinopathy*, is defined as having at least 10 optic disc areas of retinal capillary nonperfusion on fluorescein angiography. Ischemic cases are usually associated with poor vision, an afferent pupillary defect, dense central scotoma, and peripheral field constriction. Marked venous dilation, more extensive 4-quadrant hemorrhage, retinal edema (Fig 6-11), and variable numbers of cotton-wool spots are frequently found as well. Fluorescein angiography circulation times are typically prolonged and widespread capillary nonperfusion is demonstrated. Because of inner retinal dysfunction due to ischemia, the b- to a-wave amplitude ratio is decreased in electroretinographic bright-flash, dark-adapted testing. The CVOS showed that the natural history of ischemic CRVO is generally poor, with only approximately 10% of eyes achieving vision better than 20/400. With anti-VEGF treatment, the prognosis may be somewhat better in all but the most ischemic cases.

Hemiretinal vein occlusion (HRVO), which shares features with both CRVO and BRVO, has been associated with a congenital variation in central vein anatomy; it may involve either the superior or inferior half of the retina (Fig 6-12).

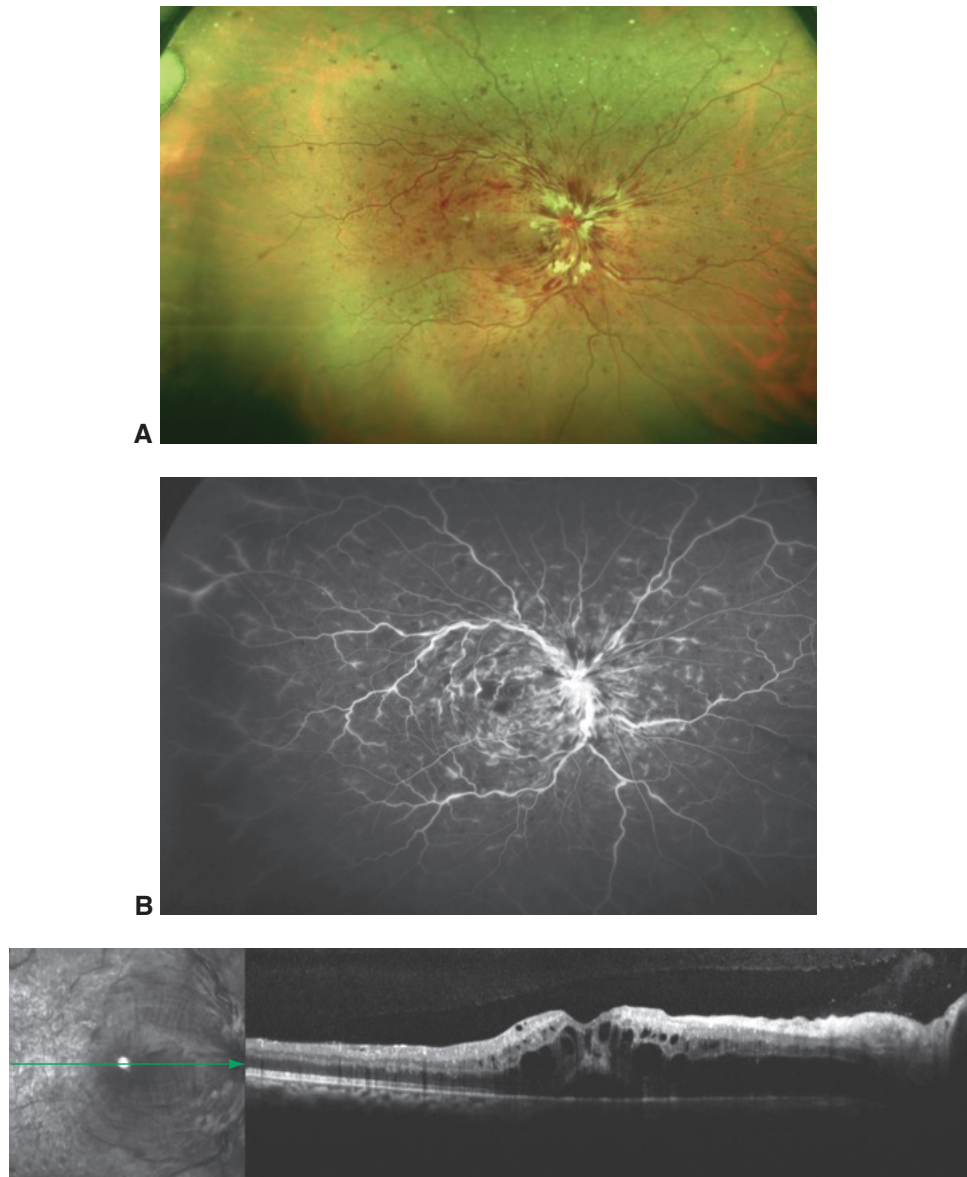


Figure 6-9 Moderate to severe nonischemic CRVO. **A**, Ultra-wide-field fundus photograph of moderate to severe nonischemic, or perfused, CRVO in an eye with 20/80 visual acuity. Dilated retinal veins and retinal hemorrhages are present in all 4 quadrants. Cotton-wool spots can be seen near the optic nerve head. **B**, A fluorescein angiography image taken at 1 minute, 8 seconds reveals relatively intact perfusion of the retinal capillary bed but dilated vessels and peripheral leakage from the large vessels. There are some areas of capillary nonperfusion in the superior macula. **C**, An SD-OCT scan shows severe cystoid retinal edema with a serous foveal detachment. After 2.5 years of anti-vascular endothelial growth factor (VEGF) treatment with bevacizumab, the patient maintains a visual acuity of 20/40. (Courtesy of Colin A. McCannel, MD.)

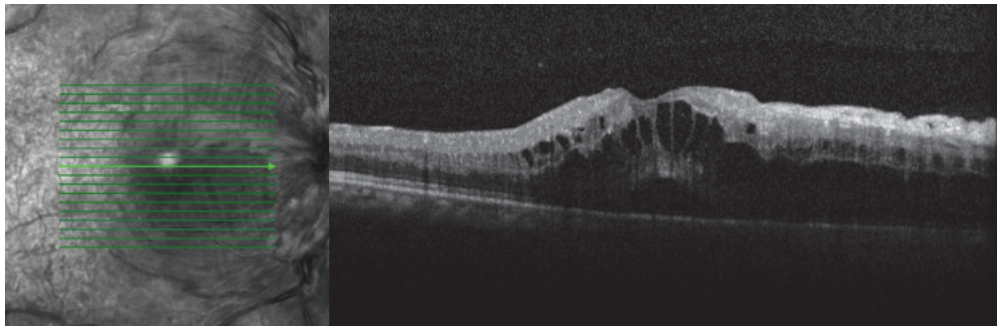


Figure 6-10 Macular OCT of eye shown in Figure 6-9 demonstrates severe CME with foveal detachment. There is also mild to moderate inner retinal hyperreflectivity, consistent with some degree of ischemia. However, the fluorescein images of the retina (Fig 6-9) show that perfusion is present. (*Courtesy of Colin A. McCannel, MD.*)

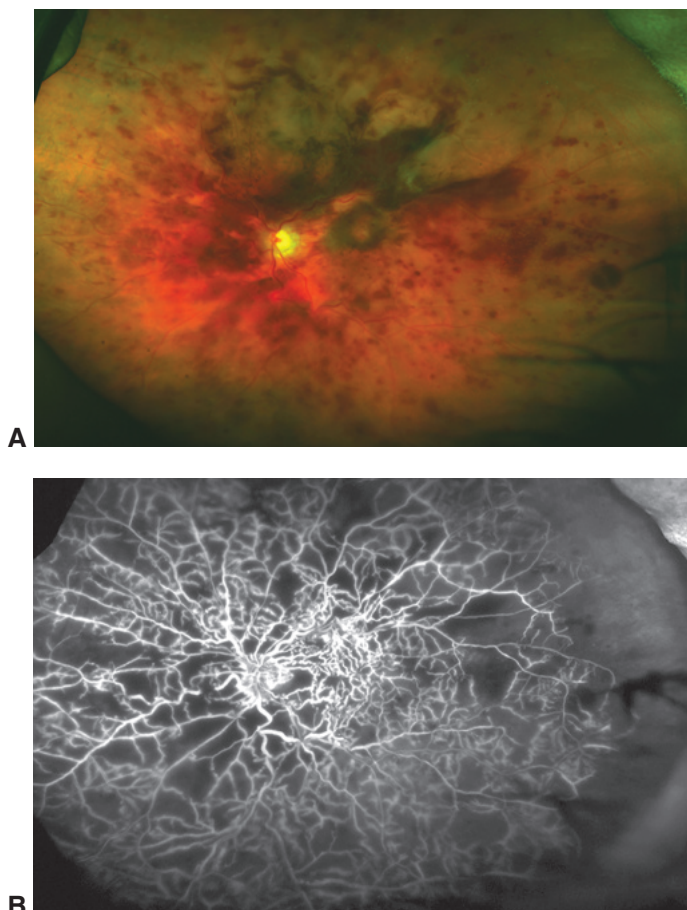


Figure 6-11 Ischemic CRVO. **A**, Ultra-wide-field fundus photograph of severe, or ischemic, CRVO in an eye with hand motions visual acuity. The veins are dilated, and extensive retinal hemorrhages are present. **B**, Ultra-wide-field fluorescein angiography image corresponding to **A** taken 40 seconds after injection reveals widespread retinal capillary nonperfusion, which causes the midsize and larger retinal vessels to stand out from the gray-black, nonperfused areas. (*Courtesy of Colin A. McCannel, MD.*)

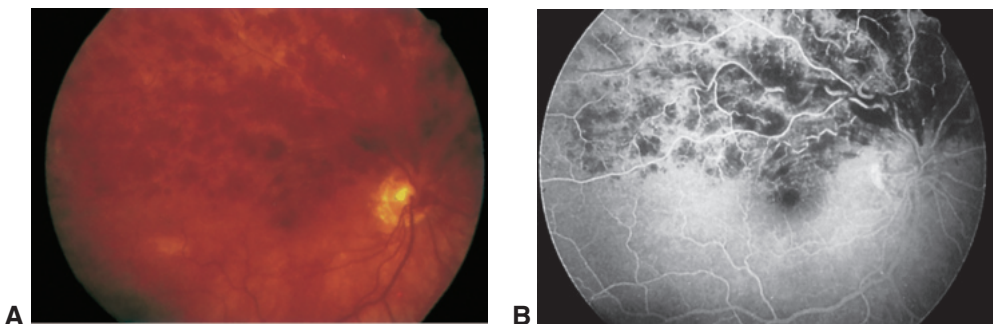


Figure 6-12 Hemiretinal vein occlusion. **A**, Fundus photograph shows superior involvement with intraretinal hemorrhage. **B**, Fluorescein angiography image shows blockage of underlying details in areas of hemorrhage. Note that the foveal avascular zone is largely intact.

Histologic studies suggest that most forms of CRVO share a common mechanism: thrombosis of the central retinal vein at or posterior to the level of the lamina cribrosa. It is postulated that, in some cases, a thickened central retinal artery may impinge on the central retinal vein, causing turbulence, endothelial damage, and thrombus formation. When thrombosis is more anterior, fewer collaterals are available, resulting in greater ischemia.

Iris neovascularization in CRVO

Among eyes with severely ischemic CRVO, the incidence of anterior segment neovascularization, iris or angle, is high (up to 60%); this development occurs on average 3–5 months after the onset of symptoms. If not detected promptly, neovascular glaucoma may develop. The CVOS found that poor visual acuity is the risk factor most predictive of iris neovascularization in central venous occlusive disease. Other risk factors include large areas of retinal capillary nonperfusion and intraretinal blood.

Baseline and early natural history report. The Central Vein Occlusion Study. *Arch Ophthalmol.* 1993;111(8):1087–1095.

Klein R, Moss SE, Meuer SM, Klein BE. The 15-year cumulative incidence of retinal vein occlusion: the Beaver Dam Eye Study. *Arch Ophthalmol.* 2008;126(4):513–518.

Risk factors and causes of CRVO

The most important risk factor for the development of CRVO is age; 90% of patients are older than 50 years at the time of onset. Mild CRVOs generally occur at a younger age. The Eye Disease Case-Control Study and other studies found the following additional risk factors associated with CRVO:

- systemic arterial hypertension
- open-angle glaucoma
- diabetes mellitus
- hyperlipidemia
- hypercoagulability

It is common for patients presenting with CRVO to have elevated intraocular pressure (IOP) or frank open-angle glaucoma, either only in the affected eye or in both eyes; if

CRVO is present in 1 eye, it is important to assess the fellow eye for glaucoma. CRVO can also lead to a transient shallowing of the anterior chamber that, in some instances, leads to angle-closure glaucoma.

Oral contraceptives and diuretics have been implicated as risk factors for the development of CRVO. Although rare, predisposing hypercoagulable conditions may be present; these abnormalities include hyperhomocysteinemia, protein S deficiency, protein C deficiency, and disorders associated with vasculitis such as sarcoidosis and systemic lupus erythematosus. However, when CRVO occurs in patients older than 50 years, it is generally considered unnecessary to pursue an elaborate systemic workup.

Differential diagnosis of CRVO

It is particularly important to recognize that *hyperviscosity retinopathy* can mimic a typical CRVO. However, the retinal findings in hyperviscosity retinopathy are generally bilateral and are usually related to dysproteinemia, for example, that associated with Waldenström macroglobulinemia, multiple myeloma, or blood dyscrasias (eg, polycythemia vera). In many cases, the hyperviscosity can be reversed by treating the underlying condition. To assess for these conditions, diagnostic testing may include complete blood count, serum protein electrophoresis, and a measure of whole-blood viscosity. *Ocular ischemic syndrome* can also mimic CRVO, but hemorrhages are limited to the deeper retinal layers and vascular tortuosity is absent. Unusual diseases that affect the blood vessel wall, blood-clotting mechanisms, or blood viscosity may also produce a CRVO-like picture.

Central Vein Occlusion Study Group. Natural history and clinical management of central retinal vein occlusion. *Arch Ophthalmol*. 1997;115(4):486–491.

Fuller JJ, Mason JO III. Retinal vein occlusions: update on diagnostic and therapeutic advances. *Focal Points: Clinical Modules for Ophthalmologists*. San Francisco: American Academy of Ophthalmology; 2007, module 5.

Evaluation and management of CRVO

To determine whether the vein occlusion is nonischemic or ischemic, the examiner should assess the patient's visual acuity, visual fields, and relative afferent defect via ophthalmoscopy, fluorescein angiography, OCT, and electroretinography. It is important to perform gonioscopy regularly during follow-up to check for angle neovascularization.

If the evaluation indicates that common risk factors for CRVO are absent, or if the patient is less than 50 years of age, a thorough investigation should be considered, possibly including a workup for thrombophilia.

Patients with CRVO should be warned about the possibility of worsening vision; eyes that initially appear perfused sometimes develop progressive ischemia. During the CVOS, 16% of initially nonischemic CRVOs converted to ischemia by 4 months of follow-up; by 36 months, the percentage had increased to 34%.

Follow-up In the absence of treatment, patients with CRVO should be monitored monthly during the first 6 months for evidence of progression and development of anterior segment neovascularization or neovascular glaucoma. Patients treated with anti-VEGF agents should be observed for a similar duration after discontinuation of the drugs.

Complications The most common complications of CRVO are vitreous hemorrhage, anterior segment neovascularization, and neovascular glaucoma. Vitreous hemorrhage may occur in the absence of obvious neovascularization, and neovascular glaucoma can occur from angle neovascularization with or without iris neovascularization.

Stem MS, Talwar N, Comer GM, Stein JD. A longitudinal analysis of risk factors associated with central retinal vein occlusion. *Ophthalmology*. 2013;120(2):362–370.

Treatment of CRVO

Pharmacologic management Pharmacologic management is currently the mainstay of RVO management. See the section Pharmacologic Management of Retinal Vein Occlusion for a discussion of this topic.

Surgical management of CRVO

MACULAR LASER SURGERY The CVOS demonstrated that grid pattern laser in CRVO with macular edema does not improve visual acuity and is therefore not recommended.

PANRETINAL PHOTOCOAGULATION The CVOS found that prophylactic panretinal photocoagulation (PRP) did not result in a statistically significant decrease in the incidence of iris neovascularization. In fact, 20% of participants who received the prophylactic PRP still developed iris neovascularization. Therefore, patients at high risk of iris neovascularization should be closely monitored. Although the CVOS investigators recommended waiting until an undilated gonioscopic examination revealed at least 2 clock-hours of iris neovascularization before performing PRP, in clinical practice PRP is often performed at the first sign of iris neovascularization, particularly when close follow-up is not possible or seems unlikely. Wide-field angiography provides expanded visualization of peripheral nonperfusion in CRVO; however, there is no evidence to support altered treatment criteria based on this information.

Central Vein Occlusion Study Group. A randomized clinical trial of early panretinal photocoagulation for ischemic central vein occlusion. The Central Vein Occlusion Study Group N report. *Ophthalmology*. 1995;102(10):1434–1444.

PARS PLANA VITRECTOMY CRVOs complicated by vitreous hemorrhage may benefit from pars plana vitrectomy. Vitrectomy is used for vision rehabilitation or to accomplish retinal ablative treatment in the management of anterior segment neovascularization and neovascular glaucoma. For neovascular glaucoma, a glaucoma valve may be implanted concurrently.

OTHER SURGICAL APPROACHES Several surgical approaches have been abandoned due to lack of evidence for their efficacy and/or their high complication rates. These approaches include creation of peripheral laser anastomosis between a retinal vein and the choroidal circulation, radial relaxing incision of the optic nerve scleral ring to decompress the central retinal vein, and retinal vein cannulation with infusion of tissue plasminogen activator (tPA).

Pharmacologic Management of Retinal Vein Occlusion

Pharmacologic management has become the mainstay treatment of CME secondary to RVO. Because studies are increasingly not separating BRVO and CRVO when evaluating

pharmacologic treatment of macular edema secondary to retinal venous occlusive disease, they are discussed together in this section.

Intravitreal anti-VEGF therapy

The initial studies of anti-VEGF therapy of RVO were BRAVO (Study of the Efficacy and Safety of Ranibizumab Injection in Patients With Macular Edema Secondary to Branch Retinal Vein Occlusion) and CRUISE (Study of the Efficacy and Safety of Ranibizumab Injection in Patients With Macular Edema Secondary to Central Retinal Vein Occlusion). In these studies, monthly injections of either 0.5- or 0.3-mg *ranibizumab* or sham injections were administered for the treatment of macular edema secondary to venous occlusions. At 6 months, 15 or more ETDRS letters were gained in BRAVO in 61.1%, 55.2%, and 28.8% of eyes treated with 0.5- or 0.3-mg *ranibizumab* or sham injection, respectively; in CRUISE, the letters were gained in 47.7%, 46.2%, and 16.9% of eyes.

Similar results were achieved with intravitreal *aflibercept* (also called *VEGF-Trap*) in the VIBRANT (Study to Assess the Clinical Efficacy and Safety of VEGF Trap-Eye in Patients With Branch Retinal Vein Occlusion), COPERNICUS (Vascular Endothelial Growth Factor Trap-Eye: Investigation of Efficacy and Safety in Central Retinal Vein Occlusion; conducted within North America), and GALILEO (similar protocol, but conducted outside North America) studies. The benefits were maintained during the second 6 months of these aflibercept studies, during which as-needed treatment was administered.

Bevacizumab is also effective for the management of CME secondary to RVO, as demonstrated in several controlled and uncontrolled studies (Fig 6-13). In SCORE2 (Study of Comparative Treatments for Retinal Vein Occlusion 2) bevacizumab was shown to be noninferior to aflibercept in the treatment of macular edema secondary to CRVO. In CRAVE (Comparison of Anti-VEGF Agents in the Treatment of Macular Edema from Retinal Vein Occlusion), the 98 patients who were randomized to receive either monthly bevacizumab or ranibizumab treatment for macular edema secondary to CRVO and BRVO showed no significant differences in central foveal thickness reduction or visual acuity improvement. As a result of these comparative efficacy studies and the general clinical impression of the equivalency of the anti-VEGF agents in the treatment of RVO, many practitioners use the 3 anti-VEGF drugs interchangeably. In practice, anti-VEGF agent administration strategies for RVO treatment include monthly dosing, as-needed treatment, and treat-and-extend approaches.

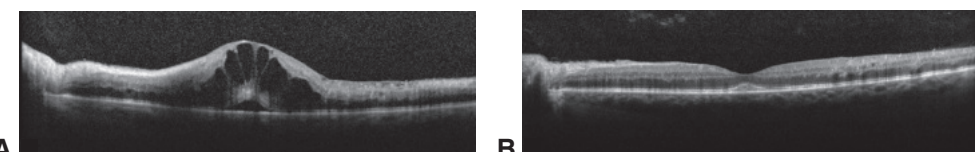


Figure 6-13 CME secondary to CRVO, before and after treatment. **A**, SD-OCT scan shows severe CME with foveal detachment in a patient with a nonischemic CRVO. Visual acuity was 20/200. **B**, One month after intravitreal injection of bevacizumab, 1.25 mg, the cystic changes and foveal detachment resolved, and the visual acuity was 20/25. (Courtesy of Colin A. McCannel, MD.)

- Brown DM, Campochiaro PA, Bhisitkul RB, et al. Sustained benefits from ranibizumab for macular edema following branch retinal vein occlusion: 12-month outcomes of a phase III study. *Ophthalmology*. 2011;118(8):1594–1602.
- Campochiaro PA, Brown DM, Awh CC, et al. Sustained benefits from ranibizumab for macular edema following central retinal vein occlusion: twelve-month outcomes of a phase III study. *Ophthalmology*. 2011;118(10):2041–2049.
- Scott IU, VanVeldhuisen PC, Ip MS, et al; SCORE2 Investigator Group. Effect of bevacizumab vs aflibercept on visual acuity among patients with macular edema due to central retinal vein occlusion: the SCORE2 randomized clinical trial. *JAMA*. 2017;317(20):2072–2087.

Intravitreal corticosteroids

Intravitreal corticosteroids were the first pharmacological therapy that appeared efficacious for retinal vein occlusion; however, their specific risks include cataract formation (common) and steroid-induced elevation of IOP (in 20%–65% of individuals). When making patient care decisions, clinicians must weigh these risks against the benefits as well as any available alternative treatments. SCORE (Standard Care Versus Corticosteroid for Retinal Vein Occlusion) found that *intravitreal triamcinolone* injection in eyes with BRVO was comparable in efficacy to macular grid laser treatment with respect to 3 or more lines of visual acuity gain. Because eyes receiving triamcinolone were more likely to develop a cataract or experience elevated IOP, the study investigators concluded that macular grid laser therapy remained the benchmark against which other treatments should be compared. In the CRVO arm of the SCORE study, at 1 year follow-up, 27% of eyes treated with 1 mg of *triamcinolone* and 26% of eyes treated with 4 mg of triamcinolone had improved by 15 ETDRS letters or more, compared with 7% of eyes in the observation group.

The GENEVA study (Randomized, Sham-Controlled Trial of Dexamethasone Intravitreal Implant in Patients With Macular Edema due to Retinal Vein Occlusion) explored the use of a *dexamethasone* (0.7-mg) intravitreal implant to treat macular edema secondary to venous occlusive disease. A statistically significant 15-letter or more improvement from baseline corrected distance visual acuity (CDVA) was achieved between 30 and 90 days, with the greatest response (29%) at day 60. At day 180, there was no longer a significant difference between the sham (18%) and treatment groups (22% for the *dexamethasone* 0.7 mg group). The COMRADE (Clinical Efficacy and Safety of Ranibizumab Versus Dexamethasone for Central Retinal Vein Occlusion) study compared the dexamethasone (0.7-mg) implant with monthly ranibizumab treatment. At the first 3 monthly follow-up visits, the efficacy of the two treatments was similar; however, at months 4–6, the eyes treated with ranibizumab had significantly better visual acuity scores, and at month 6, the mean ETDRS letters gained for the ranibizumab group and the dexamethasone (0.7-mg) implant group were 12.86 versus 2.96 letters, respectively ($P < .001$).

- Haller JA, Bandello F, Belfort R Jr, et al; OZURDEX GENEVA Study Group. Randomized, sham-controlled trial of dexamethasone intravitreal implant in patients with macular edema due to retinal vein occlusion. *Ophthalmology*. 2010;117(6):1134–1146.

- Hoerauf H, Feltgen N, Weiss C, et al; COMRADE-C Study Group. Clinical efficacy and safety of ranibizumab versus dexamethasone for central retinal vein occlusion (COMRADE C): a European label study. *Am J Ophthalmol.* 2016;169:258–267.
- Scott IU, Ip MS, VanVeldhuizen PC, et al; SCORE Study Research Group. A randomized trial comparing the efficacy and safety of intravitreal triamcinolone with standard care to treat vision loss associated with macular edema secondary to branch retinal vein occlusion: the Standard Care vs Corticosteroid for Retinal Vein Occlusion (SCORE) study report 6. *Arch Ophthalmol.* 2009;127(9):1115–1128.

Systemic anticoagulation

Systemic anticoagulation is not recommended for the treatment of RVO. Case series suggest the patient may experience worse outcomes due to increased bleeding in the retina.

Ocular Ischemic Syndrome and Retinopathy of Carotid Occlusive Disease

Ocular ischemic syndrome (OIS) comprises the ocular symptoms and signs attributable to chronic severe ocular hypoperfusion caused by ipsilateral carotid obstruction or ophthalmic artery obstruction.

Symptoms and Signs of Ocular Ischemic Syndrome

Symptoms of OIS typically include gradual vision loss that develops over a period of weeks to months, aching pain localized to the orbital area of the affected eye, and prolonged vision recovery after exposure to bright light. Anterior segment signs include iris neovascularization in two-thirds of eyes and an anterior chamber cellular response in about one-fifth of eyes. Although iris and angle neovascularization are common, only one-half of eyes with this condition show an increase in IOP; the low or normal IOP in the other half is most likely caused by impaired aqueous production.

Ocular ischemic syndrome can cause a retinopathy similar in appearance to a partial occlusion of the central retinal vein; therefore, it was originally called venous stasis retinopathy. Typical retinal findings include narrowed arteries, dilated but not very tortuous veins, hemorrhages, microaneurysms, and neovascularization of the optic nerve head, retina, or both (Fig 6-14). The retinal hemorrhages in carotid occlusive disease are usually deep and round and are more often located in the midperipheral retina. A helpful method for differentiating between the 2 entities is to measure the retinal artery pressure, either by using an ophthalmodynamometer, or by gently pushing on the eye during the examination and observing the central retinal artery. An eye with CRVO will have normal artery pressure, whereas one with carotid occlusive disease will have low artery pressure, and the artery will therefore collapse easily.

Fluorescein angiography reveals delayed choroidal filling in 60% of eyes, prolonged arteriovenous transit time in 95% of eyes, and prominent vascular staining (particularly of the arteries) in 85% of eyes. Electroretinography demonstrates global amplitude reduction in disorders that affect the blood supply to the photoreceptors as well as the inner retina. An electronegative electroretinogram occurs if the blood supply to the inner retina

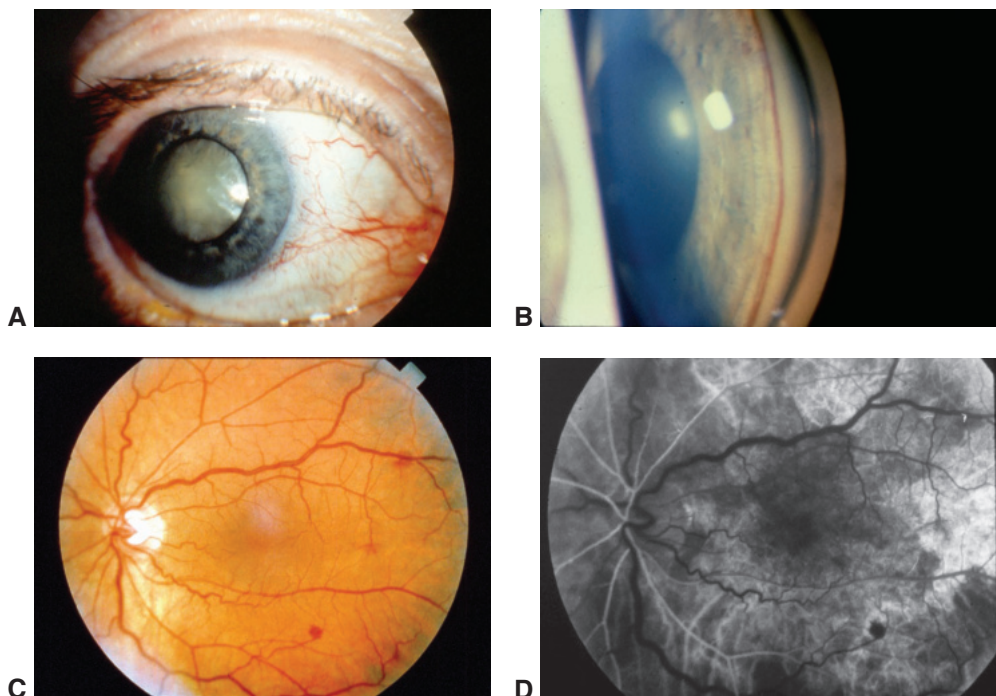


Figure 6-14 Ocular ischemic syndrome (OIS). **A**, Clinical photograph of an eye with OIS displays features of conjunctival injection, cataract, and rubeosis iridis. **B**, Gonioscopic appearance of neovascularization of the iridocorneal angle due to OIS. **C**, Fundus photograph of an eye with OIS shows features of venous dilation, midperipheral intraretinal hemorrhages, and attenuated arterioles. **D**, Fluorescein angiography image taken at 19 seconds (arterial phase) demonstrates a prolonged arm-to-retina circulation time and a patchy choroidal filling pattern. (Courtesy of Neal H. Atebara, MD.)

is compromised as in CRVO or central retinal artery occlusion (CRAO), while supply to the photoreceptors is preserved.

Etiology and Course of Ocular Ischemic Syndrome

The most common etiology of OIS is atherosclerosis. Other causes include Eisenmenger syndrome, carotid artery dissection, temporal arteritis, and other inflammatory conditions. Most patients are older than 55 years. Typically, a 90% or greater ipsilateral obstruction is necessary to cause OIS. Approximately 20% of cases involve both eyes.

The visual prognosis for eyes with OIS is uncertain, but when rubeosis iridis is also present, visual acuity in more than 90% of cases will decline to 20/200 or worse within 1 year after diagnosis. For this reason, timely diagnosis is essential.

Approximately one-half of patients with OIS also have ischemic cardiovascular disease; one-fourth have had a previous cerebrovascular accident; and one-fifth have peripheral atherosclerotic vascular disease so severe that a previous surgical procedure was necessary. The stroke rate is higher than that of the general population, and the 5-year mortality is approximately 40%, mostly resulting from complications of cardiovascular disease.

Treatment of Ocular Ischemic Syndrome

The most definitive treatment for OIS appears to be carotid artery stenting and endarterectomy, although visual acuity outcomes are variable. Unfortunately, these procedures are ineffective when there is 100% obstruction, which is often the case. Extracranial to intracranial bypass surgery has been attempted but has been shown to be ineffective for preventing loss of vision or stroke. In eyes with iris neovascularization and low or normal IOP as a result of impaired ciliary body perfusion and decreased aqueous formation, carotid reperfusion can lead to increased aqueous formation and a severe rise in IOP. Full-scatter PRP results in regression of anterior segment neovascularization in approximately two-thirds of cases. Anti-VEGF therapy has also been shown to cause regression of anterior segment neovascularization in patients with OIS.

Brown GC, Sharma S. Ocular ischemic syndrome. In: Schachat AP, Wilkinson CP, Hinton DR, Sadda SR, Wiedemann P, eds. *Ryan's Retina*. 6th ed. Philadelphia: Elsevier/Saunders; 2018:chap 62.

Arterial Occlusive Disease

The blood supply to the inner layers of the retina is derived entirely from the central retinal artery, unless a cilioretinal artery is present (20%–25% of eyes). Retinal ischemia results from disease processes that affect the vessels anywhere from the common carotid artery to the intraretinal arterioles. The signs and symptoms of arterial obstruction depend on the vessel involved: occlusion of a peripheral arteriole may be asymptomatic, whereas an ophthalmic artery occlusion can cause total blindness.

Capillary Retinal Arteriole Obstruction (Cotton-Wool Spots)

Acute obstruction in the distribution of the radial peripapillary capillary net leads to the formation of a nerve fiber layer (NFL) infarct, or cotton-wool spot, which causes impaired axoplasmic transport in the NFL (Fig 6-15). These inner retinal ischemic spots are superficial, white, and typically one-fourth optic disc area or less in size. They usually fade in 5–7 weeks, although spots present in association with diabetic retinopathy often remain longer. A subtle retinal depression caused by inner retinal ischemic atrophy may develop in an area of prior ischemia. The effect on visual function, including loss of visual acuity and field defects, is related to the size and location of the occluded area.



Figure 6-15 Fundus photograph shows a cotton-wool spot. (Courtesy of Gary C. Brown, MD.)

The most common cause of cotton-wool spots is diabetic retinopathy (discussed in Chapter 5). Other causes include

- systemic arterial hypertension
- HIV-associated retinopathy
- anemia (severe)
- radiation retinopathy
- sickle cell retinopathy
- cardiac embolic disease
- carotid artery obstructive disease
- vasculitis
- collagen vascular disease
- leukemia

If even 1 cotton-wool spot is discovered in the fundus in an otherwise apparently healthy eye, the clinician should initiate a workup for the most likely underlying etiologies.

Brown GC, Brown MM, Hiller T, Fischer D, Benson WE, Magargal LE. Cotton-wool spots. *Retina*. 1985;5(4):206–214.

Branch Retinal Artery Occlusion

Although an acute BRAO may be subtle and unapparent on initial ophthalmoscopic examination, within hours to days, it can lead to edematous opacification caused by infarction of the inner retina in the distribution of the affected vessel (Fig 6-16). In time, the occluded vessel recanalizes, perfusion returns, and the edema resolves; however, a permanent visual field defect remains. A retinal arterial occlusion that occurs outside of the posterior pole may be clinically asymptomatic.

Occlusion at any site is caused by embolization or thrombosis of the affected vessel. There are 3 main varieties of emboli:

1. cholesterol emboli (Hollenhorst plaques) arising in the carotid arteries (Fig 6-17)
2. platelet-fibrin emboli associated with large-vessel arteriosclerosis
3. calcific emboli arising from diseased cardiac valves

In rare cases, emboli might be caused by cardiac myxoma, long-bone fractures (fat emboli), infective endocarditis (septic emboli), and intravenous drug use (talc emboli). Although



Figure 6-16 Inferotemporal branch retinal artery obstruction. The fundus photograph shows opacification of the retina in the distribution of the occluded vessel (inferior macula). In this case, the visual acuity was 20/30 at presentation but returned to 20/20 over several weeks. (Courtesy of Gary C. Brown, MD.)



Figure 6-17 Hollenhorst plaque. Fundus photograph shows a Hollenhorst plaque lodged at a bifurcation of the superior arcade arteriole (arrow). Hollenhorst plaques do not typically cause vascular obstruction and can remain at a bifurcation indefinitely. Occasionally, they can be observed to move with blood flow. (Courtesy of Tara A. McCannel, MD, PhD.)

rare, migraine can cause ocular arterial occlusions in patients younger than 30–40 years. Other possible causes of emboli include

- arrhythmias
- mitral valve prolapse
- oral contraceptive use or pregnancy
- coagulation disorders
- trauma
- sickle cell disease
- inflammatory and infectious etiologies such as toxoplasmic retinochoroiditis and syphilis
- connective tissue disorders, including GCA

Initial management is directed toward determining the underlying systemic etiologic factors. Retinal arterial occlusions should be referred *urgently* to an emergency department for a stroke workup. No specific ocular therapy has been found to be consistently effective in improving the visual prognosis. Lowering IOP and applying intermittent pressure on the globe (“ocular massage”) may dislodge an embolus from a large central vessel toward a more peripheral location, but the efficacy of these maneuvers in improving vision outcomes is unproven.

Hayreh SS, Podhajsky PA, Zimmerman MB. Branch retinal artery occlusion: natural history of visual outcome. *Ophthalmology*. 2009;116(6):1188–1194.

Wang JJ, Cugati S, Knudtson MD, et al. Retinal arteriolar emboli and long-term mortality: pooled data analysis from two older populations. *Stroke*. 2006;37(7):1833–1836.

Cilioretinal Artery Occlusion

A distinct clinical entity is the occlusion of the cilioretinal artery, which arises from the short posterior ciliary vessels rather than the central retinal artery. These vessels, which are present in about 18%–32% of eyes, usually contribute to some portion of the macular circulation. Most commonly, their occlusion occurs in patients with a central retinal vein occlusion; it is postulated that the increased hydrostatic pressure associated with CRVO can reduce blood flow in the cilioretinal artery to the point of stagnation.

When cilioretinal artery occlusion occurs in isolation, GCA should be considered.

Hayreh SS, Fraterrigo L, Jonas J. Central retinal vein occlusion associated with cilioretinal artery occlusion. *Retina*. 2008;28(4):581–594.

Paracentral Acute Middle Maculopathy

Paracentral acute middle maculopathy (PAMM) refers to acute ischemic events that affect the deep macular capillary layers. It is best visualized as hyperreflective bands on SD-OCT. There are 2 variants: type 1 affects the superficial capillary plexus in the outer plexiform layer (OPL)/inner nuclear layer (INL) region, and type 2 affects the deep capillary plexus in the OPL/outer nuclear layer (ONL) region. Visual consequences vary; upon resolution, type 1 lesions produce INL thinning, and type 2 lesions cause disturbance of the ellipsoid or inner segment and outer segment line.

Sarraf D, Rahimy E, Fawzi AA, et al. Paracentral acute middle maculopathy: a new variant of acute macular neuroretinopathy associated with retinal capillary ischemia. *JAMA Ophthalmol*. 2013;131(10):1275–1287.

Central Retinal Artery Occlusion

Sudden, complete, and painless loss of vision in one eye is characteristic of CRAO. The retina becomes opaque and edematous, particularly in the posterior pole, where the nerve fiber and ganglion cell layers are thickest (Fig 6-18). The orange reflex from the intact choroidal vasculature beneath the foveola thus stands out in contrast to the surrounding opaque neural retina, producing a cherry-red spot. Even prior to the appearance of the cherry-red spot, OCT imaging reveals a normal macular profile with diffuse hyperreflectivity and loss of internal layer definition (Activity 6-2; Fig 6-19). A cilioretinal artery may preserve some degree of macular vision if the area of retina perfused by it includes a sufficient portion of the maculopapillary bundle as well as the perifovea (see Chapter 1, Fig 1-8).



ACTIVITY 6-2 OCT Activity: SD-OCT scan of an eye with CRAO and cilioretinal artery sparing.
Courtesy of Colin A. McCannel, MD.



With time, the central retinal artery reopens or recanalizes and the retinal edema clears; however, the effect on visual acuity is usually permanent because the inner retina has been infarcted. In one study, 66% of eyes had final visual acuity worse than 20/400,

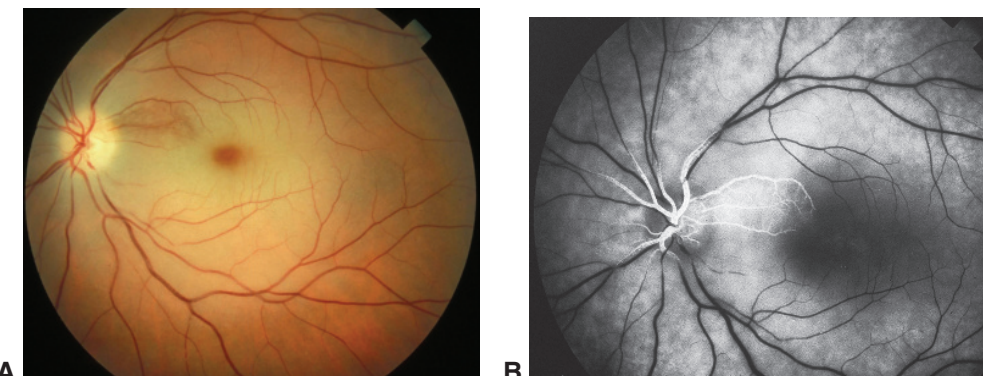


Figure 6-18 Central retinal artery occlusion (CRAO). **A**, Fundus photograph shows superficial macular opacification and a cherry-red spot in the foveola. **B**, Angiography image reveals preservation of a sector of superonasal macula related to cilioretinal vessels, perfused in this image. The patient had hand motions visual acuity. (*Courtesy of Hermann D. Schubert, MD.*)

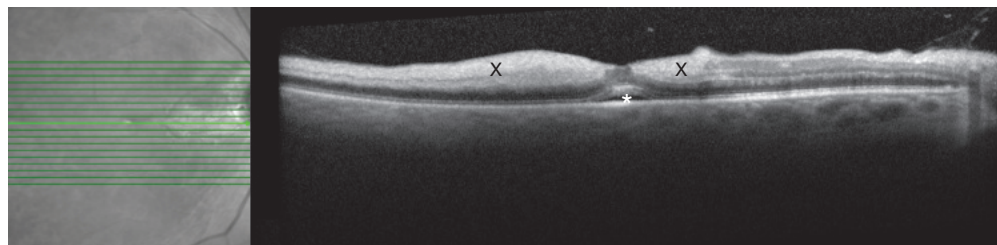


Figure 6-19 SD-OCT scan of a case of CRAO similar to the one shown in Figure 6-18 with cilioretinal artery sparing shows hyperreflectivity in the area of clinical opacification of the inner two-thirds of the retina in the affected areas (X). All retinal layers are identifiable in the area of retina perfused by the cilioretinal artery, adjacent to the optic nerve head. The retina in the fovea is spared from opacification, resulting in the appearance of a cherry-red spot on examination. Subfoveal fluid (asterisk) is variably present in these cases. (*Courtesy of Colin A. McCannel, MD.*)

and 18% of eyes had 20/40 or better. Most cases of 20/40 or better visual acuity occur in the presence of a patent cilioretinal artery (see Fig 6-18; also see Chapter 1, Fig 1-8). Vaso-occlusive vision loss to the level of no light perception is usually caused by choroidal vascular insufficiency from partial or complete ophthalmic artery occlusion or occlusions of the ciliary arteries in conjunction with occlusion of the central retinal artery (Fig 6-20). Studies in nonhuman primates have suggested that irreversible damage to the sensory retina occurs after 90 minutes of complete CRAO. Nevertheless, clinical return of vision can occur in some instances even if the obstruction has persisted for many hours.

CRAO is most often caused by embolization or atherosclerosis-related thrombosis occurring at the level of the lamina cribrosa. Less common causes are hemorrhage under an atherosclerotic plaque, thrombosis, trauma, spasm, and a dissecting aneurysm within the central retinal artery.

Emboli within the carotid distribution may cause transient ischemic attacks, amaurosis fugax, or both. Bright cholesterol emboli, or Hollenhorst plaques, typically located

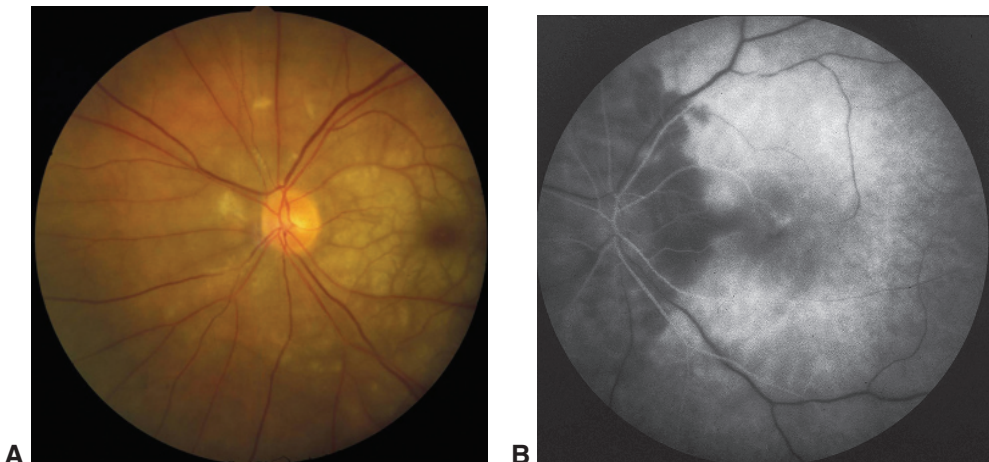


Figure 6-20 Central retinal and parent short ciliary artery occlusion. **A**, Fundus photograph of acute central retinal and short ciliary artery obstruction. Severe retinal opacification is present. The patient's visual acuity was no light perception. **B**, Fluorescein angiography image taken 3 minutes after injection reveals hypofluorescence of the retinal vessels, the nasal choroid, and the optic nerve head, corresponding to an occlusion of the central retinal artery and nasal parent ciliary artery. The latter results in ischemia in the distribution of the short posterior ciliary arteries with a vertical watershed of choroidal perfusion. (Courtesy of Hermann D. Schubert, MD.)

at retinal arterial bifurcations, suggest a carotid atheromatous origin and may be an indication for endarterectomy if accompanied by relevant symptoms and findings. Systemic etiologic considerations, such as those listed earlier in this chapter for BRAO, are important and require evaluation. The leading cause of death in patients with retinal arterial obstruction is cardiovascular disease with an elevated risk of myocardial infarction within the first 7 days following onset of the obstruction. Immediate referral for brain imaging in a stroke center is indicated, along with evaluation of the carotid arteries via Doppler ultrasound or computed tomography angiography (CTA) and of the cardiac valves via transesophageal echocardiography. Studies have reported that as many as 78% of patients may have undiagnosed risk factors.

GCA accounts for approximately 1%–2% of CRAO cases. In cases of CRAO in which emboli are not readily visible, a thorough evaluation for GCA should be considered. The risk of GCA increases with increasing age. The erythrocyte sedimentation rate (ESR), C-reactive protein level, and fibrinogen levels—markers of inflammation—are usually elevated and can be checked. A complete blood count may detect an elevated platelet count, which is also suggestive of GCA; the blood count also aids in the interpretation of the ESR. If GCA is suspected as a cause, systemic corticosteroid therapy should be instituted promptly because the second eye can become involved by ischemia within hours to days after the first. In addition, a temporal artery biopsy should be performed shortly thereafter to confirm the diagnosis and justify the need for prolonged corticosteroid treatment. See BCSC Section 5, *Neuro-Ophthalmology*, for further discussion of GCA.

Ahn SJ, Woo SJ, Park KH, Jung C, Hong JH, Han MK. Retinal and choroidal changes and visual outcome in central retinal artery occlusion: an optical coherence tomography study. *Am J Ophthalmol*. 2015;159(4):667–676.

- Atkins EJ, Bruce BB, Newman NJ, Biousse V. Translation of clinical studies to clinical practice: survey on the treatment of central retinal artery occlusion. *Am J Ophthalmol.* 2009;148(1):172–173.
- Callizo J, Feltgen N, Pantenburg S, et al; European Assessment Group for Lysis in the Eye. Cardiovascular risk factors in central retinal artery occlusion: results of a prospective and standardized medical examination. *Ophthalmology.* 2015;122(9):1881–1888.
- Falkenberry SM, Ip MS, Blodi BA, Gunther JB. Optical coherence tomography findings in central retinal artery occlusion. *Ophthalmic Surg Lasers Imaging.* 2006;37(6):502–505.
- Park SJ, Choi NK, Yang BR, et al. Risk and risk periods for stroke and acute myocardial infarction in patients with central retinal artery occlusion. *Ophthalmology.* 2015;122(11):2336–2343.

Management of CRAO

If therapy for CRAO is to be instituted, it should be undertaken without delay. Unfortunately, treatment is effective in only a small fraction of cases. Simple therapeutic approaches, such as reducing IOP by administering IOP-lowering medications and performing ocular massage, are not without benefit. However, outcomes from both anterior chamber paracentesis and carbogen (a mixture of 95% oxygen and 5% carbon dioxide) vasodilatory inhalation therapy have shown inconsistent success, as have hyperbaric oxygen therapy, catheterization of the ophthalmic artery with tPA infusion, and transvitreal Nd:YAG embolysis. Initial management should also include an evaluation directed toward determining the underlying systemic etiologic factors, and an *urgent* referral to an emergency department for a stroke workup should be undertaken.

Iris neovascularization develops in approximately 18% of eyes within 1–12 weeks after acute CRAO, with a mean time interval of approximately 4–5 weeks. Full-scatter PRP results in regression of anterior segment neovascularization in approximately two-thirds of cases. Anti-VEGF therapy in conjunction with PRP has been reported to have value as well.

Ophthalmic Artery Occlusion

Ophthalmic artery occlusion is very rare. Clinically, the disorder typically produces vision loss to the level of light perception or no light perception because simultaneous nonperfusion of the choroid and retina results in ischemia of all retinal layers. A cherry-red spot may not be present; both the inner retina and outer retina become opacified from the infarction, resulting in an absence of contrast difference between foveal and perifoveal retina that would produce such a spot.

Ophthalmic artery occlusion may be caused by dissection of the internal carotid artery, orbital mucormycosis, or embolization. An increasing number of ophthalmic artery occlusions caused by various cosmetic facial-filler injections, particularly into the periocular and brow area, have been reported, as popularity for such procedures has increased (Fig 6-21). In autopsy studies of patients who died during active GCA, up to 76% had some degree of ophthalmic artery affected by vasculitis; clinically, however, ophthalmic artery occlusion is rare in GCA.



Figure 6-21 Fundus photographic montage of the left eye of a 44-year-old woman following an ipsilateral injection of synthetic calcium hydroxylapatite gel into her left lateral lower eyelid for cosmetic purposes. Sudden loss of vision ensued to the level of no light perception. An ophthalmic artery occlusion occurred from presumed retrograde flow of the injectable cosmetic filler into the ophthalmic artery by way of anastomotic arteries in the orbit bridging the internal and external carotid circulations. The white filler material is visible in the retinal circulation and choroidal blood vessels. (*Courtesy of Kathryn Sun, MD, PhD, Thomas F. Essman, MD, and Brenda Schoenauer, CDOS.*)

Arterial Macroaneurysms

Retinal arterial macroaneurysms are acquired ectasias of the first 3 orders of retinal arterioles. Large macroaneurysms can actually traverse the full thickness of the retina. Vision loss may occur from embolic or thrombotic occlusion of the end arteriole (white infarct) or from sub–internal limiting membrane, intraretinal, subretinal, or vitreous hemorrhage, often in combination. Other retinal findings may include capillary telangiectasia and remodeling, as well as retinal edema and exudate involving the macula (Fig 6-22). Often, there are multiple arterial macroaneurysms, although only 10% of cases are bilateral. Arterial macroaneurysms are associated with systemic arterial hypertension in about two-thirds of cases and may occur in the area of previous vascular occlusions. Sclerosis and spontaneous closure often accompany macroaneurysm-related hemorrhage; bleeding more than once is rare.

Laser photocoagulation treatment may be considered if increasing edema in the macula threatens central visual function. In most instances, moderate-intensity laser treatment of the retina—performed immediately adjacent to the macroaneurysm using 2–3 rows of large-spot-size (200–500 μm) applications—results in closure. Some specialists prefer direct treatment. Caution should be used when treating macroaneurysms that occur in macular arterioles because a primary complication of the disease and its therapy



Figure 6-22 Fundus photograph of a retinal arterial macroaneurysm with some exudate in the superior macula, resulting from leakage of the lesion, and mild hemorrhage. (Courtesy of Colin A. McCannel, MD.)

is thrombosis with retinal arterial obstruction distal to the macroaneurysm. Anti-VEGF treatment has been reported to hasten resolution of macular edema from macroaneurysms without improving ultimate visual outcome.

- Cho HJ, Rhee TK, Kim HS, et al. Intravitreal bevacizumab for symptomatic retinal arterial macroaneurysm. *Am J Ophthalmol.* 2013;155(5):898–904.
- Lee EK, Woo SJ, Ahn J, Park KH. Morphologic characteristics of retinal arterial macroaneurysm and its regression pattern on spectral-domain optical coherence tomography. *Retina.* 2011;31(10):2095–2101.
- Pitkänen L, Tommila P, Kaarniranta K, Jääskeläinen JE, Kinnunen K. Retinal arterial macroaneurysms. *Acta Ophthalmol.* 2014;92(2):101–104.

Other Retinal Vascular Diseases

Sickle Cell Retinopathy

Sickle cell anemia is the most common inherited blood disorder in the United States. The sickle cell hemoglobinopathies of greatest ocular importance are those in which mutant hemoglobins S, C, or both are inherited instead of normal hemoglobin A (see BCSC Section 2, *Fundamentals and Principles of Ophthalmology*). Sickle cell hemoglobinopathies are most prevalent in the Black population, and affect about 10% of African Americans (Table 7-1). Thalassemia, in which the α - or β -polypeptide chain is defective, is rare but frequently causes retinopathy. Although sickling and solubility tests (sickle cell preparations) are reliable indicators of the presence of hemoglobin S and are therefore excellent for sickle cell anemia screening, these tests do not distinguish between heterozygous and homozygous states in the hemoglobinopathies. Patients who test positive on sickle cell preparations should also undergo hemoglobin electrophoresis testing.

Scott AW, Lutty GA, Goldberg MF. Hemoglobinopathies. In: Schachat AP, Wilkinson CP, Hinton DR, Sadda SR, Wiedemann P, eds. *Ryan's Retina*. Vol 1. 6th ed. Philadelphia: Elsevier/Saunders; 2018:chap 60.

Nonproliferative Sickle Cell Retinopathy

The retinal changes in nonproliferative sickle cell retinopathy (NPSR) are caused by arteriolar and capillary occlusion. Anastomosis and remodeling occur in the periphery,

Table 7-1 Incidence of Sickle Cell Hemoglobinopathies in North America

Hemoglobinopathy	Incidence in Population (%)	Incidence of Proliferative Retinopathy in Subgroups
Any sickle hemoglobin	10	—
Sickle cell trait (AS)	8	Uncommon
Hemoglobin C trait (AC)	2	Uncommon
Sickle cell homozygote (SS)	0.4	3% ^a
Sickle cell hemoglobin C (SC)	0.2	33% ^a
Sickle cell thalassemia (SThal)	0.03	14% ^a
Homozygous C (CC)	0.016	Unknown

^a Approximate.

Used with permission from Fekrat S, Goldberg MF. Sickle retinopathy. In: Regillo CD, Brown GC, Flynn HW Jr, eds. *Vitreoretinal Disease: The Essentials*. New York: Thieme; 1999:333. ©Thieme.

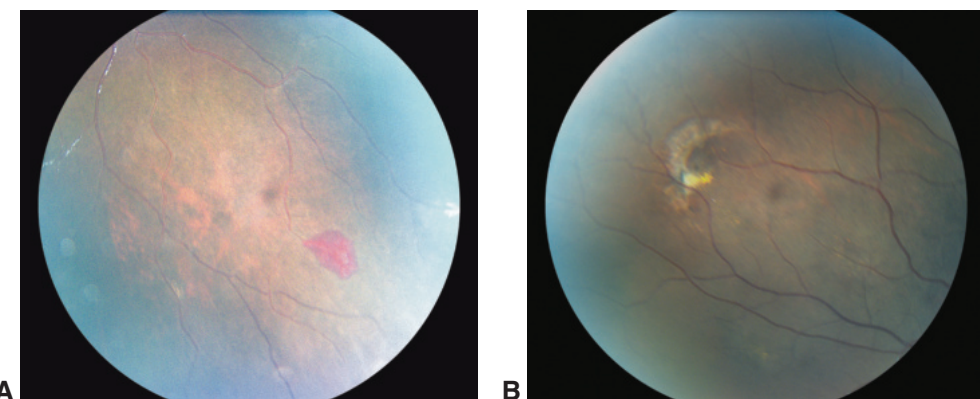


Figure 7-1 Salmon-patch hemorrhage in sickle cell retinopathy. **A**, Peripheral fundus photograph of a patient with sickle cell disease shows a retinal hemorrhage unrelated to proliferation; instead, it is the result of infarction of the retina from a vascular occlusion—a *salmon patch*. **B**, Peripheral fundus photograph of an iridescent, or refractile, patch that represents an area of previous, now resorbed, retinal hemorrhage (salmon patch). (Courtesy of G. Baker Hubbard III, MD.)

as does the resorption of blood around the infarct. Salmon-patch hemorrhages represent areas of intraretinal hemorrhage that occur after a peripheral retinal arteriolar occlusion. Refractile spots are old, resorbed hemorrhages with hemosiderin deposition within the inner retina just beneath the internal limiting membrane (ILM) (Fig 7-1). Black “sunburst” lesions are localized areas of retinal pigment epithelial hypertrophy, hyperplasia, and pigment migration in the peripheral retina, probably caused by hemorrhage.

Occlusion of parafoveal capillaries and arterioles is one cause of decreased visual acuity in patients with sickle cell retinopathy. These changes can be detected on angiography, particularly with optical coherence tomography angiography (OCTA), and may be subtle (Fig 7-2) or catastrophic (Fig 7-3). Spontaneous occlusion of the central retinal artery may also develop in patients with sickle cell hemoglobinopathies.

Proliferative Sickle Cell Retinopathy

Proliferative sickle cell retinopathy (PSR) occurs most commonly with sickle cell hemoglobin C (SC), at a rate of approximately 33%. It occurs less commonly with sickle cell thalassemia (SThal), at a rate of approximately 14%. Sickled cell homozygote (SS) disease results in more systemic complications but has a very low incidence of proliferative retinopathy, approximately 3%. Proliferative retinopathy is rare with sickle cell trait (AS). The ocular complications result from ischemia secondary to infarction of the retinal tissue by means of arteriolar, precapillary arteriolar, capillary, or venular occlusions; they include retinal neovascularization, preretinal or vitreous hemorrhage, and tractional retinal detachment.

PSR has been classified into 5 stages based on the following pathogenetic sequence:

1. Peripheral arteriolar occlusions (stage 1) lead to peripheral nonperfusion and
2. peripheral arteriovenular anastomoses (stage 2), which are dilated, preexisting capillary channels.

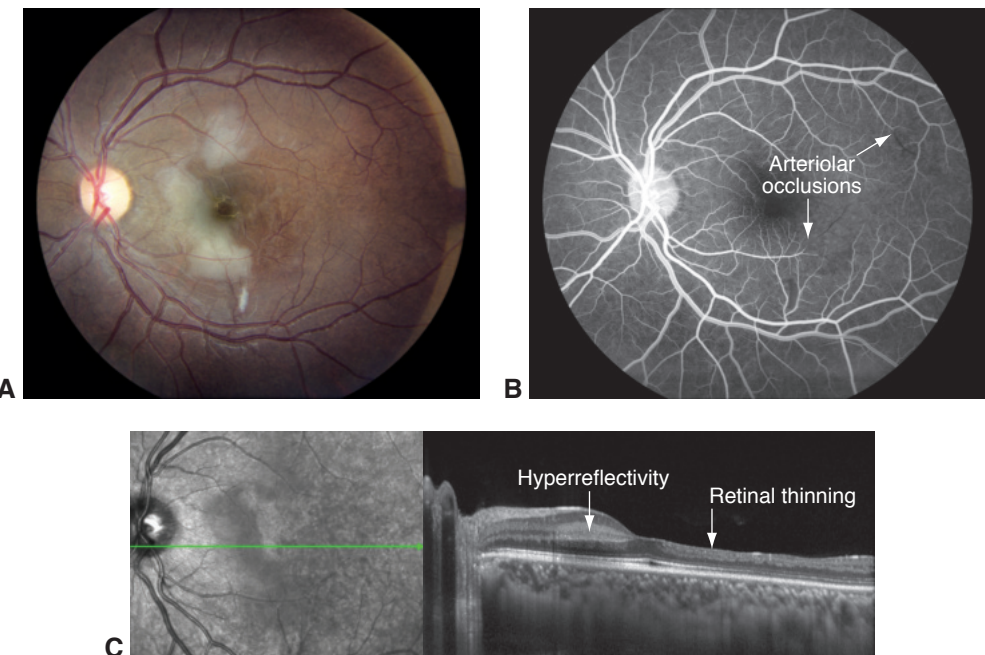


Figure 7-2 Retinal arteriolar occlusions in nonproliferative sickle cell retinopathy (NPSR). **A**, Color fundus photograph of patchy parafoveal creamy retinal infarctions in the left eye of a 21-year-old woman with sickle cell (Hb SS) disease; the sickling crisis was dehydration-induced. **B**, Fluorescein angiogram demonstrates occlusion of multiple small retinal arterioles (arrows); however, none correspond to the areas of opacified retina. Similar findings were present in the other eye. The patient maintained good central visual function. **C**, Optical coherence tomography (OCT) demonstrates *hyperreflectivity* in the middle retina corresponding to an area of creamy retinal infarction, suggesting ischemia of the intermediate and deep capillary plexus. There is temporal *retinal thinning* with loss of the inner retinal layers, indicating previous infarctions in that area. (Courtesy of Michael Dollin, MD.)

3. Preretinal sea fan neovascularization (stage 3) may occur at the posterior border of areas of nonperfusion and lead to
4. vitreous hemorrhage (stage 4) and
5. tractional retinal detachment (stage 5).

PSR is one of many retinal vascular diseases in which extraretinal fibrovascular proliferation occurs in response to retinal ischemia. Whereas the neovascularization in eyes with proliferative diabetic retinopathy (PDR) generally begins postequatorially, the neovascularization in PSR is located more peripherally (Fig 7-4). Another way in which PSR can be differentiated from PDR is that in PSR, spontaneous regression of the peripheral neovascularization by autoinfarction frequently occurs, resulting in a white sea fan neovascularization (Fig 7-5). Table 7-2 presents a differential diagnosis of peripheral retinal neovascularization.

Elagouz M, Jyothi S, Gupta B, Sivaprasad S. Sickle cell disease and the eye: old and new concepts. *Surv Ophthalmol*. 2010;55(4):359–377.

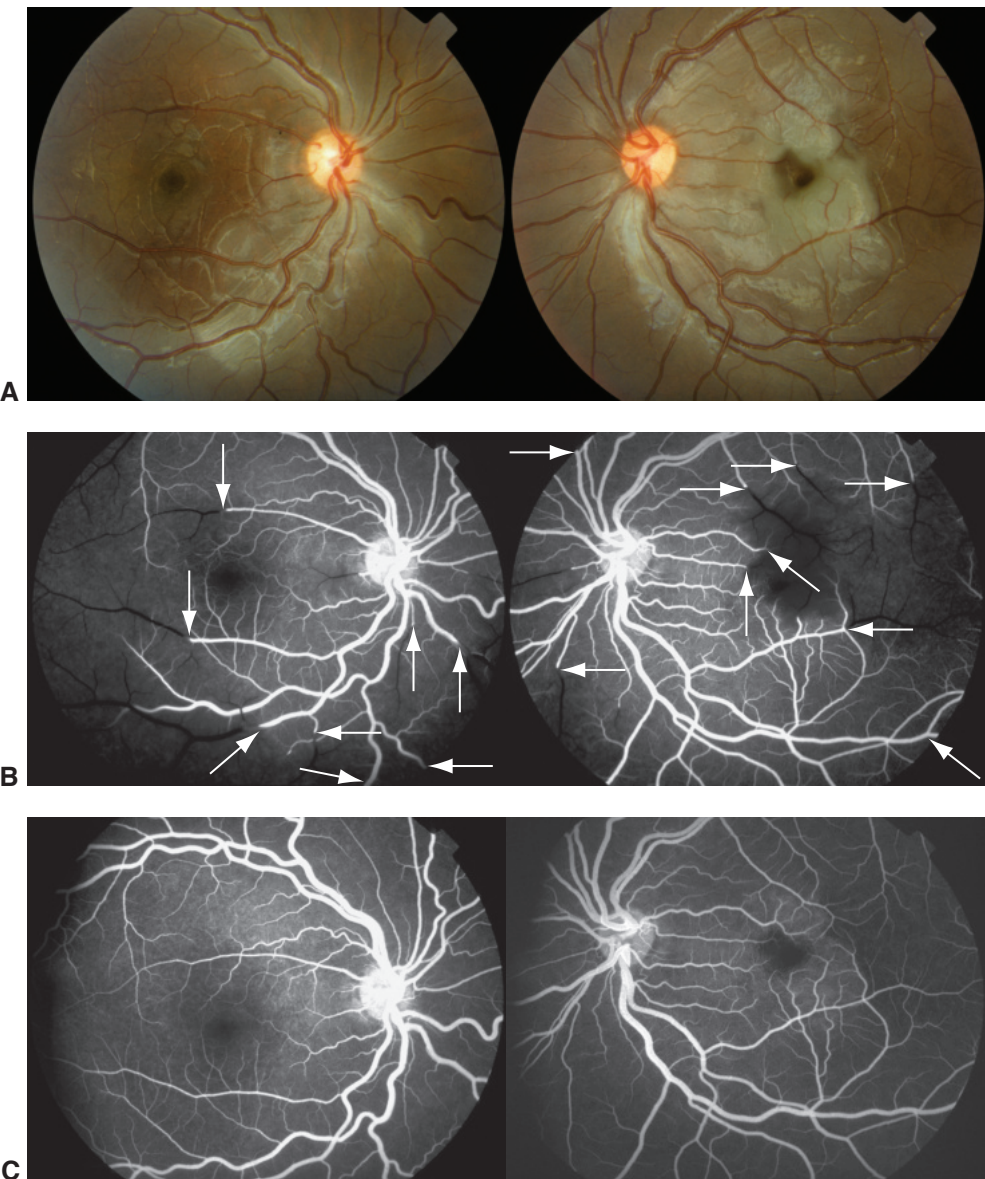


Figure 7-3 Bilateral, multiple branch retinal artery occlusions (BRAOs) in NPSR. **A**, Fundus photographs show multiple acute BRAOs (arrows) in a 5 ½-year-old boy with Hb SS during a massive sickling episode. **B**, Fluorescein angiography images show numerous medium and large arteriolar vessel occlusions. **C**, The patient was treated promptly with a hypertransfusion protocol, which resulted in dramatic reperfusion of the retina. However, the corrected distance visual acuity did not improve beyond 20/200 in either eye. (*Courtesy of Brian Leonard, MD.*)

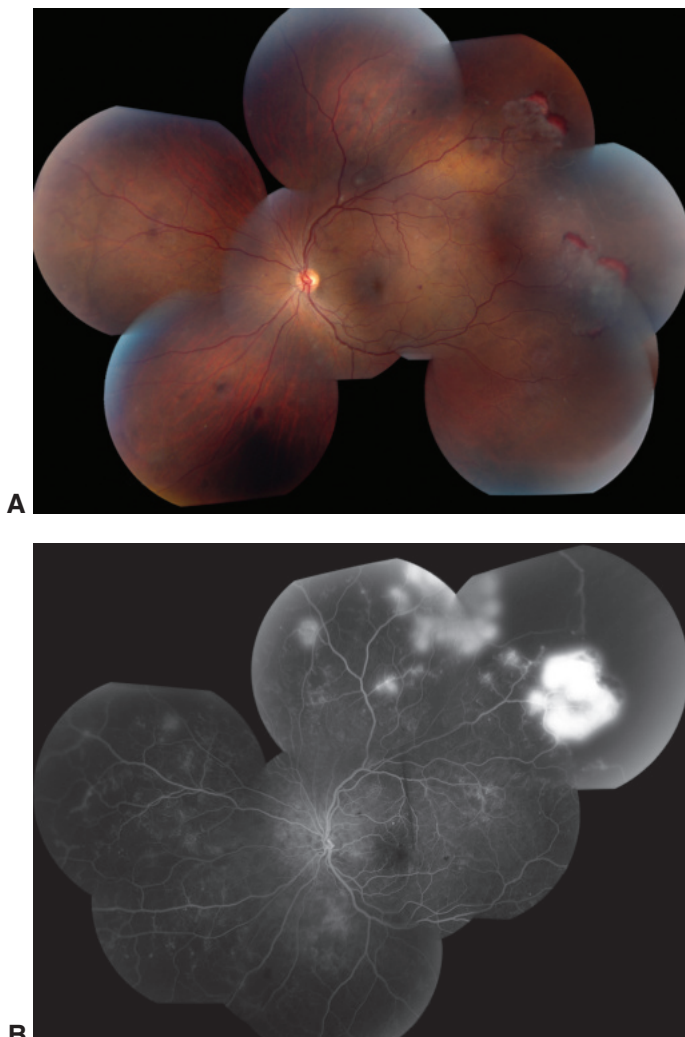


Figure 7-4 Wide-field fundus montage images of the left eye of a 26-year-old African American man with a history of sickle cell hemoglobin C (SC) disease. **A**, Hemorrhaging has occurred at the anterior border of the proliferative lesions. **B**, The wide-field montage fluorescein angiogram shows leakage from the sea fan lesions in the periphery and peripheral nonperfusion anterior to the sea fans. (*Courtesy of Asheesh Tewari, MD.*)



Figure 7-5 Fundus photograph of peripheral neovascularization (sea fan neovascularization) with autoinfarction, as illustrated by the white atrophic vessels. (*Courtesy of Harry W. Flynn, Jr, MD.*)

Table 7-2 Differential Diagnosis of Peripheral Retinal Neovascularization

Vascular diseases with ischemia
Proliferative diabetic retinopathy (PDR)
Branch retinal vein occlusion (BRVO)
Branch retinal arteriolar occlusion (BRAO)
Carotid cavernous fistula
Sickling hemoglobinopathies (eg, SC, SS)
Other hemoglobinopathies (eg, AC, AS)
Idiopathic retinal vasculitis, aneurysms, and neuroretinitis (IRVAN)
Retinal embolization (eg, talc emboli)
Retinopathy of prematurity (ROP)
Familial exudative vitreoretinopathy (FEVR)
Hyperviscosity syndromes (eg, chronic myelogenous leukemia)
Aortic arch syndromes/ocular ischemic syndromes
Eales disease
Coats disease
Inflammatory diseases with possible ischemia
Birdshot uveitis
Multiple sclerosis
Retinal vasculitis (eg, systemic lupus erythematosus)
Sarcoidosis
Toxoplasmosis
Uveitis, including pars planitis
Miscellaneous conditions
Choroidal melanoma
Incontinentia pigmenti
Long-standing retinal detachment
Retinitis pigmentosa
Retinoschisis

Modified from Jampol LM, Ebroon DA, Goldbaum MH. Peripheral proliferative retinopathies: an update on angiogenesis, etiologies, and management. *Surv Ophthalmol*. 1994;38(6):519–540.

Other Ocular Abnormalities in Sickle Cell Hemoglobinopathies

Many patients with SS or SC disease exhibit segmentation of blood in the conjunctival blood vessels. Numerous comma-shaped thrombi dilate and occlude capillaries, most often in the inferior bulbar conjunctiva and fornix (referred to as the comma sign). Similarly, small vessels on the surface of the optic nerve head can exhibit intravascular occlusions, manifested as dark red spots (called the nerve head sign of sickling). Angioid streaks have been reported clinically in up to 6% of cases of SS disease and in persons with sickle cell trait (Hb AS). The pathogenetic basis of this association is uncertain.

Management of Sickle Cell Retinopathy

All Black patients presenting with a traumatic hyphema should be screened for a sickling hemoglobinopathy (including Hb AS trait) because of the increased risk of complications in the presence of rigid sickled erythrocytes. Control of intraocular pressure (IOP) may be difficult, and ischemic optic neuropathy may result from even short intervals of a modest increase in IOP. Early anterior chamber washout in the presence of a hyphema with increased IOP is recommended. In addition, carbonic anhydrase inhibitors should

be used cautiously in sickle cell patients as they may worsen sickling through the production of systemic acidosis.

McLeod DS, Merges C, Fukushima A, Goldberg MF, Lutty GA. Histopathologic features of neovascularization in sickle cell retinopathy. *Am J Ophthalmol*. 1997;124(4):455–472.

Photocoagulation

Peripheral scatter photocoagulation applied to the ischemic peripheral retina generally causes regression of neovascular fronds and thus decreases the risk of vitreous hemorrhage. The decision to treat PSR with scatter photocoagulation should be made cautiously, however, because retinal tears and subsequent rhegmatogenous retinal detachment can occur and do so more commonly after such treatment in PSR than in proliferative diabetic retinopathy.

Vitreoretinal surgery

Surgery may be indicated for nonclearing vitreous hemorrhage and for rhegmatogenous, tractional, schisis, or combined retinal detachment. Retinal detachment usually begins in the ischemic peripheral retina. The tears typically occur at the base of sea fans and are often precipitated by photocoagulation treatment, as previously mentioned. Anterior segment ischemia or necrosis has been reported in association with 360° scleral buckling procedures, particularly when combined with extensive diathermy or cryopexy. During surgery, care should be taken to ensure adequate patient hydration and supplemental nasal oxygenation. Precautions for vitrectomy also include the judicious use of expansile gases to minimize IOP elevations postoperatively, which increase the risk of vascular occlusions. Exchange transfusion before vitreoretinal surgery is not recommended.

Vasculitis

Retinal vasculitis from any cause may progress through the stages of inflammation, ischemia, neovascularization, and subsequent hemorrhagic and tractional complications. The early clinical manifestations are generally nonspecific, consisting of perivascular infiltrates and sheathing of the retinal vessels (vascular wall thickening with vessel involution; Fig 7-6). Involvement of exclusively retinal arteries or veins is uncommon. Veins tend to become



Figure 7-6 Fundus photograph of retinal vasculitis in an eye of a patient with Crohn disease. Retinal hemorrhages and edema are present, as is prominent sheathing of the retinal vessels. (Courtesy of Gary C. Brown, MD.)

inflamed earlier and more frequently than arterioles, and combinations are the rule. Retinal vasculitis may be caused by

- Behçet disease
- cat-scratch disease
- certain medications, such as rifabutin
- giant cell arteritis
- inflammatory bowel disease
- Lyme disease
- multiple sclerosis
- pars planitis
- polyarteritis nodosa
- sarcoidosis
- syphilis
- systemic lupus erythematosus
- toxoplasmosis
- viral retinitis

Masquerade syndromes should also be considered. See BCSC Section 9, *Uveitis and Ocular Inflammation*, for further discussion of most of these conditions and Section 5, *Neuro-Ophthalmology*, for discussion of multiple sclerosis and giant cell arteritis.

A primary occlusive retinal vasculopathy for which no cause can be found is termed *Eales disease*. This condition is an occlusive vasculopathy that usually involves the peripheral retina of both eyes and often results in extraretinal neovascularization with vitreous hemorrhage. It typically occurs in males, and there may be associated tuberculin hypersensitivity.

Susac syndrome is characterized by multiple branch retinal arterial occlusions and can be associated with hearing loss and, in rare cases, with strokes. It is most commonly diagnosed in women in their third decade, and there is no known cause. Susac syndrome is treated with corticosteroids or immunosuppression.

Chronic embolism or thrombosis without inflammation may result in a clinical picture that is indistinguishable from past retinal vasculitis. Evaluation includes a search for possible causes: cardiac valvular disease, cardiac arrhythmias, ulcerated atheromatous disease of the carotid vessels, and hemoglobinopathies.

Idiopathic retinal vasculitis, aneurysms, and neuroretinitis (IRVAN) describes a syndrome characterized by the presence of retinal vasculitis, multiple macroaneurysms, neuroretinitis, and peripheral capillary nonperfusion. Systemic investigations are generally noncontributory, and oral prednisone has demonstrated little benefit. Capillary nonperfusion is often sufficiently severe to warrant panretinal photocoagulation (PRP).

Cystoid Macular Edema

Cystoid macular edema (CME) is characterized by intraretinal edema contained in honeycomb-like cystoid spaces. The source of the edema is abnormal perifoveal retinal capillary permeability, which is visible on fluorescein angiography as multiple small

focal leaks and late pooling of the dye in extracellular cystoid spaces. Optical coherence tomography (OCT) findings in CME include diffuse retinal thickening with cystic areas of low reflectivity (reduced reflectivity), more prominently in the inner nuclear and outer plexiform layers. The OCT findings correlate with histologic studies that indicate swelling in and between müllerian glia. On occasion, a nonreflective cavity that is consistent with subretinal fluid accumulation is present beneath the neurosensory retina (see Chapter 5, Fig 5-11B, and Chapter 6, Fig 6-13A). Because of the radial foveal arrangement of both the glia and Henle inner fibers, this pooling classically forms a “flower-petal” (petaloid) pattern (Fig 7-7). Severe cases may be associated with vitritis (vitreous cells) and optic nerve head swelling.

Etiologies of CME

Abnormal permeability of the perifoveal retinal capillaries may occur in a wide variety of conditions, including diabetic retinopathy, central retinal vein occlusion (CRVO), branch retinal vein occlusion (BRVO), any type of uveitis (particularly pars planitis), and retinitis pigmentosa. In addition, CME may occur after any ocular surgery, such as cataract extraction (in which case the CME is termed *Irvine-Gass Syndrome*), retinal detachment surgery, vitrectomy, glaucoma procedures, photocoagulation, and cryopexy. It can also be triggered or worsened by drugs, for example the prostaglandin analogues used to treat glaucoma or anticancer drugs such as interferon.

Subretinal disease processes (eg, choroidal neovascularization, choroidal hemangioma, or subclinical retinal detachment) must also be considered when CME is detected; see Chapter 4 of this volume.

The differential diagnosis of CME in which fluorescein angiography fails to show leakage includes conditions such as X-linked hereditary retinoschisis, Goldmann-Favre disease, and retinitis pigmentosa, in addition to the effects of treatment by nicotinic acid, MEK inhibitors, and taxanes (see also Chapter 15 in this volume).

Incidence of CME

Cataract surgery is one of the most common causes of CME. There is a lack of uniform definition of and diagnostic criteria for pseudophakic CME; its reported incidence ranges from approximately 1% to over 30% following extracapsular cataract extraction. The incidence of clinically relevant pseudophakic CME, which is usually defined as reduced vision in the presence of petaloid CME on fluorescein angiography, is 1%–2% in the absence of additional risk factors. Thus, most cases of pseudophakic CME are mild and asymptomatic; in other words, OCT or fluorescein angiography demonstrates CME, but the patient’s visual acuity is unaffected. The peak incidence occurs 6–10 weeks postoperatively, with spontaneous resolution occurring clinically in approximately 95% of uncomplicated cases, usually within 6 months. More severe CME may result in permanent vision loss. Many factors affect the incidence of CME. The presence of predisposing disease, as mentioned in the section Etiologies of CME, is an important factor. Factors affecting the incidence and severity of CME after intraocular surgery, particularly cataract

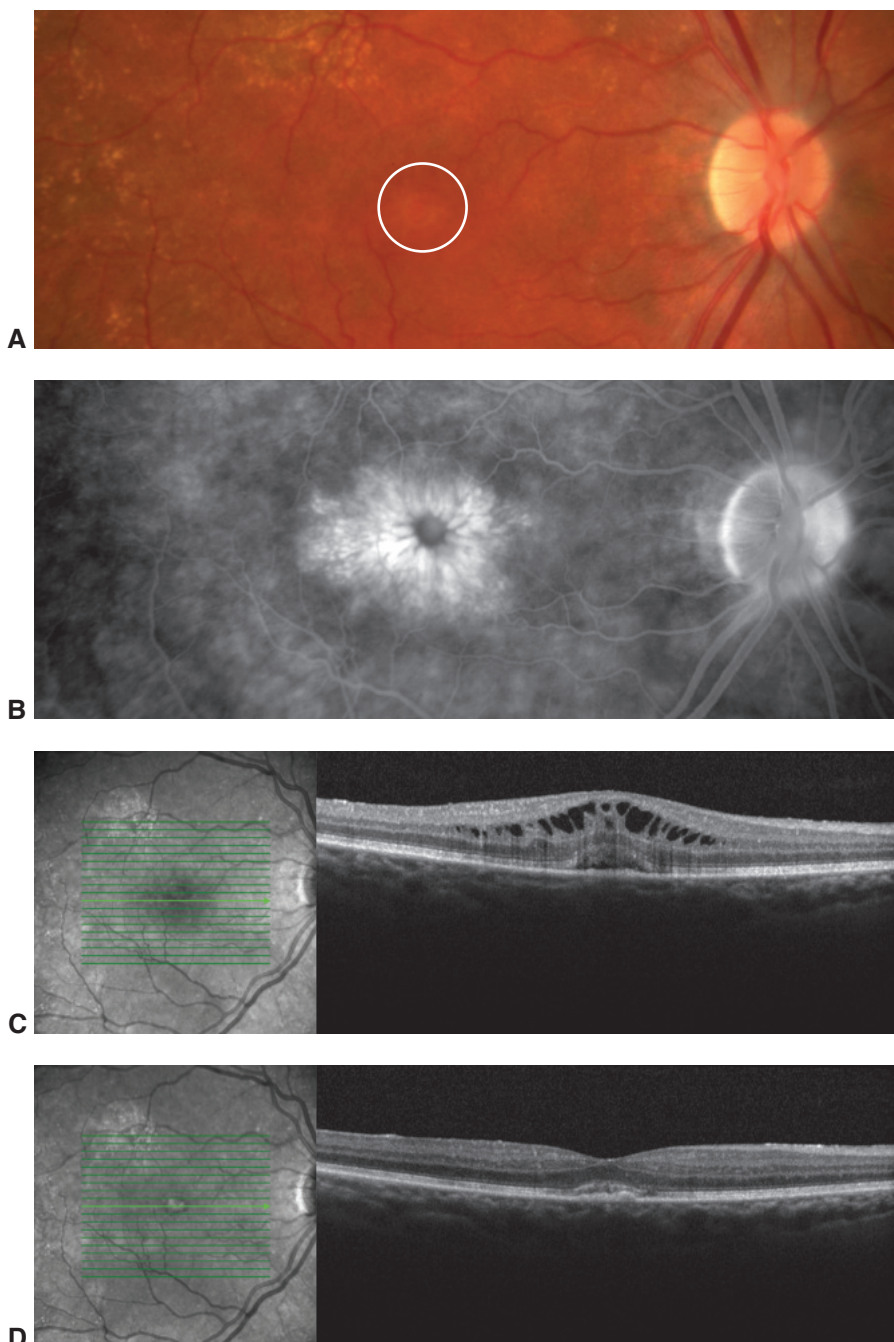


Figure 7-7 Pseudophakic cystoid macular edema (CME). **A**, Color fundus photograph of an optic nerve head and macula 3 months after complex cataract surgery. A small incidental grayish-yellow adult vitelliform dystrophy lesion is present in the subfoveal region (*circled*). **B**, A mid-phase fluorescein angiography image demonstrates cystic hyperfluorescence, with a classic petaloid pattern. As is typical in eyes with pseudophakic CME, there is mild hyperfluorescence of the nasal portion of the optic nerve head. **C**, OCT shows cystic retinal thickening and a subfoveal vitelliform lesion. **D**, Following 8 weeks of topical steroid and nonsteroidal anti-inflammatory therapy, OCT shows that the CME has fully resolved. (Courtesy of Brian Leonard, MD.)

surgery, include the degree of postoperative inflammation and the presence or absence of surgical complications such as vitreous loss or iris prolapse. For further discussion of CME, see BCSC Section 11, *Lens and Cataract*.

Johnson MW. Etiology and treatment of macular edema. *Am J Ophthalmol*. 2009;147(1):11–21.

Treatment of CME

Therapy's effect on CME is difficult to evaluate because of the high rate of spontaneous resolution. Pharmacologic therapy using a combination of topical corticosteroids and nonsteroidal anti-inflammatory drugs (NSAIDs) has become commonplace for prophylaxis and is supported by the medical literature for established edema. If CME is severe or refractory to topical therapy, periocular (eg, posterior sub-Tenon triamcinolone acetonide) or intraocular injection of steroid preparations are appropriate escalations of therapy. Systemic acetazolamide treatment may be successful for treatment of CME, especially in chronic cases such as associated with retinitis pigmentosa. For information about treating CME associated with diabetic retinopathy or ocular venous occlusive disease, see Chapters 5 and 6 of this volume.

If CME is associated with vitreous adhesions to the iris or a corneoscleral wound, vitrectomy or Nd:YAG laser treatment to interrupt the vitreous strands may be helpful. In cases of CME caused by epiretinal membranes or vitreomacular traction, surgical intervention may be appropriate (see Chapter 20 of this volume).

Coats Disease

Coats disease is characterized by the presence of vascular dilatations (retinal telangiectasia), including ectatic arterioles, microaneurysms, venous dilations (phlebectasias), and fusiform capillary dilatations, which are frequently associated with exudative retinal detachment. Usually only 1 eye is involved, and there is a marked male predominance (85%). To date, researchers have not identified an associated gene or chromosome or any hereditary pattern, and no association between Coats disease and systemic disease has been found.

In an eye with Coats disease, the abnormal vessels are compromised, resulting in the leakage of serum and other blood components, which accumulate in and under the retina. Any portion of the peripheral and macular capillary system may be involved. Although angiography demonstrates the presence of retinal capillary nonperfusion, posterior segment neovascularization is unusual. The clinical findings vary widely, ranging from mild retinal vascular abnormalities and minimal exudation to extensive areas of retinal telangiectasia associated with massive leakage and exudative retinal detachment. The severity and rate of progression appear greater in children under the age of 4 years, in whom massive exudative retinal detachment with the retina apposed to the lens may simulate retinoblastoma or other causes of leukocoria (called Coats reaction; Fig 7-8; also see BCSC



Figure 7-8 Coats disease. **A**, Ultra-wide-field fundus photograph of a patient with Coats disease showing dilated vessels with aneurysmal changes in the inferior temporal periphery as well as moderate to severe accumulation of exudate in the macula. **B**, Corresponding fluorescein angiography image shows nonperfusion in the peripheral retina and around the abnormal blood vessels. The aneurysms, characteristic of Coats disease, hyperfluoresce brightly and leak. (Courtesy of Colin A. McCannel, MD.)

Section 6, *Pediatric Ophthalmology and Strabismus*, for the differential diagnosis of leukocoria or xanthocoria (yellow pupil).

Patients with peripheral areas of leaky vascular anomalies typically present with lipid deposition in an otherwise angiographically normal macula, because “hard” exudate tends to accumulate in the macula. Similar findings in adults probably represent late decompensation of preexisting vascular anomalies. Occasionally, the initial finding is a

submacular lipogranuloma or subretinal fibrosis. The differential diagnosis for Coats disease may include

- dominant (familial) exudative vitreoretinopathy
- facioscapulohumeral muscular dystrophy
- retinopathy of prematurity (ROP)
- retinal hemangioblastomas (von Hippel–Lindau syndrome)

For milder cases of lipid exudation, additional considerations are diabetic retinopathy, BRVO, juxtapapillary retinal telangiectasia, and radiation retinopathy.

Treatment of Coats disease generally consists of ablation with photocoagulation or cryotherapy, and, in severe cases, retinal reattachment surgery. Photocoagulation and cryotherapy are effective in obliterating the vascular anomalies and in halting progression. Several treatments may be necessary, and long-term follow-up is important to detect and treat recurrences or disease progression. Intravitreal anti–vascular endothelial growth factor (VEGF) therapy may be a useful adjunctive treatment that is resistant to ablative therapy alone.

Macular Telangiectasia

Macular telangiectasia is subdivided into 3 general types:

- Type 1: unilateral parafoveal telangiectasia, congenital or acquired
- Type 2: bilateral parafoveal telangiectasia (Fig 7-9)
- Type 3: bilateral parafoveal telangiectasia with retinal capillary obliteration

Macular Telangiectasia Type 1

Macular telangiectasia type 1 (MacTel 1), also termed *aneurysmal telangiectasia*, typically occurs unilaterally, predominantly in young males, and with characteristic aneurysmal dilatations of the temporal macular vasculature with surrounding CME and yellowish exudates. MacTel 1 is considered a macular variant of Coats disease. Peripheral vascular changes may also occur. Anti-VEGF therapy is generally ineffective. However, afibercept, which blocks *placental growth factor* in addition to VEGF, elicits a treatment response in eyes with MacTel 1, implicating placental growth factor in the pathogenesis of the disease.

Macular Telangiectasia Type 2

Macular telangiectasia type 2 (MacTel 2, also called *juxtafoveal telangiectasis*), which is the most common form of macular telangiectasis, is a rare progressive bilateral idiopathic neurodegenerative disease of the macular, perifoveal, retina. Characteristic findings begin to appear in affected individuals in the fifth to seventh decades of life; they include a reduced foveolar reflex, greying appearance and loss of retinal transparency, superficial retinal crystalline deposits, mildly ectatic capillaries, slightly dilated blunted

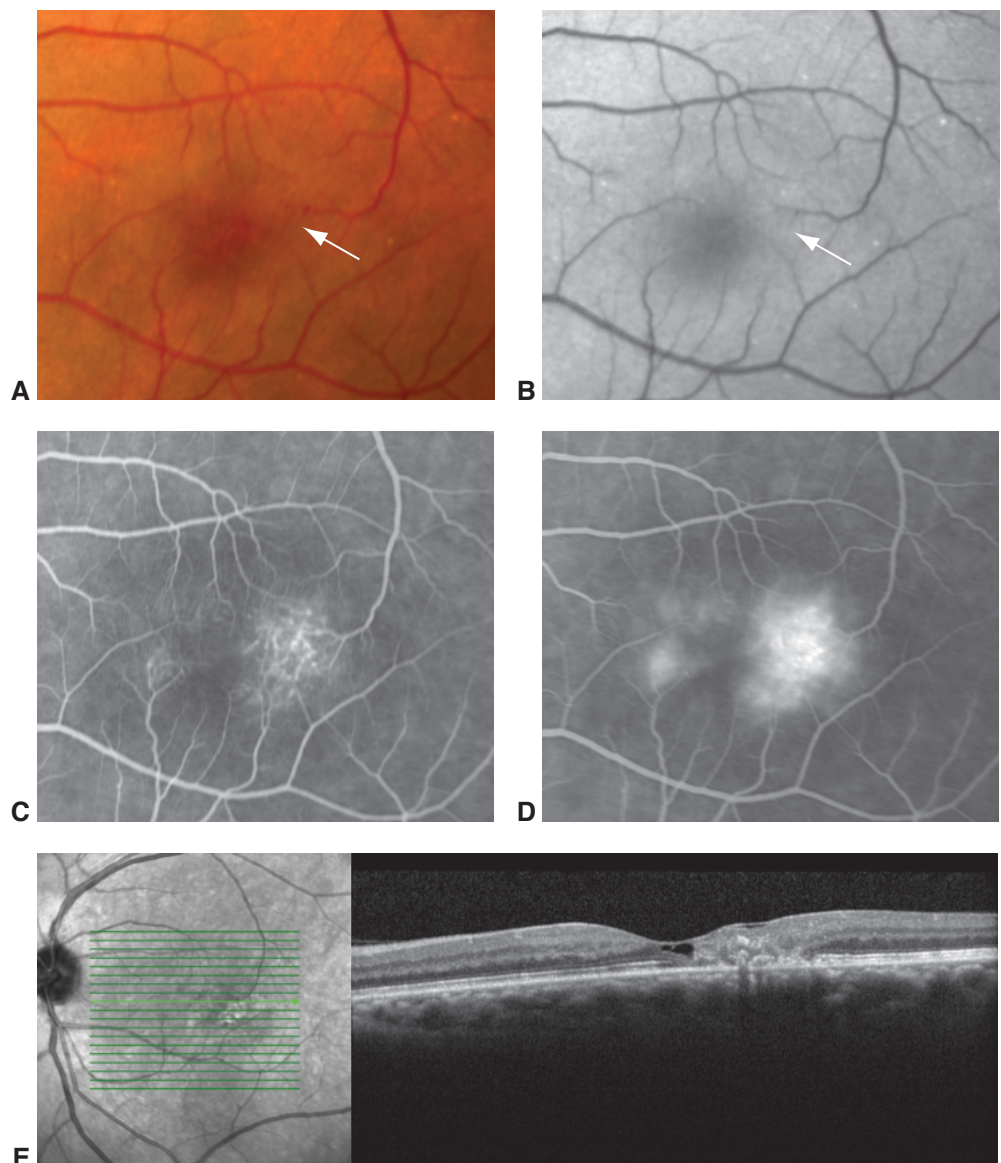


Figure 7-9 Macular telangiectasia, type 2 (MacTel 2). **A**, Fundus photo of a left macula demonstrates subtle loss of retinal transparency temporal to the foveal center (arrow). **B**, Red-free image shows subtle microvascular "dots" (arrow). **C**, Fluorescein angiography image shows ectatic retinal capillaries and dilated blunted venules. **D**, A later image shows late fluorescein leakage from these vascular defects. **E**, OCT demonstrates "collapse" of deep retinal layers toward the choroid, temporal to the fovea. (Courtesy of Brian Leonard, MD.)

venules, progression to pigment hyperplasia, and foveal atrophy. Subretinal neovascularization occurs frequently during the natural disease course. Many of the clinical features of MacTel 2 are characterized by dysfunction of both neural and vascular retinal elements, suggesting that a macular Müller cell defect plays an essential role in the pathogenesis of this disease.

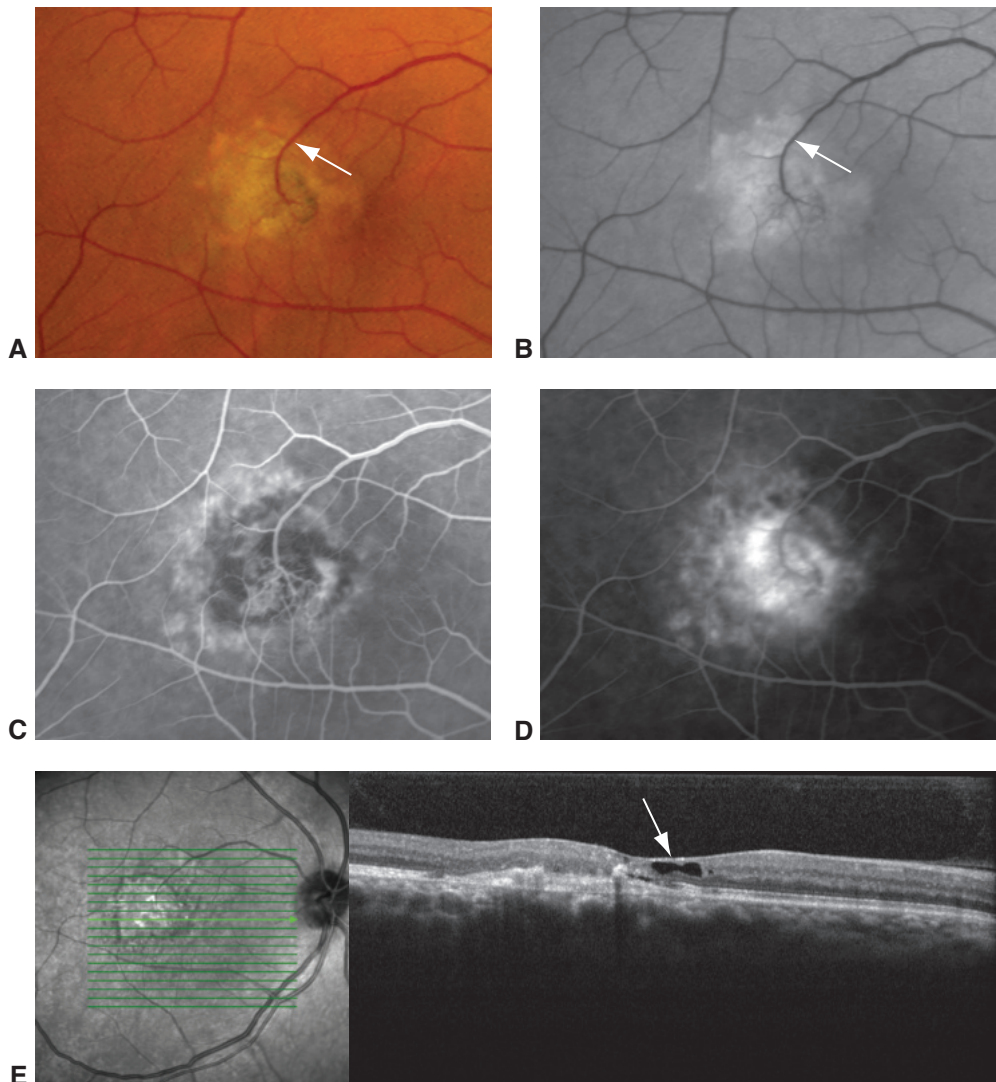


Figure 7-10 Advanced MacTel 2 (same patient as Fig 7-9). **A**, Fundus photograph of the right eye shows the chorioretinal venous shunt vessel (arrow). This patient receives recurring intravitreal anti-vascular endothelial growth factor (VEGF) treatments for a subretinal neovascular membrane. **B**, Red-free image of the eye shown in **(A)**. **C**, Mid-phase fluorescein angiography image demonstrates subretinal neovascularization with superficial and deep components. **D**, Later-phase fluorescein angiography image shows late staining of the neovascular membrane complex. **E**, OCT demonstrates the neovascular membrane complex and MacTel 2-like hyporeflective cavities within the inner foveal layers (arrow). (Courtesy of Brian Leonard, MD.)

The telangiectatic vessels are readily apparent on fluorescein angiography and usually leak. OCT imaging typically demonstrates a thinned central macular retina, including the fovea, with inner lamellar oblong foveal cavitations in which the long axis is parallel to the retinal surface (Fig 7-10; also see Fig 7-9). OCTA visualizes the deep capillary plexus changes of MacTel 2 (Fig 7-11). To date, there is no evidence for an effective treatment

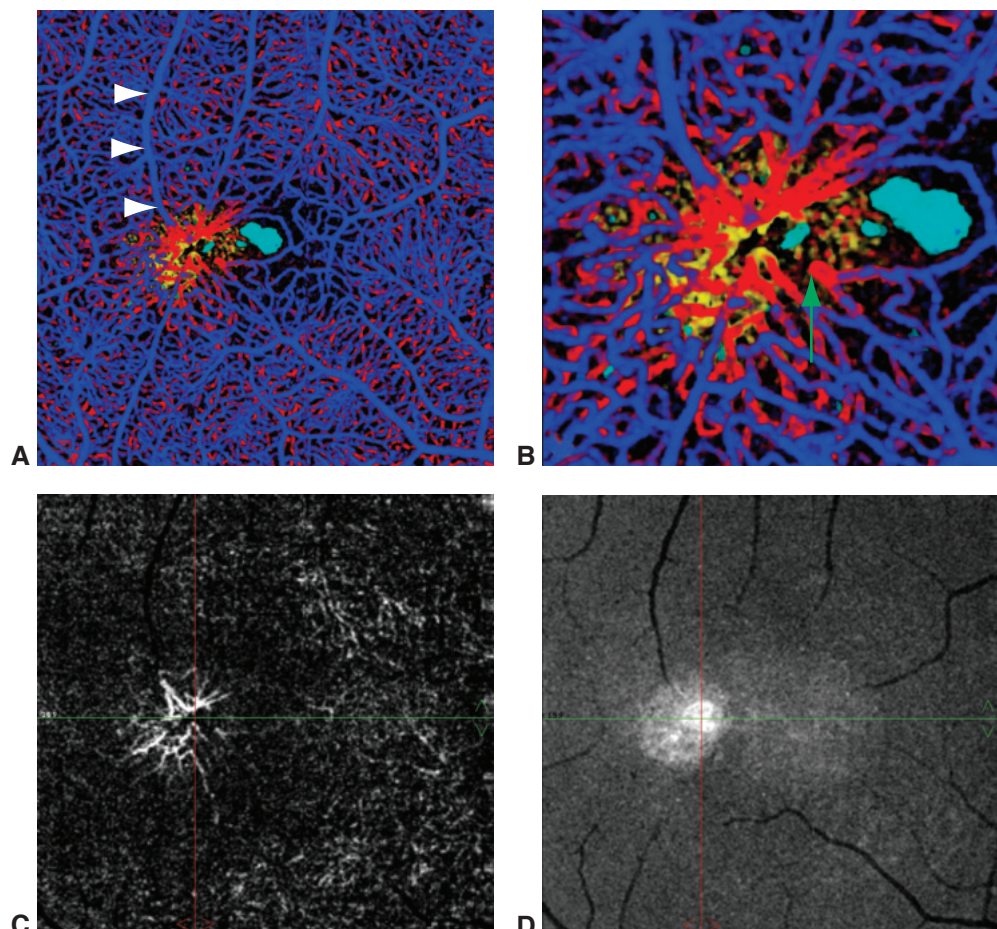


Figure 7-11 MacTel 2 OCT and OCT angiography (OCTA) imaging. **A**, Volume-rendered OCTA image of a right eye with MacTel 2. At the level of the superficial vascular plexus, the vessels are blue; at the deep plexus they are red; and deep to the deep plexus, they are yellow. Retinal cavitations are real. A contraction in the temporal juxtapfoveal region causes a dragging of the perifoveal capillary ring temporally. Note the dragging of vessels such as the large retinal vein (arrowheads), producing an appearance of a right-angle vein. **B**, OCTA image shows enlargement of the area of contracture in the temporal juxtapfoveal macula. Note the angled capillary segments (green arrow) that point toward the epicenter of the contracture. **C**, A slab OCTA image shows the outer nuclear layer, a region that is ordinarily avascular. The slab is taken at the same level as the arrow shown in **(E)**. Note the angled vascular segments. **D**, The corresponding slab structural OCT shows a hyperreflective region where the vessels are located.

(Continued)

of MacTel 2. Intravitreal anti-VEGF therapy is used for the management of subretinal neovascularization.

Macular Telangiectasia Type 3

Type 3 macular telangiectasia is an extremely rare vasocclusive process that affects the parafoveal region and is distinct from type 1 and 2 macular telangiectasias.

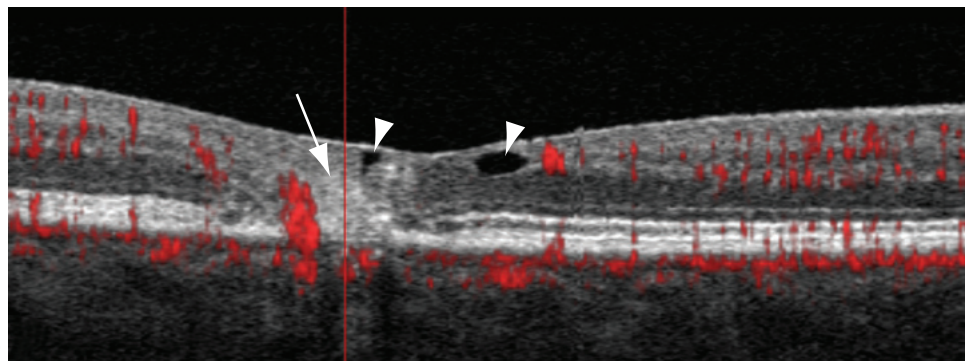


Figure 7-11 (continued) E, This B-scan structural OCT shows a flow overlay in red. The scan was taken at the location of the green line shown in **(C)** and **(D)**. The hyperreflective material extends nearly the full thickness of the retina (arrow). The red lines in **(C)**, **(D)**, and **(E)** are all at the same location. Note the considerable flow (red color) on the temporal side. Nasal to the hyperreflective region are cavitations (arrowheads). Over time, cavitations change in size, shape, and number. (Courtesy of Richard F. Spaide, MD.)

Clemons TE, Gillies MC, Chew EY, et al; MacTel Research Group. Baseline characteristics of participants in the natural history study of macular telangiectasia (MacTel). MacTel Project report no. 2. *Ophthalmic Epidemiol.* 2010;17(1):66–73.

Yannuzzi LA, Bardal AM, Freund KB, Chen KJ, Eandi CM, Blodi B. Idiopathic macular telangiectasia. *Arch Ophthalmol.* 2006;124(4):450–460.

Phakomatoses

Conventionally, many of the syndromes referred to as phakomatoses (“mother spot”) are grouped loosely by the common features of ocular and extraocular or systemic involvement of a congenital nature. Most, but not all, are hereditary. Except for Sturge-Weber syndrome, the phakomatoses involve the neuroretina and its circulation. For further discussion of the phakomatoses, see BCSC Section 5, *Neuro-Ophthalmology*, and Section 6, *Pediatric Ophthalmology and Strabismus*.

Von Hippel–Lindau Syndrome

The phakomatosis *von Hippel–Lindau (VHL) syndrome* (also called *familial cerebello retinal angiomas*) is caused by a tumor suppressor gene mutation on the short arm of chromosome 3 (3p26–p25), the inheritance of which is autosomal dominant with incomplete penetrance and variable expression. The disease is characterized by retinal and central nervous system hemangioblastomas and visceral manifestations (see BCSC Section 6, *Pediatric Ophthalmology and Strabismus*); the diagnosis can be confirmed with genetic testing. Central nervous system tumors include hemangioblastomas of the cerebellum, medulla, pons, and spinal cord in 20% of patients with VHL syndrome. Systemic manifestations include renal cell carcinoma, pheochromocytomas, endolymphatic sac tumors, cysts of the kidney, pancreas, and liver, and bilateral papillary cystadenomas of the epididymis (men) or broad ligament of the uterus (women). Diagnosis of a retinal

hemangioblastoma warrants a systemic workup and genetic testing. Cerebellar hemangioblastoma and renal cell carcinoma are the leading causes of death in patients with VHL syndrome. Patients may incur severe disability from central nervous system lesions and their treatments.

A fully developed retinal lesion is a spherical orange-red tumor fed by a dilated, tortuous retinal artery and drained by an engorged vein (Fig 7-12). Hemangioblastomas of the optic nerve head and peripapillary region are often flat and difficult to recognize. Multiple hemangioblastomas may be present in the same eye, and bilateral involvement occurs in 50% of patients. Leakage from a hemangioblastoma may cause decreased vision from macular exudates (Fig 7-13) with or without exudative retinal detachment. Vitreous hemorrhage or tractional detachment may also occur.



Figure 7-12 Fundus photograph from a patient with von Hippel-Lindau syndrome shows a peripheral retinal hemangioblastoma with surrounding exudate and retinal detachment. The feeder arteriole and draining venule are dilated.

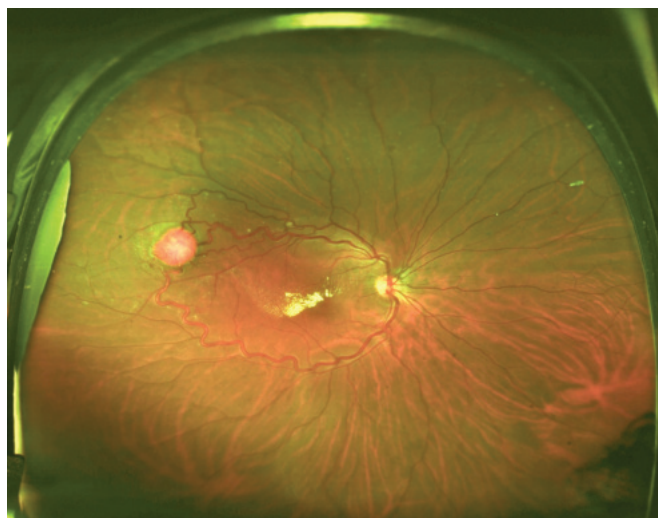


Figure 7-13 Ultra-wide-field fundus photograph of a patient with von Hippel-Lindau syndrome, showing retinal hemangioblastoma in the near periphery and associated exudative maculopathy. (Courtesy of Colin A. McCannel, MD.)

Ocular management includes destructive treatment of all identified retinal hemangioblastoma with careful follow-up to detect recurrence or the development of new lesions. Successful treatment is facilitated by early diagnosis, because the lesions usually enlarge with time. Wide-angle fluorescein angiography can assist in detecting small, early lesions (Fig 7-14). Photocoagulation and cryotherapy are used to treat and destroy the angiomatic lesions directly. Photodynamic therapy with verteporfin can also be used, but the treatment effect has a limited duration because the treatment does not destroy the lesions. Successful treatment results in shrinkage of the hemangioblastoma, attenuation

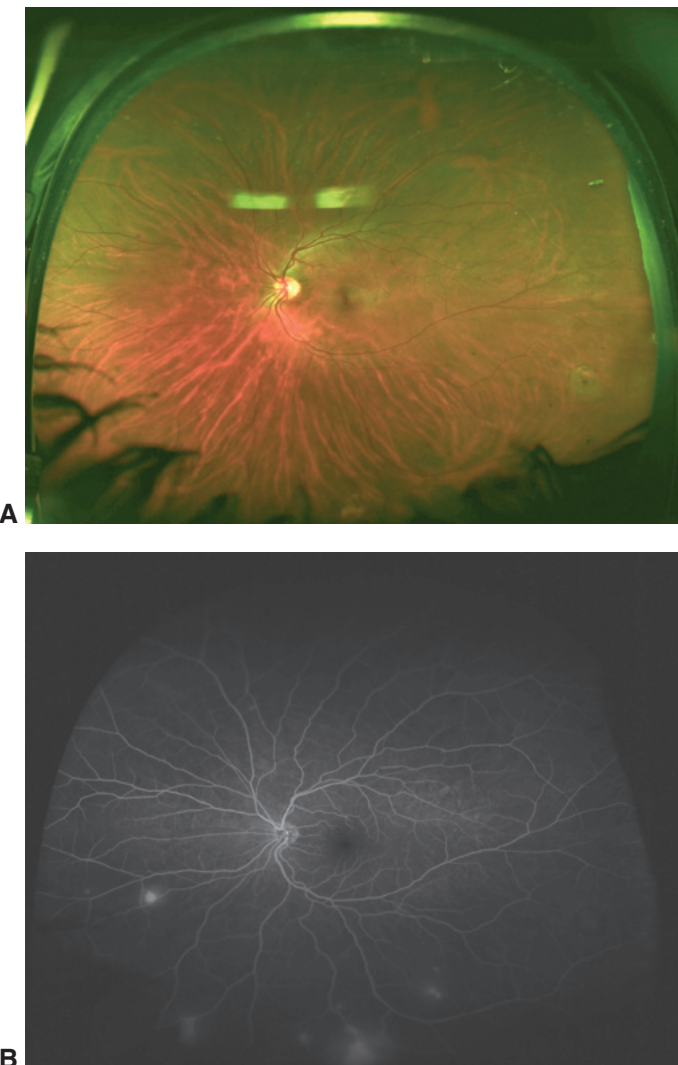


Figure 7-14 Wide-angle imaging of von Hippel-Lindau syndrome. **A**, Ultra-wide-angle fundus photography image of the left eye of a 26-year-old woman with von Hippel-Lindau syndrome. No obvious lesions are visible. **B**, The corresponding ultra-wide-angle fluorescein angiography image demonstrates multiple foci of leakage that are small, early retinal hemangioblastomas, some of which are not easily visible clinically or in the photograph. (*Courtesy of Colin A. McCannel, MD.*)

of the afferent vessels, and resorption of the subretinal fluid. Cryotherapy may be used to treat larger lesions, but it can cause a temporary and marked increase in the amount of exudation and sometimes exudative retinal detachment. Anti-VEGF therapy does not usually result in a meaningful, long-term treatment effect.

Retinal hemangioblastomas may also occur sporadically without systemic involvement; these are termed *von Hippel lesions*. Another form of retinal angiomas, *acquired vasoproliferative lesions*, are idiopathic or, in rare cases, may be present as a late complication of ROP, retinitis pigmentosa, or other conditions. These lesions do not have the dilated feeder and draining vessels seen with hemangioblastomas.

Gaudric A, Krivacic V, Duquid G, Massin P, Giraud S, Richard S. Vitreoretinal surgery for severe retinal capillary hemangiomas in von Hippel-Lindau disease. *Ophthalmology*. 2011; 118(1):142–149.

Wyburn-Mason Syndrome

In Wyburn-Mason syndrome, congenital retinal arteriovenous malformations occur in conjunction with similar ipsilateral vascular malformations in the brain, face, orbit, and mandible. The lesions are composed of blood vessels without an intervening capillary bed (racemose hemangioma). The abnormalities may range from a single arteriovenous communication to a complex anastomotic system. In the eye, the lesions are usually asymptomatic, unilateral, and located in the retina and optic nerve. Typically, they do not show leakage on fluorescein angiography. Intraosseous vascular malformations that may occur in the maxilla and mandible can lead to unexpected hemorrhaging during dental extractions. Most commonly, racemose hemangiomas in the retina are isolated and are not part of the full syndrome.

Retinal Cavernous Hemangioma

Although most cases of cavernous hemangioma are sporadic and restricted to the retina or optic nerve head, they may occur in a familial (autosomal-dominant) pattern and may be associated with intracranial and skin hemangiomas. For this reason, cavernous hemangioma may be considered one of the phakomatoses.

Retinal cavernous hemangioma is characterized by the formation of grapelike clusters of thin-walled saccular angiomatic lesions in the inner retina or on the optic nerve head (Fig 7-15). The blood flow in these lesions is derived from the retinal circulation and is relatively stagnant, producing a characteristic picture on fluorescein angiography. These dilated saccular lesions fill slowly during angiography, the sluggish blood flow results in plasma-erythrocyte layering. Fluorescein leakage is characteristically absent, correlating with the absence of subretinal fluid and exudate in the retinal cavernous hemangioma and serving to differentiate the condition from retinal telangiectasia, retinal hemangioblastomas, and racemose hemangioma of the retina.

These hemangiomas usually remain asymptomatic but may bleed into the vitreous in rare instances. Vitreous traction is thought to be the cause of the hemorrhage in these cases. Treatment of retinal cavernous hemangiomas is usually not indicated unless vitreous hemorrhage recurs, in which case photocoagulation or cryotherapy may be effective. See also BCSC Section 4, *Ophthalmic Pathology and Intraocular Tumors*.

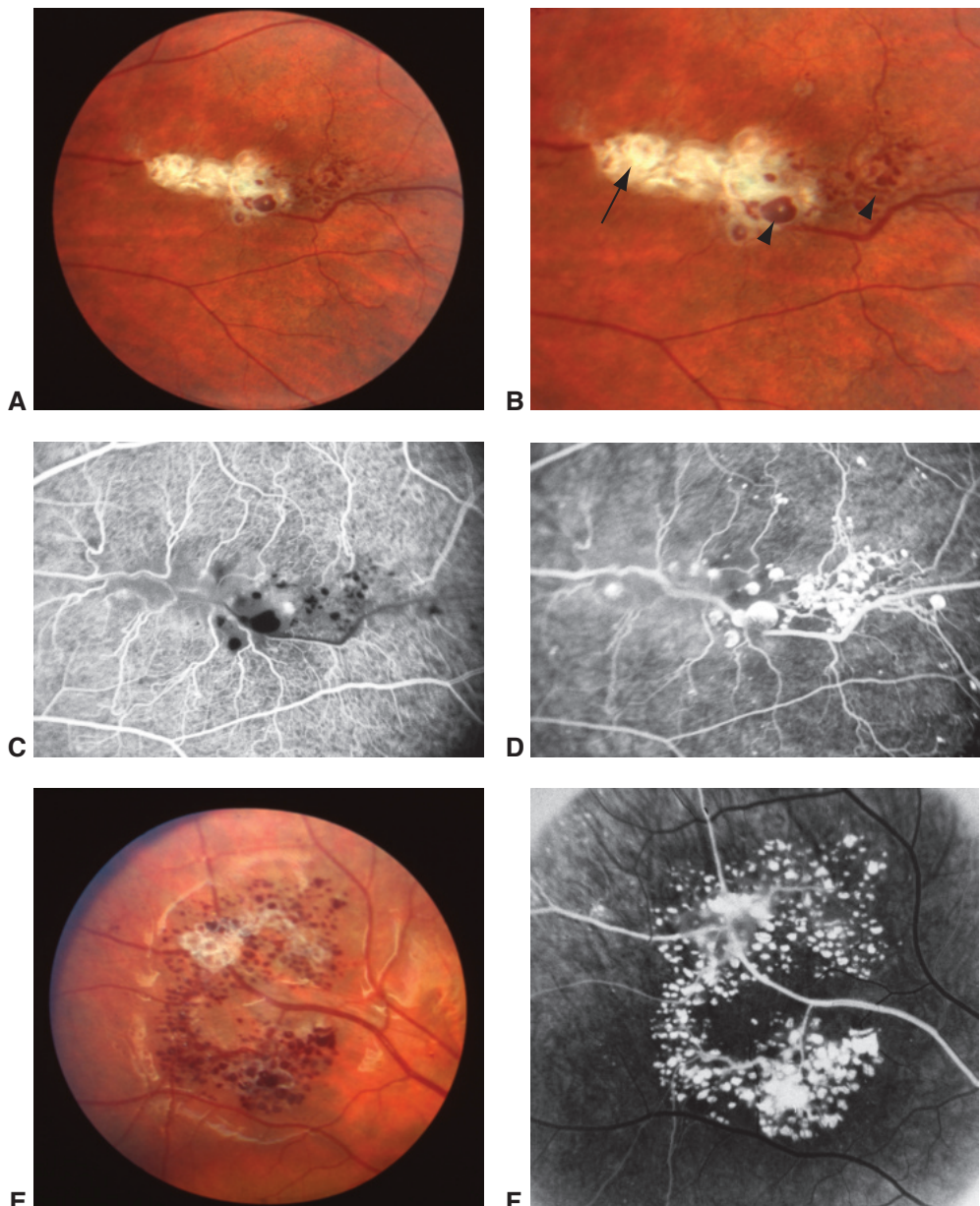


Figure 7-15 Retinal cavernous hemangioma. **A**, Fundus photograph of the left eye shows a retinal cavernous hemangioma in the temporal retina. **B**, These tumors characteristically appear as a grape-like saccular cluster of dark intraretinal venous aneurysms (arrowheads), typically located along the course of a retinal vein, without a feeding artery. White, fibroglial tissue is commonly present on the tumor surface (arrow), suggesting previous vitreous or preretinal hemorrhage. **C**, Early fluorescein angiography typically shows the very slow appearance of dye within the venous aneurysms. **D**, The tumor eventually fills with dye, without leakage. **E**, Fundus photograph of the right eye in a 12-year-old boy shows a larger characteristic retinal cavernous hemangioma in the temporal retina. **F**, Fluorescein angiography image of this tumor also demonstrates late filling of the intraretinal venous aneurysms, without leakage of dye. (Courtesy of Brian Leonard, MD.)

Radiation Retinopathy

Exposure to ionizing radiation can damage the retinal vasculature. Radiation retinopathy typically has a delayed onset, is slowly progressive, and causes microangiopathic changes that clinically resemble diabetic retinopathy. Radiation retinopathy depends on dose fractionation and can occur after either external-beam or local plaque therapy, typically within months to years after radiation treatment. In general, radiation retinopathy is observed around 18 months after treatment with external-beam radiation and earlier with brachytherapy. Because radiation retinopathy appears very similar to other vascular diseases, eliciting a history of radiation treatment is important in establishing the diagnosis. An exposure to doses of 30–35 grays (Gy) or more is usually required to induce clinical symptoms; occasionally, however, retinopathy may develop after as little as 15 Gy of external-beam radiation. Studies have shown retinal damage in 50% of patients receiving 60 Gy and in 85%–95% of patients receiving 70–80 Gy. The total dose, volume of retina irradiated, and fractionation scheme are important in determining the threshold dose for radiation retinopathy. See BCSC Section 4, *Ophthalmic Pathology and Intraocular Tumors*, for further discussion of these therapies.

Clinically, affected patients may be asymptomatic or may describe decreased visual acuity. Ophthalmic examination may reveal signs of retinal vascular disease, including cotton-wool spots, retinal hemorrhages, microaneurysms, perivascular sheathing, capillary telangiectasis, macular edema, and optic nerve head edema. Capillary nonperfusion, documented by fluorescein angiography, is commonly present, and extensive retinal ischemia can lead to neovascularization of the retina, iris, or optic nerve head (Fig 7-16).

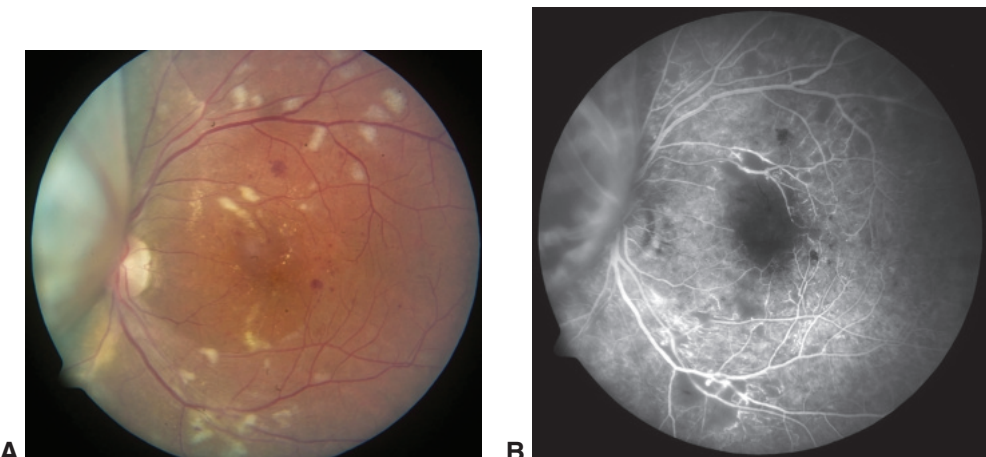


Figure 7-16 Radiation retinopathy. Images of an eye that has undergone plaque brachytherapy for treatment of choroidal melanoma. The melanoma can be seen nasally, obscuring part of the optic nerve head. Typical radiation retinopathy changes are apparent. **A**, In the fundus photograph, cotton-wool spots, exudates (“hard” exudates), and intraretinal blot hemorrhages are visible. **B**, The fluorescein angiography image shows microvascular abnormalities (representative of capillary nonperfusion) superior to the fovea and adjacent to an enlarged foveal avascular zone. Additional areas of nonperfusion are noted in the macula and near periphery. (Courtesy of Tara A. McCannel, MD, PhD.)

Other possible complications include optic atrophy, central retinal artery occlusion, CRVO, choroidal neovascularization, vitreous hemorrhage, neovascular glaucoma, and tractional retinal detachment. Vision outcome is primarily related to the extent of the macular involvement with CME, exudative maculopathy, or capillary nonperfusion. Occasionally, vision loss may be caused by acute optic neuropathy.

Anti-VEGF may be an effective treatment for radiation retinopathy. Laser photocoagulation is less effective because it creates retinal atrophy and laser scar pigment creep.

Patel SJ, Schachat AP. Radiation retinopathy. In: Albert DM, Miller JW, Azar DT, Blodi BA, eds. *Albert & Jakobiec's Principles and Practice of Ophthalmology*. 3rd ed. Philadelphia: Saunders; 2008:chap 175.

Valsalva Retinopathy

A sudden rise in intrathoracic or intra-abdominal pressure (eg, as during coughing, vomiting, lifting, or straining for a bowel movement) may increase intraocular venous pressure sufficiently to rupture small superficial capillaries in the macula. The hemorrhage is typically located under the ILM, where it may create a hemorrhagic detachment of the ILM. Vitreous hemorrhage and subretinal hemorrhage may be present. Vision is usually only mildly reduced and the prognosis is excellent, with spontaneous resolution usually occurring within months after onset. The differential diagnosis of Valsalva retinopathy includes posterior vitreous separation, which may cause an identical hemorrhage or a macroaneurysm. Therefore, in all cases, a peripheral retinal tear or an aneurysm along an arteriole must be ruled out.

Purtscher Retinopathy and Purtscherlike Retinopathy

After acute compression injuries to the thorax or head, a patient may experience loss of vision associated with Purtscher retinopathy in 1 or both eyes. Cotton-wool spots, polygonal shaped areas of retinal whitening (Purtscher flecken), hemorrhages, and retinal edema are found most commonly surrounding the optic nerve head, and fluorescein angiography reveals evidence of arteriolar obstruction and leakage. Occasionally, patients present with optic nerve head edema and an afferent pupillary defect. Vision may be permanently lost from infarction, and optic atrophy may develop.

Purtscher retinopathy is thought to be a result of injury-induced complement activation, which causes granulocyte aggregation and leukoembolization. This process in turn can occlude small arterioles. When the occlusion of a precapillary arteriole affects the radial peripapillary capillary network, cotton-wool spots develop, which are foci of axoplasmic stasis in the nerve fiber layer; these areas of retinal whitening have indistinct borders and can obscure or partially overlie retinal blood vessels. When capillaries in lamina deeper than the radial peripapillary network are blocked, the fundoscopic correlate is instead Purtscher flecken, which manifest as intraretinal whitening with a clear zone on either side of the retinal arterioles, venules, and precapillary arterioles.

Even in the absence of trauma, various other conditions may activate complement and produce a similar fundus appearance. Because Purtscher's original description involved

trauma, cases with similar fundus findings are termed *Purtscherlike retinopathy* (Fig 7-17; Table 7-3). For example, the retinopathy associated with acute pancreatitis, which appears identical to traumatic Purtscher retinopathy, is probably also caused by complement-mediated leukoembolization. Other conditions that may cause these changes include

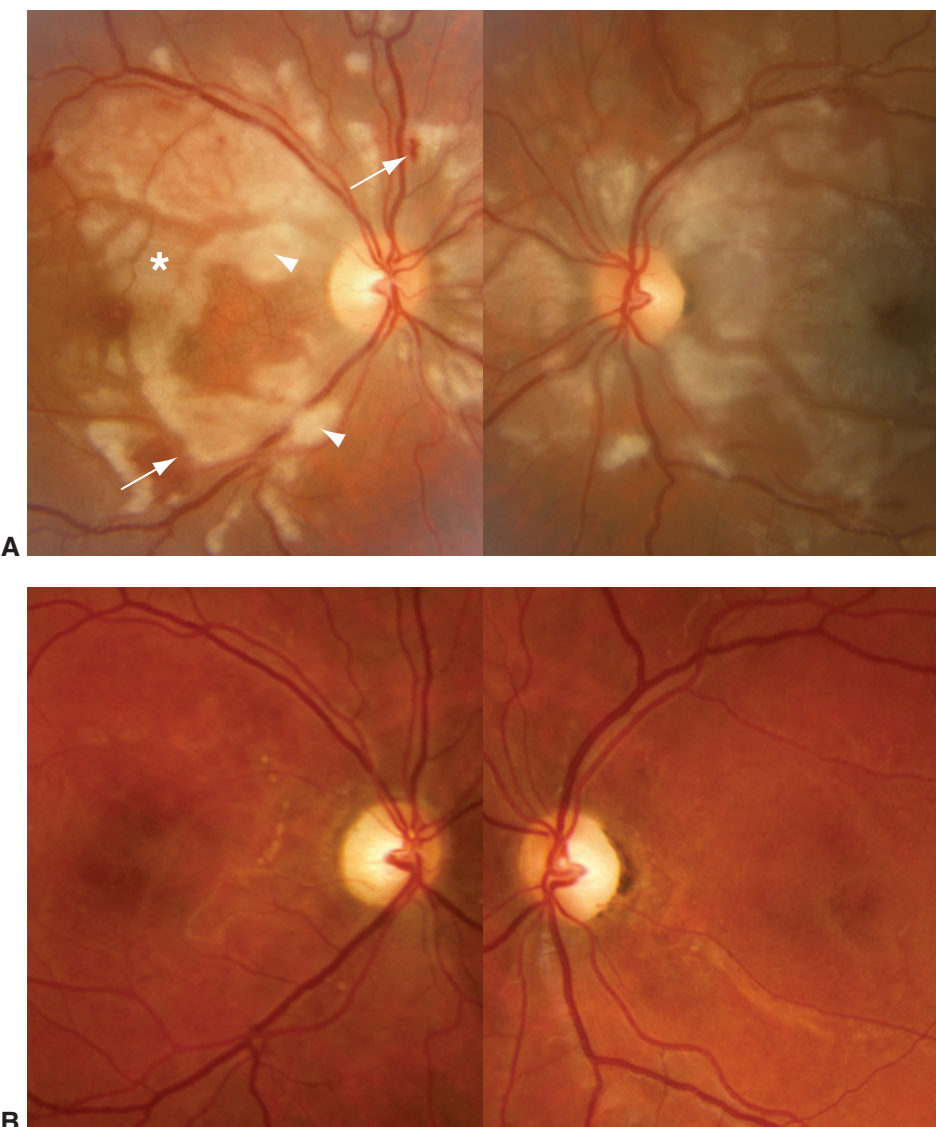


Figure 7-17 Purtscherlike retinopathy. **A**, Fundus photos of a 20-year-old woman were taken 1 day after an uncomplicated delivery of a healthy baby. The patient had noted profound, persistent bilateral vision loss beginning 1 hour after parturition. Intraretinal hemorrhages (arrows) and bright superficial cotton-wool spots (arrowheads) were present, in addition to extensive areas of well demarcated Purtscher flecken (asterisk) with characteristic sparing of the perivasculär retina. The flecken are likely the result of occlusion of the precapillary arterioles. **B**, Corresponding fundus photos taken 4 years later demonstrate optic atrophy and deep macular pigmentary atrophy. Visual acuity was 20/200 OD and 20/800 OS. (Courtesy of Brian Leonard, MD.)

Table 7-3 Conditions Associated With Purtscher or Purtscherlike Retinopathy

Trauma
Head injury
Chest compression
Long-bone fractures (fat embolism syndrome)
Acute pancreatitis
Chronic renal failure
Autoimmune diseases
Systemic lupus erythematosus
Thrombotic thrombocytopenic purpura
Scleroderma
Dermatomyositis
Sjögren syndrome
Amniotic fluid embolism
Retrobulbar anesthesia
Orbital steroid injection
Early postpartum state

Modified with permission from Fekrat S, Goldberg MF. Sickle retinopathy. In: Regillo CD, Brown GC, Flynn HW Jr, eds. *Vitreoretinal Disease: The Essentials*. New York: Thieme; 1999:538. ©Thieme.

collagen-vascular diseases (such as systemic lupus erythematosus), childbirth, and amniotic fluid embolism.

Fat embolism following crushing injuries or long-bone fractures may cause similar retinal findings. Intraretinal hemorrhages are usually scattered in the paramacular area, and the cotton-wool spots of fat embolism are generally smaller and situated more peripherally in the retina than they are in Purtscher retinopathy.

Terson Syndrome

Terson syndrome is recognized as a vitreous and sub-ILM or subhyaloid hemorrhage caused by an abrupt intracranial hemorrhage. Although the exact mechanism is not known, it is suspected that the acute intracranial hemorrhage causes an acute rise in the intraocular venous pressure, resulting in a rupture of peripapillary and retinal vessels. Approximately one-third of patients with subarachnoid or subdural hemorrhage have associated intraocular hemorrhage, which may include intraretinal and subretinal bleeding. Terson syndrome occurs primarily in individuals between 30 and 50 years old, but it can occur at any age. In most cases, visual function is unaffected once the hemorrhage clears. Spontaneous improvement generally occurs, although vitrectomy is occasionally required to clear the ocular media.

Agarwal A. *Gass' Atlas of Macular Diseases*. 5th ed. Philadelphia: Saunders; 2012:724–726.

Retinopathy of Prematurity



This chapter includes related videos, which can be accessed by scanning the QR codes provided in the text or going to www.aao.org/bcscvideo_section12.

Introduction

Retinopathy of prematurity (ROP) is a complex disease process initiated in part by a lack of complete or normal retinal vascularization in premature infants. ROP has a typical progression pattern, but the earlier disease stages may regress spontaneously at any time. The absence of retinal vessels in portions of the immature retina can result in retinal ischemia, leading to the release of growth factors that promote vascular growth. The normal vascular-growth process is disturbed, and vessels proliferate into the vitreous cavity at the border of the vascular and avascular retina. As the disease progresses, vitreous hemorrhage and tractional retinal detachment can occur. The end stage of untreated ROP is the development of a dense, white, fibrovascular plaque behind the lens and complete tractional retinal detachment. The former name of this condition, *retrolental fibroplasia*, describes the end stage of ROP. The main risk factors for developing this condition are prematurity and low birth weight. Also see BCSC Section 6, *Pediatric Ophthalmology and Strabismus*, for additional discussion of ROP.

Epidemiology

In the United States, ROP that is severe enough to require treatment occurs in approximately 1100–1500 infants annually. Among these infants, 400–600 will never achieve vision better than 20/200. In resource-limited regions of the world, there has been a rise in the incidence of ROP that corresponds to the establishment of neonatal intervention initiatives to treat premature infants who would not previously have survived. In many instances, there has been an unfortunate lag between successes in saving premature infants and successes in diagnosing and managing their subsequent ROP.

Terminology and Classification

An international classification of ROP was developed so that the disease could be consistently described, staged, and studied. Four classification concepts have prognostic and pathophysiologic importance: the location, or *zone*, of involvement; the disease

severity, or *stage*; the *extent* of disease in clock-hours of involvement; and whether or not *plus disease* is present. Table 8-1 goes into further detail about this important terminology.

Table 8-1 Descriptive Terminology for Acute Retinopathy of Prematurity

Location

Zone I: posterior retina within a 60° circle centered on the optic nerve

Zone II: annulus centered on the nerve and extending from zone I to the nasal serra

Zone III: remaining temporal peripheral retina

Extent: number of clock-hours involved

Severity

Stage 0: immature retinal vasculature without pathologic changes

Stage 1: presence of a demarcation line between vascularized and nonvascularized retina (Fig 8-1)

Stage 2: presence of a demarcation line that has height, width, and volume (ridge); small, isolated tufts of neovascular tissue lying on the surface of the retina, commonly called "popcorn," may be present (Fig 8-2)

Stage 3: a ridge with extraretinal fibrovascular proliferation that may be mild, moderate, or severe, as judged by the amount of proliferative tissue present (Fig 8-3)

Stage 4: partial retinal detachment

A. extrafoveal

B. retinal detachment including fovea (Fig 8-4)

Stage 5: total retinal detachment with funnel configuration; combinations are listed in order of frequency: top row is the most common configuration and bottom row the least common configuration (Fig 8-5)

Anterior	Posterior
Open	Open
Narrow	Narrow
Open	Narrow
Narrow	Open

Plus disease: vascular dilatation (venous) and tortuosity (arteriolar or venous) of posterior retinal vessels in at least 2 quadrants of the eye; iris vascular dilatation and vitreous haze may be present (Fig 8-6)

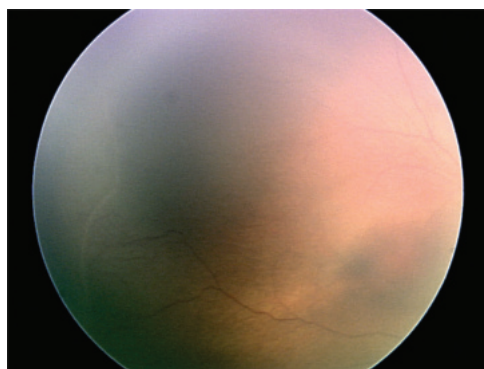


Figure 8-1 Stage 1 retinopathy of prematurity (ROP). Fundus photograph reveals a faint demarcation line present temporally. (Courtesy of Colin A. McCannel, MD.)



Figure 8-2 Stage 2 ROP. Fundus photograph shows an elevated ridge of mesenchymal tissue at the border of the vascularized (reddish) and avascular (grayish) retina. (Courtesy of Colin A. McCannel, MD.)

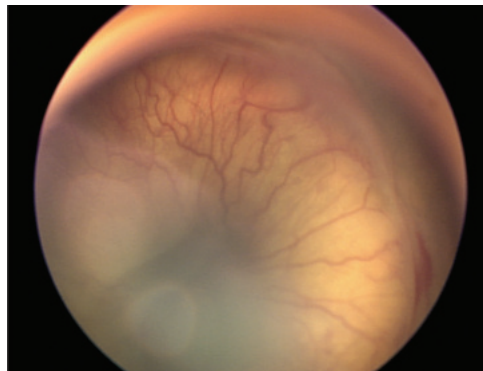


Figure 8-3 Stage 3 ROP. Fundus photograph shows an eye with severe stage 3 ROP with marked preretinal proliferations. Some vitreous and preretinal hemorrhage is visible (lower right). (Courtesy of Colin A. McCannel, MD.)

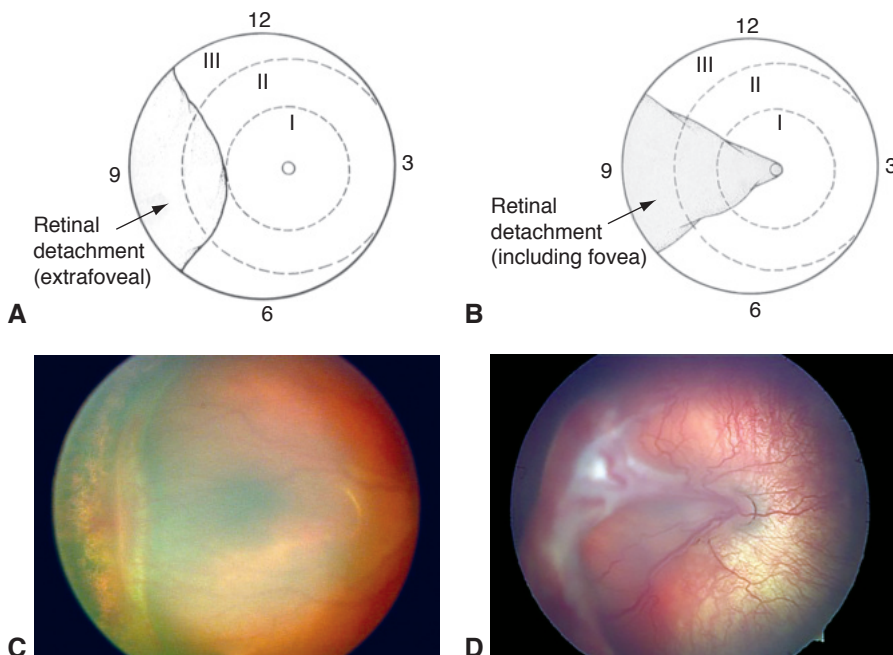


Figure 8-4 Stage 4 ROP. **A**, Schematic representation shows stage 4A ROP. **B**, In this representation of stage 4B ROP, the roman numerals in each circle indicate the zones, as per the international classification, and the arabic numerals indicate clock-hours. **C**, Wide-angle clinical photograph shows a stage 4A retinal detachment in an eye with ROP. **D**, Wide-angle clinical photograph shows a stage 4B retinal detachment. (Parts A, B courtesy of J. Arch McNamara, MD; parts C, D courtesy of Audina M. Berrocal, MD.)

Based on this terminology, ROP can be classified into several disease stages and severities to aid clinicians in making management and treatment decisions (Table 8-2). *Aggressive posterior ROP* (also referred to as *rush disease*) is characterized by the presence of vascularization that ends in zone I or very posterior zone II and is accompanied by plus disease. *Threshold disease* is characterized by at least 5 contiguous clock-hours of extraretinal neovascularization or 8 cumulative clock-hours of extraretinal neovascularization in association with plus disease and location of the retinal vessels within

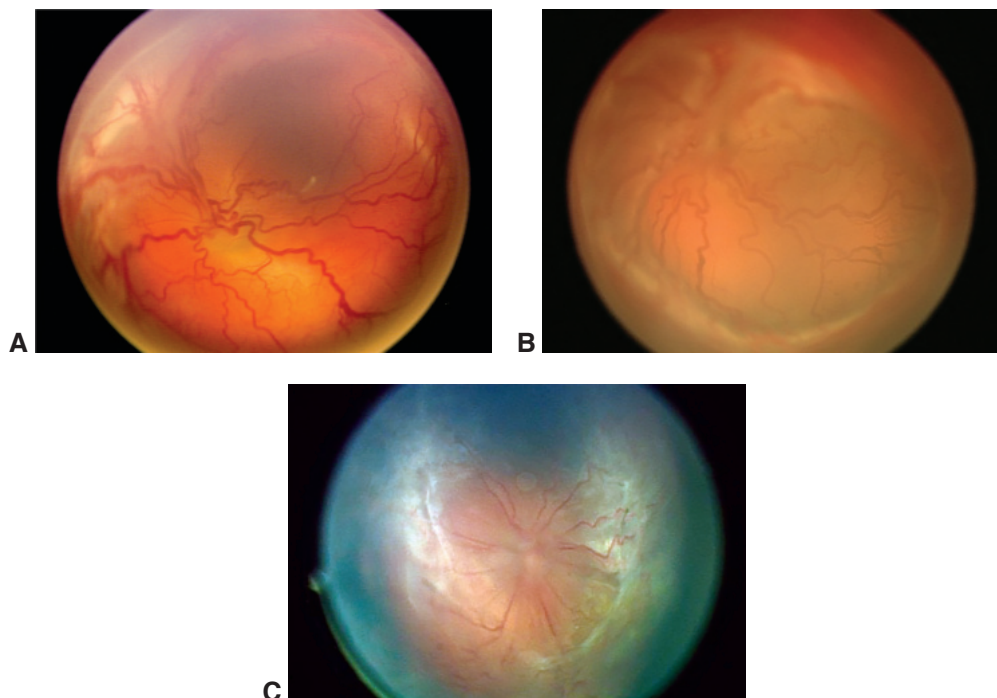


Figure 8-5 Stage 5 ROP. Each of the wide-angle fundus photographs shows examples of total ROP retinal detachment (**A–C**). The marked contraction of the preretinal fibrosis acts like a purse string. Even at this stage—an open-funnel stage 5 retinal detachment—the arborizing pattern of the retinal blood vessels approaching the preretinal proliferation is visible. Additionally, tortuous dilated vessels, also called plus disease, are present in each image. (Part A courtesy of Colin A. McCannel, MD; parts B, C courtesy of Audina M. Berrocal, MD.)

Table 8-2 Classification of Acute Retinopathy of Prematurity (ROP)

Aggressive posterior ROP (also referred to as rush disease)

Vascularization ends in zone I or very posterior zone II and is accompanied by plus disease; may progress rapidly

Threshold disease

5 contiguous clock-hours of extraretinal neovascularization

or

8 cumulative clock-hours of extraretinal neovascularization in association with plus disease and location of the retinal vessels within zone I or II

Prethreshold disease

All zone I and zone II changes, except zone II stage 1, and zone II stage 2 without plus disease, that do not meet threshold treatment criteria, and subdivided into type 1 and type 2 disease:

Type 1

zone I, any stage ROP with plus disease, or
zone I, stage 3 ROP without plus disease, or
zone II, stage 2 or 3 ROP with plus disease

Type 2

zone I, stage 1 or 2 ROP without plus disease, or
zone II, stage 3 ROP without plus disease

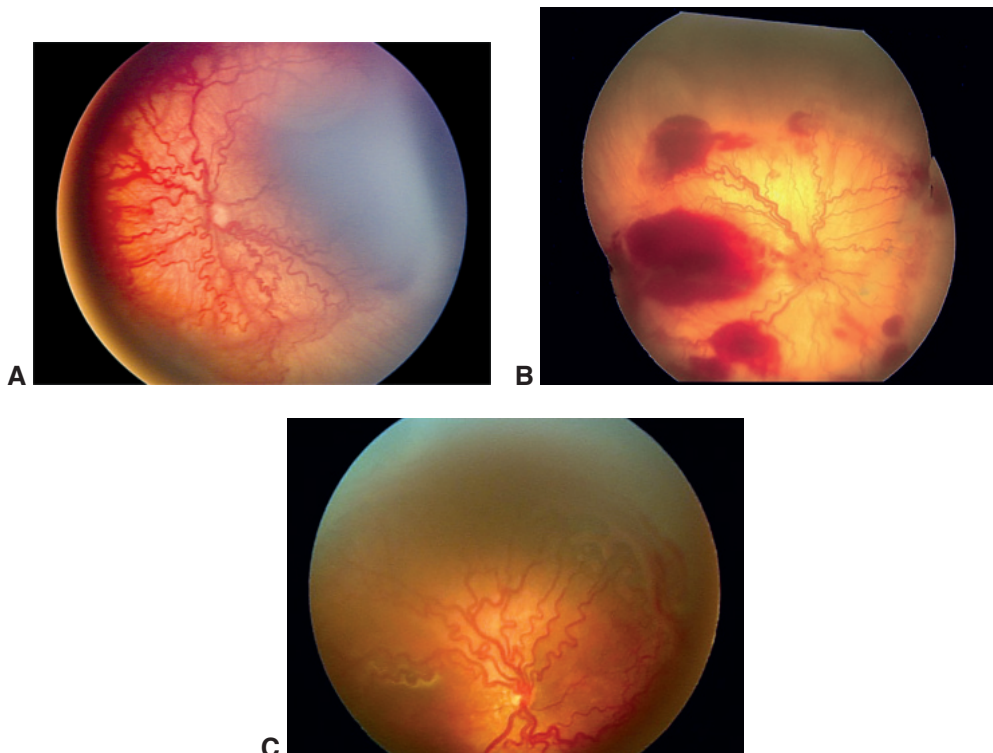


Figure 8-6 Fundus photographs show pronounced plus disease in eyes with ROP. The retinal arteries and veins are dilated and tortuous. **A**, The avascular retina and preretinal proliferations can be seen inferiorly and inferotemporally (bottom right). **B**, Preretinal hemorrhage is visible, originating from the proliferative disease. **C**, Photograph shows an eye with plus disease without notable preretinal fibrosis. (Part A courtesy of Colin A. McCannel, MD; parts B, C courtesy of Audina M. Berrocal, MD.)

zone I or II (Fig 8-7). *Prethreshold disease* is a term created by the Early Treatment for Retinopathy of Prematurity (ETROP) study; it encompasses all zone I and zone II ROP changes that do not meet threshold treatment criteria, except for zone II stage 1 and zone II stage 2 without plus disease. Prethreshold disease can be further divided into high-risk prethreshold ROP, or *type 1 ROP*, and lower-risk prethreshold ROP, or *type 2 ROP* (see Table 8-2).

An eye is classified according to the most advanced disease noted; however, documentation should reflect all zones and stages observed, including their relative extent. Eyes with ROP in zone III typically have a good visual prognosis. The more posterior the zone at the time of recognition of the disease, the more nonperfused retina there is and thus the more worrisome the prognosis.

International Committee for the Classification of Retinopathy of Prematurity. The International Classification of Retinopathy of Prematurity revisited. *Arch Ophthalmol.* 2005;123(7):991–999.

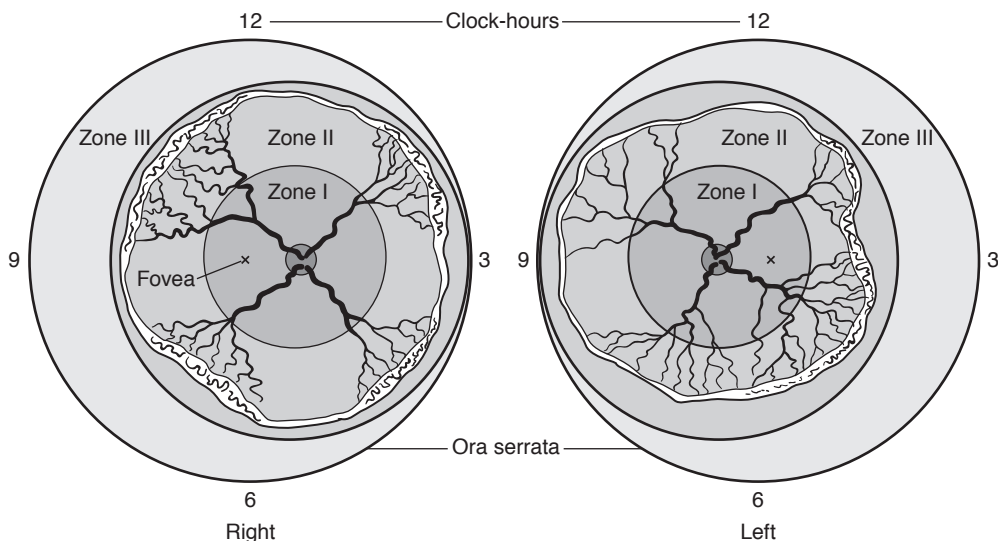


Figure 8-7 Illustrations of threshold disease, as characterized in the Multicenter Trial of Cryotherapy for Retinopathy of Prematurity. Right, 8 cumulative, noncontiguous clock-hours of stage 3 disease. Left, 5 contiguous clock-hours of proliferation. (Illustration by Mark M. Miller.)

Pathophysiology of ROP

Typically, retinal vascularization begins at approximately week 16 of gestation, proceeds from the optic nerve head to the periphery, and is completed nasally by approximately 36 weeks' gestation and temporally by 40 weeks' gestation. When this pattern of vascularization is disrupted, ROP may develop. Although the current understanding of the pathophysiology of ROP is incomplete, it is thought of as a 2-phase process. In the first phase, which occurs before approximately 31 weeks' gestational age, typical vascular development ceases. This cessation occurs largely as the result of a decrease in the levels of hormones and growth factors that govern normal vascular development in the eye, such as vascular endothelial growth factor (VEGF) and insulin-like growth factor 1 (IGF-1). The drop in the expression and levels of these growth factors is thought to be caused by an increase in the infant's systemic oxygen tension that occurs following birth and the commencement of breathing by the infant.

The second phase of ROP begins at approximately 31–34 weeks' gestational age. It is characterized by an abundance of growth factors secreted by the ischemic retina—particularly VEGF and IGF-1, among others—as well as by oxidative damage to endothelial cells, which leads to disorganized vascular growth. Initially, this process causes the formation of a visible tissue ridge (ROP stages 1, 2). As the disease progresses, vascular growth proliferates into the vitreous cavity (ROP stage 3). Eventually, growth factor and hormone shifts cause involution of the blood vessels with cicatricial contraction, which can lead to tractional retinal detachment (ROP stages 4, 5).

The more peripheral the neovascularization and the smaller its size and extent on the retina, the better the outlook is for spontaneous regression with minimal scarring. Active

neovascularization with shunting of blood flow is associated with dilation and increased tortuosity of the retinal vessels posteriorly. A notable finding in active disease is the increased and abnormal terminal arborization of retinal vessels as they approach the shunt or ridge. In addition, microvascular abnormalities (eg, microaneurysms, areas of capillary nonperfusion, and dilated vessels) may be visible posterior to the ridge.

In the vasoproliferative phase, new vessels varying widely in size and extent arise from retinal vessels just posterior to the shunt. These new vessels can induce contracture of the firmly attached vitreous gel, which results in progressive tractional retinal detachment. Vitreous hemorrhage can occur in stages 3–5, as can exudative retinal detachment.

Hartnett ME, Penn JS. Mechanisms and management of retinopathy of prematurity. *N Engl J Med.* 2012;367(26):2515–2526.

Natural Course

Although the systemic and/or local tissue factors that influence progression and regression of ROP are not known, the time course is predictable. ROP is a transient disease in the majority of infants, and spontaneous regression occurs in 85% of eyes. The initial clinical sign of regression is the development of a clear zone of retina beyond the shunt, followed by the development of straight vessels crossing the shunt and an arteriovenous feeder extending into the avascular retina.

Threshold ROP eventually develops in approximately 7%–10% of infants with a birth weight of 1250 g or less. Eyes that demonstrate progression undergo a gradual transition from the active to the cicatricial stage of ROP, which is associated with variable degrees of fibrosis, contracture of the proliferative tissue, vitreous and retinal traction, macular distortion, vitreous and retinal hemorrhages, and/or retinal detachment.

Associated Conditions and Late Sequelae

Conditions more likely to occur in eyes with regressed ROP include the following:

- myopia with astigmatism
- anisometropia
- strabismus
- amblyopia
- cataract
- glaucoma
- macular pigment epitheliopathy
- retinal tears
- abnormal vitreoretinal interface/adhesions
- retinal detachment (all types)
- anomalous foveal anatomy

Though rare, both angle-closure and pupillary-block glaucoma may occur in myopic eyes with cicatricial ROP. Angle-closure glaucoma typically occurs before 10 years of age, but it can occur well into adulthood in affected individuals. Rhegmatogenous retinal detachment, exudative retinopathy, and recurrent vitreous hemorrhages can also occur

later in life. ROP and its sequelae can cause problems throughout a patient's life; therefore, long-term monitoring is crucial.

Unfortunately, even with the current guidelines for screening and treatment, approximately 400–600 infants become legally blind from ROP each year in the United States. Poor outcomes from ROP may be perceived as medical malpractice and therefore pose a risk for litigation by patients or their families. The Ophthalmic Mutual Insurance Company (www.OMIC.com) offers numerous tools to assist ophthalmologists in limiting their liability risk.

Day S, Menke AM, Abbott RL. Retinopathy of prematurity malpractice claims: the Ophthalmic Mutual Insurance Company experience. *Arch Ophthalmol*. 2009;127(6):794–798.

Screening Recommendations

The Cryotherapy for Retinopathy of Prematurity Cooperative Group determined that signs of ROP were present in 66% of infants with a birth weight of 1250 g or less and in 82% of infants with a birth weight of less than 1000 g. Recommendations for the screening examination of premature infants at risk for ROP have been issued in a joint statement of the American Academy of Pediatrics, Section on Ophthalmology; the American Association for Pediatric Ophthalmology and Strabismus; and the American Academy of Ophthalmology (available at www.aao.org/clinical-statement/screening-examination-of-premature-infants-retinop). Screening should consist of a dilated fundus examination using binocular indirect ophthalmoscopy. Alternatively, there are telemedicine (photographic) screening approaches that can substitute for the indirect ophthalmoscopic examination (see the section Fundus Photographic Screening of ROP).

One caveat of paramount importance to recognize is that screening criteria and risk factors developed in one country do not necessarily apply in another country, especially if the level or quality of available medical or perinatal care is not comparable. For example, in some countries ROP is seen in babies with a higher birth weight than in the United States; thus, screening criteria need to be developed that reflect local experiences.

Screening Criteria

All infants with a birth weight of less than 1500 g or a gestational age of 30 weeks or less should be screened. In addition, infants with a birth weight between 1500 g and 2000 g or a gestational age greater than 30 weeks, with an unstable clinical course, and who are believed to be at high risk by their attending pediatricians or neonatologists should be screened. The first examination should generally be performed between 4 and 6 weeks of postnatal age or, alternatively, between 31 and 33 weeks' postconceptional or postmenstrual age, whichever is later.

Systemic IGF-1 levels and weight gain are also associated with ROP risk. Taken together, the rate of weight gain and IGF-1 levels are more predictive of ROP development than is either value alone. A newer model—the weight, IGF-1, neonatal ROP (WINROP) algorithm—is being assessed for more targeted screening efforts, replacing the conventional screening criteria. In some studies, this model has been 100% sensitive in detecting at-risk infants while identifying as many as 90% of infants that do not need screening. The

WINROP model has led to interest in developing other, preferably simpler, algorithms to identify infants at risk for ROP who will require screening.

Screening Intervals

After each evaluation, the follow-up interval should be determined based on the disease features; more severe disease indicates a need for shorter follow-up intervals.

1-Week or Less Follow-up

- immature vascularization: zone I—no ROP
- immature retina extends into posterior zone II, near the boundary of zone I
- stage 1 or 2 ROP: zone I
- stage 3 ROP: zone II
- the presence or suspected presence of aggressive posterior ROP

1- to 2-Week Follow-up

- immature vascularization; posterior zone II
- stage 2 ROP: zone II
- unequivocally regressing ROP: zone I

2-Week Follow-up

- stage 1 ROP: zone II
- immature vascularization: zone II—no ROP
- unequivocally regressing ROP: zone II

2- to 3-Week Follow-up

- stage 1 or 2 ROP: zone III
- regressing ROP: zone III

Retinal screening examinations can usually be discontinued when any one of the following criteria is met:

- zone III retinal vascularization attained without previous zone I or II ROP (if there is examiner doubt about the zone or if the postmenstrual age is less than 35 weeks, confirmatory examinations may be warranted);
- full retinal vascularization for 360°—that is, normal within 1 disc diameter of the ora serrata. This criterion should be used for all cases treated for ROP solely with bevacizumab;
- postmenstrual age of 50 weeks and no prethreshold disease or more severe ROP is present; or
- regression of ROP (care must be taken to ensure that there is no abnormal vascular tissue present that is capable of reactivation and progression in zone II or III).

Fierson WM; American Academy of Pediatrics Section on Ophthalmology; American Academy of Ophthalmology; American Association for Pediatric Ophthalmology and Strabismus; American Association of Certified Orthoptists. Screening examination of premature infants for retinopathy of prematurity. *Pediatrics*. 2013;131(1):189–195.

Table 8-3 Definitions of Clinically Significant Retinopathy of Prematurity (CSROP) and ROP Requiring Treatment

CSROP
(i) zone I, any ROP without plus disease
(ii) zone II, stage 2 with no plus disease or up to 1 quadrant of plus disease
(iii) zone II, stage 3 with no plus disease or up to 1 quadrant of plus disease
ROP requiring treatment (according to ETROP criteria)
(i) zone I, any ROP with plus disease
(ii) zone I, stage 3 ROP without plus disease
(iii) zone II, stages 2 or 3 ROP, with 2 or more quadrants of plus disease

Modified with permission from Photographic Screening for Retinopathy of Prematurity (Photo-ROP) Cooperative Group; Balasubramanian M, Capone A Jr, Hartnett ME, Pignatto S, Trese MT. The Photographic Screening for Retinopathy of Prematurity Study (Photo-ROP): study design and baseline characteristics of enrolled patients. *Retina*. 2006;26(7 Suppl):S4–10.

Fundus Photographic Screening of ROP

Ultra-wide-angle (120°) fundus photography of premature infant eyes is very useful for documenting the findings, for assessing any progression, and for use in fundus photographic screening. Remote screening of photographic fundus images has established itself as an efficient and cost-effective method for screening premature infants for ROP. A study by the Photographic Screening for Retinopathy of Prematurity (Photo-ROP) Cooperative Group concluded that remote interpretation of weekly digital fundus images was a useful adjunct to conventional bedside ROP screening by indirect ophthalmoscopy. The study also concluded that because of limitations of image quality in some cases, there continues to be a need for the availability of an ophthalmologist skilled at examining premature infant eyes. In addition, the study established that if clinically significant ROP or treatment requiring ROP (Table 8-3) is present, an evaluation by an ophthalmologist for assessment and possible treatment is warranted.

Prevention and Risk Factors

As ROP became a clinically distinct and recognized entity in the 1950s, supplemental oxygen administration was implicated as a major causative factor. After substantial reductions in oxygen use in neonatal intensive care units, the incidence of ROP decreased dramatically. However, many of the infants incurred adverse neurologic outcomes as an unintended consequence of that oxygen restriction, and infant death rates rose. Once oxygen was again used more liberally, neurologic outcomes and survival improved, with the consequence of a resurgence of ROP.

Preventing ROP begins with preventing prematurity through optimal prenatal, perinatal, and postnatal care. Avoiding extremely low birth weight and short gestational ages may be the most important factors in prevention. There is mounting evidence that the postnatal clinical course alters risk as well; that is, very sick premature infants are at greater risk of developing ROP. Specific factors shown to increase the risk of ROP are sepsis, blood transfusion, and a slow rate of postnatal weight gain.

Diet has been recognized as an additional risk factor. Several studies are currently under way to assess nutritional interventions for reducing the risk of ROP; one such

intervention is addition of the sugar inositol to the neonate's diet (formula) or parenteral nutrition.

BOOST II United Kingdom Collaborative Group; BOOST II Australia Collaborative Group;

BOOST II New Zealand Collaborative Group, Stenson BJ, Tarnow-Mordi WO, Darlow BA,

et al. Oxygen saturation and outcomes in preterm infants. *N Engl J Med.* 2013;368(22):

2094–2104.

Treatment

In 1988, the Cryotherapy for ROP study demonstrated that ablation of the avascular anterior retina in ROP eyes with threshold disease reduced by approximately half the incidence of unfavorable outcomes (eg, macular dragging, retinal detachment, and retrothalamic cicatrix formation). Treatment reduced these sequelae from 47% to 25% at 1 year follow-up, and visual results were shown to parallel anatomical results. At 10 years, eyes that received cryotherapy were still much less likely to be blind than untreated control eyes.

The ETROP trial randomly assigned 1 eye of infants with bilateral, high-risk, prethreshold ROP to receive early ablation of the avascular retina and the fellow eye to receive conventional management according to Cryotherapy for ROP study methods. High risk was determined using a computational model based on the natural history cohort of the Cryotherapy for ROP study; this model used demographic characteristics of the infants and clinical features of ROP to classify eyes with prethreshold ROP as either high risk or low risk. In infants with high-risk prethreshold ROP, earlier treatment was associated with a reduction in unfavorable visual acuity outcomes (from 19.5% to 14.5%; $P=.01$) and a reduction in unfavorable structural outcomes (from 15.6% to 9.1%; $P<.001$) at 9 months. The study determined that the clinical categorization of prethreshold eyes into type 1 or type 2 ROP achieved very similar results to the computational model for risk assessment to prethreshold eyes.

Any eyes meeting the criteria for type 1 ROP should be considered for peripheral retinal ablative treatment, whereas type 2 ROP eyes can be monitored in short intervals; laser ablative treatment can be considered if type 2 ROP eyes progress to type 1 ROP or threshold ROP. The authors of the ETROP study pointed out that the prethreshold treatment algorithm did not account for all other known risk factors for ROP progression, such as systemic disease, and that clinical judgment is still required for optimal disease management.

Early Treatment for Retinopathy of Prematurity Cooperative Group. Revised indications for the treatment of retinopathy of prematurity: results of the Early Treatment for Retinopathy of Prematurity Randomized Trial. *Arch Ophthalmol.* 2003;121(12):1684–1694.

Shulman JP, Hobbs R, Hartnett ME. Retinopathy of prematurity: evolving concepts in diagnosis and management. *Focal Points: Clinical Modules for Ophthalmologists.* San Francisco: American Academy of Ophthalmology; 2015, module 1.

Laser and Cryoablation Surgery

Ablation treatment of threshold or prethreshold type 1 ROP should be performed with laser surgery rather than cryoablation surgery whenever possible, because laser surgery is associated with less treatment-related morbidity. Treatment should be administered

within 72 hours of determining its need and applied using the indirect ophthalmoscope in a confluent or subconfluent scatter pattern to the avascular retina anterior to the ridge (Fig 8-8). In the horizontal meridians, laser treatment should be applied in a lighter pattern to avoid damage to the long ciliary vessels and nerves; damage to these structures can lead to severe anterior segment ischemia. Although the use of retinal cryoablation surgery is now rare (in the United States), the technique may still have a role in the treatment of eyes with media opacities or persistent tunica vasculosa lentis, or when a laser is not available. Because respiratory or cardiorespiratory arrest can occur in up to 5% of treated infants, treatment should be performed in conjunction with pediatric consultation and with systemic monitoring. Use of systemic analgesia is also advisable to minimize stress and risk to the infant. Some neonatologists prefer that infants undergo treatment with general anesthesia in an operating room.

Brown GC, Tasman WS, Naidoff M, Schaffer DB, Quinn G, Bhutani VK. Systemic complications associated with retinal cryoablation for retinopathy of prematurity. *Ophthalmology*. 1990;97(7):855–858.

Connolly BP, McNamara JA, Sharma S, Regillo CD, Tasman W. A comparison of laser photo-coagulation with trans-scleral cryotherapy in the treatment of threshold retinopathy of prematurity. *Ophthalmology*. 1998;105(9):1628–1631.

Laser ROP Study Group. Laser therapy for retinopathy of prematurity. *Arch Ophthalmol*. 1994; 112(2):154–156.

Anti-VEGF Drugs

The BEAT-ROP (Bevacizumab Eliminates the Angiogenic Threat of Retinopathy of Prematurity) Cooperative Group conducted a prospective, randomized, multicenter trial to assess intravitreal bevacizumab monotherapy for zone I or zone II posterior stage 3 ROP with plus disease. Compared with conventional laser therapy, a statistically significant treatment benefit for bevacizumab was demonstrated for zone I ROP, whereas zone II

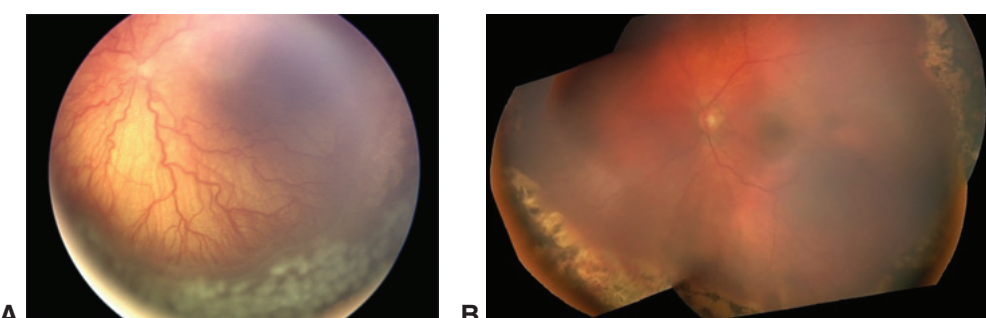


Figure 8-8 Wide-angle photograph shows a fundus after it has undergone laser photocoagulation for threshold ROP. **A**, Plus disease is visible posteriorly, and avascular retina is apparent in the inferior and inferior temporal fundus (bottom right). Arborization of the vasculature leading up to the ridge and associated fibrovascular proliferation is pronounced. **B**, In a different patient, the image shows the pigment clumping, denoting healed laser photocoagulation, and the normalization of the retinal vasculature posteriorly. (Part A courtesy of Colin A. McCannel, MD; part B courtesy of Audina M. Berrocal, MD.)

disease had similar outcomes with either treatment. Normal peripheral retinal vascularization could continue after treatment with intravitreal bevacizumab, whereas laser therapy led to permanent destruction of the peripheral retina. Recurrences occurred significantly later with bevacizumab than with laser therapy. Therefore, prolonged, close follow-up is essential. The study was too small and the follow-up period too short to allow proper evaluation of the safety of intravitreal bevacizumab for the treatment of ROP. Infants treated with anti-VEGF monotherapy have an incidence of recurrence of 8.3% and a mean recurrence time of 51.2 weeks. Findings from the RAINBOW study also suggested the superiority of intravitreal ranibizumab 0.2 mg over laser photocoagulation in infants with any treatment requiring ROP. The use of ranibizumab may have a theoretical advantage over bevacizumab because of the much more rapid systemic clearance of ranibizumab. If available, fluorescein angiography is valuable for follow-up of treated patients to assess eyes for reactivation or progression of the retinopathy.

To date, few data are available that assess the safety, especially the long-term safety, of using anti-VEGF therapy to treat ROP. Furthermore, there is mounting evidence that the disease can recur or reactivate following anti-VEGF treatment, which is rarely seen following ablative therapy. Continued investigation of long-term safety and efficacy data remains critical for understanding the exact role of anti-VEGF therapy in the management of this unique population.

Mintz-Hittner HA, Kennedy KA, Chuang AZ; BEAT-ROP Cooperative Group. Efficacy of intravitreal bevacizumab for stage 3+ retinopathy of prematurity. *N Engl J Med.* 2011; 364(7):603–615.

Stahl A, Lepore D, Fielder A, et al. Ranibizumab versus laser therapy for the treatment of very low birthweight infants with retinopathy of prematurity (RAINBOW): an open-label randomised controlled trial. *Lancet.* 2019;394(10208):1551–1559.

Intravitreal injection technique

Intravitreal injections can be performed at the patient's bedside in the neonatal intensive care unit (NICU) (Video 8-1). The neonatal nurse prepares the infant for the injection. The eye is sterilized with a 5% betadine solution. A sterile eyelid speculum for each eye is used to retract the lids. Given an infant's small eye size, the injection site should be 1.5 mm posterior to the limbus, compared with 3–4 mm in adults. Meticulous attention must be paid to the lens anatomy to avoid puncturing it with the injection needle, because the lens is larger in premature infants relative to the overall eye size compared with adults. Risks associated with the injection include ocular hypertension, cataracts, endophthalmitis, bleeding, and retinal detachment.



VIDEO 8-1 Intravitreal injection at bedside.

Courtesy of Audina M. Berrocal, MD.

Access all Section 12 videos at www.aoa.org/bcscvideo_section12.



Vitrectomy and Scleral Buckling Surgery

Eyes with stage 4 ROP (progressive, active-phase ROP) require surgical intervention using scleral buckling or a lens-sparing vitrectomy to alleviate the vitreoretinal traction causing retinal detachment. Eyes undergoing surgical intervention at stage 4A—rather than at

later stages 4B or 5—have more favorable outcomes. Lens-sparing vitrectomy for stage 4A ROP may reduce the progression to stages 4B and 5 ROP; given the improved visual outcome, this is the preferred approach. New microincisional instrumentation is available to facilitate surgery in the smaller-sized infant eyes.

For eyes with stage 5 disease, vitrectomy combined with dissection of the fibrovascular membranes and adherent vitreous has been successful in fully or partially reattaching the retina in approximately 30% of eyes (Video 8-2). Nevertheless, only 25% of retinas in eyes with initial partial or total reattachment after surgery remained fully attached a median of 5 years later. Among the patients whose retinas were initially reattached, only 10% eventually have ambulatory vision. If a drainage retinotomy is performed or an iatrogenic retinal break occurs during a vitrectomy for ROP, the prognosis for that eye becomes uniformly poor.

**VIDEO 8-2** Stage 5 ROP surgery.

Courtesy of Audina M. Berrocal, MD.



Capone A Jr, Trese MT. Lens-sparing vitreous surgery for tractional stage 4A retinopathy of prematurity retinal detachments. *Ophthalmology*. 2001;108(11):2068–2070.

Quinn GE, Dobson V, Barr CC, et al. Visual acuity of eyes after vitrectomy for retinopathy of prematurity: follow-up at 5 1/2 years. The Cryotherapy for Retinopathy of Prematurity Cooperative Group. *Ophthalmology*. 1996;103(4):595–600.

CHAPTER 9

Choroidal Disease

This chapter describes noninflammatory choroidal diseases that also involve the retina. Inflammatory disorders of the retina and choroid are discussed in Chapter 11. See also BCSC Section 9, *Uveitis and Ocular Inflammation*. Intraocular tumors, such as melanoma, are covered in BCSC Section 4, *Ophthalmic Pathology and Intraocular Tumors*.

Central Serous Chorioretinopathy

Central serous chorioretinopathy (CSC) causes an idiopathic serous detachment of the retina related to leakage at the level of the retinal pigment epithelium (RPE), secondary to hyperpermeability of the choriocapillaris, as seen on indocyanine green angiography. The condition was originally described in 1866 by von Graefe, who called it recurrent central retinitis. In the 1940s, the condition became known, through the influence of Duke-Elder, as central serous retinopathy. Many papers published during that era found that the condition occurred most often in young men, with a male-female incidence ratio of approximately 10:1. These papers, which were published during World War II, were based predominantly on studies of military conscripts. In 1955, Bennett published reports on a series of patients with central serous retinopathy and determined that the majority had a “tense obsessional or inadequate personality” or experienced “worry or over-work.” He stated that there had been a “great awakening of interest in the effects of stress on the organism acting through the nervous and endocrine systems,” thus highlighting the influence of psychological factors. Maumenee later performed fluorescein angiography on patients with CSC and found a leak at the level of the RPE, not from retinal vessels (the previously hypothesized source of leakage). Gass described the fluorescein angiographic findings and suggested that laser photocoagulation could be used to treat affected patients. Gass also stated that the disease was secondary to hyperpermeability of the choriocapillaris, a finding which was confirmed decades later via ICG angiography.

Demographics

CSC occurs primarily in persons between the ages of 35 and 55 years, with a male-female ratio of 3:1; at present there are no reliable statistics suggesting any association with race. Patients describe a variety of symptoms, including sudden onset of blurred or dim vision, micropsia, metamorphopsia, paracentral scotomas, decreased color vision, and

prolonged afterimages. Visual acuity ranges from 20/20 to 20/200, but in most patients, it is better than 20/30. Decreased visual acuity can often be improved with a small hyperopic correction. CSC can show several clinical variations in its expressions. In an acute manifestation, the retina has a round or oval elevation in the macular region; it often involves the fovea. Fluorescein angiography shows leaks from the RPE that may appear, early in the angiographic sequence, as a dot (the “dot” form) or as a tree-shaped movement of dye in the subretinal space (the “smokestack” form) (Fig 9-1). In some circumstances, vigorous leaks can cause deposition of a grayish white, feathered-edge subretinal material that is generally believed to be fibrin. In chronic CSC, the RPE shows granular pigmentation; fluorescein angiography reveals many small, sometimes inconspicuous leaks; and there is widespread shallow detachment with areas of atrophy of the photoreceptors (see Fig 9-1).

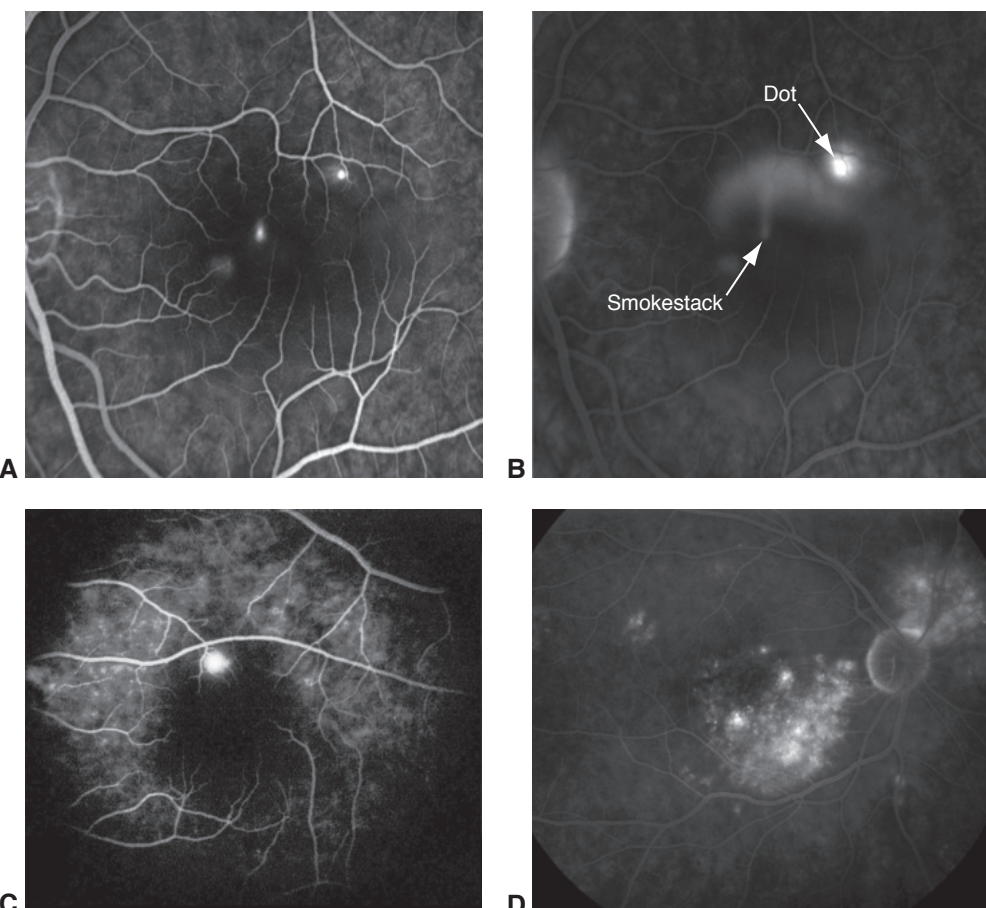


Figure 9-1 Fluorescein angiographic forms of the leaks in central serous chorioretinopathy (CSC). **A**, In the early phase, the patient was seen to have 2 main leaks. **B**, Later in the angiogram, the leaks show two different morphologies; the *smokestack* and the *dot* varieties. **C**, Acute CSC generally presents as 1 or up to a few leaks. **D**, Chronic forms of CSC exhibit many small leaks. (Courtesy of Richard F Spaide, MD.)

As mentioned, CSC is associated with stress and with a tense, driven personality. Systemic associations include endogenous hypercortisolism (Cushing syndrome), hypertension, sleep apnea, use of psychopharmacologic medications, and pregnancy. Use of systemic corticosteroids is associated with CSC, but curiously, use of intraocular corticosteroids does not appear to be associated with the condition.

Imaging

The extent of the detachment can be documented with color fundus photographs. Auto-fluorescence imaging shows the accumulation of shed outer segments in the subretinal space, as well as distributed defects of the RPE. It has been theorized that the white dots seen under the retina are macrophages with fluorophores from phagocytized outer segments (Fig 9-2). Eyes with chronic CSC can display descending tracts during both fluorescein and autofluorescence imaging (Fig 9-3). Enhanced depth imaging optical coherence tomography (EDI-OCT) shows thickening of the choroid and, in areas where thickening is most prominent, posterior loculation of fluid in the deep choroid. Figure 9-4 shows the internal structure of a healthy choroid, while Figure 9-5 shows the

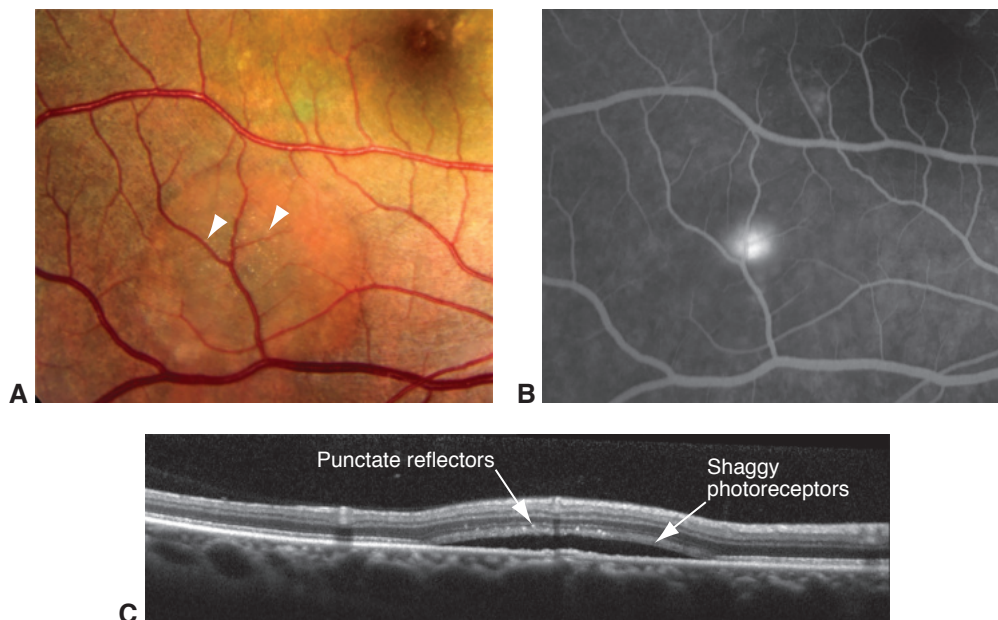


Figure 9-2 CSC with white dots. **A**, A color fundus photograph shows an ovoid elevation of the retina that has white dots on the undersurface (arrowheads). **B**, Fluorescein angiography reveals a single leakage point. **C**, The elevated retina, seen in cross section, has a thick coat on its inner surface that has autofluorescent characteristics consistent with retinal outer segment-derived fluorophores. These fluorophores are therefore considered to be derived from the outer segments that could not be phagocytized by the retinal pigment epithelium (RPE) because of the physical separation, caused by the fluid, of the retina and RPE. The region of shaggy photoreceptors contains punctate dots that are highly reflective; it has been theorized that these dots are macrophages. (Courtesy of Richard F. Spaide, MD.)

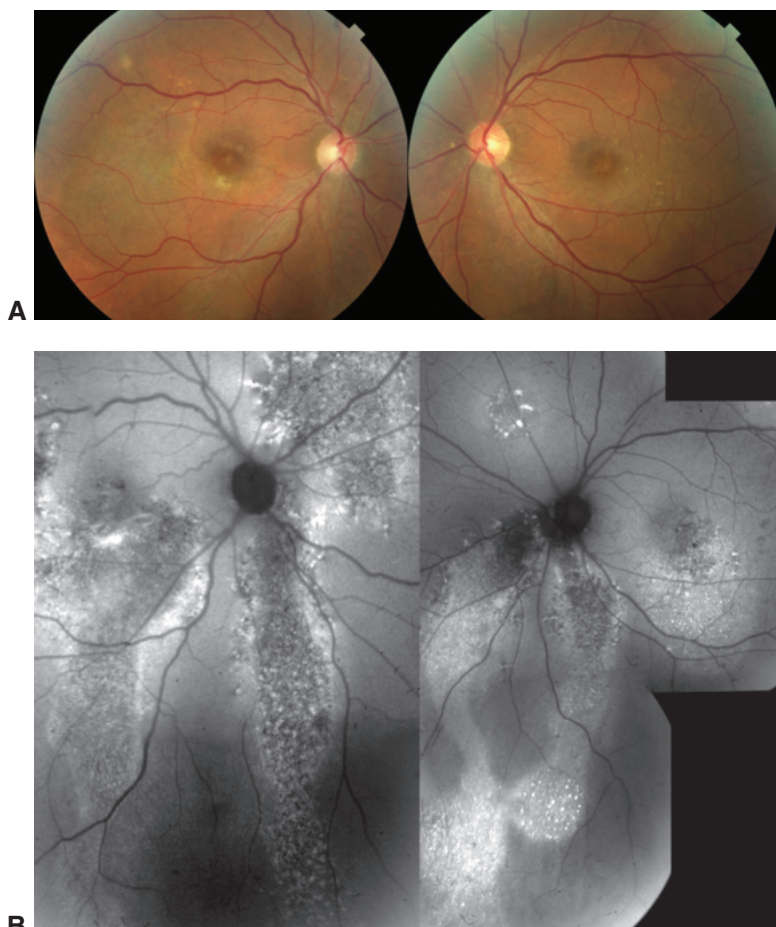


Figure 9-3 Autofluorescence abnormalities in CSC. **A**, Color photographs show the right and left eyes of a patient with CSC. Although subtle pigmentary changes are visible, it can be difficult to discern where fluid has accumulated. **B**, Autofluorescent images show widespread abnormalities induced by the presence of subretinal fluid, particularly the descending tracts caused by the fluid. (Used with permission from Imamura Y, Fujiwara T, Spaide RF. Fundus autofluorescence and visual acuity in central serous chorioretinopathy. *Ophthalmology*. 2011;118[4]:700–705.)

choroid in 1 healthy eye and in 3 eyes with CSC. Although ICG angiography is able to visualize choroidal vascular hyperpermeability (Fig 9-6), it has largely been supplanted by OCT, even for detecting possible coexisting choroidal neovascularization (CNV), which may be present in up to 20% of cases in individuals over the age of 50 years. OCT angiography seems to be adept at detecting type 1 CNV in these patients.

Imamura Y, Fujiwara T, Margolis R, Spaide RF. Enhanced depth imaging optical coherence tomography of the choroid in central serous chorioretinopathy. *Retina*. 2009;29(10):1469–1473.

Spaide RF, Klancnik JM Jr. Fundus autofluorescence and central serous chorioretinopathy. *Ophthalmology*. 2005;112(5):825–833.

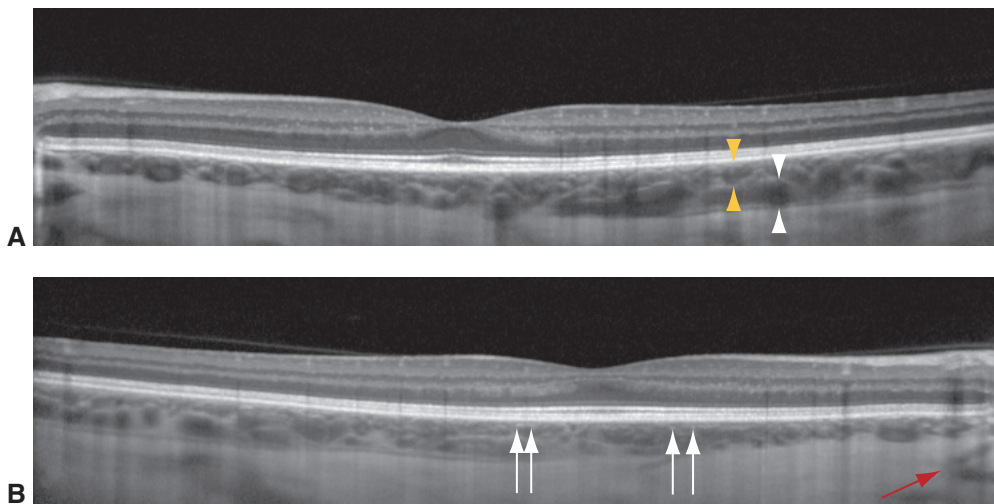


Figure 9-4 The internal structure of the healthy choroid. The choroidal vessels decrease in diameter from the outer to the inner choroid. **A**, The larger vessels (white arrowheads) are dark in the center with a thick hyperreflective wall. The medium-sized vessels (yellow arrowheads) have a smaller hyporeflective area in the center and a hyperreflective wall. **B**, As vessel diameter decreases, the central hyporeflective area decreases until it is not visible. At that size, the vessel appears as a white hyperreflective structure (arrows). Note the delineation of the hyporeflective line near the junction with the inner sclera, which appears to be in the suprachoroidal space. The red arrow points to a vessel coursing through the sclera. (Used with permission from Mrejen S, Spaide RF. Optical coherence tomography: imaging of the choroid and beyond. *Surv Ophthalmol*. 2013;58[5]:387–429.)

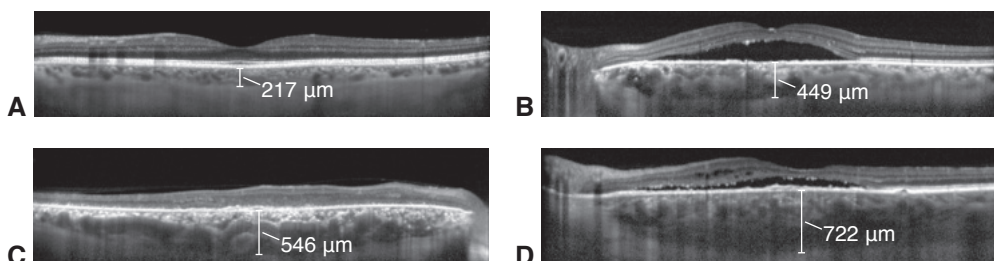


Figure 9-5 The choroid is seen in cross section using enhanced depth imaging optical coherence tomography (EDI-OCT). Subfoveal choroidal thickness was measured vertically from the outer border of the RPE to the inner border of the sclera (brackets) in a healthy eye in a 55-year-old man (**A**) and in 3 representative eyes with CSC: in a 44-year-old man (**B**), a 57-year-old man (**C**), and a 63-year-old man (**D**). (Used with permission from Imamura Y, Fujiwara T, Margolis R, Spaide RF. Enhanced depth imaging optical coherence tomography of the choroid in central serous chorioretinopathy. *Retina*. 2009; 29[10]:1469–1473.)

Differential Diagnosis

As discussed, CSC appears to be caused by hyperpermeability of choroidal vessels. Other entities that may be considered in the differential diagnosis include type 1 CNV and polyposidal choroidal vasculopathy (PCV), which is a variant of type 1 CNV. The fluorescein angiographic findings can overlap significantly; both show leakage of fluorescein and the

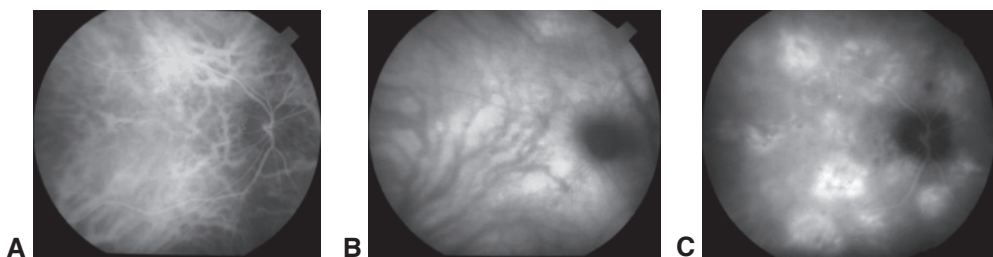


Figure 9-6 Stages of indocyanine green (ICG) angiography in CSC. **A**, Early after injection, the dye can be seen within the choroidal vessels. **B**, During the middle phase of the angiogram, choriocapillaris hyperpermeability results in the appearance of multiple hyperfluorescent clouds. **C**, Later in the angiogram, the dye has largely been removed from the choroidal vessels. Dye that has leaked into the stroma has diffused posteriorly, silhouetting the larger choroidal vessels. (Used with permission from Spaide RF, Hall L, Haas A, et al. Indocyanine green videoangiography of older patients with central serous chorioretinopathy. *Retina*. 1996;16(3):203–213.)

visualization of the structures underlying the RPE is poor. If CNV is present, OCT demonstrates an irregular wavy, shallow elevation of the RPE by a layer of material with heterogeneous reflectivity. The neovascularization seen in association with CSC are generally easy to detect with OCT angiography. What complicates the issue, particularly regarding treatment, is that type 1 CNV and PCV appear to be associated with CSC; they may be its sequelae.

Treatment

CSC is destructive and therefore can cause visually significant scotomas. Secondary CNV occurs in the immediate postoperative period in up to 2% of eyes that have been treated with photocoagulation. Laser photocoagulation is not associated with a reduced rate of recurrence. Verteporfin photodynamic therapy (PDT) reduces or eliminates subretinal fluid and is associated with few complications, the most common of which is atrophy, which occurs in about 4% of treated eyes. Recurrence after successful PDT is rare. Laser photocoagulation has no effect on choroidal thickness, while PDT decreases choroidal thickness and reduces choroidal vascular hyperpermeability. Use of mineralocorticoid receptor antagonists (eplerenone or spironolactone) has shown anecdotal benefit; however, a recent randomized, placebo-controlled trial using eplerenone in cases of chronic CSC showed no benefit of the medication over placebo.

- Maruko I, Iida T, Sugano Y, Ojima A, Ogasawara M, Spaide RF. Subfoveal choroidal thickness after treatment of central serous chorioretinopathy. *Ophthalmology*. 2010;117(9):1792–1799.
Warrior DJ, Hoang QV, Freund KB. Pachychoroid pigment epitheliopathy. *Retina*. 2013;33(8):1659–1672.

Choroidal Perfusion Abnormalities

The choroid has arterial supply from approximately 20 short posterior ciliary arteries and 2 anterior ciliary arteries. A network of branching arterioles distributes the blood throughout the choroid in a segmental fashion (Fig 9-7), ultimately leading to the choriocapillaris,

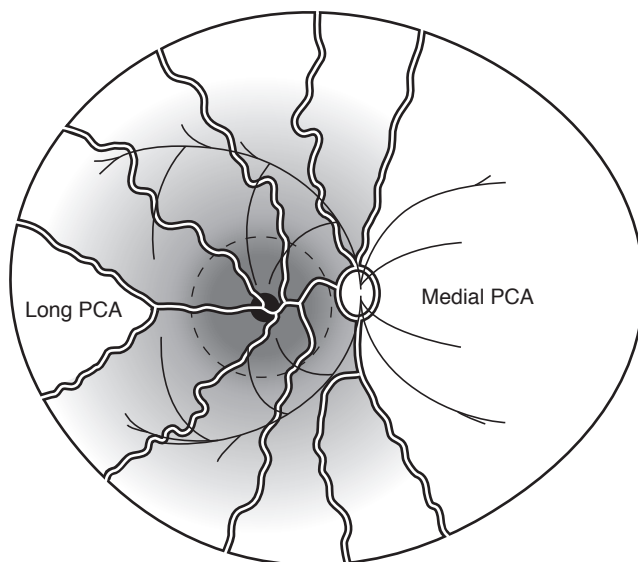


Figure 9-7 Diagram of the choroidal distribution of the short posterior ciliary arteries (PCAs) and long PCA branches arising from the temporal (lateral) PCA, and their watershed zones. Details of the branches from the medial PCA are not indicated. Dashed circle indicates the macular region. (Used with permission from Hayreh SS. Submacular choroidal vascular pattern: experimental fluorescein fundus angiographic studies. Albrecht Von Graefes Arch Klin Exp Ophthalmol. 1974;192(3):181–196.)

and helps reduce the blood pressure as well. Although the vessels in the choriocapillaris exhibit relatively uniform patterns in any given region of the eye, the pressure gradients imposed by the feeding arterioles and draining venules establish a lobular perfusion pattern. Abnormalities in choroidal blood flow can be divided into several main categories based on the underlying disease process.

Arteritic Disease

In arteritic diseases such as *giant cell arteritis* (Fig 9-8) or *granulomatosis with polyangiitis* (formerly, Wegener granulomatosis) (Fig 9-9), inflammatory occlusion can cause sectoral areas of nonperfusion. Fluorescein or ICG angiography is typically performed in cases in which an arteritic cause of vision loss is suspected, because flow defects in the choroid are often undetected by ophthalmoscopy alone.

Nonarteritic Disease

Nonarteritic problems with flow could occur due to embolic or systemic disease or as part of the manifestation of severe hypertension. Emboli from the heart, corticosteroids or calcium hydroxyapatite injection, and intravascular coagulation all have the potential to occlude choroidal vessels. Vascular occlusion could also occur in patients with lupus anticoagulants. *Thrombotic thrombocytopenic purpura* causes a classic pentad of findings: (1) microangiopathic hemolytic anemia, (2) thrombocytopenia, (3) fever, (4) neurologic dysfunction, and (5) renal dysfunction. Patients with this condition may have

Figure 9-8 Giant cell arteritis. ICG angiography image 1 day after this patient had severe vision loss secondary to arteritic anterior ischemic optic neuropathy revealed a wedge-shaped area of choroidal nonperfusion (curved arrow). The apex of the wedge of nonperfusion points toward the area of the occluded short PCA. (Courtesy of Richard F. Spaide, MD.)

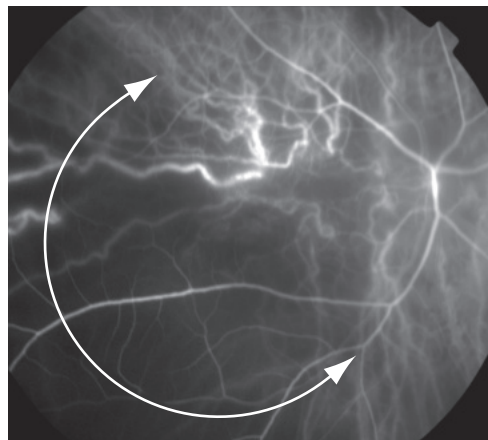
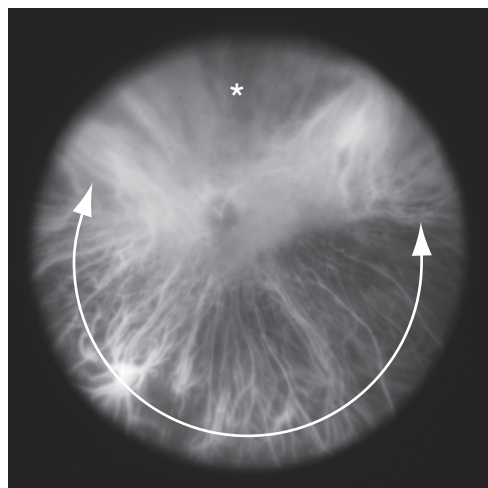


Figure 9-9 Granulomatosis with polyangiitis (formerly, Wegener granulomatosis). The early phase of wide-angle ICG angiography of the left eye reveals a widespread filling defect of the arterioles and choriocapillaris in the inferior fundus (curved arrow) and in a segmental area of the superior fundus (asterisk). (Reprinted from Iida T, Spaide RF, Kantor J. Retinal and choroidal arterial occlusion in Wegener's granulomatosis. Am J Ophthalmol. 2002;133[1]:151–152. Copyright © 2002, with permission from Elsevier.)



multifocal yellow placoid areas and associated serous detachment of the retina. Similar fundus findings may occur in patients with *disseminated intravascular coagulation*, in which consumption of coagulation proteins, involvement of cellular elements, and release of fibrin degradation products lead to hemorrhage from multiple sites and ischemia from microthrombi.

Similar fundus findings occur in patients with acute hypertension, such as *malignant hypertension* or *eclampsia* (Fig 9-10). In addition to retinal and optic nerve head abnormalities, these disorders also commonly lead to serous detachment of the retina associated with areas of yellow placoid discoloration of the RPE (see Fig 9-10). The perfusion abnormalities may range from focal infarction of the choriocapillaris to fibrinoid necrosis of larger arterioles. Resolution of smaller infarcts, which initially appear tan in color, produces small patches of atrophy and pigmentary hyperplasia called *Elschnig spots*.

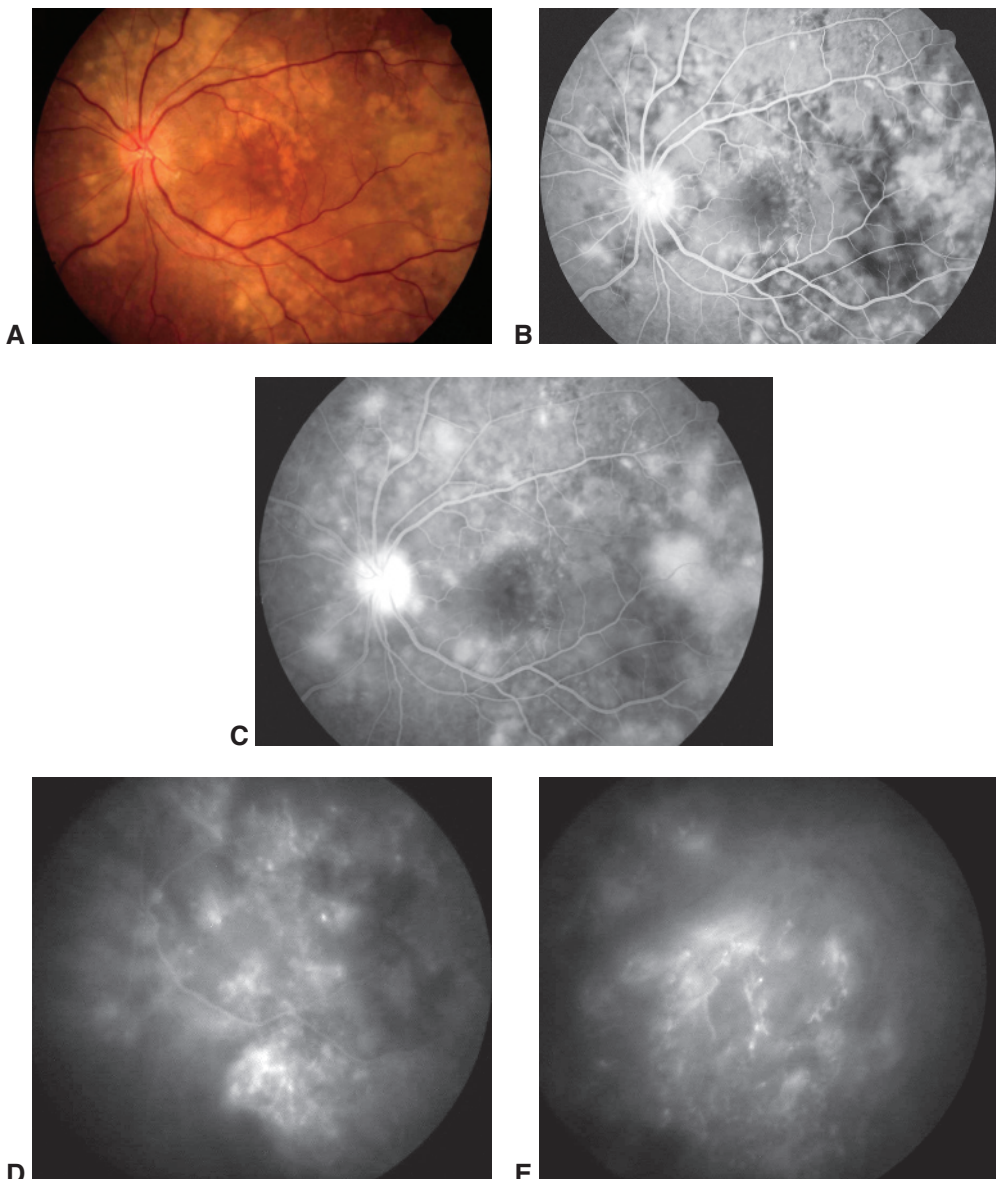


Figure 9-10 Preeclampsia with HELLP (*hemolysis, elevated liver enzymes, and low platelet count*) syndrome. **A**, Color fundus photograph reveals a serous detachment of the retina and multiple yellowish placoid areas at the level of the RPE and inner choroid. **B**, Early-phase fluorescein angiography image shows reticular patterns of decreased choroidal perfusion bordering areas of hyperfluorescence. Early leakage from the level of the RPE is evident and becomes more apparent in the later phases of the study (**C**). There is also staining of and leakage from the optic nerve. **D**, ICG angiography image shows profound choroidal vascular filling defects alternating with areas of abnormal vessel leakage and staining, a rare finding. **E**, In the late phase, numerous arterioles show staining of their walls, indicating severe vascular damage. (*Used with permission from Spaide RF, Goldbaum M, Wong DW, Tang KC, Iida T. Serous detachment of the retina. Retina. 2003;23(6):820–846.*)

Infarction of an arteriole can lead to *Siegrist streaks*, while sector-shaped abnormalities are called *Amalric triangles*.

Older patients may have areas of slow blood flow in the choroid, causing choroidal filling defects. The flow problems may result from low inflow pressure. Histologic sections of eyes of older patients may reveal intimal hyperplasia and medial hypertrophy with a decrease in the lumen size. This change may also adversely affect blood flow. Decreased flow in the segmentally arranged choroid can cause areas of particularly decreased perfusion between areas of low perfusion; these are called *watershed defects*.

Choriocapillaris Blood Flow Abnormalities

Choroidal blood flow defects affect lobule-sized areas of the choroid or areas supplied by arterioles and therefore affect one to several choroidal lobules. Many ocular diseases (eg, acute posterior multifocal placoid pigment epitheliopathy) characteristically produce lesions that are the putative size of a choroidal lobule. The advent of OCT angiography has uncovered another problem in choroidal circulation. The choriocapillaris develops multiple areas of signal voids, consistent with decreased perfusion. These areas increase in size and number with age; they are also larger and more numerous in patients with hypertension, pseudodrusen, or, interestingly, late age-related macular degeneration in the *fellow eye*. In addition, these defects exhibit power law probability distributions, which may be useful in gauging ocular and systemic health. These characteristic OCT angiographic findings are consistent with histologic studies showing an increasing number of ghost vessels in the choriocapillaris (a sign of vessel death), basal linear deposits, and subretinal drusenoid deposits with increasing age. Hayreh characterized the segmental nature of blood flow in the choroid from larger to smaller vessels and finally to the choriocapillaris lobule. The data from OCT angiography descends another unit of scale to show potential defects in capillary flow within parts of a choroidal lobule. Some diseases are known to be associated with RPE atrophy in addition to geographic atrophy; they include pseudoxanthoma elasticum and maternally inherited diabetes mellitus and deafness. Even in the absence of the development of RPE atrophy, these patients can exhibit remarkable loss of the choriocapillaris (Fig 9-11). Curiously, pseudodrusen also develop in patients with pseudoxanthoma elasticum.

Hayreh SS. Posterior ciliary artery circulation in health and disease: the Weisenfeld lecture.
Invest Ophthalmol Vis Sci. 2004;45(3):749–757; 748.

Increased Venous Pressure

Although rare, choroidal blood flow abnormalities may be related to venous outflow problems, including those caused by *dural arteriovenous malformations* or *carotid-cavernous fistulas* (Fig 9-12). Diagnosis of choroidal blood flow abnormalities often requires dye-based angiography, and occasionally a stethoscope (to detect a bruit). These patients should be referred for appropriate medical evaluation.

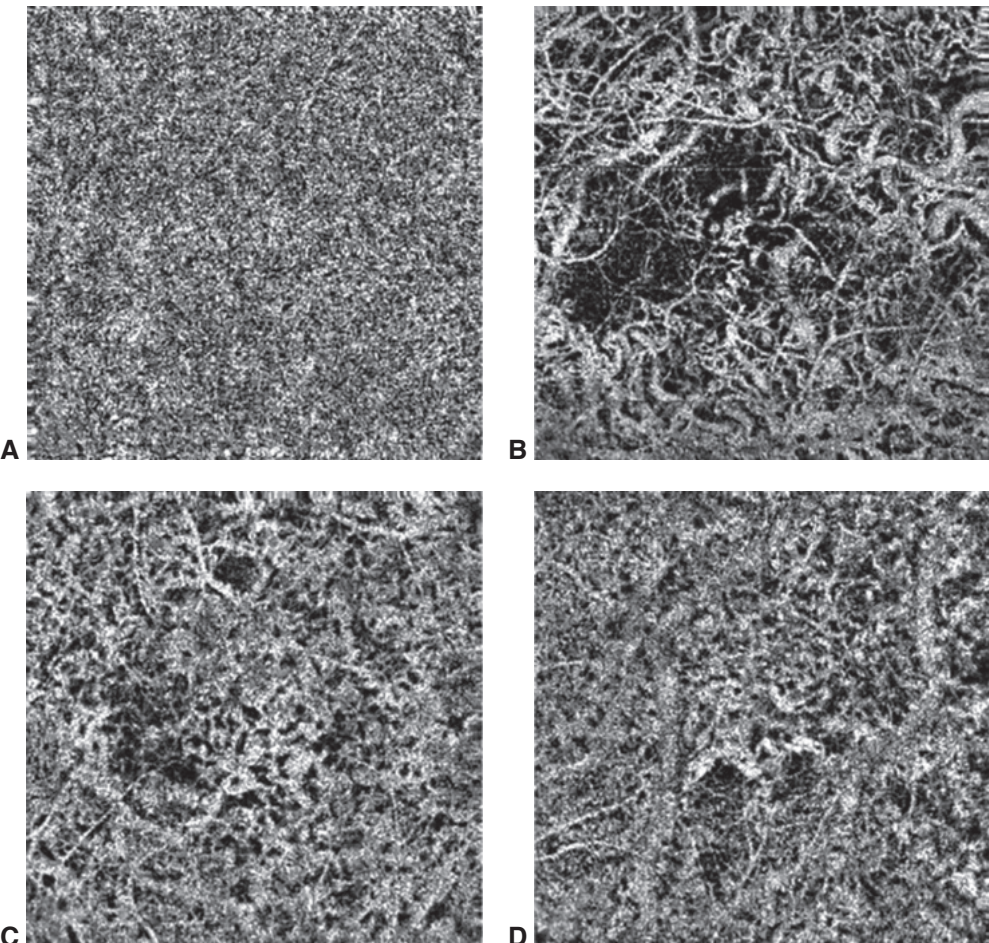


Figure 9-11 OCT angiography images of the choriocapillaris in a healthy patient and in patients with pseudoxanthoma elasticum (PXE). The eyes with PXE show no evidence of RPE atrophy. **A**, A healthy 63-year-old patient with no ocular disease. **B**, A 55-year-old patient and **C** and **D**, two 63-year-old patients, all with PXE. There is remarkable loss of the choriocapillaris. (From Spaide RF. Choriocapillaris signal voids in maternally inherited diabetes and deafness and in pseudoxanthoma elasticum. Retina. 2017;37(11):2008–2014.)

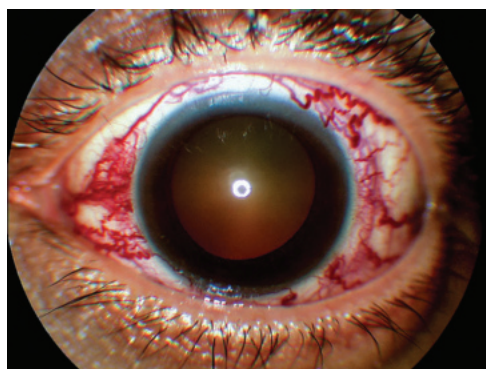


Figure 9-12 Photograph showing dilated episcleral vessels (after administration of topical phenylephrine hydrochloride) in a patient with a dural arteriovenous malformation. (Used with permission from Chung JE, Spaide RF, Warren FA. Dural arteriovenous malformation and superior ophthalmic vein occlusion. Retina. 2004;24(3):491–492.)

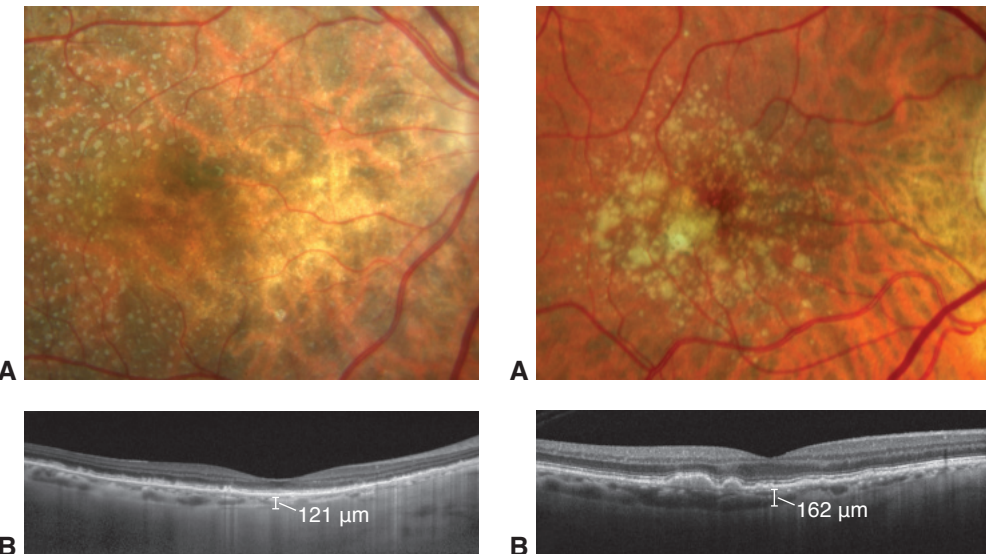


Figure 9-13 Pseudodrusen and the choroid. **A**, Color fundus photograph showing an eye that has prominent pseudodrusen. **B**, The true nature of the pseudodrusen is seen as subretinal drusenoid deposits. The subfoveal choroidal thickness is 121 μm . (Used with permission from Spaide RF. Disease expression in nonexudative age-related macular degeneration varies with choroidal thickness. *Retina*. 2018;38(4):708–716.)

Figure 9-14 Drusen and the choroid. **A**, An eye with typical soft drusen. **B**, The subfoveal choroidal thickness is 162 μm . The choroid is thinner in eyes with pseudodrusen (subretinal drusenoid deposits) than in those with drusen. (Used with permission from Spaide RF. Disease expression in nonexudative age-related macular degeneration varies with choroidal thickness. *Retina*. 2018;38(4):708–716.)

Age-Related Choroidal Atrophy

The thickness of the choroid decreases with higher amounts of myopia and increasing age. The eyes of some older patients have choroids that are much thinner than expected. These same eyes tend to have *pseudodrusen*, which resemble drusen in appearance but are caused by collections of subretinal drusenoid deposits above the RPE. Like eyes with drusen, eyes with subretinal drusenoid deposits have an increased risk for CNV, particularly types 2 and 3, and geographic atrophy. More than 90% of eyes with geographic atrophy also have pseudodrusen. Unlike eyes with drusen, eyes with subretinal drusenoid deposits exhibit poorer microperimetry performance and markedly prolonged dark adaptation (Figs 9-13, 9-14).

Spaide, RF. Disease expression in nonexudative age-related macular degeneration varies with choroidal thickness. *Retina*. 2018;38(4):708–716.

Choroidal Folds

Folds in the choroid, sometimes called *chorioretinal folds*, occur secondary to several diseases. Forces external to the eye, such as an indenting tumor or thyroid eye disease, can cause folds in the choroid. The sclera may be thickened by posterior scleritis,

thereby crowding the choroid. A relatively common cause, one that is also poorly characterized, is the development of choroidal folds in middle-aged adults, some of whom acquire an increased amount of hyperopia. One theory is these patients, who develop bilaterally symmetric horizontal or oblique choroidal folds, may have an inflammatory disease that causes scleral shortening and flattening of the posterior sclera. Engorgement of the choroid causes an expansion of the tissue, which is limited by the sclera. The engorgement can be the result of inflammation and a diffusely infiltrative condition such as lymphoma. Reduced intraocular pressure can cause ciliochoroidal effusions and curvilinear choroidal folds in the posterior pole, a condition known as *hypotony maculopathy*. Medications such as topiramate can cause idiopathic swelling of the choroid with creation of chorioretinal folds and ciliochoroidal effusions without hypotony. Increased intracranial pressure can cause fine folds that course circumferentially around the optic nerve head; these folds are called *Patton lines*. Localized choroidal folds can be seen in association with CNV, choroidal neoplasms, and scleral buckles (Fig 9-15).

Spaide RF, Goldbaum M, Wong DW, Tang KC, Iida T. Serous detachment of the retina. *Retina*. 2003;23(6):820–846.

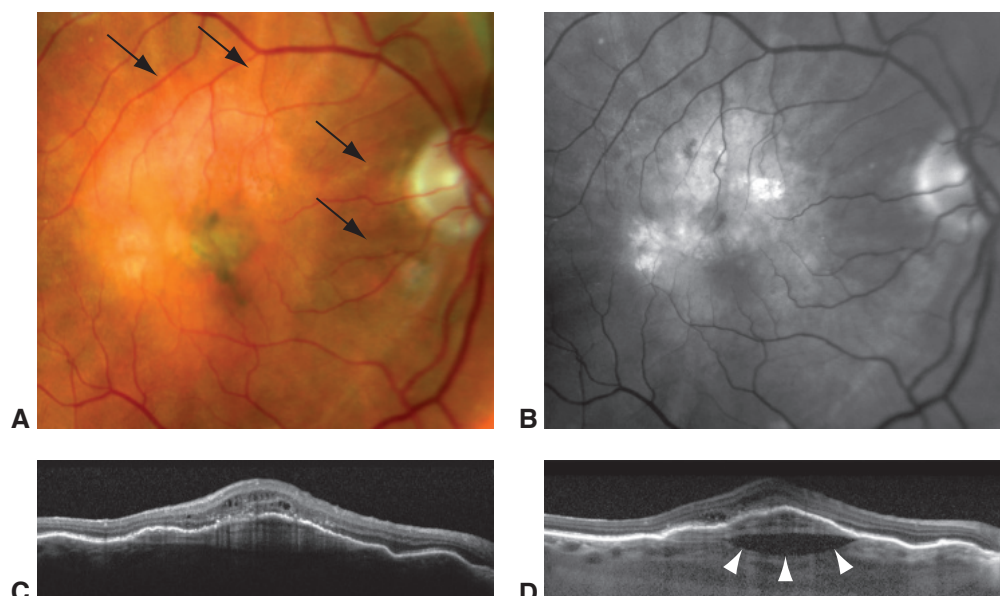


Figure 9-15 Multimodal imaging of the right eye of a 95-year-old man in whom chorioretinal folds developed after intravitreal anti-vascular endothelial growth factor therapy to treat a fibrovascular pigment epithelial detachment (PED). **A**, Color and **B**, red-free photographs show chorioretinal folds (arrows) radiating from the retracted borders of the fibrovascular PED. **C**, A conventional OCT scan shows little exudation except for a few intraretinal cystic changes. Note the multilamellar hyperreflective structure on the back surface of the partly collapsed PED. **D**, An EDI-OCT scan shows recurrent fluid exudation (arrowheads) at the base of the fibrovascular PED secondary to choroidal neovascularization on the back surface of the hyperreflective lamellar material. (Used with permission from Mrejen S, Spaide RF. Optical coherence tomography: imaging of the choroid and beyond. *Surv Ophthalmol*. 2013;58(5):387–429.)

Choroidal Hemangiomas

Isolated *choroidal hemangiomas* are reddish-orange, well-circumscribed tumors of varying thickness that can affect the macula either directly or through subretinal fluid (Fig 9-16). Circumscribed hemangiomas transilluminate readily and exhibit highly echographic patterns on ultrasonography. During dye-based angiography, hemangiomas show very early filling of large vessels. *Sturge-Weber syndrome* (encephalofacial cavernous hemangiomatosis) causes a diffuse hemangioma that may present first as glaucoma or amblyopia in children. The areas corresponding to the hemangioma have a typical tomato ketchup appearance, and the underlying choroidal markings are not visible. The

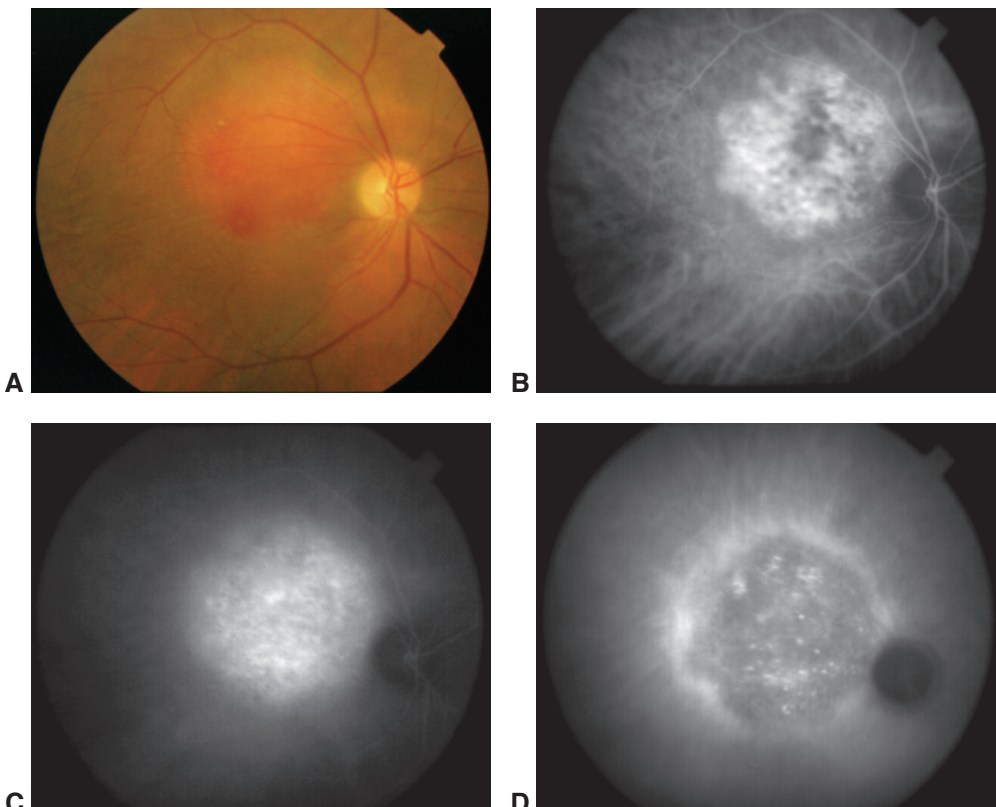


Figure 9-16 Choroidal hemangioma. **A**, Fundus photograph of the typical reddish-orange elevation of a circumscribed choroidal hemangioma. **B**, Soon after ICG injection, the vascular composition of the hemangioma is revealed. **C**, Hyperfluorescence of the tumor occurs in the middle phase of the angiogram study from a combination of dye within and leakage from the vessels of the hemangioma. **D**, In the late phase of the study, the dye "washes out" of the lesion, leaving hyperfluorescent staining in the adjacent tissues. (Used with permission from Spaide RF, Goldbaum M, Wong DW, Tang KC, Iida T. Serous detachment of the retina. *Retina*. 2003;23(6):820-846.)

choroidal hemangiomas in Sturge-Weber syndrome are sometimes overlooked because they are diffuse and may blend imperceptibly into adjacent normal choroid. An ipsilateral facial nevus flammeus (port-wine stain) is also typically present in patients with this syndrome.

The alterations caused by choroidal hemangiomas include cystic retinal edema, hard exudate, neurosensory detachment, and calcification and ossification in the choroid. Hemangiomas have been treated with laser photocoagulation, cryopexy, external-beam and plaque radiation, and PDT. The success rate for treatment of diffuse hemangiomas with visual acuity improvement is poor. PDT with verteporfin may have the lowest risk of treatment-related morbidity.

Beardsley RM, McCannel CA, McCannel TA. Recurrent leakage after Visudyne photodynamic therapy for the treatment of circumscribed choroidal hemangioma. *Ophthalmic Surg Lasers Imaging Retina*. 2013;44(3):248–251.

Blasi MA, Tiberti AC, Scupola A, et al. Photodynamic therapy with verteporfin for symptomatic circumscribed choroidal hemangioma: five-year outcomes. *Ophthalmology*. 2010; 117(8):1630–1637.

Madreperla SA, Hungerford JL, Plowman PN, Laganowski HC, Gregory PT. Choroidal hemangiomas: visual and anatomic results of treatment by photocoagulation or radiation therapy. *Ophthalmology*. 1997;104(11):1773–1778.

Tsipursky MS, Golchet PR, Jampol LM. Photodynamic therapy of choroidal hemangioma in Sturge-Weber syndrome, with a review of treatments for diffuse and circumscribed choroidal hemangiomas. *Surv Ophthalmol*. 2011;56(1):68–85.

Uveal Effusion Syndrome

In *uveal effusion syndrome*, abnormal scleral composition or thickness reduces trans-scleral aqueous outflow, inhibiting net fluid movement through the posterior eye wall. Choroidal and ciliary body thickening, RPE alterations, and exudative retinal detachment may occur. The choroid is often so thick that OCT imaging is not possible, but the gross thickening can be imaged with ultrasonography. Fluorescein angiography usually shows a leopard-spot pattern of hypofluorescence without focal leakage (Fig 9-17). Visual function may fluctuate. Although scleral window surgery may yield anatomical restitution, the visual results may be less satisfactory because of chronic, irreversible changes caused by the condition. A high index of suspicion for uveal effusion syndrome should be maintained for young patients with hyperopia whose disorder has been diagnosed as either CSC or retinal detachment without a retinal hole or tear. In some patients, intravitreal triamcinolone may cause resolution of fluid.

Elagouz M, Stanescu-Segall D, Jackson TL. Uveal effusion syndrome. *Surv Ophthalmol*. 2010; 55(2):134–145.

Johnson MW, Gass JD. Surgical management of the idiopathic uveal effusion syndrome. *Ophthalmology*. 1990;97(6):778–785.

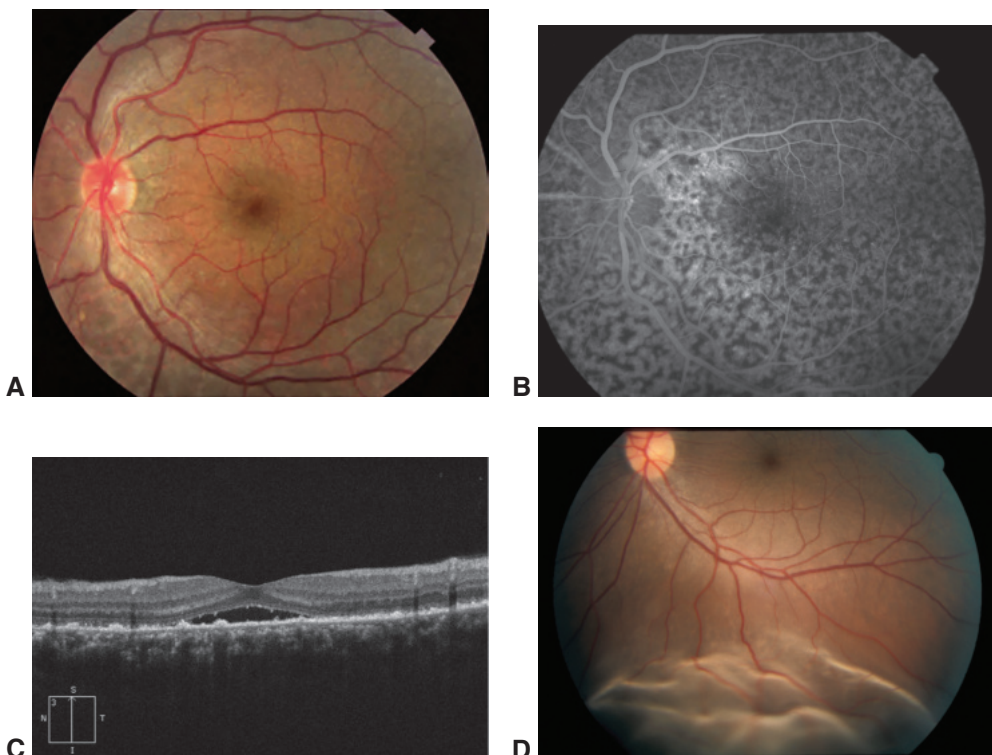


Figure 9-17 Idiopathic uveal effusion. **A–C**, In this patient's left eye, the visual acuity was reduced to 20/70, and systemic workup was negative. **A**, Fundus photograph demonstrates blunted foveal reflex and irregular, subtle subretinal deposits. **B**, Corresponding fluorescein angiography image reveals a diffuse leopard-spot pattern of blocking with intervening window defects involving the entire posterior pole. **C**, OCT scan reveals a small amount of subfoveal fluid and outer retinal deposits. Not shown is a peripheral serous retinal detachment. **D**, Fundus photograph from a separate case of recent-onset uveal effusion shows the typical appearance of serous retinal detachment syndrome as well as an underlying choroidal detachment, which is common for this condition. (Parts A–C courtesy of Ronald C. Gentile, MD; part D courtesy of Colin A. McCannel, MD.)

Bilateral Diffuse Uveal Melanocytic Proliferation

A rare paraneoplastic disorder affecting the choroid, *bilateral diffuse uveal melanocytic proliferation* (BDUMP) causes diffuse thickening of the choroid, reddish or brownish choroidal discoloration, serous retinal detachment, and cataracts (Fig 9-18). The bilateral proliferation of benign melanocytes is usually associated with or often heralds systemic cancer. These proliferations can look like large nevi. Most patients with BDUMP also exhibit nummular loss of the RPE, an anatomical change that differs distinctly from large nevi or thickening of the choroid. These areas of RPE loss are hypoautofluorescent during autofluorescence imaging, but hyperfluorescent during fluorescein angiography. OCT shows mounds of residual material, presumed to be persistent RPE cells between areas

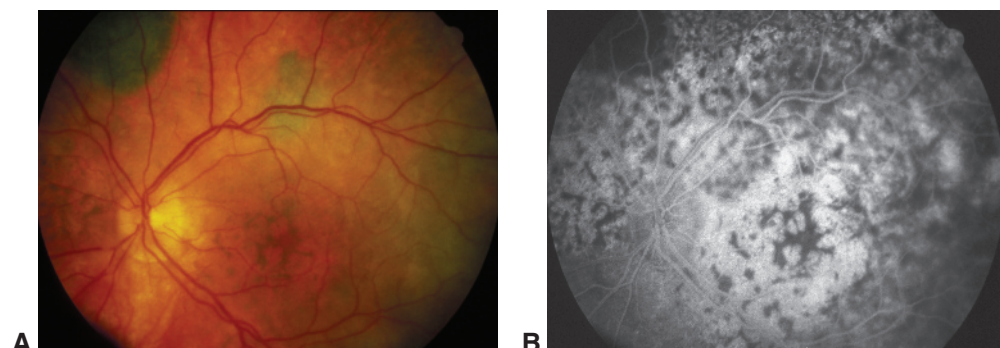


Figure 9-18 Bilateral diffuse uveal melanocytic proliferation. **A**, Note the large nevuslike regions of increased pigmentation in this fundus photograph. **B**, Fluorescein angiography image demonstrates decreased fluorescence in the region of the melanocytic proliferation in the superonasal portion. There is a giraffe-spot pattern to the fluorescence in the posterior pole, secondary to nummular loss of the RPE in the hyperfluorescent areas. (Courtesy of Mark Johnson, MD.)

of loss. Tumors commonly associated with BDUMP are cancers of the ovary, uterus, and lung, but BDUMP may also occur with cancers of the kidney, colon, pancreas, gallbladder, breast, and esophagus.

- Gass JD, Gieser RG, Wilkinson CP, Beahm DE, Pautler SE. Bilateral diffuse uveal melanocytic proliferation in patients with occult carcinoma. *Arch Ophthalmol*. 1990;108(4):527–533.
Wu S, Slakter JS, Shields JA, Spaide RF. Cancer-associated nummular loss of the pigment epithelium. *Am J Ophthalmol*. 2005;139(5):933–935.

CHAPTER 10

Myopia and Pathologic Myopia

There has been an explosion in the prevalence of myopia around the world. Although the more severe manifestations of myopia, variously termed *pathologic myopia* or *high myopia*, are found in a smaller proportion of the population, this subset accounts for many of the vision problems that occur in eyes with myopia. Pathologic myopia could be defined as the development of the pathologic changes associated with myopia. Most studies use a myopic refractive error greater than –6 diopters (D) or an axial length of 26.5 mm or more as a threshold for pathologic myopia. However, cutoffs based on refractive error or axial length in which the probability of pathologic changes to occur are increased are not sharp demarcations.

Currently, pathologic myopia is found in 1%–2% of individuals in the United States, approximately 5% in Italy, 5%–8% in Japan, 15% in Singapore, and 38% in university students in Taiwan. Many factors might contribute to the occurrence of myopia; determining a cause has proved difficult as findings from one study have not necessarily been replicated in other studies. Numerous studies have been conducted to examine whether there are any genetic associations to the occurrence of pathologic myopia, but again, there are no universal findings. Given the rapid and widespread acquisition of myopia, especially pathologic myopia in diverse populations, the development of myopia may be due to elements of emmetropization gone awry. Common factors among patients with pathologic myopia seem to include a lack of outdoor activities at a young age and are related to concentrated near work. Societal transitions from hunting or agrarian activities to dependence on modern manufacturing or knowledge workers created a generational shift in the proportion of myopic people. In East Asia, young people are pressured to do well on examinations to gain entrance into universities, because graduates of those universities have desirable well-paying jobs that also help promote economic and scientific advances for their respective countries. Because it is highly unlikely any of these pressures will abate over the next generations, research into myopia prevention and treatment is a major public health issue. Pathologic myopia and its consequences rank at the top or near the top of the list of causes of vision decrease or blindness in many countries; with its increase in prevalence, it will likely become even more important in the future.

Prevention

Prevention of pathologic myopia is a complex and evolving topic. Pathologic myopia has only been recognized as a problem relatively recently. The various animal models may have only limited applicability to humans; to date, there have been only limited studies

with human participants. In addition, the epidemiologic data vary. Participation in outdoor activities is thought to be a contributing factor in reducing the incidence of myopia; this finding is supported by experimental animal model data showing that periods of blue light exposure decrease the amount of myopia that develops. Some theories posit chromatic aberration in the eye is operative in causing myopia; red light is focused at a deeper level than blue light.

In 1891, Taylor recommended atropine, blue glasses, and the application of leeches for the treatment of progressive myopia. Much later, McBrien and his coworkers demonstrated that atropine could slow the development of form-deprivation myopia via a mechanism that was independent of accommodation. Numerous studies have been conducted using atropine eyedrops, including eyedrops at very low concentrations, with a slight decrease in the amount of myopia that develops. Although the use of leeches has been discontinued, progress since the time of Taylor has been limited in scope and effect (and in fact, we have no data to discount the importance of leeches).

- Chia A, Lu QS, Tan D. Five-year clinical trial on atropine for the treatment of myopia 2: Myopia control with atropine 0.01% eyedrops. *Ophthalmology*. 2016;123(2):391–399.
McBrien NA, Moghaddam HO, Reeder AP. Atropine reduces experimental myopia and eye enlargement via a nonaccommodative mechanism. *Invest Ophthalmol Vis Sci*. 1993;34(1):205–215.
Spaide RF, Ohno-Matsui K, Yannuzzi LA. *Pathologic Myopia*. New York: Springer-Verlag; 2014.
Taylor CB. *Lectures on Diseases of the Eye*. London: Kegan Paul, Trench and Co; 1891.

The Retina

In the central macula, the retinal thickness in eyes with pathologic myopia is not that different from that in emmetropic eyes, particularly in younger individuals. In older subjects with marked thinning of the choroid, there may be loss of the outer retinal bands and apparent thinning of the central macula (Fig 10-1). Outside of the macula, the retinal thickness in eyes with pathologic myopia is thinner than that in emmetropic eyes. Lattice degeneration is more commonly found in myopic eyes. With increasing age, the vitreous starts to detach in all eyes, starting with smaller areas of detachment bordering areas of attachment; this is also true for myopic eyes. Vitreous traction in areas of persistent attachment can cause retinal tears and then detachment, or may even cause subretinal fluid to occur in association with small atrophic holes in lattice degeneration. The proportion of retinal detachment secondary to holes as compared with tears increases with more exaggerated amounts of myopia. Repairing retinal detachment may be more difficult in patients with high myopia because of the thinner retina, a higher prevalence of lattice degeneration, the thinner sclera (which can complicate buckle placement), the more posterior location of retinal breaks, and the possibility of multiple retinal defects.

Traction on the retina in eyes with larger amounts of myopia can affect broader areas of the retina, independent of vitreous attachment. The posterior portion of the retina can remain attached to the retinal pigment epithelium (RPE) despite broad areas of traction. Retinal thickness increases because of the fluid accumulation within the retina and distention of the cellular elements in the retina.

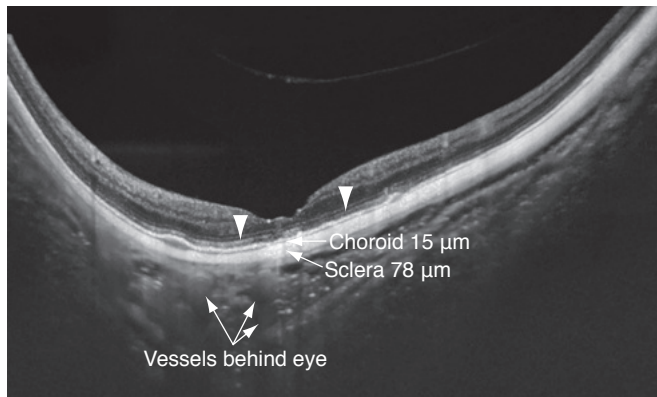


Figure 10-1 Swept-source optical coherence tomography (SS-OCT) image demonstrates some of the many abnormalities that can be present in a highly myopic eye. The magnitude and thickness of the reflection from the ellipsoid layer (arrowheads) shows a rough correlation to the thickness of the underlying choroid, but do vary with the location in the image because of a number of factors, including defocus of the illumination beam and astigmatism. The subfoveal choroid is 15 μm thick and the subfoveal sclera is 78 μm thick. Both measurements are less than 10% of their expected values. The layers of this eye are so thin that it is possible to image structures in the orbit behind the eye, including blood vessels. Note the unusual shape of the eye, which is due to the presence of a staphyloma. (Courtesy of Richard F. Spaide, MD.)

Myopic macular schisis most commonly involves Henle fiber layer but can also involve the inner nuclear layer, the ganglion cell layer, and the region underneath the internal limiting membrane (ILM). The traction can be related to vitreous traction from attached vitreous, but eyes with myopic macular schisis can still have vitreous traction with posterior vitreous detachment (Fig 10-2). Myopic macular retinoschisis can occur in eyes with posterior vitreous detachment that, at the time of surgery, are found to have minimal amounts of adherent residual vitreous. After posterior vitreous detachment, a skim coat of vitreous remains on the surface of the retina and appears to cause traction. Varying amounts of epiretinal membrane may also contribute to the traction. Peeling of the ILM causes resolution of the schisis, typically near the area where the ILM was peeled, leading to the conclusion the ILM may be altered in eyes with myopic macular retinoschisis. An alternate possibility is that many of these eyes have progressive myopia with continued ocular expansion. The ILM may not necessarily be remodeled, and thus it may not expand like the outer retina.

More advanced tractional changes can lead to retinal detachment over staphylomas and to myopic macular holes. Macular holes in eyes with high myopia have a lower proportion of successful repair than in emmetropic eyes and frequently require the use of the inverted ILM technique in which the ILM is folded over the hole prior to fluid gas exchange. In addition, in eyes with high myopia macular holes may lead to extensive or complete retinal detachment (see Chapter 16, Fig 16-20 in this volume).

Traction appears to affect the retinal vessels in pathologic myopia. The retinal vessels can straighten, particularly the maculopapillary bundle, with occasional microaneurysm formation, and there can be a slight elevation of the arcade vessels. Paravascular cavitations and lamellar holes may also be found, but these defects do not appear to have any clinically meaningful effect.

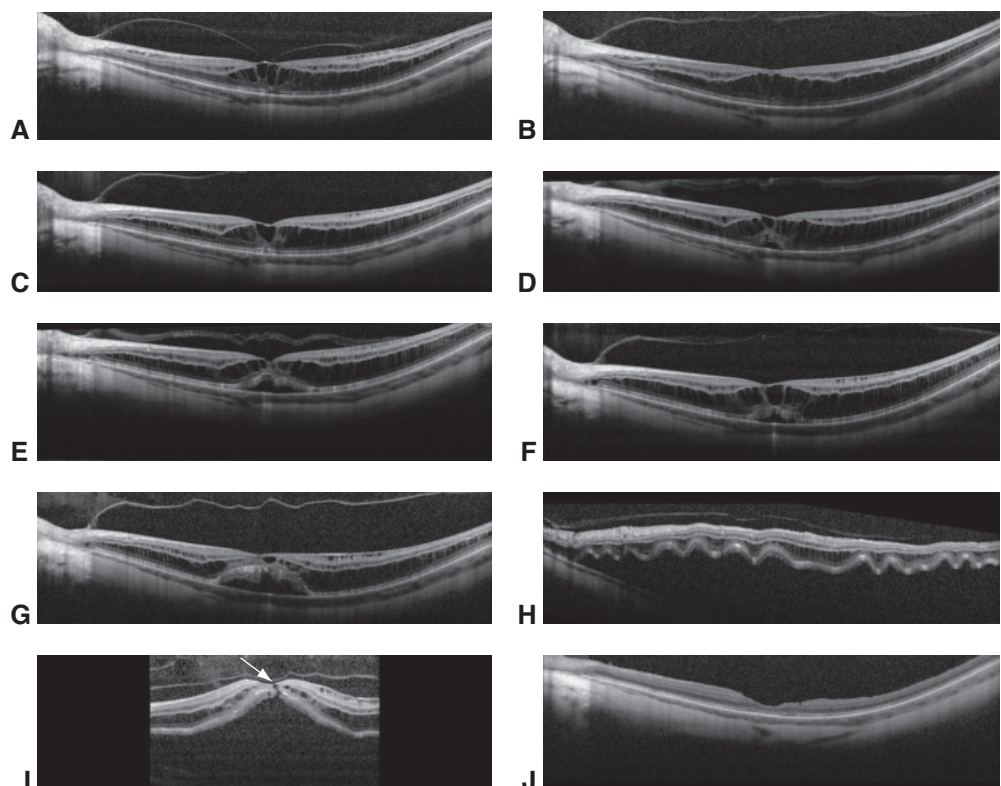


Figure 10-2 Successive OCT examinations of a female patient with myopic macular schisis. At presentation, the patient had a perifoveal vitreous detachment (**A**) that separated (**B**). **C**, Four months later, a larger fovea cavitation developed. **D**, One month after that, a localized detachment of the fovea occurred. **E**, One month after the image in **D** was taken, the detachment was slightly larger (**F**). **G**, At 4-month follow-up, the macular detachment had increased in size. **H**, One month later, she returned with a substantial loss of central vision. Imaging revealed a large retinal detachment with edematous folding of the outer retina. **I**, A small macular hole caused the larger detachment (arrow). **J**, The macular hole was repaired by vitrectomy with internal limiting membrane removal, which resulted in resolution of the retinal detachment and the myopic macular schisis. (Courtesy of Richard F. Spaide, MD.)

Bruch Membrane

Located between the RPE and the choriocapillaris, Bruch membrane forms early in the development of the eye and appears to undergo varying amounts of remodeling over time. However, this may not be true in eyes with more advanced amounts of myopia. In these eyes, the Bruch membrane opening shifts so that the nasal portion of the optic nerve head is undermined by Bruch membrane. The nerve fibers must course around the nasal portion of the Bruch membrane opening; this has been referred to as “supertraction” or “supertraction crescent.” Corresponding temporal displacement of the posterior part of Bruch membrane opening is related to the myopic macular crescent typically located on the temporal side of the optic nerve. The lack of choroidal circulation in this region creates a white appearance due to the visualization of the sclera.

Ocular expansion puts stress on Bruch membrane, potentially leading to fine ruptures called *lacquer cracks*. The outer lamella of Bruch membrane is the basement membrane of the choriocapillaris. The cracks disrupt not only the avascular membrane, but may also rupture the capillaries in the choriocapillaris, resulting in subretinal hemorrhages. These hemorrhages can be difficult to differentiate from those caused by choroidal neovascularization (CNV), which is discussed in the following section. Lacquer cracks offer a region of ingress for CNV (Fig 10-3). Extension of lacquer cracks through the center of the fovea can cause distortion and loss of visual acuity. If many lacquer cracks develop, a region of pigmentary granularity can form. In late-stage myopic degeneration, large dehiscences in Bruch membrane may occur.

Choroidal Neovascularization

An important pathologic change common to eyes with pathologic myopia is the development of CNV. Early manifestations of CNV in pathologic myopia include decreased or distorted vision. The clinical findings include subretinal hemorrhage, elevation and

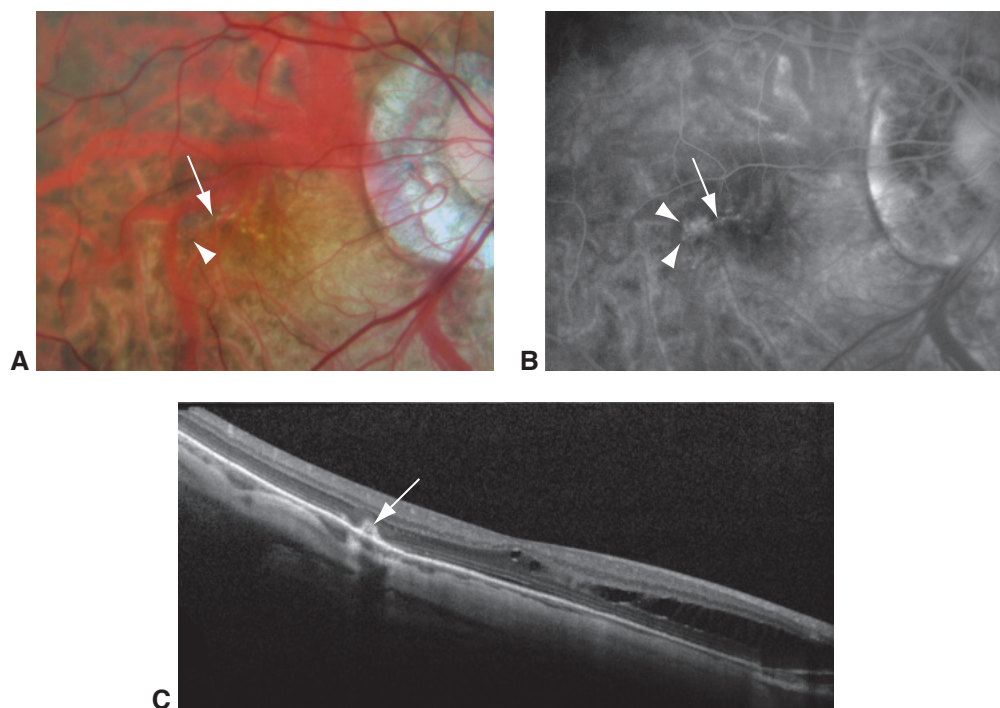


Figure 10-3 Myopic choroidal neovascularization (CNV) emanating from a lacquer crack. **A**, A patient with -16 diopter myopia developed a small scotoma near the center of the visual field. Note the lacquer cracks (arrow) and associated pigmentary changes (arrowhead). **B**, Fluorescein angiography image shows a hyperfluorescent lesion consistent with CNV. **C**, OCT scan shows a small elevated lesion (arrow) and also nonassociated macular schisis. (Used with permission from Spaide RF. Choroidal Neovascularization. In: Spaide RF, Ohno-Matsui K, Yannuzzi LA, eds. Pathologic Myopia. New York: Springer-Verlag; 2014: 211–230.)

infiltration of the outer retina by vascular invasion, accumulation of subretinal fluid, and a localized area of pigmentary change. It is easy to overlook the findings of CNV in highly myopic eyes using ophthalmoscopy alone.

The size and apparent exudation of CNV appears to vary inversely with the amount of myopia. Myopic CNV does not cause retinal edema as commonly as age-related macular degeneration does. Myopic CNV is often seen in close association with lacquer cracks, or it may occur as an extension from a region of chorioretinal atrophy. In the United States, it is not uncommon to find CNV in young myopic women who show signs of multifocal choroiditis and panuveitis, either at the time or later. These eyes may develop damage from the CNV, from inflammation, or from both; each component requires careful treatment. Myopic CNV was first treated with thermal laser photocoagulation and then later treated with photodynamic therapy, but both approaches were suboptimal. The advent of injections of anti-vascular endothelial growth factor (anti-VEGF) agents was a major advance; this treatment caused regression of the neovascularization without causing immediate collateral damage (Fig 10-4). To control the CNV, episodic reinjection of medications may be necessary. Some patients may need frequent reinjections, including patients with CNV developing at the edge of a staphyloma or with untreated multifocal choroiditis and panuveitis. With or without treatment, CNV in pathologic myopia may become hyperpigmented; this lesion is called a Fuchs spot. With longer follow-up, areas of atrophy often develop at or adjacent to the pigmented lesions, and the atrophy eventually encompasses the central macula.

The Choroid in Pathologic Myopia

More than 70% of the blood flow to the eye goes to the choroid, a structure that provides oxygen to the choroid, RPE, and the outer retina in addition to acting as a heat sink, absorbing stray light, participating in immune response and host defense, and acting as an integral part in the process of emmetropization. Optical coherence tomography (OCT), particularly either swept-source OCT (SS-OCT) or enhanced depth imaging OCT (EDI-OCT) using spectral-domain OCT (SD-OCT), can image the full thickness of the choroid in myopic eyes.

One study found that the mean subfoveal choroid thickness in children aged 11–12 years was 369 ± 81 μm in girls and 348 ± 72 μm in boys. With increasing age, the choroid becomes thinner; for example, the typical subfoveal choroidal thickness in an emmetropic 60-year-old might be approximately 220–260 μm . Eyes with myopia, particularly those progressing into the range of pathologic myopia, undergo ocular expansion starting in late childhood, and this expansion is also associated with thinning of the choroid (Fig 10-5). A group of patients with myopia with a mean age of 59.7 years had a mean refractive error of -11.9 D and a mean subfoveal choroidal thickness of 93 μm , with a relatively large standard deviation of 63 μm . The thinning of the choroid per decade of life is approximately the same in myopic eyes as in nonmyopic eyes. Therefore, older individuals, or individuals with higher amounts of myopia, may have remarkably thin choroids. The most significant predictor of visual acuity in highly myopic eyes with no macular pathology is subfoveal choroidal thickness. Eyes with pathologic myopia have

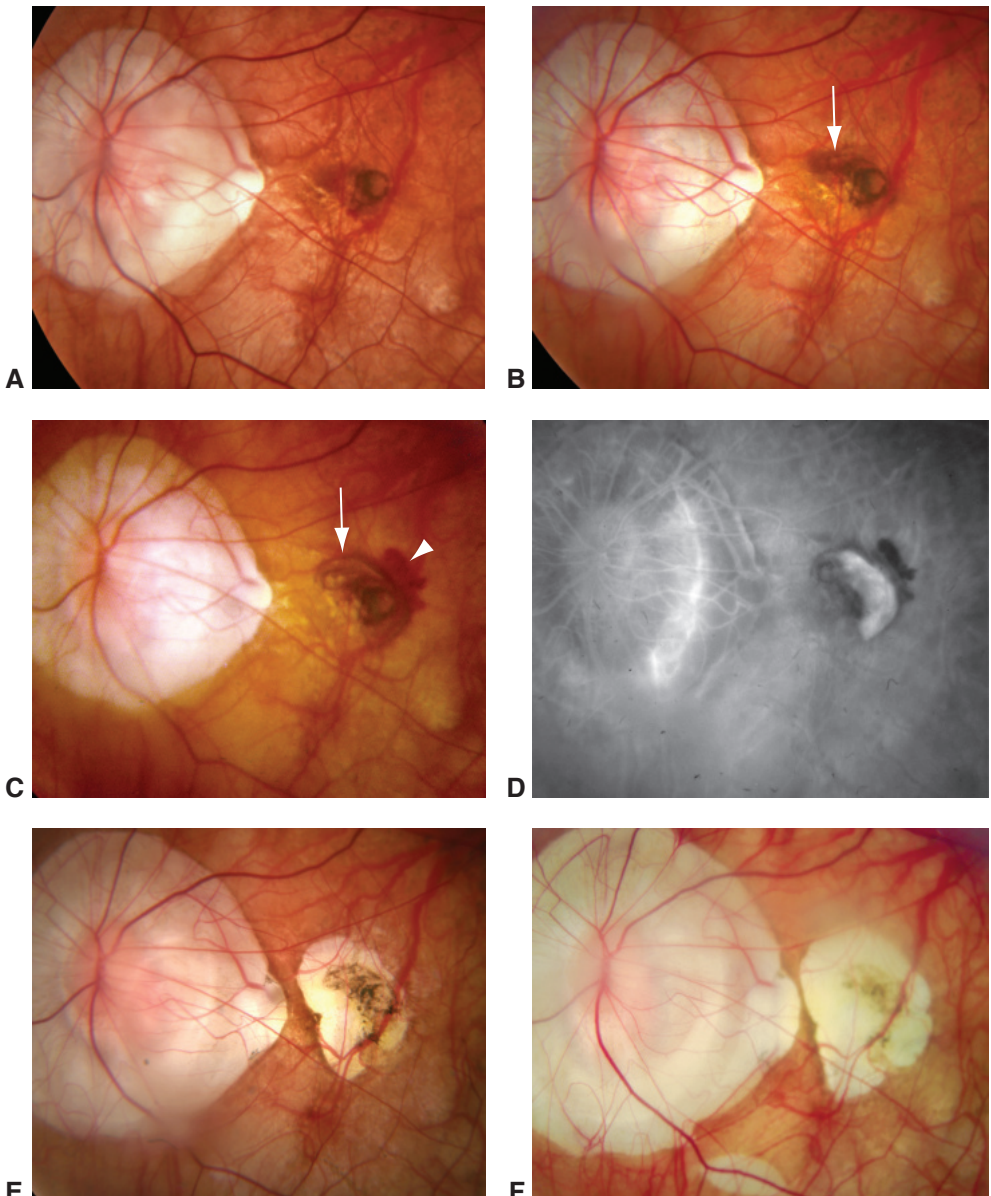


Figure 10-4 Expansion of CNV after treatment with photodynamic therapy followed by bevacizumab. **A**, This patient was treated with photodynamic therapy for myopic choroidal neovascularization with leakage. Note the rings of pigment centrally, indicating successive expansions of the lesion. **B**, After treatment, the lesion expanded even more. Note the increased pigment (arrow). **C**, After several photodynamic therapy treatments, the lesion expanded further (arrow), and a hemorrhage developed (arrowhead). Visual acuity was 20/80. **D**, Fluorescein angiography image reveals the extent of the neovascularization. The patient was given an injection of intravitreal bevacizumab 1.25 mg. **E**, The patient received 2 additional injections over time. Six years after first being treated with bevacizumab, the patient has some residual hyperpigmentation, but also a wide area of pigmentary loss. Visual acuity was 20/60. **F**, Nearly 10 years after injection, the atrophy continued to expand. (Courtesy of Richard F. Spaide, MD.)

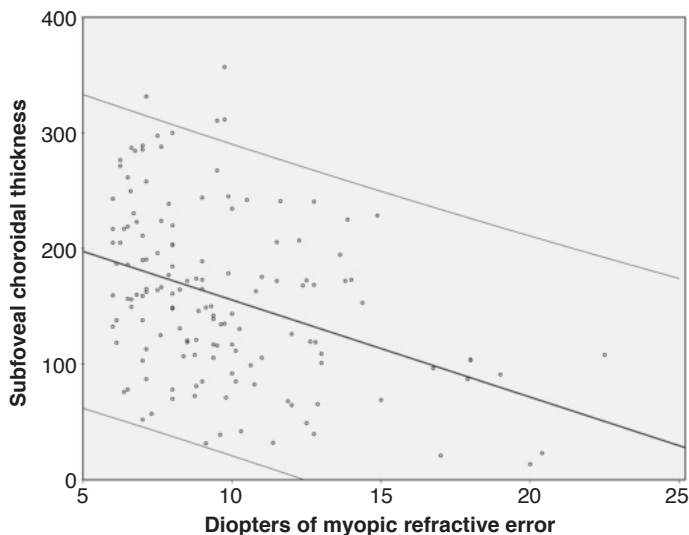
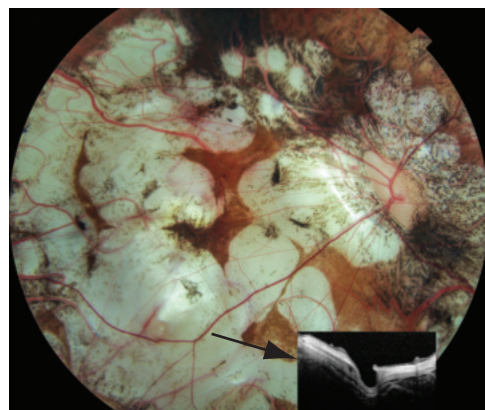


Figure 10-5 Graph of subfoveal choroidal thickness versus myopic refractive error in a group of 145 highly myopic eyes with no macular pathology. The trend line demonstrates the decrease in choroidal thickness with increasing refractive error, and the thinner bordering lines show the 95% confidence interval of the trend line. (Used with permission from Nishida Y, Fujiwara T, Imamura Y, Lima LH, Kurosaka D, Spaide RF. Choroidal thickness and visual acuity in highly myopic eyes. *Retina*. 2012;32(7):1229–1236.)

many reasons to lose visual acuity, and some of these are quite dramatic, such as retinal detachment. However, later in life many more highly myopic eyes suffer smaller amounts of visual acuity loss associated with decreasing choroidal thickness.

When the choroid becomes very thin, the pigmentation of the RPE often becomes granular. The larger choroidal vessels, or what is left of them, are easily visible. The choroid may show a repeating pattern of pigmentation, blood vessel, pigmentation, blood vessel and so on in a pattern known as a *tessellation*. Eventually the choroid may become so thin that the choroidal tissue and the overlying RPE are no longer supported (Fig 10-6). This produces ovoid areas of white, called patchy atrophy, in which the underlying sclera is shown. If the central macula is involved, the patient's visual acuity will be poor. In eyes with larger areas of atrophy, even Bruch membrane can rupture, leaving a truly bare sclera.

Figure 10-6 End-stage chorioretinal atrophy in pathologic myopia. Note the patches of full-thickness tissue loss; these appear white because of the direct visualization of the sclera. The emissary openings in the sclera become enlarged. *Inset*, an OCT image taken at the origin of the arrow, demonstrates remarkable thinning of the sclera and a near absence of scleral tissue in the emissary opening itself. (Courtesy of Richard F. Spaide, MD.)



Around the optic nerve, between 5% and 10% of highly myopic eyes will have a yellow-orange pocket, which was at one time thought to be a localized retinal detachment, but more refined OCT imaging revealed it to be an acquired cavitation in the choroid (Fig 10-7). Therefore, these lesions are called *peripapillary intrachoroidal cavitations*.

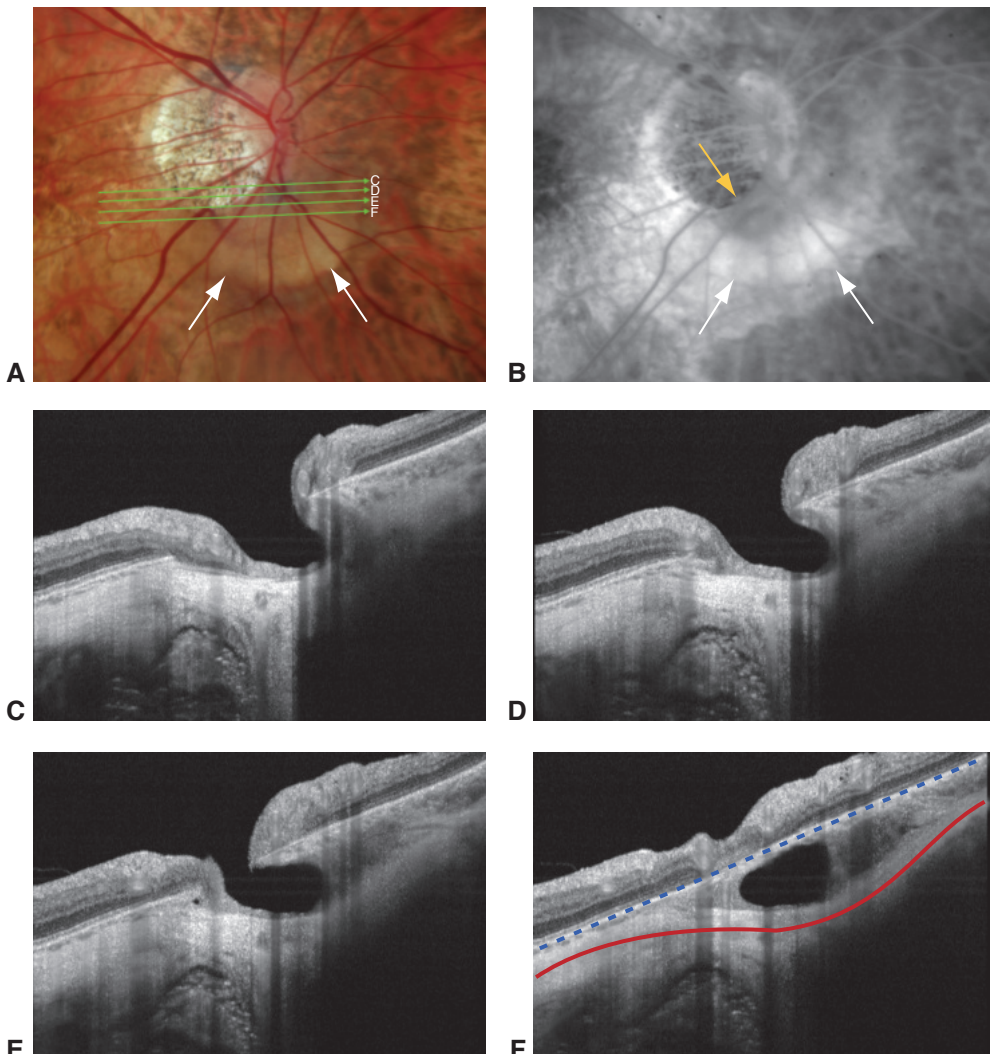


Figure 10-7 Peripapillary intrachoroidal cavitation. **A**, Color fundus photograph shows the yellow-orange region of the intrachoroidal cavitation (white arrows). The green arrows show the locations of subsequent OCT sections. **B**, Fluorescein angiography image shows a modest late collection of dye within the cavity (white arrows). Note the upper edge of the cavity is sharply demarcated (yellow arrow). The edge of the retinal defect is more clearly evident than in the color photograph. **C–F**, Successive serial sections taken using SS-OCT show the inner retinal defect and the extension of the cavitation into the choroid. A veil of tissue extends through the thickness of the choroid at the border of the cavitation. In **F**, the hyperreflective band that corresponds to the retinal pigment epithelium is nearly straight, as illustrated by the blue dashed line. The red line follows a posterior bowing at the center-point thickness in the sclera. (Used with permission from Spaide RF, Akiba M, Ohno-Matsui K. Evaluation of peripapillary intrachoroidal cavitation with swept source and enhanced depth imaging optical coherence tomography. Retina. 2012;32(6):1037–1044.)

EDI-OCT demonstrated that these cavitations are associated with a posterior bowing of the sclera around the nerve.

- Li XQ, Jeppesen P, Larsen M, Munch IC. Subfoveal choroidal thickness in 1323 children aged 11 to 12 years and association with puberty: the Copenhagen Child Cohort 2000 Eye Study. *Invest Ophthalmol Vis Sci*. 2014;55(1):550–555.
- Nickla DL, Wallman J. The multifunctional choroid. *Prog Retin Eye Res*. 2010;29(2):144–168.
- Nishida Y, Fujiwara T, Immamura Y, Lima LH, Kurosaka D, Spaide RF. Choroidal thickness and visual acuity in highly myopic eyes. *Retina*. 2012;32(7):1229–1236.
- Ohno-Matsui K, Jonas JB, Spaide RF. Macular Bruch membrane holes in highly myopic patchy chorioretinal atrophy. *Am J Ophthalmol*. 2016;166:22–28.
- Spaide RF, Akiba M, Ohno-Matsui K. Evaluation of peripapillary intrachoroidal cavitation with swept source and enhanced depth imaging optical coherence tomography. *Retina*. 2012;32(6):1037–1044.

The Sclera

The thickness of the sclera in a nonmyopic eye varies considerably with location; the thickest area, which is around the optic nerve, can be slightly more than 1 mm, whereas the area immediately under the rectus muscle insertions may be as thin as 0.3 mm. When ocular expansion related to myopia begins, the eye elongates, but the amount of material that makes up the sclera does not increase (see Fig 10-1). The collagen fibers become thinner, the typical gradient in fiber thickness in the sclera is lost, and the amount of extracellular matrix decreases. Over time, the sclera in a myopic eye shows more elasticity and greater viscoelastic creep. These factors appear to be necessary to allow the myopic eye to expand, but why it expands is unknown.

Form-deprivation or lens-induced errors in the eye are followed by axial length changes in animal models. Optic nerve sectioning or the destruction of the ciliary nerve does not prevent the development of experimental myopia. Form deprivation of a hemifield results in expansion of the eye that is conjugate with that hemifield, even if the optic nerve is sectioned. These findings support the hypothesis that remodeling of the eye results from local effects within the eye, beginning with signaling that originates in the retina and choroid and eventually affects the sclera. Connection to the brain does not appear to be necessary. Eyes that develop axial myopia lengthen, but in comparison to the posterior pole, the periphery becomes relatively hyperopic. Peripheral hyperopia can induce myopia in animal models, and curiously myopia can develop in eyes with peripheral hyperopia even if the posterior portion of the retina has been destroyed.

Ocular expansion can vary regionally, inducing formation of areas of the sclera that have differing radii of curvature. A regional expansion of the eye that produces a protrusion is called a staphyloma. These protrusions follow several patterns, but typically involve 3 general areas of the eye: (1) the area around the nerve, (2) the macular region, which leads to exaggerated thinning of the choroid and possibly myopic traction maculopathy, and (3) the inferior or inferotemporal portion of the eye (Fig 10-8). The superior portion of the eye has one radius of curvature while the inferior portion has another, and there is a visible boundary between these two curves. If the boundary occurs above the optic nerve, the optic nerve head will appear grossly tilted and rotated. If

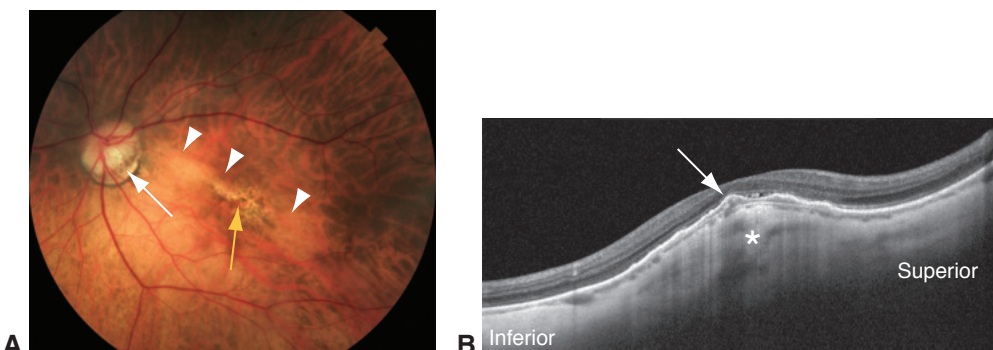


Figure 10-8 Inferior staphyloma syndrome, also known as tilted disc syndrome. **A**, Color fundus photograph shows that the color of the superior fundus is darker than the staphylomatous inferior staphyloma. At the border between the two regions (arrowheads) there is a pigmentary change in the macula (yellow arrow). Because this border runs through the superior border of the optic nerve head, the patient has a tilted disc (arrow). **B**, A vertical OCT taken through the fovea shows the two curves. At the ridge between them, there is choroidal neovascularization (arrow) associated with a small amount of submacular fluid. The sclera is typically thicker at the border zone (asterisk) than anywhere in the neighboring areas. (Courtesy of Richard F. Spaide, MD.)

the boundary bisects the fovea, several alterations may be seen. In later life, there may be atrophy along the boundary line that affects the RPE under the fovea, and either subretinal fluid without CNV or frank CNV may also develop in these eyes. Because this last staphyloma may be accompanied by a set of possible ocular manifestations, it has been referred to as *inferior staphyloma syndrome* or *tilted disc syndrome*. The origin of the accumulation of subretinal fluid without CNV is not known. In some patients, the choroid may show slight regional thickening around the change in curvature, but nearly all patients show a localized thickening of the sclera, which may limit outflow through the sclera (see Fig 10-8).

Diether S, Schaeffel F. Local changes in eye growth induced by imposed local refractive error despite active accommodation. *Vision Res*. 1997;37(6):659–668.

Ohno-Matsui K, Akiba M, Moriyama M, et al. Acquired optic nerve and peripapillary pits in pathologic myopia. *Ophthalmology*. 2012;119(8):1685–1692.

Smith EL 3rd, Hung LF, Huang J, Blasdel TL, Humbird TL, Bockhorst KH. Effects of optical defocus on refractive development in monkeys: evidence for local, regionally selective mechanisms. *Invest Ophthalmol Vis Sci*. 2010;51(8):3864–3873.

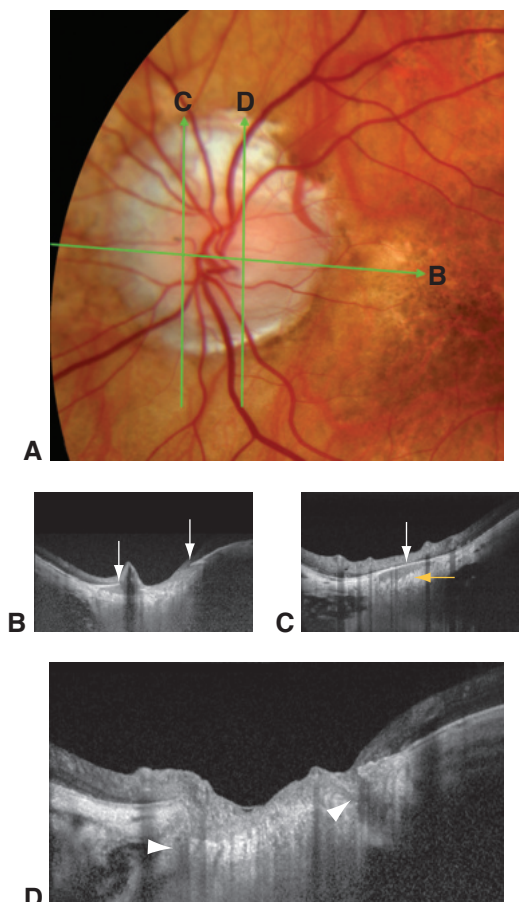
Smith EL 3rd, Ramamirtham R, Qiao-Grider Y, et al. Effects of foveal ablation on emmetropization and form-deprivation myopia. *Invest Ophthalmol Vis Sci*. 2007;48(9):3914–3922.

Wildsoet CF, Schmid KL. Optical correction of form deprivation myopia inhibits refractive recovery in chick eyes with intact or sectioned optic nerves. *Vision Res*. 2000;40(23):3273–3282.

The Optic Nerve

In eyes with pathologic myopia, the optic nerve head is undercut by a shifted Bruch membrane opening, the scleral canal may be stretched and tilted, the circle of Zinn–Haller is greatly enlarged, and the optic nerve may ordinarily appear stretched and pallorous.

Figure 10-9 Optic nerve changes in pathologic myopia. **A**, The optic nerve head seen in the color fundus photograph does not accurately show the size of the Bruch membrane opening. **B**, The enhanced depth imaging OCT shows the actual Bruch membrane opening (arrows). Note how far Bruch membrane extends into what appears to be the nerve (left arrow). **C**, A vertical section through (C) in the color photograph shows the extent of Bruch membrane. The arrow shows Bruch membrane extending into the nerve tissue. The nerve fibers have to arch nasally under Bruch membrane to reach the lamina cribrosa (yellow arrow). **D**, A vertical section through (D) in the color photograph shows 2 dehiscences (arrowheads) in the lamina cribrosa. Although this is a common finding in both glaucoma and pathologic myopia, it is not known whether every patient with a lamina defect in high myopia also has glaucoma. When an eye with glaucoma develops a Drance hemorrhage, there is typically an appearance of a lamina cribrosa dehiscence; however, in pathologic myopia dehiscences in the lamina are not typically seen to have any associated hemorrhage. (Courtesy of Richard F. Spaide, MD.)



Glaucoma is much more common in highly myopic eyes and frequently goes undetected. Measuring the retinal nerve fiber layer with OCT is problematic because of the varying shape of the eye, the potential for schisis, and because normative databases were developed for eyes that are not pathologically myopic. Visual field tests may show defects because of the shape of the eye, some of which can be “fixed” by using a refractive correction for that portion of the eye. Dehiscences in the lamina cribrosa are common in eyes with high myopia (Fig 10-9).

CHAPTER 11

Focal and Diffuse Choroidal and Retinal Inflammation

A variety of inflammatory disorders are associated with yellow-white lesions of the retina and choroid. This chapter highlights various focal and diffuse retinal and choroidal inflammatory disorders that can cause such lesions and includes epidemiology and descriptions of clinical features associated with these disorders. When the term *standard treatment* is used to describe therapy, options for inflammatory eye disease include corticosteroids in the acute phase and immunosuppressive agents for suppressive therapy. Other therapies or disease-specific treatment options are also outlined as appropriate. See BCSC Section 9, *Uveitis and Ocular Inflammation*, for more in-depth information on these disorders, further detail on treatment approaches, and additional illustrations.

Agarwal A. *Gass' Atlas of Macular Diseases*. 2 vols. 5th ed. Philadelphia: Saunders; 2012: 805–1064.

Foster CS, Vitale AT, Jakobiec FA. *Diagnosis and Treatment of Uveitis*. 2nd ed. New Delhi: Jaypee Brothers Medical Publishers; 2013.

Freund KB, Sarraf D, Mieler WF, Yannuzzi LA. *The Retina Atlas*. 2nd ed. Philadelphia: Saunders; 2017:399–492.

Noninfectious Retinal and Choroidal Inflammation

White Dot Syndromes

The term *white dot syndromes* has been used to refer to the following conditions (Table 11-1):

- acute posterior multifocal placoid pigment epitheliopathy (APMPPE)
- serpiginous choroidopathy
- multiple evanescent white dot syndrome (MEWDS)
- birdshot uveitis
- multifocal choroiditis (MFC)
- multifocal choroiditis and panuveitis syndrome (MCP)
- punctate inner choroidopathy (PIC)

Table 11-1 White Dot Syndromes: Comparative Findings and Course

Disease	Laterality	Age/Sex	Notable Findings	Course	Treatment
APMPPE	Bilateral	Young / M=F	Early hypofluorescence and late hyperfluorescence on fluorescein angiogram, cerebral vasculitis in rare cases	Spontaneous resolution with good visual prognosis; recurrences rare	No proven treatment. Evaluate for cerebral vasculitis if indicated
Serpiginous choroidopathy	Bilateral	Middle age / M=F	Angiogram findings similar to acute APMPPE	Central vision loss due to scarring; chronic, progressive	Standard autoimmune disease treatment
MEWDS	Unilateral	Young / F>M	Central foveal granularity with surrounding hyperfluorescence of dots in wreath-like pattern	Spontaneous resolution with good visual prognosis; recurrences rare	No proven treatment
Birdshot uveitis	Bilateral	Older / F>M	Nyctalopia, vitritis, strong association with HLA-A29	Vision loss due to CME; chronic, progressive	Standard autoimmune disease treatment
MFC	Bilateral	Young / F>M	Chorioretinal lesions evolve to burnt-out or punched-out scars	Central vision loss due to CNV; chronic, progressive	Standard autoimmune disease treatment
PIG	Bilateral	Young / F>M	No vitritis; in the acute phase, there are small (100–300 µm), round, yellow lesions in the macula. Older lesions can resemble MFC	Central vision loss due to CNV; self-limited or chronic, progressive	Standard autoimmune disease treatment

APMPPE = acute posterior multifocal placoid pigment epitheliopathy; CME = cystoid macular edema; CNV = choroidal neovascularization; MEWDS = multiple evanescent white dot syndrome; MFC = multifocal choroiditis; PIG = punctate inner choridopathy.

Many authorities now believe that MFC and PIC are part of a spectrum of the same condition; in this chapter, both of these entities are referred to as MFC (discussed in the section “Multifocal choroiditis”). Acute zonal occult outer retinopathy (AZOOR), acute macular neuroretinopathy (AMN), and acute idiopathic maculopathy (AIM), also discussed in this chapter, are often included in discussions of the more classic white dot syndromes listed above because of their presumed inflammatory etiology and the frequently shared symptoms of decreased vision, scotomas, and photopsias.

Acute posterior multifocal placoid pigment epitheliopathy

Acute posterior multifocal placoid pigment epitheliopathy (APMPPE; also known as AMPPPE or AMPPE) is an uncommon, bilateral inflammatory disorder characterized by the acute onset of blurred vision, scotomas, and, in some patients, photopsias. Approximately one-third of patients describe an antecedent flulike illness. Men and women are affected equally; onset usually occurs in youth to middle age. Mild anterior chamber and vitreous inflammation may be present. The lesions, which are typically multiple, yellow-white, placoid, and variable in size, occur at the level of the outer retina (retinal pigment epithelium, RPE) and inner choroid (choriocapillaris) (Fig 11-1). Recurrences are uncommon. The etiology is unknown, although the condition is characterized by hypoperfusion of the choriocapillaris that results in injury to the overlying RPE.

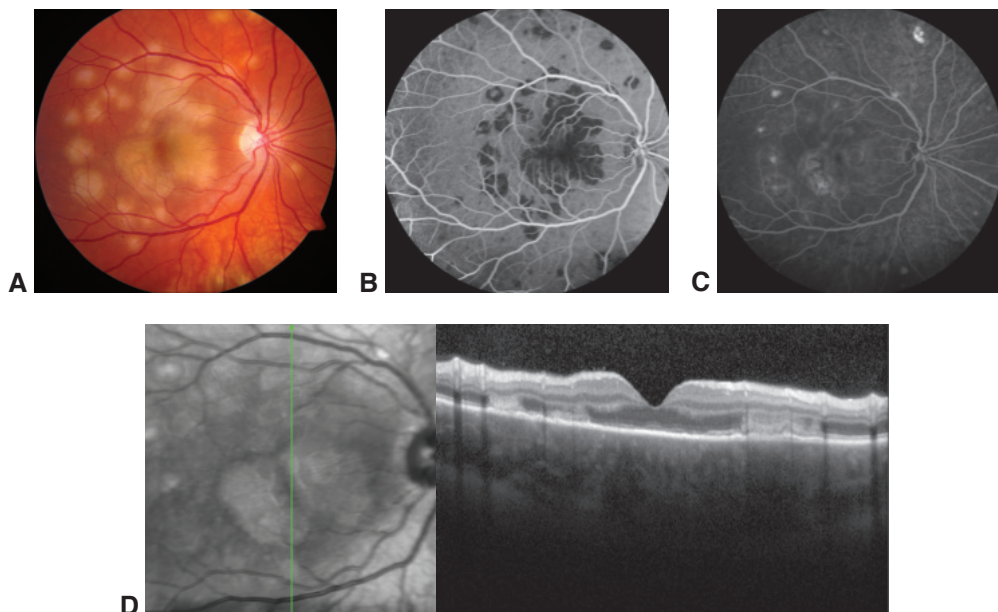


Figure 11-1 Acute posterior multifocal placoid pigment epitheliopathy (APMPPE). **A**, Color fundus photograph of the right eye of a 19-year-old male patient shows multiple yellowish placoid lesions in the posterior pole. The left eye (not pictured) was also involved. Early (**B**) and late-phase (**C**) fluorescein angiography demonstrate hypofluorescence (due to decreased choriocapillaris perfusion and/or thickening of the retinal pigment epithelium [RPE]), and hyperfluorescence, respectively. **D**, Vertical optical coherence tomography (OCT) scan demonstrates outer retinal involvement of the lesions. (Courtesy of Stephen J. Kim, MD.)

Systemic involvement—especially cerebral vasculitis—can occur, although it is uncommon. APMPE-like lesions can be present in patients with sarcoidosis, syphilis, and tuberculosis; therefore, testing to exclude these conditions should be considered.

Acutely, fluorescein angiography (FA) of active lesions shows early blockage followed by progressive late leakage and staining. Indocyanine green (ICG) angiography shows early and late (persistent) hypofluorescence, corresponding to and often extending beyond those lesions identified clinically and on FA. Optical coherence tomography (OCT) images taken through active lesions reveal outer retinal lesions associated with disruption of the outer retinal hyperreflective bands. Autofluorescence in and around active lesions varies over time and may be either increased or decreased at presentation; it tends to decrease as disease activity subsides. With time, hypoautofluorescence develops in areas of RPE disruption. The fundus appearance and visual symptoms typically improve within weeks. The long-term prognosis tends to be good, but severe vision loss can result from RPE and/or photoreceptor injury.

Treatment for APMPE is not typically indicated, although systemic corticosteroids may be considered in cases with central macular involvement and are required in cases with cerebral vasculitis. Severe APMPE may be difficult to distinguish from serpiginous choroidopathy (discussed in the following section); that difficulty led to the introduction of the term *ampiginous* to characterize the APMPE-serpiginous choroidopathy disease continuum. Other, related placoid disorders include persistent placoid maculopathy, which is characterized by central macular involvement, a longer healing time, and a high risk of choroidal neovascularization (CNV) formation, as well as relentless placoid chorioretinitis, which is characterized by the frequent occurrence of smaller, geographically distributed lesions that typically require immunosuppressive treatment.

Steiner S, Goldstein DA. Imaging in the diagnosis and management of APMPE. *Int Ophthalmol Clin.* 2012;52(4):211–219.

Serpiginous choroidopathy

Serpiginous choroidopathy, also known as *geographic choroiditis* or *helicoid peripapillary choroidopathy*, is an uncommon, often vision-threatening, recurring inflammatory disorder involving the outer retina (the RPE) and inner choroid (the choriocapillaris). Classically, lesions first appear at or near the optic nerve head and extend centrifugally in a serpentine pattern. With numerous recurrences, a serpiginous (pseudopodial) or geographic (maplike) pattern of chorioretinal scarring develops (Fig 11-2). Findings on clinical examination and through multimodal imaging of active serpiginous lesions resemble those of acute APMPE. Lesions tend to occur near or adjacent to inactive scars from prior episodes of inflammation. Persistent scotomas and decreased central vision are common symptoms. Serpiginous choroidopathy tends to affect men and women equally; onset typically occurs in middle age.

In endemic areas, such as India, tuberculosis is recognized as producing serpiginous-like lesions, leading some clinicians to describe such lesions as *tubercular serpiginous-like choroiditis*. In patients with serpiginous-like lesions, evaluation for tuberculosis, sarcoidosis, and syphilis should be considered. Standard autoimmune disease treatment options are typically needed to stabilize the condition and prevent recurrences.

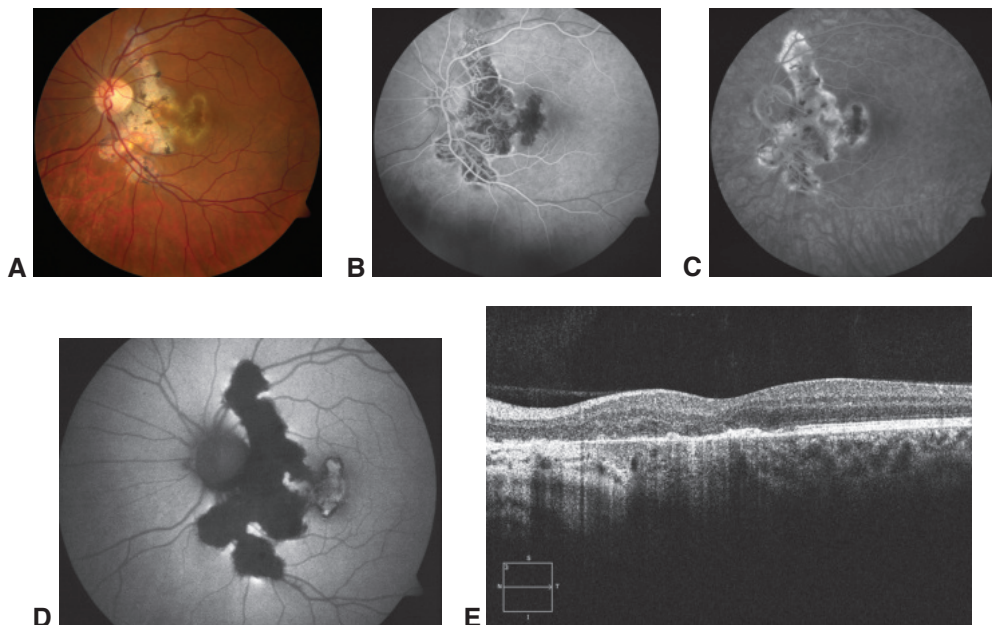


Figure 11-2 Serpiginous choroidopathy. **A**, Color fundus photograph shows an old peripapillary chorioretinal scar with an active serpentine lesion extending centrifugally into the fovea. **B**, Early-phase fluorescein angiogram demonstrates classic hypofluorescence, with hyperfluorescence of the edge of the older peripapillary chorioretinal scar. **C**, Late-phase angiogram demonstrates hyperfluorescence of involved areas. **D**, Autofluorescence image demonstrates a complete absence of autofluorescence in the area of older chorioretinal scarring, but not in the area of active extension. **E**, OCT image demonstrates disorganization of outer retinal layers and choroid nasal to and underneath the fovea that corresponds to the involved areas. (Courtesy of Stephen J. Kim, MD.)

Bansal R, Gupta A, Gupta V. Imaging in the diagnosis and management of serpiginous choroiditis. *Int Ophthalmol Clin.* 2012;52(4):229–236.

Multiple evanescent white dot syndrome

Multiple evanescent white dot syndrome (MEWDS) is an acute-onset syndrome characterized by multiple small gray, white, or yellow-white dots at the level of the outer retina (RPE level) in and around the posterior pole (Fig 11-3). In some patients, an unusual transient foveal granularity consisting of tiny yellow-orange flecks at the level of the RPE also develops; this is highly suggestive of the condition. Abnormalities on ICG angiography suggest simultaneous choroidal involvement. Mild anterior chamber cell reaction or vitritis may be present. Affected individuals are typically young to middle aged; women are affected more often than men. Symptoms tend to be unilateral and include decreased vision, scotomas, and sometimes photopsias. Temporal visual field abnormalities and an enlarged blind spot are common, and an afferent pupillary defect is often present. The etiology of MEWDS is unknown, although one-third of patients describe a flulike prodrome.

FA reveals multiple, punctate, hyperfluorescent dots associated with the spots observed clinically, typically in a wreath-like cluster. Mild, late leakage and staining of the optic nerve head is often observed. ICG angiography shows hypofluorescence around

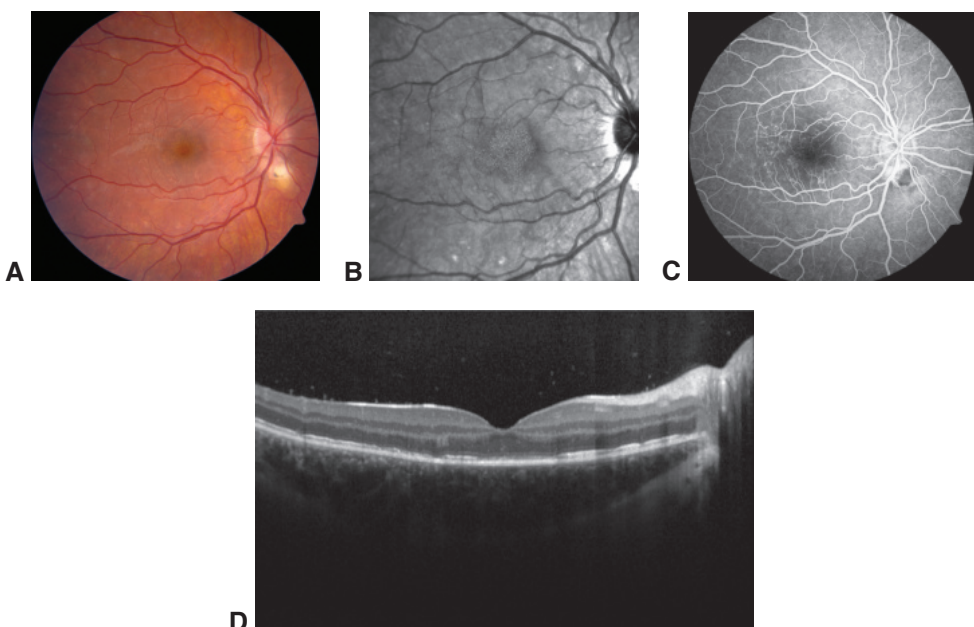


Figure 11-3 Multiple evanescent white dot syndrome (MEWDS). **A**, Color fundus photograph demonstrates foveal granularity consisting of tiny yellow-orange flecks that can be easily visualized in a red-free image (**B**). **C**, Angiography image demonstrates classic hyperfluorescent punctate lesions in a wreath-like cluster. **D**, OCT image demonstrates disruption of the outer retina and RPE. (Courtesy of Shriji N. Patel, MD.)

the optic nerve head as well as multiple hypofluorescent dots, which are typically more numerous than those observed either clinically or on FA. OCT images taken through active lesions reveal dome-shaped outer retinal lesions associated with disruption of the outer retinal hyperreflective bands. Fundus autofluorescence imaging often shows focal hyperautofluorescence in the area of the white dots. On electroretinogram (ERG) testing, some patients show delayed 30-Hz flicker responses and decreased bright-flash, dark-adapted a-wave amplitudes. The symptoms and fundus findings start to improve in most patients in 2–6 weeks without treatment. In rare cases, MEWDS can be recurrent or bilateral, cause persistent scotomas or visual field defects, or be associated with the late development of CNV.

Birdshot uveitis

Birdshot uveitis, or *vitiliginous chorioretinitis*, is bilateral and affects women more often than men, typically in late middle age. Early symptoms include floaters and blurred or decreased vision. Later in the course of disease, nyctalopia, diminished contrast sensitivity, and decreased color vision may occur. Examination reveals vitreous inflammation, which is typically mild and is associated with multiple yellow-white choroiditis spots that are often most prominent inferonasal to the optic nerve head (Fig 11-4). Fluorescein angiography often shows leakage from the retinal vessels and optic nerve head, frequently producing cystoid macular edema (CME). Variable amounts of outer retinal atrophy can

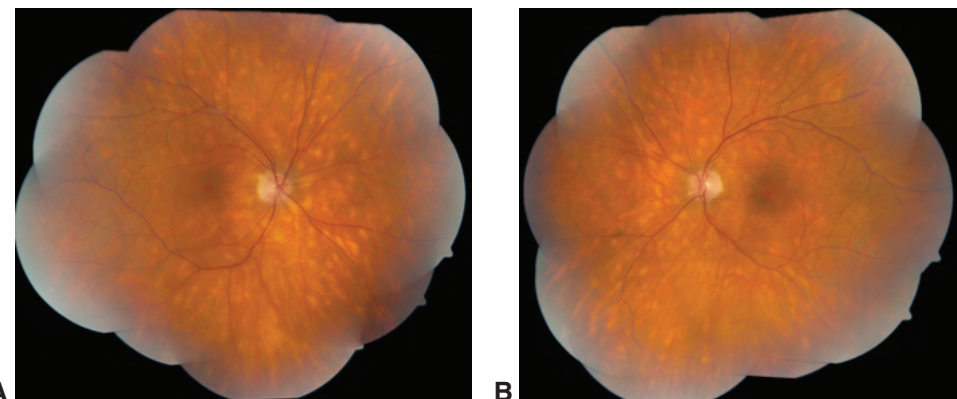


Figure 11-4 Color fundus photograph montage of the right (**A**) and left (**B**) eyes of a patient with birdshot uveitis demonstrate multiple creamy, yellow-white choroiditis lesions scattered around the posterior pole. The images are slightly hazy due to vitritis. (Courtesy of Stephen J. Kim, MD.)

also be present, resulting in window defects. Choroidal lesions are best visualized using ICG angiography. OCT and fundus autofluorescence can be used to assess the extent of outer retinal atrophy.

The disease is chronic, progressive, and prone to recurrent episodes of inflammation. Vision loss may be caused by CME, epiretinal membrane formation, and/or outer retinal atrophy, which can be extensive and is associated with optic atrophy in advanced cases. Most patients with birdshot uveitis are white and test positive for HLA-A29 (>90%); birdshot uveitis has the strongest association documented between a disease and HLA class I. Disease activity and progression may be assessed in the office using multimodal imaging (FA, ICG angiography, spectral-domain OCT, enhanced depth OCT, and fundus autofluorescence) and through periodic electrophysiologic (ERG), color vision, and visual field testing—each of which may show a degree of dysfunction far greater than that suggested by Snellen visual acuity assessments. Standard autoimmune disease treatment options are employed.

Multifocal choroiditis

Use of the terms *idiopathic multifocal choroiditis*, *multifocal choroiditis with panuveitis* (MFCPU), *recurrent multifocal choroiditis* (RMC), *punctate inner choroiditis* or *choroidopathy* (PIC), and *pseudo-presumed ocular histoplasmosis syndrome* (pseudo-POHS), among others, is both inconsistent and confusing in the literature. Current recommendations suggest that only the term *multifocal choroiditis* (MFC) should be used to refer to the occurrence of discrete chorioretinitis lesions in the absence of an identifiable underlying infection (such as tuberculosis or histoplasmosis) or systemic inflammation (such as sarcoidosis). In MFC, lesions are commonly clustered in the macula and around the optic nerve head, although they can also occur in the mid- and far periphery (Fig 11-5), and are frequently aligned in a curvilinear manner—configurations that are sometimes referred to as *Schlaegel lines*. Affected individuals are typically young, myopic, and female. Clinical examination usually reveals little or no anterior chamber or vitreous inflammation,

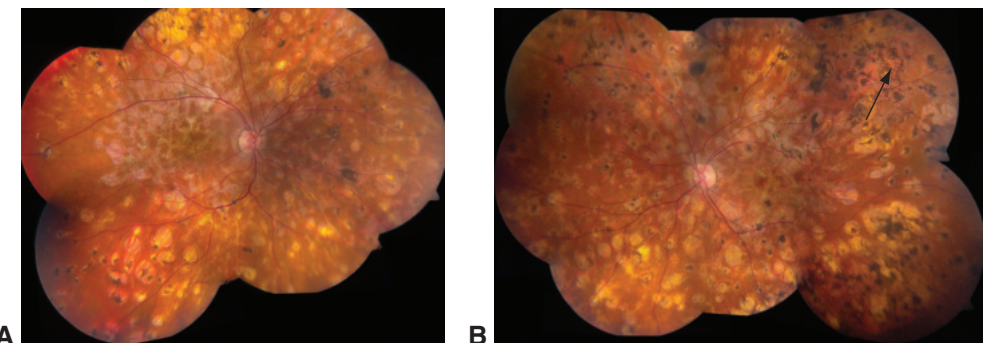


Figure 11-5 Color fundus photograph montage of the right (**A**) and left (**B**) eyes showing multifocal chorioretinal scars, some with a punched-out appearance, in a patient with end-stage multifocal choroiditis (MFC) with panuveitis. (Courtesy of Stephen J. Kim, MD.)

although patients can have mild to moderate vitreous inflammation—a presentation some clinicians mean when using the term *MFCPU*. Blurred or decreased vision and scotomas are the most common symptoms. Decreased central vision results most frequently from direct central macular involvement or from the development of CNV, which occurs in one-third of patients (Fig 11-6). Subretinal fibrosis can occur in and around lesions and, when the central macula is involved, can also limit vision. Standard treatment options for autoimmune disease are employed.

Essex RW, Wong J, Jampol LM, Dowler J, Bird AC. Idiopathic multifocal choroiditis: a comment on present and past nomenclature. *Retina*. 2013;33(1):1–4.

Acute zonal occult outer retinopathy

Acute zonal occult outer retinopathy (AZOOR), a presumed inflammatory disorder, damages broad zones of the outer retina in 1 or both eyes. AZOOR typically occurs in young

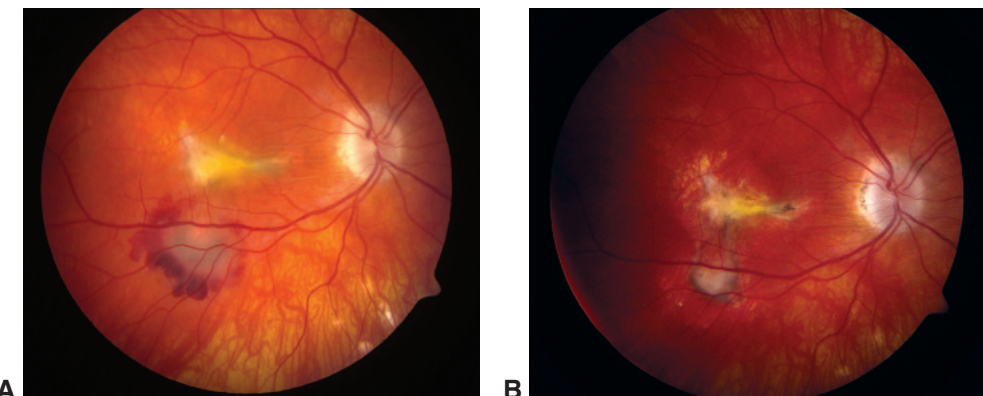


Figure 11-6 Choroidal neovascularization (CNV). **A**, Fundus photograph of a patient with MFC with panuveitis with central subfoveal fibrosis. **B**, After resolution of CNV, subretinal fibrosis is present. (Courtesy of Stephen J. Kim, MD.)

women with myopia, and onset is acute and unilateral. Three-fourths of cases progress to bilateral involvement. Initial symptoms include photopsia, nasal visual field loss, and sometimes an enlarged blind spot; visual acuity is affected in rare instances. On initial presentation, the fundus may appear normal or show evidence of mild vitritis (Fig 11-7). Nearly 25% of patients have an afferent pupillary defect. Angiographic findings may include retinal and optic nerve head capillary leakage, especially in patients with evidence of vitritis. On ERG, a delayed 30-Hz flicker response is common; multifocal ERG (mfERG) shows decreased responses in areas of the visual field defect. Visual field testing may show scotomas, which can enlarge over weeks or months.

Some patients recover from AZOOR, whereas others have persistent, large visual field defects, which tend to stabilize over 6 months. Permanent visual field loss is often associated with late development of fundus changes. Depigmentation of large zones of RPE usually corresponds to scotomas (see Fig 11-7); narrowed retinal vessels may be visible within these areas. In some patients, the late fundus appearance may resemble cancer-associated retinopathy or retinitis pigmentosa. FA images tend to appear normal early on but become abnormal in eyes with RPE alterations. ICG angiography may show areas of late hypofluorescence. OCT typically reveals outer retinal atrophy, including disruption of the ellipsoid zone and the outer nuclear layer in involved areas. Confocal near-infrared

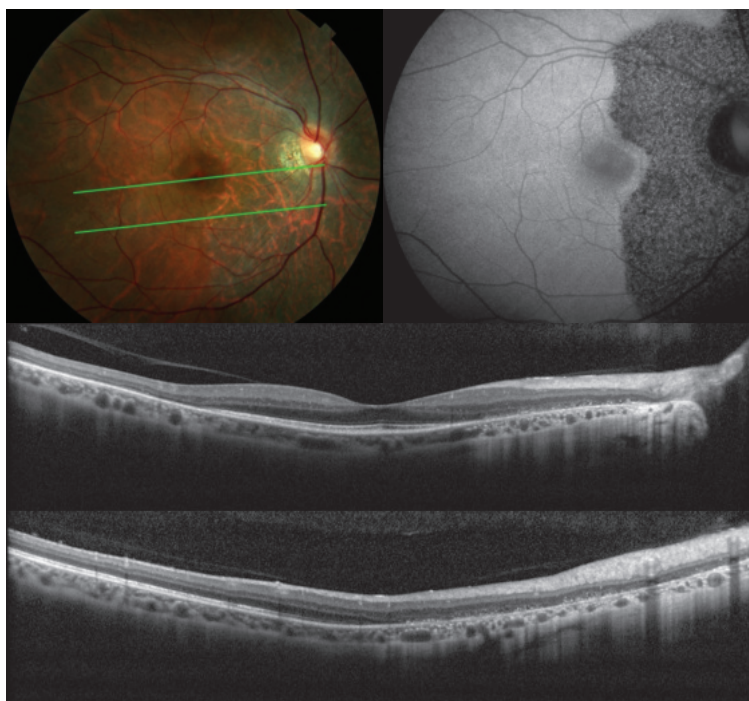


Figure 11-7 Acute zonal occult outer retinopathy (AZOOR). Annular depigmentation of the RPE can be seen around the optic nerve (top left). Autofluorescence (top right) demonstrates areas of hypofluorescence corresponding to RPE loss. The fovea appears normal. OCT images (bottom) demonstrate outer retinal atrophy in the involved area. (Courtesy of Richard F. Spaide, MD.)

reflectance imaging shows hyporeflective areas that correspond to areas of lost ellipsoid zone. Autofluorescence is typically decreased in areas of involvement and is occasionally associated with either punctate or a peripheral rim of hyperautofluorescence. Immunosuppression does not alter the course of the disease.

Gass JD, Agarwal A, Scott IU. Acute zonal occult outer retinopathy: a long-term follow-up study. *Am J Ophthalmol*. 2002;134(3):329–339.

Acute macular neuroretinopathy

Acute macular neuroretinopathy (AMN) is a rare condition characterized by the acute onset of paracentral scotomas in 1 or both eyes in young, otherwise healthy patients. Women outnumber men nearly 6 to 1 in this condition. Clinically, reddish-brown teardrop or wedge-shaped lesions are observed around the fovea. The tips of these lesions point centrally; the lesions correspond in size and location to the subjective paracentral scotomas. The lesions can be difficult to see on fundus examination or with color photography but are apparent on near-infrared imaging. The retinal vessels and optic nerve are unaffected, and there is no vitreous inflammation. High-resolution OCT is particularly helpful for visualizing the lesions and has revealed 2 patterns: (1) type 1, which is characterized by involvement of the middle retina or inner nuclear layer; and (2) type 2, which is characterized by involvement of the outer retina—including both the outer nuclear layer and the hyperreflective bands associated with the photoreceptors of the ellipsoid zone. Both patterns are believed to result from ischemia of the deep capillary plexus of the central retina.

The lesions typically resolve over several weeks to months with corresponding visual recovery; alternatively, the scotomas persist. The pathogenesis of AMN is unclear. Several associations have been noted, however, including a preceding flulike illness, the use of oral contraceptives or caffeine, and injection of adrenaline or epinephrine. Lesions resembling AMN can occur following mild to moderate, blunt, or whiplash-type trauma. Whether these lesions are AMN or traumatic maculopathy is controversial (Fig 11-8).

Fawzi AA, Pappuru RR, Sarraf D, et al. Acute macular neuroretinopathy: long-term insights revealed by multimodal imaging. *Retina*. 2012;32(8):1500–1513.

Acute idiopathic maculopathy

Acute idiopathic maculopathy (AIM) is a rare disorder that presents with sudden, severe central or paracentral vision loss, typically in younger individuals following a flulike illness. Men and women are affected equally. Initially, only central unilateral lesions were described, but both bilateral and eccentric macular lesions have since been added to the disease spectrum. The main clinical finding is an exudative neurosensory macular detachment with little or no vitreous inflammation and variable discoloration of the underlying RPE. Mild optic nerve head swelling, retinal hemorrhages, vasculitis, and subretinal infiltrates occur infrequently. Fluorescein angiography typically shows progressive irregular hyperfluorescence at the level of the RPE, followed in the late stages by pooling in the detachment space. ICG angiography shows early and persistent hypoangiogenesis. High-resolution OCT imaging documents the size and extent of the

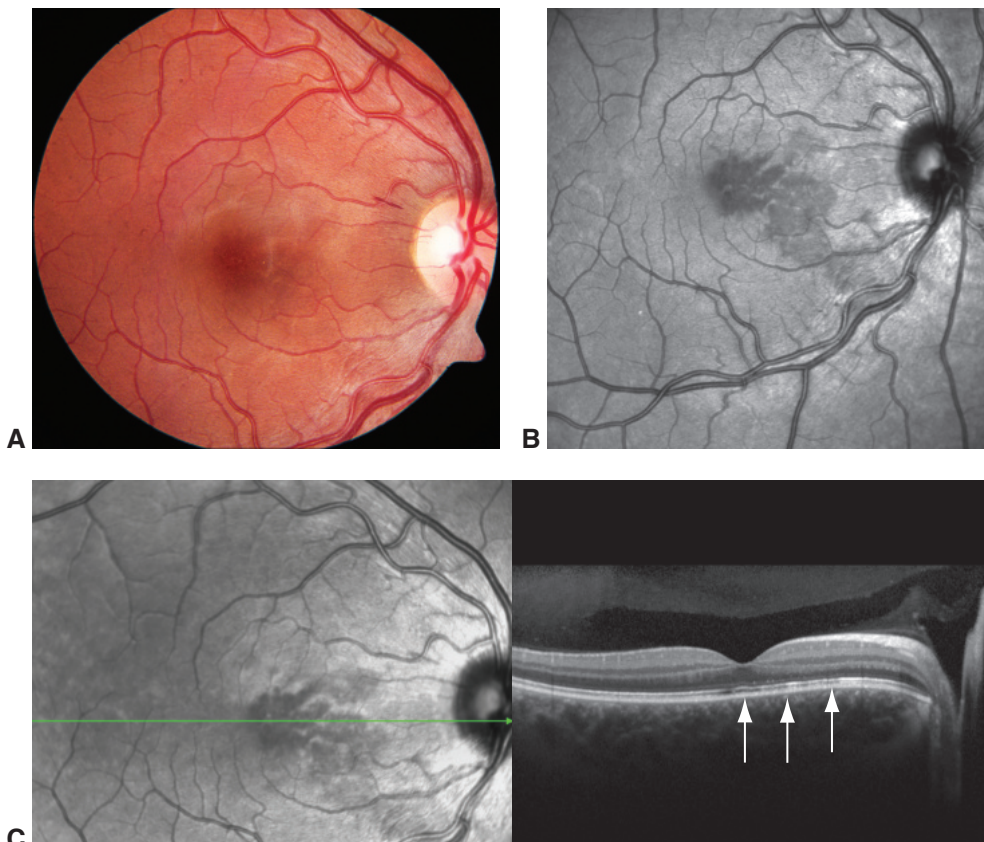


Figure 11-8 Acute macular neuroretinopathy following whiplash-type trauma. Reddish-brown wedge-shaped lesions nasal to the fovea are difficult to see in a color fundus photograph (**A**), but they are apparent in a near-infrared image (**B**). **C**, OCT image demonstrates involvement of the external limiting membrane and ellipsoid zone (arrows). (Courtesy of Milam A. Brantley, MD, PhD.)

detachment space and shows loss of the hyperreflective outer retinal bands associated with the photoreceptors and RPE. The lesions resolve spontaneously but leave a bull's-eye pattern of RPE alteration, which on FA shows central hypofluorescence and surrounding hyperfluorescence. There is typically near-complete recovery of vision over weeks to months. The cause is unknown, although isolated cases have been associated with coxsackievirus infection.

Yannuzzi LA, Jampol LM, Rabb MF, Sorenson JA, Beyrer C, Wilcox LM Jr. Unilateral acute idiopathic maculopathy. *Arch Ophthalmol*. 1991;109(10):1411–1416.

Chorioretinal Autoimmune Conditions

The following sections detail selected autoimmune diseases that affect the retina and choroid. These conditions are generally treated using standard autoimmune treatment options. Specific treatment considerations are mentioned when applicable.

Inflammatory vasculitis

Behçet disease Behçet disease is a complex systemic disorder characterized by recurrent attacks of inflammation and vascular occlusion involving multiple organ systems. There are no specific tests to confirm a diagnosis of Behçet disease, but it is associated with the major histocompatibility complex HLA-B5 allele, and more specifically with HLA-B51 (the predominant split antigen). The diagnosis is based on clinical criteria (Table 11-2). Recurrent oral ulceration affects nearly all patients, and cutaneous lesions such as erythema nodosum are common. Central nervous system involvement may develop in more than 50% of patients and should be suspected in any patient with neurologic signs. Other systemic manifestations include arthritis, epididymitis, and intestinal ulcers. Behçet disease tends to affect men more than women and is particularly common in Japan, Southeast Asia, the Middle East, and the Mediterranean region. The etiology is unknown.

Uveitis is common in patients with this disorder; it may be anterior, posterior, or diffuse (panuveitis). Posterior segment involvement may include vitritis, an occlusive retinal vasculitis, intraretinal hemorrhages, macular edema, focal areas of retinal necrosis, and ischemic optic neuropathy. Recurring episodes of retinal vasculitis may lead to severe ischemia and retinal neovascularization, which should be treated with panretinal photocoagulation. Despite treatment, the visual prognosis is often poor because of progressive retinal ischemia from recurring episodes of occlusive vasculitis. Use of biologic agents, such as inhibitors of tumor necrosis factor alpha, as well as interferon, has shown promise. Treatment with azathioprine and cyclosporine has been shown to reduce ocular manifestations in well-designed prospective trials.

Masuda K, Nakajima A, Urayama A, Nakae K, Kogure M, Inaba G. Double-masked trial of cyclosporin versus colchicine and long-term open study of cyclosporin in Behçet's disease. *Lancet*. 1989;1(8647):1093–1096.

Tugal-Tutkun I. Imaging in the diagnosis and management of Behçet disease. *Int Ophthalmol Clin*. 2012;52(4):183–190.

Yazici H, Pazarli H, Barnes CG, et al: A controlled trial of azathioprine in Behçet's syndrome. *N Engl J Med*. 1990;322(5):281–285.

Lupus vasculitis *Systemic lupus erythematosus* (SLE) is a systemic autoimmune disorder that most commonly affects women of childbearing age. Black and Hispanic women are at higher risk than are White women. As a multisystem disease, SLE can involve almost every ocular and periocular structure. Approximately 3%–10% of patients with SLE have retinal findings ranging from asymptomatic cotton-wool spots and intraretinal hemorrhages to

Table 11-2 International Clinical Criteria for Behçet Disease

Recurrent oral ulcerations (aphthous or herpetiform) at least 3 times in 1 year in addition to 2 of the following:

- Recurring genital ulcerations
 - Ocular inflammation
 - Skin lesions (erythema nodosum, pseudofolliculitis, papulopustular lesions, acneiform nodules)
 - Positive pathergy test
-

Adapted from the International Study Group for Behçet's Disease. Criteria for diagnosis of Behçet's disease. *Lancet*. 1990;335(8697):1078–1080.

macular infarction with severe central vision loss (Fig 11-9). Lupus choroidopathy is less common and presents as multifocal serous retinal detachments. The retinal and choroidal pathology is vascular and thought to be autoimmune in nature.

The presence of retinal vascular occlusion, including cotton-wool spots, is indicative of active systemic inflammation and should prompt treatment. Sarcoidosis can cause retinal vasculitis (Fig 11-10) and should be evaluated as a possible alternative.

Intermediate uveitis

The Standardization of Uveitis Nomenclature (SUN) Working Group defined intermediate uveitis as a subset of posterior uveitis where the vitreous is the major site of inflammation. Eighty percent of intermediate uveitis cases are idiopathic. The most commonly identified causes in North America and Europe are sarcoidosis and multiple sclerosis. The diagnostic term *pars planitis* should be used only for the subset of intermediate uveitis where a “snowbank” or “snowball” formation occurs in the absence of an associated systemic disease or infection.

Intermediate uveitis is typically bilateral and can occur in children, adolescents, or adults. Common symptoms include floaters and decreased vision. Characteristic ocular manifestations include vitreous inflammation, inflammatory debris overlying the pars plana (snowbanks), and aggregates of vitreous cells (snowballs). Both snowbanks and

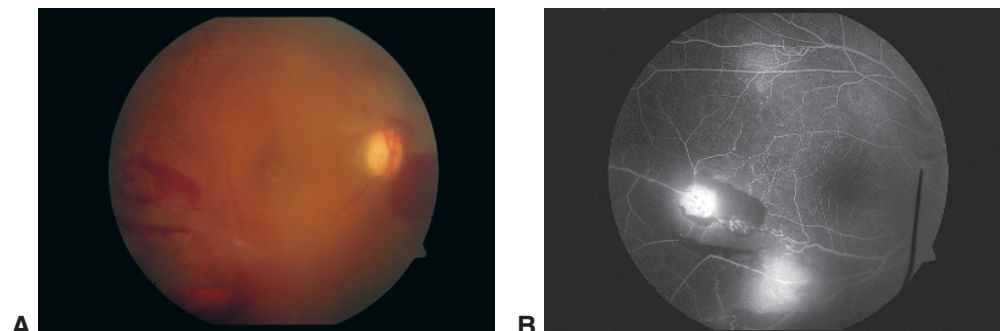


Figure 11-9 Vasculitis secondary to systemic lupus erythematosus. **A**, Color fundus photograph shows vitreous hemorrhage secondary to neovascularization. **B**, Late-phase fluorescein angiography image reveals choroidal and retinal nonperfusion, perivascular staining, and leakage due to neovascularization. (Courtesy of Matthew A. Thomas, MD.)

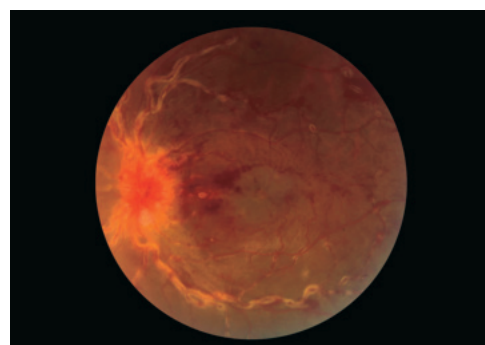


Figure 11-10 Sarcoidosis. Color fundus photograph shows retinal vascular sheathing. (Courtesy of Ramin Schadlu, MD.)

snowballs are most often observed inferiorly. Peripheral neovascularization may form along the inferior snowbank in 5%–10% of cases and can lead to vitreous hemorrhage with tractional or rhegmatogenous retinal detachment. When active, segmental phlebitis, optic nerve head leakage, and CME are common. Epiretinal membrane formation also occurs.

Vitreous cells or segmental phlebitis in the absence of decreased vision can be observed without treatment. Active CME is best treated with corticosteroids.

Vidovic-Valentincic N, Kraut A, Hawlina M, Stunf S, Rothova A. Intermediate uveitis: long-term course and visual outcome. *Br J Ophthalmol*. 2009;93(4):477–480.

Vogt-Koyanagi-Harada disease

Vogt-Koyanagi-Harada (VKH) disease (or syndrome) is a systemic autoimmune disorder in which T lymphocytes are directed against melanocytes in the eye, auditory system, meninges, and skin. VKH disease most commonly affects people of Asian, American Indian, Asian Indian, Mediterranean, and Middle Eastern descent. Ocular findings are typically bilateral and include vitreous inflammation associated with serous retinal detachment. Optic nerve head hyperemia and edema are common. Fluorescein angiography studies can be particularly helpful in monitoring disease activity and often show multiple RPE leaks in the areas of detachment, a finding referred to as the “starry night” or “Milky Way” sign. A “sunset glow” fundus appearance can be seen due to choroidal depigmentation as the uveitis subsides (Fig 11-11).

A diagnosis of VKH disease should only be made in patients who have not had a penetrating ocular injury or ocular surgery in either eye, to help distinguish this disease from sympathetic ophthalmia. VKH disease is termed *probable* when characteristic ocular inflammation occurs in the absence of skin or neurologic findings; it is termed *incomplete*

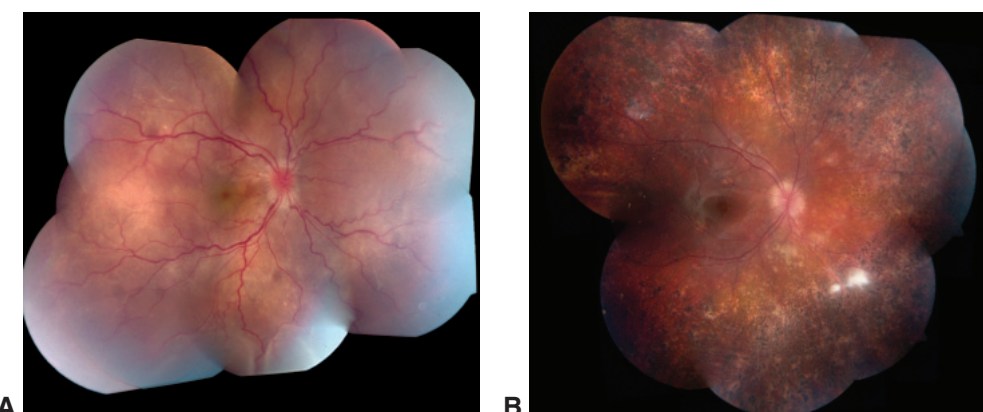


Figure 11-11 Vogt-Koyanagi-Harada (VKH) disease. **A**, Color fundus photograph montage of the right eye taken during an acute uveitic phase in a patient with a presenting visual acuity of 20/400 in both eyes demonstrate vitritis, optic nerve head swelling, diffuse serous detachments with inferior dependency, and dilated and tortuous vasculature. **B**, Montage fundus photographs of the right eye taken 2 years later during the chronic (convalescent) phase demonstrate diffuse chorioretinal scarring and the classic “sunset glow” fundus due to loss of choroidal pigment. Visual acuity improved to 20/20 in both eyes. (Courtesy of Stephen J. Kim, MD.)

if either skin or neurologic findings, but not both, are present; and it is termed *complete* when both skin and neurologic findings develop.

The clinical course of VKH disease can be divided into 3 phases:

1. *prodromal phase*: characterized by a flulike illness with symptoms that can include headache, meningismus, tinnitus, and dysacusis
2. *acute uveitic phase*: closely follows the prodromal phase; characterized by pain, photophobia, and vision loss accompanied by the onset of bilateral panuveitis with serous retinal detachments
3. *chronic (convalescent) phase*: the uveitis subsides, but depigmentation of the skin and uvea can occur; ocular depigmentation may develop at the limbus (“Sugirura” sign), the trabecular meshwork (“Ohno” sign), or within the choroid (“sunset glow” sign)

VKH disease tends to respond to standard treatments. A delay in diagnosis and treatment is associated with an increased risk of depigmentation of the skin and eye and with an increased rate of ocular complications, including cataract, glaucoma, and subretinal fibrosis.

Sympathetic Ophthalmia

Sympathetic ophthalmia, a rare condition that occurs after a penetrating ocular injury or ocular surgery, is caused by exposure of the immune system to sequestered uveal antigens. Its ocular findings are clinically and histologically indistinguishable from those in VKH disease. Inflammation of the exciting (injured or operated) and sympathizing (fellow) eye may occur days to decades after the initial insult. As in VKH disease, the inflammation is bilateral and is characterized by the presence of panuveitis, often associated with areas of serous retinal detachment and focal choroiditis (nummular chorioretinal lesions). Nonocular complications, such as vitiligo or poliosis, can occur but are much less common than in VKH disease. Moreover, in the rare instances when sympathetic ophthalmia does follow either injury or surgery, standard treatments almost always control the inflammation. Therefore, enucleation or evisceration of an injured eye to minimize risk of sympathetic ophthalmia should be undertaken only when the eye is painful, structurally disorganized, and has no light perception. Optimally, the enucleation should occur within 14 days of the trauma; it is thought immune activation against otherwise sequestered antigens in the eye does not occur until later. However, this 14-day timeline is becoming increasingly controversial.

Castiblanco CP, Adelman RA. Sympathetic ophthalmia. *Graefes Arch Clin Exp Ophthalmol*. 2009;247(3):289–302.

Uveitis Masquerade: Intraocular Lymphoma

Primary vitreoretinal lymphoma was previously referred to as *reticulum cell sarcoma*, *histiocytic lymphoma*, and *non-Hodgkin lymphoma of the central nervous system*. Most cases are aggressive large B-cell tumors. Half of all cases of primary vitreoretinal lymphoma occur in patients older than 60 years. Most patients with primary vitreoretinal lymphoma will

develop central nervous system (CNS) involvement. Conversely, of patients who present with CNS involvement, approximately 20% will have intraocular involvement. HIV infection is associated with an increased risk of lymphoma that ranges from 50-fold (with potent antiretroviral therapy) to more than 500-fold (prior to—or without access to—potent antiretroviral therapy). Clinical features that are suggestive of lymphoma include an incomplete or transient response to corticosteroid treatment, the presence of atypical vitreous cells, which may be uncharacteristically white and/or align in sheets, and the presence of subretinal infiltrates, which may be transient and/or shift location over time (Fig 11-12). Optic nerve head edema and serous retinal detachment can also occur. Patients with suspected primary vitreoretinal lymphoma should undergo magnetic resonance imaging (MRI) of the brain with contrast as well as a spinal tap for cytologic studies to evaluate for CNS involvement. A confirmatory CNS or vitreoretinal biopsy is usually performed. It is notoriously difficult to arrive at a diagnosis based on tests of a vitreous specimen because of the low cell concentrations and the propensity of lymphoma cells to undergo autolysis. Because corticosteroids will also reduce cell count, it is best to stop any corticosteroid treatments for a period of weeks before a planned biopsy. Best results are achieved with rapid test processing and analysis by cytology, immunoglobulin or T-cell receptor gene rearrangement studies, flow cytometry, and cytokine analyses. Current management practices involve both chemotherapy and radiation treatment. Intravitreal injection of methotrexate and rituximab can be effective at controlling intraocular disease, but the recurrence rate is high and long-term prognosis guarded.

In contrast, *uveal lymphoma* is usually more indolent and is associated with systemic lymphoma in up to one-third of cases. Characteristic clinical findings include uveal thickening, which often produces a birdshot uveitis-like fundus appearance, with or without serous retinal detachment (Fig 11-13). Episcleral involvement may manifest anteriorly as salmon-colored conjunctival infiltration or posteriorly as a juxtascleral mass on ultrasound. Biopsy of affected tissues can confirm the diagnosis. Evaluation for systemic involvement includes use of computed tomography (CT) or combined CT and positron emission tomography (PET) imaging of the thorax, abdomen, and pelvis.

Chan CC, Sen HN. Current concepts in diagnosing and managing primary vitreoretinal (intraocular) lymphoma. *Discov Med*. 2013;15(81):93–100.

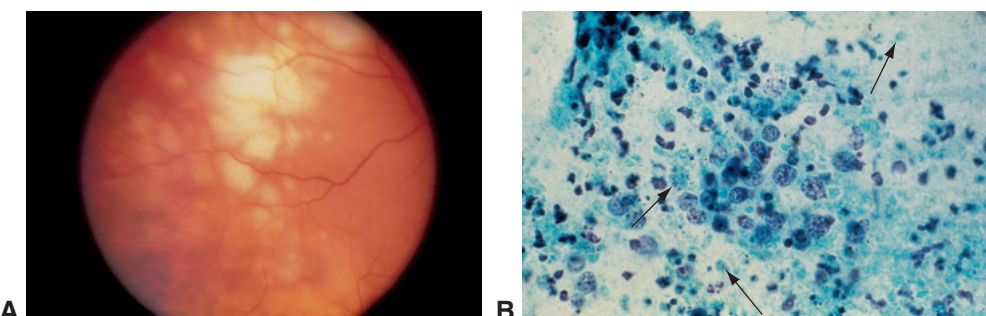


Figure 11-12 Intraocular lymphoma. **A**, Color fundus photograph shows sub-retinal pigment epithelial infiltrates. **B**, Cytologic preparation of vitreous cells reveals many atypical cells with large nuclei and multiple nucleoli. Cell ghosts (arrows) are also present. (Courtesy of David J. Wilson, MD.)

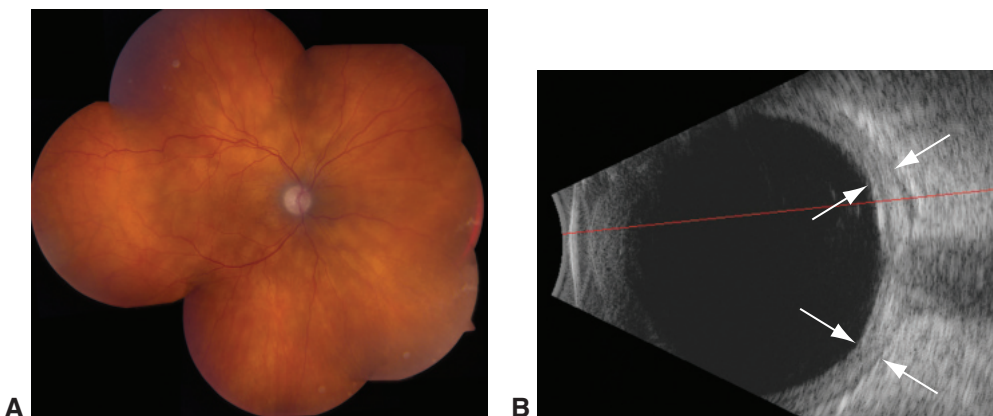


Figure 11-13 Uveal lymphoma. **A**, Fundus photograph demonstrates birdshot uveitis–like fundus appearance. **B**, B-scan ultrasound reveals characteristic uveal thickening (arrows). (Courtesy of Stephen J. Kim, MD.)

Infectious Retinal and Choroidal Inflammation

The following sections briefly describe selected infectious diseases that can cause retinal and choroidal inflammation.

Cytomegalovirus Retinitis

Cytomegalovirus (CMV) *retinitis* is the most common infectious congenital syndrome worldwide and can result in congenital CMV retinitis (see BCSC Section 6, *Pediatric Ophthalmology and Strabismus*, Chapter 28 for more in-depth information on this disorder). CMV retinitis is also the most common ocular opportunistic infection in adult patients with advanced AIDS and usually occurs when CD4⁺ T-cell counts are less than 50/ μ L. Patients with CMV retinitis typically present with floaters or decreased visual acuity. Clinically, CMV retinitis has a characteristic appearance that consists of opacification of the necrotic retina, typically along retinal vessels and often with areas of hemorrhage. Periphlebitis and even “frosted branch” angiitis may be prominent features. The degree of vitreous inflammation is highly variable. Early CMV retinitis may resemble the cotton-wool spots associated with HIV-related retinopathy. Although the diagnosis is often made clinically, polymerase chain reaction (PCR)–based analysis of ocular fluids may be diagnostic in unclear cases.

CMV retinitis can be treated with ganciclovir or foscarnet, administered systemically or intravitreally. High-dose induction therapy is typically given for 2–3 weeks, after which maintenance therapy is continued until immune reconstitution results in restoration of anti-CMV T-cell immunity—usually at CD4⁺ T-cell counts greater than 200/ μ L. Immune recovery uveitis and its complications, most notably CME and epiretinal membrane formation, occurs in approximately 20% of HIV-seropositive patients following immune reconstitution. Up to 50% of eyes with CMV retinitis eventually develop a rhegmatogenous retinal detachment.

CMV retinitis can occur in the absence of HIV infection. This scenario is uncommon, however, and is almost always associated with relative immune suppression, such as that

which occurs with use of systemic corticosteroids, noncorticosteroid immunosuppressive agents, or chemotherapeutics.

Lalezary M, Recchia FM, Kim SJ. Treatment of congenital cytomegalovirus retinitis with intravitreal ganciclovir. *Arch Ophthalmol*. 2012;130(4):525–527.

Takakura A, Tessler HH, Goldstein DA, et al. Viral retinitis following intraocular or periocular corticosteroid administration: a case series and comprehensive review of the literature. *Ocul Immunol Inflamm*. 2014;22(3):175–182.

Non-CMV Necrotizing Herpetic Retinitis

Both varicella-zoster virus (VZV) and herpes simplex virus (HSV) can cause necrotizing retinitis in patients, whether immunocompromised or not. Unlike CMV, these infections can progress rapidly and therefore should be treated aggressively. Two distinct clinical syndromes have been described: (1) *acute retinal necrosis* (ARN) syndrome and (2) *progressive outer retinal necrosis* (PORN) syndrome. Characteristic features of ARN include the presence of 1—or more typically, multiple—foci of retinitis, which usually occur in the periphery and are associated with occlusive retinal vasculitis and moderate to severe anterior chamber and vitreous inflammation (Fig 11-14).

PORN occurs in patients who are severely immunocompromised, usually as the result of AIDS, and consists of rapidly progressive, multifocal necrotizing retinitis with little or no anterior chamber or vitreous inflammation. Initial involvement of the peripheral retina is most common, with rapid progression and coalescence of lesions (Fig 11-15).

Evaluation for these infections should include serologic testing for syphilis as well as intraocular fluid aspiration for use in PCR analysis in order to identify DNA from VZV, HSV, CMV, and *Toxoplasma gondii*. Because ARN and PORN progress rapidly, treatment should commence immediately upon suspicion of either. Some specialists initiate therapy with intraocular injection of ganciclovir or foscarnet, particularly when the macula or optic nerve is threatened. High-dose antiviral therapy, using either intravenous acyclovir or oral

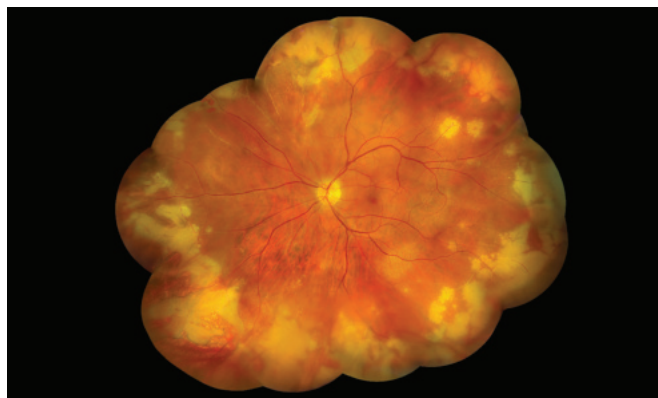


Figure 11-14 Peripheral necrotizing herpetic retinitis (acute retinal necrosis). Color fundus photograph montage shows intraretinal hemorrhage and full-thickness opacification of the retina. (Courtesy of Mark W. Johnson, MD, and Richard Hackel, CRA. Used with permission from Aizman A, Johnson MW, Elner SG. Treatment of acute retinal necrosis syndrome with oral antiviral medications. *Ophthalmology*. 2007;114(2):307–312.)

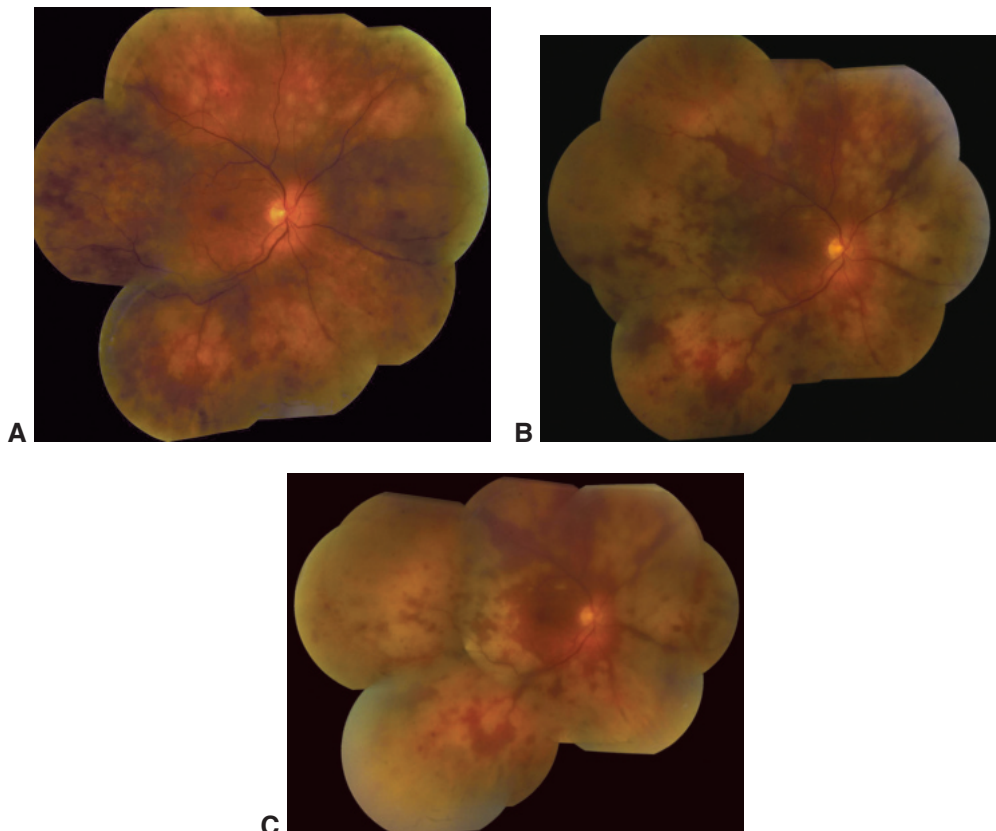


Figure 11-15 Progressive outer retinal necrosis (PORN) syndrome. The color fundus photograph montages show the rapid progression of retinitis from initial presentation (**A**), day 3 (**B**), and day 6 (**C**). An aqueous biopsy was positive for varicella-zoster polymerase chain reaction (PCR). (Courtesy of Daniel F. Martin, MD and Stephen J. Kim, MD.)

valacyclovir (2 grams three times daily) for a minimum of 7 days, should be administered. Thereafter, immunocompetent patients should be treated with oral suppressive therapy; treatment duration can vary from several months to long-term, even lifelong treatment. Patients with HIV/AIDS should be treated at least until the CD4⁺ cell count exceeds 200/ μ L, or perhaps indefinitely (Table 11-3). Once antiviral therapy is initiated, systemic corticosteroids can be added in nonimmunocompromised patients and then tapered over 3–6 weeks.

Schoenberger SD, Kim SJ, Thorne JE, et al. Diagnosis and treatment of acute retinal necrosis: a report by the American Academy of Ophthalmology. *Ophthalmology*. 2017;124(3): 382–392.

Endogenous Bacterial Endophthalmitis

Endogenous bacterial endophthalmitis results from hematogenous seeding of the eye, typically during transient bacteremia. Although decreased vision and eye pain are common symptoms, many patients do not have any constitutional symptoms. A wide range

Table 11-3 Treatment Options for Herpetic Retinitis Caused by Cytomegalovirus (CMV), Varicella-Zoster Virus (VZV), or Herpes Simplex Virus (HSV)

Intraocular treatments			
CMV, VZV, HSV			
Systemic treatments			
	Drug	Induction/high dose	Maintenance/suppression
CMV			
	Ganciclovir ^a	5 mg/kg, intravenously, every 12 hours for 2 weeks	Valganciclovir, 900 mg, once or twice daily or Ganciclovir intraocular implant
	Foscarnet ^{a,b}	90 mg/kg, intravenously, every 12 hours for 2 weeks	
VZV/HSV			
	Acyclovir ^a	10 mg/kg, intravenously, every 8 hours	800 mg, orally, 5 times daily
	Valacyclovir ^a	2 g, orally, 3 times daily	1 g, orally, 3 times daily
	Prednisone (optional)	0.5 mg/kg/day for 3–6 weeks ^c	

^aStandard adult dosages. Monitoring of kidney function is required, as kidney toxicity can occur.

^bMonitoring of bone marrow function is required, as suppression can occur.

^cAfter antiviral therapy is initiated.

of bacteria can cause endogenous bacterial endophthalmitis. In North America, 40% of cases occur in patients with endocarditis, most typically caused by either *Staphylococcus* or *Streptococcus* species. In contrast, 60% of endogenous endophthalmitis cases in Asia occur in patients with liver abscesses caused by *Klebsiella pneumoniae*. Nearly one-third of cases occur in patients who have urinary tract infections, most often caused by *Escherichia coli*. Other cases can be associated with intravenous drug use or with procedures known to produce bacteremia, particularly placement of indwelling catheters.

Clinical presentation can vary and depends on both the size of the inoculum and the virulence of the organism; it ranges from a focal chorioretinitis (Fig 11-16) with little vitreous inflammation to a dense panophthalmitis that obscures the view of the posterior



Figure 11-16 Color fundus photograph of focal endogenous bacterial endophthalmitis.
(Courtesy of Janet L. Davis, MD.)

segment. The patient should undergo systemic evaluation for the source of infection and initiate treatment with systemic antibiotics. Additionally, intravitreal injection of broad-spectrum antibiotics should be considered.

Durand ML. Endophthalmitis. *Clin Microbiol Infect*. 2013;19(3):227–234.

Fungal Endophthalmitis

Endophthalmitis caused by fungal infections may be either endogenous or exogenous. *Exogenous fungal endophthalmitis* is uncommon in North America and Europe. In contrast, in tropical regions such as India, fungi account for up to one-fifth of culture-positive cases following surgery or trauma. *Endogenous fungal endophthalmitis* is rare regardless of setting and typically occurs in either severely immunocompromised patients with persistent fungemia or otherwise healthy intravenous drug users following transient fungemia. Clinical presentation is often subacute, and the diagnosis is typically delayed for weeks. *Aspergillus* (Fig 11-17) and *Fusarium* are the most commonly identified causative species. Fungal keratitis may also progress to endophthalmitis, most typically when caused by *Fusarium*. Treatment is frequently difficult and typically involves vitrectomy, intravitreal injection of amphotericin B (5 µg/0.1 ml) and/or voriconazole (0.1 mg/0.1 ml), and systemic antifungal therapy. Two-thirds of patients with fungal endophthalmitis lose useful vision.

Wykoff CC, Flynn HW Jr, Miller D, Scott IU, Alfonso EC. Exogenous fungal endophthalmitis: microbiology and clinical outcomes. *Ophthalmology*. 2008;115(9):1501–1507.

Yeast (Candida) endophthalmitis

Endogenous yeast endophthalmitis is most frequently caused by *Candida* species. Affected patients frequently have previously used indwelling catheters or have undergone long-term antibiotic treatment or immunosuppressive therapy. Many also have a history of hyperalimentation, recent abdominal surgery, or diabetes mellitus. The initial intraocular inflammation is usually mild to moderate, and yellow-white choroidal or chorioretinal lesions may be single or multiple (Fig 11-18). Subretinal infiltrates may coalesce into a

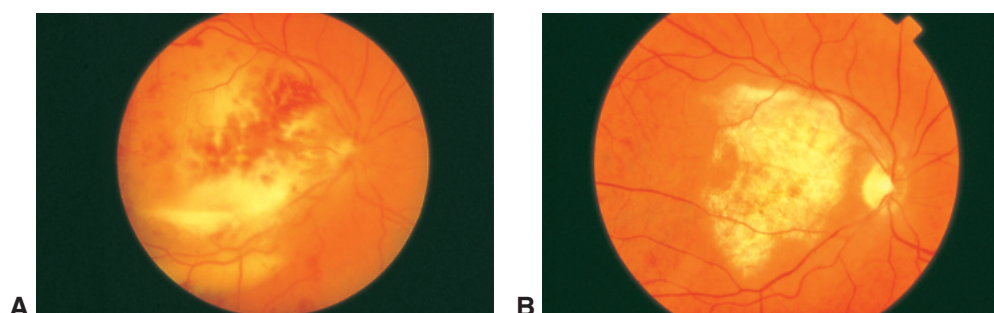


Figure 11-17 Color fundus photographs of endophthalmitis caused by infection with *Aspergillus* species. **A**, Features present include mild vitritis, a diffuse macular chorioretinal lesion with subretinal and subhyaloid hypopyon, intraretinal hemorrhage, and papillitis. **B**, Same eye 2 months after treatment shows macular scar, preserved overlying retinal vessels, and temporal optic nerve head pallor. Final visual acuity was 20/400. (From Weishaar PD, Flynn HW Jr, Murray TG, et al. Endogenous *Aspergillus* endophthalmitis. Clinical features and treatment outcomes. *Ophthalmology*. 1998;115(1):60.)

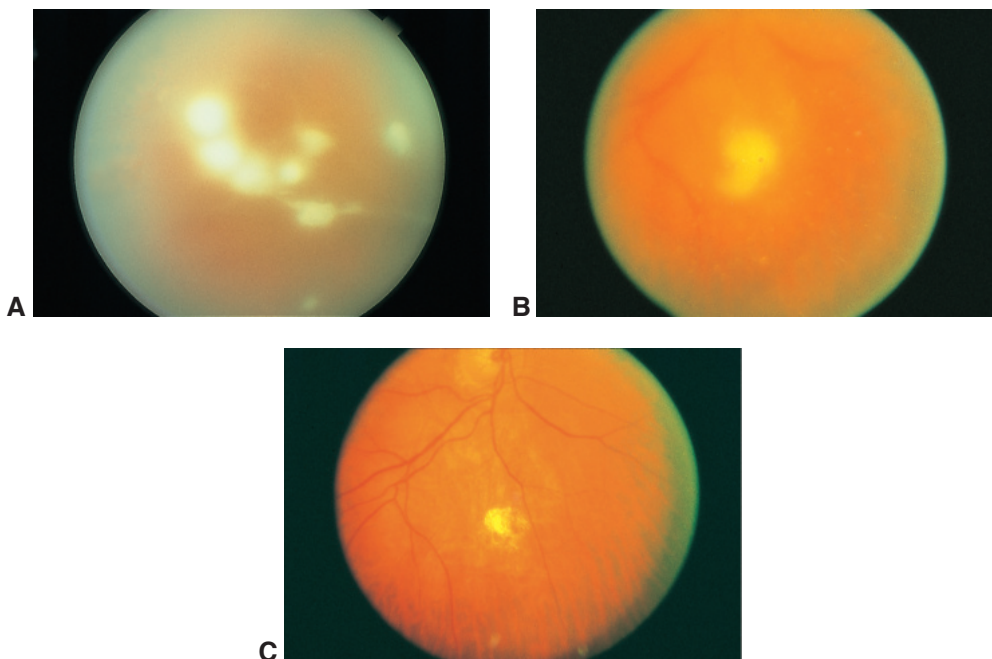


Figure 11-18 Color fundus photographs of endogenous yeast (*Candida*) endophthalmitis. **A**, Note the vitreous infiltrates in a “string-of-pearls” configuration. **B**, Photograph shows a patient with endogenous endophthalmitis before treatment. **C**, After treatment with vitrectomy and intravitreal amphotericin B, the endogenous endophthalmitis shown in **B** was resolved. (Courtesy of Harry W. Flynn, Jr, MD.)

mushroom-shaped white nodule that projects through the retina into the vitreous. Exogenous *Candida* endophthalmitis is rare.

The diagnosis of *Candida* endophthalmitis is usually made according to the history, clinical setting, and presence of characteristic fundus features. Intraocular culture specimens are best obtained during pars plana vitrectomy, because it is difficult to culture the localized vitreous clusters of fungus from specimens taken via diagnostic vitreous tap. After completion of the vitrectomy, intravitreal injection of amphotericin B or voriconazole at standard doses is usually performed.

The ophthalmologist should seek consultation with a specialist in infectious diseases to evaluate the patient for systemic disease and assist with treatment planning. If the macula is not involved, visual prognosis after treatment is generally good. Focal chorioretinal lesions are often successfully treated with systemic medications alone. Intravenous fluconazole and voriconazole penetrate the eye well and have been used to treat focal lesions.

Oude Lashof AM, Rothova A, Sobel JD, et al. Ocular manifestations of candidemia. *Clin Infect Dis.* 2011;53(3):262–268.

Tuberculosis

Even though one-third of the world’s population has been exposed to *Mycobacterium tuberculosis*, active *M tuberculosis* uveitis is uncommon, even in endemic areas. Suggestive



Figure 11-19 Ocular tuberculosis. Color fundus photograph shows a choroidal granuloma superotemporal to the optic nerve head. (Courtesy of Janet L. Davis, MD.)

clinical findings include solitary (Fig 11-19) or multifocal choroiditis, serpiginous-like chorioretinitis, and Eales disease–like peripheral nonperfusion in association with uveitis. Patients suspected of having tuberculous uveitis should undergo testing for prior *M tuberculosis* exposure, including a chest X-ray and either purified protein derivative (PPD) skin testing or a blood-based interferon-gamma release assay.

Once the diagnosis of ocular tuberculosis is either confirmed or strongly suggested, the patient should be treated for extrapulmonary tuberculosis as recommended by either the US Centers for Disease Control and Prevention or the World Health Organization.

Abouammoh M, Abu El-Asrar AM. Imaging in the diagnosis and management of ocular tuberculosis. *Int Ophthalmol Clin.* 2012;52(4):97–112.

Gupta A, Bansal R, Gupta V, Sharma A, Bambery P. Ocular signs predictive of tubercular uveitis. *Am J Ophthalmol.* 2010;149(4):562–570.

Syphilitic Chorioretinitis

Uveitis is often the presenting sign of syphilis but can occur at any stage of the infection. Syphilitic uveitis is confirmed through serologic testing with both the specific and sensitive fluorescent treponemal antibody absorption (FTA-ABS) test and the nonspecific VDRL or rapid plasma reagin (RPR) tests, which are complementary to each other. Additional confirmatory tests include the *Treponema pallidum* particle agglutination assay (TP-PA) and the microhemagglutination assay for *T pallidum* antibodies (MHA-TP). Patients with uveitis who test positive for syphilis on serologic tests should also have their cerebrospinal fluid anti-treponemal antibody titers measured before and, when present, after completion of therapy to document a complete response to treatment.

Many patients with syphilitic uveitis present with a nondescript panuveitis, which supports the need for routine syphilis testing in all sexually active adults with uveitis. Specifically suggestive clinical findings include inflammatory ocular hypertensive syndrome, iris roseola, and retinochoroiditis. The retinochoroiditis is often diaphanous—appearing less opaque than either herpetic or toxoplasmic necrotizing retinitis—and is accompanied by overlying inflammatory accumulations termed *retinal precipitates*. A distinctive form of syphilitic outer retinitis termed *acute syphilitic posterior placoid chorioretinitis* (ASPPC) is characterized by the presence of a placoid, round or oval, yellow-white lesion that involves or is near the macula (Fig 11-20). Because coinfection is common, all patients with

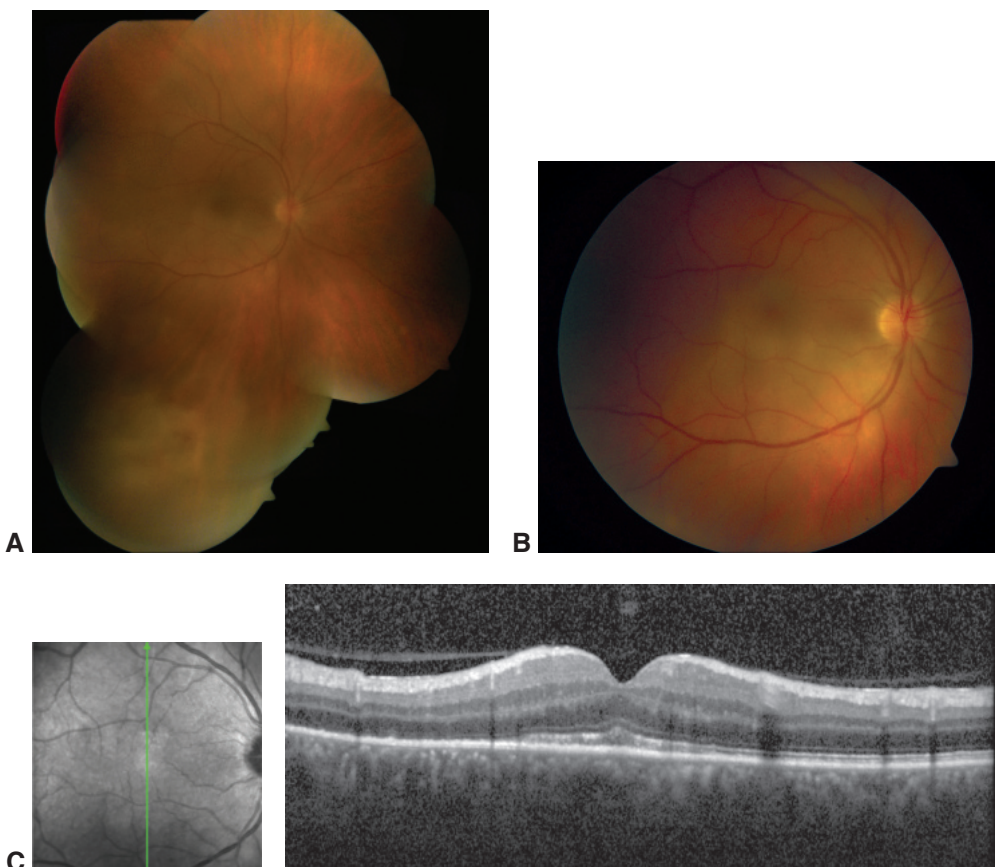


Figure 11-20 Syphilitic retinochoroiditis. **A**, Color fundus photograph montage shows a right eye with vitritis. **B**, Fundus photograph shows placoid yellow lesions in the macula and inferior periphery representing acute syphilitic posterior placoid chorioretinitis (ASPPC). **C**, OCT image demonstrates location of ASPPC in the outer retina. (Courtesy of Stephen J. Kim, MD.)

syphilis should be tested for HIV. Patients with syphilitic uveitis should be treated for neurosyphilis.

Cunningham ET Jr, Eandi CM, Pichi F. Syphilitic uveitis. *Ocul Immunol Inflamm*. 2014; 22(1):2–3.

Cat-Scratch Disease

Cat-scratch disease is associated with 2 ocular syndromes: (1) Parinaud oculoglandular syndrome, which consists of conjunctival inflammation with preauricular adenopathy, and (2) Leber stellate neuroretinitis, which includes macular star formation and optic nerve head swelling, often associated with a peripapillary serous macular detachment (Fig 11-21). Small, focal areas of retinitis or chorioretinitis occur frequently in patients with neuroretinitis. In rare cases, an optic nerve head angiomatic lesion can develop. Immunocompetent adults with cat-scratch disease are treated with doxycycline, 100 mg



Figure 11-21 Color fundus photograph of neuroretinitis shows optic nerve head swelling and a macular star formation resulting from cat-scratch disease (*Bartonella henselae*). (Courtesy of George Alexandakis, MD.)

twice daily for 4–6 weeks. Oral erythromycin can be used in children. Prolonged treatment with doxycycline and rifampin can be used in immunocompromised adults or in patients with persistent infection.

Toxoplasmic Retinochoroiditis

Toxoplasmic retinochoroiditis is the most common cause of posterior segment infection worldwide. The causative organism, *Toxoplasma gondii*, is an obligate, intracellular parasitic protozoan. Because seropositivity for *T gondii* is very common, seropositivity alone does not confirm that uveitis is related to toxoplasmosis. Congenital disease occurs via acquisition of the organism by a pregnant woman exposed to tissue cysts or oocytes in uncooked meat or substances contaminated with cat feces (see also BCSC Section 6, *Pediatric Ophthalmology and Strabismus*, Chapter 28). The typical ocular finding in congenital toxoplasmosis is a chorioretinal scar, usually in the macula and often bilateral. Most cases of toxoplasmosis are currently assumed to be acquired postnatally, although proving this assumption can be difficult. A positive serologic test result for immunoglobulin M (IgM) anti-*T gondii* antibodies supports the diagnosis of an acquired disease.

Decreased vision and floaters are the most common presenting symptoms of toxoplasmic retinochoroiditis. Clinically, the disorder consists of a focal area of intense, necrotizing retinochoroiditis, typically with moderate to severe overlying vitreous inflammation (Fig 11-22). Recurring disease is indicated by an adjacent or nearby retinochoroidal scar. Multiple active lesions are rare and should prompt HIV testing. HIV-seropositive patients with ocular toxoplasmosis have a high risk of CNS involvement and therefore should undergo magnetic resonance imaging with contrast. Elderly patients may present with more aggressive disease due to their relative immunosuppression.

Active ocular toxoplasmosis is commonly treated with antibiotics, despite the lack of well-designed randomized controlled trials. The simplest approach is treatment with trimethoprim-sulfamethoxazole. Classic therapy uses sulfadiazine with pyrimethamine and prednisone (prescribed with folinic acid and accompanied by regular monitoring of blood cell counts); the addition of clindamycin results in so-called quadruple therapy. None of these approaches has been shown to be superior to another with regard to final vision outcome, lesion size, or recurrence rate. Treatment typically lasts 4–6 weeks, and complete healing of active lesions occurs over 4–6 months. When used, systemic

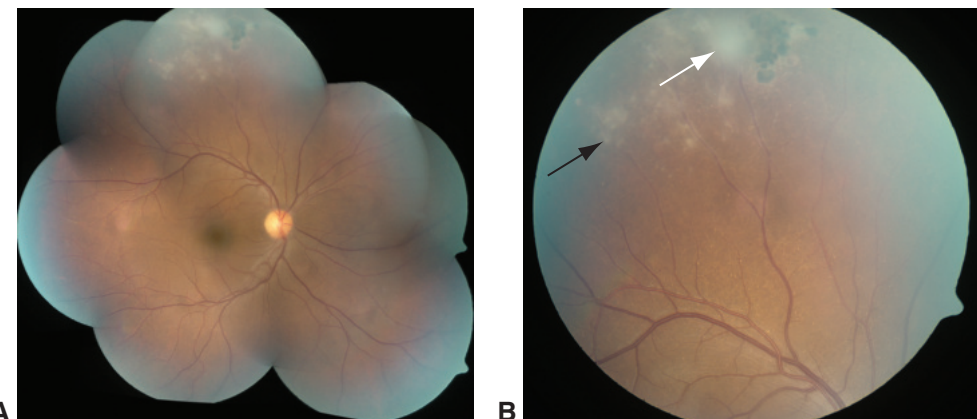


Figure 11-22 Toxoplasmic retinochoroiditis. **A**, Color fundus photograph montage of a patient with recurring toxoplasmic retinochoroiditis. **B**, Color fundus photograph shows white focal retinitis (white arrow) with overlying vitreous inflammation, which creates a “headlight in the fog” appearance, with an adjacent pigmented retinochoroidal scar. There is accompanying perivasculitis and nonspecific exudates, in addition to distinct lobular periarteriolar collections of cells (black arrow) called Kyrieleis plaques. (Courtesy of Stephen J. Kim, MD.)

corticosteroids should be given under antibiotic cover. Use of long-acting, depot periocular or intraocular corticosteroid injections should be avoided. Long-term, maintenance treatment with trimethoprim-sulfamethoxazole has been used to decrease the attack rate in patients experiencing frequent recurrences or in severely immunosuppressed patients. Intravitreal clindamycin with or without dexamethasone has been used to treat vision-threatening lesions or for patients who are intolerant of or fail to respond to systemic therapy.

Holland GN. Ocular toxoplasmosis: a global reassessment. Part I: epidemiology and course of disease. *Am J Ophthalmol*. 2003;136(6):973–988.

Holland GN. Ocular toxoplasmosis: a global reassessment. Part II: disease manifestations and management. *Am J Ophthalmol*. 2004;137(1):1–17.

Kim SJ, Scott IU, Brown GC, Brown MM, Ho AC, Ip MS, Recchia FM. Interventions for toxoplasma retinochoroiditis: a report by the American Academy of Ophthalmology. *Ophthalmology*. 2013;120(2):371–378.

Toxocariasis

Toxocariasis is a parasitic infection caused by 1 of 2 roundworms: *Toxocara canis* or *Toxocara cati*, which are common intestinal parasites of dogs and cats, respectively. Humans are infected following ingestion of soil or vegetables contaminated by the ova. Although ocular toxocariasis is part of a systemic infestation by the nematode, systemic manifestations such as visceral larval migrans, fever, and eosinophilia are relatively uncommon. Children and young adults are affected disproportionately. Common symptoms include decreased vision and floaters. The condition is unilateral in most cases and typically has 1 of 3 presentations: (1) a peripheral granuloma, which often produces a traction band that extends toward the macula (Fig 11-23) and occasionally mimics unilateral intermediate uveitis

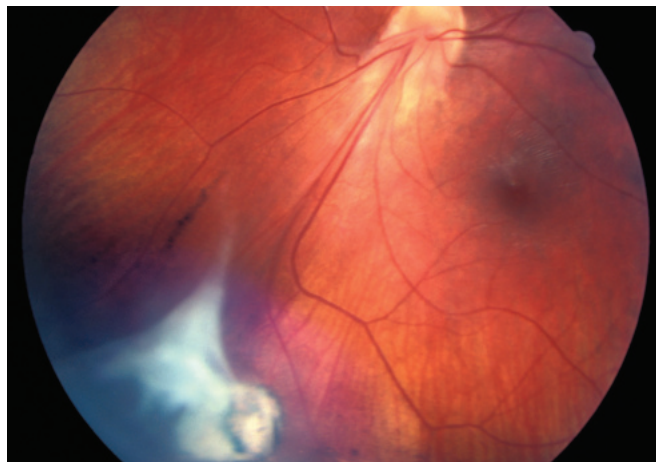


Figure 11-23 Color fundus photograph from a 6-year-old boy with reduced and distorted vision. The image shows a peripheral toxocariasis cyst with associated fibrosis (bottom left). The fibrosis results in considerable traction, and the macula is dragged inferiorly and distorted. (Courtesy of Colin A. McCannel, MD.)

with snowbank formation; (2) a posterior pole granuloma, which can decrease vision dramatically when the central macula is involved; or (3) a moderate to severe panuveitis that can mimic endogenous endophthalmitis. Enzyme-linked immunosorbent assay (ELISA) analysis of serum or intraocular fluids can help establish the diagnosis in these cases but is relatively insensitive. Vitreous inflammation, CME, and tractional retinal detachment are the most common causes of vision loss. Most specialists assume that the uveitis of toxocariasis represents an immune response to antigens released from a dead or dying worm. Thus, treatment typically involves use of local or systemic corticosteroids, and antihelminthic therapy has little or no therapeutic role.

Woodhall D, Starr MC, Montgomery SP, et al. Ocular toxocariasis: epidemiologic, anatomic, and therapeutic variations based on a survey of ophthalmic subspecialists. *Ophthalmology*. 2012;119(6):1211–1217.

Lyme Disease

Lyme disease is caused by the spirochete *Borrelia burgdorferi*, which is transmitted to humans by ticks from animal reservoirs: primarily rodents, deer, birds, cats, and dogs. Early systemic manifestations consist of myalgias, arthralgias, fever, headache, malaise, and a characteristic skin lesion known as *erythema migrans* or a bull's-eye rash, which consists of an annulus of erythema surrounding an area of central clearing. In later stages, as neurologic or musculoskeletal findings manifest, ocular inflammation may develop but is uncommon. Lyme disease-related ocular findings include keratitis, scleritis, and uveitis, which may include anterior chamber or vitritis inflammation, retinal vasculitis, papillitis, or optic neuritis. Chronic uveitis in patients who reside in or have traveled to an endemic area or who have had a recent tick bite or an *erythema migrans*-like skin lesion should suggest the possibility of Lyme disease. Initial serologic testing is performed using

a sensitive ELISA. If an ELISA result is positive or equivocal, then separate IgM immunoblotting (if symptoms have been present for fewer than 30 days) and IgG immunoblotting should be performed on the same blood sample. A diagnosis of Lyme disease is supported only when both tests are positive. The 2 tests are designed to be used together; thus, the initial ELISA test should not be skipped. Treatment for early disease consists of tetracycline, doxycycline, or penicillin. Advanced disease may require intravenous ceftriaxone or penicillin.

Raja H, Starr MR, Bakri SJ. Ocular manifestations of tick-borne diseases. *Surv Ophthalmol*. 2016;61(6):726–744.

Diffuse Unilateral Subacute Neuroretinitis

Diffuse unilateral subacute neuroretinitis (DUSN) is a rare condition that typically occurs in otherwise healthy, young patients and is caused by the presence of a mobile subretinal nematode. Prompt diagnosis and treatment of the condition can help prevent vision loss, which can be severe. The clinical findings in DUSN can be divided into acute and end-stage manifestations. In the acute phase, patients frequently have decreased visual acuity, vitritis, papillitis, and clusters of gray-white or yellow-white outer retinal and choroidal lesions. The clustering of the lesions is important because it often helps localize the causative nematode. The degree of vision loss is often greater than might be expected from the clinical examination. Left untreated, late sequelae ultimately develop, which include optic atrophy, retinal arterial narrowing, and diffuse RPE disruption with severe vision loss. The late findings can be misinterpreted as unilateral retinitis pigmentosa.

The causative nematodes in DUSN have yet to be definitively established, although *Toxocara* species, *Baylisascaris procyonis*, and *Ancylostoma caninum* have all been implicated. Raccoon exposure appears to be common in patients in North America. The characteristic lesions are believed to result from a single nematode migrating within the subretinal space. If the nematode can be observed, which occurs in less than half of cases, it should be destroyed using laser photocoagulation. After the worm is killed, vision usually stabilizes.

de Amorim Garcia Filho CA, Gomes AH, de A Garcia Soares AC, de Amorim Garcia CA.

Clinical features of 121 patients with diffuse unilateral subacute neuroretinitis. *Am J Ophthalmol*. 2012;153(4):743–749.

West Nile Virus Chorioretinitis

West Nile virus (WNV) infection is transmitted to humans by an infected mosquito of the genus *Culex*, with birds serving as the primary reservoir. Human infection is most often subclinical, although a febrile illness occurs in approximately 20% of cases. Ocular manifestations usually occur in very ill diabetic patients with encephalitis. The manifestation most typically observed is a multifocal chorioretinitis that is usually bilateral and includes lesions arranged in distinctive curvilinear clusters that often follow the course of retinal nerve fibers (Fig 11-24). Vision typically remains good unless the lesions involve the central macula.

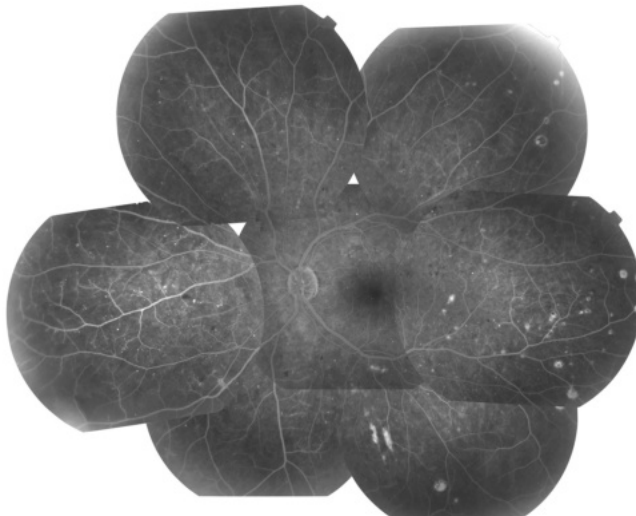


Figure 11-24 Fundus photograph montage of West Nile virus chorioretinitis. Fluorescein angiography images show punched-out lesions that characteristically arrange in almost confluent streaks in some areas. Alterations caused by nonproliferative diabetic retinopathy are also apparent; West Nile virus chorioretinitis typically occurs in diabetic patients. (Courtesy of Robert Beardsley, MD, and Colin A. McCannel, MD.)

Zika Virus Chorioretinitis

Zika virus (ZIKV) is a member of the virus family *Flaviviridae* and is related to yellow fever virus, dengue virus, and West Nile virus. Zika is primarily spread by the female *Aedes aegypti* mosquito; infection in adults is often asymptomatic or results in only mild symptoms. Infection during pregnancy, however, can result in severe microcephaly and other brain malformations in some infants. Macular and optic nerve abnormalities have been reported in some patients with ZIKV.

Ebola Virus Panuveitis

Ebola virus (EBOV) causes a severe and fatal hemorrhagic fever in humans; the mortality rate is as high as 90%. Among survivors, uveitis has been described; there has been 1 report of severe panuveitis that occurred after the patient experienced a complete systemic recovery but still had persistent viral replication in the aqueous humor.

Chikungunya Virus Retinitis

Chikungunya virus (CHIKV) is a member of the *Alphavirus* genus. The most common symptoms of CHIKV infection are fever and joint pain. Several ocular findings have been reported, including retinitis and optic neuritis, but anterior uveitis may be the most common presentation.

Congenital and Stationary Retinal Disease

Color Vision (Cone System) Abnormalities

Patients may present with color vision defects, or dyschromatopsia, that are either static or progressive. Static dyschromatopsia is usually, although not always, congenital. Whereas congenital color vision defects are stationary and usually affect both eyes equally, acquired color vision defects may be progressive and/or uniocular. This chapter describes the nonprogressive forms of color vision loss. For further discussion of optic neuropathies that may lead to acquired forms of vision loss, please refer to BCSC Section 5, *Neuro-Ophthalmology*.

Congenital Color Deficiency

Congenital color vision defects are traditionally classified by an individual's performance on color-matching tests. A person with normal color vision (*trichromatism*, or *trichromacy*) can match any colored light by varying a mixture of 3 different-colored lights, or primary colors (eg, a long-wavelength red, middle-wavelength green, and short-wavelength blue light).

Individuals with *anomalous trichromatism* make up the largest group of color-deficient persons; they include approximately 5%–6% of males. These individuals can also use 3 primary colors to match a given color; however, because 1 of their cone photopigments has an abnormal absorption spectrum, they use different proportions of colors than those used by persons with normal color vision. Anomalous trichromacy ranges in severity. Some individuals have only a mild abnormality and may, for example, fail some of the subtle Ishihara test plates but have no trouble naming colors or passing the less-sensitive screening tests such as the Farnsworth Panel D-15 hue test (see Chapter 3 in this volume). Others have poor color discrimination and may appear to have dichromacy on some of the color vision tests.

Hereditary congenital color vision defects are most frequently X-linked-recessive, red-green abnormalities; they affect 5%–8% of males and 0.5% of females. Acquired defects are more frequently of the blue-yellow, or tritan, variety and affect males and females equally. Table 12-1 shows the traditional classification of color vision deficits based on color-matching test results.

Table 12-1 Classification and Male-Population Incidence of Color Vision Defects

Color Vision	Inheritance	Incidence in Male Population (%)
Hereditary		
<i>Trichromatism</i>		
Normal	—	92.0
Deutanomalous	XR	5.0
Protanomalous	XR	1.0
Tritanomalous	AD	0.0001
<i>Dichromatism</i>		
Deutanomalous	XR	1.0
Protanomalous	XR	1.0
Tritanomalous	AD	0.001
<i>Achromatopsia (monochromatism)</i>		
Typical (rod monochromatism)	AR	0.0001
Atypical (blue-cone monochromatism)	XR	Unknown
Acquired		
Tritanomalous (blue-yellow)	Unknown	Unknown
Protanomalous-deutanomalous (red-green)	Unknown	Unknown

AD=autosomal dominant; AR=autosomal recessive; XR=X-linked recessive.

Individuals who need only 2 primary colors to make a color match have *dichromacy*. It is assumed that such individuals lack 1 of the cone photopigments. Approximately 2% of males have dichromacy.

An absence of color discrimination, or *achromatopsia*, means that any spectral color can be matched with any other solely by intensity adjustments. The congenital achromatopsias are disorders of photoreceptor function. Essentially, there are 2 forms of achromatopsia: (1) *rod monochromatism*, and (2) *S-cone monochromatism (blue-cone monochromatism)*. Both disorders typically present with congenital nystagmus, poor visual acuity, and photophobia. Electrotretinography (ERG) testing helps differentiate achromatopsia from congenital motor nystagmus or ocular albinism, both of which are associated with normal cone ERGs (see Chapter 3, Fig 3-2).

Rod monochromatism (complete achromatopsia) is the most severe form; affected individuals have normal rod function but no detectable cone function and see the world in shades of gray. Patients may have full to partial expression of the disorder, with visual acuity ranging from 20/80 to 20/200. Nystagmus is usually present in childhood and may improve with age. Characteristically, the ERG pattern in patients with rod monochromatism shows an absence of cone-derived responses and normal rod responses. Dark adaptometry shows no cone plateau and no cone–rod break. The disorder exhibits autosomal-recessive inheritance.

In *S-cone (or blue-cone) monochromatism*, the function of rods and S cones is normal, but L- and M-cone function is absent. The condition is usually X-linked and can be difficult to distinguish clinically from rod monochromatism in the absence of a family history or results from specialized color or ERG testing. Individuals with S-cone monochromatism exhibit preserved S-cone ERG responses, severely reduced cone flicker ERGs, and normal rod ERGs. These individuals typically have a visual acuity of

approximately 20/80, which is better than the visual acuity found in individuals with typical rod monochromatism.

Dingcai C. Color vision and night vision. In: Schachat AP, Wilkinson CP, Hinton DR, Sadda SR, Wiedemann P, eds. *Ryan's Retina*. Vol 1. 6th ed. Philadelphia: Elsevier/Saunders; 2018: 325–339.

Wu DM, Amani AF. Abnormalities of cone and rod function. In: Schachat AP, Wilkinson CP, Hinton DR, Sadda SR, Wiedemann P, eds. *Ryan's Retina*. Vol 2. 6th ed. Philadelphia: Elsevier/Saunders; 2018:1006–1017.

Night Vision (Rod System) Abnormalities

Congenital Night-Blinding Disorders With Normal Fundi

Congenital stationary night blindness (CSNB) is a nonprogressive disorder of night vision. CSNB has 3 genetic subtypes:

1. X-linked (most common)
2. autosomal recessive
3. autosomal dominant (rare)

Snellen visual acuities of patients with CSNB range from normal to occasionally as poor as 20/200, but most cases of decreased vision are associated with significant myopia. The appearance of the fundus is usually normal, except for myopic changes in some cases. Patients commonly present with difficulty with night vision; nystagmus and reduced visual acuity may also be presenting symptoms. Some CSNB patients never report nyctalopia (night blindness), perhaps because they are accustomed to it. Some patients may have a paradoxical pupillary response, in which the pupil dilates when the ambient light dims. Dark-adaptometry curves reveal markedly reduced responses (Fig 12-1).

Electroretinography is important in the diagnosis of CSNB. The most common ERG pattern seen in patients with CSNB is the *negative* ERG (the Schubert-Bornschein form of CSNB), in which the bright-flash, dark-adapted ERG has a normal (or near-normal) a-wave but a markedly reduced b-wave. The normal a-wave excludes significant rod photoreceptor dysfunction, and the result thus facilitates the differentiation of CSNB from the potentially blinding disorder retinitis pigmentosa (RP; see Chapter 3).

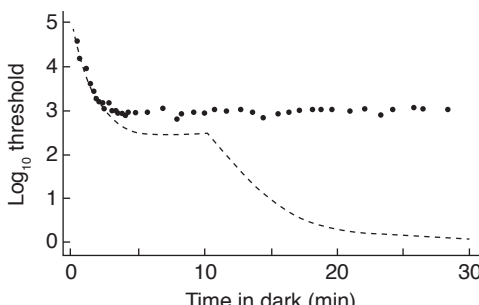


Figure 12-1 Dark-adaptometry curve in congenital stationary night blindness (CSNB). The dark-adaptometry curve of this patient (dotted curve) with CSNB shows no rod adaptation. Dashed curve indicates normal response. (Used with permission from Ripps H. Night blindness revisited: from man to molecules. Proctor lecture. Invest Ophthalmol Vis Sci. 1982;23(5):588–609.)

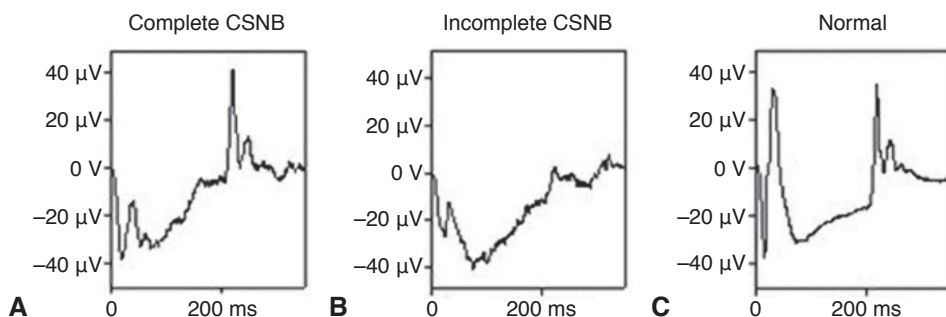


Figure 12-2 Electroretinography (ERG) patterns of on- and off-responses in CSNB. The stimulus has a 200-millisecond (ms) duration to enable independent recording of the ERG responses to onset and offset. **A**, The pattern of a patient with “complete” CSNB shows a negative-waveform on-response but a normal off-response. **B**, The pattern of a patient with “incomplete” CSNB shows both on- and off-response abnormalities. **C**, Pattern of a subject with normal responses. (Courtesy of Graham E. Holder, PhD.)

X-linked CSNB has been categorized into 2 types: “complete” and “incomplete.” Patients with complete CSNB (cCSNB) have an undetectable rod-specific, dim-flash, dark-adapted ERG and psychophysical thresholds that are mediated by cones. Patients with incomplete CSNB (iCSNB) have some detectable rod function on ERG and an elevated dark-adaptation final threshold (Fig 12-2). The differential diagnosis of CSNB includes melanoma-associated retinopathy (MAR), which demonstrates an identical ERG pattern to CSNB, but which usually presents with acquired night blindness and shimmering photopsias.

Congenital Night-Blinding Disorders With Fundus Abnormality

Fundus albipunctatus results from a mutation in *RDH5* (12q13–q14). *RDH5* encodes 11-*cis*-retinol dehydrogenase, a microsomal enzyme in the retinal pigment epithelium (RPE) that is involved in the regeneration of rhodopsin. Patients with fundus albipunctatus have very delayed rhodopsin regeneration, and although levels eventually normalize, the process may require many hours in the dark. Affected individuals are night blind from birth and usually exhibit yellow-white dots in the posterior pole extending into the midperiphery, but sparing the fovea (Fig 12-3). ERG responses commonly show a cone-isolated retina pattern, with undetectable rod-specific ERG, and a severely reduced bright-flash dark-adapted ERG (arising in dark-adapted cones) that normalizes with sufficiently extended dark adaptation. Some patients may have a normal fundus but characteristic ERG findings and molecular confirmation of the mutation; visual acuity and color vision are usually good in these patients.

The differential diagnosis of fundus albipunctatus includes *retinitis punctata alba*, a disorder related to mutation in *RLBP1*, which encodes cellular retinaldehyde-binding protein. In this condition, which is a progressive rod–cone dystrophy, the white dots may be finer than those of *fundus albipunctatus*, and there may be attenuation of the retinal vessels. ERG responses are usually very abnormal; although they show some recovery with extended dark adaptation, they do not normalize.

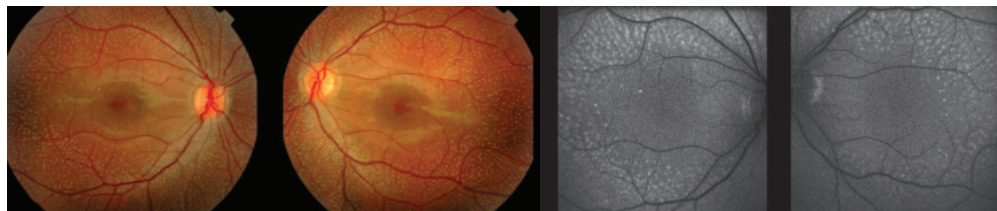


Figure 12-3 Fundus photographs and fundus autofluorescence images of a patient with fundus albipunctatus, showing multiple spots of unknown material scattered primarily throughout the deep retina. (Used with permission from Sergouniotis PI, Sohn EH, Li Z, et al. Phenotypic variability in RDH5 retinopathy (fundus albipunctatus). *Ophthalmology*. 2011;118(8):1661–1670.)

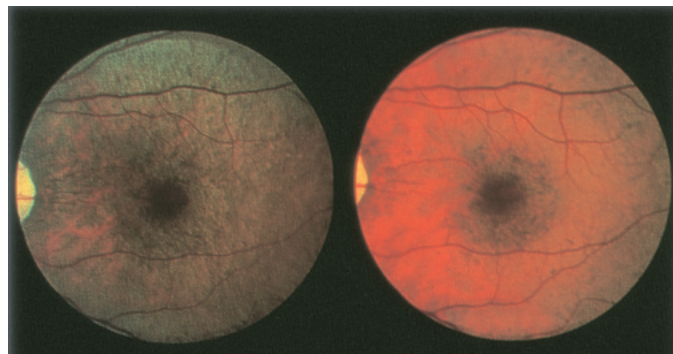


Figure 12-4 Fundus photographs of eyes with the Mizuo-Nakamura phenomenon. The fundus of this patient with X-linked cone dystrophy is unremarkable in a dark-adapted state (right) but has a yellow iridescent sheen after exposure to light (left).

Patients with *Oguchi disease* are also night blind from birth. This condition is due to either a mutation in the gene *SAG* (2q37), which encodes arrestin, or in *GRK1* (13q34), which encodes rhodopsin kinase. This very rare disorder is most common in Japanese patients. The fundus in eyes with Oguchi disease is normal after dark adaptation but shows a peculiar yellow iridescent sheen alteration after even brief exposure to light (the *Mizuo-Nakamura phenomenon*; Fig 12-4).

Cukras CA, Zein WM, Caruso RC, Sieving PA. Progressive and “stationary” inherited retinal degenerations. In: Yanoff M, Duker JS, eds. *Ophthalmology*. 4th ed. St. Louis: Elsevier/Saunders; 2013:480–490.

Zeitz C, Robson AG, Audo I. Congenital stationary night blindness: an analysis and update of genotype-phenotype correlations and pathogenic mechanisms. *Prog Retin Eye Res*. 2015; 45:58–110.

CHAPTER 13

Hereditary Retinal and Choroidal Dystrophies

Classification

The *Online Mendelian Inheritance in Man* (OMIM) website lists more than 750 genetic disorders with significant involvement of the retina, choroid, or both. The online Retinal Information Network, *RetNet*, lists more than 300 distinct genes or genetic loci associated with various retinal or choroidal dystrophies. Table 13-1 summarizes known retinal dystrophies and their associated genes and loci. Despite their numerous distinctive clinical features, these conditions are characterized by multiple genes that give rise to the same phenotype (*genetic heterogeneity*) as well as diverse phenotypes that share common causative genes (*variable expressivity*). Conversely, defects in a particular gene can give rise to different phenotypes; this is referred to as pleiotropy.

The disorders have been divided by 2 anatomic classifications: (1) apparent topography or (2) layer of involvement, such as retina, macula, retinal pigment epithelium (RPE), choroid, and vitreous/retina; however, these distinctions do not always correspond to the sites of the causative gene expression. A second system of organization classifies the disorders based on the inheritance pattern of the disease; however, some genes have variants that can give rise to either autosomal or X-linked dominant or autosomal or X-linked recessive inheritance, respectively. A third approach classifies the disorders by disease phenotype based on clinical examination and electrophysiological and psychophysical testing, but many genes can give rise to overlapping phenotypes.

For convenience, this chapter organizes the retinal and choroidal dystrophies based on clinical phenotypes and anatomic involvement, rather than on molecular genetics. Thus, the reader will note that some genes are causative across multiple phenotypes, and only in rare instances is a specific phenotype defined by a unique causative gene. Disorders with primary diffuse photoreceptor involvement are classified separately from those with predominantly macular involvement, for which the symptoms and prognoses generally differ. The diffuse photoreceptor dystrophy category of disorders is further subcategorized into rod-dominant, cone-dominant, and choroidal syndromes and diseases.

Daiger SP, Sullivan LS, Bowne SJ. Genetic mechanisms of retinal disease. In: Schachat AP, Wilkinson CP, Hinton DR, Sadda SR, Wiedemann P, eds. *Ryan's Retina*. Vol 2. 6th ed. Philadelphia: Elsevier/Saunders; 2018:711–721.

Table 13-1 Genes and loci associated with inherited retinal dystrophies

Disease Category	Mapped Loci (Not Identified)	Mapped and Identified Genes
Bardet-Biedl syndrome, autosomal recessive	None	<i>ADIPOR1, ARL6, BBIPI1, BBS1, BBS2, BBS4, BBS5, BBS7, BBS9, BBS10, BBS12, C8orf37, CEP19, CEP290, IFT172, IFT27, INPP5E, KCNJ13, LZTFL1, MKKS, MKS1, NPHP1, SDCCAG8, TRIM32, TTC8, PRDM13, RGR, TEAD1</i>
Chorioretinal atrophy or degeneration, autosomal dominant	None	<i>CORD4, CORD17, RCD1</i>
Cone or cone-rod dystrophy, autosomal dominant	<i>CORD8</i>	<i>AIPL1, CRX, GUCA1A, GUCY2D, PITPNM3, PROM1, PRPH2, RIMS1, SEMA4A, UNC119</i>
Cone or cone-rod dystrophy, autosomal recessive	<i>COD2</i>	<i>ABCA4, ADAM9, ATF6, C21orf37, CACNA2D4, CDHRY1, CEP78, CERKL, CNGA3, CNGB3, CNNM4, GNAT2, IFT81, KCNV2, PDE6C, PDE6H, POC1B, RAB28, RAX2, RDH5, RPGRIP1, TTLL5</i>
Congenital stationary night blindness, autosomal dominant	None	<i>CACNA1F, RPGR, GNAT1, PDE6B, RHO</i>
Congenital stationary night blindness, autosomal recessive	None	<i>CABP4, GNAT1, GNB3, GPR179, GRK1, GRM6, LRIT3, RDH5, SAG, SLC24A1, TRPM1</i>
Congenital stationary night blindness, X-linked	None	<i>CACNA1F, NYX</i>
Deafness, alone or syndromic, autosomal dominant	None	<i>ESPN, WFS1</i>
Deafness, alone or syndromic, autosomal recessive	None	<i>CDH23, CIB2, DFNB31, MYO7A, PCDH15, PDZD7, USH1C</i>
Leber congenital amaurosis, autosomal dominant	None	<i>CRX, IMPDH1, OTX2</i>
Leber congenital amaurosis, autosomal recessive	None	<i>AIPL1, CABP4, CCT2, CEP290, CLUAP1, CRB1, CRX, DTHD1, GDF6, GUCY2D, IFT140, IQCB1, KCNJ13, LCAS5, LRAT, NMNAT1, PRPH2, RD3, RDH12, RPPE65, RPGRIP1, SPATA7, TULP1</i>
Macular degeneration, autosomal dominant	<i>BCAMD, MCDR3, MCDR4, MCDR5, MDDC</i>	<i>BEST1, C1QTNF5, CTNNNA1, EFEMP1, ELavl4, FSCN2, GUCA1B, HMGN1, IMPG1, OTX2, PRDM13, PROM1, PRPH2, RP1L1, TIMP3</i>
Macular degeneration, autosomal recessive	None	<i>ABCA4, CFH, DRAV2, IMPG1, MFSD8</i>
Macular degeneration, X-linked	None	<i>RPGR</i>
Ocular-retinal developmental disease, autosomal dominant	None	<i>VCAN</i>
Optic atrophy, autosomal dominant	<i>OPA4, OPA5, OPA8</i>	<i>AFG3L2, MFN2, NR2F1, OPA1</i>
Optic atrophy, autosomal recessive	<i>OPA6</i>	<i>ACO2, NBAS, RTN4IP1, TMEM126A</i>
Optic atrophy, X-linked	<i>OPA2</i>	<i>TMM8A</i>

Retinitis pigmentosa, autosomal dominant	<i>RP63</i>	<i>ADIPOR1, ARL3, BEST1, CA4, CRX, FSCN2, GUCA1B, HK1, IMPDH1, IMPG1, KLHL7, NR2E3, NRL, PRPF3, PRPF4, PRPF6, PRPF8, PRPF31, PRPH2, RDH12, RHO, ROM1, RP1, RP9, RPE65, SAG, SEMA4A, SNRNP200, SPP2, TOPORS</i>
Retinitis pigmentosa, autosomal recessive	<i>RP22, RP29</i>	<i>ABCA4, AGBL5, AHR, ARHGEF18, ARL6, ARL2BP, BBS1, BBS2, BEST1, C2orf71, C8orf37, CERKL, CLCC1, CLRN1, CNGA1, CNGB1, CRB1, CYP4V2, DHDDS, DHX38, EMC1, EYS, FAM161A, GPR125, HGSNAT, IDH3B, IFT140, IFT172, IMPG2, KIAA1549, KIZ, LRAT, MAK, MERTK, MVK, NEK2, NEUROD1, NR2E3, NRL, PDE6A, PDE6B, PDE6G, POMGNT1, PRCD, PROM1, RBP3, REEP6, RGR, RHO, RIBP1, RP1, RP1L1, RPE65, SAG, SAMD11, SLC7A14, SPATA7, TRNT1, TTC8, TULP1, USH2A, ZNF408, ZNF513</i>
Retinitis pigmentosa, X-linked Syndromic/systemic diseases with retinopathy, autosomal dominant	<i>RP6, RP24, RP34</i>	<i>OFD1, RP2, RPGR</i>
Syndromic/systemic diseases with retinopathy, autosomal recessive	<i>CORD1</i>	<i>ABCC6, AFG3L2, ATXN7Z, COL11A1, COL2A1, JAG1, KCNJ13, KIF11, MFN2, OPA3, PAZ2, TREX1, VCAN</i>
Syndromic/systemic diseases with retinopathy, autosomal recessive	<i>FHASD, MRST, WFS2</i>	<i>ABCC6, ABHD12, ACBD5, ACO2, ADAMTS18, ADIPOR1, AFG3L2, AH11, ALMS1, CC2D2A, CEP164, CEP290, CLN3, COL9A1, CSPPP1, ELOVL4, EXOSC2, FLVCR1, GNPTG, HARS, HGSNAT, HMX1, IFT140, IFT81, INPP5E, INV/S, IQCB1, LAMA1, LRP5, MKS1, MTTP, NPHP1, NPHP3, NPHP4, OPA3, PANK2, PCYT1A, PEX1, PEX2, PEX7, PHYH, PLK4, PNPLA6, POC5, POC1B, PRPS1, RDH11, RPRGP1L, SDCCAG8, SLC25A46, TMEM216, TMEM237, TRNT1, TTPA, TUB, TUBGCP4, TUBGCP6, WDPCP, WDR19, WFS1, ZNF423</i>
Syndromic/systemic diseases with retinopathy, X-linked	<i>OFD1, TIMM8A</i>	<i>ABHD12, ADGRV1, ARSG, CDH23, CEP78, CEP250, CIB2, CLRN1, DFNB31, ESPN, HARS, MYO7A, PCDH15, USH1C, USH1G, USH2A, BEST1, CAPN5, CRB1, ELOVL1, FZD4, ITM2B, LRP5, MAPKAPK3, MIR204, OPN1SW, RB1, RCBTB1, TSPAN12, ZNF408</i>
Usher syndrome, autosomal recessive		<i>ASRG1, BEST1, C12orf65, CDH3, CNGA3, CNGB3, CNNM4, CYP4V2, LRP5, MFRP, MVK, NBAS, NR2E3, OAT, PLA2G5, PROM1, RBP4, RCBTB1, RGSG9, RGSG9BP, RLBP1</i>
Other retinopathy, autosomal dominant	<i>CACD, CODA1, EVR3, MCDR4</i>	<i>KSS, LHON, MT-ATP6, MT-TH, MT-TL1, MT-TP, MT-TS2</i>
Other retinopathy, autosomal recessive	<i>RNANC, VRD1</i>	<i>CACNA1F, CHM, DMD, NDP, OPN1LW, OPN1MW, PGK1, RS1</i>
Other retinopathy, mitochondrial		
Other retinopathy, X-linked	<i>None</i>	
	<i>PRD</i>	

Modified from *Gene and Locus Symbols by Disease Category (One or More Diseases per Gene/Locus)*, RetNet (Retinal Information Network) website; <https://sph.uth.edu/retnet/sum-dis.htm#B-diseases>. Accessed July 22, 2020. Courtesy of Stephen P. Daiger, PhD, the University of Texas Health Science Center at Houston; and the Foundation Fighting Blindness.

Note: Diseases and genes in boldface represent targets of gene therapy (either completed or in clinical trials). www.clinicaltrials.gov. Accessed July 23, 2020.

OMIM, Online Mendelian Inheritance in Man website. www.omim.org. Accessed July 25, 2020.

RetNet, Retinal Information Network website. <https://sph.uth.edu/retnet/>. Accessed July 25, 2020.

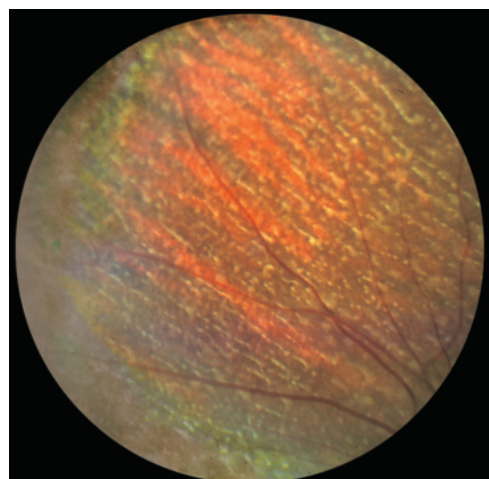
General Diagnostic Considerations

Heredity diseases of the eye have bilateral symmetric involvement, with rare exceptions. If ocular involvement is unilateral, other causes—such as birth defects, intrauterine or antenatal infections, or inflammatory diseases—should be considered. Because retinal degenerations can also occur as part of a systemic disorder, obtaining a thorough medical history is crucial (see Chapter 14), as is ruling out any reversible or treatable cause of retinal dysfunction, such as vitamin A deficiency, autoimmune disorders, or paraneoplastic or infectious retinopathy.

Clinical diagnostic evaluation, assessment of disease severity, and monitoring the progression of chorioretinal dystrophies usually involve some combination of electroretinography, fundus autofluorescence, optical coherence tomography (OCT), and perimetric testing. Several photoreceptor dystrophies have typical phenotypes, such as the deep retinal white dots or flecks in *retinitis punctata albescens* (Fig 13-1), choriocapillaris atrophy in *choroideremia* (CHM), retinal thickening and loss of laminations resulting from mutations in *CRB1*, crystalline deposits associated with *Bietti crystalline dystrophy* (*CYP4V2*), or the preserved para-arteriolar RPE in *CRB1*-related retinopathy. Distinctive phenotypes are the exception, however, and in most cases of photoreceptor dystrophy, there are diffuse pigment epithelial changes that are secondary effects of the diffuse photoreceptor degeneration.

Generally, panretinal dystrophies or degenerations of the RPE and retina are divided into 2 groups: (1) nonsyndromic retinopathies and (2) syndromic retinopathies. The term *nonsyndromic panretinal dystrophies* refers to hereditary disorders that diffusely involve

Figure 13-1 Color fundus photograph of a patient with *retinitis punctata albescens*, showing numerous deep retinal white dots.
(Courtesy of John R. Heckenlively, MD.)



photoreceptor and pigment epithelial function; these conditions are characterized by progressive visual field loss, central vision loss, and abnormal electroretinogram (ERG) responses. The disease process is confined to the eyes and is not associated with other systemic manifestations. In *syndromic (secondary) panretinal dystrophies*, the retinal degeneration is associated with single- or multiple-organ system disease, such as hearing loss (Usher syndrome) or multisystem disorders (see Chapter 14). Occasionally, when the etiology is unknown and no associated disease is present, the term *pigmentary retinopathy* is used to describe the disorder.

General Genetic Considerations

All inheritance patterns are represented among currently known inherited retinal dystrophies. Thus, obtaining an accurate and complete family history is essential in determining the dystrophy's inheritance pattern (ie, autosomal dominant, autosomal recessive, X-linked recessive, X-linked dominant, or mitochondrial). However, patients with retinal dystrophies may have a negative family history for a variety of reasons, including lack of information, variable expressivity and/or incomplete penetrance within the family, or de novo mutations. It is helpful to examine relatives for any signs of asymptomatic retinal degeneration.

Molecular genetic testing can help establish an inheritance pattern; de novo mutations in X-linked and autosomal dominant genes can be occasionally observed in sporadic rod–cone or cone dystrophy cases. The expression of these disorders can vary widely even within family members that share the same causative mutations. Molecular genetic testing helps differentiate the specific causative genes within this phenotypic group; it can be useful for family planning purposes because of the multiple possible inheritance patterns.

Genes that were previously thought to only give rise to stationary conditions, such as congenital stationary night blindness and achromatopsias, have since been linked to some progressive cases. In some cases, both dominant and recessive forms have been seen, resulting from mutations in the same gene. Molecular genetic testing is also useful for identifying syndromic versus nonsyndromic causes of retinal dystrophies, but it does not predict the penetrance, expressivity, and/or rate of progression of these conditions. Testing in asymptomatic individuals to determine a potential future risk of vision loss is generally not warranted (unless a treatment is available). Clinicians can consult the American Academy of Ophthalmology's guidelines for genetic testing and consider the use of genetic counseling services when offering testing to their patients and family members.

Stone EM, Aldave AJ, Drack AV, et al. Recommendations for genetic testing of inherited eye diseases: report of the American Academy of Ophthalmology task force on genetic testing. *Ophthalmology*. 2012;119(11):2408–2410.

General Management Considerations

Management of patients with retinal degeneration should include ophthalmic evaluations every 1–2 years. Follow-up visits are appropriate to address refractive management and monitor for the development of cystoid macular edema (CME), cataract, glaucoma,

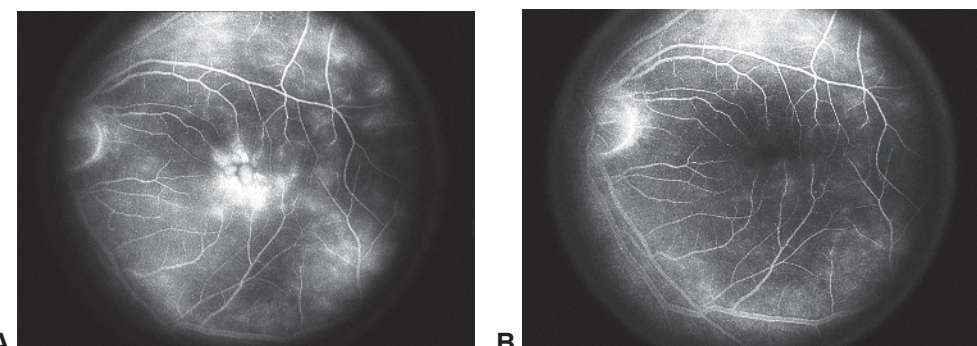


Figure 13-2 Cystoid macular edema (CME) responsive to treatment in inherited retinal dystrophies. **A**, Fluorescein angiography image shows dye leakage. **B**, Eye of the same patient after 2 weeks of treatment with oral acetazolamide. CME related to inherited retinal dystrophies is not always evident on angiography. (*Courtesy of Michael F. Marmor, MD.*)

and retinal exudation. CME, which develops in 10%–20% of patients with retinal degenerations, especially retinitis pigmentosa, can be managed in a subset of these patients with oral and/or topical carbonic anhydrase inhibitors, such as acetazolamide (Fig 13-2) or with periocular or intravitreal steroids. Cataract surgery has a higher complication rate in part due to zonular instability. Following surgery, posterior capsular opacification and CME are more common. Assessment of optic nerve for the development of glaucoma or optic nerve head drusen (common in retinitis pigmentosa) is important. Approximately 2%–5% of patients with panretinal dystrophies will develop areas of an acquired Coats reaction (ie, hyperpermeability and exudation of the retinal vessels, which can lead to exudative retinal detachments). These areas require treatment to preserve vision.

Patients with retinal dystrophies may understandably fear that they will become blind in the near future. The clinician should help these patients understand that total blindness is an infrequent endpoint, but also that the diseases' impact on visual function (eg, reduced visual acuity, reduced visual field) may affect their activities and quality of life. The clinician should also explain that while most patients retain vision for decades, the progression of this condition is variable, and that it is possible to adapt to the various aspects of vision loss. Patients and their family members often experience guilt or fear of passing on the condition to their progeny; they may benefit from psychological and genetic counseling. Patients with subnormal visual acuity may benefit from low-vision aids, while patients with advanced disease may need vocational rehabilitation and mobility training. The clinician should refer patients for these services before the patients are seriously limited by vision loss. To learn about the American Academy of Ophthalmology's Initiative in Vision Rehabilitation and obtain a patient handout, visit the Low Vision and Vision Rehabilitation page on the ONE Network at www.aao.org/low-vision-and-vision-rehab.

Stem cell and gene therapies are being developed to modify the natural history of retinal and chorioretinal degenerations, or even to restore function already lost.

Diffuse Dystrophies

Diffuse Photoreceptor Dystrophies

Rod–cone dystrophies (*retinitis pigmentosa*)

Patients with rod–cone dystrophies, usually referred to as *retinitis pigmentosa* (RP)—a term no longer preferred but still widely used—often present with history of nyctalopia (night blindness) and reports of vision changes that relate to visual field loss. The history may not be clear; patients may assume that their visual function is normal, because it is “normal” for them not to be able to see in the dark. It is important to ask the patient (and family members, in some instances) questions that properly assess them for vision dysfunction. Typical fundus findings in RP include arteriolar narrowing, with or without optic nerve head pallor, and variable amounts of bone spicule–like pigment changes resulting from intraretinal pigment deposition by macrophages that migrate into the retina to process degenerating retinal cells (Fig 13-3). This form of pigment deposition within the retina occurs in regions of outer retinal atrophy (eg, following retinal detachment or inflammatory retinopathies) and is not specific to hereditary retinopathies. The peripheral retina and RPE may be atrophic even if intraretinal pigment is absent (*RP sine pigmento*), and the macula typically shows a loss of the foveal reflex and irregularity of the vitreoretinal interface. Autofluorescence imaging can often identify additional areas of retinal involvement that are not evident on clinical examination. Vitreous cells, CME, epiretinal membranes, optic nerve drusen, and posterior subcapsular cataracts are commonly observed in eyes with panretinal dystrophies (Fig 13-4). Eyes with rod–cone degenerations typically develop partial- to full-ring scotomas in midequatorial regions; these often expand into the periphery, leaving only a small central island of visual field (Fig 13-5).

The ERG response in eyes with rod–cone dystrophies typically shows a loss or a marked reduction in rod-derived responses, more than in cone-derived responses. Both a- and b-waves are reduced because the photoreceptors are primarily involved. The b-waves are characteristically prolonged in time as well as diminished in amplitude. Individuals with the carrier state of X-linked recessive RP often show a mild reduction or delay in b-wave responses. Eyes with postinflammatory retinopathies (eg, retinopathies resulting from rubella) often have better preservation of the ERG than eyes with comparably appearing pigmentary changes from a hereditary retinopathy. In these cases, although the rod and cone amplitudes are reduced, the implicit times are usually within normal ranges, because the remaining photoreceptors are essentially normal. In contrast, in patients with a hereditary retinopathy, the remaining photoreceptors are impaired by the genetic condition and the ERG response shows prolonged implicit times. In *conventional testing* of many rod–cone dystrophies, the ERG responses may initially present as undetectable or become undetectable over time. An undetectable ERG signal is not diagnostic; while it represents severe retinal dysfunction, it doesn’t necessarily correlate to the patient’s level of visual function. Unless the patient has a treatable condition, such as vitamin A deficiency or an autoimmune retinopathy, repetitive ERG testing has minimal benefit for monitoring disease progression.

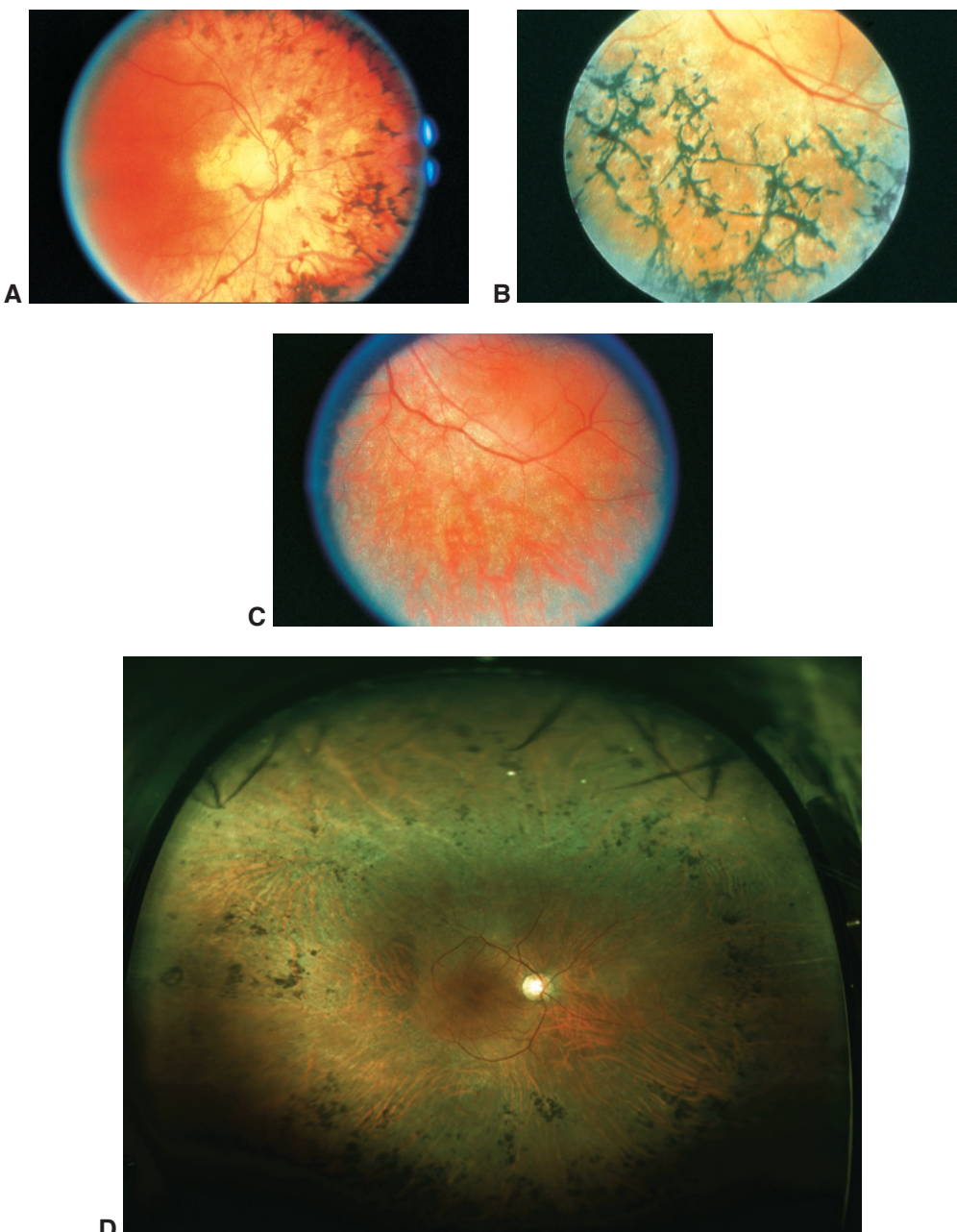


Figure 13-3 Different fundus photographic appearances in retinitis pigmentosa (RP). **A**, Posterior fundus, showing arteriolar attenuation and a dull macula. **B**, Fundus with dense, peripheral intraretinal pigmentary changes. **C**, Fundus shows peripheral atrophy but virtually no intraretinal pigment. **D**, Ultra-wide-angle fundus image of a patient with RP. Extensive pigmentary abnormalities, including intraretinal pigment and retinal pigment epithelium (RPE) alterations, are visible. (Parts A and C courtesy of Michael F. Marmor, MD; part B courtesy of Carl D. Regillo, MD; part D courtesy of Colin A. McCannel, MD.)

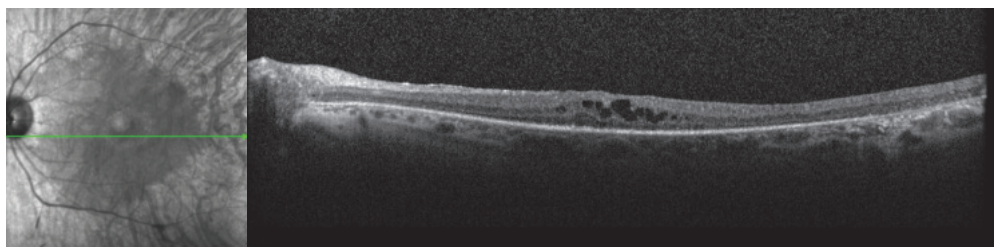


Figure 13-4 Spectral-domain optical coherence tomography (SD-OCT) image of the macula of an eye with RP. Both CME and epiretinal membrane are present. Intraretinal fluid is characteristically present in the inner nuclear layer. Note the absence of any outer segment signal outside of the area of the fovea, as well as the thicker-than-normal appearance of the retinal nerve fiber layer near the optic nerve head. (Courtesy of Michael B. Gorin, MD, PhD.)

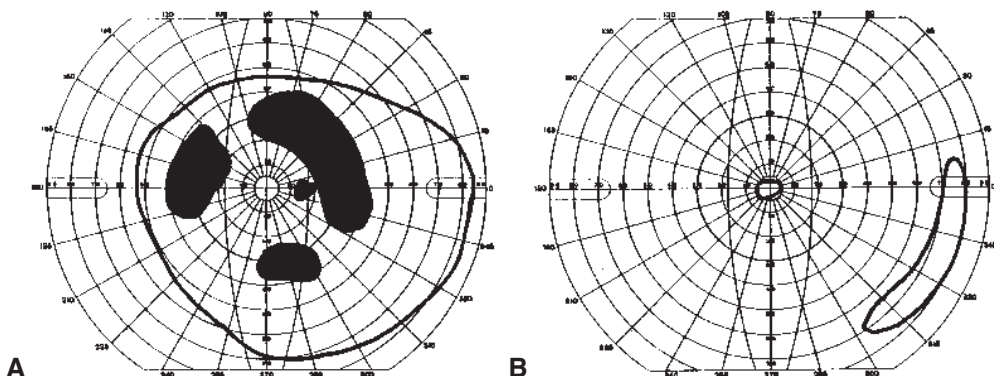


Figure 13-5 Examples of visual fields in RP, obtained with a Goldmann III-4 test object. **A**, Early disease: midperipheral scotomas. **B**, Late disease: severe loss, sparing only a central tunnel and a far-peripheral island, which may eventually disappear. (Courtesy of Michael F. Marmor, MD.)

Sectorial RP refers to disease that involves only 1 or 2 sectors of the fundus. This condition is generally symmetric in both eyes, which helps rule out acquired damage (eg, from trauma, vascular insult, or inflammation) (Fig 13-6). *Unilateral RP* is extremely rare; there has only been a single reported case within a family with a germline mutation. Most cases of unexplained unilateral pigmentary retinopathy are postinflammatory or posttraumatic. Most cases of *pigmented paravenous retinopathy* are postinflammatory, have interocular asymmetry, and are usually nonprogressive.

When evaluating suspected panretinal dystrophy in a patient with a negative family history (*sporadic retinal dystrophy*), it is important to consider acquired causes of retinal degeneration that can mimic hereditary conditions, including previous bilateral ophthalmic artery occlusions, diffuse uveitis, infections (eg, syphilis), paraneoplastic syndromes, and retinal drug toxicity. Syndromic forms of pigmentary retinopathy associated with metabolic or other organ system disease must also be considered (see Chapter 14). Age of onset, pattern of progression, interocular asymmetry, and comorbidities and exposures can help to distinguish these conditions.

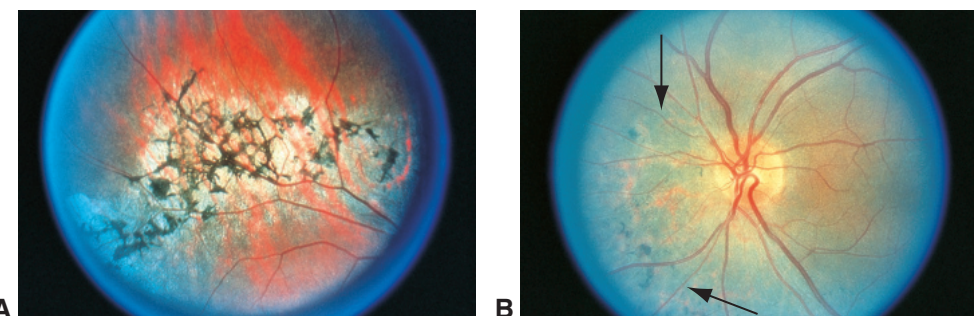


Figure 13-6 Color fundus photographs of delimited forms of inherited retinal dystrophies. Note the sharp demarcation between the areas of degeneration and other regions of the fundus that appear quite healthy. It is important to assess interocular symmetry and the pattern of cell damage to consider acquired forms of retinopathy (such as pigmented paravenous retinopathy). **A**, Fundus with degenerative changes near the arcades. **B**, Fundus with sectorial RP (between arrows), showing vascular narrowing and spicules only in the inferonasal quadrant. (Courtesy of Michael F. Marmor, MD.)

Gregory-Evans K, Pennesi ME, Weleber RG. Retinitis pigmentosa and allied disorders. In: Schachat AP, Wilkinson CP, Hinton DR, Sadda SR, Wiedemann P, eds. *Ryan's Retina*. Vol 2. 6th ed. Philadelphia: Elsevier/Saunders; 2018:861–935.

Management Nutritional supplements have been advocated as therapy for RP. One large study reported that high daily doses of vitamin A palmitate (15,000 IU/day) can slow the decline in ERG response and visual fields in eyes with RP by approximately 20% per year. A slight benefit from omega-3 and omega-6 fatty-acid supplementation has also been reported. The modest benefit of high-dose vitamin A supplementation must be weighed against the risks of long-term liver toxicity, vitamin A-related intracranial hypertension, and teratogenicity.

Excessive light exposure may play a role in retinal degenerations caused by rhodopsin mutations and/or genes that contribute to lipofuscin accumulation, such as *ABCA4*. Recommendations for patients to employ UV-absorbing sunglasses and brimmed hats for protection from high levels of light exposure seem prudent, despite the absence of direct evidence of benefit.

Efforts to restore at least some vision in patients rendered completely blind from RP include the use of electronic chips that interface with the remaining retina tissue. One such device, the Argus II Retinal Prosthesis System (Second Sight Medical Products, Sylmar, California), is now commercially available, and others are in development.

Makiyama Y, Oishi A, Otani A, et al. Prevalence and spatial distribution of cystoid spaces in retinitis pigmentosa: investigation with spectral domain optical coherence tomography. *Retina*. 2014;34(5):981–988.

Salvatore S, Fishman GA, Genead MA. Treatment of cystic macular lesions in hereditary retinal dystrophies. *Surv Ophthalmol*. 2013;58(6):560–584.

Cone and cone–rod dystrophies

Patients with cone dystrophy present with progressive loss of visual acuity and color discrimination, often accompanied by hemeralopia (day blindness) and photophobia (discomfort



Figure 13-7 Color fundus photograph of cone dystrophy, showing the bull's-eye pattern of central atrophy.

and/or pain in the presence of normal levels of light). Onset of symptoms typically occurs in the teenage years or later adulthood. Ophthalmoscopy may be normal early in the course of the disease. Because of this, patients with cone dystrophies may be suspected of malingering. In other patients, ophthalmoscopy may reveal the typical symmetric bull's-eye pattern of macular atrophy (Fig 13-7), or more severe atrophy, such as demarcated circular macular lesions. Mild to severe temporal optic atrophy and tapetal retinal reflexes (with a glistening greenish or golden sheen) may also be present. Unlike macular dystrophies, the cone dystrophies are more associated with color discrimination symptoms and photophobia, and as such, they must be differentiated from color vision defects (see Chapter 12).

When cone dystrophy is suspected, a full-field ERG is the appropriate test. Cone dystrophies are diagnosed when ERG results indicate an abnormal or undetectable photopic ERG response and a normal or near-normal rod-isolated ERG response. When present, the cone flicker ERG response is almost invariably delayed, in keeping with generalized cone-system dysfunction. Peripheral visual fields may remain normal. The cone dystrophies are progressive and are a heterogeneous group of hereditary diseases with more than 25 identified causative genes. In some patients, secondary rod photoreceptor involvement develops in later life, leading to overlap between progressive cone dystrophies and cone–rod dystrophies.

Similar to patients with cone dystrophies, patients with *cone–rod dystrophies* typically present with reduced central visual acuities and symptoms of dyschromatopsia and photophobia. On *visual field testing*, some patients show a tight ring or central scotoma within the central 20° or 30° of the visual field. Ophthalmoscopy may initially be normal; later, it may demonstrate intraretinal pigment in areas of retinal atrophy in the fundus periphery, and patients may report progressive night blindness. The diagnostic hallmark of a cone–rod dystrophy is that the cone-derived full-field ERG responses are more abnormal than the rod ERG responses.

Leber congenital amaurosis

The early-onset retinal dystrophies are collectively termed *Leber congenital amaurosis* (LCA) (also see BCSC Section 6, *Pediatric Ophthalmology and Strabismus*, Chapter 25). LCA is

characterized by severely reduced vision from birth, usually associated with wandering nystagmus. Infants exhibit limited to absolutely no visual responses, and visual acuities tend to range between 20/200 to no light perception (NLP). Some infants with LCA rub or poke their eyes (the *oculodigital reflex*) to create visual stimulation, as do other infants with poor vision.

In the early stages, obvious fundus changes are rare, and molecular genetic testing offers the best method of distinguishing stationary and progressive hereditary retinopathies. In addition, because there are both syndromic and nonsyndromic forms of LCA, a molecular genetic diagnosis can help identify potential systemic features that warrant medical management. Some forms of LCA involve developmental defects, while others appear to represent degenerations of normally formed retina. Postinfectious etiologies should be considered based on clinical history and clinical findings. Central macular atrophic lesions (sometimes incorrectly referred to as macular colobomas) are often seen in eyes with LCA, in addition to early-onset cataracts and keratoconus in older children. Most children with nonsyndromic LCA have normal intelligence, and some of the observed psychomotor impairment may be secondary to sensory deprivation.

The ERG response is typically minimal or undetectable, but ERG testing is not able to establish whether the condition is stationary (congenital stationary night blindness [CSNB] or achromatopsia) or progressive (rod–cone dystrophy or cone–rod dystrophy). OCT can help identify whether the failure of foveal maturation that is associated with ocular albinism and is also detected in dystrophy-related macular edema is present.

Currently, 3 autosomal dominant and 18 recessive mutations that cause LCA have been identified. There is some overlap in the genes responsible for LCA and those that cause later-onset retinal dystrophies (both rod–cone and cone–rod). One form of LCA bearing a mutation in *RPE65* has been treated successfully by gene therapy in clinical trials using an adeno-associated virus. In 2018, the FDA issued the first approval for a gene therapy, Luxturna, for the treatment of this condition in individuals aged 1 year or older.

Enhanced S-cone disease

The most prominent features of enhanced S-cone (or blue-cone; “S” refers to short wavelength) disease (ESCD), also known as Goldmann-Favre syndrome, include night blindness, increased sensitivity to blue light, pigmentary retinal degeneration, an optically empty vitreous, hyperopia, pathognomonic ERG abnormalities, and varying degrees of peripheral to midperipheral visual field loss (Fig 13-8). The posterior pole may show round, yellow, sheenlike lesions along the arcades, accompanied by areas of diffuse degeneration. Deep nummular pigmentary deposition is usually observed at the level of the RPE around the vascular arcades. Macular (and sometimes peripheral) schisis may be present, overlapping the phenotype of X-linked retinoschisis. The ERG response includes no detectable dim-flash, rod-specific signal; delayed and simplified responses to a brighter flash that have the same waveform under both dark-adapted and light-adapted conditions; and a flicker ERG response of lower amplitude than that of the single-flash photopic a-wave.

In eyes with ESCD there is an overabundance of blue cones, a reduced number of red and green cones, and few, if any, functional rods. This condition is unique in that it is both a developmental and degenerative photoreceptor retinopathy. ESCD is autosomal recessive and results from homozygous or compound heterozygous mutations in *NR2E3*.

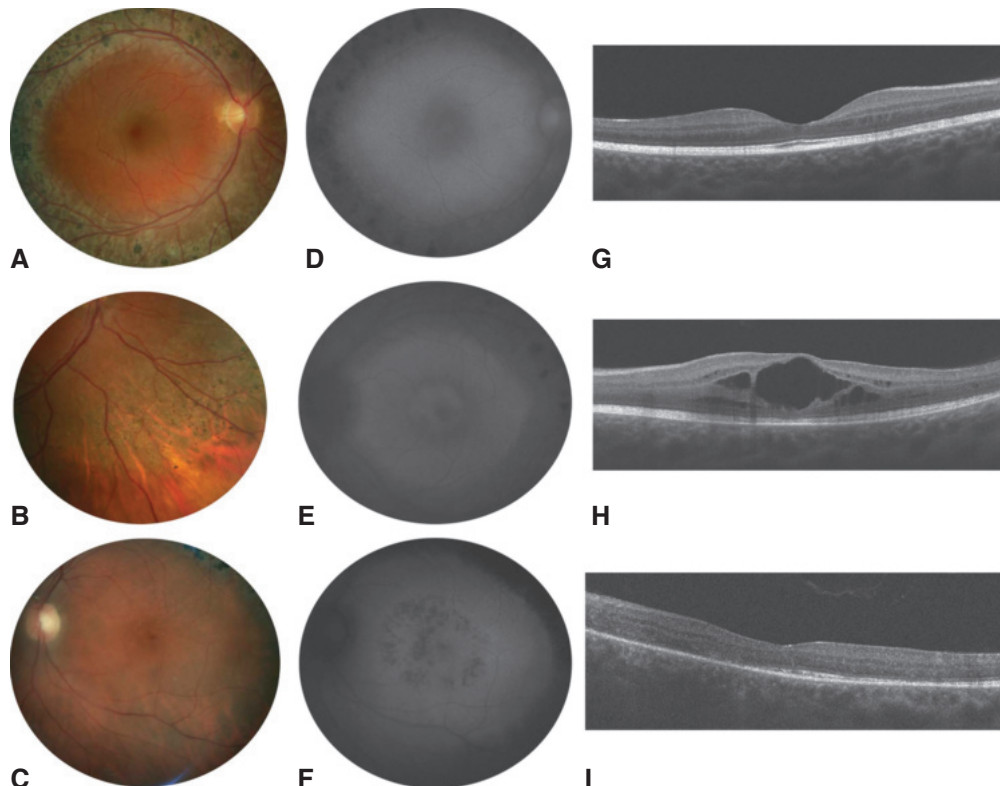


Figure 13-8 Clinical characteristics of enhanced S-cone disease (ESCD). In the early stages, the fundus may be normal. In older subjects, the fundus usually shows 360° nummular pigmentary changes outside the vascular arcades at the level of the RPE (**A–C**). The macula may show changes resulting from schisis or nonspecific pigment epithelial changes (**C**). The autofluorescence is variable (**D–F**). There may be hyperautofluorescence within the arcades that either spares or involves the foveal region. SD-OCT imaging of the macula may be normal (**G**) or show schitic and/or cystoid changes (**H**) or outer retinal abnormalities (**I**). (Used with permission from Vincent A, Robson AG, Holder GE. Pathognomonic (diagnostic) ERGs. A review and update. *Retina*. 2013;33(1):5–12.)

Choroidal Dystrophies

Widespread primary retinal or RPE disease that causes advanced atrophy of the choriocapillaris occurs in choroideremia, gyrate atrophy, Bietti crystalline dystrophy, and phenothiazine-related retinal toxicity (see also Chapter 15). In fundus autofluorescence imaging, hypoautofluorescence in the areas of atrophy is typically observed in all of these conditions and is therefore helpful for monitoring the disease progression.

Choroideremia

Patients with choroideremia have night blindness and show progressive peripheral visual field loss over 3–5 decades. Most patients maintain good visual acuity until a central island of foveal vision is lost. The degeneration initially manifests as mottled areas of pigmentation in the anterior equatorial region and macula. The anterior areas gradually degenerate



Figure 13-9 Fundus photograph of a patient with choroideremia. (From Fishman GA, Birch DG, Holder GE, Brigell MG. Electrophysiologic Testing in Disorders of the Retina, Optic Nerve, and Visual Pathways. 2nd ed. Ophthalmology Monograph 2. San Francisco: American Academy of Ophthalmology; 2001:67.)

to confluent scalloped areas of RPE and choriocapillaris loss; larger choroidal vessels are preserved (Fig 13-9). The retinal vessels also appear normal, and there is no optic atrophy.

On fluorescein angiography imaging, the changes are pronounced: the scalloped areas of missing choriocapillaris appear hypofluorescent next to brightly hyperfluorescent areas of perfused choriocapillaris with intact overlying RPE. Fundus autofluorescence imaging shows a characteristic speckled pattern of autofluorescence in the nonatrophic areas. The ERG response is abnormal early in the course of the disease and is generally extinguished by midlife. Because phenotypes can overlap with other conditions, especially other choroidal dystrophies, the clinical and imaging features should not be considered pathognomonic.

Choroideremia is X-linked and caused by mutations in *CHM*, which is constitutively expressed and encodes geranylgeranyl transferase Rab escort protein. Carriers of choroideremia are usually asymptomatic and have normal ERGs. However, they often show patches of subretinal black mottled pigment, and on occasion, older female carriers show a lobular pattern of choriocapillaris and RPE loss. Gene-therapy trials for choroideremia are ongoing.

Edwards TL, Jolly JK, Groppe M, et al. Visual acuity after retinal gene therapy for choroideremia. *N Engl J Med*. 2016;374(20):1996–1998.

Russell S, Bennett J, Wellman JA, et al. Efficacy and safety of voretigene neparvovec (AAV2-hRPE65v2) in patients with RPE65-mediated inherited retinal dystrophy: a randomised, controlled, open-label, phase 3 trial. *Lancet*. 2017;390(10097):849–860.

Gyrate atrophy

Patients affected by *gyrate atrophy* usually develop night blindness during the first decade of life, and experience progressive loss of visual field and visual acuity later in the course of the disease. Macular edema is commonly present. In the early stages of the disease,



Figure 13-10 Gyrate atrophy. Wide-angle color fundus photograph shows scalloped edges of the remaining posterior retina, as is typically seen in gyrate atrophy. A crescent of nasal macular atrophy is also present. (Courtesy of Colin A. McCannel, MD.)

patients have large, geographic, peripheral paving-stone-like areas of atrophy of the RPE and choriocapillaris, which gradually coalesce to form a characteristic scalloped border at the junction of normal and abnormal RPE (Fig 13-10). Gyrate atrophy is an autosomal recessive dystrophy caused by mutations in the gene for ornithine aminotransferase (*OAT*). The diagnosis is supported by elevated plasma levels of ornithine. If started at a young age, aggressive dietary restriction of arginine intake and, in some cases, vitamin B6 supplementation can slow or halt progression of the retinal degeneration. The clinical diagnosis can be confirmed by measuring elevated serum or plasma ornithine levels as well as by genetic testing for mutations of *OAT*.

Bietti crystalline dystrophy

Individuals with Bietti crystalline dystrophy develop symptoms of nyctalopia, decreased vision, and paracentral scotomas in the second to fourth decades. On examination, intraretinal yellow-white crystals are visible in the posterior retina and in the peripheral cornea near the limbus. As the disease progresses, widespread retinochoroidal atrophy develops and peripheral vision worsens. In eyes with advanced disease, the intraretinal crystals may not be evident. This condition is a very rare, autosomal recessive disorder caused by mutations in the gene *CYP4V2*. There is no known treatment.

Macular Dystrophies

Stargardt Disease

Stargardt disease is the most common juvenile macular dystrophy and a common cause of central vision loss in adults younger than 50 years. The visual acuity in Stargardt disease typically ranges from 20/50 to 20/200.

The classic Stargardt phenotype is characterized by a juvenile-onset foveal atrophy surrounded by discrete, yellowish, round or pisciform flecks at the level of the RPE (Fig 13-11A). If the flecks are widely scattered throughout the fundus with central sparing, the condition, which used to be referred to as *fundus flavimaculatus*, is now known to result from mutations in the same genes and can be present in families with the classic Stargardt phenotype. On fluorescein angiography, 80% or more of patients with Stargardt

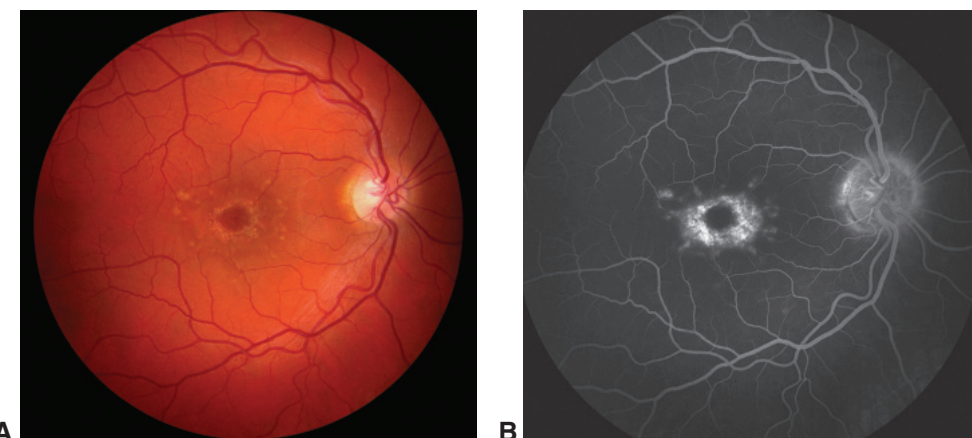


Figure 13-11 Stargardt disease. **A**, Color fundus photograph shows paramacular yellowish flecks and “beaten-bronze” central macular atrophy. **B**, Fluorescein angiography image of the same eye shows a dark choroid, hyperfluorescence associated with flecks, and bull’s-eye pattern of macular transmission defect. (Courtesy of Mark W. Johnson, MD.)

disease have a “dark choroid,” or, in other words, blocking of choroidal fluorescence that highlights the retinal circulation (Fig 13-11B). Fundus autofluorescence imaging is a more reliable means of demonstrating elevated background autofluorescence and characteristic findings, including peripapillary sparing of the RPE changes, central macular hypoautofluorescence, and, over time, an outward expanding pattern of hyperautofluorescent flecks, which leave hypoautofluorescent areas in their wake. Full-field ERGs are not diagnostic for this condition; however, individuals with significantly abnormal responses generally have more severe and progressive disease.

The age of onset and presentation of the clinical features in Stargardt disease varies, sometimes even among individuals within the same family. The condition is usually slowly progressive with the accumulation of lipofuscin-like material in the RPE (Fig 13-12). Once the central vision is involved, the loss of visual acuity can be relatively rapid, over months to a few years, and then plateaus. However, if the central fovea area is spared, it is not unusual for a patient to be unaware that they are affected until adulthood. In later stages,

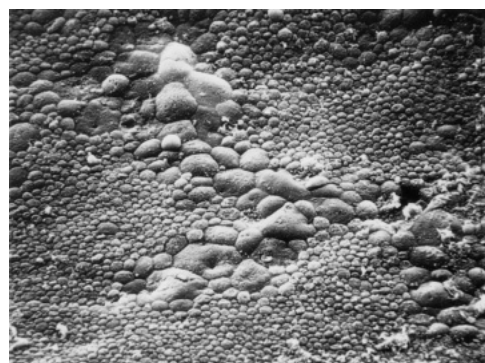


Figure 13-12 Scanning electron micrograph of the RPE in Stargardt disease. The flecks represent regions of RPE cells engorged with abnormal lipofuscin-like material. (From Eagle RC Jr, Lucier AC, Bernardino VB Jr, Yanoff M. Retinal pigment epithelial abnormalities in fundus flavimaculatus: a light and electron microscopic study. Ophthalmology. 1980;87(12):1189–1200.)

atrophic maculopathy, with or without lipofuscin flecks and panretinal degeneration, can be observed.

The majority of cases of Stargardt disease are autosomal recessive and are due to mutations in the *ABCA4* gene. However, autosomal dominant transmission patterns can result from mutations in other genes, most notably *PRPH2*. The *ABCA4* gene encodes an adenosine triphosphate (ATP)-binding cassette (ABC) transporter protein expressed by rod outer segments and RPE. See Table 13-1 for a list of additional genetic causes. Based on animal models of *ABCA4*-related disease, vitamin A supplementation accelerates the accumulation of lipofuscin pigments in the RPE and, in conjunction with blue light, also accelerates retinal cell death. Drug therapies to reduce lipofuscin accumulation, gene therapies, and stem cell treatments are currently undergoing clinical trials.

Best Disease or Best Vitelliform Dystrophy

Individuals affected by Best disease frequently develop a yellow, egg yolk–like (vitelliform) macular lesion in childhood, which eventually breaks down, leaving a mottled geographic atrophic appearance (Fig 13-13). Late in the course of the disease, the geographic atrophy may be difficult to distinguish from other types of macular degeneration or dystrophy. Some patients (up to 30% in some series) have extrafoveal vitelliform lesions in the fundus. The macular appearance in all stages is deceptive, as most patients maintain relatively good visual acuity throughout the course of the disease. Even patients with “scrambled-egg” macular lesions typically have visual acuities from 20/30 to 20/60. In approximately 20% of patients, a choroidal neovascular membrane develops in at least 1 eye during the course of the disease and, if untreated, may result in poor vision.

The ERG response is characteristically normal, but the electro-oculogram (EOG) result is almost always abnormal, even in “unaffected,” asymptomatic individuals who have the causative genetic variant but have normal-appearing fundi. The light rise of the EOG (see Chapter 3) is typically severely reduced or absent. Before ordering an EOG to rule out Best disease, clinicians should ensure that the full-field ERG is normal. Molecular genetic studies are more sensitive in detecting carriers than electrophysiologic testing is. In addition to incomplete penetrance, there is also variable expressivity, and some cases may show multifocal vitelliform lesions rather than a single subfoveal lesion.

Best disease is an autosomal dominant maculopathy caused by mutations in the *BEST1* gene (*VMD2*). The encoded protein bestrophin localizes to the basolateral plasma membrane of the RPE and functions as a transmembrane ion channel. Although some *BEST1* variants will cause autosomal dominant disease, other mutations, when present as homozygous or compound heterozygous variants, can give rise to autosomal recessive bestrophinopathy (ARB). Unlike Best disease, ARB is associated with progressive retinal dysfunction on the full-field ERG, loss of visual acuity, diffuse irregularity of the RPE, and dispersed punctate flecks, which are distinct from extramacular vitelliform lesions.

Agarwal A. *Gass' Atlas of Macular Diseases*. 5th ed. Philadelphia: Saunders; 2012:278–280.

Boon CJ, Klevering BJ, Leroy BP, Hoyng CB, Keunen JE, den Hollander AJ. The spectrum of ocular phenotypes caused by mutations in the *BEST1* gene. *Prog Retin Eye Res*. 2009;28(3):187–205.

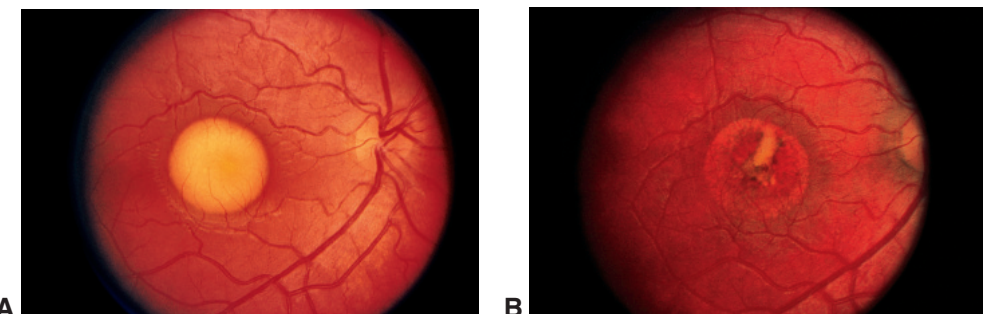


Figure 13-13 Color fundus photographs of Best vitelliform dystrophy. **A**, Characteristic “yolk” stage, during which visual acuity is typically good. **B**, Atrophy and scarring after the yolk breaks down. (Courtesy of Mark W. Johnson, MD.)

Adult-Onset Vitelliform Lesions

Several types of symmetric yellow deposits that resemble Best disease may develop in the macula of older adults. The most common disorder, *adult-onset foveomacular vitelliform dystrophy*, is one of the *pattern dystrophies* (discussed later in this chapter). It is characterized by yellow subfoveal lesions that are bilateral, round or oval, and typically one-third disc diameter in size; they often contain a central pigmented spot (Fig 13-14). Occasionally, when the lesions are larger, they may be misdiagnosed as Best disease or even as age-related macular degeneration (AMD). This dystrophy generally appears in the fourth to sixth decades in patients who either are visually asymptomatic or have mild blurring and metamorphopsia. Eventually, the lesions may fade, leaving an area of RPE atrophy, but most patients retain reading vision in at least 1 eye throughout their lives. Autosomal dominant inheritance has been recognized in some affected families. The most common causative gene is *PRPH2*, and there is evidence of genetic heterogeneity for this phenotype. In some cases of post-surgical CME, acute onset of foveomacular subretinal deposits in the absence of drusen or intraretinal fluid have been seen; these respond well to standard therapy.

Patients with numerous basal laminar (cuticular) drusen may develop an unusual *vitelliform exudative macular detachment* (Fig 13-15). The yellowish subretinal fluid blocks background fluorescence early, often stains late in the angiogram study, and may be mistaken for choroidal neovascularization. Patients with yellowish macular detachments often maintain good visual acuity for many months but may eventually lose central vision because of geographic atrophy or choroidal neovascularization and disciform scarring.

In some patients with large, soft drusen, there is a large, central coalescence of drusen, or *drusenoid RPE detachment*, which may occasionally mimic a macular vitelliform lesion (Fig 13-16). Such lesions often have pigment mottling on their surface and are surrounded by numerous other individual or confluent soft drusen. They may remain stable (and allow for good vision) for many years, but eventually they tend to flatten and evolve into geographic atrophy.

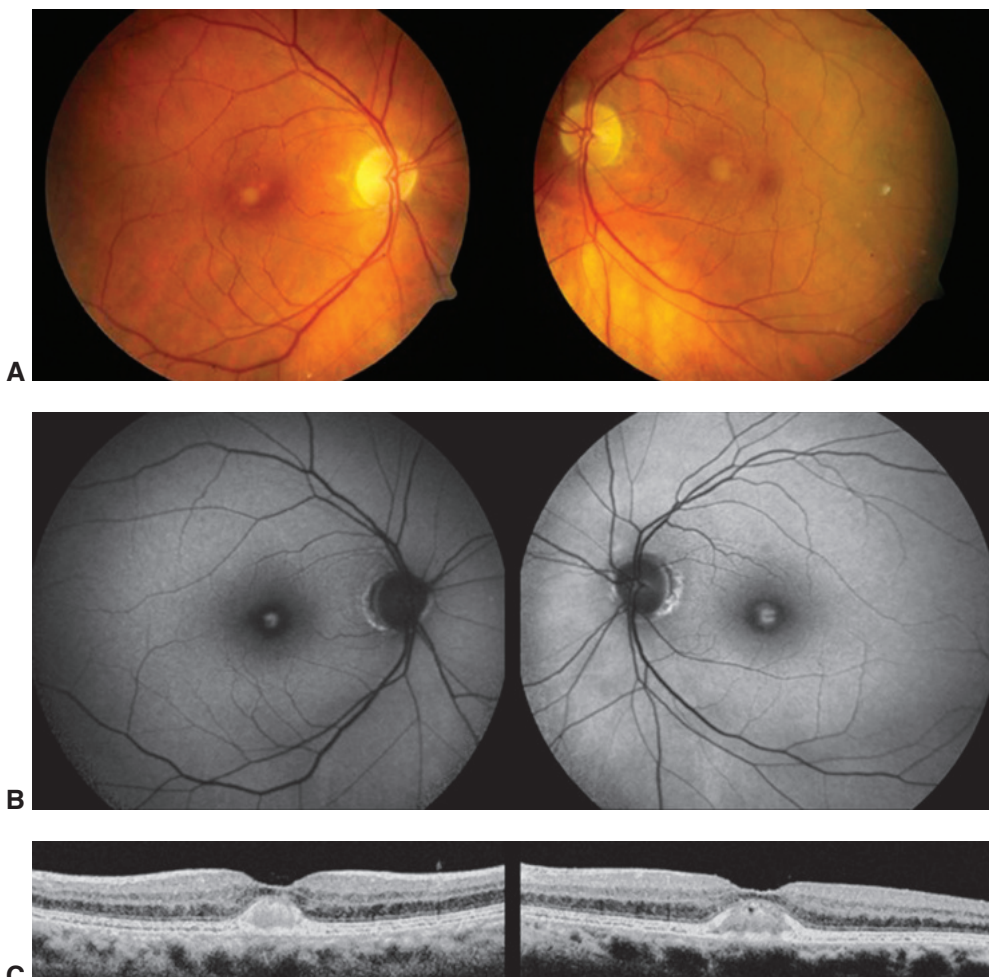


Figure 13-14 Adult-onset foveomacular vitelliform dystrophy. Left panels in each part are images of the right eye, and right panels are images of the left eye of the same patient. **A**, Color fundus photographs demonstrate small, round, yellow subfoveal lesions. **B**, These lesions show hyperautofluorescence on autofluorescence imaging. **C**, SD-OCT images show the reflective, dome-shaped subfoveal material elevating the overlying neurosensory retina. (Courtesy of Stephen J. Kim, MD.)

Early-Onset “Drusenoid” Macular Dystrophies

Early-onset drusen typically manifests at younger ages than do drusen in most cases of AMD. Though they are frequently referred to as “familial or autosomal dominant drusen,” the clinician needs to establish whether other family members are affected before assuming an inheritance pattern. In addition, although early-onset drusen are presumed to be genetically determined, the inheritance pattern in the majority of young patients is never established; many cases may be multigenic and related to the same pathways that give rise to AMD.

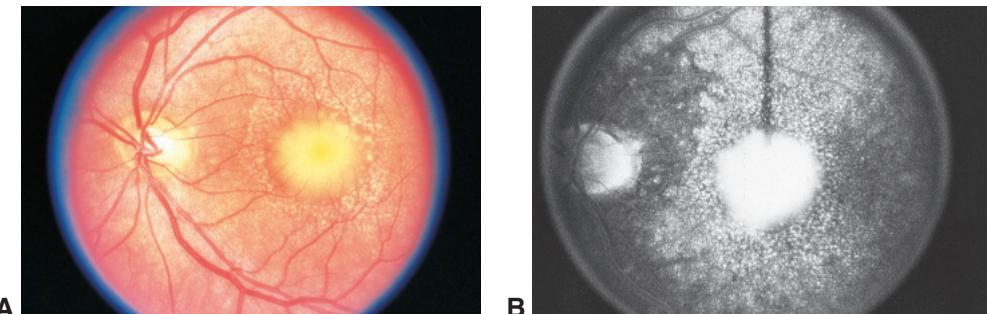


Figure 13-15 Vitelliform exudative macular detachment. **A**, Color fundus photograph of a vitelliform lesion in the setting of numerous cuticular (basal laminar) drusen. **B**, Corresponding late-phase fluorescein angiography image shows staining of drusen and vitelliform lesion. (Courtesy of Michael F. Marmor, MD.)

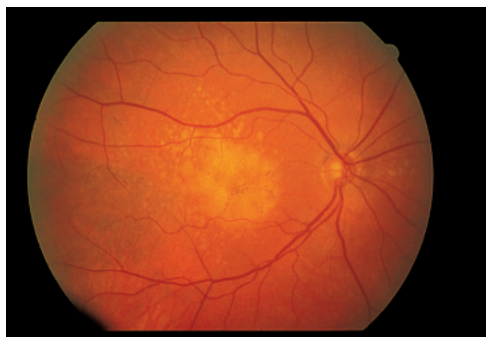


Figure 13-16 Color fundus photograph shows central coalescence of large drusen simulating a macular vitelliform lesion. (Courtesy of Mark W. Johnson, MD.)

Drusen are usually numerous and vary in size, typically extending beyond the vascular arcades and nasal to the optic nerve head (Fig 13-17). Early-onset drusen have been classified into 3 entities: (1) large colloid drusen, (2) Malattia Leventinese, and (3) cuticular drusen (Fig 13-18). On fundus examination, *large colloid drusen* appear as large, yellowish, and bilateral lesions located in the macula and/or the periphery of the retina. The vitelliform lesions are hyperautofluorescent and are thought to be made up of lipofuscin,

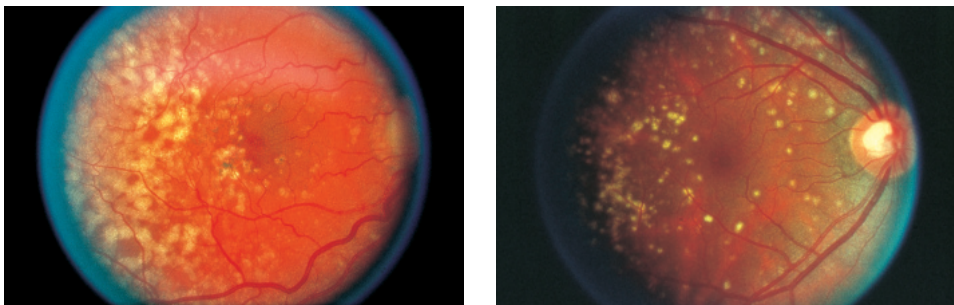


Figure 13-17 Color fundus photographs of different manifestations of early-onset drusen. Variable size and distribution of the drusen are evident. (Courtesy of Michael F. Marmor, MD.)

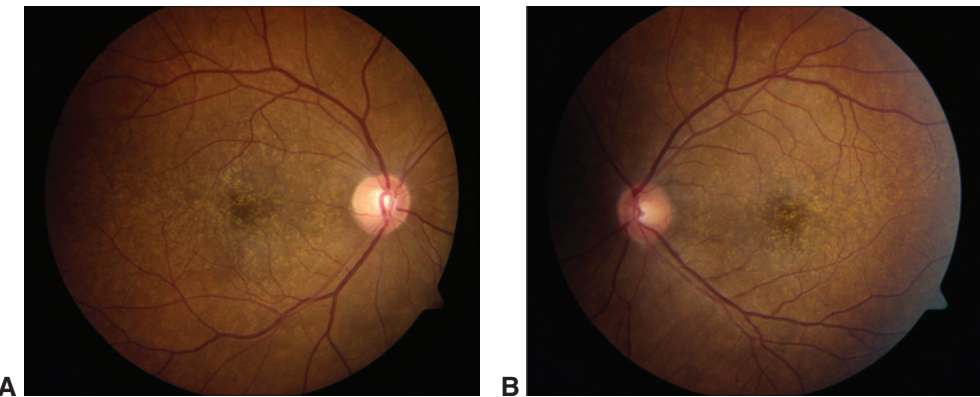


Figure 13-18 Basal laminar (cuticular) drusen. Color fundus photographs of the left (**A**) and right (**B**) eyes of a 38-year-old man with numerous round, yellow drusen scattered in the macula. Basal laminar (cuticular) drusen result from nodular thickening of the basement membrane of the RPE and are more easily seen on angiography and in young patients with brunette fundi. (Courtesy of Stephen J. Kim, MD.)

while the associated surrounding cuticular drusen and/or subretinal drusenoid deposits are generally not autofluorescent. *Malattia Leventinese* and *Doyne honeycomb dystrophy* are essentially the same condition and often show a distinctive pattern of radial extensions of small and intermediate-sized deposits emanating from the fovea. The condition is caused by a shared single autosomal dominant mutation in the gene *EFEMP1*, which to date has not been associated with AMD risk. However, the causative genes in several juvenile and early-onset macular dystrophies are the same as the genes that have been implicated in the complex genetic disorder of AMD.

Sorsby macular dystrophy (SMD), a dominantly inherited disease resulting from *TIMP3* mutations, involves the development of bilateral, subfoveal, choroidal neovascular lesions at approximately 40 years of age (Fig 13-19). As the macular lesions evolve, they take on the appearance of geographic atrophy, with pronounced clumps of black pigmentation around the central ischemic and atrophic zone (a pseudoinflammatory appearance). An early sign of the disease is the presence of numerous fine drusenlike

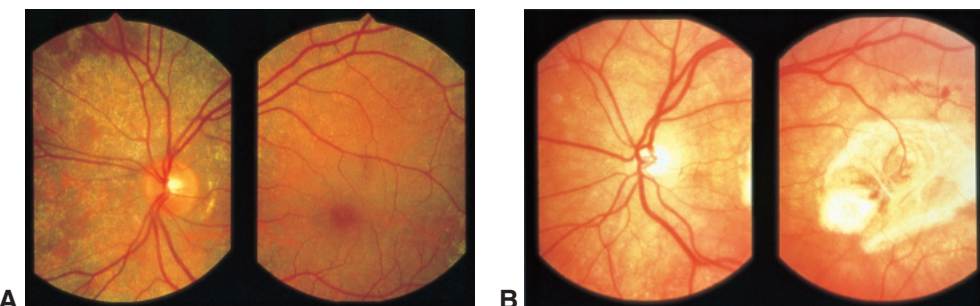


Figure 13-19 Color fundus photographs of Sorsby macular dystrophy. **A**, Characteristic pale drusen. **B**, Late disciform scarring after the development of choroidal neovascularization. (Courtesy of Alan Bird, MD.)

deposits or a confluent plaque of faintly yellow material beneath the RPE of the posterior pole. Both common and rare variants of *TIMP3* have been implicated in the pathogenesis of AMD. Other drusenlike deposits that manifest before age 50 include those associated with several hereditary basement membrane abnormalities that lead to significant renal disease, including Alport syndrome, membranoproliferative glomerulonephritis type II, and atypical hemolytic uremia syndromes. Recognition of these conditions and confirmation with molecular genetic testing is critical because of the initial occult nature of the renal disease, which can be life-threatening. The genes known to lead to these Mendelian disorders are also implicated in the causation of AMD.

Pattern Dystrophies

The pattern dystrophies are a group of disorders characterized by the development, typically in midlife, of various patterns of yellow, orange, or gray pigment deposition at the level of the RPE in the macular area. These dystrophies may be subdivided into 4 major patterns according to the distribution of pigment deposits: (1) adult-onset foveomacular vitelliform dystrophy (discussed earlier in this chapter), (2) butterfly-type pattern dystrophy (Fig 13-20), (3) reticular-type pattern dystrophy (Fig 13-21), and (4) fundus

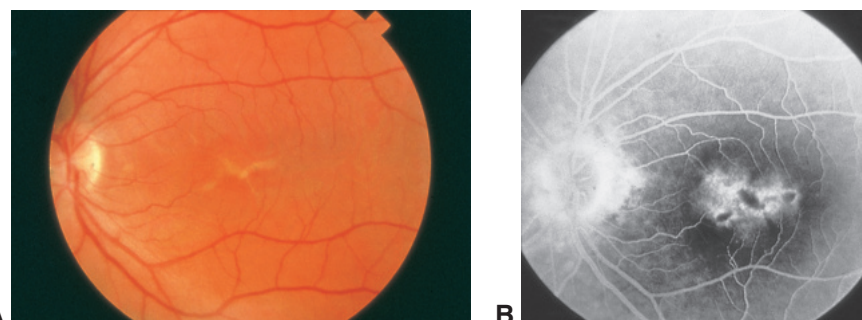


Figure 13-20 Butterfly-type pattern dystrophy. **A**, Color fundus photograph from a 56-year-old woman shows a typical yellow macular pigment pattern. **B**, Fluorescein angiography image shows blocked fluorescence of the pigment lesion itself and a rim of hyperfluorescence from surrounding RPE atrophy. (Used with permission from Song M-K, Small KW. Macular dystrophies. In: Regillo CD, Brown GC, Flynn HW Jr, eds. Vitreoretinal Disease: The Essentials. New York: Thieme; 1999:297. © Thieme.)

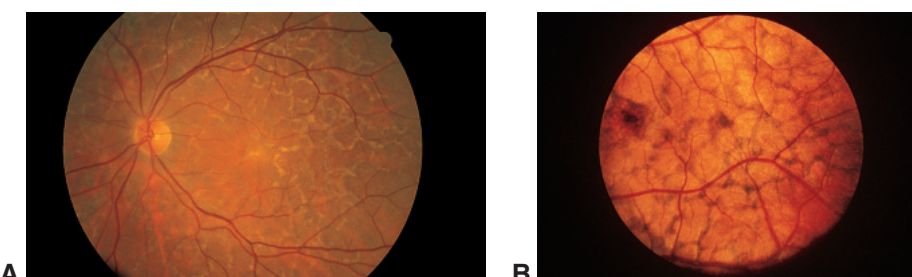


Figure 13-21 Color fundus photographs show 2 examples of reticular-type pattern dystrophy, characterized by a "fishnet" pattern of yellowish-orange (**A**) or brown (**B**) pigment deposition in the posterior fundus. (Courtesy of Mark W. Johnson, MD.)

pulverulentus (coarse pigment mottling). Patients are often asymptomatic. The most common presenting symptom of the pattern dystrophies is diminished visual acuity or mild metamorphopsia. The risk of developing choroidal neovascularization is low, but geographic macular atrophy may eventually develop.

The inheritance is often autosomal dominant, but other modes of inheritance have been observed, including autosomal recessive and mitochondrial. The majority of the cases of autosomal dominant pattern dystrophy have been associated with mutations in *PRPH2*, but other genes and conditions can give rise to similar phenotypes, including pseudoxanthoma elasticum and some mitochondrial disorders.

Atypical and “Occult” Macular Dystrophies

Atypical macular dystrophies include *central areolar choroidal dystrophy* for which *PRPH2*, *GUCY2D*, and 2 other genetic loci have been implicated in autosomal dominant inheritance (Fig 13-22). *North Carolina macular dystrophy* is an autosomal dominant, completely penetrant congenital and stationary maldevelopment of the macula. There is very large phenotypic variability with 3 grades of severity: grade 1, drusen; grade 2, confluent drusen; and grade 3, colobomatous-like excavated defects in the macula that sometimes resemble toxoplasmosis. (Fig 13-23). The visual acuity in eyes with North Carolina macular dystrophy can be surprisingly good, given the appearance of the macula. However, choroidal neovascularization and fibrosis can develop, resulting in visual acuity deterioration.

Although many of the macular dystrophies result in abnormal RPE pigmentation and/or accumulation of lipofuscin or drusenlike deposits, some forms of macular dystrophy, often referred to as *occult macular dystrophy*, do not have these associated findings. These patients frequently present with seemingly unexplained loss of central vision. ERG testing is uninformative in these cases, and the most striking clinical findings are disruption (either discrete or diffuse) of the central ellipsoid layer on OCT. The differential diagnosis can include *solar retinopathy* as well as *early macular telangiectasia* (which itself may be a type of polygenic macular dystrophy) and *acute macular neuroretinopathy* (either unilateral or bilateral). Mutations in *RP1L1* and *MFSD8* have been reported to give rise to this phenotype.



Figure 13-22 Color fundus photograph of central areolar choroidal dystrophy in a patient with autosomal dominant inheritance pattern. (Courtesy of Mark W. Johnson, MD.)

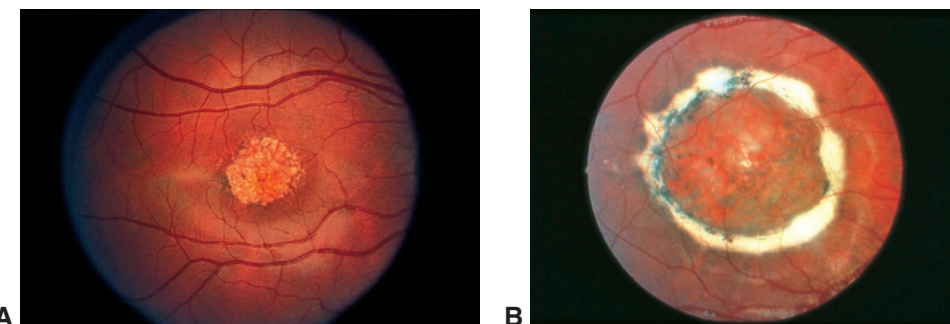


Figure 13-23 Color fundus photographs show clinical variations in North Carolina macular dystrophy. **A**, Fundus of a 7-year-old patient with a cluster of peculiar yellowish-white atrophic lesions in the macula. **B**, Example of a severe, almost colobomatous, macular defect. (Part A courtesy of Mark W. Johnson, MD; part B courtesy of Kent Small, MD.)

Inner Retinal Dystrophies

X-Linked Retinoschisis

Retinoschisis refers to a splitting of the neurosensory retina. The phenotype of congenital X-linked retinoschisis (XLRS) is variable, even within families. In pediatric patients, foveal schisis, which appears as small, cystoid spaces and fine radial striae in the central macula (Fig 13-24), can be best seen with OCT and fundus autofluorescence imaging. Other presenting signs include parafoveal white dots. Schisis is occasionally absent on OCT imaging, even in molecularly confirmed disease. Central vision may initially be quite good and may remain stable for long periods but can eventually decline to 20/200 or worse.

Peripheral retinoschisis may occur in up to 50% of patients. In severe cases involving peripheral schisis, there may be extensive areas of inner retinal elevation resembling total

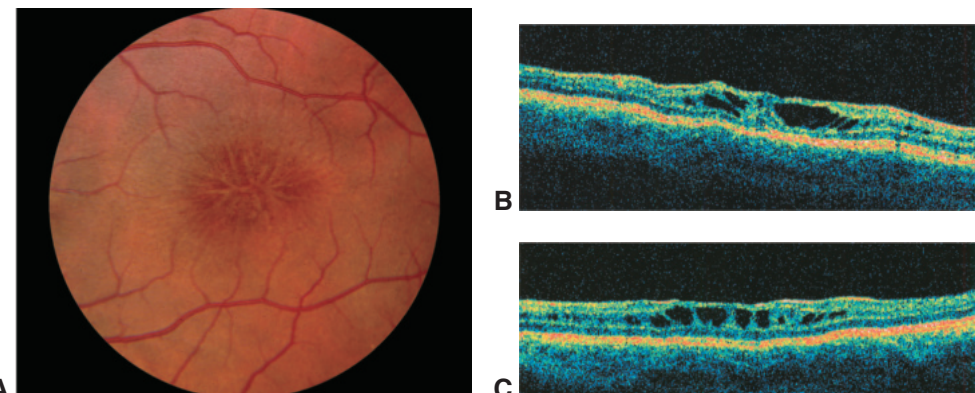


Figure 13-24 Juvenile retinoschisis. **A**, Color fundus photograph shows the characteristic pattern of macular schisis, a more consistent finding than peripheral changes. Vertical (**B**) and horizontal (**C**) OCT scans demonstrate schisis spaces in the middle layers of the macula. (Courtesy of Mark W. Johnson, MD.)

or subtotal retinal detachment. Histologic studies have shown that the splitting in peripheral XLRS occurs in the outer plexiform and nerve fiber layers. Pigmentary deposits may develop in peripheral areas destroyed by the disease process, so advanced cases of XLRS may be mistaken for RP. Boys with XLRS frequently present with vitreous hemorrhages from torn retinal vessels in areas of retinoschisis. Areas of peripheral schisis and the associated absolute scotomas are best monitored by widefield perimetry (eg, HVF 60-4) because photographic documentation can be extremely difficult.

The panretinal involvement and inner retinal location of the disease are reflected in the ERG response, which has a negative waveform in which the a-wave is normal or near normal, but the b-wave is reduced (see Chapter 3, Fig 3-2).

In XLRS, the gene *RS1* encodes an adhesion protein called *retinoschisin*, which is crucial for the structural integrity of the retina provided by the Müller cells. Treatment with topical and/or oral carbonic anhydrase inhibitors can be effective in reducing the intraretinal fluid in the central schisis cavities and may help to preserve long-term central vision function. A clinical trial of a gene therapy for this condition was initiated in 2016.

Retinal Degenerations Associated With Systemic Disease

For many of the conditions discussed in this chapter, a correct diagnosis could lead to meaningful, and in some cases, life-saving therapies or interventions. This is a highly heterogeneous group of systemic diseases that often require specialty care due to potentially severe associated morbidities and mortality. Important diagnostic and prognostic questions that arise in evaluating a patient who presents with retinal degeneration include the following:

- Is the degeneration hereditary or acquired?
- Is the condition stable or progressive?
- Can a precise diagnosis be made?

Retinal Degeneration With Systemic Involvement

Pigmentary retinopathy and retinal degenerations may be associated with a wide spectrum of genetic or acquired diseases. The term *pigmentary retinopathy* refers broadly to a panretinal disturbance of the retina and retinal pigment epithelium (RPE). Pigment deposits define most pigmentary retinopathies and typically present in the form of pigment clumps or spicules, but some diseases have a generalized depigmentation characterized by atrophy and little or no pigment deposition. This section summarizes some important examples of these disorders (Table 14-1).

Infantile-Onset to Early Childhood-Onset Syndromes

Leber congenital amaurosis (LCA) should be considered in any infant suspected of poor or declining vision if a severely diminished or extinguished electroretinogram (ERG) signal is present at birth (also see Chapter 13). If the ERG signal is diminished and the changes are progressive, evaluation should include careful screening for congenital syndromes and metabolic disorders that affect the retina.

den Hollander AI, Roepman R, Koenekoop RK, Cremers FP. Leber congenital amaurosis: genes, proteins and disease mechanisms. *Prog Retin Eye Res.* 2008;27(4):391–419.

Bardet-Biedl Syndrome

Bardet-Biedl syndrome comprises several different diseases with a similar constellation of findings, including pigmentary retinopathy (with or without pigment deposits), obesity,

Table 14-1 Selected Systemic Diseases With Pigmentary Retinopathies

Disorder	Features
Autosomal dominant disorders	
Arteriohepatic dysplasia (Alagille syndrome)	Intrahepatic cholestatic syndrome, posterior embryotoxon, Axenfeld anomaly, congenital heart disease, flattened facies and bridge of nose, bony abnormalities, myopia, pigmentary retinopathy
Charcot-Marie-Tooth disease Myotonic dystrophy (Steinert disease)	Pigmentary retinopathy, degeneration of lateral horn of spinal cord, optic atrophy Muscle wasting, "Christmas tree" cataract, retinal degeneration, pattern dystrophy or reticular degeneration; ERG response subnormal to abnormal
Oculodentodigital dysplasia Syndrome	Thin nose with hypoplastic alae, narrow nostrils, abnormality of fourth and fifth fingers, hypoplastic dental enamel, congenital cataract, colobomas
Olivopontocerebellar atrophy Stickler syndrome (arthro-ophthalmopathy)	Retinal degeneration (peripheral and/or macular), cerebellar ataxia, possible external ophthalmoplegia Progressive myopia with myopic retinal degeneration, arthropathy including joint hypermobility and arthritis, midfacial hypoplasia, high arched or cleft palate, bifid uvula; retinal detachment common; ERG response subnormal to abnormal
Waardenburg syndrome	Hypertelorism, wide bridge of nose, cochlear deafness, white forelock, heterochromia iridis, poliosis, pigment disturbance of RPE, choroidal vitiligo; ERG response normal to subnormal
Wagner hereditary vitreoretinal degeneration	Narrowed and sheathed retinal vessels, pigmented spots in the retinal periphery and along retinal vessels, choroidal atrophy and optic atrophy, extensive liquefaction and membranous condensation of vitreous body; subnormal ERG response; overlapping features with Stickler syndrome
Autosomal recessive disorders	
Bardet-Biedl syndrome	Pigmentary retinopathy, bull's-eye maculopathy, mild cognitive disabilities, polydactyly, obesity, hypogenitalism, progressive visual field loss; ERG response severely diminished to undetectable
Bietti crystalline dystrophy	Yellow-white crystals scattered in posterior pole, round subretinal pigment deposits, confluent loss of RPE and choriocapillaris on fluorescein angiogram, possible crystals in limbal cornea
Spinocerebellar degeneration Homocystinuria	Ataxia, limb incoordination, nerve deafness, maculopathy, retinal degeneration, optic atrophy
Mannosidosis	Fine pigmentary or cystic degeneration of retina, marfanoid appearance, myopia, lens subluxation or dislocation, cardiovascular abnormalities (thromboses), glaucoma, cognitive disabilities
Mucopolysaccharidosis type I H (Hurler syndrome)	MacroGLOSSIA, flat nose, large head and ears, skeletal abnormalities, possible hepatosplenomegaly, storage material in retina; resembles Hurler syndrome
Mucopolysaccharidosis type I S (Scheie syndrome)	Early corneal clouding, gargoyle facies, deafness, cognitive disabilities, dwarfism, skeletal abnormalities, hepatosplenomegaly, optic atrophy; subnormal ERG response
Mucopolysaccharidosis type III (Sanfilippo syndrome)	Coarse facies, aortic regurgitation, stiff joints, early clouding of the cornea, normal life span, normal intellect, pigmentary retinopathy Milder somatic stigmata than in Hurler syndrome, but severe pigmentary retinopathy

Disorder	Features
Neonatal adrenoleukodystrophy	Pigmentary retinopathy, optic atrophy, seizures, hypotonia, adrenal cortical atrophy, psychomotor impairment; extinguished ERG response
Neuronal ceroid lipofuscinoses (Batten disease)	Haltia-Santavuori, onset 8–18 months with rapid deterioration, fine granular inclusions Jansky-Bieleschowsky, onset 2–4 years, rapid CNS deterioration, curvilinear body inclusions Lake-Cavanagh, onset 4–6 years, ataxia, dementia, curvilinear and fingerprint inclusions
Refsum disease	Elevations of phytanic acid, pigmentary retinopathy, optic atrophy, partial deafness, cerebellar ataxia, ichthyosis
Usher syndrome	Congenital deafness (profound or partial), pigmentary retinopathy, vestibular areflexia
Zellweger (cerebrohepatorenal) syndrome	Muscular hypotonia, high forehead and hypertelorism, hepatomegaly, deficient cerebral myelination, nystagmus, cataract, microphthalmia, retinal degeneration; undetectable ERG response
X-linked pigmentary retinopathies	
Incontinentia pigmenti (Bloch-Sulzberger syndrome)	Skin pigmentation in lines and whorls, alopecia, dental anomalies, optic atrophy, falciform folds, cataract, nystagmus, strabismus, patchy mottling of fundi, conjunctival pigmentation
Mucopolysaccharidosis type II (Hunter syndrome)	Minimal or no corneal clouding, mild clinical course; onset of signs at age 2–4 years; full lips, large rounded cheeks, broad nose, enlarged tongue (macroglossia), cognitive disabilities, pigmentary retinopathy; subnormal ERG response; over time, voice changes from vocal cord enlargement; possible airway obstruction from airway narrowing
Pelizaeus-Merzbacher disease	Infantile progressive leukodystrophy, cerebellar ataxia, limb spasticity, cognitive impairment, possible pigmentary retinopathy with absent foveal reflex
Mitochondrial disorders	
Kearns-Sayre syndrome; maternally inherited	Progressive external ophthalmoplegia, ptosis, pigmentary retinopathy and/or macular atrophy, heart block (Kearns-Sayre syndrome); normal to abnormal ERG response
diabetes and deafness (MIDD); mitochondrial encephalopathy, lactic acidosis, strokelike episodes (MELAS)	

CNS = central nervous system; ERG = electroretinogram; RPE = retinal pigment epithelium.

Data from Rimoin DL, Connor JM, Pyeritz RE, Korf BR, eds. *Emery and Rimoin's Principles and Practice of Medical Genetics*. 3 vols. 4th ed. New York: Churchill Livingstone; 2002:chap 137.

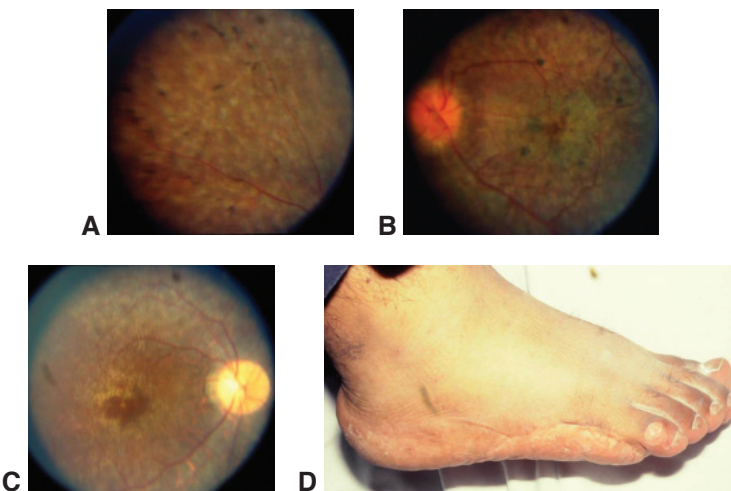


Figure 14-1 Bardet-Biedl syndrome. **A, B,** Color fundus photographs show pigmentary alterations in the periphery and macula. **C,** Color fundus photograph of the sibling of the patient in **(A)** and **(B)** demonstrates similar macular changes. **D,** Clinical photograph of a patient's foot with 6 toes (polydactyly). (Courtesy of David Sarraf, MD.)

polydactyly, hypogonadism, and cognitive disability. Patients with Bardet-Biedl syndrome typically demonstrate a severe but variable form of rod-cone dystrophy, usually sine pigmento, with a bull's-eye atrophic maculopathy (Fig 14-1). These disorders were previously classified as autosomal recessive, but molecular studies strongly suggest that many are multigenic, with 2 or even 3 different mutations contributing to the phenotype. Increasing evidence suggests that the primary functions of the proteins affected in Bardet-Biedl syndrome are to mediate and regulate microtubule-based intracellular transport processes.

M'hamdi O, Ouertani I, Chaabouni-Bouhamed H. Update on the genetics of Bardet-Biedl syndrome. *Mol Syndromol.* 2014;5(2):51–56.

Hearing Loss and Pigmentary Retinopathy: Usher Syndrome

Usher syndrome is the most common name used to describe the association of retinitis pigmentosa (RP) with congenital sensorineural hearing loss, whether partial or profound. The prevalence of Usher syndrome is thought to be 3 cases per 100,000 persons. There are 3 types of Usher syndrome; patients with type 1 have early and profound deafness, RP, and vestibular areflexia. Type 2 patients are born with moderate to severe hearing loss and develop RP within their second decade but have normal vestibular function. Type 3 patients have progressive hearing loss, variable RP, and sporadic vestibular function.

All forms show autosomal recessive inheritance. Currently, 16 genetic loci have been identified as associated with Usher syndrome. The proteins encoded by these genes are part of a dynamic protein complex present in the cilia of the inner ear and in the cone outer segments of the photoreceptor cells of the retina. Other genetic conditions and environmental factors that may also lead to pigmentary retinopathy and hearing loss include Alport, Alström, Cockayne, and Hurler syndromes; spondyloepiphyseal dysplasia congenita; Refsum disease; and congenital rubella.

Mathur P, Yang J. Usher syndrome: hearing loss, retinal degeneration and associated abnormalities. *Biochim Biophys Acta*. 2015;1852(3):406–420.

Neuromuscular Disorders

Pigmentary retinopathy associated with neuromuscular pathology is present in a variety of disorders (see Table 14-1). ERG abnormalities found in these neurologic disorders confirm the presence of retinopathy but are not diagnostic for any one disorder.

Although *Duchenne muscular dystrophy* does not cause a pigmentary retinopathy, it deserves mention because the ERG signal shows a negative waveform similar to that found in patients with congenital stationary night blindness (CSNB)—specifically, a normal a-wave but a reduced b-wave (see Chapters 3 and 12). This ERG response suggests a defective “on-response” pathway, but patients with this disorder do not have night blindness. Interestingly, Duchenne muscular dystrophy is caused by mutations in the gene for *dystrophin*, a protein that is abundant in muscle but also found in neural synaptic regions and in the retina.

Barboni MT, Nagy BV, de Araújo Moura AL, et al. ON and OFF electroretinography and contrast sensitivity in Duchenne muscular dystrophy. *Invest Ophthalmol Vis Sci*. 2013;54(5):3195–3204.

Other Organ System Disorders

Most retinopathies associated with other organ systems are rare and genetic, and clinicians may find the Online Mendelian Inheritance in Man website (www.omim.org) useful in recognizing them.

Renal diseases

Several forms of congenital renal disease may be associated with retinal degeneration. *Familial juvenile nephronophthisis* is one of the family of renal-retinal dysplasia (and ciliopathy) characterized by autosomal recessive inheritance and childhood onset of end-stage renal disease. Individuals with Joubert syndrome have cerebellar malformation (a characteristic “molar tooth” deformity that can be observed on magnetic resonance imaging of the brain) and may also have associated chorioretinal coloboma. Patients with Bardet-Biedl syndrome commonly have urethral reflux with pyelonephritis and kidney damage, whereas patients with Alström syndrome, another retinal ciliopathy, may demonstrate obesity, short stature, and cardiomyopathy in addition to renal disease. Jeune syndrome is a retinal ciliopathy that is complicated by cystic kidney disease and asphyxiating thoracic dystrophy.

Liver disease

Patients with Alagille syndrome present with hepatorenal abnormalities including cholestatic jaundice and have several characteristic ocular findings, including posterior embryotoxin and pigmentary retinopathy, that can have a peripapillary and macular predilection.

Gastrointestinal disease

Familial adenomatous polyposis (FAP, also known as *Gardner syndrome*) is associated with pigmented lesions that are similar to those found in congenital hypertrophy of the RPE. However, the lesions in FAP are smaller, ovoid, more variegated, and typically multiple

and bilateral. The presence of more than 4 widely spaced, small (<0.5-disc-diameter) lesions per eye and bilateral involvement suggest FAP. Note that congenital grouped pigmentation (“bear tracks”) is not associated with FAP. Caused by mutations in the adenomatous polyposis gene (*APC*), FAP has an autosomal dominant inheritance pattern with incomplete expression. The pigmented retinal lesions are an important marker for identifying family members at risk for colonic polyps, which have a high malignant potential.

Dermatologic diseases

Ichthyosis, comprising abnormal scaling, dryness, and tightness of the skin, may be found in conjunction with the pigmentary retinopathy of Refsum disease and the crystalline maculopathy of Sjögren-Larsson syndrome. *Incontinentia pigmenti (Bloch-Sulzberger syndrome)* is a rare, X-linked disorder that presents only in females; the mutation is lethal in males. It is characterized by streaky skin lesions and abnormalities of the teeth and central nervous system (CNS). Ocular involvement occurs in approximately one-third of affected females and includes pigmentary abnormalities as well as peripheral retinal non-perfusion and neovascularization that may cause tractional and cicatricial retinal detachment (also see BCSC Section 6, *Pediatric Ophthalmology and Strabismus*). *Pseudoxanthoma elasticum* is associated with a “plucked-chicken” skin appearance, peripapillary angioid streaks, and a *peau d'orange* fundus appearance (see Chapter 4).

Holmström G, Thorén K. Ocular manifestations of incontinentia pigmenti. *Acta Ophthalmol Scand.* 2000;78(3):348–353.

Traboulsi EI. Ocular manifestations of familial adenomatous polyposis (Gardner syndrome). *Ophthalmol Clin North Am.* 2005;18(1):163–166.

Dental disease

Amelogenesis imperfecta is a genetic disease that causes abnormalities in dentition development resulting from defective enamel production. When associated with a cone-rod dystrophy this condition is referred to as *Jalili syndrome* and has a wide range of clinical retinal manifestations, including macular coloboma and pigmentary retinopathy.

Paraneoplastic and Autoimmune Retinopathies

Occasionally, retinal degeneration is a complication of cancer resulting from a paraneoplastic immunologic mechanism. BCSC Section 9, *Uveitis and Ocular Inflammation*, explains the role of the immune system in this process. The 2 main paraneoplastic retinopathy syndromes are (1) *cancer-associated retinopathy* (CAR; Fig 14-2) and (2) *melanoma-associated retinopathy* (MAR). The characteristic ERG findings in MAR are a preserved dark adapted a-wave followed by a strikingly reduced b-wave, resulting in an electronegative ERG, which is similar to the ERG findings in CSNB. Patients with MAR usually present with an acquired night blindness and shimmering photopsias.

A third entity, *autoimmune retinopathy*, refers to an acquired, presumed immunologically mediated, retinal degeneration that resembles paraneoplastic retinopathy but without any identifiable systemic malignancy.

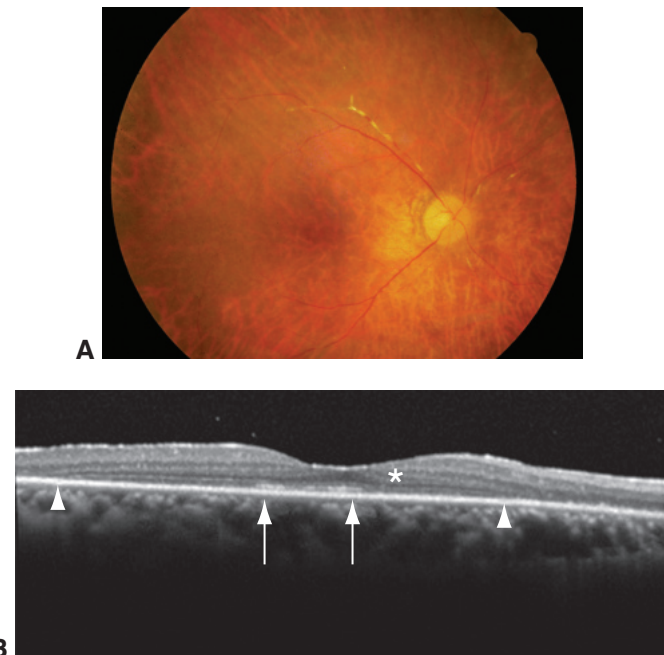


Figure 14-2 Cancer-associated retinopathy (CAR). **A**, Color fundus photograph of CAR in a patient with ovarian carcinoma. Note the severe vascular attenuation without obvious pigmentary alterations. **B**, Fourier-domain cross-sectional optical coherence tomography (OCT) of an eye with CAR that shows hyperreflectivity (asterisk) and disruption (arrowheads) of the outer nuclear layer external limiting membrane as well as decreases in reflectivity of the inner segment ellipsoid zone (arrows). (Part A courtesy of John R. Heckenlively, MD; part B used with permission from Mesiwala NK, Shemonski N, Sandrian MG, et al. Retinal imaging with en face and cross-sectional optical coherence tomography delineates outer retinal changes in cancer-associated retinopathy secondary to Merkel cell carcinoma. J Ophthalmic Inflamm Infect. 2015;5(1):53.)

Bilateral diffuse uveal melanocytic proliferation (BDUMP) is a paraneoplastic syndrome characterized by multiple melanocytic lesions of the choroid that may be associated with rapidly progressive posterior subcapsular cataract, iris and ciliary body cysts, and exudative retinal detachment. BDUMP has been associated with various systemic malignancies (see Chapter 9). *Acute exudative polymorphous vitelliform maculopathy*, which is characterized by multiple waxing and waning subretinal vitelliform lesions, has been reported in association with metastatic cutaneous melanoma and other systemic malignancies.

Fox AR, Gordon LK, Heckenlively JR, et al. Consensus on the diagnosis and management of nonparaneoplastic autoimmune retinopathy using a modified Delphi approach. *Am J Ophthalmol*. 2016;168:183–190.

Grange L, Dalal M, Nussenblatt RB, Sen HN. Autoimmune retinopathy. *Am J Ophthalmol*. 2014;157(2):266–272.

Rahimy E, Sarraf D. Paraneoplastic and non-paraneoplastic retinopathy and optic neuropathy: evaluation and management. *Surv Ophthalmol*. 2013;58(5):430–458.

Metabolic Diseases

When evaluating patients with retinal degeneration, it is important to consider metabolic diseases. Some disorders, such as albinism and conditions associated with CNS abnormalities, are covered in BCSC Section 6, *Pediatric Ophthalmology and Strabismus*. Other metabolic disorders, such as abetalipoproteinemia and Refsum disease, are among the differential diagnostic concerns for RP, even though the retinopathy associated with these disorders may be granular and atypical.

Albinism

In albinism, the synthesis of melanin is reduced or absent. When the reduction in melanin biosynthesis affects the eyes, skin, and hair follicles, the disease is called *oculocutaneous albinism*. These disorders usually have an autosomal recessive inheritance pattern. If the skin and hair appear normally pigmented and only ocular pigmentation is affected, the condition is called *ocular albinism*. Ocular albinism typically has an X-linked inheritance pattern. Female carriers of X-linked ocular albinism may show partial iris transillumination and fundus pigment mosaicism.

Regardless of the type of albinism, ocular involvement generally conforms to 1 of 2 clinical patterns: (1) congenitally subnormal visual acuity (typically 20/100–20/400) and nystagmus or (2) normal or minimally reduced visual acuity without nystagmus. The first pattern is true albinism; the second has been termed *albinoidism* because of its milder visual consequences. Both patterns share the clinical features of photophobia, iris transillumination, and hypopigmented fundi. They differ according to whether or not the fovea develops normally; in true albinism, the fovea is hypoplastic, with no foveal pit or reflex and no evident luteal pigment (Fig 14-3). The gold standard for diagnosis of true albinism is the finding of characteristic abnormalities of the flash and pattern visual evoked potentials (VEPs). Compared with a normal symmetric response, in albinism, a single eye stimulation will result in an asymmetric occipital response because there is a greater number of decussating fibers.

Oculocutaneous albinism has 2 forms with potentially lethal systemic implications. The first, *Chédiak-Higashi syndrome*, combines albinism with neutropenia and an extreme susceptibility to infections as well as other complications such as bleeding (caused by deficient platelets). The second, *Hermansky-Pudlak syndrome*, is characterized by a platelet defect that causes easy bruising and bleeding. In the United States, most patients with Hermansky-Pudlak syndrome are of Puerto Rican descent.

King RA, Jackson IJ, Oetting WS. Human albinism and mouse models. In: Wright AF, Jay B, eds. *Molecular Genetics of Inherited Eye Disorders*. Chur, Switzerland: Harwood Academic; 1994:89–122.

Central Nervous System Metabolic Abnormalities

Although a comprehensive description is beyond the scope of this chapter, the following discussion includes some of the major inherited metabolic diseases known to affect the CNS and retina (see Table 14-1). See BCSC Section 6, *Pediatric Ophthalmology and Strabismus*, for a listing of the ocular findings in inborn errors of metabolism.

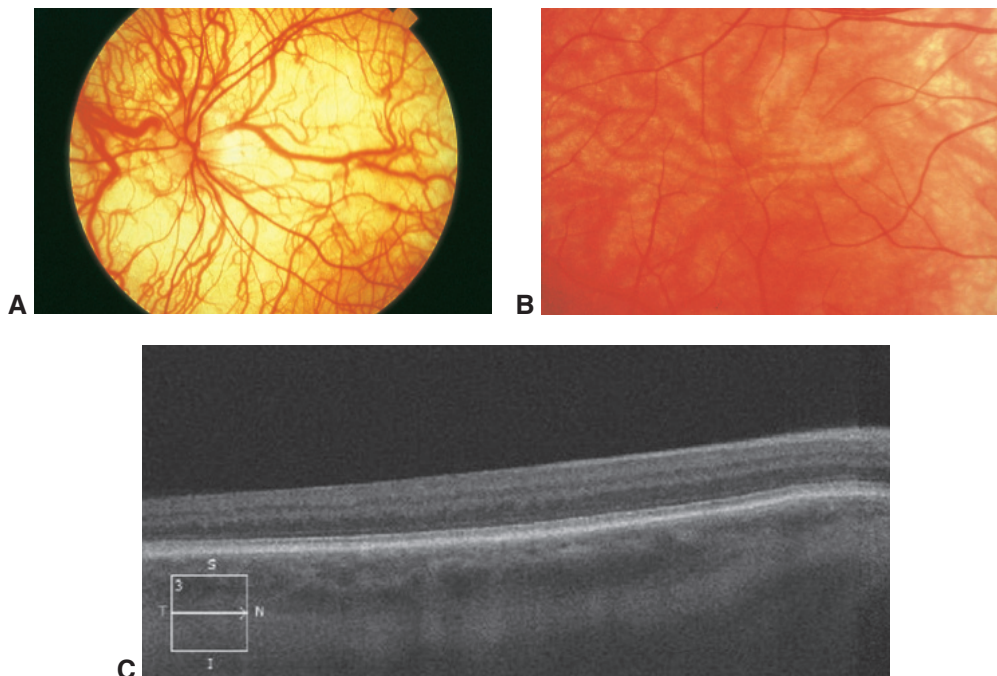


Figure 14-3 Albinism. **A**, Color fundus photograph shows generalized fundus hypopigmentation. **B**, High-magnification color fundus photograph shows foveal hypoplasia. No foveal reflex or luteal pigment is evident. **C**, SD-OCT image shows the lack of a foveal pit. Eccentric fixation was also present, resulting in superior decentration of the scans. (Parts A, B courtesy of Carl D. Regillo, MD; part C courtesy of David Browning, MD.)

Neuronal ceroid lipofuscinoses

The neuronal ceroid lipofuscinoses (NCLs) are a group of autosomal recessive diseases caused by the accumulation of waxy lipopigments (eg, ceroid and lipofuscin) within the lysosomes of neurons and other cells. These disorders usually become evident in early childhood and are characterized by progressive dementia, seizures, and loss of vision associated with a pigmentary retinopathy in early-onset cases. A diagnosis can be made with genetic testing, in addition to a peripheral blood smear or biopsy of conjunctival or other tissues looking for the characteristic curvilinear, fingerprint-like or granular inclusions on electron microscopy. The infantile and juvenile types of NCLs are associated with pigmentary retinopathies (see Table 14-1). Ocular findings in infantile NCL include optic atrophy; macular pigmentary changes including bull's-eye atrophic maculopathy, mottling of the fundus periphery, and retinal vascular attenuation; and reduced or absent ERG signals (Fig 14-4). The 2 adult forms of NCL do not have ocular manifestations.

Abetalipoproteinemia and vitamin A deficiency

Abetalipoproteinemia is an autosomal recessive disorder in which apolipoprotein B is not synthesized, which causes fat malabsorption, fat-soluble vitamin deficiencies, and retinal and spinocerebellar degeneration. Supplementation with vitamins A and E is needed to prevent or ameliorate the retinal degeneration. The most common form of vitamin A



Figure 14-4 Color fundus photograph from a patient with Batten disease (juvenile neuronal ceroid lipofuscinosis) shows vascular attenuation and central retinal atrophy with mottled pigmentation and a wrinkled, cellophane-like surface. (Used with permission from Hansen MS, Hove MN, Jensen H, Larsen M. Optical coherence tomography in juvenile neuronal ceroid lipofuscinosis. *Retin Cases Brief Rep.* 2016;10(2):137–139.)

deficiency retinopathy occurs in patients who have undergone gastric bypass surgery for obesity or small-bowel resection for Crohn disease. These patients have malabsorption of fat-soluble vitamins and may develop a blind loop syndrome, in which an overgrowth of bacteria consumes vitamin A. Patients experience nyctalopia, and if the condition remains untreated, eventually demonstrate vision loss and diffuse, drusenlike spots similar to those observed in retinitis punctata albescens.

Peroxisomal disorders and Refsum disease

The peroxisomal disorders are mostly autosomal recessive diseases caused by the dysfunction or absence of peroxisomes or peroxisomal enzymes, which leads to defective oxidation and accumulation of very-long-chain fatty acids. *Zellweger syndrome* is the prototype of peroxisomal diseases. Severe infantile-onset retinal degeneration is associated with hypotonia, psychomotor impairment, seizures, characteristic facies, renal cysts, and hepatic interstitial fibrosis. Death usually occurs in infancy. Patients with *neonatal adrenoleukodystrophy* also present in infancy but generally survive until the age of 7–10 years (Fig 14-5).

Similar but less severe findings are present in *infantile Refsum disease*, which is characterized by pigmentary retinopathy with reduced or extinguished ERG signals, cerebellar ataxia, polyneuropathy, anosmia, hearing loss, and cardiomyopathy. Diagnosis is made by demonstrating elevated plasma levels of phytanic acid or reduced phytanic acid oxidase activity in cultured fibroblasts. Dietary restriction of phytanic acid precursors may slow or stabilize the neuropathy but typically not the retinal degeneration.

Mucopolysaccharidoses

The systemic *mucopolysaccharidoses* (MPSs) are caused by inherited defects in catabolic lysosomal enzymes that degrade the glycosaminoglycans dermatan sulfate, keratan sulfate, and heparan sulfate. The MPSs are transmitted as autosomal recessive traits except for type II, which is an X-linked recessive disorder (see Table 14-1).

Only those MPSs in which heparan sulfate is stored are associated with retinal dystrophy. These include MPS type I H (*Hurler syndrome*) and MPS type I S (*Scheie syndrome*),



Figure 14-5 Neonatal adrenoleukodystrophy. Color fundus photograph shows retinal arteriolar attenuation, diffuse pigmentary alterations, and mild optic atrophy. (Courtesy of Mark W. Johnson, MD.)

the clinical features of which include coarse facies, cognitive disabilities, corneal clouding, and retinal degeneration. The retinal pigmentary changes may be subtle, but the ERG response is abnormal. MPS type II (*Hunter syndrome*) also features pigmentary retinopathy but corneal clouding, if present, is only mild; patients have coarse facies and short stature and may show cognitive disabilities. In MPS type III (*Sanfilippo syndrome*), somatic stigmata are mild, but pigmentary retinopathy is severe.

Other lysosomal metabolic disorders

Tay-Sachs disease (GM₂ gangliosidosis type I), caused by a deficient subunit A of hexosaminidase A, is the most common ganglioside storage disease. Glycolipid accumulation in the brain and retina causes cognitive disability and blindness, and death generally occurs between the ages of 2 and 5 years. Ganglion cells surrounding the fovea become filled with ganglioside and appear grayish or white, causing a cherry-red spot (Fig 14-6).

The chronic nonneuronopathic adult form of *Gaucher disease* does not have cerebral involvement. This disease is characterized by large accumulations of glucosylceramide in the liver, spleen, lymph nodes, skin, and bone marrow. Some patients have a cherry-red spot; others show whitish superficial lesions in the midperiphery of the fundus. Spectral-domain optical coherence tomography (SD-OCT) analysis demonstrates multiple characteristic hyperreflective lesions located along the retinal surface.

The various types of *Niemann-Pick disease* are caused by the absence of different sphingomyelinase isoenzymes. Type A (acute neuronopathic) Niemann-Pick disease shows a cherry-red spot in about 50% of cases. Type B (chronic) Niemann-Pick disease, also known as *sea-blue histiocyte syndrome*, is the mildest, and although there is no functional involvement of the CNS, patients have a macular halo that is considered diagnostic (Fig 14-7).

Fabry disease (angiokeratoma corporis diffusum) is an X-linked condition caused by mutations in the gene encoding alpha-galactosidase A. Ceramide trihexoside accumulates

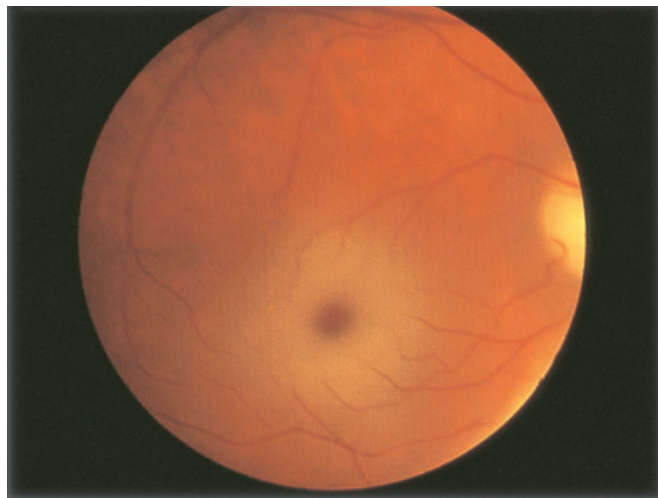


Figure 14-6 Tay-Sachs disease. Color fundus photograph shows a cherry-red spot.



Figure 14-7 Chronic Niemann-Pick disease. Color fundus photograph shows a macular halo. (Courtesy of Mark W. Johnson, MD.)

in the smooth muscle of blood vessels in the kidneys, skin, gastrointestinal tract, CNS, heart, and reticuloendothelial system. Ocular signs include corneal verticillata (whorls), tortuous conjunctival vessels, tortuous and dilated retinal vessels, and lens changes. Tortuosity of conjunctival and retinal vessels is also characteristic of fucosidosis, a rare lysosomal storage disorder caused by buildup of complex sugars due to reduced or absent activity of the alpha-L-fucosidase enzyme.

Gregory-Evans K, Pennesi ME, Weleber RG. Retinitis pigmentosa and allied disorders. In: Schachat AP, Wilkinson CP, Hinton DR, Sadda SR, Wiedemann P, eds. *Ryan's Retina*.

6th ed. Philadelphia: Elsevier/Saunders; 2018:861–935.

Haltia M. The neuronal ceroid-lipofuscinoses: from past to present. *Biochim Biophys Acta*. 2006;1762(10):850–856.

Amino Acid Disorders

In *cystinosis*, intralysosomal cystine accumulates because of a deficiency in the carrier protein cystinosin that typically transports it out of lysosomes. Three types are recognized, all autosomal recessive: (1) nephropathic, (2) late-onset (or intermediate), and (3) benign. Cystine crystals accumulate in the cornea and conjunctiva in all 3 types, but retinopathy develops only in patients with the nephropathic type who present early (8 to 15 months of age) with progressive renal failure, growth delays, renal rickets, and hypothyroidism. The retinopathy is characterized by areas of patchy depigmentation of the RPE alternating with irregularly distributed pigment clumps and associated fine retinal crystals, but no significant visual disturbance. Treatment with cysteamine may be beneficial. Bietti crystalline dystrophy may also cause crystalline keratopathy and retinopathy associated with patchy loss of the choriocapillaris and RPE and with associated photoreceptor loss.

Mitochondrial Disorders

Chronic progressive external ophthalmoplegia (CPEO) belongs to a group of diseases collectively termed *mitochondrial myopathies* (Fig 14-8), in which mitochondria are abnormally

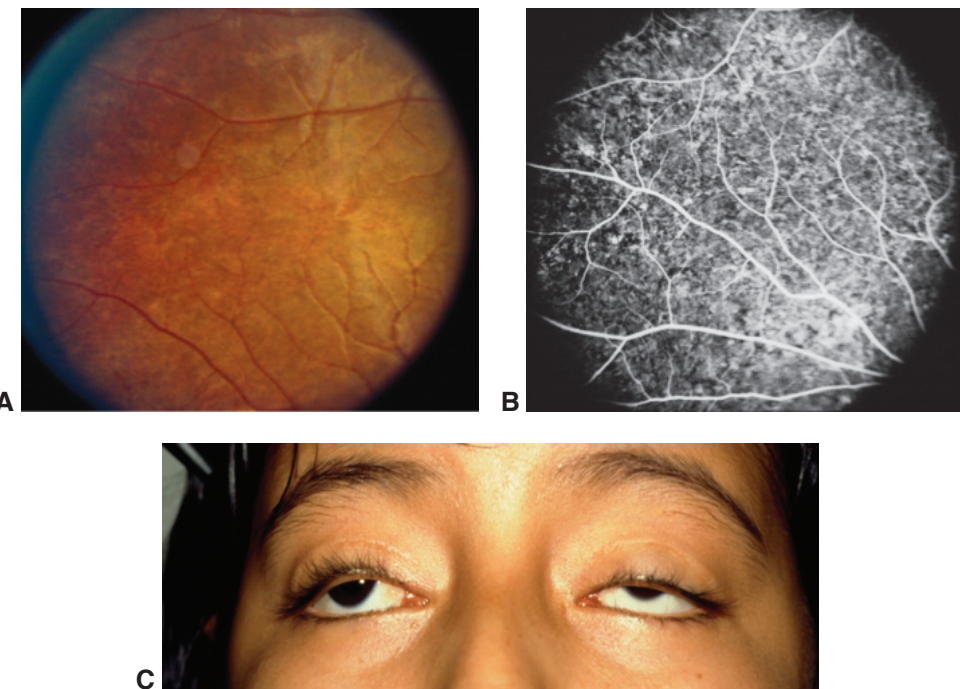


Figure 14-8 Chronic progressive external ophthalmoplegia (CPEO) and mitochondrial associated retinopathy. **A**, Color fundus photograph shows diffuse retinal pigment epithelial mottling. **B**, Corresponding mottled hyper- and hypo-fluorescence in the arteriovenous-phase fluorescein angiography image. **C**, Color photograph shows bilateral ptotic eyelids and eyes in a misaligned exotropic position from poor extraocular muscle function consistent with CPEO caused by a mitochondrial mutation. (Courtesy of David Sarraf, MD.)

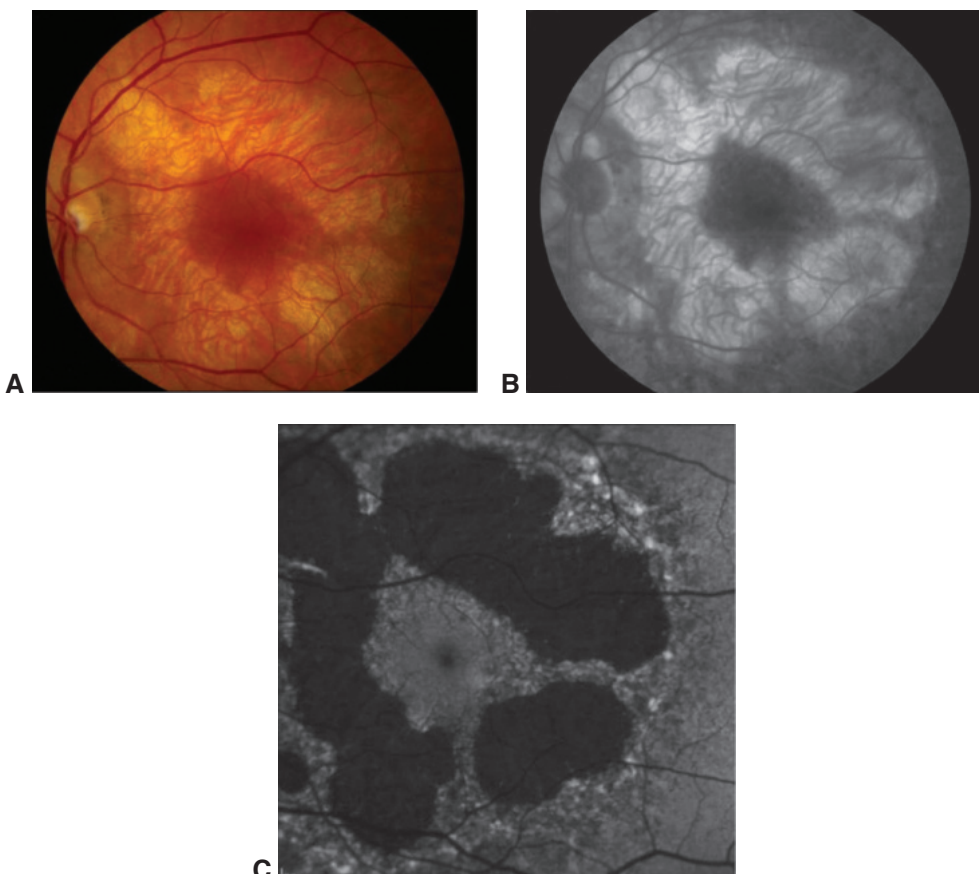


Figure 14-9 Maternally inherited diabetes and deafness (MIDD). Color fundus photograph (**A**), late fluorescein angiography frame (**B**), and fundus autofluorescence image (**C**) show retinal pigment epithelial atrophy in a perifoveal distribution in a patient with MIDD caused by a mitochondrial mutation. These findings were all symmetrically present in the fellow eye. (Courtesy of Herb Cantrill, MD.)

shaped and increased in number. Muscle biopsy specimens may reveal ragged red fibers. In addition to CPEO, the syndrome is associated with atypical RP and various systemic abnormalities. When associated with cardiomyopathy and cardiac conduction defects (heart block), the disorder is known as *Kearns-Sayre syndrome*; onset is usually before the age of 10 years. The severity of the pigmentary retinopathy is highly variable. Many patients retain good visual function and a normal ERG signal. Other mitochondrial myopathies with pigmentary retinopathy include *MIDD* (maternally inherited diabetes and deafness; Fig 14-9), *MELAS* (mitochondrial encephalomyopathy, lactic acidosis, and stroke), and *NARP* (neurogenic muscle weakness, ataxia, and retinitis pigmentosa) syndromes.

CHAPTER 15

Systemic Drug-Induced Retinal Toxicity

Retinal toxicities caused by systemic therapeutics may be categorized according to the level and pattern of toxicity. Broadly, these toxicities consist of (1) abnormalities at the level of the RPE/photoreceptor complex, (2) occlusive retinopathy or microvasculopathy, (3) ganglion cell and optic nerve toxicities, and (4) other manifestations of toxicity that include macular edema, crystalline retinopathy, and alterations in color vision and electroretinogram (ERG) signals.

Drugs Causing Abnormalities of the Retinal Pigment Epithelium/Photoreceptor Complex

Chloroquine Derivatives

Although retinal toxicity from *chloroquine* use remains a problem in many parts of the world, it is rare in the United States, where this medication has largely been replaced by the much safer, related drug *hydroxychloroquine*. These medications are used for the treatment of malaria and rheumatologic and dermatologic disorders. Both medications bind to melanin in the RPE, which may concentrate or prolong their effects. Although the incidence of toxicity is low, it is a serious concern because associated vision loss rarely recovers and may even progress after the drug is discontinued. Patients and their primary care physicians must be made aware of the ophthalmic risks and the need for regular screening examinations to detect retinal toxicity at an early stage, before vision loss occurs. Typical symptoms can include paracentral scotomas, central visual decline, and/or reading difficulty.

The earliest signs of toxicity include bilateral paracentral visual field defects and/or inner segment ellipsoid loss in a paracentral location, which appears as the “flying saucer” sign on spectral-domain optical coherence tomography (SD-OCT) imaging. However, most patients of Asian descent will show initial damage in a more peripheral extramacular distribution. With continued drug exposure, progressive pigmentary changes may develop, and a bilateral atrophic bull’s-eye maculopathy may ensue (Fig 15-1). End-stage cases of advanced toxicity may show panretinal degeneration that simulates retinitis pigmentosa; this degeneration can occur from long-term exposure to either drug or from acute overdosing of chloroquine. In some patients, corneal intraepithelial deposits, usually referred to as *corneal verticillata*, may also be observed.

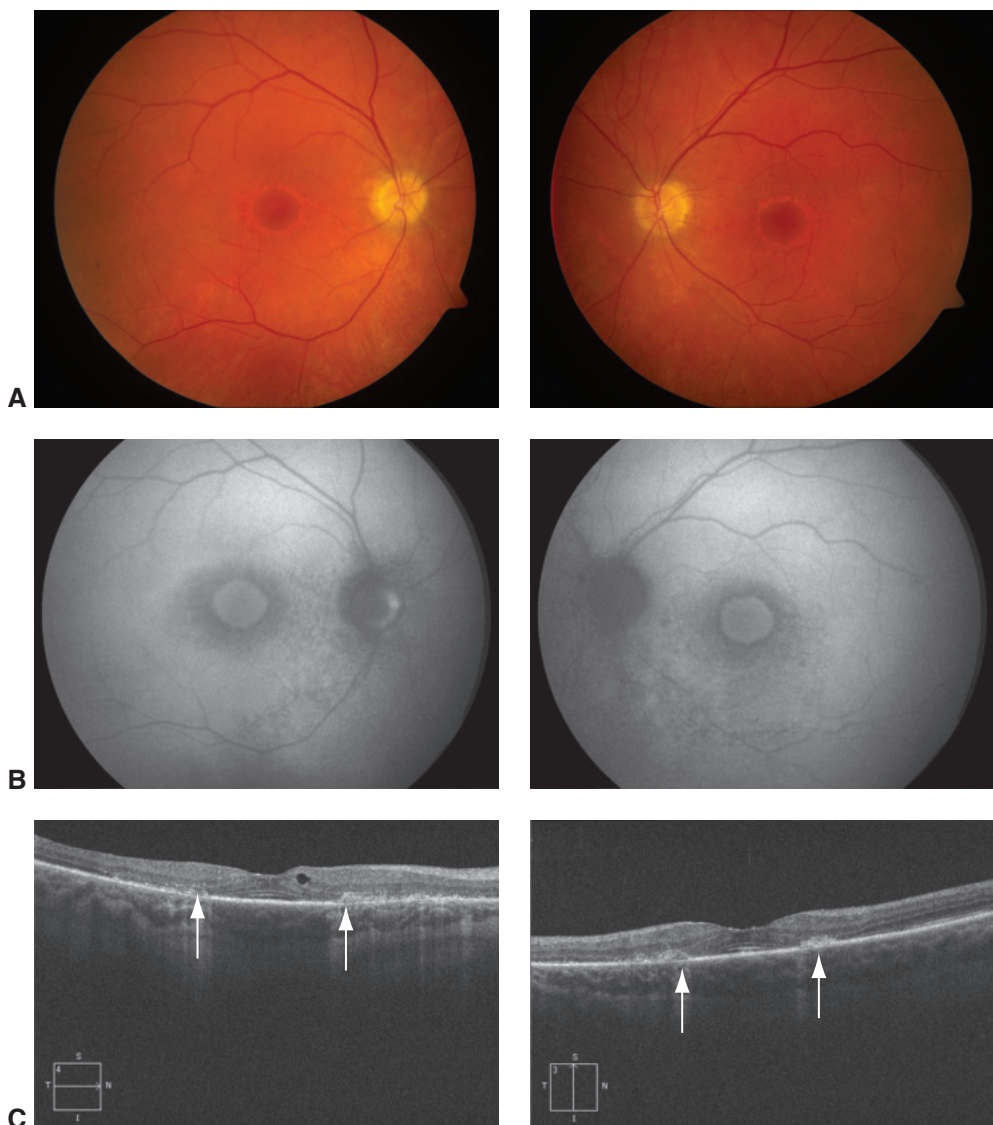


Figure 15-1 Bilateral, symmetric bull's-eye maculopathy in a patient with hydroxychloroquine toxicity. **A**, Color fundus photographs of left and right eyes. **B**, Corresponding fundus autofluorescence images. **C**, Spectral-domain optical coherence tomography (SD-OCT) images demonstrating the characteristic “flying-saucer” sign (arrows): the ovoid appearance of the central fovea due to preservation of the outer retinal structures in the central fovea surrounded by loss of the outer retinal structures in the perifoveal location. (*Courtesy of Stephen J. Kim, MD.*)

Ophthalmic screening of patients receiving chloroquine or hydroxychloroquine is aimed primarily at early detection and minimization of toxicity. As summarized in a 2016 Clinical Statement from the American Academy of Ophthalmology (www.aoa.org/clinical-statement/revised-recommendations-on-screening-chloroquine-h), the risk of toxicity is low for individuals who have no complicating conditions and take less than 6.5 mg/kg/day

of hydroxychloroquine or 3 mg/kg/day of chloroquine. The most recent data suggest that a hydroxychloroquine dosage of 5.0 mg/kg/day and a chloroquine dosage of 2.3 mg/kg/day based on the patient's real body weight may be safer across all body mass indexes than the dosage recommendation of 6.5 mg/kg/day and 3 mg/kg/day, respectively using the patient's ideal body weight.

Cumulative total doses greater than 1000 g of hydroxychloroquine and 460 g of chloroquine place patients at high risk of toxicity. Additional risk factors include duration of use (>5 years), kidney disease, concomitant use of tamoxifen (5-fold increase), and concomitant retinal disease such as age-related macular degeneration (AMD). The latter can also make early detection of toxicity difficult. Furthermore, well-documented but rare cases of hydroxychloroquine maculopathy have occurred with "safe" daily doses and in the absence of other risk factors.

Baseline evaluation for patients beginning treatment with a chloroquine derivative should include a complete ophthalmic examination. For follow-up comparison, the ophthalmologist should employ SD-OCT as well as automated threshold field testing with a white pattern (Humphrey white 10-2 protocol), although some clinicians prefer red for its increased sensitivity. Current guidelines recommend a baseline fundus examination within the first year of use, then annual screening after 5 years of use in patients at low risk for toxicity. Many practitioners, however, screen patients every 6 to 12 months with a combination of Humphrey 10-2 and SD-OCT until 5 years and then every 6 months thereafter. Patients who are at risk of toxicity or have unclear symptoms can be further assessed with fundus autofluorescence and multifocal electroretinography (mfERG). Signs of toxicity include a paracentral ring of hyperautofluorescence or hypoautofluorescence and paracentral mfERG depressions. Cessation of the drug at the first sign of toxicity is recommended.

- Marmor MF, Kellner U, Lai TY, Melles RB, Mieler WF; American Academy of Ophthalmology. Recommendations on screening for chloroquine and hydroxychloroquine retinopathy (2016 revision). *Ophthalmology*. 2016;123(6):1386–1394.
- Melles RB, Marmor MF. Pericentral retinopathy and racial differences in hydroxychloroquine toxicity. *Ophthalmology*. 2015;122(1):110–116.
- Melles RB, Marmor MF. The risk of toxic retinopathy in patients on long-term hydroxychloroquine therapy. *JAMA Ophthalmol*. 2014;132(12):1453–1460.

Phenothiazines

Phenothiazines, including *chlorpromazine* and *thioridazine*, are concentrated in uveal tissue and RPE by binding to melanin granules. High-dose chlorpromazine therapy commonly causes abnormal pigmentation of the eyelids, interpalpebral conjunctiva, cornea, and anterior lens capsule. Anterior and posterior subcapsular cataracts may also develop. However, pigmentary retinopathy from chlorpromazine therapy is unusual.

In contrast, high-dose thioridazine treatment can cause development of a severe pigmentary retinopathy within a few weeks or months of dosing initiation (Fig 15-2). Toxicity is rare at doses of 800 mg/day or lower. Initially, patients experience blurred vision, and the fundus shows coarse retinal pigment epithelial stippling in the posterior pole. Eventually, patchy nummular atrophy of the RPE and choriocapillaris may develop. The late stages

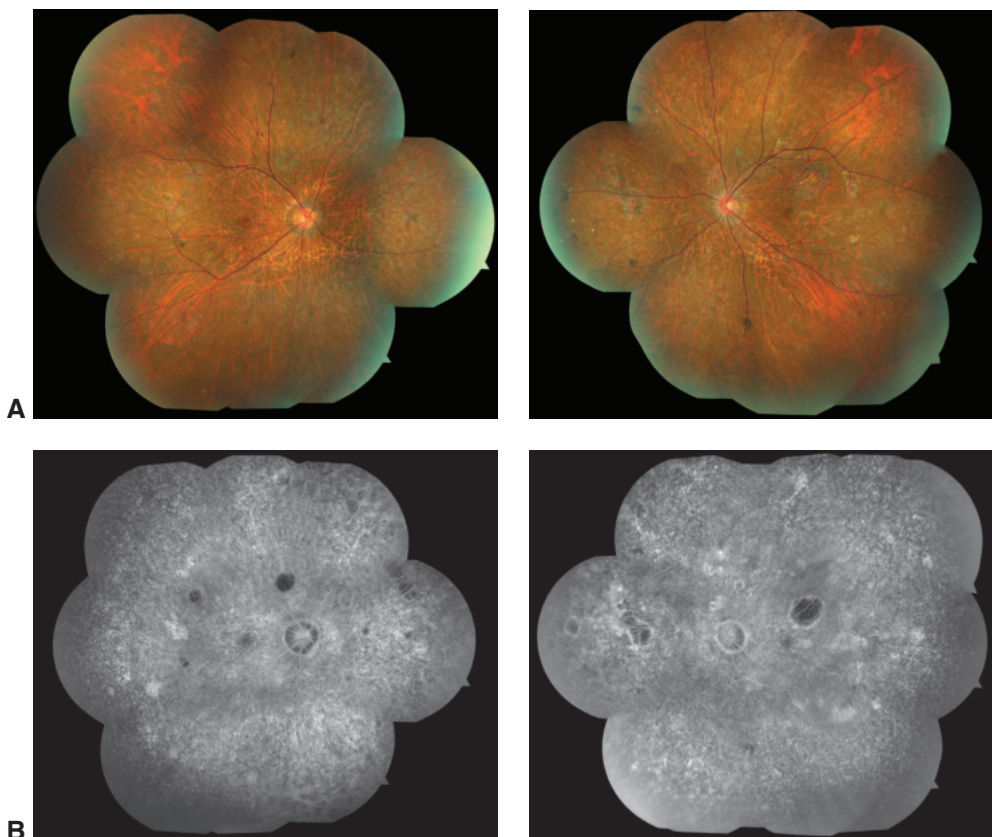


Figure 15-2 Thioridazine toxicity in a patient with schizophrenia. **A**, Color fundus photograph montages of right and left eyes. **B**, Corresponding fluorescein angiography montages. Note the diffuse nummular loss of retinal pigment epithelium (RPE) in the posterior pole and periphery of each eye. (Courtesy of David Sarraf, MD.)

may be mistaken for choroioderemia or Bietti crystalline dystrophy; late-stage symptoms include visual field loss and nyctalopia (night blindness).

Generally, patients taking thioridazine are not monitored ophthalmoscopically because toxicity is rare at standard doses. However, symptomatic patients or patients suspected of having toxicity, especially those who have taken high doses of the drug, should undergo a full retinal evaluation.

Miscellaneous Medications

Other systemic medications that can induce toxicity of the RPE include clofazimine, deferoxamine, and nucleoside reverse transcriptase inhibitors (NRTIs). *Clofazimine* is a phenazine dye used to treat dapsone-resistant leprosy and various autoimmune disorders, such as psoriasis and systemic lupus erythematosus. Its toxicity manifests as a bull's-eye maculopathy. *Deferoxamine* is an iron-chelating agent, which can cause reticular or vitelliform retinal pigment epithelial changes in the macula and can be associated with macular

edema caused by retinal pigment epithelial pump failure. NRTIs such as *dideoxyinosine* have been used in the systemic treatment of patients infected with HIV to inhibit replication of the virus. However, this class of medications can cause mitochondrial toxicity and damage to tissues with high oxygen requirements, such as the optic nerve and RPE. Patients may develop peripheral vision loss associated with a bilateral, symmetric, and midperipheral pattern of concentric mottling and atrophy of the RPE and choriocapillaris. The fundus changes are most readily identified with fundus autofluorescence imaging.

MEK inhibitors, a class of drugs used as chemotherapeutic agents in the treatment of metastatic cancers, can cause a condition similar to central serous chorioretinopathy. This condition is characterized by multifocal serous retinal detachments (Fig 15-3). In rare instances, the use of *sildenafil* has been associated with serous macular detachment and central serous chorioretinopathy, presumably caused by choroidal vascular dilation and choroidal congestion manifesting as increased choroidal thickness on enhanced depth

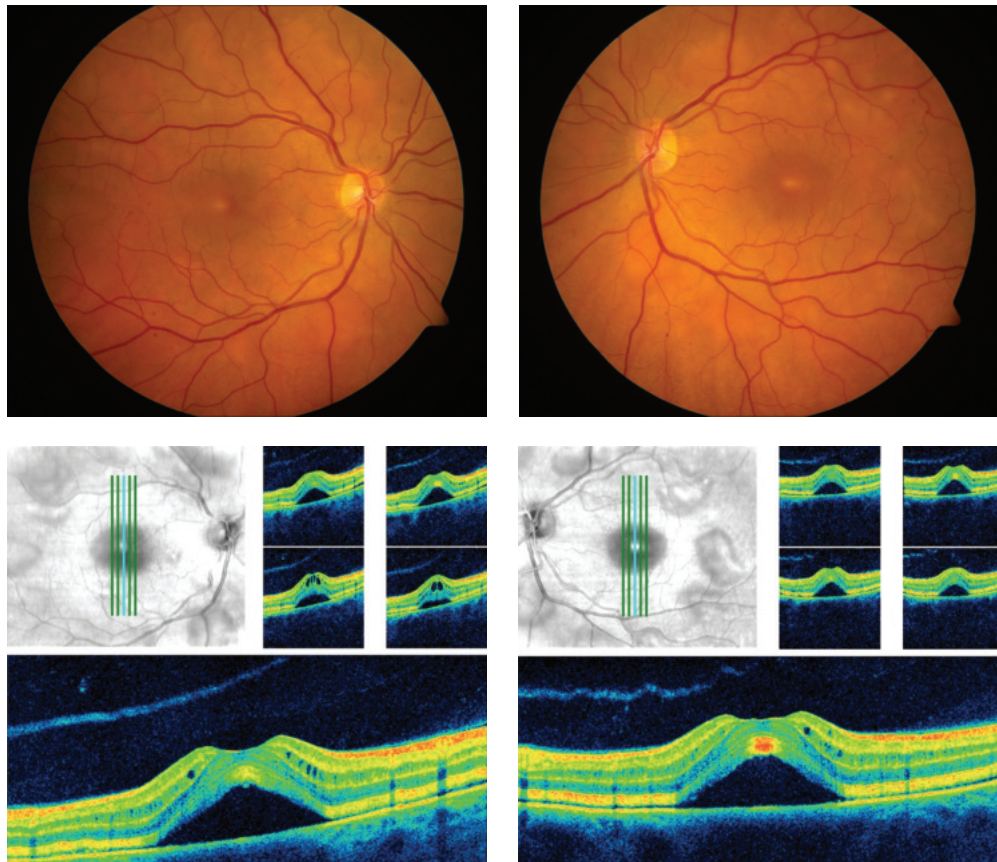
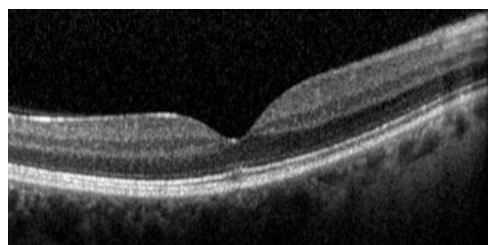


Figure 15-3 MEK toxicity. Color fundus photographs and OCT images of both eyes demonstrate multifocal serous detachments involving the fovea and around the arcades. Patient reported decreased vision 3 weeks after starting the MEK inhibitor trametinib for metastatic cutaneous melanoma. (Courtesy of Stephen J. Kim, MD.)

Figure 15-4 SD-OCT image shows maculopathy in the right eye of a patient with a 10-day history of a central white spot that developed after inhalation of an alkyl nitrite ("popper") for recreational purposes. Note the central presence of inner segment ellipsoid disruption. (Courtesy of Maziar Lalezary, MD.)



imaging (EDI) SD-OCT. *Corticosteroids* are the most common medications to be associated with the development of central serous chorioretinopathy.

Alkyl nitrites ("poppers") are a class of drugs used for recreation. They are inhaled to induce euphoria and relax smooth muscles, usually in preparation for sexual activity; in rare cases, these drugs can cause a toxic maculopathy. Patients are typically young and present with central scotoma or photopsia. Fundus examination may demonstrate a yellow spot on the fovea. SD-OCT imaging may reveal focal disruption of the central inner segment ellipsoid band, indicating an abnormality of the foveal cones (Fig 15-4). Pentosan polysulfate, the only FDA-approved medication for interstitial cystitis, has recently been associated with a pigmentary maculopathy that affects exposed females, with characteristic bilateral findings of parafoveal pigmentary changes, dense hypo- and hyperautofluorescence, and nodular thickening of the RPE on OCT.

- Davies AJ, Kelly SP, Naylor SG, et al. Adverse ophthalmic reaction in poppers users: case series of 'poppers maculopathy'. *Eye (Lond)*. 2012;26(11):1479–1486.
- Gabrielian A, MacCumber MM, Kukuyev A, Mitsuyasu R, Holland GN, Sarraf D. Didanosine-associated retinal toxicity in adults infected with human immunodeficiency virus. *JAMA Ophthalmol*. 2013;131(2):255–259.
- McCannel TA, Chmielowski B, Finn RS, et al. Bilateral subfoveal neurosensory retinal detachment associated with MEK inhibitor use for metastatic cancer. *JAMA Ophthalmol*. 2014;132(8):1005–1009.

Drugs Causing Occlusive Retinopathy or Microvasculopathy

Interferon alfa-2a is an antiviral and immunomodulatory drug used for the treatment of viral hepatitis. This treatment may be complicated by the development of cotton-wool spots and retinal hemorrhages. Affected patients may experience symptoms such as paracentral visual field defects. Ergot alkaloids (vasoconstrictors used to treat migraines) and oral contraceptives have been associated with thrombotic complications, including retinal vein and retinal artery occlusions. *Procainamide* can induce systemic lupus erythematosus and cause extensive "pruning" of second-order retinal vessels and infarction of the retina, leading to severe vision loss.

The aminoglycosides *amikacin* and especially *gentamicin*—administered intraocularly but not systemically—can cause macular infarction and severe macular ischemia, leading to irreversible central vision loss. These agents' narrow therapeutic window has caused their use to decline. Recently, hemorrhagic occlusive retinal vasculitis (HORV) has been associated with intracameral *vancomycin* use for prophylaxis of endophthalmitis in rare

instances. HORV is associated with widespread retinal vascular occlusion and subsequent nonperfusion. The pathogenesis is unclear but is presumed to be a type III hypersensitivity reaction mediated by antibody/antigen complex deposition causing small vessel vasculitis.

Raza A, Mittal S, Sood GK. Interferon-associated retinopathy during the treatment of chronic hepatitis C: a systematic review. *J Viral Hepat.* 2013;20(9):593–599.

Witkin AJ, Shah AR, Engstrom RE, et al. Postoperative hemorrhagic occlusive retinal vasculitis: expanding the clinical spectrum and possible association with vancomycin. *Ophthalmology.* 2015;122(7):1438–1451.

Drugs Causing Ganglion Cell and Optic Nerve Toxicity

Quinine is used as a muscle relaxant for leg cramps and as an antimalarial. It has a narrow therapeutic index that is safe at doses under 2 g, but it causes morbidity at doses greater than 4 g and mortality at doses greater than 8 g. At toxic levels, acute severe vision loss may occur as a result of retinal ganglion cell toxicity, mimicking a central retinal artery occlusion. A cherry-red spot may be observed, and SD-OCT imaging may demonstrate ganglion cell layer thickening and hyperreflectivity. Diffuse inner-retinal atrophy will ensue, accompanied by retinal vascular attenuation and optic atrophy. Full-field ERG testing will show a negative waveform signal, similar to that observed with a central retinal artery occlusion (Fig 15-5). Blindness caused by quinine toxicity is permanent.

Methanol toxicity causes acute blindness. Posterior segment manifestations include acute transient optic nerve head and macular edema. In histologic studies of acute methanol toxicity, the retina, RPE, and optic nerve demonstrate vacuolization, a sign of cell death. Eventually, optic atrophy and occasionally retinal vascular attenuation caused by diffuse ganglion cell loss may develop. Full-field ERG testing shows an electronegative waveform. The most commonly reported sequela of methanol toxicity is optic atrophy.

Narkewicz MR, Rosenthal P, Schwarz KB, et al; PEDS-C Study Group. Ophthalmologic complications in children with chronic hepatitis C treated with pegylated interferon. *J Pediatr Gastroenterol Nutr.* 2010;51(2):183–186.

Drugs Causing Macular Edema

The *taxanes* are a class of microtubule inhibitors that include *paclitaxel*, albumin-bound paclitaxel, and *docetaxel*. These drugs are employed as chemotherapeutics for the treatment of various cancers, including breast carcinoma. In rare cases, they are associated with cystoid macular edema (CME) that is visible on examination or SD-OCT but not on fluorescein angiography. Similarly, the cholesterol-lowering agent *nicotinic acid* can produce angiographically silent CME. Initially, central vision may be impaired, but full recovery follows discontinuation of the drug and resolution of the cystoid edema.

The glitazones *rosiglitazone* and *pioglitazone* are oral hypoglycemics used for the treatment of diabetes mellitus. They can cause severe fluid retention, leading to pulmonary edema, and are occasionally associated with the development or exacerbation of macular edema. *Fingolimod*, which is an oral agent used in the management of relapsing forms

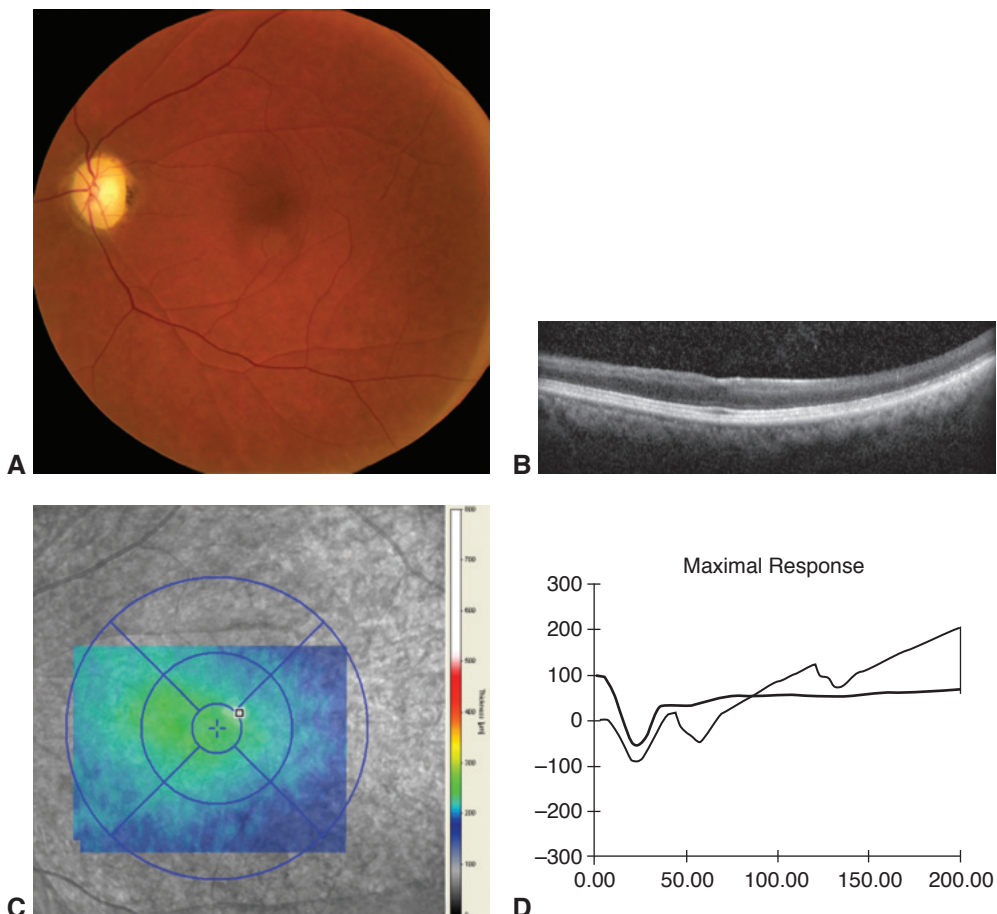


Figure 15-5 Quinine toxicity. **A**, Color fundus photograph shows optic nerve head pallor and retinal vascular attenuation. **B**, SD-OCT image demonstrates diffuse inner-retinal atrophy. **C**, OCT map analysis shows diffuse retinal thinning. **D**, Full-field electroretinogram shows an electronegative response (the positive b-wave amplitude is less than the negative a-wave amplitude). (Courtesy of David Sarraf, MD.)

of multiple sclerosis, can infrequently cause macular edema, usually within 3 months of initiation of treatment; the edema resolves with cessation. Topical prostaglandin F_{2α} analogs have been reported in small case series to cause macular edema. Deferoxamine may also cause secondary macular edema caused by RPE toxicity, as mentioned earlier in the chapter.

Drugs Causing Crystalline Retinopathy

Crystalline retinopathies can be caused by systemic medications and other agents and can be associated with ocular and systemic diseases not discussed in this chapter (Table 15-1). *Tamoxifen* is an antiestrogen drug used as adjuvant therapy following primary treatment

Table 15-1 Causes of Crystalline Retinopathy**Systemic diseases**

- Primary hereditary hyperoxaluria (primary oxalosis)
- Cystinosis
- Sjögren-Larsson syndrome

Drug-induced causes

- Tamoxifen toxicity
- Canthaxanthine toxicity
- Talc emboli (caused by chronic intravenous drug abuse with methylphenidate)
- Nitrofurantoin toxicity
- Methoxyflurane anesthesia (secondary oxalosis)
- Ethylene glycol ingestion (secondary oxalosis)
- Triamcinolone acetonide injection–associated crystalline maculopathy (caused by intravitreal triamcinolone injection)
- West African crystalline maculopathy (long-term kola nut ingestion)

Ocular diseases

- Bietti crystalline dystrophy
- Calcific drusen
- Gyrate atrophy
- Retinal telangiectasia

for breast cancer. Retinopathy is rare at typical doses (20 mg daily), but crystalline retinopathy has been reported in patients receiving high-dose tamoxifen therapy (daily doses greater than 200 mg or cumulative doses greater than 100 g). The maculopathy is characterized by brilliant inner-retinal crystalline deposits clustered around the fovea and may be associated with CME and significant vision loss in severe cases; it may be irreversible. More recently, in rare instances SD-OCT imaging has revealed central loss of the inner segment ellipsoid band in patients receiving low-dose tamoxifen therapy, without crystals visible on fundoscopic examination (Fig 15-6).

A crystalline maculopathy may also occur after ingestion of high doses of *canthaxanthine*, a widely available carotenoid used to simulate tanning. The inner-retinal, glistening canthaxanthine deposits distribute in a doughnut pattern around the macula, with a predilection for the juxtapapillary region, but they do not typically cause vision loss and may resolve after the medication is discontinued.

Intravascular crystalline deposits of oxalate have been observed after the ingestion of ethylene glycol and after prolonged administration of *methoxyflurane* anesthesia (an agent that is no longer used in the United States) in patients with renal dysfunction. Other retinal crystals that may be deposited intravascularly include talc emboli, which are injected along with drugs such as methylphenidate in long-term intravenous drug abusers. The refractile talc deposits usually embolize in the smaller-caliber perifoveal retinal arterioles and may cause peripheral retinal neovascularization in rare cases; they do not typically cause vision loss.

West African crystalline maculopathy was first reported in elderly persons from the Igbo tribe of Nigeria but has been noted in patients from other countries in this region as well. Affected individuals are typically diabetic and demonstrate benign, inert

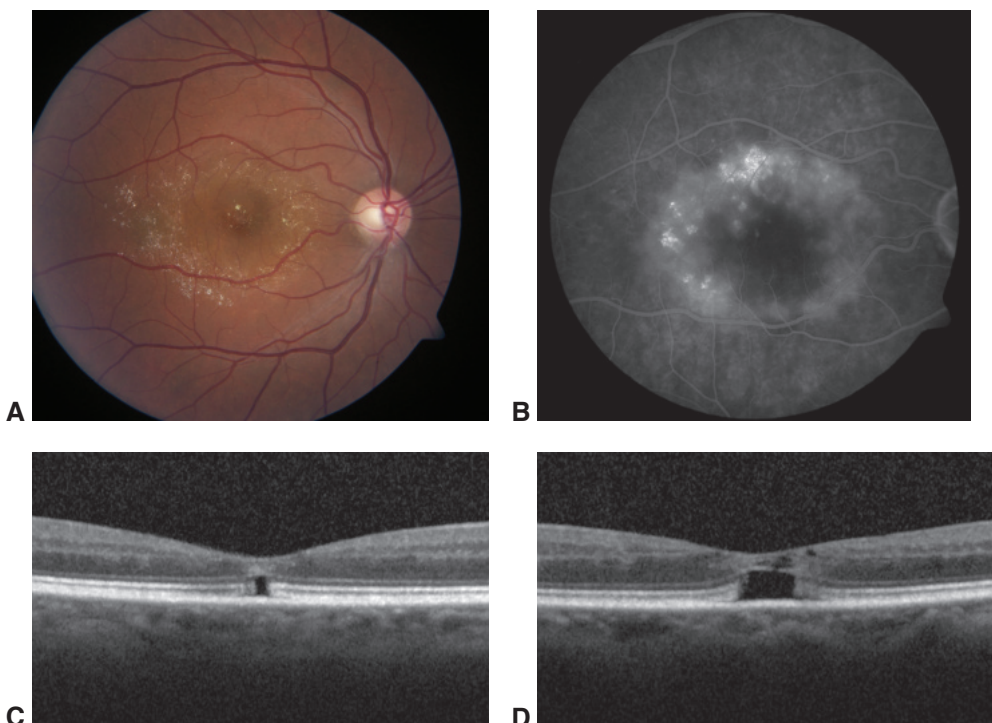


Figure 15-6 Tamoxifen retinopathy. **A**, Color fundus photograph shows tamoxifen retinopathy of the right eye in a male patient who had received high-dose therapy for treatment of glioblastoma of the brain. **B**, Corresponding fluorescein angiography image shows parafoveal cystoid macular edema associated with the extrafoveal tamoxifen deposits. **C**, **D**, SD-OCT images of left and right eyes from a case of low-dose tamoxifen retinopathy, which caused central disruption and loss of the ellipsoid band in each eye. (Parts A and B courtesy of David Sarraf, MD; parts C and D courtesy of Rishi Doshi, MD, and Jorge Fortun, MD.)

inner-retinal refractile crystals of the fovea that are yellow-green in color (Fig 15-7). These crystals, which have been linked to long-term ingestion of kola nuts, are not associated with vision loss.

Drenser K, Sarraf D, Jain A, Small KW. Crystalline retinopathies. *Surv Ophthalmol*. 2006;51(6):535–549.

Drugs Causing Abnormalities in Color Vision and Electroretinography

Phosphodiesterase 5 (PDE-5) inhibitors such as *sildenafil* and *tadalafil* can also partially inhibit phosphodiesterase 6 (PDE-6), an integral enzyme in the phototransduction cascade. Transient blue tinting of vision and temporarily abnormal ERG responses (including a delayed cone b-wave implicit time) have been observed in patients taking high doses of sildenafil. These changes may occur in up to 50% of patients ingesting doses greater than

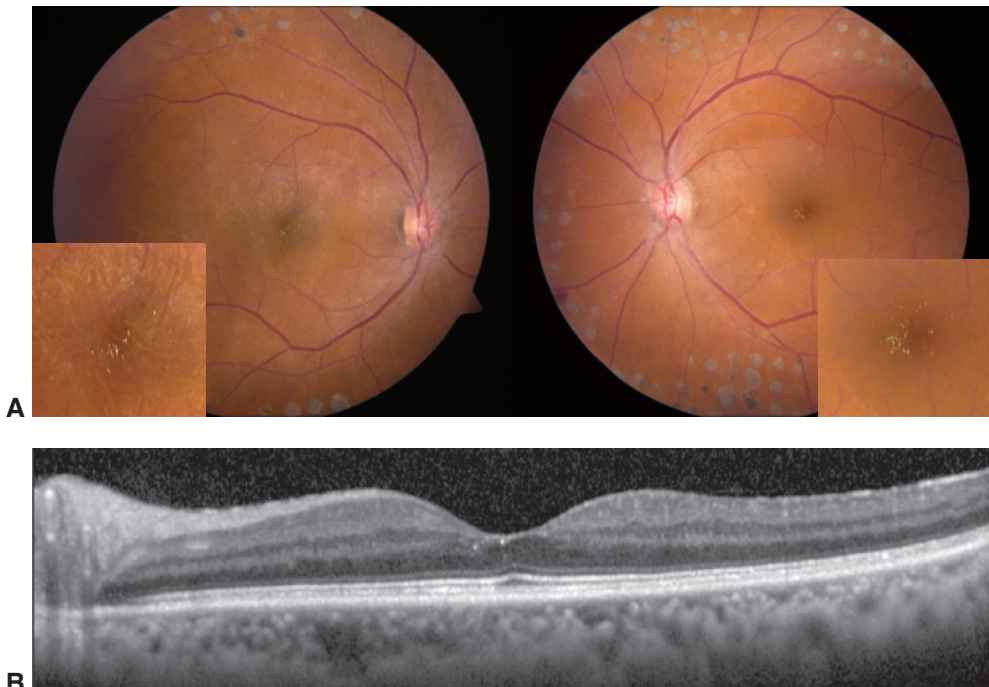


Figure 15-7 West African crystalline maculopathy. **A**, Fundus photographs of a patient from Nigeria with diabetes mellitus and previous panretinal photoocoagulation scars. The distinct yellow-green refractile crystals in the fovea are better visualized in the magnified *inset* images. **B**, OCT image of the left eye shows the crystals located in the inner retina. (*Courtesy of Stephen J. Kim, MD.*)

100 mg, but no permanent retinal toxic effects have been reported. Reversible yellow tinting of vision, or *xanthopsia*, may be caused by the cardiac glycoside *digitalis*.

Some patients taking *isotretinoin* for the treatment of acne have reported poor night vision and have been found to have abnormal dark-adaptation curves and ERG responses. Toxicity seems to be infrequent but is more likely in patients undergoing repetitive courses of therapy. The changes are largely reversible.

The antiepileptic drug *vigabatrin* can cause visual field constriction and ERG abnormalities, including depression of the 30-Hz cone amplitude.

Miscellaneous Drugs Causing Ocular Toxicities

The use of *rifabutin* has been associated with vision loss arising from anterior and posterior uveitis with hypopyon and hypotony. Certain sulfur-derived medications such as *acetazolamide* and *topiramate* can cause medication-induced myopia and associated retinal and choroidal folds and macular edema. Vision loss may be mild (caused by isolated macular folds) or severe (caused by ciliochoroidal effusion, leading to angle-closure glaucoma) and

may be reversed with early recognition and prompt discontinuation of the drug. There are rare reports of *bupropion* causing choroidal effusion.

Historically, and more recently on the Internet, *silver* has been erroneously claimed to have medicinal benefits. Overingestion can cause slate-gray or blue coloring of the skin, referred to as *argyria*. Ocular argyrosis may develop after colloidal silver ingestion over a period longer than 1 year; this condition manifests as ocular pigmentation, black tears, and a dark choroid. The dark choroid is caused by brown-black granules diffusely deposited in Bruch membrane, which can lead to “leopard spotting” and drusenlike deposition.

CHAPTER 16

Retinal Detachment and Predisposing Lesions



This chapter includes a related activity, which can be accessed by scanning the QR code provided in the text or going to www.aao.org/bcscactivity_section12.

This chapter reviews the most common lesions and antecedent events that lead to the development of retinal breaks and the subsequent mechanism of retinal detachment. After reading the chapter, the reader should be comfortable with the diagnosis and management of retinal detachment and its predisposing lesions.

Posterior Vitreous Detachment

The vitreous gel is attached most firmly at the *vitreous base*, a circumferential zone straddling the ora serrata that extends approximately 2 mm anterior and 4 mm posterior to the ora. Vitreous collagen fibers at this base are so firmly attached to the retina and pars plana epithelium that the vitreous cannot be separated without tearing these tissues. The vitreous is also firmly attached at the margin of the optic nerve head, at the macula, along major vessels, at the margins of lattice degeneration, and at chorioretinal scars.

Most retinal tears result from traction caused by spontaneous or traumatic *posterior vitreous detachment* (PVD) (Fig 16-1). The predisposing event is syneresis (collapse) of the central vitreous. There is increasing evidence that age-related PVD is insidious and slowly progressive over many years. A PVD typically begins with a shallow separation in the perifoveal cortical vitreous. Liquid vitreous enters through a cortical tear and detaches the macular vitreous cortex, causing a partial vitreous detachment. The early stages are usually asymptomatic and occult; in most eyes, the evolving PVD remains subclinical for years until separation from the optic nerve head margin (the area of Martegiani) occurs. This separation from the optic nerve head is often accompanied by symptoms associated with the appearance of a Weiss ring. The vitreous gel remains attached at the vitreous base. Vitreous traction on the retina can produce a retinal break, usually at the posterior edge of the vitreous base (Fig 16-2).

The prevalence of PVD increases with age. Other conditions associated with vitreous syneresis, synchysis (liquefaction), and PVD include aphakia, pseudophakia with open posterior capsule, inflammatory disease, trauma, vitreous hemorrhage, and axial myopia. Whether the vitreous is attached to or separated from the surface of the retina may be



Figure 16-1 Posterior vitreous detachment. Color fundus photograph (**A**) shows attached vitreous and (**B**) shows an acute Weiss ring over the fovea with obscuration (arrow) occurring several days later. (Courtesy of Stephen J. Kim, MD.)

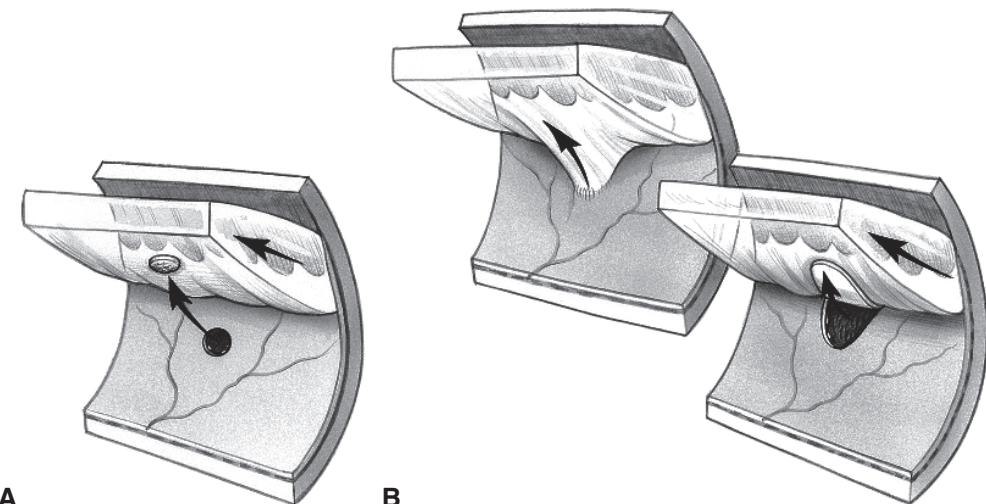


Figure 16-2 Schematic representations of mechanisms of retinal tear formation associated with posterior vitreous separation. **A**, Round or oval hole. **B**, Flap tear: posterior extension of vitreous base with firm vitreoretinal attachment. (Illustration by Christine Gralapp, based on illustrations by Tim Hengst.)

difficult to determine using biomicroscopy. Clinical studies typically reveal a low incidence of PVD in patients younger than 50 years. Autopsy studies demonstrate PVD in fewer than 10% of patients under age 50 years but in 63% of those over age 70 years.

Many patients do not report acute symptoms when a PVD occurs. Symptoms of PVD at the initial examination include the entoptic phenomena of photopsias (flashing lights), multiple floaters, and the appearance of a curtain or cloud across the visual field. Patients with these symptoms should be examined promptly, and office staff should be made aware of the urgency of these symptoms. Photopsias are caused by the physical stimulus of vitreoretinal traction on the retina. Floaters are caused by vitreous opacities such as blood, glial cells

torn from the optic nerve head, or aggregated collagen fibers, all of which can cast shadows on the retina.

Vitreous hemorrhage may arise from avulsion of superficial retinal or prepapillary vessels or from rupture of retinal vessels that cross retinal tears. Important predictors of subsequent new retinal breaks are vitreous hemorrhage at the initial examination and an increase in the number of floaters after the initial examination. Overall, 7%–18% of all patients with acute symptomatic PVD have retinal tears. If vitreous hemorrhage is present, then 50%–70% have retinal tears, versus only 7%–12% without vitreous hemorrhage. Patients with an acute PVD complicated by a retinal tear are 7 times more likely to present with vitreous pigment or granules than are those without a tear.

van Overdam KA, Bettink-Remeijer MW, Klaver CC, Mulder PG, Moll AC, van Meurs JC. Symptoms and findings predictive for the development of new retinal breaks. *Arch Ophthalmol*. 2005;123(4):479–484.

Examination and Management of Posterior Vitreous Detachment

Indirect ophthalmoscopy with scleral depression or slit-lamp biomicroscopy with a 3-mirror lens or indirect contact lens are used to clinically diagnose PVD and rule out retinal breaks or detachment. In unclear cases, optical coherence tomography (OCT) can be employed to confirm the state of the vitreous gel on the optic nerve head and macula. Re-examination of the patient 2–4 weeks following presentation may be appropriate, because as the PVD evolves over time, new retinal breaks may occur. Additional risk factors to consider in follow-up determination include aphakia, myopia, fellow-eye history, family history of retinal detachment, and signs of Stickler syndrome. All patients should be instructed to return to the ophthalmologist immediately if they notice a change in symptoms, such as increasing numbers of floaters or the development of visual field loss.

If a large vitreous hemorrhage precludes a complete examination, bilateral ocular patching and bed rest, with the patient's head elevated 45° or more for a few days, may allow the hemorrhage to settle sufficiently to permit detection of breaks in a superior location. Echography may be performed to find flap tears and rule out retinal detachment and other fundus lesions. If the cause of the hemorrhage cannot be found, the patient should be reexamined at frequent, regular intervals, and early vitrectomy should be considered to reduce the risk of retinal detachment.

Byer NE. Natural history of posterior vitreous detachment with early management as the premier line of defense against retinal detachment. *Ophthalmology*. 1994;101(9):1503–1514.

Lesions That Predispose Eyes to Retinal Detachment

Lattice Degeneration

Lattice degeneration, a vitreoretinal interface abnormality, is present in 6%–10% of the general population and is bilateral in one-third to one-half of affected patients. It occurs more commonly in—but is not limited to—myopic eyes; a familial predilection is present.

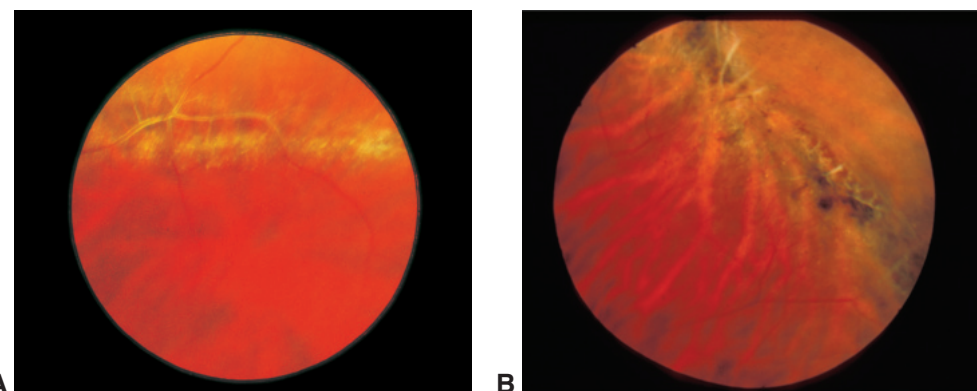


Figure 16-3 Lattice degeneration. **A**, Color fundus photograph of lattice degeneration as viewed without scleral indentation. Vascular sheathing is apparent where the vessel crosses the area of lattice. Characteristic white lattice lines are visible. **B**, Color fundus photograph of another example of lattice degeneration demonstrates associated hyperpigmentation, which is commonly observed. (*Part A used with permission from Byer NE. Peripheral Retina in Profile: A Stereoscopic Atlas. Torrance, CA: Criterion Press; 1982.*)

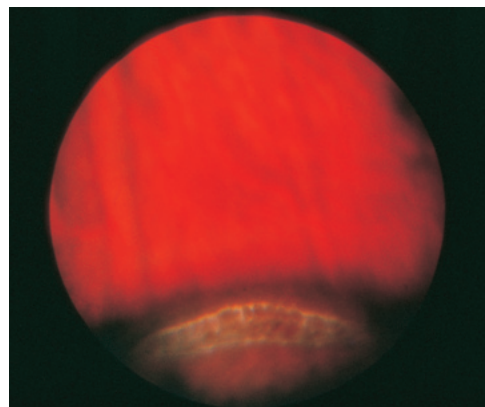


Figure 16-4 Fundus photograph of lattice degeneration as viewed with scleral indentation. (*Reproduced with permission from Byer NE. Peripheral Retina in Profile: A Stereoscopic Atlas. Torrance, CA: Criterion Press; 1982.*)

Lattice degeneration may predispose eyes to retinal breaks and detachment. The most important histologic features include varying degrees of atrophy and irregularity of the inner layers, an overlying pocket of liquefied vitreous, condensation, and adherence of vitreous at the margin of the lesion (Figs 16-3, 16-4, 16-5).

Lattice degeneration is found in approximately 20%–30% of all eyes that present with rhegmatogenous retinal detachments (discussed later in this chapter). However, because the lattice degeneration is not necessarily causative, prophylactic laser treatment is not universally recommended. When lattice degeneration is the cause of retinal detachment, a tractional tear at the lateral or posterior margin of the lattice lesion or, less commonly, an atrophic hole within the zone of lattice itself occurs (Fig 16-6). Retinal detachments secondary to atrophic holes typically occur in young patients with myopic eyes and no vitreous detachment; they are generally asymptomatic until fixation is involved.

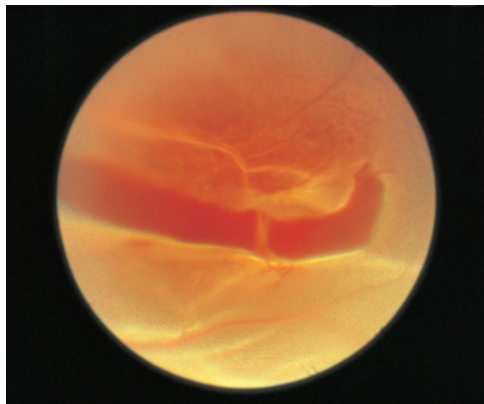


Figure 16-5 Color fundus photograph of lattice degeneration shows a large, posteriorly located flap tear and associated detachment. Note vessel bridging the tear. (Used with permission from Byer NE. Peripheral Retina in Profile: A Stereoscopic Atlas. Torrance, CA: Criterion Press; 1982.)

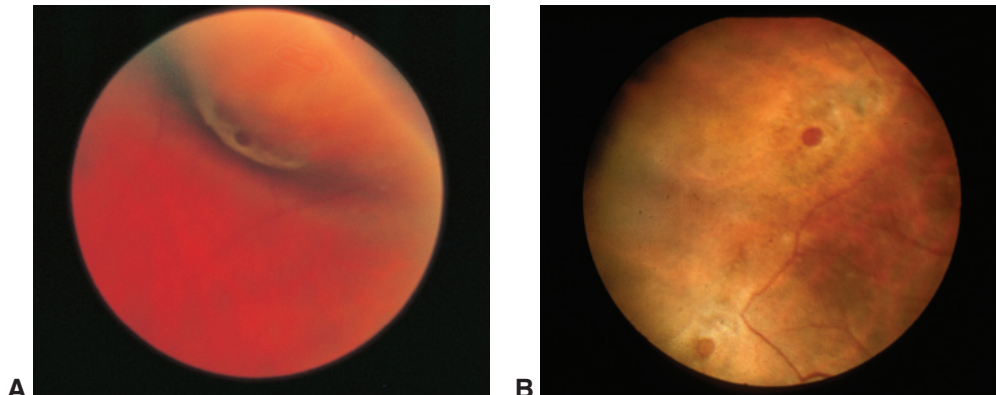


Figure 16-6 Lattice degeneration with atrophic hole. **A**, Fundus photograph of lattice degeneration with a small atrophic hole as viewed with scleral depression. **B**, Fundus photograph of an example of an atrophic hole as may be observed in lattice degeneration without scleral depression. (Part A courtesy of Norman E. Byer, MD.)

Byer NE. Lattice degeneration of the retina. *Surv Ophthalmol*. 1979;23(4):213–248.

Byer NE. Long-term natural history of lattice degeneration of the retina. *Ophthalmology*. 1989;96(9):1396–1402.

Vitreoretinal Tufts

Peripheral retinal tufts are small, peripheral, focal areas of elevated glial hyperplasia associated with vitreous or zonular attachment and traction. Tractional tufts are classified according to anatomical, pathogenetic, and clinical distinctions into the following groups:

- noncystic retinal tufts (Fig 16-7)
- cystic retinal tufts
- zonular traction retinal tufts (Fig 16-8)

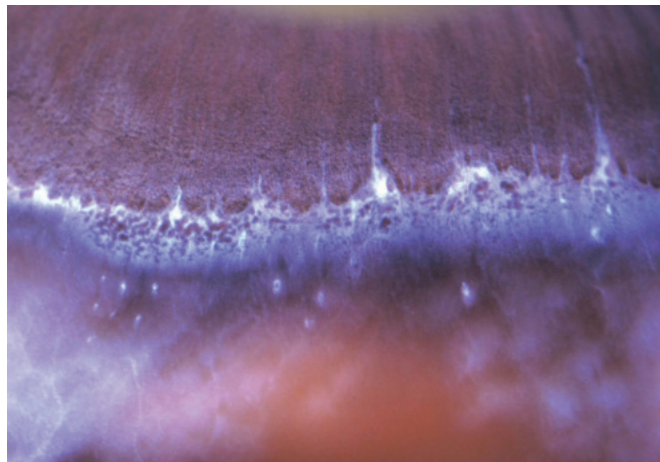


Figure 16-7 Color photograph of a gross eye specimen shows a cluster of white surface nodules with characteristic gross appearance and location of noncystic retinal tufts. (Used with permission from Foos RY, Silverstein RN, eds. System of Ocular Pathology. Vol. 3. Los Angeles: iPATH Press; 2004.)

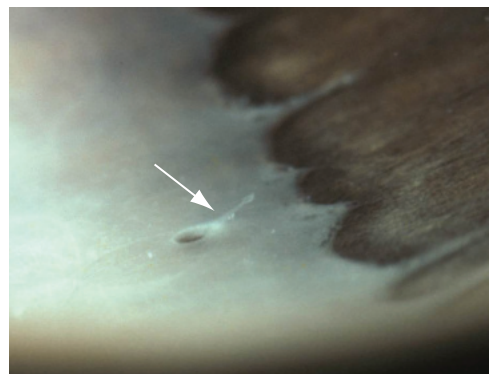


Figure 16-8 Color photograph of a gross eye specimen shows a small zonular traction tuft (arrow) with cystic base. Note that the tuft points anteriorly toward the peripheral lens. (Used with permission from Foos RY, Silverstein RN, eds. System of Ocular Pathology. Vol. 3. Los Angeles: iPATH Press; 2004.)

Retinal pigment epithelial hyperplasia may surround the tuft. Cystic and zonular traction retinal tufts, both with firm vitreoretinal adhesions, may predispose eyes to retinal tears and detachment.

Byer NE. Cystic retinal tufts and their relationship to retinal detachment. *Arch Ophthalmol*. 1981;99(10):1788–1790.

Meridional Folds, Enclosed Ora Bays, and Peripheral Retinal Excavations

Meridional folds are folds of redundant retina, usually located superonasally. They are usually associated with dentate processes but may also extend posteriorly from ora bays. Occasionally, tears associated with PVD occur at the most posterior limit of the folds (see Chapter 1, Fig 1-3). Retinal tears can also occur at or near the posterior margins of enclosed ora bays, which are oval islands of pars plana epithelium located immediately posterior to the ora serrata and completely or almost completely surrounded by peripheral retina (Fig 16-9). Occasionally, tears may occur at the site of peripheral retinal excavations, which represent a

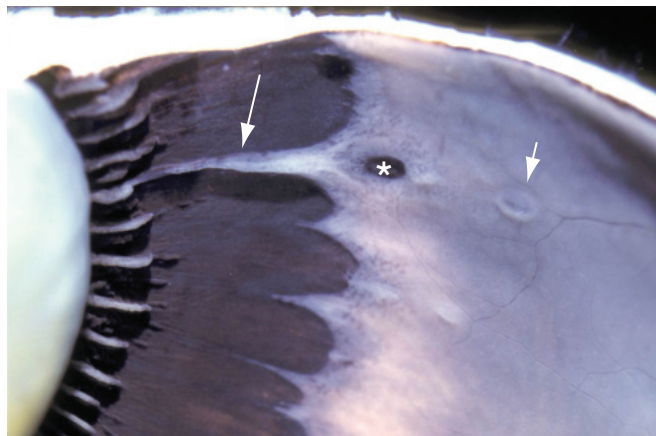


Figure 16-9 Color photograph of a gross eye specimen shows a meridional complex, consisting of an atypical and large dentate process (arrow) that is continuous with a ciliary process of the pars plicata and an area of enclosed pars plana and ora bay (asterisk). Slightly posterior to the complex is a small area in the same meridian that appears to be excavated but is in fact a cyst (small arrow). (Used with permission from Foos RY, Silverstein RN, eds. System of Ocular Pathology. Vol. 3. Los Angeles: iPATH Press; 2004.)

mild form of lattice degeneration. The excavations may have firm vitreoretinal adhesions and are found adjacent to, or up to 4 disc diameters posterior to, the ora serrata. They are often aligned with meridional folds.

Engstrom RE Jr, Glasgow BJ, Foos RY, Straatsma BR. Degenerative diseases of the peripheral retina. In: Tasman W, Jaeger EA, eds. *Duane's Clinical Ophthalmology on DVD-ROM*. Vol 3. Philadelphia: Lippincott Williams & Wilkins; 2013:chap 26.

Lesions That Do Not Predispose Eyes to Retinal Detachment

Paving-Stone Degeneration

Paving-stone (or cobblestone) degeneration is characterized by peripheral, small, discrete areas of atrophy of the outer retina; it appears in 22% of individuals older than 20 years (Fig 16-10). The atrophic areas may occur singly or in groups and are sometimes confluent. On histologic examination, these “paving stones” are characterized by atrophy of the retinal pigment epithelium (RPE) and outer retinal layers, attenuation or absence of the choriocapillaris, and adhesions between the remaining neuroepithelial layers and Bruch membrane. These lesions are most common in the inferior quadrants, anterior to the equator. Ophthalmoscopically, they appear yellowish white and are sometimes surrounded by a rim of hypertrophic RPE. Because the RPE is absent or hypoplastic, large choroidal vessels are visible beneath the lesions.

Retinal Pigment Epithelial Hyperplasia

When stimulated by chronic low-grade traction, retinal pigment epithelial cells proliferate. Diffuse retinal pigment epithelial hyperplasia may be observed straddling the ora serrata, in latitudes that correspond roughly to the insertion of the vitreous base. They

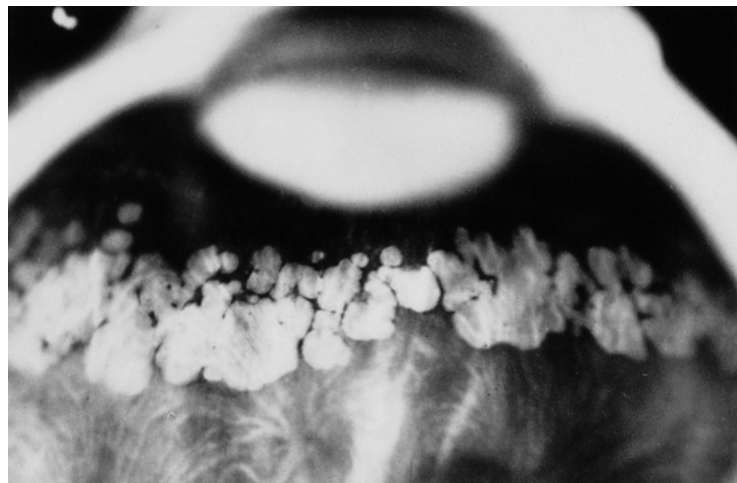


Figure 16-10 Gross appearance of paving-stone degeneration. (Used with permission from Green VR. *Pathology of the retina*. In: Frayer WC, ed. Lancaster Course in Ophthalmic Histopathology, unit 9, Philadelphia: FA Davis; 1988:181.)

may also occur focally on the pars plana and peripheral retina, especially in areas of focal traction such as vitreoretinal tufts and lattice degeneration. Areas of previous inflammation and trauma may also be sites of retinal pigment epithelial hyperplasia.

Retinal Pigment Epithelial Hypertrophy

Acquired retinal pigment epithelial hypertrophy is a degenerative change associated with aging that commonly occurs in the periphery, often in a reticular pattern. Histologically, it is characterized by large cells and by large, spherical melanin granules. Similar histologic features are present in congenital hypertrophy of the RPE (eg, grouped pigmentation, or “bear tracks”).

Peripheral Cystoid Degeneration

Typical peripheral cystoid degeneration, characterized by zones of microcysts in the far-peripheral retina, is present in almost all adults over the age of 20 years. Although retinal holes may form in these areas, they rarely cause retinal detachment. *Reticular peripheral cystoid degeneration* is almost always located posterior to typical peripheral cystoid degeneration. It usually occurs in the inner retina and presents with a linear or reticular pattern that follows the retinal vessels. This form is found in approximately 20% of adults and may, in some instances, develop into reticular degenerative retinoschisis.

Retinal Breaks

A retinal break is defined as any full-thickness defect in the neurosensory retina. Breaks are clinically significant in that they may allow liquid from the vitreous cavity to enter the potential space between the sensory retina and the RPE, thereby causing a rhegmatogenous

retinal detachment. Some breaks are caused by atrophy of inner retinal layers (holes); others result from vitreoretinal traction (tears). Breaks resulting from trauma are discussed in the next section. Retinal breaks may be classified as

- flap, or horseshoe, tears
- giant retinal tears
- operculated holes
- retinal dialyses
- atrophic retinal holes

A *flap tear* occurs when a strip of retina is pulled anteriorly by vitreoretinal traction, often in the course of a posterior vitreous detachment or trauma. A tear is considered symptomatic when the patient reports photopsias, floaters, or both. A *giant retinal tear* extends 90° (3 clock-hours) or more circumferentially and usually occurs along the posterior edge of the vitreous base. An *operculated hole* occurs when traction is sufficient to tear a piece of retina completely free from the adjacent retinal surface. A *retinal dialysis* is a circumferential, linear break that occurs at the ora serrata, with vitreous base attached to the retina posterior to the tear's edge; it is commonly a consequence of blunt trauma. An *atrophic hole* is generally not associated with vitreoretinal traction and has not been linked to an increased risk of retinal detachment.

American Academy of Ophthalmology Retina/Vitreous Panel. Preferred Practice Pattern Guidelines. *Posterior Vitreous Detachment, Retinal Breaks, and Lattice Degeneration*. San Francisco: American Academy of Ophthalmology; 2014. Available at: www.aao.org/ppp

Traumatic Breaks

Blunt or penetrating eye trauma can cause retinal breaks by direct retinal perforation, contusion, or vitreous traction. Fibrocellular proliferation occurring later at the site of an injury may cause vitreoretinal traction and subsequent detachment. Also see Chapter 18 in this volume.

Blunt trauma can cause retinal breaks by direct contusive injury to the globe through 2 mechanisms: (1) *coup*, adjacent to the point of trauma, and (2) *contrecoup*, opposite the point of trauma. Blunt trauma compresses the eye along its anteroposterior axis and expands it in the equatorial plane. Because the vitreous body is viscoelastic, slow compression of the eye has no deleterious effect on the retina. However, rapid compression of the eye results in severe traction on the vitreous base that may tear the retina.

Contusion injury may cause large, ragged equatorial breaks, dialysis, or a macular hole. Traumatic breaks are often multiple, and they are commonly found in the inferotemporal and superonasal quadrants. The most common injuries are dialyses, which may be as small as 1 ora bay (the distance between 2 retinal dentate processes at the latitude of the ora serrata) or may extend 90° or more. Dialyses are usually located at the posterior border of the vitreous base but can also occur at the anterior border (Fig 16-11; Activity 16-1). Avulsion of the vitreous base may be associated with dialysis and is considered pathognomonic of ocular contusion. The vitreous base can be avulsed from the underlying retina and nonpigmented epithelium of the pars plana without tearing either one; generally, however, one or both are also torn in the process. Less common types of breaks caused by blunt trauma are

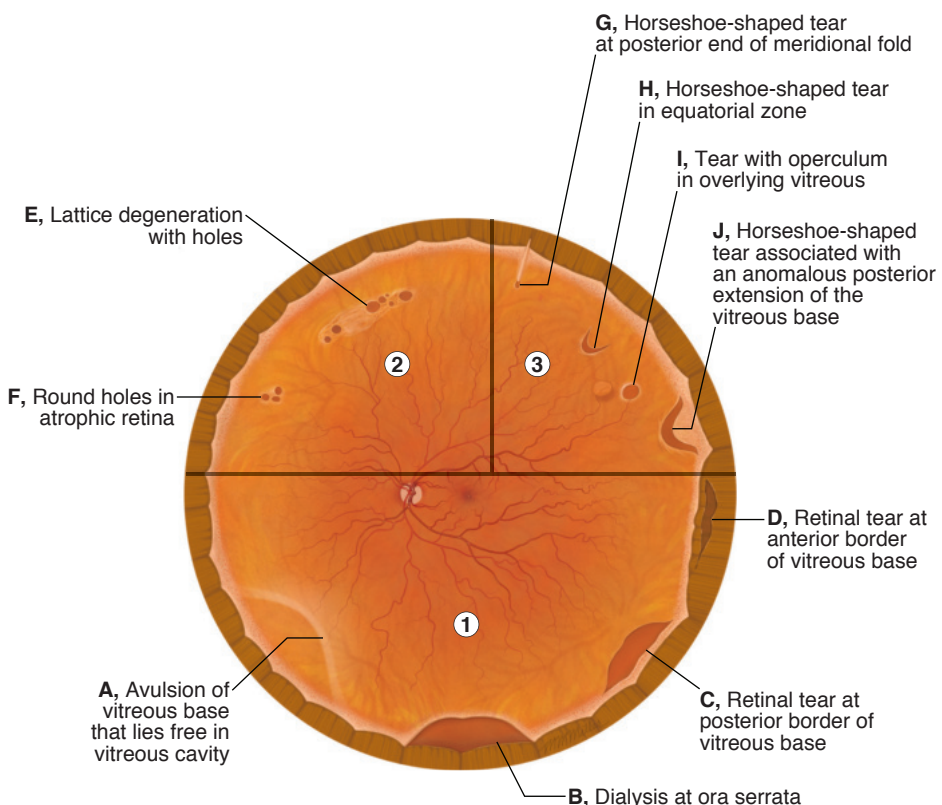


Figure 16-11 Schematic illustration of retinal tears and holes. **Part 1**, Retinal breaks at borders of the vitreous base. **A**, Avulsion of vitreous base that lies free in the vitreous cavity. **B**, Dialysis of the ora serrata. **C**, Retinal tear at the posterior border of the vitreous base. **D**, Retinal tear at the anterior border of the vitreous base. **Part 2**, Retinal breaks with areas of abnormal vitreoretinal interface (lattice degeneration). **E**, Lattice degeneration with holes. **F**, Round holes in atrophic retina. **Part 3**, Retinal breaks associated with abnormal vitreoretinal attachments. **G**, Horseshoe-shaped tear at the posterior end of a meridional fold. **H**, Horseshoe-shaped tear in the equatorial zone. **I**, Tear with operculum in the overlying vitreous. **J**, Horseshoe-shaped tear associated with an anomalous posterior extension of the vitreous base. (Illustration by Mark M. Miller.)

horseshoe-shaped tears (which may occur at the posterior margin of the vitreous base, at the posterior end of a meridional fold, or at the equator) and operculated holes.



ACTIVITY 16-1 Anatomy marker activity: Retinal tears and holes.

Courtesy of Mark M. Miller and Colin A. McCannel, MD.



Access all Section 12 activities at www.aaos.org/bcscactivity_section12.



Trauma in Young Eyes

Although young patients have a higher incidence of eye injury than do other age groups, only in rare instances does the retina detach immediately following blunt trauma, because young vitreous has not yet undergone *syneresis*, or liquefaction. The vitreous, therefore, does not allow fluid movement through the retinal tears or dialyses. With time, however,

the vitreous may liquefy over a tear, allowing fluid to pass through the break to detach the retina. The clinical presentation of the retinal detachment is usually delayed:

- 12% of detachments are identified immediately.
- 30% are identified within 1 month.
- 50% are identified within 8 months.
- 80% are identified within 24 months.

Traumatic retinal detachments in young patients may be shallow and often show signs of chronicity, including multiple demarcation lines, subretinal deposits, and intraretinal schisis.

When posterior vitreous separation is present or occurs later after trauma, retinal breaks are often associated with abnormal vitreoretinal attachments and may resemble nontraumatic breaks. Retinal detachments may occur acutely in these patients.

Prophylactic Treatment of Retinal Breaks

Any retinal break can cause a retinal detachment by allowing liquid from the vitreous cavity to pass through the break and separate the sensory retina from the RPE. However, the vast majority of retinal holes or breaks do not cause a detachment.

The ophthalmologist may consider prophylactic treatment of breaks in an attempt to reduce the risk of retinal detachment (Table 16-1). Treatment does not eliminate the risk of new tears or detachment.

The goal of prophylactic laser treatment or cryotherapy of retinal breaks is the creation of a chorioretinal adhesion around each break to prevent fluid from entering the subretinal space (Fig 16-12). If subretinal fluid is present, treatment is applied so it surrounds the area of subretinal fluid. If insufficient treatment is applied, vitreous traction can lead to anterior extension of horseshoe tears and retinal detachment. Similarly, when treating lattice degeneration, the entire lesion needs to be surrounded with treatment applications.

In considering prophylaxis, the ophthalmologist weighs numerous factors, including symptoms, family history, residual traction, size and location of the break, phakic status,

Table 16-1 Prophylactic Treatment of Retinal Breaks

Type of Retinal Lesion	Treatment
Acute symptomatic dialysis	Treat promptly
Acute symptomatic horseshoe tear	Treat promptly
Acute symptomatic operculated hole	Consider treatment
Asymptomatic atrophic round hole	Usually observed without treatment
Asymptomatic dialysis	No consensus guidelines, but consider treatment
Asymptomatic horseshoe tear (no subretinal fluid)	Consider treatment
Asymptomatic lattice degeneration, with or without holes (no subretinal fluid)	Usually does not require treatment
Asymptomatic operculated tear	Usually observed without treatment
Eyes with lattice degeneration, atrophic holes, or asymptomatic retinal tear where the fellow eye has had a retinal detachment	No consensus guidelines, but consider treatment



Figure 16-12 Widefield image shows a retinal tear inadequately surrounded by laser and subsequent retinal detachment. (Courtesy of Stephen J. Kim, MD.)

refractive error, status of the fellow eye, presence of subretinal fluid, and availability of the patient for follow-up evaluation. Prophylaxis is sometimes contraindicated in eyes with more than 6.00 diopters (D) of myopia and more than 6 clock-hours of lattice degeneration. The following discussion serves only as a broad guideline, because many clinical factors should be considered in each patient. (Also see the discussion of hereditary hyaloideoretinopathies with optically empty vitreous in Chapter 17.)

Symptomatic Retinal Breaks

Overall, 7%–18% of eyes with a symptomatic PVD are found to have 1 or more tractional tears at the time of the initial examination. Numerous clinical studies have demonstrated that acute, symptomatic breaks are at greater risk of progressing to retinal detachment, especially if there is associated vitreous hemorrhage. Therefore, *acute symptomatic flap tears* are commonly treated prophylactically.

Acute operculated holes are less likely to cause detachment because there is no residual traction on the adjacent retina, and they usually are not treated. However, if slit-lamp biomicroscopy reveals persistent vitreous traction at the margin of an operculated hole, if the hole is large or located superiorly, or if there is vitreous hemorrhage, prophylaxis should be considered.

Atrophic holes are often incidental findings in a patient who presents with an acute PVD. Generally, treatment is not recommended for these holes.

Asymptomatic Retinal Breaks

Asymptomatic flap tears progress to retinal detachment in approximately 5% of cases. Because of this low risk, treatment is not universally recommended in emmetropic, phakic eyes. However, asymptomatic flap tears accompanied by lattice degeneration, myopia, sub-clinical detachment, aphakia, pseudophakia, or a history of retinal detachment in the fellow eye have an increased risk of retinal detachment, and treatment may be considered. Asymptomatic operculated holes and atrophic holes rarely cause retinal detachment and therefore treatment is not generally recommended.

Byer NE. What happens to untreated asymptomatic retinal breaks, and are they affected by posterior vitreous detachment? *Ophthalmology*. 1998;105(6):1045–1050.

Lattice Degeneration

Although only limited data are available, an 11-year follow-up study of patients with untreated lattice degeneration and no symptomatic tears showed that retinal detachment occurred in approximately 1% of cases. Thus, the presence of lattice, with or without atrophic holes, generally does not require prophylaxis in the absence of other risk factors or symptoms. If lattice degeneration is present in a patient with additional risk factors, such as retinal detachment in the fellow eye, flap tears, pseudophakia, or aphakia, then prophylactic treatment can be considered.

Byer NE. Long-term natural history of lattice degeneration of the retina. *Ophthalmology*. 1989;96(9):1396–1401.

Wilkinson CP. Interventions for asymptomatic retinal breaks and lattice degeneration for preventing retinal detachment. *Cochrane Database Syst Rev*. 2014;(9):CD003170.

Aphakia and Pseudophakia

Because aphakic and pseudophakic eyes have higher risks of retinal detachment (1%–3%) than do phakic eyes, such patients should be warned of potential symptoms and carefully examined if symptoms occur. In a population-based 25-year follow-up study that compared eyes that underwent cataract surgery with eyes that did not, the probability ratio of retinal detachment following cataract surgery was greatest in the first year (an approximately 11-fold difference, compared with approximately 4-fold in years 5 through 20). The cumulative risk of retinal detachment steadily increased to 1.79% at 20 years. Risk factors for the development of retinal detachment following cataract surgery include male sex, younger age, myopia, increased axial length, posterior capsular tear, and absence of a PVD.

Erie JC, Raecker MA, Baratz KH, Schleck CD, Burke JP, Robertson DM. Risk of retinal detachment after cataract extraction, 1980–2004: a population-based study. *Ophthalmology*. 2006;113(11):2026–2032.

Fellow Eye in Patients With Retinal Detachment

In patients with retinal detachment, the fellow-eye risk of detachment is approximately 10% for phakic retinal detachment and as high as 20%–36% for aphakic or pseudophakic detachment. Prophylactic treatment of flap tears and lattice degeneration is often recommended.

Folk JC, Arrindell EL, Klugman MR. The fellow eye of patients with phakic lattice retinal detachment. *Ophthalmology*. 1989;96(1):72–79.

Subclinical Retinal Detachment

The term *subclinical retinal detachment* is used in various ways. Although it may refer to an asymptomatic retinal detachment, it usually describes a detachment in which subretinal fluid extends more than 1 disc diameter from the break but not more than 2 disc diameters posterior to the equator. Because approximately 30% of such detachments progress, treatment is often recommended. Treatment is advised especially for symptomatic

patients or cases involving traction on the break. A demarcation line suggests a lower risk; however, progression may occur through the demarcation line.

Brod RD, Flynn HW Jr, Lightman DA. Asymptomatic rhegmatogenous retinal detachments. *Arch Ophthalmol.* 1995;113(8):1030–1032.

Retinal Detachment

Retinal detachments are classified as rhegmatogenous, tractional, or exudative. The most common are *rhegmatogenous retinal detachments* (RRDs). The term is derived from the Greek *rhegma*, meaning “break.” RRDs are caused by fluid passing from the vitreous cavity through a retinal break into the potential space between the sensory retina and the RPE. *Tractional detachments* are caused by proliferative membranes that contract and elevate the retina; these are less common. Combinations of tractional and rhegmatogenous pathophysiologic components may also lead to retinal detachment. *Exudative*, or *secondary*, *detachments* are caused by retinal or choroidal diseases in which fluid leaks beneath the sensory retina and accumulates there.

The differential diagnosis of retinal detachment includes retinoschisis, choroidal tumors, and retinal elevation secondary to detachment of the choroid. Table 16-2 lists diagnostic features of the 3 forms of retinal detachment.

Rhegmatogenous Retinal Detachment

The Rochester epidemiology project determined that rhegmatogenous retinal detachment has an annual incidence of 12.6 per 100,000 persons in a primarily White population. A given individual’s risk is affected by the presence or absence of certain factors, including myopia, family history, fellow-eye retinal tear or detachment, recent vitreous detachment, trauma, peripheral high-risk lesions, and vitreoretinal degenerations. Current or recent use of fluoroquinolones may also be a risk factor, but the evidence for a causal relationship is controversial.

In 90%–95% of RRDs, a definite retinal break can be found, often with the help of Lincoff rules (Figs 16-13, 16-14). In the remainder, an occult break is presumed to be present. If no break can be found, the ophthalmologist must rule out all other causes of retinal elevation. Half of patients with RRD have photopsias, or *floaters*. The intraocular pressure is usually lower in the affected eye than in the fellow eye but may occasionally be higher. A Shafer sign, descriptively termed “tobacco dust” due to its small clumps of pigmented cells, is frequently present in the anterior vitreous. The retina detaches progressively from the periphery to the optic nerve head; usually it has convex borders and contours and a corrugated appearance, especially in recent retinal detachments, and undulates with eye movements. In a long-standing RRD, however, the retina may appear smooth and thin. Fixed folds resulting from *proliferative vitreoretinopathy* (PVR) almost always indicate an RRD. Shifting fluid may occur, but it is uncommon and more typical of serous retinal detachments.

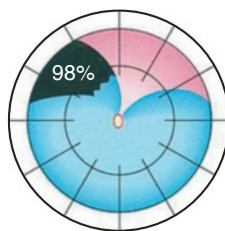
PVR is the most common cause of failure following surgical repair of an RRD. In PVR, retinal pigment epithelial, glial, and other cells grow and migrate on both the inner

Table 16-2 Diagnostic Features of the 3 Types of Retinal Detachments

	Rhegmatogenous (Primary)	Fractional	Nonrhegmatogenous (Secondary) Exudative
History	Aphakia, myopia, blunt trauma, photopsia, floaters, field defect; progressive, generally healthy Identified in 90%–95% of cases	Diabetes mellitus, prematurity, penetrating trauma, sickle cell disease, venous occlusions No primary break; may develop secondary break	Systemic factors such as malignant hypertension, eclampsia, renal failure No break, or coincidental
Extent of detachment	Extends ora to optic nerve head early, has convex borders and surfaces; gravity dependent	Frequently does not extend to ora; may be central or peripheral	Volume and gravity dependent; extension to ora is variable, may be central or peripheral
Retinal mobility	Undulating bullae or folds	Taut retina, concave borders and surfaces, peaks to traction points	Smoothly elevated bullae, usually without folds
Evidence of chronicity	Demarcation lines, intraretinal macrocysts, atrophic retina	Demarcation lines	Usually none
Pigment in vitreous	Present in 70% of cases	Present in trauma cases	Not present
Vitreous changes	Frequently synergetic; posterior vitreous detachment, traction on flap of tear	Vitreoretinal traction	Usually clear, except in uveitis
Subretinal fluid	Clear	Clear, no shift	May be turbid and shift rapidly to dependent location with changes in head position
Choroidal mass	None	None	May be present
Intraocular pressure	Frequently low	Usually normal	Varies
Transillumination	Normal	Normal	Normal; however, blocked transillumination if pigmented choroidal lesion present
Examples of conditions causing detachment	Retinal break	Proliferative diabetic retinopathy, retinopathy of prematurity, toxocariasis, sickle cell retinopathy, posttraumatic vitreous traction	Uveitis, metastatic tumor, malignant melanoma, Coats disease, Vogt-Koyanagi-Harada syndrome, retinoblastoma, choroidal hemangioma, senile exudative maculopathy, exudative detachment after cryotherapy or diathermy

Modified from Hilton GF, McLean EB, Brinton DA, eds. *Retinal Detachment: Principles and Practice*. 2nd ed. Ophthalmology Monograph 1. San Francisco: American Academy of Ophthalmology; 1995.

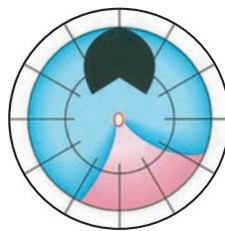
Rules to Find the Primary Break



Rule 1:

Superior temporal or nasal detachments:

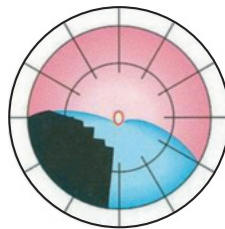
In 98%, the primary break lies within 1 $\frac{1}{2}$ clock-hours of the highest border.



Rule 2:

Total or superior detachments that cross the 12 o'clock meridian:

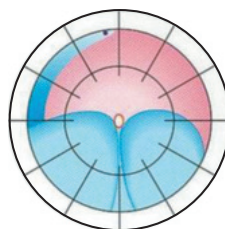
In 93%, the primary break is at 12 o'clock or in a triangle, the apex of which is at the ora serrata, and the sides of which extend 1 $\frac{1}{2}$ clock-hours to either side of 12 o'clock.



Rule 3:

Inferior detachments:

In 95%, the higher side of the detachment indicates on which side of the disc an inferior break lies.



Rule 4:

"Inferior" bullous detachment:

Inferior bullae in a rhegmatogenous detachment originate from a superior break.

Figure 16-13 Using Lincoff rules to find the primary break. (Used with permission from Kreissig I. A Practical Guide to Minimal Surgery for Retinal Detachment. Vol 1. Stuttgart, New York: Thieme; 2000:13–18. © Thieme.)

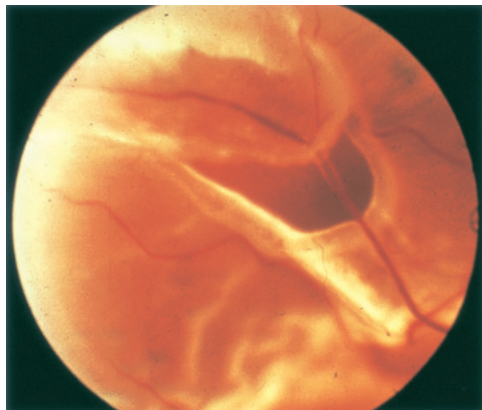


Figure 16-14 Color fundus photograph of a horseshoe retinal tear with a bridging vessel and secondary retinal detachment. Intact retinal vessels can bridge a tear, whereas some vessels crossing a flap tear can rupture and bleed into the vitreous cavity. Along with photopsia, initial symptoms may include black spots from the vitreous hemorrhage.

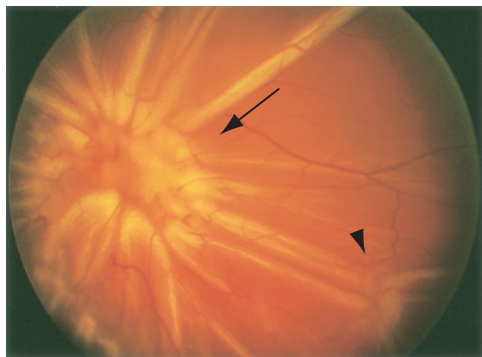


Figure 16-15 Color fundus photograph of a retinal detachment with proliferative vitreoretinopathy. Revised Retina Society classification CP-12 with diffuse retinal contraction in posterior pole (arrow) and single midperipheral starfold (arrowhead). See Table 16-3.

and outer retinal surfaces and on the vitreous face, forming membranes. Contraction of these membranes causes fixed retinal folds, equatorial traction, detachment of the nonpigmented epithelium from the pars plana, and generalized retinal shrinkage (Fig 16-15). As a result, the causative retinal breaks may reopen, new breaks may occur, or a tractional detachment may develop.

To better compare preoperative anatomy with postoperative outcomes, researchers developed a classification of PVR (Table 16-3). The 1991 classification lists 3 grades of PVR

Table 16-3 Classification of Proliferative Vitreoretinopathy, 1991

Grade	Features
A	Vitreous haze, vitreous pigment clumps, pigment clusters on inferior retina
B	Wrinkling of inner retinal surface, retinal stiffness, vessel tortuosity, rolled and irregular edge of retinal break, decreased mobility of vitreous
CP 1–12	Posterior to equator: focal, diffuse, or circumferential full-thickness folds, ^a subretinal strands ^a
CA 1–12	Anterior to equator: focal, diffuse, or circumferential full-thickness folds, ^a subretinal strands, ^a anterior displacement, ^a condensed vitreous with strands

^aExpressed in number of clock-hours involved.

Used with permission from Machemer R, Aaberg TM, Freeman HM, Irvine AR, Lean JS, Michels RM. An updated classification of retinal detachment with proliferative vitreoretinopathy. *Am J Ophthalmol*. 1991;112(2):159–165.

(A, B, and C), which correspond to increasing severity of the disease. Anterior and posterior involvement (CA, CP) are distinguished and subclassified into focal, diffuse, subretinal, circumferential, and anterior displacement. The extent of the pathology is described in clock-hours.

Han DP, Lean JS. Proliferative vitreoretinopathy. In: Albert DM, Miller JW, Azar DT, Blodi BA, eds. *Albert & Jakobiec's Principles and Practice of Ophthalmology*. Philadelphia: Saunders; 2008:chap 183.

Rowe JA, Erie JC, Baratz KH, et al. Retinal detachment in Olmsted County, Minnesota, 1976 through 1995. *Ophthalmology*. 1999;106(1):154–159.

Management of rhegmatogenous retinal detachment

The principles of surgery for retinal detachment are as follows:

- Find all retinal breaks.
- Create a chorioretinal irritation around each break.
- Close the retinal breaks.

The most important element in management of retinal detachment is a careful retinal examination, first preoperatively and then intraoperatively. Retinal breaks can be closed by several methods, all of which involve bringing the RPE and choroid into contact with the retina long enough to produce a chorioretinal adhesion that will permanently wall off the subretinal space. This process usually involves 1 of 3 approaches: (1) *scleral buckling*, (2) *vitrectomy*, or (3) *pneumatic retinopexy*. For acute, macula-on retinal detachments with symptoms, surgery is performed urgently. In contrast, in eyes with chronic retinal detachments with pigmented demarcation lines, treatment may be delayed or it may not be needed, if the eye continues to be monitored closely (Fig 16-16). See Chapter 20 for a more detailed discussion of these techniques and outcomes.

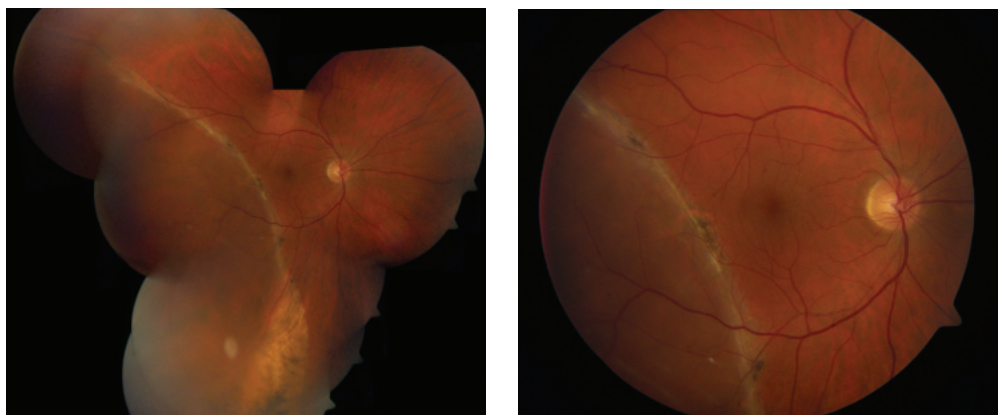


Figure 16-16 Chronic retinal detachment. At initial examination, patient presented with an asymptomatic large retinal detachment with a pigmented and atrophic demarcation line. No progression was observed over several weeks, and surgery was performed electively. (Courtesy of Stephen J. Kim, MD.)

Tractional Retinal Detachment

Vitreous membranes caused by penetrating injuries or by proliferative retinopathies such as diabetic retinopathy can pull the neurosensory retina away from the RPE, causing a tractional retinal detachment. The retina characteristically has smooth concave surfaces and contours and is immobile. The detachment can be central or peripheral and, in rare cases, can extend from the optic nerve head to the ora serrata. In most cases, the causative vitreous membrane can be seen biomicroscopically with a 3-mirror contact lens or a 60 D to 90 D indirect lens. If the traction can be released by vitrectomy, the detachment may resolve.

In some cases, traction may tear the retina and cause a combined tractional and rhegmatogenous retinal detachment. Clinically, the tractional retinal detachment loses its concave surface and assumes a convex shape more reminiscent of an RRD. However, the retinal mobility is often limited compared with that of an eye with RRD because of the tethering by proliferative tissue. In addition, corrugations characteristic of an RRD are present, and subretinal fluid, which is more extensive than in tractional retinal detachment, may extend from the optic nerve head to the ora. Treatment may require a combination of vitrectomy and a scleral buckling procedure to release the traction and seal the break.

Exudative Retinal Detachment

Recognizing whether a retinal detachment is exudative is crucial because, unlike with other types of retinal detachment, the management of exudative retinal detachment is usually nonsurgical. Exudative detachment occurs when either retinal blood vessels leak or the RPE is damaged, allowing fluid to pass into the subretinal space (Fig 16-17). Neoplasia and inflammatory diseases are the leading causes of large exudative detachments.



Figure 16-17 Color fundus photograph of an exudative retinal detachment that resulted from metastatic breast carcinoma. (Courtesy of Hermann D. Schubert, MD.)

The presence of shifting fluid strongly suggests a large exudative retinal detachment. Because the subretinal fluid responds to the force of gravity, it detaches the area of the retina in which it accumulates. For example, when the patient is sitting, the inferior retina is detached. However, when the patient becomes supine, the fluid moves posteriorly in a matter of seconds or minutes, detaching the macula. Another characteristic of exudative detachments is the smoothness of the detached retinal surface, in contrast to the corrugated appearance in eyes with RRDs. Included in the differential diagnosis is the rhegmatogenous inferior bullous detachment, which may shift and is connected to a superior tear (see Fig 16-13, rule 4). Fixed retinal folds, which usually indicate PVR, are rarely, if ever, present in exudative detachments. Occasionally, the retina is sufficiently elevated in exudative detachments to be visible directly behind the lens (eg, in Coats disease), a rare occurrence in RRDs.

Differential Diagnosis of Retinal Detachment

Retinoschisis

Typical peripheral cystoid degeneration is present in virtually all adults. Contiguous with and extending up to 2–3 mm posterior to the ora serrata, the area of degeneration has a bubbly appearance and is best visualized with scleral depression. The cystoid cavities in the outer plexiform layer contain a hyaluronidase-sensitive mucopolysaccharide. The only known complications of typical cystoid degeneration are coalescence and extension of the cavities and progression to typical degenerative retinoschisis.

Reticular peripheral cystoid degeneration is almost always located posterior to and continuous with typical peripheral cystoid degeneration, but it is considerably less common. It has a linear or reticular pattern that corresponds to the retinal vessels and a finely stippled internal surface. The cystoid spaces are in the nerve fiber layer. This condition may progress to *reticular degenerative retinoschisis* (also known as *bulbous retinoschisis*).

Although degenerative retinoschisis is sometimes subdivided into typical and reticular forms, clinical differentiation is difficult. The complications of posterior extension and progression to retinal detachment are associated with the reticular form. Retinoschisis is bilateral in 50%–80% of affected patients, often occurs in the inferotemporal quadrant, and is commonly associated with hyperopia.

In *typical degenerative retinoschisis*, the retina splits in the outer plexiform layer. The outer layer is irregular and appears pockmarked on scleral depression. The inner layer is thin and appears clinically as a smooth, oval elevation, usually in the inferotemporal quadrant but sometimes located superotemporally. Occasionally, small, irregular white dots (“snowflakes”) are present; these are footplates of Müller cells and neurons that bridge or formerly bridged the cavity. The retinal vessels may appear sclerotic. In all cases, peripheral cystoid degeneration with a typical “bubbly” appearance can be found anterior to the schisis cavity. The schisis may extend posteriorly to the equator, but complications such as hole formation, retinal detachment, or marked posterior extension are rare. The split in the retina almost never extends as far posteriorly as the macula.

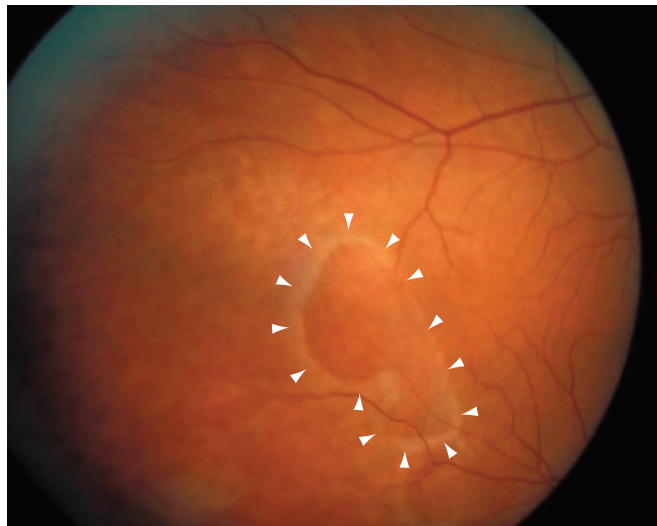


Figure 16-18 Retinoschisis with large, irregular outer-schisis-layer holes (outlined by arrowheads) and yellow dots on the inner surface. (Courtesy of Colin A. McCannel, MD.)

In *reticular degenerative retinoschisis*, the splitting occurs in the nerve fiber layer. The very thin inner layer may be markedly elevated. As in typical retinoschisis, the outer layer appears pockmarked and the retinal vessels sclerotic. Posterior extension is more common in reticular than in typical retinoschisis. Approximately 23% of cases have holes in the outer wall that may be large and have rolled edges (Fig 16-18).

Reed D, Garg AJ. Degenerative retinoschisis. In: Schachat AP, Wilkinson CP, Hinton DR, Sadda SR, Wiedemann P, eds. *Ryan's Retina*. 6th ed. Philadelphia: Elsevier/Saunders; 2018:chap 100.

Differentiation of Retinoschisis From Rhegmatogenous Retinal Detachment

Retinoschisis must be differentiated from RRD (Table 16-4). Retinoschisis causes an absolute scotoma, whereas RRD causes a relative scotoma. Tobacco dust, hemorrhage, or both are present in the vitreous with retinoschisis only in rare instances, whereas they are commonly observed with RRD. Retinoschisis has a smooth surface and usually appears dome shaped; in contrast, RRD often has a corrugated, irregular surface. In long-standing

Table 16-4 Differentiation of Rhegmatogenous Retinal Detachment and Retinoschisis

Clinical Feature	Rhegmatogenous Retinal Detachment	Retinoschisis
Surface	Corrugated	Smooth-domed
Hemorrhage or pigment	Present	Usually absent
Scotoma	Relative	Absolute
Reaction to photocoagulation	Absent	Generally present
Shifting fluid	Usually absent	Absent

RRD, however, the retina also may appear smooth and thin, similar to its appearance in retinoschisis. Whereas long-standing RRD may also show atrophy of the underlying RPE, demarcation line(s), and degenerative retinal schisis (macrocysts), the underlying RPE is normal in eyes with retinoschisis.

Retinoschisis is associated with approximately 3% of full-thickness retinal detachments. Two types of schisis-related detachments occur. In the first type, if holes are present in the outer but not the inner wall of the schisis cavity, the contents of the cavity can migrate through a hole in the outer wall and slowly detach the retina (see Fig 16-18). Demarcation lines and degeneration of the underlying RPE are common. A demarcation line in an eye with retinoschisis suggests that a full-thickness detachment is present, or was formerly present and has spontaneously regressed. This type of retinoschisis detachment usually does not progress, or it progresses slowly and seldom requires treatment.

In the second type of schisis detachment, holes are present in both the inner and outer layers. The schisis cavity may collapse, and a progressive RRD may result. Such detachments often progress rapidly and usually require treatment. The causative breaks may be located very posteriorly and thus may be difficult to repair with scleral buckling. Vitrectomy may be appropriate.

Byer NE. Long-term natural history study of senile retinoschisis with implications for management. *Ophthalmology*. 1986;93(9):1127–1137.

Gotzardis EV, Georgalas I, Petrou P, Assi AC, Sullivan P. Surgical treatment of retinal detachment associated with degenerative retinoschisis. *Semin Ophthalmol*. 2014;29(3):136–141.

Ip M, Garza-Karren C, Duker JS, et al. Differentiation of degenerative retinoschisis from retinal detachment using optical coherence tomography. *Ophthalmology*. 1999;106(3):600–605.

Xue K, Muqit MMK, Ezra E, et al. Incidence, mechanism and outcomes of schisis retinal detachments revealed through a prospective population-based study. *Br J Ophthalmol*. 2017; 101(8):1022–1026.

Macular Lesions Associated With Retinal Detachment

Optic Pit Maculopathy

Optic pits are small, hypopigmented, yellow or whitish, oval or round, excavated colobomatous defects of the optic nerve; they are usually found within the inferior temporal portion of the optic nerve head margin (Fig 16-19). Most are unilateral, asymptomatic, and congenital, but they can be acquired in the setting of glaucomatous excavation. Optic pits may lead to serous macular detachments with a poor prognosis if left untreated. The macular retinal thickening and detachment typically extend from the optic pit in an oval shape toward the fovea. OCT imaging reveals macular schisis as well as subretinal fluid. Whether the subretinal fluid is liquid vitreous or cerebrospinal fluid is controversial; a proteomic analysis of fluid in 1 adult case confirmed that vitreous was the definite source. Optic pits are among the few conditions associated with macular schisis. Various successful treatments have been reported, involving vitrectomy with gas-bubble placement.

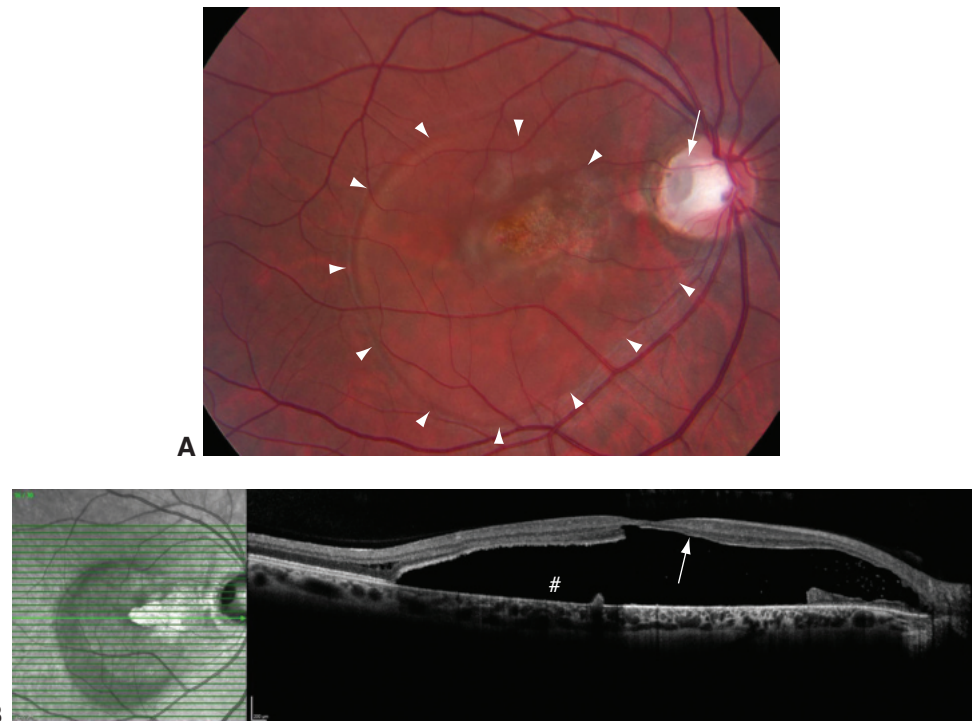


Figure 16-19 Optic nerve pit with macular detachment, retinal thinning, and retinal pigment epithelial atrophy. **A**, Fundus photograph shows an abnormal temporal optic nerve head appearance with an excavation, or pit (arrow). The adjacent retina is thickened and elevated, extending into the macula (outlined by arrowheads). **B**, Optical coherence tomography scan illustrates subretinal fluid (pound sign) associated with the optic pit. Note the degenerated outer segments (arrow) of the photoreceptors. (Courtesy of Colin A. McCannel, MD.)

The differential diagnosis of optic pits includes glaucomatous nerve damage, such as optic pit-like changes that may occur at the inferior or superior pole of the optic nerve. Optic pits are also included in the differential diagnosis of macular thickening or detachment. Careful examination of the optic nerve margin is important for recognizing this condition.

Bottoni F, Cereda M, Secondi R, Bochicchio S, Staurenghi G. Vitrectomy for optic disc pit maculopathy: a long-term follow-up study [epub ahead of print February 6, 2018]. *Graefes Arch Clin Exp Ophthalmol*. doi: 10.1007/s00417-018-3925-9.

Jain N, Johnson MW. Pathogenesis and treatment of maculopathy associated with cavitary optic disc anomalies. *Am J Ophthalmol*. 2014;158(3):423–435.

Ooto S, Mittra RA, Ridley ME, Spaide RF. Vitrectomy with inner retinal fenestration for optic disc pit maculopathy. *Ophthalmology*. 2014; 121(9):1727–1733.

Patel S, Ling J, Kim SJ, Schey KL, Rose K, Kuchtey RW. Proteomic analysis of macular fluid associated with advanced glaucomatous excavation. *JAMA Ophthalmol*. 2016;134(1):108–110.

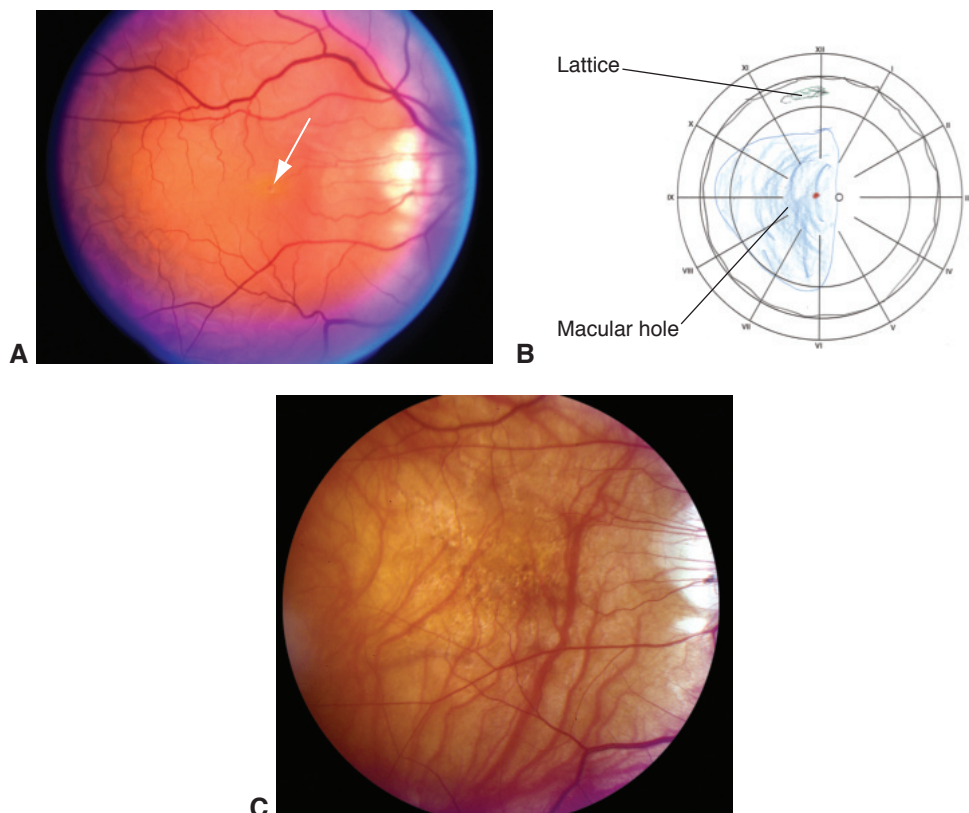


Figure 16-20 A case of rhegmatogenous retinal detachment caused by a macular hole. **A**, Fundus photograph (50-degree camera) of the detached retina with a macular hole visible in the center of the macula (arrow). **B**, A retinal drawing of the extent of the detachment. The area within the blue outline is detached; the red dot symbolizes the macular hole. At presentation, the detachment did not extend to the ora serrata; lack of such an extension is uncharacteristic even for a limited rhegmatogenous retinal detachment arising from a peripheral break. A lattice lesion with pigmentation is drawn superiorly. **C**, Fundus photograph (30-degree camera) of the macula after successful retinal reattachment using vitrectomy surgery with gas tamponade. Typical myopic fundus features include retinal pigment epithelial changes from myopic degeneration, fair pigmentation, peripapillary scleral crescent, and prominent large choroidal vessels. (Courtesy of Colin A. McCannel, MD.)

Macular Holes in High Myopia

A distinct variant of RRD is caused by macular holes, almost always in the setting of a posterior staphyloma in highly myopic eyes (Fig 16-20). Vitreous cavity fluid enters the subretinal space through the macular hole and initiates the detachment. These macular holes with retinal detachment have a far lower success rate for surgical repair than do either macular holes or typical RRDs.

Ando Y, Hirakata A, Ohara A, et al. Vitrectomy and scleral imbrication in patients with myopic traction maculopathy and macular hole retinal detachment. *Graefes Arch Clin Exp Ophthalmol.* 2017;255(4):673–680.

Ho TC, Ho A, Chen MS. Vitrectomy with a modified temporal inverted limiting membrane flap to reconstruct the foveolar architecture for macular hole retinal detachment in highly myopic eyes. *Acta Ophthalmol.* 2018;96(1):e46–e53.

Diseases of the Vitreous and Vitreoretinal Interface



This chapter includes related activities, which can be accessed by scanning the QR codes provided in the text or going to www.aao.org/bcscactivity_section12.

Posterior Vitreous Detachment

The vitreous is a transparent connective tissue composed of collagen and hyaluronan that is attached to the basal lamina of the lens, optic nerve, and retina, and fills the vitreous cavity of the eye. A posterior vitreous detachment (PVD) is the separation of the posterior cortical gel from the retinal surface, including its adhesions at the optic nerve head (the area of Martegiani), the macula, and blood vessels. At its base, the vitreous remains firmly attached to the retina—even after severe trauma—sometimes resulting in vitreous base avulsion. Because of this firm attachment, the basal cortical vitreous collagen cannot be peeled off the retina; instead, the vitreous must be “shaved” during vitrectomy, instead of being removed. See Chapter 16 in this volume for more on PVD.

With advancing age, the vitreous gel undergoes both liquefaction (synchysis) and collapse (syneresis). The viscous hyaluronan accumulates in lacunae, which are surrounded by displaced collagen fibers. The gel can then contract, possibly because of electrostatic attraction and crosslinking of adjacent collagen fibers in the absence of hyaluronan. With this contraction, the posterior cortical gel detaches toward the firmly attached vitreous base. The prevalence of PVD is increased in patients who have had cataract extractions, particularly if the posterior capsule’s integrity has been violated. Prevalence is also increased in individuals with a history of vitritis because of the loss or alteration of hyaluronan. Localized regions of the posterior cortical gel can separate slowly, over the course of many years, with few if any symptoms, compared with the more acute, symptomatic event.

The diagnosis of PVD is often made with indirect ophthalmoscopy or slit-lamp biomicroscopy, with which the posterior vitreous face may be observed a few millimeters in front of the retinal surface. In eyes with a PVD, a translucent ring of fibroglial tissue (the “Weiss” or “Vogt” ring) is frequently torn loose from the surface of the optic nerve head, and its observation helps the clinician make the diagnosis. Although a shallow detachment of the posterior cortical gel may be difficult or impossible to observe with biomicroscopy, this type of detachment may be revealed on contact B-scan ultrasonography as a thin, hyperreflective line bounding the posterior vitreous. Optical coherence tomography

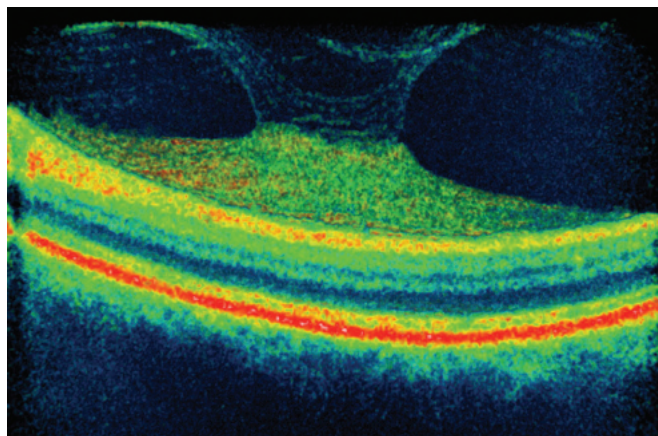


Figure 17-1 A 3-dimensional rendering of spectral-domain optical coherence tomography (SD-OCT) imaging of vitreomacular traction (VMT) syndrome. The cone of vitreous is attached to and elevates the central fovea. (Courtesy of Richard F. Spaide, MD.)

(OCT) has shown that PVDs often start as a localized detachment of the vitreous over the perifovea, called a *posterior perifoveal vitreous detachment*, later spreading anteriorly to involve larger areas.

Persistent focal attachment of the vitreous to the retina can cause a number of pathologic conditions. Vitreous contraction as well as traction caused by ocular saccades may lead to breaks, particularly at the posterior edge of the vitreous base. Persistent attachment to the macula may lead to vitreomacular traction syndrome. Focal attachment to the foveola can induce foveal cavitation and macular hole formation (Fig 17-1). Remnants of the vitreous often remain on the internal limiting membrane (ILM) after a posterior vitreous “detachment.” For this reason, some authorities state that a presumed PVD often is actually posterior vitreoschisis that is internal or external to the layer of hyalocytes. These vitreous remnants may have a role in epiretinal membrane or macular hole formation and can contribute to tractional detachments in patients with pathologic myopia and to macular edema in patients with diabetes mellitus. Plaques of these adherent remnants of cortical vitreous can often be highlighted during vitreous surgery by applying triamcinolone (Fig 17-2).

Gupta P, Yee KM, Garcia P, et al. Vitreoschisis in macular diseases. *Br J Ophthalmol*. 2011;95(3):376–380.

Sakamoto T, Ishibashi T. Hyalocytes: essential cells of the vitreous cavity in vitreoretinal pathophysiology? *Retina*. 2011;31(2):222–228.

Epiretinal Membranes

An epiretinal membrane (ERM) is a transparent, avascular, fibrocellular membrane on the inner retinal surface that adheres to and covers the ILM of the retina. Proliferation of glia, retinal pigment epithelium (RPE), or hyalocytes at the vitreoretinal interface, especially at the posterior pole, results in ERM formation.

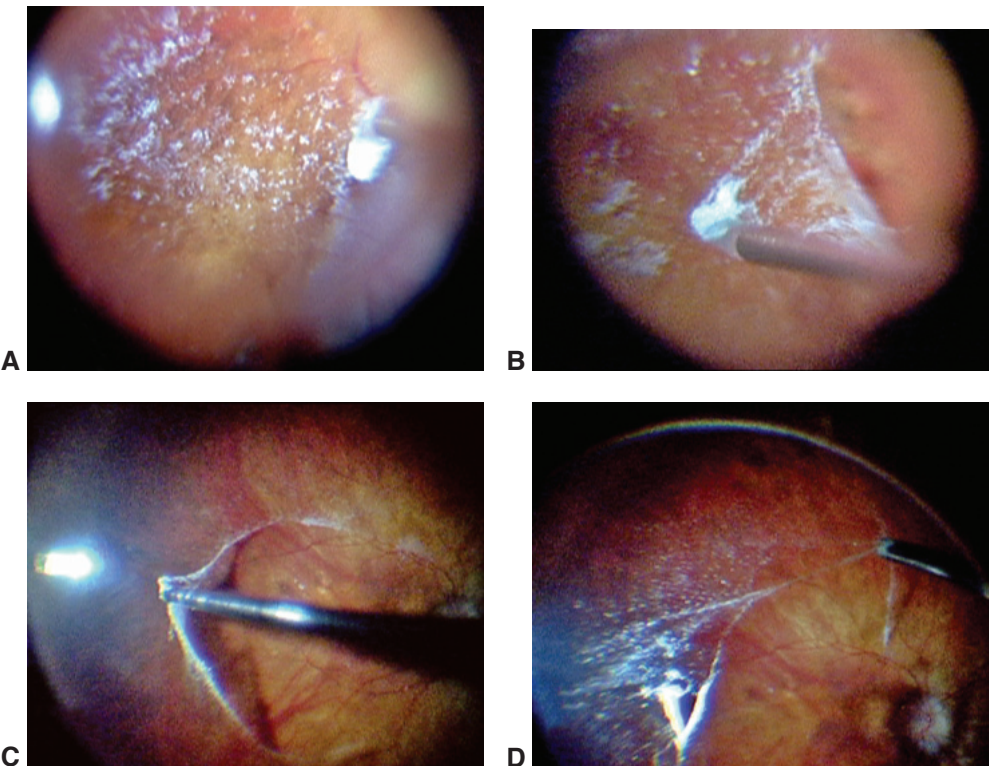


Figure 17-2 Visualization of a thin layer of adherent vitreous during vitrectomy with the use of triamcinolone. This patient appeared to have a posterior vitreous detachment (PWD) and underwent a vitrectomy. **A**, A small amount of triamcinolone was injected into the vitreous cavity; the excess was aspirated from the surface of the retina, leaving a fine distribution of triamcinolone sticking to the adherent vitreous. **B**, The vitreous membrane was elevated using a diamond-dusted silicone scraper. Note that the vitreous is difficult to see; the sheet of triamcinolone is the clue to its presence. **C**, A wide-angle viewing system then was used to visualize the elevation of the adherent vitreous, and the vitrector was set to suction only. **D**, Note the extent of the adherent vitreous sheet, which was removed with the vitrector set to cut. (Courtesy of Richard F. Spaide, MD.)

ERMs are relatively common; at autopsy, they are discovered in 2% of patients older than 50 years and in 20% older than 75 years. ERMs are most common in persons over age 50 years, and both sexes are equally affected. The incidence of bilaterality is approximately 10%–20%, and severity is usually asymmetric. Detachment or separation of the posterior vitreous is present in almost all eyes with idiopathic epiretinal membranes, and may be a requisite for ERM development. Schisis of the posterior vitreous may leave variable portions of the posterior cortical vitreous attached to the macula, allowing glial cells from the retina to proliferate along the retinal surface and hyalocytes to proliferate on posterior cortical vitreous remnants on the retinal surface. Secondary ERMs occur regardless of age or sex in association with abnormal vitreoretinal adhesions and areas of inflammation, as well as following retinal detachment or retinal bleeding.

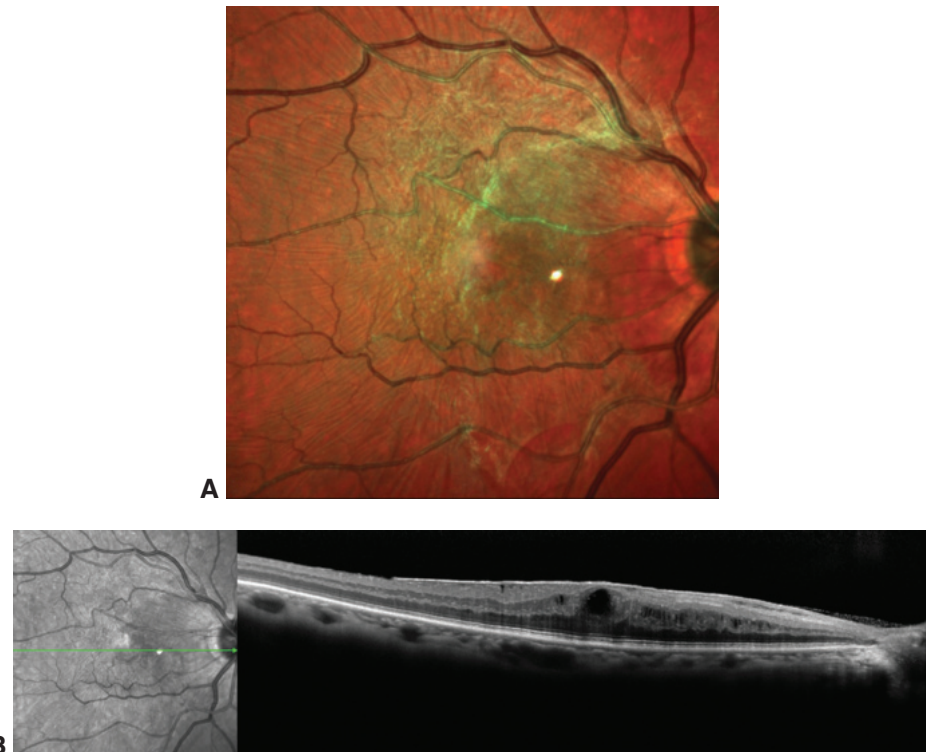


Figure 17-3 Epiretinal membrane (ERM). **A**, Scanning laser ophthalmoscope 30° fundus reflectance multicolor image reveals an ERM in the central macula with radiating striae of the internal limiting membrane (ILM) in the superior, temporal, and inferior macula. The colors in reflectance multicolor images are not exactly true to life. **B**, OCT scan through the fovea shows increased retinal thickening and cystoid edema with a large central cyst. The ERM is distorting the retinal surface temporally, which appears as several small optical voids between the ERM and the retina. (Courtesy of Colin A. McCannel, MD.)

Signs and symptoms

Epiretinal proliferation is generally located in the central macula—over, surrounding, or eccentric to the fovea (Fig 17-3). The membranes usually appear as a mild sheen or glint on the retinal surface. Over time, ERMs become more extensive, increasing retinal distortion and thickening (Figs 17-4 and 17-5; Activities 17-1 and 17-2). However, their rate of progression and severity vary greatly. In some cases, the ERM may become opaque, obscuring underlying retinal details. A “pseudohole” appearance is produced when this preretinal membrane contracts to the edge of the clivus, steepening the gentle slope around the fovea into a cylindrical depression. Occasionally, intraretinal hemorrhages or whitened patches of superficial retina representing delayed axoplasmic flow in the nerve fiber layer (NFL) and edema may be present. The cellular origin of ERMs is still under debate. Histologic examination reveals mainly RPE cells and retinal glial cells (astrocytes and Müller cells); however, myofibroblasts, fibroblasts, hyalocytes, and macrophages have also been identified.

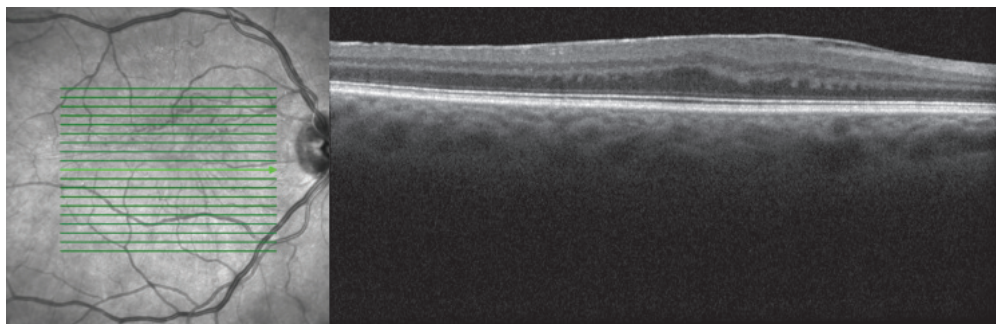


Figure 17-4 SD-OCT line cube scan of the right macula of a 61-year-old woman with ERM. The visual acuity at the time of the scan was 20/30. A loss of foveal depression can be appreciated. The outer nuclear layer is thickened and peaks toward the retinal surface. The infrared reflectance image (*left*) shows the surface wrinkling with striae radiating outward from the central macula with the ERM. See also Activity 17-1. (*Courtesy of Colin A. McCannel, MD.*)

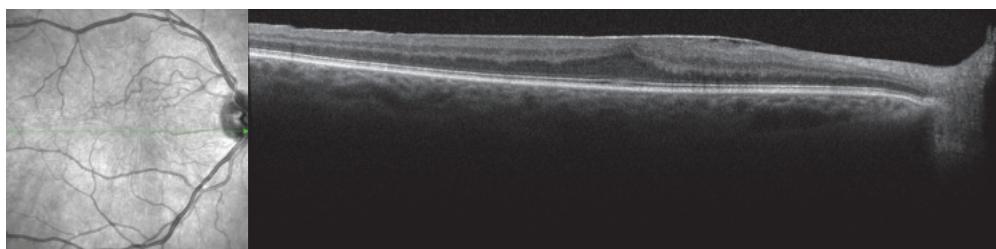


Figure 17-5 ERM progression. SD-OCT image of a patient's right macula with ERM that has developed over the previous 5 years. The ERM expanded and eventually covered the fovea with a secondary complete loss of foveal depression. In this patient, the ERM and retinal thickness did not change much after the fovea was covered. Visual acuity was initially 20/20, but declined slightly to 20/25 at the time the foveal contour was lost and has remained stable during follow-up. See also Activity 17-2. (*Courtesy of Colin A. McCannel, MD.*)



ACTIVITY 17-1 OCT Activity: Epiretinal membrane.

Courtesy of Colin A. McCannel, MD.



Access all Section 12 activities at www.ao.org/bcscactivity_section12.



ACTIVITY 17-2 OCT Activity: Epiretinal membrane progression.

Courtesy of Colin A. McCannel, MD.



Contracture of ERMs produces distortion and wrinkling of the inner surface of the retina, called *cellophane maculopathy* or *preretinal macular fibrosis*. It can range from mild to severe, with *wrinkling* or *striae* to severe *macular puckering*. Increased traction may cause shallow macular detachment, diffuse thickening, or cystic changes. Furthermore, traction on retinal vessels results in increased vascular tortuosity and straightening of the perimacular vessels. Fluorescein angiography (FA) may show staining of the optic nerve and capillary leakage in the central macula. The most common OCT findings are a highly reflective epiretinal reflective layer, loss of the normal retinal contour, and retinal

thickening. Additional findings include irregularities of the inner retinal surface and cystic edema.

Treatment

When ERMs are asymptomatic and visual acuity is good, intervention is not indicated. Asymptomatic ERMs should be monitored periodically, because they will often worsen, sometimes over a relatively short period of time, after being stable. In rare cases, an ERM may spontaneously detach from the inner retinal surface, with concomitant improvement or resolution of the retinal distortion and improvement in symptoms and vision. If the patient is bothered by reduced visual acuity or metamorphopsia, vitrectomy should be considered (see also Chapter 20). The goal of surgery is to optimize visual acuity, reduce metamorphopsia, and restore binocularly if it was affected preoperatively.

Johnson TM, Johnson MW. Epiretinal membrane. In: Yanoff M, Duker JS. *Ophthalmology*. 4th ed. St Louis: Elsevier; 2014:614–619.

Vitreomacular Traction Diseases

Vitreomacular traction diseases include abnormalities that arise from focal or broad vitreomacular adhesions in the presence of detaching or otherwise detached posterior vitreous. The 3 recognized categories of vitreomacular traction disease are: (1) vitreomacular adhesion (VMA), (2) vitreomacular traction (VMT) syndrome, and (3) macular hole. Table 17-1 summarizes a useful classification system for these categories that relies on OCT findings.

Vitreomacular adhesions

VMAs typically do not cause visual symptoms. They can be focal or diffuse and can lead to secondary traction disease, that is, VMT and macular hole.

Vitreomacular traction syndrome

In VMT syndrome, the posterior hyaloid is abnormally adherent to the macula (eg, a VMA). As the vitreous detaches, the posterior hyaloid remains tethered at the macula,

Table 17-1 The International Vitreomacular Traction Study Classification System for Vitreomacular Adhesion, Traction, and Macular Hole

Classification	Subclassification
Vitreomacular adhesion	Size: focal ($\leq 1500 \mu\text{m}$) or broad ($> 1500 \mu\text{m}$) Isolated or concurrent
Vitreomacular traction (VMT)	Size: focal ($\leq 1500 \mu\text{m}$) or broad ($> 1500 \mu\text{m}$) Isolated or concurrent
Full-thickness macular hole	Size: small ($\leq 250 \mu\text{m}$), medium ($> 250\text{--}400 \mu\text{m}$), or large ($> 400 \mu\text{m}$) Status of vitreous: with or without VMT Cause: primary or secondary

From Duker JS, Kaiser PK, Binder S, et al. The International Vitreomacular Traction Study Group classification of vitreomacular adhesion, traction, and macular hole. *Ophthalmology*. 2013;120(12):2611–2619.

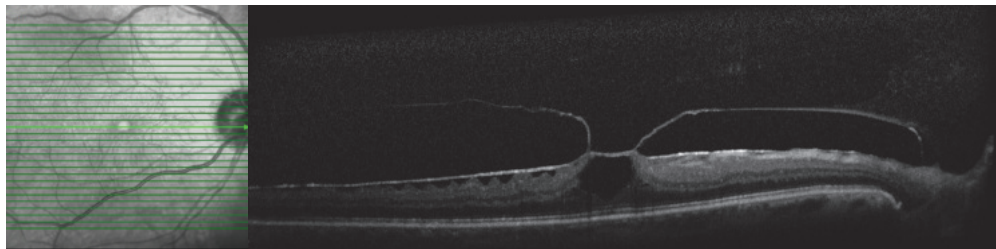


Figure 17-6 Vitreomacular traction syndrome. OCT scan of the macula through the fovea shows vitreomacular traction causing a large foveal cyst and distortion of the inner retina. An ERM is also present. (Courtesy of Tara A. McCannel, MD, PhD.)

usually the fovea, causing tractional foveal distortion, cystic edema, and, in severe cases, tractional foveal detachment. These changes lead to decreased visual acuity, metamorphopsia, and often vague reports about poor vision in the affected eye that are out of proportion to the measured visual acuity. Angiography may demonstrate leakage of fluorescein dye from macular vessels as well as from the optic nerve. OCT is useful to demonstrate the vitreoretinal interface abnormalities and the tractional effects of VMT syndrome on the foveal architecture. Chronic traction is generally understood to be harmful over the long term, particularly when cystic edema is present or when the patient's vision is affected. Spontaneous separation of the focal vitreoretinal adhesion, with resolution of all clinical features, occurs in approximately 50% of cases, and less commonly when there is an associated ERM or the adhesion is broad (Fig 17-6).

Intervention should be considered for VMT syndrome; it includes pars plana vitrectomy with membrane peeling or intravitreal injection of ocriplasmin. Vitrectomy surgery is highly successful in achieving resolution of VMT (see also Chapter 20).

Ocriplasmin is a recombinant protease with activity against fibronectin and laminin; it has a variable success rate. A multicenter clinical trial found that resolution of vitreomacular traction occurred in 26.5% of ocriplasmin-injected eyes compared with 10.1% of placebo-injected eyes over the same period. In a subset of patients with vitreomacular adhesions smaller than 1500 µm, the rate of resolution increased to 33.6%. Unfortunately, a small number of patients experienced permanent visual loss with electroretinogram (ERG) changes. This may be due to a disruption of the interphotoreceptor matrix, leading to ellipsoid layer attenuation.

Margo JA, Shocket LS, Kilma K, Johnson MA. Persistent retinal changes after intravitreal ocriplasmin. *Retin Cases Brief Rep.* 2016;10(1):48–51.

Idiopathic Macular Holes

Idiopathic macular holes occur at a rate of approximately 8 per 100,000 persons per year and have a female-to-male ratio of 2 to 1. They occur mostly in the sixth through eighth decades of life and can appear at a younger age in myopic eyes. Idiopathic macular holes are bilateral in approximately 10% of patients. Investigations using OCT suggest that idiopathic macular holes are caused by the same tractional forces as the forces associated with perifoveal vitreous detachment and thus are likely an early stage of age-related PVD.

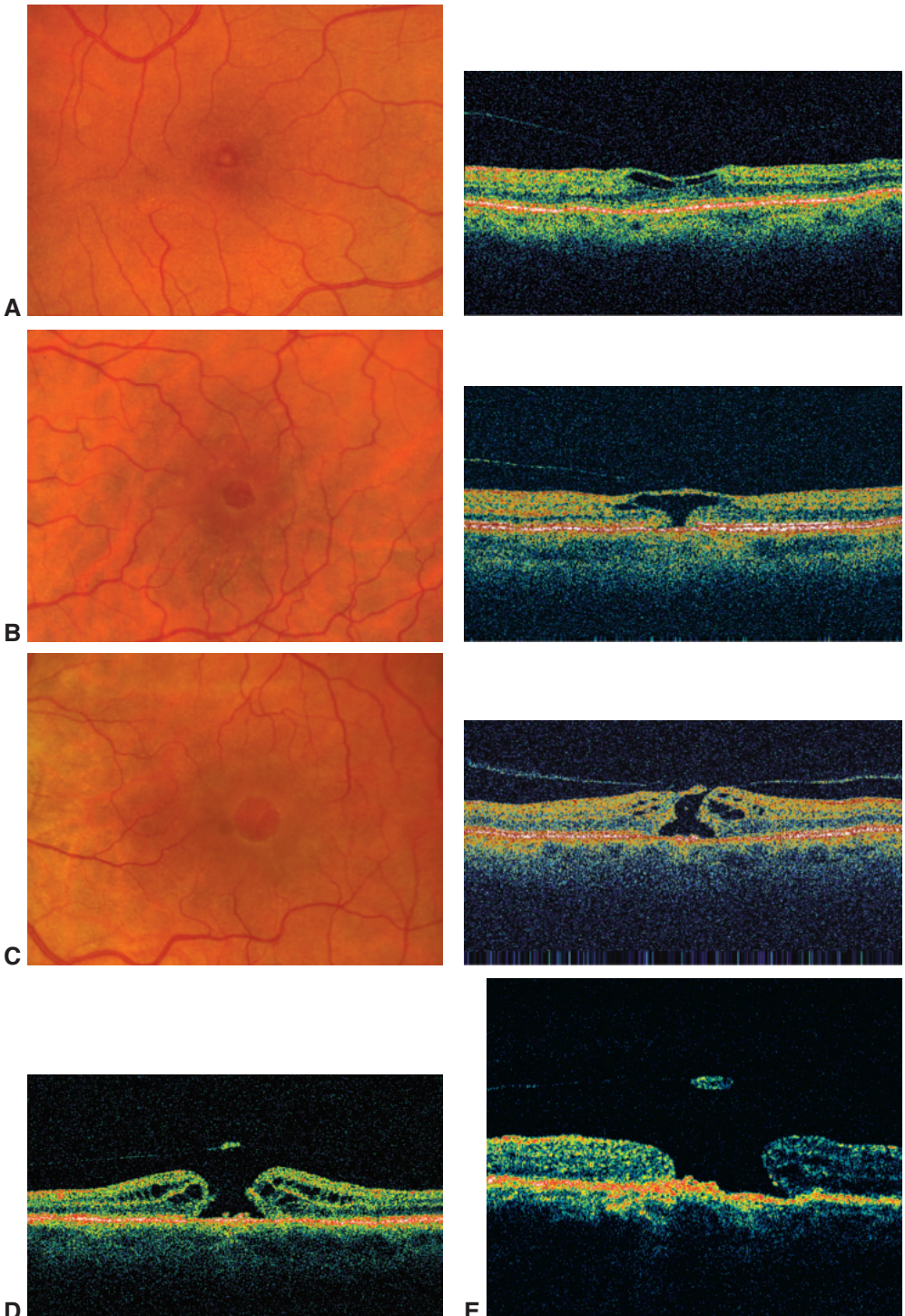


Figure 17-7 Macular holes. **A**, Color fundus photograph of stage 1A hole with horizontal splitting of retinal layers and corresponding OCT scan showing stage 1A hole. **B**, Fundus photograph and corresponding OCT scan of stage 1B hole. **C**, Fundus photograph of stage 2 hole with small opening in inner layer eccentrically and corresponding OCT scan of stage 2 hole. **D**, OCT scan of stage 3 full-thickness hole with elevation of adjacent retinal edges. **E**, OCT scan of stage 4 full-thickness hole with operculum. (Courtesy of Mark W. Johnson, MD, and Peter K. Kaiser, MD.)

The following description of the stages of macular hole formation is useful in making management decisions (Fig 17-7):

- A stage 0, or premacular, hole occurs when a PVD with persistent foveal attachment develops. Subtle loss of the foveal depression can be observed, and visual acuity is usually unaffected. Most stage 0 holes do not progress to advanced stages. This stage represents a VMA.
- A stage 1 macular hole (impending macular hole) typically causes visual symptoms of metamorphopsia and central vision decline, usually to a visual acuity range of 20/25 to 20/60. The characteristic findings are either a small yellow spot (stage 1A) or a yellow circle (stage 1B) in the fovea. OCT examination reveals that a stage 1A hole is a foveal “pseudocyst,” or horizontal splitting (schisis), associated with vitreous traction to the foveal center. A stage 1B hole indicates a break in the outer fovea, the margins of which constitute the yellow ring noted clinically. Spontaneous resolution of a stage 1 hole occurs in approximately 50% of cases without ERM. This stage represents VMT syndrome.
- A stage 2 macular hole represents an early full-thickness macular hole that is less than 400 µm in diameter. It results from the progression of a foveal schisis (pseudocyst) to a full-thickness dehiscence, as a tractional break develops in the “roof” (inner layer) of the pseudocyst. Progression to stage 2 is accompanied by a further decline in visual acuity. OCT demonstrates the full-thickness defect and the continuing attachment of the posterior hyaloid to the foveal center. This stage represents VMT syndrome with a small- to medium-sized macular hole.
- A stage 3 macular hole is a fully developed hole (≥ 400 µm in diameter), typically surrounded by a rim of thickened and detached retina. Visual acuity ranges widely. The posterior hyaloid remains attached to the optic nerve head but is detached from the fovea. An operculum suspended by the posterior hyaloid may be seen overlying the hole. On OCT, this stage represents a large macular hole with no VMT (Activity 17-3, Fig 17-8).
- A stage 4 macular hole is a fully developed hole with a complete posterior vitreous detachment, as evidenced by the presence of a Weiss ring. On OCT, this stage represents a large macular hole with no VMT.



ACTIVITY 17-3 OCT Activity: Macular hole.

Courtesy of Colin A. McCannel, MD.



The fellow-eye risk of macular hole development depends on the vitreous attachment status. If a complete vitreous detachment is present in the fellow eye, there is little, if any, risk of macular hole development. If the fellow eye has stage 1A abnormalities, however, there is a substantial risk of progression to a full-thickness macular hole. When the fellow eye is normal and its vitreous is attached, the risk of developing a macular hole in that eye is approximately 10%, the rate of bilaterality.

Management options

For stage 2 or greater macular holes, surgical intervention is recommended—specifically, pars plana vitrectomy with gas tamponade; in most recent case series, the success rate

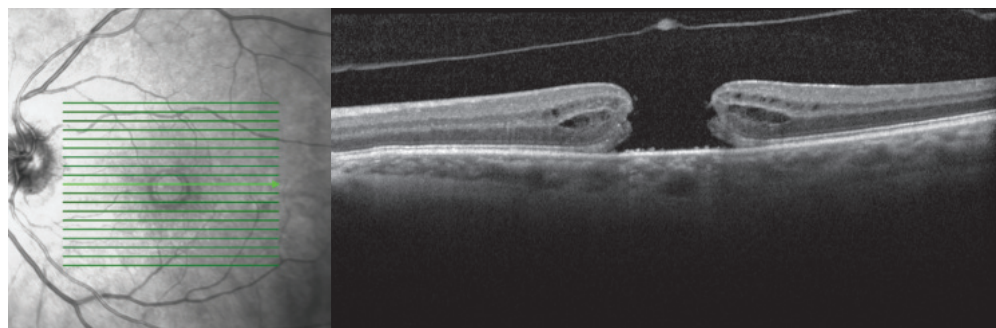


Figure 17-8 SD-OCT line cube scan of the left macula of a 62-year-old woman who suffered loss of vision 18 months prior to presentation. At the time of the scan, the visual acuity of this eye was 20/40 (eccentric fixation). The infrared reflectance image (left) shows a hole in the central macular retina. See also Activity 17-3; scrolling through the images, a discontinuity of the retina in the central macular scans can be seen, corresponding to the macular hole. The scan through the macular hole (scan 10) shows an operculum. This operculum represents a small glial plug that helps keep the fovea together; when it is pulled away by the posterior vitreous, a macular hole is facilitated. Histologic studies indicate that the number of photoreceptors attached to the plug can vary, from none to many. The prominent posterior vitreous face can also be seen; its contour suggests that it is likely attached at the optic nerve head and peripheral macula (dome-shaped configuration), which is typical in idiopathic macular holes. (*Courtesy of Colin A. McCannel, MD.*)

of this procedure for closure and vision improvement was greater than 90% (see Chapter 20 in this volume). Modifications of routine macular hole surgery are usually reserved for very large, chronic, or nonclosing holes; these include inverted ILM flaps and autologous retinal grafts composed of peripheral retina. Although these techniques may achieve anatomical hole closure, visual acuity may not improve.

Stage 1 macular holes have an approximate 50% rate of spontaneous resolution and thus are typically monitored. An alternative management option for stage 1 holes or holes that are less than 250 µm in diameter is the intravitreal injection of ocriplasmin. In the ocriplasmin phase 3 clinical trial, the closure rate of full-thickness macular holes was 40.6% overall and 58.3% for holes of less than 250 µm diameter. Ocriplasmin is most effective in eyes with focal adhesions and much less effective for broad vitreoretinal adhesions or adhesions associated with an ERM.

Duker JS, Kaiser PK, Binder S, et al. The International Vitreomacular Traction Study Group classification of vitreomacular adhesion, traction, and macular hole. *Ophthalmology*. 2013;120(12):2611–2619.

Developmental Abnormalities

Tunica Vasculosa Lentis

Although they are commonly observed, remnants of the tunica vasculosa lentis and hyaloid artery are not visually significant. Mittendorf dot, an anterior remnant, is a small, dense, and white round plaque attached to the posterior lens capsule nasally and inferiorly to its posterior pole. A prepapillary remnant known as Bergmeister papilla is a fibroglial



Figure 17-9 Color fundus photograph of a prepapillary vascular loop. (Courtesy of M. Gilbert Grand, MD.)

tuft of tissue extending into the vitreous for a short distance at the margin of the optic nerve head. The entire hyaloid artery may persist from optic nerve head to lens as multi-layered fenestrated sheaths forming the Cloquet canal.

Prepapillary Vascular Loops

Initially thought to be remnants of the hyaloid artery, prepapillary vascular loops are normal retinal vessels that have grown into Bergmeister papilla before returning to the retina (Fig 17-9). The loops typically extend less than 5 mm into the vitreous. These vessels may supply one or more quadrants of the retina. FA has shown that 95% of these vessels are arterial and 5% are venous. Complications associated with these vessels include branch retinal artery obstruction, amaurosis fugax, and vitreous hemorrhage.

Persistent Fetal Vasculature

Persistent fetal vasculature (PFV), previously known as *persistent hyperplastic primary vitreous*, is a congenital anomaly thought to result from failure of the primary vascular vitreous to regress. The disorder is unilateral in 90% of cases and usually has no associated systemic findings. Anterior, posterior, and combined forms of this developmental abnormality have been described. Most cases are sporadic, but PFV can occur as either an autosomal recessive (mutations in the *ATOH7* gene) or autosomal dominant trait. In some patients with mutations, the disease can be asymmetric and bilateral, with the fellow eye showing variable changes, including avascularity. See BCSC Section 6, *Pediatric Ophthalmology and Strabismus*, for more on PFV.

Anterior persistent fetal vasculature

In anterior PFV, the hyaloid artery remains, and a white vascularized fibrous membrane or mass is present behind the lens. Associated findings include microphthalmos, a shallow anterior chamber, and elongated ciliary processes that are visible around the small lens.

Leukocoria is often present at birth. A dehiscence of the posterior lens capsule may, in many cases, cause swelling of the lens and cataract as well as secondary angle-closure glaucoma. In addition, glaucoma may result from incomplete development of the chamber angle.

The natural course of anterior PFV may result in blindness in the most advanced cases. Lensectomy and removal of the fibrovascular retrolental membrane prevent angle-closure glaucoma in some cases; however, growth of a secondary cataract is common. Deprivational and refractive amblyopia is a serious postoperative challenge in these patients.

Anterior PFV should be considered in the differential diagnosis of leukocoria. Differentiating it from retinoblastoma is particularly important. Unlike PFV, retinoblastoma is usually not obvious at birth, is more often bilateral, and is almost never associated with microphthalmos or cataract. PFV is anterior in the eye at birth; retinoblastomas do not appear in the anterior fundus until well after birth. Ancillary testing, such as diagnostic echography and x-ray techniques to look for calcification within the retinoblastoma, can be helpful in differentiating the 2 disorders.

Posterior persistent fetal vasculature

Posterior PFV may occur in association with anterior PFV or as an isolated finding. The eye may be microphthalmic, but the anterior chamber is usually normal and the lens is typically clear and without a retrolental membrane. A stalk of tissue emanates from the optic nerve head and courses toward the retrolental region, often running along the apex of a retinal fold that may extend anteriorly from the optic nerve head, usually in an inferior quadrant. The stalk fans out circumferentially toward the anterior retina. Posterior PFV should be differentiated from retinopathy of prematurity (ROP), familial exudative vitreoretinopathy, and ocular toxocariasis. Surgical repair of posterior PFV consists of lensectomy and vitrectomy, which result in formed vision in about 70% of cases.

Goldberg MF. Persistent fetal vasculature (PFV): an integrated interpretation of signs and symptoms associated with persistent hyperplastic primary vitreous (PHPV). LIV Edward Jackson Memorial Lecture. *Am J Ophthalmol.* 1997;124(5):587–626.

Sisk RA, Berrocal AM, Feuer WJ, Murray TG. Visual and anatomic outcomes with or without surgery in persistent fetal vasculature. *Ophthalmology.* 2010;117(11):2178–2183.

Hereditary Hyaloideoretinopathies With Optically Empty Vitreous: Wagner and Stickler Syndromes

The hallmark of the group of conditions known as hereditary hyaloideoretinopathies is vitreous liquefaction (synchysis) that results in an optically empty cavity except for a thin layer of cortical vitreous behind the lens and threadlike, avascular membranes that run circumferentially and adhere to the retina. Fundus abnormalities include equatorial and perivasculär (radial) lattice degeneration. The ERG response may be subnormal.

In Wagner disease, the optically empty vitreous is accompanied by myopia, strabismus, and cataract, but there are no associated systemic findings. It is not associated with retinal detachment and has an autosomal dominant inheritance pattern.

Stickler syndrome is the most common variety of hereditary hyaloideoretinopathy with associated systemic findings (Fig 17-10) and is transmitted as an autosomal

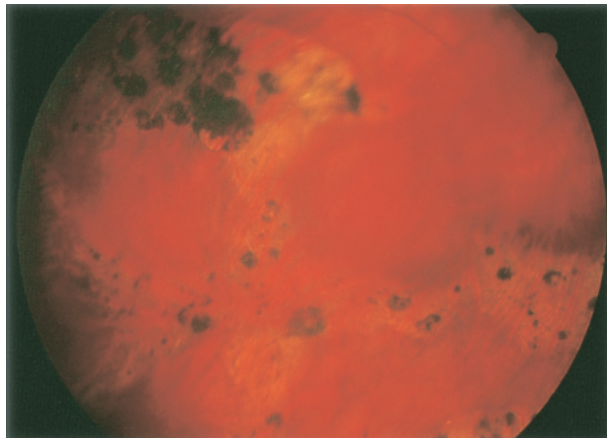


Figure 17-10 Color fundus photograph shows extensive lattice degeneration and pigmentary change in a patient with Stickler syndrome. (Courtesy of William F Mieler, MD.)

dominant trait. Most patients have a mutation in the gene *COL2A1*, which encodes type II procollagen. Various mutations may produce Stickler syndrome phenotypes of differing severity. Additional ocular abnormalities include myopia, open-angle glaucoma, and cataract. Orofacial findings include midfacial flattening and the Pierre Robin malformation complex of cleft palate, micrognathia, and glossoptosis. These abnormalities may be dramatic at birth, requiring tracheostomy, or they may not be obvious at all. Generalized skeletal abnormalities include joint hyperextensibility and enlargement; arthritis, particularly of the knees; and mild spondyloepiphyseal dysplasia. Early recognition of this syndrome is very important because of the high incidence of retinal detachment. In one case series, retinal tears were associated with mutations in *COL2A1* in 91% of cases and retinal detachments in 53%. The detachments may be difficult to repair because of multiple, posterior, or large breaks and a tendency toward proliferative vitreoretinopathy. Patients with this condition typically have cortical vitreous condensations that are firmly adherent to the retina. For this reason, prophylactic treatment of retinal breaks should be considered. (See the section Prophylactic Treatment of Retinal Breaks in Chapter 16.)

Other forms of hereditary hyaloideoretinopathy associated with systemic abnormalities include Weill-Marchesani syndrome and some varieties of dwarfism.

Maumenee IH. Vitreoretinal degeneration as a sign of generalized connective tissue diseases.

Am J Ophthalmol. 1979;88(3 Pt 1):432–449.

Rose PS, Levy HP, Liberfarb RM, et al. Stickler syndrome: clinical characteristics and diagnostic criteria. *Am J Med Genet A.* 2005;138A(3):199–207.

Familial Exudative Vitreoretinopathy

Familial exudative vitreoretinopathy (FEVR) is characterized by failure of the temporal retina to vascularize and is phenotypically similar to ROP. Retinal folds and peripheral fibrovascular proliferation as well as tractional and exudative retinal detachment are often

associated with FEVR (Fig 17-11). Temporal dragging of the macula may cause the patient to appear to have exotropia. Late-onset rhegmatogenous retinal detachments may occur. Generally, the earlier the disease presents, the more severe the manifestations.

The condition is frequently bilateral, although the severity of ocular involvement may be asymmetric. Unlike patients with ROP, individuals with FEVR are born full term and have normal respiratory status. In FEVR, the peripheral retinal vessels are dragged, straightened, and end abruptly a variable distance from the ora (brush border). Differentiation of FEVR from ROP is also aided by the family history and a careful examination of all family members. The only finding in some family members with FEVR may be a straightening of vessels and peripheral retinal nonperfusion. Parents and siblings of affected children may be mildly affected and asymptomatic. FA with peripheral sweeps or wide-field angiography is indispensable in examining family members. Treatment of the affected family members may consist of laser therapy applied to the avascular retina, guided by FA.

FEVR is usually inherited as an autosomal dominant trait, but X-linked transmission also occurs. Several different gene loci have been associated with the FEVR phenotype (Table 17-2). A number of genetic disorders can present with the retinal characteristics of FEVR, including dyskeratosis congenita, Coats plus disease, facioscapulohumeral muscular dystrophy, and progressive hemifacial atrophy (Parry-Romberg syndrome). It is important to differentiate these diseases genetically.

Ranchod TM, Ho LY, Drenser KA, Capone A Jr, Trese MT. Clinical presentation of familial exudative vitreoretinopathy. *Ophthalmology*. 2011;118(10):2070–2075.

Vitreous Opacities

Vitreous Degeneration and Detachment Associated Opacities (“Floaters”)

Synchysis and syneresis result in loss of the highly organized vitreous anatomy. The collagen fibers that make up the vitreous can coalesce, or tangle, producing small areas that are no longer transparent and can cast shadows. These shadows are perceived by patients as floaters, and patients may find them bothersome. In some cases, for example as in cases of myopic vitreopathy, a large, dense central opacity can form, obstructing vision.

Following vitreous detachment, the coalescence and tangling of vitreous collagen fibers can worsen. In addition, areas where the vitreous was attached more firmly, such as at the optic nerve, are less transparent. When these areas move away from the retinal surface, they too can cast shadows and may be perceived as floaters. Varying amounts of bleeding can occur at the time of vitreous detachment, producing vitreous opacities.

Over time, as the vitreous continues to liquefy, the vitreous opacities may sink toward the bottom and become less noticeable. Also, the brain has the capacity to learn to selectively ignore the floaters, an adaptation not unlike how people who live next to a train track eventually do not hear trains passing unless they are specifically paying attention. As a result, most patients become asymptomatic or minimally symptomatic and do not require any intervention.

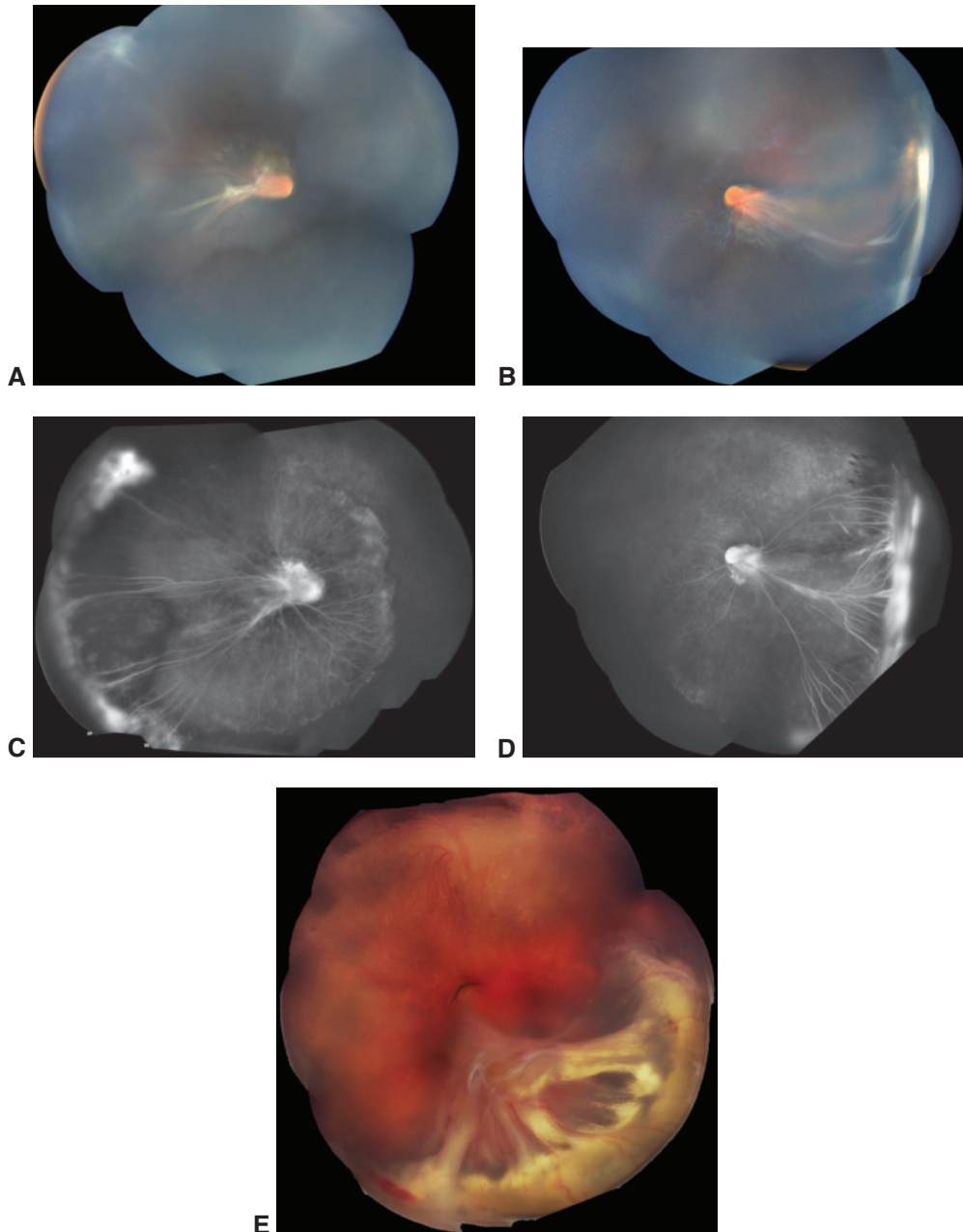


Figure 17-11 Familial exudative vitreoretinopathy (FEVR) with the *LRP5* mutation. **A–B**, The temporal retina shows a zone of nonperfusion that is horizontally V-shaped, causing a tractional macular fold. **C–D**, Fluorescein angiography images of the same patient demonstrate dragging of the vasculature. There is evidence of leakage and avascularity. **E**, Color fundus image montage from a patient with FEVR shows folding of the retina with massive exudation. (Courtesy of Audina M. Berrocal, MD.)

Table 17-2 Genes That Cause Familial Exudative Vitreoretinopathy

Gene	Disease(s)	Chromosome	Inheritance Pattern
<i>EVR1</i> (<i>FZD4</i> , 11q14.2)	Exudative vitreoretinopathy Retinopathy of prematurity	11	AD
<i>EVR2</i> (<i>NDP</i> , Xp11.3)	Exudative vitreoretinopathy Norrie disease	X	X-linked
<i>EVR3</i> (11p13–p12)	Exudative vitreoretinopathy	11	AD
<i>EVR4</i> (<i>LRP5</i> , 11q13.2)	Exudative vitreoretinopathy Endosteal hyperostosis Osteopetrosis (AD) Osteoporosis-pseudoglioma syndrome Osteosclerosis	11	AD, AR
<i>EVR5</i> (<i>TSPAN12</i> , 7q31.31)	Exudative vitreoretinopathy	7	AD

AD = autosomal dominant; AR = autosomal recessive.

Asteroid Hyalosis

In asteroid hyalosis, minute white opacities composed of calcium-containing phospholipids are found in the otherwise normal vitreous (Fig 17-12). Clinical studies have confirmed a relationship between asteroid hyalosis and both diabetes mellitus and hypertension. Asteroid hyalosis has an overall incidence of 1 in 200 persons, most frequently in people older than 50 years. The condition is unilateral in 75% of cases, and significant decreases in visual acuity are rare. When PVD occurs, compression of the material occurs

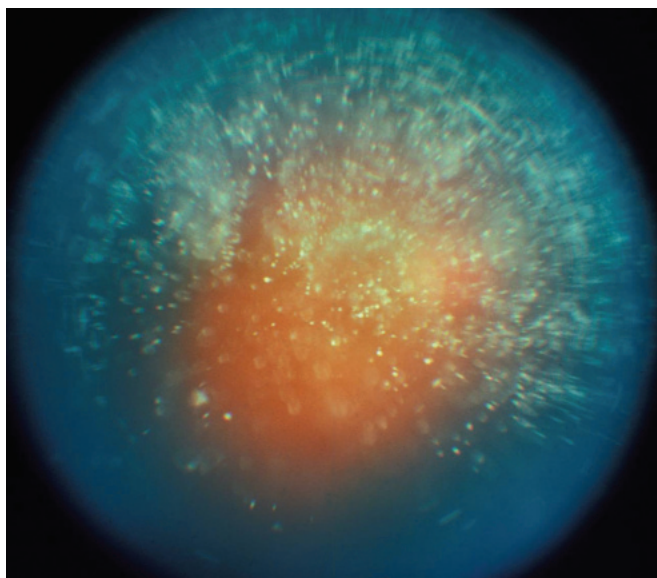


Figure 17-12 Color fundus photograph of asteroid hyalosis. (Courtesy of Hermann D. Schubert, MD.)

and visual acuity may decrease. When asteroid hyalosis blocks the view of the posterior fundus and retinal pathology is suspected, FA is usually successful in imaging the abnormalities. Occasionally, vitrectomy may be necessary to remove visually significant opacities or to facilitate treatment of underlying retinal abnormalities such as proliferative retinopathy. Many eyes with asteroid hyalosis have an abnormal vitreoretinal interface with unusual vitreoretinal adhesions. These adhesions increase the risk of retinal break formation during vitrectomy surgery.

Mochizuki Y, Hata Y, Kita T, et al. Anatomical findings of vitreoretinal interface in eyes with asteroid hyalosis. *Graefes Arch Clin Exp Ophthalmol*. 2009;247(9):1173–1177.

Vitreous Hemorrhage

A common cause of emergency visits to ophthalmology offices is sudden vision loss due to vitreous hemorrhage not associated with trauma to the eye. In adults, the most common causes include proliferative diabetic retinopathy (see Chapter 5), PVD, central retinal vein occlusion, and retinal neovascularization from a variety of causes (see Chapter 7, Table 7-2). Bleeding can be exacerbated by the use of systemic anticoagulants, so physicians need to be aware of the systemic medications the patient is taking. In cases of vitreous hemorrhage associated with an acute PVD, retinal tears are found in approximately 50%–70% of eyes and clinical retinal detachment in 8%–12%. In children, X-linked hereditary retinoschisis and pars planitis are common causes of vitreous hemorrhage; however, trauma must always be considered in the differential diagnosis (see Chapter 18).

In most cases of vitreous hemorrhage, the underlying cause can be determined by obtaining a history or on retinal examination. If the hemorrhage is too dense to permit indirect ophthalmoscopy or biomicroscopy, suggestive clues can be obtained from examination of the fellow eye. Diagnostic echography should be performed to detect any tractional tear (often superotemporally) and to rule out retinal detachment or tumor. Bilateral eye patching with bed rest for a few hours to several days, with the head of the bed elevated, may permit the intrahyaloid and retrohyaloid blood to settle, allowing for a better view of the posterior segment. If the etiology still cannot be established, the ophthalmologist should consider frequent reexamination with repeat echography until the cause is found. Alternatively, prompt diagnostic vitrectomy in nondiabetic patients can be considered and may help prevent progression of a retinal tear to retinal detachment. Ghost cell glaucoma can result from long-standing vitreous hemorrhage. Early intervention should be considered in monocular patients with vitreous hemorrhage. In addition, surgical intervention should be considered in patients whose hemorrhage does not clear.

El-Sanhouri AA, Foster RE, Petersen MR, et al. Retinal tears after posterior vitreous detachment and vitreous hemorrhage in patients on systemic anticoagulants. *Eye (Lond)*. 2011;25(8):1016–1019.

Sarrafizadeh R, Hassan TS, Ruby AJ, et al. Incidence of retinal detachment and visual outcome in eyes presenting with posterior vitreous separation and dense fundus-obscuring vitreous hemorrhage. *Ophthalmology*. 2001;108(12):2273–2278.

Witmer MT, Cohen SM. Oral anticoagulation and the risk of vitreous hemorrhage and retinal tears in eyes with acute posterior vitreous detachment. *Retina*. 2013;33(3):621–626.

Pigment Granules

In a patient without uveitis, retinitis pigmentosa, or a history of surgical or accidental eye trauma, the presence of pigmented cells in the anterior vitreous (“tobacco dust”), known as a *Shafer sign*, is highly suggestive of a retinal break (see Chapter 16).

Cholesterolosis

Numerous yellow-white, gold, or multicolored cholesterol crystals are present in the vitreous and anterior chamber in cholesterolosis, also known as *synchysis scintillans*. This condition appears almost exclusively in eyes that have undergone repeated or severe accidental or surgical trauma causing large intravitreal hemorrhages. The descriptive term *synchysis scintillans* refers to the highly refractile appearance of the cholesterol-containing crystals. In contrast to eyes with asteroid hyalosis, in which the opacities are evenly distributed throughout the vitreous cavity, eyes with cholesterolosis frequently have a PVD, which allows the crystals to settle inferiorly.

Amyloidosis

Bilateral vitreous opacification can occur as an early manifestation of the dominantly inherited form of familial amyloidosis, which is most commonly associated with a trans-thyretin mutation (Fig 17-13). Amyloid infiltration of the vitreous is rare in nonfamilial cases. In addition to the vitreous, amyloid can be deposited in the retinal vasculature, the choroid, and the trabecular meshwork.

Retinal findings include hemorrhages, exudates, cotton-wool spots, and peripheral retinal neovascularization. In addition, infiltrations may be present in the orbit, extraocular muscles, eyelids, conjunctiva, cornea, and iris. Nonocular manifestations of amyloidosis include upper- and lower-extremity polyneuropathy and central nervous system abnormalities. Amyloid can be deposited in several organs, including the heart and skin, and in the gastrointestinal tract.

Initially, the extracellular vitreous opacities appear to lie adjacent to retinal vessels posteriorly; they later develop anteriorly. At first, the opacities appear granular and have wispy fringes, but as they enlarge and aggregate, the vitreous takes on a “glass-wool” appearance. With vitreous liquefaction or PVD, the opacities may be displaced into the visual axis, causing reduced vision and photophobia.

The differential diagnosis of amyloidosis includes chronic (dehemoglobinized) vitreous hemorrhage, lymphoma, sarcoidosis, and Whipple disease. Vitrectomy may be indicated for vitreous opacities when symptoms warrant intervention, but recurrent opacities may develop in residual vitreous. Histologic examination of removed vitreous shows material with a fibrillar appearance and a staining reaction characteristic of amyloid. Birefringence and electron microscopic studies are confirmatory. Immunocytochemical studies have shown the major amyloid constituent to be a protein resembling prealbumin.

Sandgren O. Ocular amyloidosis, with special reference to the hereditary forms with vitreous involvement. *Surv Ophthalmol*. 1995;40(3):173–196.

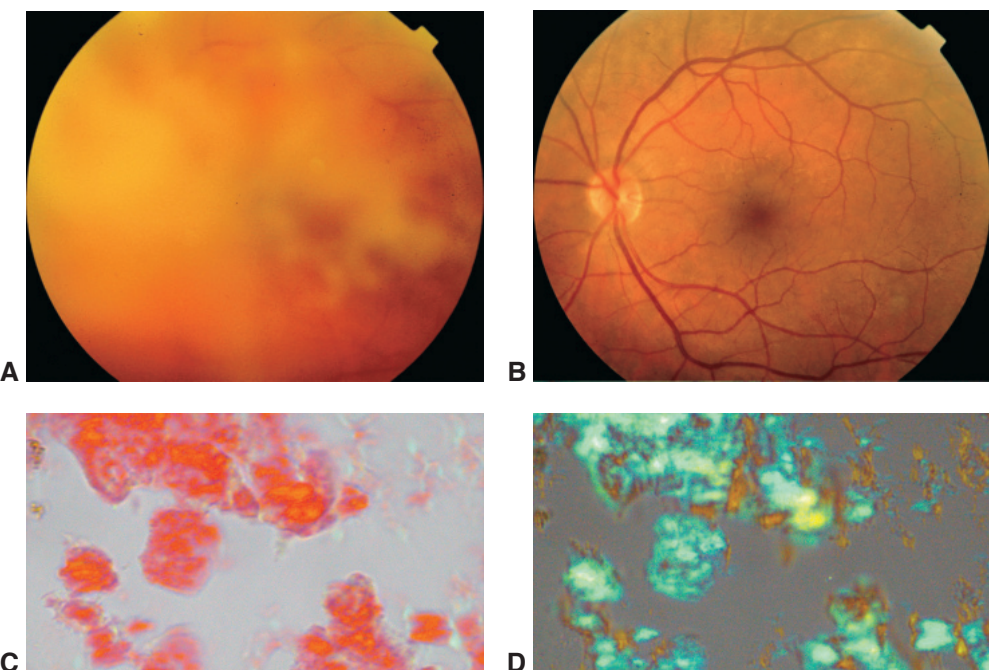


Figure 17-13 Amyloidosis. Images from a 57-year-old woman with a history of vitrectomy for floaters in the right eye. A cataract subsequently developed in the right eye and was extracted. Her vision then decreased in the left eye, which she ascribed to a cataract. **A**, Color fundus photograph of the left eye showed a dense vitreous infiltration; there was no cataract, and intraocular pressure was markedly elevated. Review of systems revealed carpal tunnel syndrome in both wrists. **B**, After vitrectomy surgery on the left eye, the color fundus photograph revealed retinal hemorrhages along the inferotemporal vascular arcade. **C**, The removed vitreous material, stained with Congo red, demonstrated birefringence (**D**). The patient was found to have a mutation affecting transthyretin. Glaucoma commonly develops in patients with transthyretin-related familial amyloidotic polyneuropathy. (Courtesy of Richard F. Spaide, MD.)

Vitreous Abnormalities Secondary to Surgery

Incarceration of vitreous in the wound during cataract or vitreous surgery can lead to many postoperative complications. Following cataract surgery with vitreous incarceration, there is increased risk of infectious endophthalmitis, epithelial ingrowth, hypotony, shallow anterior chamber, peripheral anterior synechiae, and secondary glaucoma. Incarcerated vitreous in the wound and iridovitreal adhesions may cause chronic ocular discomfort with inflammation, cystoid macular edema, and optic nerve head edema (Irvine-Gass syndrome). These complications may be reduced by disconnecting any vitreous from anterior adhesions and incarcerations through vitrectomy.

Retinal detachment can be caused by contraction of vitreous incarcerated in cataract or vitrectomy incisions. Such detachments may be rhegmatogenous or tractional and may require treatment with vitrectomy and/or scleral buckling surgery (see Chapter 20).

The risk of complications from vitreous loss during cataract surgery can be sharply reduced by careful anterior vitrectomy followed by meticulous closure of all wounds. For

further discussion of the complications of cataract surgery and their management, see BCSC Section 11, *Lens and Cataract*. For information about postoperative endophthalmitis, see BCSC Section 9, *Uveitis and Ocular Inflammation*.

Harbour JW, Smiddy WE, Rubsamen PE, Murray TG, Davis JL, Flynn HW Jr. Pars plana vitrectomy for chronic pseudophakic cystoid macular edema. *Am J Ophthalmol*. 1995;120(3):302–307.

CHAPTER 18

Posterior Segment Manifestations of Trauma



This chapter includes a related video, which can be accessed by scanning the QR code provided in the text or going to www.aao.org/bcscvideo_section12.

Ocular trauma is an important cause of visual impairment worldwide. Ocular globe trauma can be classified as follows (terminology based on the Birmingham Eye Trauma Terminology System):

- Closed-globe injuries
 - contusion (blunt trauma *without* break in eyewall)
 - lamellar laceration (partial-thickness wound of the eyewall)
 - superficial foreign bodies
- Open-globe injuries
 - rupture (blunt trauma *with* break in eyewall)
 - laceration (full-thickness wound of the eyewall, caused by a sharp object)
 - intraocular foreign bodies, penetrating or perforating
 - penetrating injury (entrance break; no exit break in eyewall)
 - perforating injury (both entrance and exit breaks in eyewall)

This chapter focuses on posterior segment injuries; therefore, lamellar lacerations and superficial foreign bodies are not discussed here.

Microsurgical techniques have improved the ability to repair corneal and scleral lacerations, and vitrectomy techniques allow management of severe intraocular injuries (see Chapter 20 in this volume). Ocular trauma is also discussed in BCSC Section 6, *Pediatric Ophthalmology and Strabismus*; Section 7, *Oculofacial Plastic and Orbital Surgery*; and Section 8, *External Disease and Cornea*.

Evaluation of the Patient After Ocular Trauma

In the initial evaluation of an ocular injury, the clinician should try to determine whether the injury is closed globe or open globe, and whether an intraocular foreign body (IOFB) is present. The evaluation includes obtaining a complete history, or as complete as possible under the circumstances, which is crucial before a patient with ocular trauma is examined (Table 18-1), and performing a thorough examination. During the examination, caution is required to avoid exacerbating the damage; for example, attempting to pry open the eye of

Table 18-1 Important Questions to Ask in Cases of Ocular Trauma

- When exactly did the injury occur?
- What was the exact mechanism of injury?
 - How forceful was the injury?
 - Was there any object that may have penetrated the eye; if so, what was the object's material (wood stick, nail, knife, etc.)?
- Is the presence of an intraocular foreign body a possibility?
 - Was the patient hammering metal on metal or working near machinery that could have caused a projectile to enter the eye?
 - Was the patient wearing spectacles or was he or she close to shattered glass?
 - Was the patient wearing eye protection?
- What was the health status of the eye before the injury?
 - Has the patient had previous ocular surgery, including laser in situ keratomileusis (LASIK), penetrating keratoplasty, and/or cataract surgery?
- Are there concomitant systemic injuries?
- What emergency measures were taken, if any (eg, tetanus shot given, antibiotics administered)?
- When was the last tetanus toxoid administered?
- When was the patient's last oral intake (in case surgery is required)?
- Was the injury work-related?

an uncooperative patient is inadvisable. If possible, the clinician should measure the visual acuity of each eye separately and evaluate the pupils for an afferent pupillary defect. To the extent possible, external, slit-lamp, and fundus examination should be performed and intraocular pressure (IOP) should be measured. Severe chemosis, ecchymosis, eyelid edema, low IOP, the presence of an entrance wound, iris damage or incarceration, cataract, or other anterior segment pathology may suggest an ocular rupture or laceration. Normal IOP and/or absence of findings on examination do not exclude an occult penetration of the globe.

If an open-globe injury is suspected but cannot be confirmed based on findings, or if lack of patient cooperation prevents a thorough examination in the clinical setting (eg, when examining a child), a thorough examination with possible surgical exploration should be performed under general anesthesia in the operating room. Optimally, the patient's consent should be obtained for immediate repair following this examination and surgical exploration.

Ocular imaging can help assess the status of the injured eye and facilitate detection of an IOFB, particularly in the presence of media opacities. In the acute setting, the 2 most helpful imaging systems are *ocular ultrasonography* (B-scan) and *computed tomography* (CT) of the eye and orbits. When an ocular ultrasound examination is performed, care must be taken to avoid causing ocular compression, which may lead to expulsion of intraocular matter. It is advisable to perform the ultrasound through the patient's closed lids, aided by copious amounts of ultrasound gel. B-scan ultrasonography can be particularly helpful in detecting nonradiopaque IOFBs, such as wood and plastic. Signs of a scleral rupture that are visible on ultrasonography include the entrapment of vitreous strands into the rupture site. Intraocular air may cause image artifacts that complicate the interpretation of ultrasonography.

Bone-free *plain-film x-ray studies* may be helpful, but these are less sensitive than ultrasonograms for detecting smaller IOFBs. CT is very helpful in detecting radiopaque

IOFBs; however, very dense IOFBs may introduce image artifacts that cause them to appear larger than they really are, making exact localization difficult. Although *magnetic resonance imaging (MRI)* is not usually used in the acute setting, it can be helpful in detecting detailed ocular anatomy and in identifying the presence and location of IOFBs, including those that are not radiopaque. However, MRI should be used only after the presence of ferromagnetic foreign bodies has been definitively ruled out, due to the possibility that the magnetic field may move such foreign bodies, causing additional damage.

Blunt Trauma Without Break in Eye Wall

In blunt trauma, the object does not penetrate the eye but may cause rupture of the eye-wall. Serious sequelae from blunt trauma affecting the anterior segment include

- angle recession (see also BCSC Section 10, *Glaucoma*)
- iridodialysis (see also BCSC Section 8, *External Disease and Cornea*)
- iritis (see also BCSC Section 9, *Uveitis and Ocular Inflammation*)
- hemorrhage into the anterior chamber (hyphema)
- subluxated or dislocated lens (see also BCSC Section 11, *Lens and Cataract*)

Serious sequelae from blunt trauma affecting the posterior segment include

- commotio retinae
- choroidal rupture
- macular hole
- choroidal hemorrhage
- retinal tears or detachment
- vitreous hemorrhage
- traumatic chorioretinal disruption (retinal sclopetaria)

See Chapter 16 for discussion of traumatic retinal breaks and retinal detachment and Chapter 20 for discussion of choroidal hemorrhage. Sequelae of the posterior segment are discussed in the following sections.

Commotio Retinae

The term *commotio retinae* refers to damage to the outer retinal layers caused by shock waves that traverse the eye from the site of impact following blunt trauma. Ophthalmoscopic examination reveals a sheenlike retinal whitening that appears some hours after the injury (Fig 18-1). This retinal whitening occurs most commonly in the posterior pole but may also be found peripherally. Spectral-domain optical coherence tomography (SD-OCT) findings suggest that the major site of disruption is in the photoreceptor and retinal pigment epithelium (RPE) layers, resulting in the observed retinal opacification. With foveal involvement, a cherry-red spot may appear because the cells involved in the whitening are not present in the foveola. Commotio retinae in the posterior pole may decrease visual acuity to as low as 20/200. Gradual visual recovery may occur if there is no associated macular pigment epitheliopathy, choroidal rupture, or macular hole formation.



Figure 18-1 Color fundus photograph reveals commotio retinae (arrows) and vitreous hemorrhage after blunt trauma.

Choroidal Rupture

When the eye is compressed along its anterior-posterior axis, tears may occur in Bruch membrane, which has little elasticity, as well as in the overlying RPE and fibrous tissue around the choriocapillaris. Adjacent subretinal hemorrhage is common. Choroidal ruptures may be single or multiple and occur typically in the periphery and concentric to the optic nerve head (Fig 18-2). Ruptures that extend through the fovea may cause permanent vision loss. There is no effective treatment.



Figure 18-2 Color fundus photograph from a patient with a posttraumatic submacular hemorrhage. The hemorrhage started to clear, revealing a choroidal rupture (arrow). The yellow material located at the inferonasal portion of the macula (arrowhead) is dehemoglobinized blood. (Courtesy of Mark Johnson, MD.)

Occasionally, choroidal neovascularization (CNV) develops as a late complication after damage to Bruch membrane (Fig 18-3). A patient with a choroidal rupture near the macula should be alerted to the risk of CNV. Subfoveal CNV, if present, is generally treated with a vascular endothelial growth factor (VEGF) inhibitor. See Chapter 4 of this volume for information on the management of CNV.

Posttraumatic Macular Hole

Blunt trauma may cause a full-thickness macular hole by various mechanisms, including contusion necrosis and vitreous traction. Holes may be observed immediately after blunt

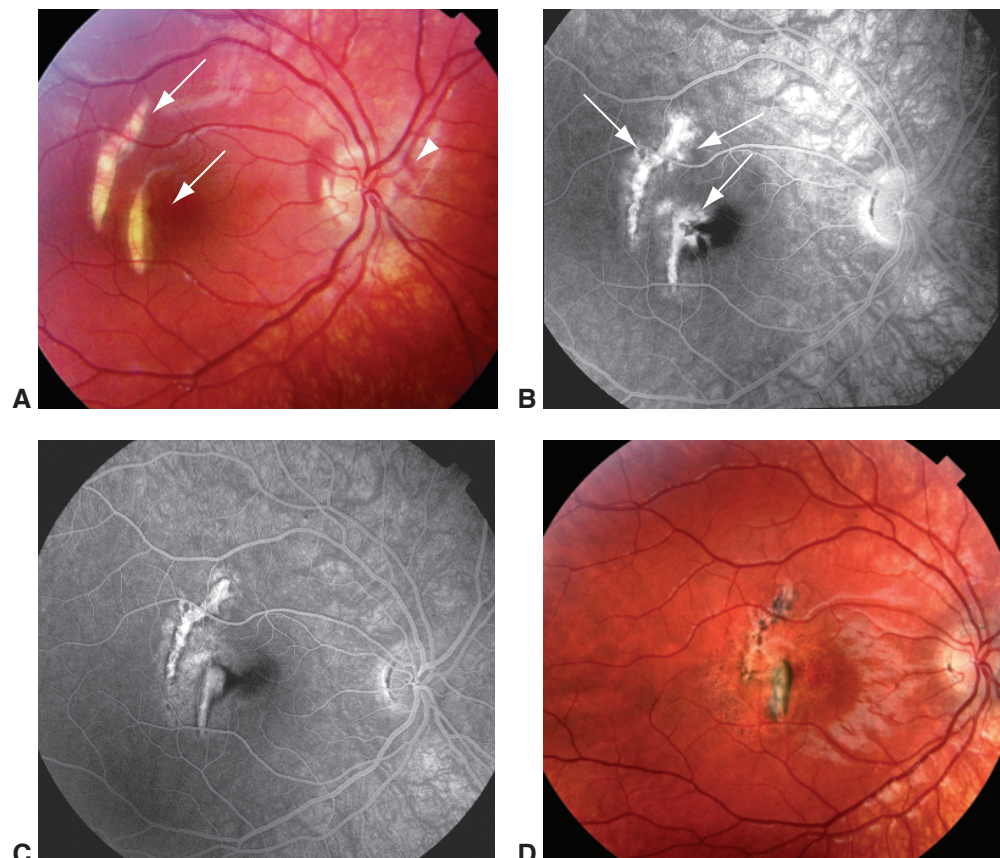


Figure 18-3 Images from a 10-year-old who was hit in the eye with a tennis ball. **A**, Color fundus photograph reveals choroidal ruptures (arrows). A subretinal hemorrhage is present around the nerve head (arrowhead). Visual acuity was 20/30. **B**, Six weeks later, visual acuity decreased to 20/400. Late-phase fluorescein angiography image shows multiple fronds of choroidal neovascularization (CNV) arising from the choroidal ruptures (arrows). **C**, Late-phase fluorescein angiography image taken 2 weeks after treatment with corticosteroids and photodynamic therapy shows the CNV has regressed dramatically. **D**, Color fundus photograph taken 6 months after treatment. The scarring around the choroidal ruptures obscures their characteristic appearance. Some pigmentary changes have occurred in the macula as well, but visual acuity is 20/25. (Courtesy of Richard F. Spaide, MD.)

trauma that causes severe commotio retinae, following a submacular hemorrhage caused by a choroidal rupture (Fig 18-4), or after a whiplash separation of the vitreous from the retina. In addition, central depressions, or macular pits (similar to those observed

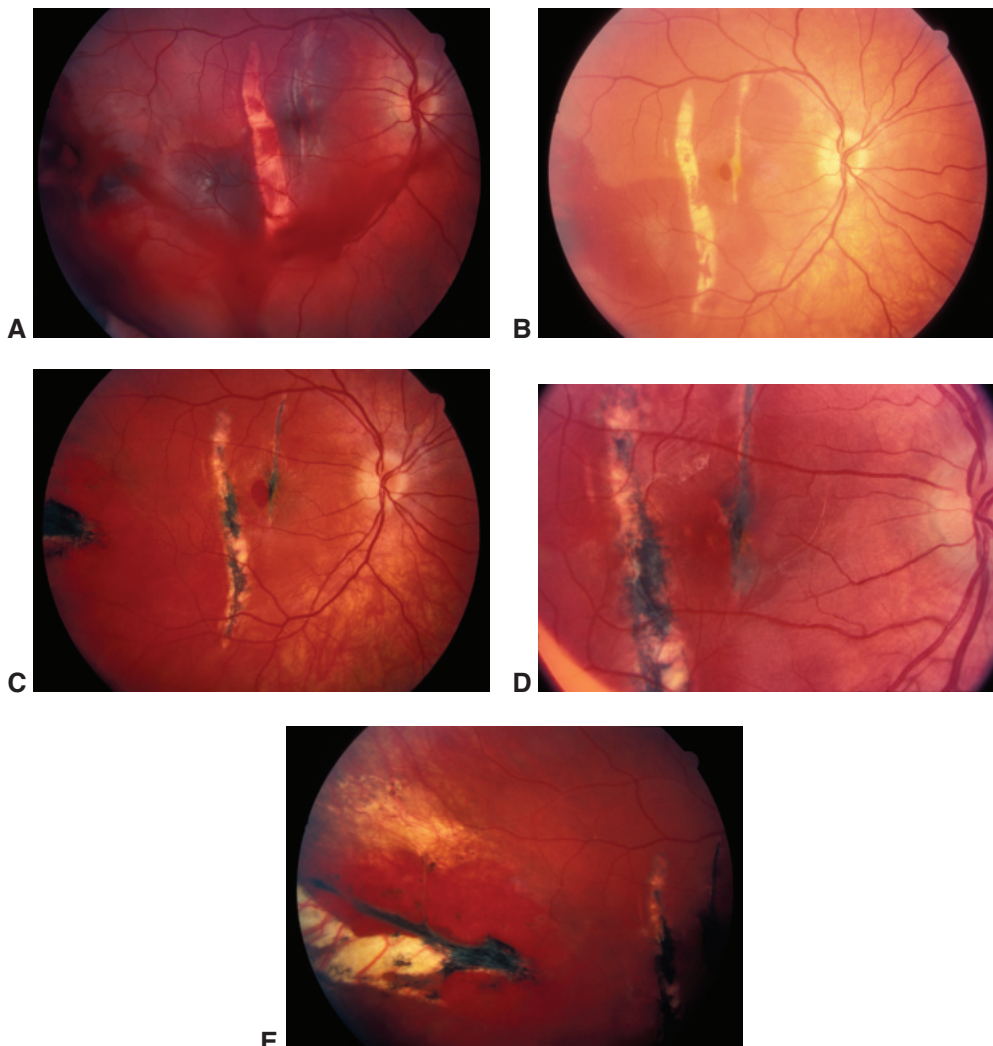


Figure 18-4 Blunt ocular trauma with traumatic choroidal rupture, subretinal hemorrhage, macular hole, and retinal sclopetaria. **A**, Fundus photograph obtained shortly after the 14-year-old boy's right eye was struck by a coin thrown forcefully at him. Choroidal rupture in the macula, submacular hemorrhage, and vitreous hemorrhage emanating from the temporal periphery are apparent. **B**, Several days later, a macular hole developed. **C**, After several weeks, the choroidal rupture was healed, leaving pigment hypertrophy and the macular hole. **D**, Fundus photograph shows a closed macular hole following vitrectomy with internal limiting membrane peeling, gas-bubble placement, and face-down positioning. Visual acuity eventually recovered to 20/60. **E**, Fundus photograph of the temporal periphery shows the sequelae of mild to moderate retinal sclopetaria, the source of the vitreous hemorrhage observed immediately after the injury. (Courtesy of Colin A. McCannel, MD.)

in patients after sun gazing), have been described following blunt trauma to the eye and whiplash injuries. Lightning and electrical injury can also cause macular holes; patients with these injuries usually have signs of cataract and can have acute peripapillary retinal whitening. Posttraumatic macular holes may close spontaneously or may be successfully closed surgically. Depending on the degree of collateral damage to the fovea, visual acuity recovery varies greatly.

Vitreous Hemorrhage

Vitreous hemorrhage is a common sequela of ocular trauma. Because a hemorrhage that is loculated at presentation can later become diffuse, a determination of the cause of the hemorrhage should always be undertaken as soon as possible. Bed rest with elevation of the head may enable the hemorrhage to settle sufficiently to allow for a more detailed ophthalmoscopic examination. If vitreous hemorrhage obscures the view of the posterior segment, B-scan or radiologic ocular imaging should be considered.

Traumatic Chorioretinal Disruption (Retinal Sclopetaria)

An unusual retinal pathology can be produced by high-speed projectile injuries to the orbit. Large areas of choroidal and retinal disruption combine with extensive subretinal, retinal, or vitreous hemorrhage. As the blood resorbs, the injured area is repaired by extensive scar formation and widespread pigmentary alteration (Fig 18-5, see also Fig 18-4).



Figure 18-5 A color fundus photograph from a patient shot with a bullet 2 months earlier in the right inferotemporal orbit, causing the sequelae of retinal sclopetaria. The bullet's path missed the globe by several millimeters, and the patient acutely lost visual acuity. The image shows large areas of subretinal proliferation and retinal pigment epithelial hyperplasia, consistent with moderate to severe retinal sclopetaria. Visual acuity returned to 20/70. (Courtesy of Richard F. Spaide, MD.)

If the macula is involved, there is significant loss of vision. Secondary retinal detachment rarely develops. The pattern of damage is ascribed to shock waves generated by the deceleration of the projectile passing close to the sclera. Blunt trauma due to injuries from paintballs or other projectiles may produce a similar fundus appearance.

Open-Globe Injuries

Open-globe injuries generally have a guarded prognosis regarding visual acuity outcomes (see the section Prognostication of Globe Injuries later in this chapter). The development of a retinal detachment is common; the detachment is usually caused by the primary injury or by traction resulting from proliferative vitreoretinopathy (PVR). In all cases of open-globe injuries, the presence of an intraocular foreign body should be ruled out.

Scleral Rupture

Severe blunt injuries can rupture the globe. Rupture injuries can be very severe; there is often expulsion of intraocular content (to varying degrees). The 2 most common locations for rupture are the limbus, particularly through previous surgical wounds, or through areas of physiological scleral thinning parallel to and under the insertions of the rectus muscles. Important diagnostic signs of rupture include a marked decrease in ocular ductions, very boggy conjunctival chemosis with hemorrhage (ecchymosis), deepened anterior chamber, and severe vitreous hemorrhage. The IOP is usually very low but may be normal or even elevated.

Lacerating and Penetrating Injuries

Lacerating injuries result from cutting or tearing of the eyewall by objects of varying sharpness. A penetrating injury of the globe is a laceration of the eyewall at a single entry site. The prognosis is related to the location and extent of the wound, as well as the associated damage and degree of hemorrhage.

Perforating Injuries

A globe-perforating injury has both entrance and exit wounds. Globe-perforating injuries may be caused by objects of varying sharpness such as needles, knives, high-velocity pellets, or small fragments of metal. An important iatrogenic cause is needle perforation during retrobulbar or peribulbar anesthesia for intraocular surgery. Studies have shown that, after perforating injuries, fibrous proliferation occurs along the scaffold of damaged vitreous between the entrance and exit wounds. The wounds are often closed by fibrosis within 5–7 days after the injury, depending on wound size. Small-gauge injuries with only a small amount of hemorrhage and no significant collateral damage often heal without serious sequelae.

Surgical Management

In most instances, primary repair of open-globe injuries consists of suturing of the corneal and scleral wounds. Although there are some theoretical reasons for performing an early vitrectomy, the priority at the time of the acute injury is to close the globe. Primary wound closure should not be delayed, particularly because closure will facilitate a later vitrectomy if it is needed. For more on vitrectomy, see Chapter 20 in this volume. Open-globe trauma surgery is best performed with the patient under general anesthesia, because injection of local anesthetics into the orbit can cause compression of the globe and expulsion of intraocular content.

Primary repair

The principles of primary repair of open-globe injuries include careful, gentle microsurgical corneoscleral wound repair, during which incarcerated uvea is repositioned or excised. If a laceration crosses the limbus, or if there is any suspicion of a scleral laceration or rupture, a gentle and generous peritomy, usually 360°, should be performed for best possible exposure. Corneal lacerations may be closed with 10-0 nylon interrupted sutures, and scleral wounds may be closed with stronger 7-0, 8-0, or 9-0 nonabsorbable sutures. Vitreous should be excised from the wound and the anterior chamber should be reformed. Any uvea or retina that protrudes should be amputated if contaminated or gently repositioned into the eye. Chapter 4 of BCSC Section 4, *Ophthalmic Pathology and Intraocular Tumors*, discusses wound healing in detail.

Any scleral laceration must be explored until its posterior extent has been located. If no laceration or rupture can be seen, and a posterior rupture is suspected, a meticulous scleral exploration, including underneath the rectus muscles, should be performed. This may necessitate disinserting one or more extraocular muscles to achieve adequate exposure. If the wound is very posterior, the site should be left to heal without suturing; attempts to suture very posterior wounds may result in expulsion of intraocular content. Some ophthalmologists advocate for placing a prophylactic encircling scleral buckle at the time of primary repair to reduce the likelihood of a later retinal detachment.

Immediate vitrectomy

Immediate vitrectomy may be necessary or advisable in some circumstances—for example, if evaluation suggests the possibility of an IOFB or endophthalmitis.

Some surgeons favor immediate vitrectomy at the time of the primary repair, before cellular proliferation (proliferative vitreoretinopathy) begins. Inducing a posterior vitreous detachment and thorough dissection of the vitreous removes some of the scaffold on which contractile membranes grow. This may reduce the risk of late complications such as tractional retinal detachments, cyclitic membrane formation, and phthisis bulbi. Separating the posterior cortical vitreous from the retina may be difficult, especially in children, young adults, and in eyes with retinal breaks or retinal detachment. If the injury is perforating, the posterior wound may present challenges because it may leak infusate, making the maintenance of IOP during surgery difficult.

Delayed vitrectomy

Most practitioners in the United States prefer initially performing a primary repair of the wound(s) to restore the globe and IOP, followed by delayed vitrectomy, if needed. Reasons that support of delayed vitrectomy include

- decreasing the risk of intraoperative hemorrhage in eyes that are acutely inflamed and congested
- allowing the cornea to clear and improve intraoperative visualization
- permitting spontaneous separation of the vitreous from the retina, which facilitates a safer and more complete vitrectomy
- allowing posterior wounds in perforating injuries to heal, so there is ocular integrity during vitrectomy

The optimal timing of vitrectomy following primary repair remains controversial. It may be best to perform vitrectomy 2–14 days following primary repair. Many advocate waiting at least 5 days if there are unsutured (posterior) wounds. Vitrectomy that is delayed more than 2 weeks following the injury may contribute to substantial worsening of proliferative vitreoretinopathy and associated worse anatomic and visual outcomes.

Typical indications for vitrectomy may include the following:

- the presence of moderate to severe vitreous hemorrhage
- other tissue damage that requires repair
- phacoanaphylactic uveitis, which may occur if the lens is damaged
- signs of developing transvitreal traction
- retinal detachment

Kuhn F. The timing of reconstruction in severe mechanical trauma. *Ophthalmic Res.* 2014;51(2):67–72.

Mieler WF, Mittra RA. The role and timing of pars plana vitrectomy in penetrating ocular trauma. *Arch Ophthalmol.* 1997;115(9):1191–1192.

Intraocular Foreign Bodies

An IOFB should always be suspected and ruled out in cases of ocular or orbital trauma. In most cases, an IOFB is either observed, or it is suggested by the presence of an entry site or the reported mechanism of injury. A detailed history helps the clinician assess the likelihood of the presence of an IOFB. As previously discussed, ocular imaging can be very helpful in the detection of IOFBs (Fig 18-6). If surgical removal of an IOFB cannot be accomplished promptly, intravitreal injection of antimicrobial agents should be considered to minimize the risk of endophthalmitis developing.

Surgical techniques for removal of intraocular foreign bodies

In the case of an IOFB, surgical planning should address the following issues:

- location of the foreign body in the eye
- surgeon's ability to visualize and localize the foreign body
- size and shape of the foreign body

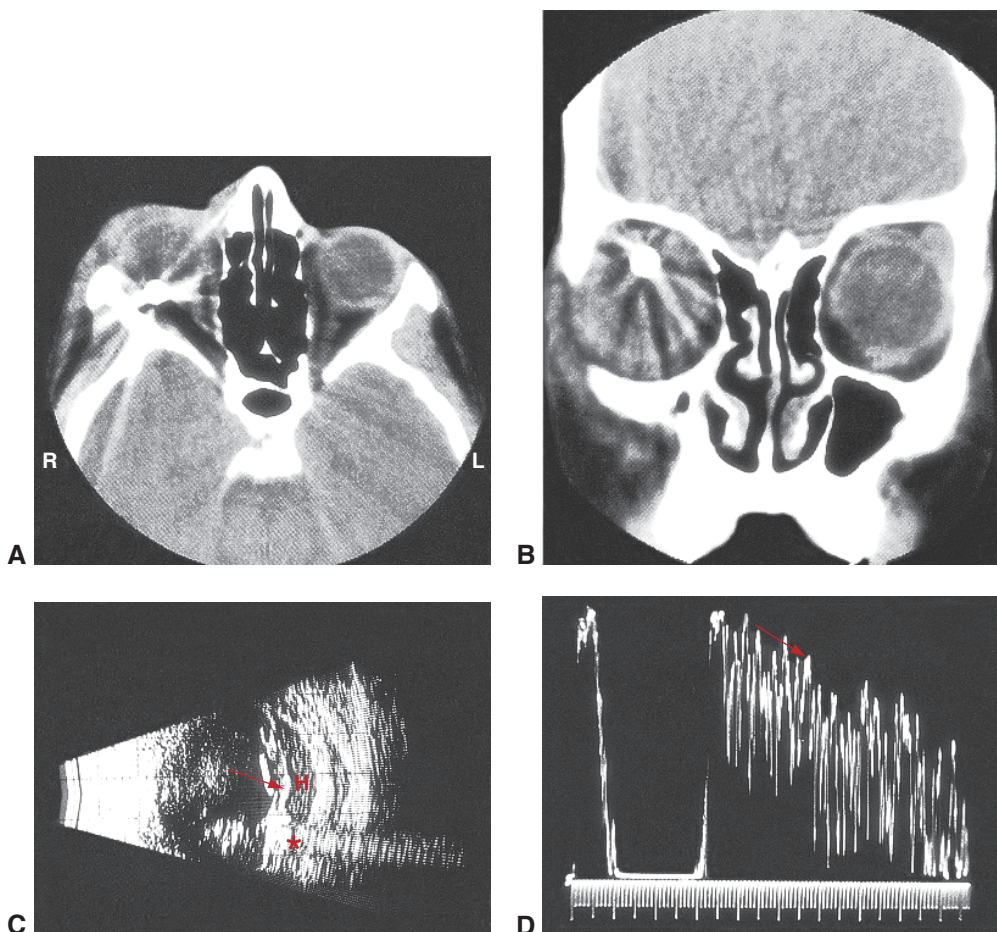


Figure 18-6 Images from a patient with an intraocular BB pellet. Axial (**A**) and coronal (**B**) computed tomography views show the pellet's position to be in the superior and posterior globe. B-scan echography (**C**) shows retinal detachment (arrow) and subretinal hemorrhage (H). A characteristic reverberation of echoes between the front and back surfaces of the round pellet gives a “trail of echoes” artifact that extends posterior to the foreign body on B-scan (asterisk) and on A-scan (**D**) (arrow).

- composition of the foreign body (ferromagnetic vs nonferromagnetic)
- encapsulation of the foreign body

Pars plana vitrectomy allows removal of traumatized vitreous and facilitates controlled microsurgical extraction of IOFBs as well as media opacities such as cataract and hemorrhage (Video 18-1). Before forceps extraction is attempted, the IOFB should be freed of all attachments. A small rare-earth magnet may be used to engage and separate the foreign body from the retinal surface. Although small foreign bodies can be removed through enlargement of the pars plana sclerotomy site, it may be safer to extract some large foreign bodies through the corneoscleral limbus or the initial wound to minimize collateral damage.


VIDEO 18-1 Removal of large metallic intraocular foreign body.

Courtesy of Nur Acar, MD.

 Access all Section 12 videos at www.aao.org/bcscvideo_section12.


Retained intraocular foreign bodies

The reaction of the eye to a retained foreign body varies widely and depends on the object's chemical composition, sterility, and location. Inert, sterile foreign bodies such as stone, sand, glass, porcelain, plastic, and cilia are generally well tolerated. If such material is found several days after the injury and does not appear to create an inflammatory reaction, it may be left in place, provided it is not obstructing vision.

Zinc, aluminum, copper, and iron are metals that are commonly reactive in the eye. Of these, zinc and aluminum tend to cause minimal inflammation and may become encapsulated. However, any very large foreign body may incite inflammation and thereby cause proliferative vitreoretinopathy. Epiretinal proliferations, tractional retinal detachment, and phthisis bulbi may result in complete loss of vision. Migration of the foreign body also can occur, especially if it contains copper.

Chalcosis Pure copper is especially toxic and causes acute *chalcosis*. Prompt removal is required to prevent severe inflammation that may lead to loss of the eye. Foreign bodies with a copper content of less than 85% (eg, brass, bronze) may cause *chronic chalcosis*. Typical findings in chronic chalcosis are deposits in Descemet membrane (a sign similar to the Kayser-Fleischer ring in Wilson disease and the result of copper's affinity for basement membranes), greenish aqueous particles, green discoloration of the iris, lens capsule ("sunflower" cataract), brownish-red vitreous opacities and strand formation, and metallic flecks on retinal vessels and the internal limiting membrane in the macular region. Late removal of copper may not cure the chalcosis; in fact, dissemination of the metal during surgery may worsen the inflammatory response.

Siderosis bulbi In *siderosis bulbi*, iron from IOFBs is deposited primarily in neuroepithelial tissues such as the iris sphincter and dilator muscles, the nonpigmented ciliary epithelium, the lens epithelium (see BCSC Section 11, *Lens and Cataract*, Chapter 5, Fig 5-14), the retina, and the RPE. Retinal photoreceptors and RPE cells are especially susceptible to damage from iron (Table 18-2). Electroretinography (ERG) changes in eyes with early siderosis include an increased a-wave and normal b-wave, a progressively diminishing b-wave amplitude over time, and eventually an undetectable signal during the final stage of iron toxicity of the retina. Serial ERGs can be helpful in monitoring eyes with small retained foreign bodies. If the b-wave amplitude decreases, removal of the foreign body is generally recommended.

Posttraumatic Endophthalmitis

Endophthalmitis occurs following 2%–7% of penetrating injuries; the incidence is higher in association with IOFBs and in rural settings. Posttraumatic endophthalmitis can progress rapidly; its clinical signs include marked inflammation featuring hypopyon, fibrin, vitreous infiltration, and corneal opacification. The risk of endophthalmitis occurring after

Table 18-2 Symptoms and Signs of Siderosis Bulbi

Symptoms
Nyctalopia
Concentrically constricted visual field
Decreased vision
Signs
Rust-colored corneal stromal staining
Iris heterochromia
Pupillary mydriasis and poor reactivity
Brown deposits on the anterior lens
Cataract
Vitreous opacities
Peripheral retinal pigmentation (early)
Diffuse retinal pigmentation (late)
Narrowed retinal vessels
Optic nerve head discoloration and atrophy
Secondary open-angle glaucoma from iron accumulation in the trabecular meshwork

penetrating ocular injury may be reduced by prompt wound closure and early removal of IOFBs. Use of prophylactic subconjunctival, intravenous, or intravitreal antibiotics is often recommended. Intravitreal or periocular aminoglycoside antibiotics should be avoided because of their high risk of retinal toxicity. Anterior chamber and vitreous cultures should be obtained, and if endophthalmitis is suspected, antibiotics should be injected.

Bacillus cereus, which rarely causes endophthalmitis in other settings, accounts for almost 25% of cases of posttraumatic endophthalmitis. Endophthalmitis caused by *B cereus* has a rapid and severe course and, once established, leads to profound vision loss and often loss of the eye. Most commonly, *B cereus* endophthalmitis is associated with soil-contaminated injuries, especially those involving foreign bodies. Gram-negative organisms are also frequent pathogens in posttraumatic endophthalmitis.

Treatment of posttraumatic endophthalmitis should cover the aforementioned pathogens. Because recommendations for antibiotic selection can change, ophthalmologists should consult a recent reference or an infectious disease specialist.

Jindal A, Pathengay A, Mithal K, et al. Endophthalmitis after open globe injuries: changes in microbiological spectrum and isolate susceptibility patterns over 14 years. *J Ophthalmic Inflamm Infect.* 2014;4(1):5.

Pronostication of Globe Injuries

The severity of the damage to the eye and its function at presentation have prognostic significance. Given the complexity of ocular trauma and its inherent unpredictable nature, there is no perfect system for prognostication of ocular injuries. However, some specific factors have been determined to have prognostic importance. Functional assessments include evaluating visual acuity and whether an afferent pupillary defect is present, and noting the injury descriptors, specifically the type of trauma and the zone of injury. The

Table 18-3 Calculating the Ocular Trauma Score

Step 1: Record any of variables present and their associated raw points.

Variables Used	Raw Points
A. Visual acuity at presentation	
NLP	60
LP/HM	70
1/200–19/200	80
20/200–20/50	90
≥20/40	100
B. Rupture	-23
C. Endophthalmitis	-17
D. Perforating injury	-14
E. Retinal detachment	-11
F. Afferent pupillary defect	-10

Step 2: Total the raw points of the applicable variables (A–F) to determine the raw score.

Step 3: Use the raw score to look up the estimate of the likelihood of various final visual acuity outcomes.

Raw Score	NLP	LP/HM	1/200–19/200	20/200–20/50	≥20/40
0–44	74%	15%	7%	3%	1%
45–65	27%	26%	18%	15%	15%
66–80	2%	11%	15%	31%	41%
81–91	1%	2%	3%	22%	73%
92–100	0%	1%	1%	5%	94%

HM = hand motions; LP = light perception; NLP = no light perception.

Adapted from Kuhn F, Maisiak R, Mann L, Mester V, Morris R, Witherspoon CD. The Ocular Trauma Score (OTS). *Ophthalmol Clin North Am*. 2002;15(2):163–165, vi.

Ocular Trauma Score assigns a point value based on these assessments (Table 18-3). In this system, visual acuity is the most important predictor of injury severity; other characteristics are assigned a negative point value that is subtracted from the visual acuity score to produce the total raw score. The higher the raw score, the better the final visual acuity prognosis (see Table 18-3). This system is a useful general guide to roughly estimate visual acuity outcomes following globe trauma.

Kuhn F, Maisiak R, Mann L, Mester V, Morris R, Witherspoon CD. The Ocular Trauma Score (OTS). *Ophthalmol Clin North Am*. 2002;15(2):163–165, vi.

Pieramici DJ, Au Eong KG, Sternberg P Jr, Marsh MJ. The prognostic significance of a system for classifying mechanical injuries of the eye (globe) in open-globe injuries. *J Trauma*. 2003;54(4):750–754.

Sympathetic Ophthalmia

Sympathetic ophthalmia is a rare complication of penetrating ocular trauma in which the fellow, uninjured eye develops a severe autoimmune inflammatory reaction. Removing an injured eye is thought to reduce the very small risk of sympathetic ophthalmia, especially

if it is done by 14 days after the injury. Thus, some advocate for prompt enucleation of eyes without vision (no light perception). Others advise against the removal of eye, because the disorder is extremely rare and treatable, and superior cosmetic and psychological outcomes are achieved with globe retention. Sympathetic ophthalmia is discussed in more detail in BCSC Section 9, *Uveitis and Ocular Inflammation*.

Avulsion of the Optic Nerve Head

A forceful backward dislocation of the optic nerve from the scleral canal can occur under several circumstances, including

- extreme rotation and forward displacement of the globe
- penetrating orbital injury, causing a backward pull on the optic nerve
- sudden increase in IOP, causing rupture of the lamina cribrosa

Total loss of vision characteristically occurs. Findings may vary from a pitlike depression of the optic nerve head to posterior hemorrhage and contusion necrosis (Fig 18-7); however, hemorrhage is usually present acutely. A B-scan ultrasound may reveal a hypoechoic defect in the area of the posterior scleral defect in the region of the optic nerve (ON). Cross-sectional neuroimaging may also be helpful in making the diagnosis.

Abusive Head Trauma

Severe shaking of infants, a form of nonaccidental trauma, is the cause of abusive head trauma (formerly known as *shaken baby syndrome*). The typical baby with abusive head trauma is almost always younger than 1 year and is frequently younger than 6 months. The presenting sign of child abuse involves the eye in approximately 5% of cases. Any

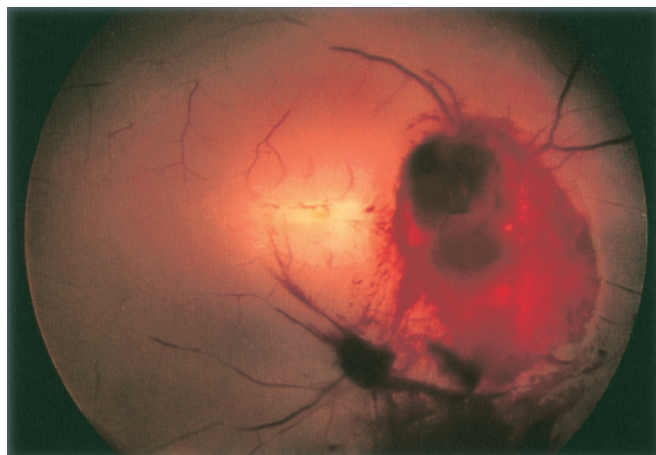


Figure 18-7 Avulsion of the optic nerve head. In this color fundus photograph, the nerve is obscured by hemorrhage, and a mixed vascular occlusion is present.

physician who suspects that child abuse might have occurred is required by law in every US state and Canadian province to report the incident to a designated government agency.

See BCSC Section 6, *Pediatric Ophthalmology and Strabismus*, for discussion of the multiple systemic symptoms associated with abusive head trauma. Ocular signs include

- retinal hemorrhages and cotton-wool spots (Fig 18-8)
- retinal folds
- hemorrhagic schisis cavities

The retinal hemorrhages associated with abusive head trauma often have a hemispheric contour. They can begin to resolve very rapidly, so it is important to examine suspected cases on presentation. The retinopathy may resemble that observed in Terson syndrome or central retinal vein occlusion, neither of which is common in infants. Retinal hemorrhages may be caused by trauma, but they are not usually associated with typical accidents, such as falls in the home.

Vitrectomy for vitreous hemorrhage should be considered if amblyopia is likely to occur but may be deferred if a bright-flash ERG response shows loss of the b-wave, which is indicative of extensive retinal damage. Fluorescein angiography shows attenuated vasculature and avascularity of the periphery.

Matthews GP, Das A. Dense vitreous hemorrhages predict poor visual and neurological prognosis in infants with shaken baby syndrome. *J Pediatr Ophthalmol Strabismus*. 1996;33(4):260–265.

Pierre-Kahn V, Roche O, Dureau P, et al. Ophthalmologic findings in suspected child abuse victims with subdural hematomas. *Ophthalmology*. 2003;110(9):1718–1723.

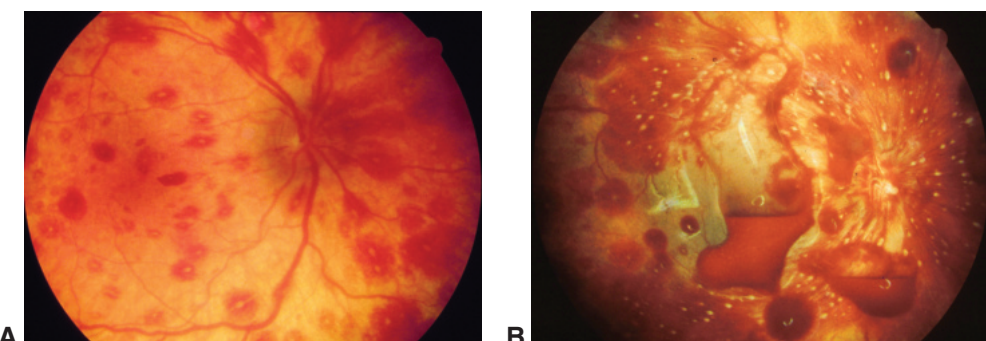


Figure 18-8 Color fundus photographs from a patient with abusive head trauma causing pre-retinal and retinal hemorrhages. **A**, Image taken several days after hospital admission, by which time many of the smaller hemorrhages had started to resorb. **B**, Numerous hemorrhages are located on and within the retina, and regions of hemorrhagic retinoschisis are observed centrally. Because the baby was upright, the red blood cells sank down into a dependent position within the larger regions of hemorrhagic retinoschisis. Some of the hemorrhages were white centered, whereas others had reflections of the flash from the fundus camera. (Used with permission from Spaide RF, Swengel RM, Scharre DW, Mein CE. Shaken baby syndrome. Am Fam Physician. 1990;41(4):1145–1152.)

Photic Damage

The eye has several mechanisms to protect itself against light damage, including pupil constriction, light absorption by melanin in the RPE, and the presence of antioxidants, such as lutein and zeaxanthin, in the macula. Light injures the retina by 3 basic mechanisms: (1) mechanical, (2) thermal, and (3) photochemical. *Mechanical injury* occurs when the power of the absorbed light is high enough to form gas or water vapor or to produce acoustic shock waves that mechanically disrupt retinal tissues. The absorbed energy may be enough to strip electrons from molecules in the target tissue, producing a collection of ions and electrons referred to as *plasma*. For example, a Q-switched Nd:YAG laser produces its therapeutic effect through mechanical light damage and uses this effect to disrupt a cloudy posterior capsule behind an intraocular lens.

Thermal injury occurs when excessive light absorption by the RPE and surrounding structures causes local elevation of the tissue temperature, leading to coagulation, inflammation, and scarring of the RPE and the surrounding neurosensory retina and choroid. A therapeutic application of thermal light injury is the retinal burn caused by laser photocoagulation. See Chapter 19 for discussion of photocoagulation.

Photochemical injury results from biochemical reactions that cause retinal tissue destruction without elevation of temperature. It is the result of the transfer of light energy to a molecule; the excess energy initiates reactions that cause tissue damage. Damaging reactions can include oxidation, photoisomerization, photochemical cleavage, and electrocyclic reactions. Such changes occur primarily at the level of the outer segments of the photoreceptors, which are more sensitive than the inner segments. Examples of photochemical injury are solar retinopathy and photic retinopathy that occurs after excessive exposure to illumination from an operating microscope.

Mainster MA, Turner PL. Photic retinal injuries: mechanisms, hazards, and prevention.

In: Schachat AP, Wilkinson CP, Hinton DR, Sadda SR, Wiedemann P, eds. *Ryan's Retina*. Vol 2. 6th ed. Philadelphia: Elsevier/Saunders; 2018:chap 93.

Solar Retinopathy

Solar retinopathy, also known as *foveomacular retinitis*, *eclipse retinopathy*, or *solar retinitis*, is a thermally enhanced photochemical retinal injury caused by direct or indirect gazing at the sun; it may also occur after viewing a solar eclipse without proper protection. The extent of the damage depends on the duration and intensity of the exposure. Younger patients with clearer lenses are at a higher risk of solar retinopathy. Symptoms include decreased vision, central scotomas, dyschromatopsia, metamorphopsia, micropsia, and frontal or temporal headache within hours of exposure. Visual acuity is typically reduced to 20/25–20/100 but may be worse depending on the degree of exposure. Most patients recover within 3–6 months, with visual acuity returning to the level of 20/20–20/40, but there may be residual metamorphopsia and paracentral scotomas. Typical findings include a central opacified area of the fovea acutely and depigmentation after the acute changes resolve (Fig 18-9). No known beneficial treatment exists, and therefore prevention through education is critically important.

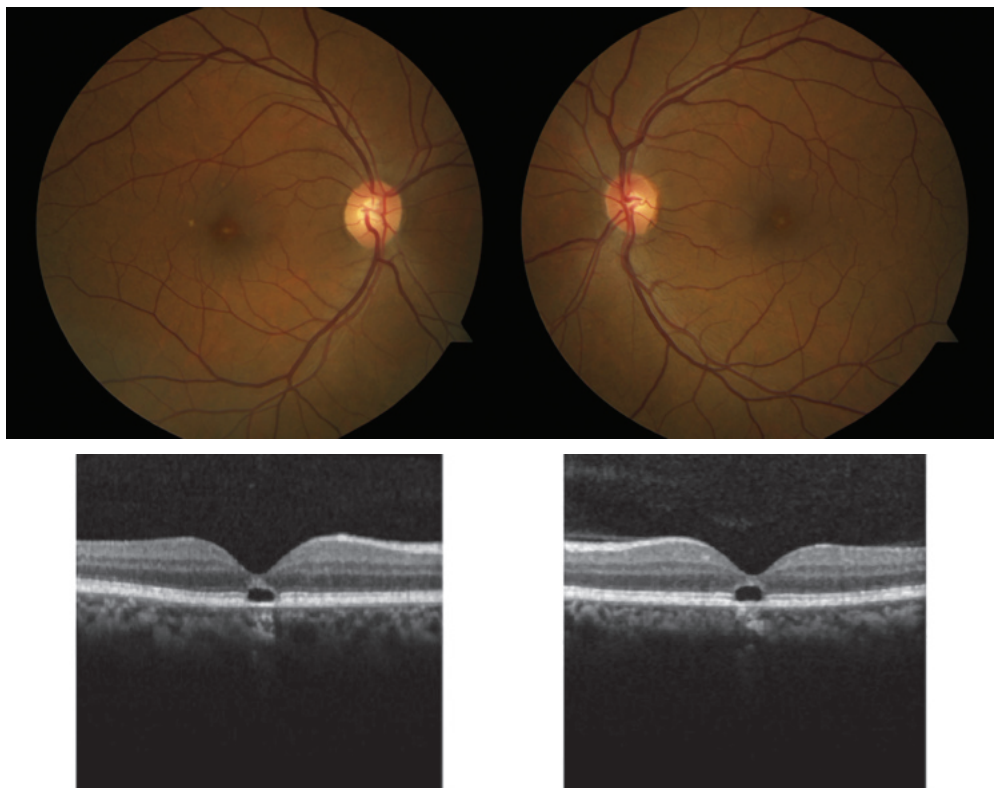


Figure 18-9 Solar retinopathy. The fundus photos show central foveal hypopigmentation. On OCT imaging, outer retinal cavitation in the fovea is typically seen. (Courtesy of David Sarraf, MD.)

Comander J, Gardiner M, Loewenstein J. High-resolution optical coherence tomography findings in solar maculopathy and the differential diagnosis of outer retinal holes. *Am J Ophthalmol*. 2011;152(3):413–419.e6.

Phototoxicity From Ophthalmic Instrumentation

The potential for photochemical damage from exposure to modern ophthalmic instruments has been studied extensively. Injuries have been reported from operating microscopes and from fiber-optic endoilluminating probes used in vitrectomies. The incidence of photic retinopathy after contemporary cataract surgery is not known. However, cases continue to be reported after intraocular surgery. The incidence increases with prolonged operating times but can occur even with surgery times as short as 30 minutes. In retinal surgery, photic injury is more likely to occur with prolonged, focal exposure, especially when the light probe is held in close proximity to the retina, as it may be during macular hole and epiretinal membrane procedures.

Most affected patients are asymptomatic, but some will notice a paracentral scotoma on the first postoperative day. Depending on the severity of the damage, vision may return to normal after some time, or it may progressively deteriorate. Acutely affected patients

may have a deep, irregular, oval-shaped, yellow-white retinal lesion adjacent to the fovea that resembles the shape of the light source. The lesion typically evolves to become a zone of mottled RPE that transmits background hyperfluorescence on fluorescein angiography.

Reports of photic macular lesions occurring after intraocular surgery underscore the need for prevention. During ocular surgery, the risk of photic retinopathy may be reduced by minimizing exposure time, avoiding the use of intense illumination, using oblique illumination when possible during parts of the surgery, filtering out short-wavelength blue light and UV light, and using shielding. BCSC Section 11, *Lens and Cataract*, lists several precautions for minimizing retinal light toxicity. See also BCSC Section 3, *Clinical Optics*.

van den Biesen PR, Berenschot T, Verdaasdonk RM, van Weelden H, van Norren D.

Endoillumination during vitrectomy and phototoxicity thresholds. *Br J Ophthalmol*. 2000; 84(12): 1372–1375.

Youssef PN, Sheibani N, Albert DM. Retinal light toxicity. *Eye*. 2011;25(1):1–14.

Occupational Light Toxicity

Occupational exposure to bright lights can lead to retinal damage. A common cause of this type of occupational injury is arc welding without the use of protective goggles. The damage from the visible blue light of the arc welder leads to photochemical damage similar to that observed in solar retinopathy. Occupational injury from stray laser exposure is also a serious concern.

Handheld Laser-Pointer Injury

The availability of high-power green and blue handheld laser devices has created a serious emerging source of immediate accidental or purposeful sight-threatening macular injury. These devices are easily obtainable via the Internet and resemble the much safer, ubiquitous low-power red laser pointers. These devices also present the risk of causing secondary harmful effects by visually incapacitating people undertaking visually demanding functions, such as firefighters and airline pilots, even if they do not cause retinal damage.

Alsulaiman SM, Alrushood AA, Almasaud J, et al; King Khaled Eye Specialist Hospital

Collaborative Retina Study Group. High-power handheld blue laser-induced maculopathy: the results of the King Khaled Eye Specialist Hospital Collaborative Retina Study Group. *Ophthalmology*. 2014;121(2):566–572.e1.



PART III

Selected Therapeutic Topics

Laser Therapy for Posterior Segment Diseases

Basic Principles of Photocoagulation

Photocoagulation uses light energy to coagulate tissue. After light energy is applied to the target tissue, it converts into thermal energy, and the tissue temperature rises above 65°C, causing denaturation of tissue proteins and coagulative necrosis.

Current posterior segment laser delivery systems span the visible light spectrum of 400–700 nm (green, yellow, red) and venture into the infrared wavelengths (>700 nm). Delivery systems may employ a transpupillary approach with slit-lamp or indirect ophthalmoscopic delivery, endophotocoagulation during vitrectomy, or transscleral application with a contact probe.

The effectiveness of photocoagulation depends on the transmission of light through ocular media and the absorption of that light by pigment in the target tissue. Light is absorbed principally by ocular tissues that contain melanin, xanthophyll, or hemoglobin. Figure 19-1 illustrates the absorption spectra of the key pigments found in ocular tissues:

- *Melanin* is an effective absorber of green, yellow, red, and infrared wavelengths.
- Macular *xanthophyll* readily absorbs blue but minimally absorbs yellow and red wavelengths.
- *Hemoglobin* easily absorbs blue, green, and yellow but has minimal absorption of red wavelengths.

Choice of Laser Wavelength

Laser wavelength selection depends on the specific goals of treatment and the degree to which the photocoagulation must be targeted to the particular tissue while sparing adjacent healthy tissue. The *area* (depth and diameter) of effective coagulation is directly related to the *intensity* and *duration* of irradiation. For a specific set of laser parameters (spot size, duration, and power), the intensity of the burn obtained depends on the clarity of the ocular media and the degree of pigmentation.

The *green laser* produces light that is absorbed well by melanin and hemoglobin and less completely by xanthophyll. Because of these characteristics and the absence of undesirable short (blue) wavelengths, the green laser has replaced the blue-green laser for treatment of retinal vascular abnormalities and choroidal neovascularization (CNV).

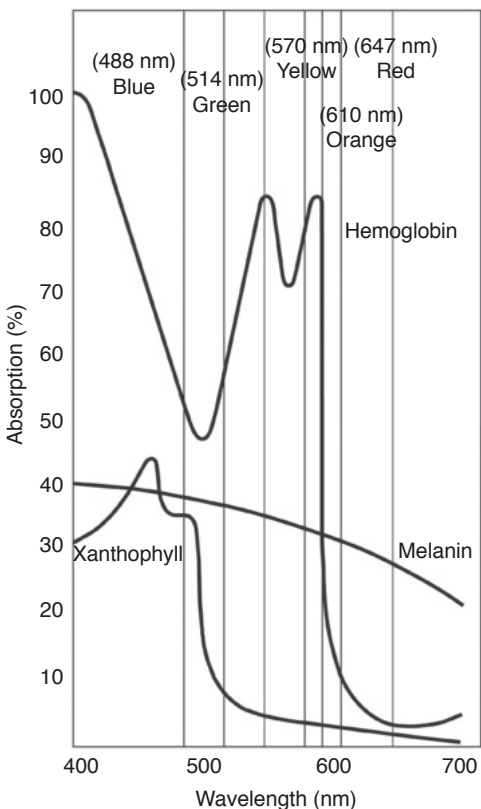


Figure 19-1 Absorption spectra of xanthophyll, hemoglobin, and melanin. (From Folk JC, Pulido JS. Laser Photocoagulation of the Retina and Choroid. Ophthalmology Monograph 11. San Francisco: American Academy of Ophthalmology; 1997:9.)

The *red laser* penetrates through nuclear sclerotic cataracts and moderate vitreous hemorrhages better than lasers with other wavelengths do. In addition, it is minimally absorbed by xanthophyll and thus may be useful in treatments near the fovea. The red laser causes deeper burns with a higher rate of patient discomfort and inhomogeneous absorption at the level of the choroid. The *infrared laser* has characteristics similar to those of the red laser with even deeper tissue penetration.

The *yellow laser* has, among its advantages, minimal scatter through nuclear sclerotic lenses, low xanthophyll absorption, and little potential for photochemical damage. It appears to be useful for destroying vascular structures while causing minimal damage to adjacent pigmented tissue; thus, it may be valuable for treating retinal vascular and choroidal neovascular lesions. For typical laser wavelengths of specific lasers, see BCSC Section 3, *Clinical Optics*, Chapter 2.

Laser effects on posterior segment tissues include photochemical and thermal effects and vaporization. Photochemical reactions can be induced by ultraviolet or visible light that is absorbed by tissue molecules or by molecules of a photosensitizing medication (eg, verteporfin), producing cytotoxic reactive oxygen species (eg, free radicals). Absorption of laser energy by pigment results in a temperature rise by tens of degrees and subsequent protein denaturation; the exact temperature rise depends on laser wavelength, laser power, duration of laser application, and spot size. Vaporization is generated by the rise in

water temperature above the boiling point, which causes microexplosions, as can occur in overly intense burns. For further discussion of laser light characteristics and light–tissue interactions, see BCSC Section 3, *Clinical Optics*, Chapter 2.

Atebara NH, Thall EH. Principles of lasers. In: Yanoff M, Duker JS. *Ophthalmology*. 4th ed.

Philadelphia: Elsevier/Saunders; 2014:32–37.

Palanker D, Blumenkranz MS. Retinal laser therapy: biophysical basis and applications. In:

Schachat AP, Wilkinson CP, Hinton DR, Sadda SR, Wiedemann P, eds. *Ryan's Retina*. Vol 1.

6th ed. Philadelphia: Elsevier/Saunders; 2018:chap 41.

Practical Aspects of Laser Photocoagulation

Anesthesia

Topical, peribulbar, or retrobulbar anesthesia may be needed to facilitate delivery of laser photocoagulation. The risks of peribulbar and retrobulbar injection should be considered when choosing among these forms of anesthesia.

Lenses

Two types of contact lenses are available to assist in slit-lamp delivery of photocoagulation:

1. negative-power planoconcave lenses
2. high-plus-power lenses

The planoconcave lenses provide an upright image with superior resolution of a small retinal area. Most clinicians favor use of these lenses for macular treatments. Mirrored planoconcave lenses facilitate viewing and photocoagulation of more peripheral retina; the exact location in view depends on the angle of the mirror used. Planoconcave lenses generally provide the same retinal spot size as that selected on the slit-lamp setting.

High-plus-power lenses provide an inverted image with some loss of fine resolution, but they offer a wide field of view, which facilitates efficient treatment over a broad area. The macula may be kept in view while the midperiphery of the retina is being treated, making these lenses ideal for panretinal photocoagulation. High-plus-power lenses provide a spot size that is magnified over the laser setting size; the magnification factor depends on the lens used (Table 19-1).

Parameters and indications

Selection of laser setting parameters depends on the treatment goals, the clarity of the ocular media, and the fundus pigmentation. As a general rule, smaller spot sizes require less energy than larger spot sizes, and longer-duration exposures require less energy than shorter-duration exposures to achieve the same intensity effects. The following sections present guidelines for conventional laser treatments.

Macular laser Although its use is declining, laser photocoagulation still has a role in the management of some forms of macular edema, extrafoveal CNV, and focal retinal pigment epithelium (RPE) abnormalities with leakage, such as those seen in central serous chorioretinopathy. To avoid causing central scotomas and perifoveal capillary dropout, treatment should not be administered within 500 µm of the foveal center. Macular laser

Table 19-1 Magnification Factors for Common Laser Lenses

Lens	Magnification	Laser Spot Magnification
Panretinal photocoagulation lenses		
Ocular Mainster PRP 165	0.51×	1.96×
Ocular Mainster Wide Field PDT	0.68×	1.5×
Ocular Pro Retina	0.5×	2.0×
Rodenstock Panfunduscope	0.7×	1.43×
Volk Equator Plus	0.44×	2.27×
Volk HR Wide Field	0.5×	2.0×
Volk QuadrAspheric	0.51×	1.97×
Volk SuperQuad 160	0.5×	2.0×
Focal laser lenses		
Goldmann 3-mirror (central)	0.93×	1.08×
Ocular Fundus Laser	0.93×	1.08×
Ocular Mainster High Magnification	1.25×	0.8×
Ocular PDT 1.6×	0.63×	1.6×
Ocular Reichel-Mainster 1× Retina	0.95×	1.05×
Ocular Reichel-Mainster 2× Retina	0.5×	2.0×
Ocular Yannuzzi Fundus	0.93×	1.08×
Volk Area Centralis	1.06×	0.94×
Volk Centralis Direct	0.9×	1.11×
Volk Fundus 20	1.44×	0.7×
Volk Fundus Laser	1.25×	0.8×
Volk HR Centralis	1.08×	0.93×
Volk HR Wide Field	0.5×	2.0×
Volk PDT Lens	0.66×	1.5×
Volk SuperMacula 2.2	1.49×	0.67×

treatment for edema generally employs a smaller spot size (50–200 µm) and shorter duration (≤ 0.1 second) to achieve smaller, less-intense burns. For diabetic macular edema, green or yellow direct laser therapy should be applied to all leaking microaneurysms located between 500 µm and 3000 µm from the center of the macula. For more diffuse leakage or zones of capillary nonperfusion, a light-intensity grid pattern using a green or yellow laser is applied to all areas of diffuse leakage more than 500 µm from the center of the macula and 500 µm from the temporal margin of the optic nerve head. A similar strategy is employed in treating macular edema caused by branch retinal vein occlusion. In the treatment of CNV or RPE leakage spots, the aim is to achieve a more intense burn of the entire lesion or area of leakage.

Peripheral retinal photocoagulation Peripheral retinal photocoagulation may be delivered with either a slit-lamp or indirect ophthalmoscopic delivery system. The latter system offers less control over precise spot size or burn intensity. In panretinal photocoagulation (PRP) or laser retinopexy, the aim is to achieve somewhat intense, larger laser burns. For PRP, the laser spot size typically is 200–500 µm, and laser power is adjusted to achieve gray or light cream-colored burns. Applications, or burns, are usually one-half to one burn width apart (see Chapter 5, Fig 5-8) and should spare the macula. For initial PRP

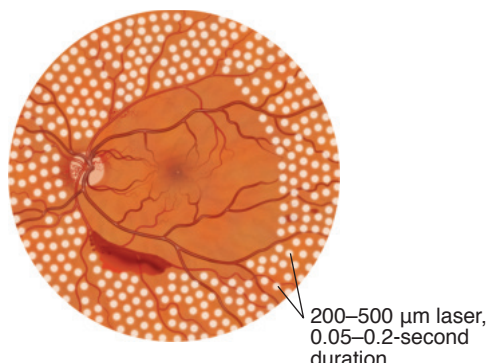


Figure 19-2 Illustration of the posterior extent of full panretinal photocoagulation (peripheral treatment not shown). (Illustration by Mark Miller.)

treatment, some practitioners leave approximately 1–2 disc diameters of retina outside of the macula and optic nerve head untreated, whereas others treat up to the arcade vessels and up to the optic nerve (Fig 19-2). The initial treatment pattern can be concentrated more densely in the inferior retina to help minimize temporal and inferior visual field loss and to facilitate retreatment in the case of vitreous hemorrhage. The long ciliary nerves in the 3- and 9-o'clock meridians should be avoided, if possible, and any coexisting macular edema should be treated beforehand to avoid exacerbation after PRP. Typically, 1200–1400 laser applications of 500-µm spot size—the equivalent of smaller burns—are placed.

Laser retinopexy is used to create a chorioretinal adhesion around retinal tears or for demarcation of a (small) retinal detachment; it uses spot sizes of 200–500 µm, and its goal is creating whitish, but not snow-white, burns. Usually, 2–3 rows of photocoagulation around the break are considered appropriate to achieve the desired adhesion.

Laser ablation of retinal vascular lesions Vascular lesions are often treated using a large spot size ($\geq 500 \mu\text{m}$), lower power, and long duration so each lesion slowly heats up and coagulates “from the inside out.” High-intensity burns whiten the surface of the lesions, after which visible-light laser does not penetrate well, making it difficult to achieve the treatment goal.

Alternative laser delivery systems and strategies

New technologies and concepts have led to novel treatment systems and strategies. Recent innovations in slit-lamp delivery systems include pattern scanners that deliver an entire array of laser applications with each foot-pedal depression; the high-intensity laser pulses are ultrashort (20–50 milliseconds) and are delivered in rapid succession. This approach possibly increases the efficiency of treatment, but it may not achieve an effect equivalent to traditional laser treatment on a spot-number-to-spot-number comparison.

Some systems incorporate real-time retinal image overlay and registration with the laser delivery system. This configuration allows for computer-assisted planning and precise targeting of the retinal lesions during treatments.

Delivery systems that apply subthreshold (barely visible to invisible) laser spots administer laser in micropulses (≤ 0.1 millisecond) that can confine heat conduction to the

RPE while limiting thermal damage to the photoreceptors and choriocapillaris. These systems have been shown to be effective in treating diabetic macular edema and have the potential to reduce the number and size of scotomas. Titration of burn intensity and monitoring of the area of placement of invisible laser spots during laser delivery is enhanced in commercial laser systems using endpoint software technology.

Baumal CR, Ip M, Puliafito CA. Light and laser injury. In: Yanoff M, Duker JS.

Ophthalmology. 4th ed. Philadelphia: Saunders/Elsevier; 2013:461–466.

Chappelow AV, Tan K, Waheed NK, Kaiser PK. Panretinal photocoagulation for proliferative diabetic retinopathy: pattern scan laser versus argon laser. *Am J Ophthalmol*. 2012;153(1):137–142.e2.

Complications of Photocoagulation

The most serious complications of photocoagulation are caused by the use of excessive energy or misdirected light. Complications that may be associated with photocoagulation include inadvertent corneal burns, which can lead to opacities. Treatment of the iris may cause iritis and create zones of atrophy. Pupillary abnormalities may arise from thermal damage to the long ciliary nerves in the suprachoroidal space or the iris sphincter muscle. Absorption by lens pigments may create lenticular burns and resultant opacities. Optic neuropathy may occur from treatment directly to or adjacent to the optic nerve head, and nerve fiber damage may follow intense absorption in zones of intraretinal hemorrhage, increased pigmentation, or retinal thinning. Chorioretinal complications include foveal burns, Bruch membrane ruptures, creation of retinal or choroidal lesions, and exudative choroidal or retinal detachment. Retinal nerve fiber layer damage resulting from laser treatment can have more widespread vision loss than the local area. For example, if the damage occurs in the peripapillary retinal nerve fiber layer, arcuate scotomas can develop; when the papillomacular bundle is damaged, central vision loss can result.

Accidental foveal burns

Great care should be taken to identify the fovea by means of biomicroscopy; this step may be aided by comparing the appearance with recent fluorescein angiography images. Frequent reference to the foveal center throughout the procedure is helpful to maintain orientation. In some instances, the risk of foveal burns may be reduced by immobilizing the globe with peribulbar or retrobulbar anesthesia, especially when juxtapfoveal treatment is being performed.

Bruch membrane ruptures

Small spot size, high power, and short duration of applications all increase the risk of a rupture in Bruch membrane, which may subsequently give rise to hemorrhage from the choriocapillaris and development of CNV.

Retinal lesions

Intense photocoagulation may cause full-thickness retinal holes. Similarly, intense treatment may create fibrous proliferation, striae, and foveal distortion, with resultant metamorphopsia or diplopia. Focal treatment with small-diameter, high-intensity burns may

cause vascular occlusion or perforate blood vessels, leading to preretinal or vitreous hemorrhage. In addition, extensive panretinal treatment may induce or exacerbate macular edema, particularly in patients with diabetes mellitus.

Choroidal lesions

Treatment of CNV may be complicated by subretinal hemorrhage, choroidal ischemia, and additional CNV or chorioretinal anastomosis. If active subretinal hemorrhage occurs during treatment, it should be addressed immediately by increasing digital pressure on the contact lens while continuing to treat the remaining portions of the CNV lesion in order to minimize obscuration of landmarks by hemorrhage. Progressive atrophy of the RPE may develop at the margin of photocoagulation scars, resulting in enlarged scotomas. Also, photocoagulation may precipitate tears of the pigment epithelium.

Exudative retinal and choroidal detachment

Extensive, intense photocoagulation may lead to massive chorioretinal edema and resultant serous retinal and choroidal detachment (Fig 19-3). The latter, in turn, can lead to narrowing of the anterior chamber angle from forward rotation of the ciliary body, resultant elevated intraocular pressure, and, rarely, aqueous misdirection. This reaction peaks 1–3 days after treatment and resolves spontaneously within a few weeks. Corticosteroids may be helpful to treat massive exudation.

Avoiding laser photocoagulation complications

As discussed, awareness and avoidance of the fovea during laser treatment is paramount. Selection of proper wavelength, power, exposure time, and spot size is also important. Proper titration of laser power and exposure time may be necessary to achieve the desired tissue effect. Waiting for proper pupillary dilation can help limit iris damage. Careful pre-operative explanation of the laser procedure to the patient and comfortable positioning of the patient will facilitate cooperation and steady fixation, thereby improving safety.

Palanker D, Lavinsky D, Blumenkranz MS, Marcellino G. The impact of pulse duration and burn grade on size of retinal photocoagulation lesion: implications for pattern density. *Retina*. 2011;31(8):1664–1669.

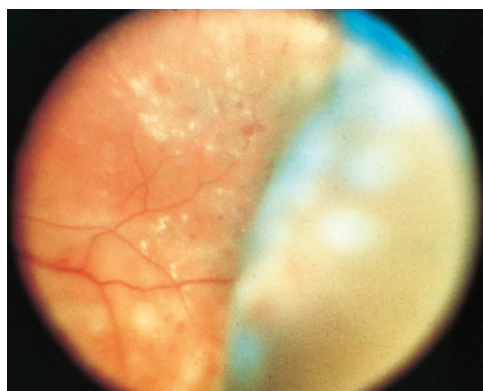


Figure 19-3 Color fundus photograph shows choroidal detachment that occurred following panretinal scatter photocoagulation for diabetic retinopathy. (Courtesy of M. Gilbert Grand, MD.)

Transpupillary Thermotherapy

Transpupillary thermotherapy (TTT) acts in a subthreshold manner by slightly raising the choroidal temperature, thus causing minimal thermal damage to the RPE and overlying retina. TTT is administered with an infrared laser (810 nm) using beam sizes from 0.8 mm to 3.0 mm, power settings between 250 mW and 750 mW, and a 1-minute exposure time. For choroidal melanoma, TTT may be considered as a stand-alone treatment for tumors less than 4 mm thick, but for thicker tumors, a combination of TTT and plaque radiotherapy results in better local tumor control than TTT alone.

Photodynamic Therapy

Photodynamic therapy (PDT) using the photosensitizing drug verteporfin is approved by the US Food and Drug Administration for treating certain types of subfoveal CNV in age-related macular degeneration and subfoveal CNV that is secondary to ocular histoplasmosis syndrome and myopia. Because more effective treatments have become available, PDT has generally fallen out of favor for the management of CNV, but it continues to be a valuable option for the management of some ocular tumors and central serous chorioretinopathy.

PDT is a 2-step procedure:

1. intravenous administration of the photosensitizing drug, which localizes to endothelial cells of vessels present in CNV and tumors
2. local activation of the drug by a laser wavelength preferentially absorbed by the sensitizing drug

The low-intensity laser energy produces a photochemical reaction, leading to the formation of reactive oxygen species and free radicals. These radicals cause endothelial cell damage, platelet adherence, vascular thrombosis, and capillary closure.

Complications of Photodynamic Therapy

The most serious adverse effects of PDT are photosensitivity reactions that range from mild to second-degree burns of sun-exposed skin. This can be avoided by having the patient minimize exposure to sunlight for 5 days after treatment. In the Treatment of Age-Related Macular Degeneration with Photodynamic Therapy (TAP) Study Group report, severe vision loss occurred in 0.7%–2.2% of patients within 7 days of PDT treatment of subfoveal lesions. Additionally, verteporfin infusion-related transient lower-back, side, and chest pain were reported in 2.0%–2.5% of patients. In efforts to minimize choriocapillaris nonperfusion and ischemia, treatment using half-fluence PDT (25 J/cm² energy; 300 mW/cm² light intensity) has become more common, and it may be as effective as standard-fluence PDT.

Vitreoretinal Surgery and Intravitreal Injections



This chapter includes related videos, which can be accessed by scanning the QR codes provided in the text or going to www.aao.org/bcscvideo_section12.

Pars Plana Vitrectomy

Pars plana vitrectomy is typically used for removing vitreous opacities (vitreous hemorrhage), relieving vitreoretinal traction, restoring the normal anatomical relationship of the retina and retinal pigment epithelium (RPE), and accessing the subretinal space. This vitreoretinal surgical technique involves a closed-system approach in which 3 ports are placed 3–4 mm posterior to the surgical limbus. One port is typically dedicated to infusion of balanced salt solution into the vitreous cavity, by which intraocular pressure (IOP) can be maintained at a desired level. Epinephrine can be added to the infusion solution for mydriasis and to induce vasoconstriction to reduce intraoperative bleeding, but it may promote ischemia and increase inflammation. Dextrose is often added to infusions to reduce cataractogenesis for phakic diabetic patients. The remaining ports are used to access the vitreous cavity with tools such as a fiber-optic endoilluminator to visualize the posterior segment and other instruments to manipulate, dissect, or remove intraocular tissues, fluids, and objects.

Vitrectomy is performed using an operating microscope in conjunction with a contact lens or noncontact viewing system. Direct and indirect visualization are possible; the latter requires the use of an inverting system to orient the image. The advantages of indirect visualization include a wider viewing angle, which enables visualization through media opacities and miotic pupils, as well as when the eye is filled with gas. Although direct viewing systems offer greater magnification and enhanced stereopsis, their field of view is smaller. Many vitreoretinal surgeons use both types of viewing systems, selecting the type according to the pathology.

Various instruments, visualization aids, and vitreous substitutes are used during vitreoretinal surgery. Advanced instrumentation includes the high-speed vitreous cutter, intraocular forceps, endolaser probe, micro-pic, intraocular scissors, extrusion cannula, and fragmatome, among others. Examples of visualization aids include indocyanine green (ICG) or brilliant blue G (BBG) dyes and triamcinolone suspension. These substances aid

in the visualization of the internal limiting membrane (ILM) and, in the case of triamcinolone, also help identify the vitreous. Perfluorocarbon (PFC) liquids, which are heavier than water, can be used to temporarily stabilize the retina during dissection and facilitate anterior drainage of subretinal fluid during retinal detachment repair. Tamponade of the retina can be achieved using air, gas, or silicone oil as a vitreous substitute. Commonly used gases include sulfur hexafluoride (SF_6) and perfluoropropane (C_3F_8), which last approximately 2 and 8 weeks, respectively, at nonexpansile, isovolumic concentrations.

The development of smaller-gauge vitrectomy instrumentation has facilitated transconjunctival, sutureless vitrectomy techniques. With these systems, surgeons place 23-gauge, 25-gauge, or 27-gauge trocar cannulas to align conjunctival and scleral openings and to allow instrument insertions. These cannulas obviate the need for opening the conjunctiva, including cautery, and the wounds generally do not usually require suture closure when constructed with self-sealing architecture. Before small-gauge vitrectomy instrumentation, 20-gauge was the norm. The diameter of 20-gauge sclerotomies is 1 mm, compared to 0.7 mm, 0.5 mm, and 0.4 mm for 23-gauge, 25-gauge, and 27-gauge instrumentation, respectively. Potential advantages of small-gauge vitrectomy include fewer intraoperative iatrogenic retinal tears, shortened operative time, increased postoperative patient comfort, faster visual recovery, and reduced conjunctival scarring.

Fujii GY, de Juan E Jr, Humayun MS, et al. Initial experience using the transconjunctival suture-less vitrectomy system for vitreoretinal surgery. *Ophthalmology*. 2002;109(10):1814–1820.

Vitrectomy for Selected Macular Diseases

Macular Epiretinal Membranes

Epiretinal membranes (ERMs) have a variable clinical course. There are generally 2 indications for surgery: (1) reduced visual acuity or (2) distortion causing dysfunction of binocular vision. In general, epiretinal membrane peel (Video 20-1) is advised if visual acuity is reduced to 20/40–20/60 or worse. Separately, dysfunction of binocular vision that involves difficulty with fusion of 1 distorted and 1 normal-vision image is an indication for surgery, even if the patient's visual acuity is still good (Fig 20-1).



VIDEO 20-1 Vitrectomy for epiretinal membrane peel.

Courtesy of Colin A. McCannel, MD.

Access all Section 12 videos at www.aao.org/bcscvideo_section12.



After surgery, approximately two-thirds of patients achieve an improvement in visual acuity of 2 or more lines. Maximal improvement may take up to 6–12 months (Fig 20-2). Although improvement in patients with metamorphopsia is nearly universal, complete resolution usually does not occur.

Vitreomacular Traction Diseases

Vitreomacular traction syndrome

Vitreomacular traction (VMT) syndrome is a distinct vitreoretinal interface disorder that is differentiated clinically from typical ERM. Whereas ERM formation generally results

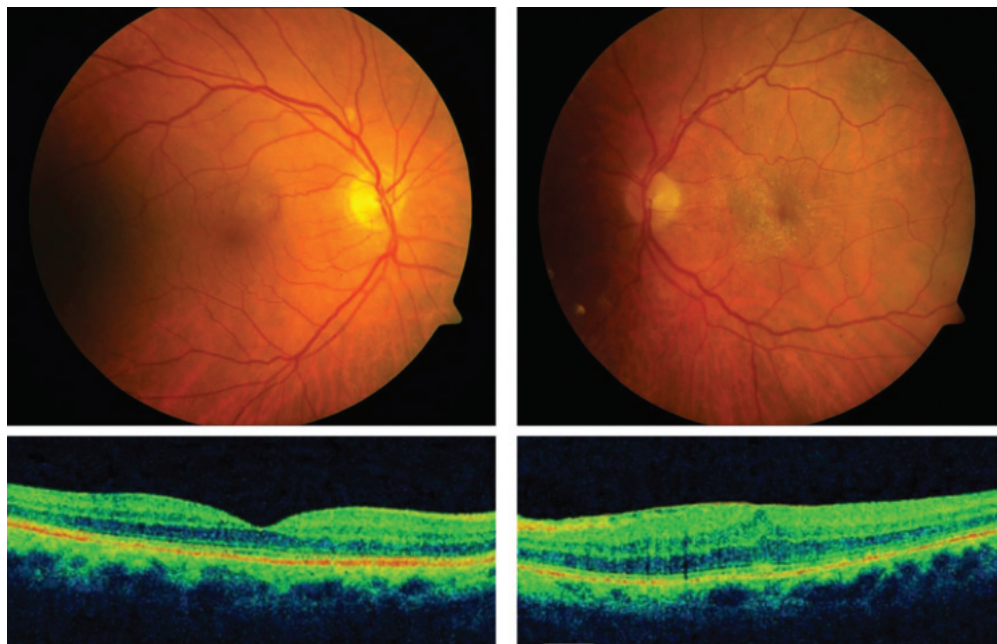


Figure 20-1 Epiretinal membrane (ERM). *Top row*, color fundus photographs of a normal right eye and a left eye with a macular ERM that shows distortion of the foveal architecture and retinal striae. *Bottom row*, corresponding optical coherence tomography (OCT) images confirm preretinal traction from the ERM, associated loss of foveal contour, and macular thickening in the left eye. Visual acuity was 20/50 in the left eye with central distortion. This patient was a candidate for pars plana vitrectomy surgery. (Courtesy of Stephen J. Kim, MD.)

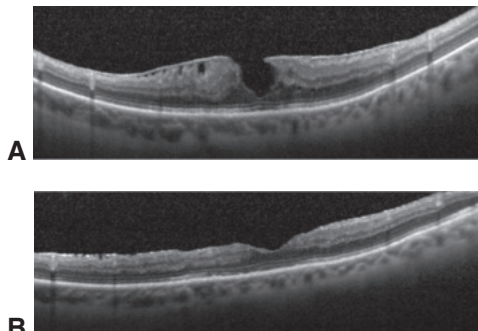
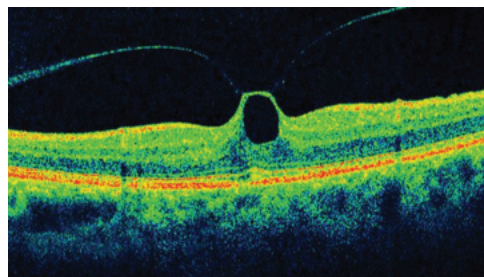


Figure 20-2 OCT images of an ERM forming a pseudohole in a patient with visual distortion and reduced visual acuity (20/50). **A**, A preretinal membrane distorts the retinal contour and intraretinal edema. **B**, Image taken 2 months after surgery shows continued restoration of normal macular contour and the absence of the preretinal membrane and traction; visual acuity had improved to 20/25. (Courtesy of Edward F. Cherney, MD.)

from complete posterior vitreous detachment, VMT syndrome stems from anomalous, incomplete posterior vitreous separation at the macula. The fundus examination in VMT syndrome is often normal. The disorder may create focal elevation of the fovea (Fig 20-3) and, occasionally, a shallow retinal detachment. VMT syndrome is best diagnosed and differentiated from ERMs with the aid of optical coherence tomography (OCT); in eyes with this syndrome the hyaloid classically inserts onto a tractionally elevated macular retina, usually the fovea. Symptoms include decreased vision and distortion. VMT syndrome is often progressive and is associated with a greater loss of vision than are ERMs alone. Surgical treatment consists of a pars plana vitrectomy and peeling of the cortical vitreous

Figure 20-3 Vitreomacular traction syndrome in a patient with visual acuity of 20/60 and mild ophthalmoscopic findings. OCT scan shows a partial posterior detachment with persistent hyaloidal insertion at the center of the macula. Note the elevated fovea with complete loss of contour and inner schisis cavity. Pars plana vitrectomy with membrane peeling led to an improved visual acuity of 20/25 and resolution of symptomatic distortion. (Courtesy of Stephen J. Kim, MD.)



from the surface of the retina. Intraoperative use of triamcinolone may aid visualization of the cortical vitreous. See Chapter 17 for further discussion of VMT syndrome.

Voo I, Mavrofrides EC, Puliafito CA. Clinical applications of optical coherence tomography for the diagnosis and management of macular diseases. *Ophthalmol Clin North Am.* 2004; 17(1):21–31.

Idiopathic macular holes

Vitrectomy surgery is not generally recommended for stage 1 macular holes because approximately 50% of them will resolve spontaneously. It is definitely indicated for all recent full-thickness macular holes (stages 2, 3, and 4). Early intervention for full-thickness macular holes is important; shorter time intervals between the development and the closure of macular holes have been associated with improved anatomical and functional outcomes.

Surgery for full-thickness macular holes typically consists of a pars plana vitrectomy, separation and removal of the posterior cortical vitreous, optional removal of the ILM, and use of an intraocular air or gas tamponade (Video 20-2). Various studies have demonstrated that ILM peeling improves the rate of hole closure, particularly for larger stage 3 or 4 holes, and reduces reopening rates. ILM inverted flaps is a newer surgical technique used to repair macular holes, but there is no consensus on whether this technique improves visual acuity in patients with large macular holes (Video 20-3). The intraoperative use of dyes (eg, ICG, trypan blue, BBG) or other visualization techniques (eg, triamcinolone) to aid in peeling the ILM is widely practiced, despite potential toxicity. Duration of face-down positioning ranges from a few hours to 2 or more weeks. Since the early 2000s, most studies have reported macular hole closure at rates higher than 90% (Fig 20-4). After successful closure, it is uncommon for the hole to reopen; however, this may occur if severe cystoid macular edema or ERM develops.



VIDEO 20-2 Vitrectomy for macular hole repair with ILM peeling.

Courtesy of Colin A. McCannel, MD.



VIDEO 20-3 Inverted ILM flap for macular hole closure.

Courtesy of María H. Berrocal, MD.



Kelly NE, Wendel RT. Vitreous surgery for idiopathic macular holes. Results of a pilot study. *Arch Ophthalmol.* 1991;109(5):654–659.

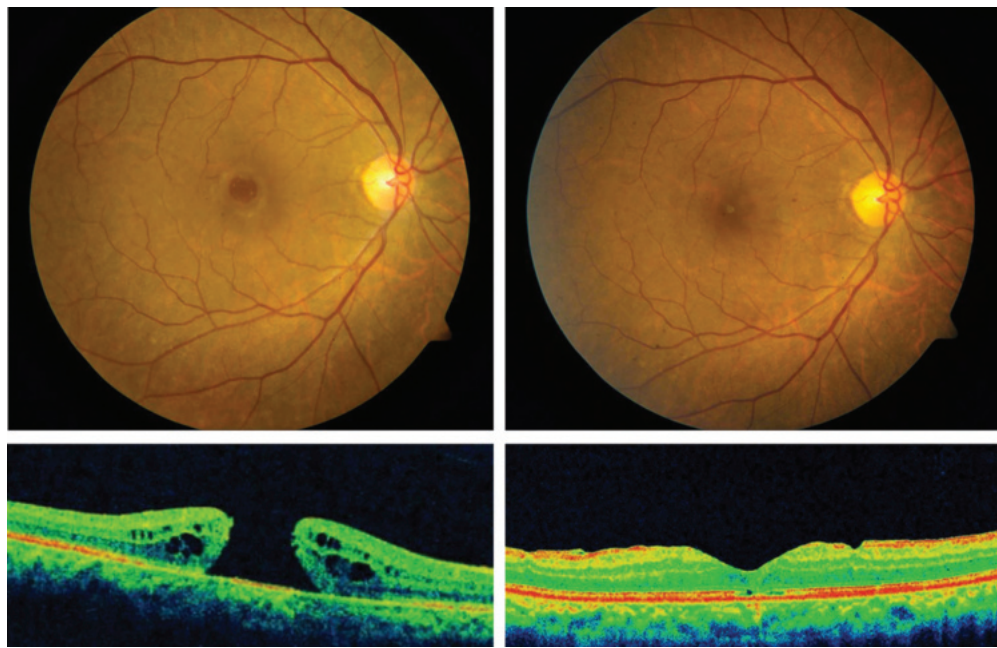


Figure 20-4 Idiopathic macular hole. *Left*, Color fundus photograph and corresponding OCT image of a patient with a full-thickness macular hole who had experienced reduced visual acuity (20/100) for 3 months. *Right*, Postoperative color fundus photograph and OCT image of the same patient. After vitrectomy, membrane peeling, and fluid–gas exchange, the macular hole closed, visual acuity improved to 20/25, and normal foveal anatomy was restored. (Courtesy of Stephen J. Kim, MD.)

Kumagai K, Furukawa M, Ogino N, Uemura A, Demizu S, Larson E. Vitreous surgery with and without internal limiting membrane peeling for macular hole repair. *Retina*. 2004;24(5):721–727.

Submacular Hemorrhage

Vitrectomy for submacular hemorrhage remains unproven and controversial. The clinical course of submacular hemorrhages can vary. Patients with neovascular age-related macular degeneration (AMD) and larger submacular hemorrhages generally have poor visual outcomes. For removal of thick submacular hemorrhages, pars plana vitrectomy techniques can be considered. The surgery involves pneumatic displacement of subretinal blood away from the macular center without attempting to remove the hemorrhage. This technique can be performed with a vitrectomy, subretinal injection of tissue plasminogen activator (tPA) via a 39-gauge to 41-gauge cannula, and partial air–fluid exchange. Postoperative face-down positioning can result in substantial inferior extramacular displacement of the blood (Fig 20-5). Intravitreal injection of expansile gas (eg, SF₆ or C₃F₈) and face-down positioning, with or without adjunctive intravitreal tPA administration, has also been performed in an office setting. Resolution of submacular hemorrhage with improvement of visual acuity can be achieved with administration of anti-VEGF agents alone, particularly if the blood is of mild thickness. Following treatment of the submacular hemorrhage, most patients require chronic treatment for the exudative AMD, usually with anti-VEGF injections.

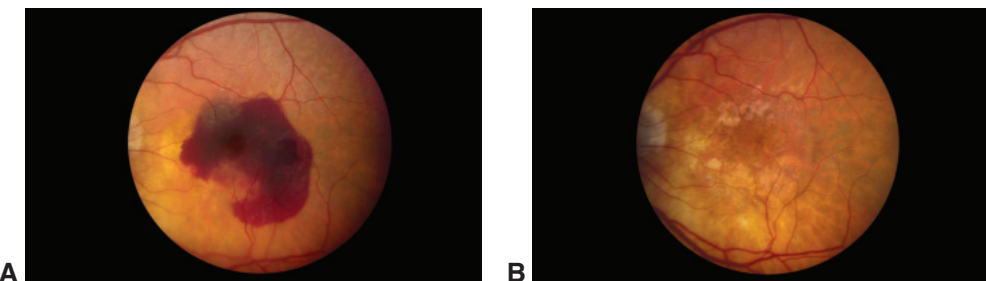


Figure 20-5 Fundus photographs of submacular hemorrhage in age-related macular degeneration (AMD). **A**, Patient had a submacular hemorrhage for 5 days and counting-fingers vision. **B**, After vitrectomy with subretinal infusion of tissue plasminogen activator and pneumatic displacement, dry atrophic changes are apparent. Visual acuity improved to 20/100. (Courtesy of Nancy M. Holekamp, MD.)

Vitrectomy for Vitreous Opacities

Surgery to remove vitreous opacities or symptomatic floaters is becoming more common; however, proper case selection is necessary. Surgery and its possible complications are not a good match in many cases. However, if the vitreous opacities affect reading, driving, or visual performance in general, vitrectomy surgery may be an appropriate solution. YAG laser photodisruption can be used as an alternative to surgical removal of floaters. However, there is very little scientific literature assessing the efficacy and complications of this technique, resulting in limited adoption.

Vitrectomy for Complications of Diabetic Retinopathy

Advances in vitreoretinal surgical techniques have facilitated earlier surgical intervention in patients with diabetic retinopathy, with reduced surgical morbidity and decreased surgical duration. These advances include the routine use of intraocular endolasers, widefield noncontact viewing systems, smaller-gauge surgical instrumentation, bimanual surgical techniques, and perioperative anti-VEGF injections. In addition, the use of anti-VEGF agents prior to vitrectomy for proliferative diabetic retinopathy (PDR) reduces intraoperative bleeding as well as surgical duration, the incidence of intraoperative retinal breaks, and the number of endodiathermy applications. Pre-operative use of anti-VEGF agents can help reduce intraoperative bleeding but can lead to traction retinal detachment if surgery is significantly delayed following the injection.

Vitreous Hemorrhage

Vitreous hemorrhage is a common complication in patients with PDR. Vitrectomy is indicated when a vitreous hemorrhage fails to clear spontaneously after approximately 4 weeks to 3 months; the timing of the surgery is determined by the surgeon's preference and the patient's visual requirements. Possible indications for more prompt intervention include monocularity, bilateral vitreous hemorrhages or ultrasonic evidence of a retinal tear, underlying

rhegmatogenous retinal detachment, or tractional retinal detachment that threatens the macula. In the absence of ophthalmoscopic visualization, serial ultrasonography helps the clinician assess the anatomical condition of the retina. If surgery is indicated, treatment involves a pars plana vitrectomy with removal of vitreous hemorrhage (Video 20-4) and release of the hyaloid from fronds of retinal neovascularization. Vitreoretinal traction at the optic nerve head and along the arcade vessels, if present, is addressed at the time of surgery, along with any macular ERMs. Complete panretinal photocoagulation and hemostasis should generally be achieved during the procedure. To prevent bleeding or rebleeding, the eye may be filled with air or a short-acting gas to tamponade possible bleeding sites.


VIDEO 20-4 Vitrectomy for vitreous hemorrhage.

Courtesy of Colin A. McCannel, MD.


Diabetic Tractional Retinal Detachment

Tractional retinal detachment (TRD) occurs when the hyaloid contracts but fronds of neovascular ingrowth prevent it from separating from the retinal interface. The tractional forces are transmitted to full-thickness retina and, in the absence of a retinal break, cause schisis and/or detachment of the underlying retina from its corresponding RPE (Fig 20-6). Vitrectomy is indicated when progression of a TRD threatens or involves the macula. In certain complex cases, spontaneous breaks can also occur in an atrophic retina under traction, resulting in combined traction and rhegmatogenous detachments; this variety of TRD is also a strong indication for earlier surgical intervention. Although panretinal

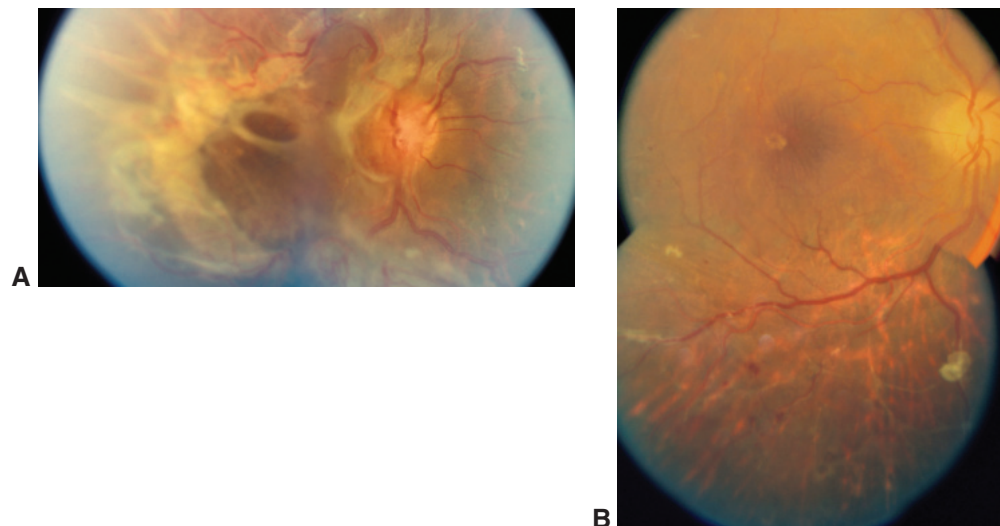


Figure 20-6 Color fundus photograph montages of diabetic tractional retinal detachment. **A**, Fibrovascular proliferation and a contracted posterior hyaloid along the retinal arcade vessels and over the macula cause elevation and distortion of the retinal surface at the arcade vessels and in the temporal macula. **B**, After surgery, the macula and vessels are flattened. (*Courtesy of Colin A. McCannel, MD.*)

photocoagulation should precede vitrectomy whenever possible, it can be more difficult to accomplish in the presence of vitreous hemorrhage. A preoperative adjunctive intravitreal injection of an anti-VEGF agent may induce regression of neovascularization, facilitating dissection and minimizing intraoperative bleeding.

Vitrectomy for TRD is performed to relieve vitreoretinal traction that interferes with retinal reattachment. In this procedure, the cortical vitreous and posterior hyaloid are removed from the retinal surface, particularly in areas of retinal neovascularization. Point adhesions of cortical vitreous to surface retinal neovascularization can be relieved by unimanual or bimanual techniques using various instruments, including scissors or the vitrectomy cutter. Surgical approaches to fibrovascular tissue include segmentation and delamination. In segmentation, bands of fibrovascular tissue causing traction are cut, but the epiretinal proliferations are not completely removed. In delamination, the epiretinal proliferations are completely, or nearly completely, dissected off the retinal surface to relieve the traction.

After tractional membranes are removed, diathermy may be used to treat fibrovascular tufts and achieve hemostasis, and supplementary laser treatment may be used in the periphery to reduce ischemia.

Brunner S, Binder S. Surgery for proliferative diabetic retinopathy. In: Schachat AP, Wilkinson CP, Hinton DR, Sadda SR, Wiedemann P, eds. *Ryan's Retina*. Vol 3. 6th ed. Philadelphia: Elsevier/Saunders; 2018.

Diabetic Macular Edema

The current mainstays of treatment for diabetic macular edema are intravitreal anti-VEGF, corticosteroid pharmacotherapy, and photocoagulation (for more information regarding pharmacologic agents, please see Chapter 5 of this volume). However, vitrectomy with membrane peeling may be considered for recalcitrant cases in which the posterior hyaloid or epiretinal membrane is taut. In these instances, the surgeon performs a pars plana vitrectomy with mechanical release of a taut hyaloid, peeling of epiretinal membrane, and stripping of the ILM as necessary.

Vitrectomy for Posterior Segment Complications of Anterior Segment Surgery

Postoperative Endophthalmitis

Postoperative endophthalmitis is classified based on the time of onset in the eye; *acute onset* occurs within 6 weeks following surgery, and *delayed onset* occurs more than 6 weeks following surgery. A specific subtype of endophthalmitis that occurs *following filtering bleb surgery* has a markedly different spectrum of causative organisms.

Acute-onset postoperative endophthalmitis

Clinical features of acute-onset postoperative endophthalmitis include the following signs: intraocular inflammation, often with hypopyon, conjunctival vascular congestion, and corneal and eyelid edema; symptoms include pain and loss of vision. Common

causative organisms are coagulase-negative *Staphylococcus* species, *Staphylococcus aureus*, *Streptococcus* species, and gram-negative organisms. Monitoring includes obtaining intraocular cultures. An anterior chamber specimen is typically obtained by using a 30-gauge needle on a tuberculin syringe. A vitreous specimen can be obtained either by needle tap or by using a vitrectomy instrument. A needle tap of the vitreous is typically accomplished using a 25-gauge, 1-inch needle on a 3-mL syringe (to provide greater vacuum) introduced through the pars plana and directed toward the midvitreous cavity. Vitreous specimens are more likely to yield a positive culture result than are simultaneously obtained aqueous specimens. Management includes administering intravitreal antibiotics; the antibiotics commonly used include ceftazidime and vancomycin. Ceftazidime has largely replaced amikacin or gentamicin in clinical practice because of concerns of potential aminoglycoside toxicity. Intravitreal dexamethasone may reduce posttreatment inflammation, but its role in endophthalmitis management remains controversial.

The use of vitrectomy for acute-onset postoperative endophthalmitis is guided by the results of the Endophthalmitis Vitrectomy Study (EVS; Clinical Trial 20-1). In the EVS, patients were randomly assigned to undergo either vitrectomy or vitreous tap/biopsy. Both

CLINICAL TRIAL 20-1

Endophthalmitis Vitrectomy Study (EVS)

Objective: Evaluate the role of pars plana vitrectomy and intravenous antibiotics in management of postoperative bacterial endophthalmitis.

Participants: Patients with clinical signs and symptoms of bacterial endophthalmitis in an eye after cataract surgery or lens implantation; onset of infection is within 6 weeks of surgery.

Randomization: Patients were randomly assigned to immediate pars plana vitrectomy or to immediate tap and inject. Patients were randomly assigned to receive systemic antibiotics or no systemic antibiotics and evaluated at regular intervals after treatment.

Outcome measures: Standardized visual acuity testing and media clarity.

Outcomes:

1. No difference in final visual acuity or media clarity whether or not systemic antibiotics (amikacin/ceftazidime) were employed.
2. No difference in outcomes between the 3-port pars plana vitrectomy group and the immediate tap/biopsy group for patients with better than light perception visual acuity at the study entry examination.
3. For patients with light perception visual acuity, much better results in the immediate pars plana vitrectomy group:
 - a. Three times more likely to achieve $\geq 20/40$ (33% vs 11%)
 - b. Two times more likely to achieve $\geq 20/100$ (56% vs 30%)
 - c. Less likely to incur $< 5/200$ (20% vs 47%)

Clinical impact: Study completed in 1995. Revolutionized treatment of post-cataract surgery endophthalmitis by making tap and inject an office procedure for most eyes.

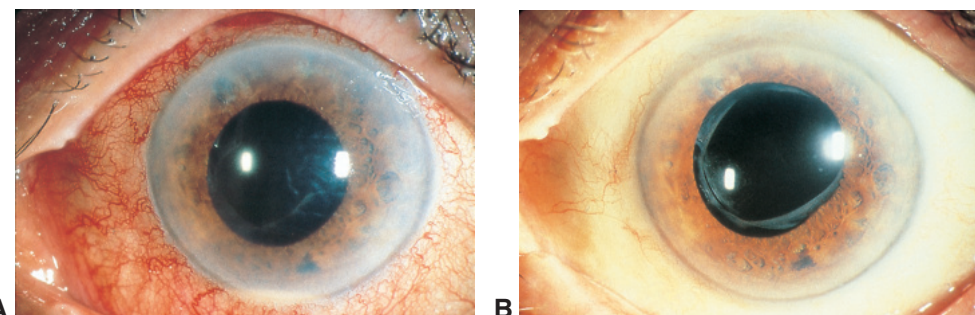


Figure 20-7 Acute-onset endophthalmitis. **A**, Patient with marked epibulbar hyperemia, iritis, hypopyon, and endophthalmitis 5 days after cataract surgery. **B**, After a needle tap of vitreous and injection of intravitreal antibiotics, the inflammation resolved and visual acuity improved to 20/30. (Courtesy of Harry W. Flynn, Jr, MD.)

groups received intravitreal and subconjunctival antibiotics (vancomycin and amikacin). The EVS concluded that vitrectomy surgery was indicated in patients with acute-onset (within 6 weeks of cataract extraction) postoperative endophthalmitis with light perception vision (Fig 20-7). Patients with hand motions visual acuity or better had equivalent outcomes in both treatment groups.

Endophthalmitis Vitrectomy Study Group. Results of the Endophthalmitis Vitrectomy Study.

A randomized trial of immediate vitrectomy and of intravenous antibiotics for the treatment of postoperative bacterial endophthalmitis. *Arch Ophthalmol.* 1995;113(12):1479–1496.

Chronic (delayed-onset) endophthalmitis

Chronic endophthalmitis has a progressive or indolent course over months or years. Common causative organisms are *Propionibacterium acnes*, coagulase-negative *Staphylococcus* spp, and fungi. Endophthalmitis caused by *P acnes* characteristically induces a peripheral white plaque within the capsular bag and an associated chronic granulomatous inflammation. An injection of antibiotics into the capsular bag or vitreous cavity does not usually eliminate the infection; instead, the preferred treatment is pars plana vitrectomy, partial capsulectomy with selective removal of intracapsular white plaque, and injection of 1 mg intravitreal vancomycin, adjacent to or inside the capsular bag. If the condition recurs after vitrectomy, removal of the entire capsular bag, with removal or exchange of the intraocular lens (IOL), should be considered (Fig 20-8).

Clark WL, Kaiser PK, Flynn HW Jr, Belfort A, Miller D, Meisler DM. Treatment strategies and visual acuity outcomes in chronic postoperative *Propionibacterium acnes* endophthalmitis. *Ophthalmology*. 1999;106(9):1665–1670.

Endophthalmitis associated with conjunctival filtering blebs

Except for the additional sign of a purulent bleb, the clinical features of conjunctival filtering bleb-associated endophthalmitis are similar to those of acute-onset postoperative endophthalmitis. These features include conjunctival vascular congestion and noticeable intraocular inflammation, often with hypopyon (occurring months or years after glaucoma filtering surgery). The initial infection may involve the bleb only (*blebitis*), without anterior chamber or vitreous involvement. Blebitis without endophthalmitis can be treated with

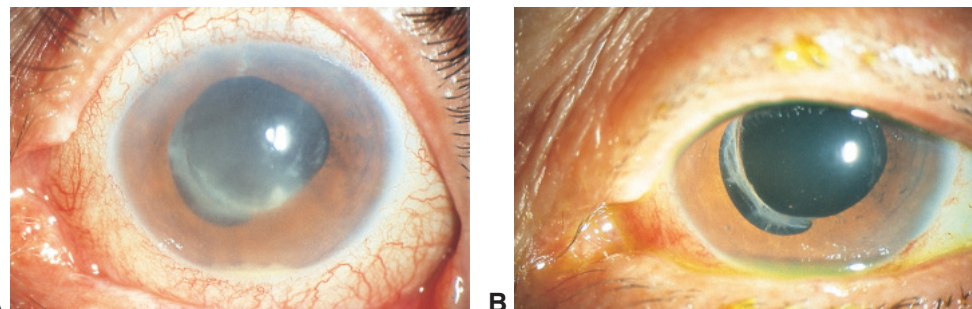


Figure 20-8 Chronic (delayed-onset) postoperative endophthalmitis. **A**, Endophthalmitis in a patient with progressive intraocular inflammation 3 months after cataract surgery. **B**, Same patient after pars plana vitrectomy, capsulectomy, and injection of intravitreal antibiotics. Culture results confirmed a diagnosis of *Propionibacterium acnes* endophthalmitis. (Courtesy of Harry W. Flynn, Jr, MD.)

frequent applications of topical and subconjunctival antibiotics and close follow-up. However, if blebitis progresses to bleb-associated endophthalmitis, patients are treated with intravitreal antibiotics with or without vitrectomy. Bleb-associated endophthalmitis typically occurs months to years after surgery, and causative organisms include *Streptococcus* spp, *Haemophilus* species, and other gram-positive organisms. The recommended intravitreal antibiotics are similar to those used in acute-onset postoperative endophthalmitis. However, the most common causative organisms in bleb-associated endophthalmitis (ie, *Streptococcus* or *Haemophilus* spp) are more virulent than the most frequently encountered organisms in endophthalmitis that occurs after other intraocular surgeries (such as cataract surgery). Even with prompt treatment, the visual outcomes in bleb-associated endophthalmitis are generally worse than for acute-onset endophthalmitis after cataract surgery (Fig 20-9). Management of filtering bleb-associated endophthalmitis is similar to acute-onset postoperative endophthalmitis; however, vitrectomy may be more commonly considered.

Retained Lens Fragments After Phacoemulsification

The incidence of posteriorly displaced, or retained, lens fragments ranges from 0.3%–1.1% in reported series. Retained lens fragments may cause severe intraocular

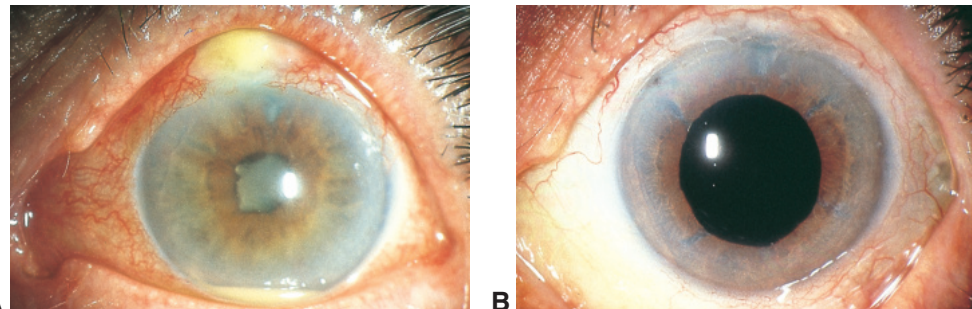


Figure 20-9 Bleb-associated endophthalmitis. **A**, Patient with endophthalmitis who had a sudden onset of decreased vision, redness, and pain 2 years after glaucoma filtering surgery. **B**, Same patient after treatment with pars plana vitrectomy and injection of intravitreal antibiotics. (Courtesy of Harry W. Flynn, Jr, MD.)

Table 20-1 General Recommendations for Management of Retained Lens Fragments**For the anterior segment surgeon**

- Attempt retrieval of displaced lens fragments only if fragments are readily accessible.
- Perform anterior vitrectomy as necessary to avoid vitreous prolapse into the wound.
- Insert an intraocular lens if possible.
- Close the cataract wound with interrupted sutures.
- Prescribe topical medications as needed.
- Refer the patient to a vitreoretinal consultant.

For the vitreoretinal surgeon

- Observe eyes with minimal inflammation and/or a small lens fragment.
- Continue topical medications as needed.
- Schedule vitrectomy
 - if inflammation or IOP is not controlled.
 - if a nuclear fragment is present.
- Delay vitrectomy if necessary to allow clearing of corneal edema.
- Perform maximal core vitrectomy before phacofragmentation.
- Start with low fragmentation power (5%–10%) for more efficient removal of the nucleus.
- Prepare for secondary intraocular lens insertion if necessary.
- Examine the retinal periphery for retinal tears or retinal detachment.

IOP=intraocular pressure.

Modified with permission from Flynn HW Jr, Smiddy WE, Vilar NF. Management of retained lens fragments after cataract surgery. In: Saer JB, ed. *Vitreo-Retinal and Uveitis Update: Proceedings of the New Orleans Academy of Ophthalmology Symposium*. The Hague, Netherlands: Kugler; 1998:149, 150.

inflammation and secondary glaucoma. Nuclear fragments usually continue to cause chronic intraocular inflammation, whereas cortical remnants usually spontaneously reabsorb (Table 20-1).

Indications for vitrectomy include secondary glaucoma, lens-induced uveitis, and the presence of large nuclear fragments. In the 4 largest reported series, 52% of patients with retained lens fragments had an IOP of at least 30 mm Hg before vitrectomy. Removal of the lens fragments reduced this incidence by 50% or more in these series. Pars plana vitrectomy, with or without use of a fragmatome, is the preferred approach to remove harder pieces of the lens nucleus (Video 20-5). Following lens fragment removal, the retinal periphery should be examined for the presence of retinal tears or retinal detachment.


VIDEO 20-5 Vitrectomy for removal of retained lens fragment.

Courtesy of Colin A. McCannel, MD.



Reported studies with long-term follow-up have found that retinal detachment occurs in about 15% of eyes with retained lens fragments. Aggressive attempts to retrieve posterior lens fragments using a limbal approach are sometimes complicated by retinal detachments caused by giant retinal tears. Giant retinal tears are more commonly found 180° away from the incision used for cataract surgery.

Aaberg TM Jr, Rubsamen PE, Flynn HW Jr, Chang S, Mieler WF, Smiddy WE. Giant retinal tear as a complication of attempted removal of intravitreal lens fragments during cataract surgery. *Am J Ophthalmol*. 1997;124(2):222–226.

Modi YS, Epstein A, Smiddy WE, Murray TG, Feuer W, Flynn HW Jr. Retained lens fragments after cataract surgery: outcomes of same-day versus later pars plana vitrectomy. *Am J Ophthalmol.* 2013;156(3):454–459.

Vanner EA, Stewart MW. Vitrectomy timing for retained lens fragments after surgery for age-related cataracts: a systematic review and meta-analysis. *Am J Ophthalmol.* 2011;152(3):345–357.

Posteriorly Dislocated Intraocular Lenses

Posterior chamber intraocular lenses (PCIOLs) may become dislocated despite seemingly satisfactory capsular support at the time of the initial surgery. Factors to consider when placing a sulcus-fixated IOL include the presence of zonular dehiscence, total amount of anterior capsular support (eg, >180°), size of the eye, and haptic-to-haptic diameter of the IOL. Foldable IOLs have a 12.5–13.0-mm haptic-to-haptic length. This length, which is frequently smaller than the sulcus-to-sulcus diameter into which these haptics must fit, may contribute to postoperative subluxation or dislocation of the IOL. A flexible IOL may also become dislocated following Nd:YAG laser capsulotomy performed soon after cataract surgery. Late dislocation of the IOL (from several months to decades after surgery) is less common but may occur as a result of trauma or spontaneous loss of zonular support in eyes with pseudoexfoliation syndrome. Treatment options in such cases include observation only, surgical repositioning, IOL exchange, or IOL removal.

In vitrectomy for posteriorly dislocated IOLs, all vitreous adhesions to the IOL are removed in order to minimize vitreous traction to the retina when the lens is manipulated back into the anterior chamber. The IOL may be placed into the ciliary sulcus provided there is adequate support. If capsular support is inadequate, the IOL may be fixated by suturing the haptics to the iris (*iris fixation*) or sclera (*scleral fixation*) or by placing the haptics into intrascleral tunnels (*intrascleral fixation*). Alternatively, the PCIOL can be removed through a limbal incision and exchanged for an anterior chamber IOL (ACIOL; Video 20-6).



VIDEO 20-6 Vitrectomy for retrieval of posteriorly dislocated IOL.

Courtesy of Colin A. McCannel, MD.



Smiddy WE, Flynn HW Jr. Managing retained lens fragments and dislocated posterior chamber IOLs after cataract surgery. *Focal Points: Clinical Modules for Ophthalmologists.* San Francisco: American Academy of Ophthalmology; 1996, module 7.

Cystoid Macular Edema

Cystoid macular edema (CME) that develops after anterior segment surgery usually resolves spontaneously. Treatment with corticosteroid and nonsteroidal anti-inflammatory eye drops is the first-line approach for patients with persistent CME. Periocular or intravitreal corticosteroids may be used in recalcitrant cases. Oral acetazolamide may also be useful in some cases. Pars plana vitrectomy with removal of obvious vitreous adhesions to anterior segment structures may promote resolution of CME and improve visual acuity in select cases (Fig 20-10). An IOL may require repositioning, exchange, or removal if it is deemed that the IOL is irritating the iris by chafing or capture.

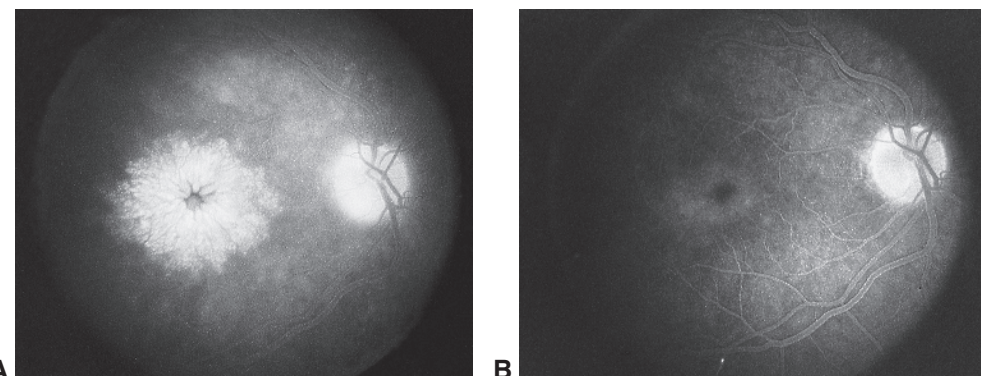


Figure 20-10 Fundus photographs of pseudophakic cystoid macular edema (CME). **A**, Patient has nonresolving CME, vitreous strands adhering to the cataract wound, and a dislocated intraocular lens (IOL). **B**, Same patient after pars plana vitrectomy, removal of vitreous strands, repositioning of IOL, and periocular administration of corticosteroids. CME has markedly improved. (Courtesy of Harry W. Flynn, Jr, MD.)

Suprachoroidal Hemorrhage

Suprachoroidal hemorrhage may occur during or after any form of intraocular surgery, particularly glaucoma surgery, in which large variations in IOP are commonplace. By definition, such hemorrhages accumulate in the supraciliary and suprachoroidal space, a potential space between the sclera and uvea that is modified by uveal adhesions and entries of vessels. Hemorrhages may be limited or massive and involve 1–4 quadrants. When retinal surfaces touch one another, dictated by scleral spur and the entries of the short posterior ciliary vessels and nerves, the choroidal hemorrhage is termed *appositional*, or “kissing.” These hemorrhages may be further classified as nonexpulsive or expulsive; the expulsive type involves extrusion of intraocular contents. Reported risk factors for suprachoroidal hemorrhage include

- advanced age
- aphakia
- arteriosclerotic cardiovascular disease
- glaucoma
- hypertension
- intraoperative tachycardia
- myopia
- Sturge-Weber-associated choroidal hemangiomas

Transient hypotony is a common feature of all incisional ocular surgery; in a small percentage of patients, it may be associated with suprachoroidal hemorrhage from rupture of the long or short posterior ciliary arteries.

Surgical management strategies are controversial. Most studies recommend immediate closure of ocular surgical incisions and removal of vitreous incarceration in the wound, if possible; the primary goal is to prevent or limit expulsion. Successful intraoperative drainage of a suprachoroidal hemorrhage is rare, however, because the blood coagulates rapidly. Most surgeons recommend observation of suprachoroidal hemorrhages

for 7–14 days to allow some degree of liquefaction of the hemorrhage. Determining the timing of secondary surgical intervention is aided by B-scan ultrasound, through evaluation of echographic features of clot liquefaction. Indications for surgical drainage include recalcitrant pain, increased IOP, retinal detachment, and appositional choroidal detachments associated with ciliary body rotation and angle closure. Furthermore, prolonged IOP elevation in the presence of an anterior chamber hemorrhage (hyphema) increases the risk of corneal blood staining and is an indication for surgical intervention.

In surgical management of suprachoroidal hemorrhage, an anterior chamber infusion line is placed to maintain IOP (Video 20-7, Fig 20-11). A full-thickness sclerotomy is then placed subjacent to the site of maximum accumulation of blood. After the suprachoroidal blood drains, pars plana vitrectomy may be performed. Appositional and closed-funnel suprachoroidal hemorrhage, prolonged elevation of IOP, and retinal detachment all portend a poor visual prognosis.



VIDEO 20-7 Drainage of suprachoroidal hemorrhage.

Courtesy of Koen A. van Overdam, MD.



Scott IU, Flynn HW Jr, Schiffman J, Smiddy WE, Murray TG, Ehlies F. Visual acuity outcomes among patients with appositional suprachoroidal hemorrhage. *Ophthalmology*. 1997;104(12):2039–2046.

Needle Penetration of the Globe

Factors predisposing patients to needle penetration of the globe include

- axial high myopia
- inexperience of the practitioner
- poor patient cooperation at the time of the injection
- posterior staphyloma
- previous scleral buckling surgery
- scleromalacia

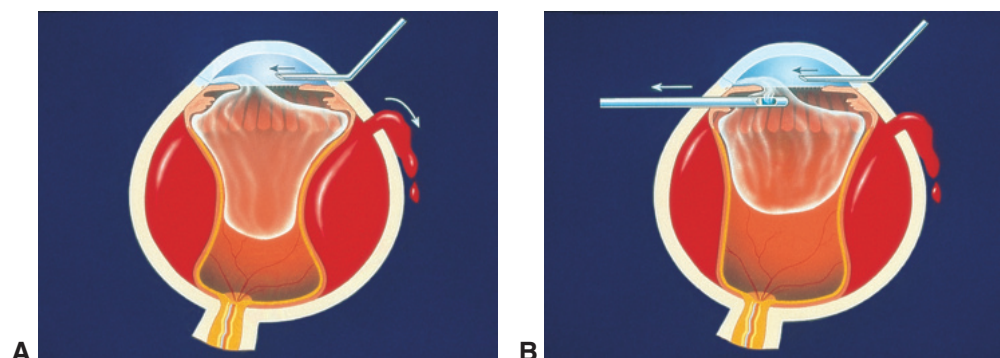


Figure 20-11 Schematics of suprachoroidal hemorrhage. **A**, Anterior infusion and simultaneous drainage of suprachoroidal hemorrhage through pars plana sclerotomy. **B**, Pars plana vitrectomy removes vitreous prolapse while drainage of suprachoroidal hemorrhage continues. (Courtesy of Harry W. Flynn, Jr, MD.)

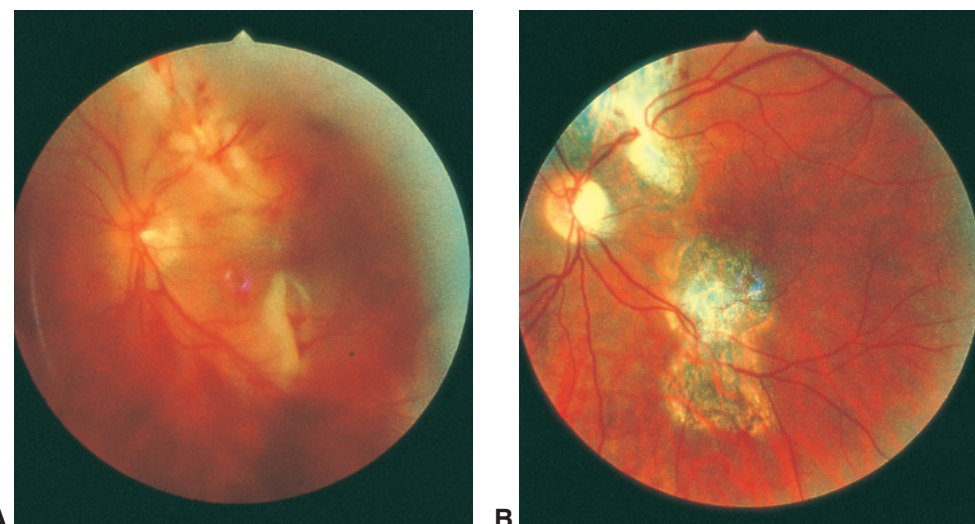


Figure 20-12 Color fundus photographs show damage from needle penetration of the globe. **A**, Needle penetration of the globe caused multiple retinal breaks, including damage to the macula. **B**, After retinal detachment, treatment consisted of vitrectomy, fluid–gas exchange, and endolaser photocoagulation of retinal breaks. Retinal reattachment was achieved, but the patient's visual acuity remained very poor. (*Courtesy of Harry W. Flynn, Jr, MD.*)

Management options vary with the severity of the intraocular damage. Often, blood obscures and surrounds the retinal penetration site, making laser treatment difficult. Observation or transscleral cryotherapy may be considered in such cases. When retinal detachment is present, early vitrectomy with or without scleral buckling is often recommended. Posterior pole damage from needle extension into the macula or optic nerve is associated with a very poor visual prognosis (Fig 20-12).

Rhegmatogenous Retinal Detachment Surgery

Rhegmatogenous retinal detachment occurs when a retinal break (or multiple breaks) allows ingress of fluid from the vitreous cavity into the subretinal space. Breaks can be atrophic, often associated with lattice degeneration, or they may be tractional tears, related to vitreous traction on the retina and posterior vitreous detachment (PVD). The risk of rhegmatogenous retinal detachment (RRD) in otherwise normal eyes is approximately 5 new cases in 100,000 persons per year; lifetime risk is approximately 1 in 300 persons. The most significant risk factors are high myopia, family history of retinal detachment, and fellow-eye retinal detachment. Pseudophakia is also an important risk factor; the reported incidence after cataract surgery is less than 1% but increases over time (Fig 20-13). Patient characteristics that increase the risk of pseudophakic retinal detachment include younger age at the time of cataract extraction, male sex, and longer axial length. A surgical complication such as posterior capsular rupture with vitreous loss has been estimated to increase the risk of retinal detachment by as much as 20-fold.

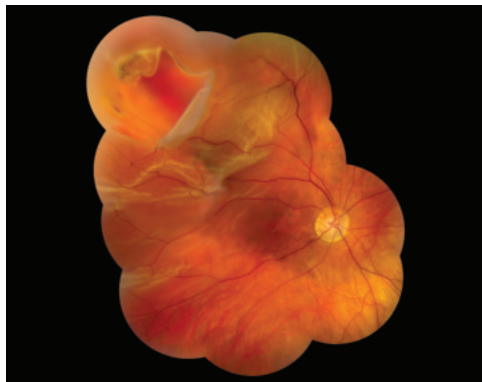


Figure 20-13 Color fundus photograph mon-tage of a patient with symptomatic retinal de-tachment from a large superotemporal break after cataract surgery. (Courtesy of Nancy M. Hole-kamp, MD.)

Management options for RRD include *laser demarcation* of the detachment, *pneumatic retinopexy*, *scleral buckling procedure*, and *vitrectomy with or without scleral buckling*. Observation can be considered for selected patients with localized retinal detachment and no associated symptoms (subclinical retinal detachment).

Selection of the treatment approach among the modalities available for retinal detachment is surgeon-dependent and remains a topic of debate among retinal surgeons. The precise configuration of the detachment, the location of the breaks, and the phakic status of the eye are all considered carefully before the method of treatment is determined.

Clark A, Morlet N, Ng JQ, Preen DB, Semmens JB. Risk for retinal detachment after phaco-emulsification: a whole-population study of cataract surgery outcomes. *Arch Ophthalmol*. 2012;130(7):882–888.

Powell SK, Olson RJ. Incidence of retinal detachment after cataract surgery and neodymium: YAG laser capsulotomy. *J Cataract Refract Surg*. 1995;21(2):132–135.

Techniques for Surgical Repair of Retinal Detachments

There are 3 surgical techniques for eyes with primary uncomplicated rhegmatogenous retinal detachment: *pneumatic retinopexy*, *scleral buckling*, and *primary vitrectomy with or without scleral buckling*. The common goals of these procedures are to identify and treat all causative retinal breaks while supporting such breaks through external and internal tamponade as needed.

Kreissig I, ed. *Primary Retinal Detachment: Options for Repair*. Berlin: Springer-Verlag; 2005.
Campo RV, Sipperley JO, Snead SR, et al. Pars plana vitrectomy without scleral buckle for pseudophakic retinal detachments. *Ophthalmology*. 1999;106(9):1811–1816.

Pneumatic retinopexy

Pneumatic retinopexy closes retinal breaks by using an intraocular gas bubble for a sufficient time to allow the subretinal fluid to reabsorb and a chorioretinal adhesion to form around the causative break(s). The classic indications for pneumatic retinopexy include

- confidence that all retinal breaks have been identified
- retinal breaks that are confined to the superior 8 clock-hours

- a single retinal break or multiple breaks within 1–2 clock-hours
- the absence of proliferative vitreoretinopathy (PVR) grade CP or CA
- a cooperative patient who can maintain proper positioning
- clear media

With direct pneumatic occlusion of the causative retinal breaks in acute detachments, subretinal fluid is often completely reabsorbed within 6–8 hours.

Transconjunctival cryopexy can be performed on the causative retinal breaks; alternatively, laser retinopexy may be performed after retinal apposition. A variety of intraocular gases (eg, air, SF₆, C₃F₈) can be used for tamponade, and a concomitant anterior chamber paracentesis is generally required to normalize the elevated IOP that results from the gas injection. The patient must maintain a predetermined head posture to place the breaks in the least dependent position (Fig 20-14).

A prospective, multicenter, randomized clinical trial comparing pneumatic retinopexy with scleral buckling demonstrated successful retinal reattachment in 73% of patients who underwent pneumatic retinopexy and in 82% of those who received scleral buckle procedures; this difference was not statistically significant. Complications from pneumatic retinopexy include subretinal gas migration, anterior chamber gas migration, endophthalmitis, cataract, and recurrent retinal detachment from the formation of new retinal breaks.

Gilca M, Duval R, Goodyear E, Olivier S, Cordahi G. Factors associated with outcomes of pneumatic retinopexy for rhegmatogenous retinal detachments: a retrospective review of 422 cases. *Retina*. 2014;34(4):693–699.

Tornambe PE, Hilton GF; The Retinal Detachment Study Group. Pneumatic retinopexy. A multicenter randomized controlled clinical trial comparing pneumatic retinopexy with scleral buckling. *Ophthalmology*. 1989;96(6):772–784.

Scleral buckling

Scleral buckling closes retinal breaks through external scleral indentation. Transscleral cryopexy is used to create a permanent adhesion between the retina and RPE at the sites of retinal breaks. The buckling material is then carefully positioned to support the causative breaks by scleral imbrication.

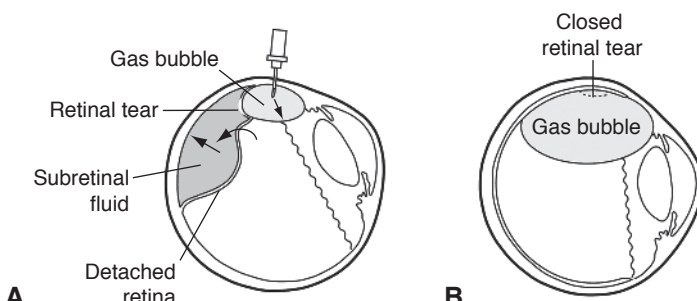


Figure 20-14 Schematic of pneumatic retinopexy. **A**, A small, expansile gas bubble is injected into the vitreous cavity. **B**, The bubble enlarges. The patient is positioned so the gas bubble occludes the retinal break, allowing for resorption of subretinal fluid. (Illustration by Dave Yates.)

The surgeon chooses the scleral buckling technique (eg, encircling, segmental, or radial placement of the sponge, sutured vs scleral tunnels) according to the number and position of retinal breaks, eye size, and associated vitreoretinal findings (eg, lattice degeneration, vitreoretinal traction, aphakia), and individual preference and training (Video 20-8, Fig 20-15).


VIDEO 20-8 Scleral buckle for rhegmatogenous retinal detachment.

Courtesy of Colin A. McCannel, MD.


An increase in the IOP related to compression from the buckling effect may indicate the need for external drainage of the subretinal fluid, anterior chamber paracentesis,

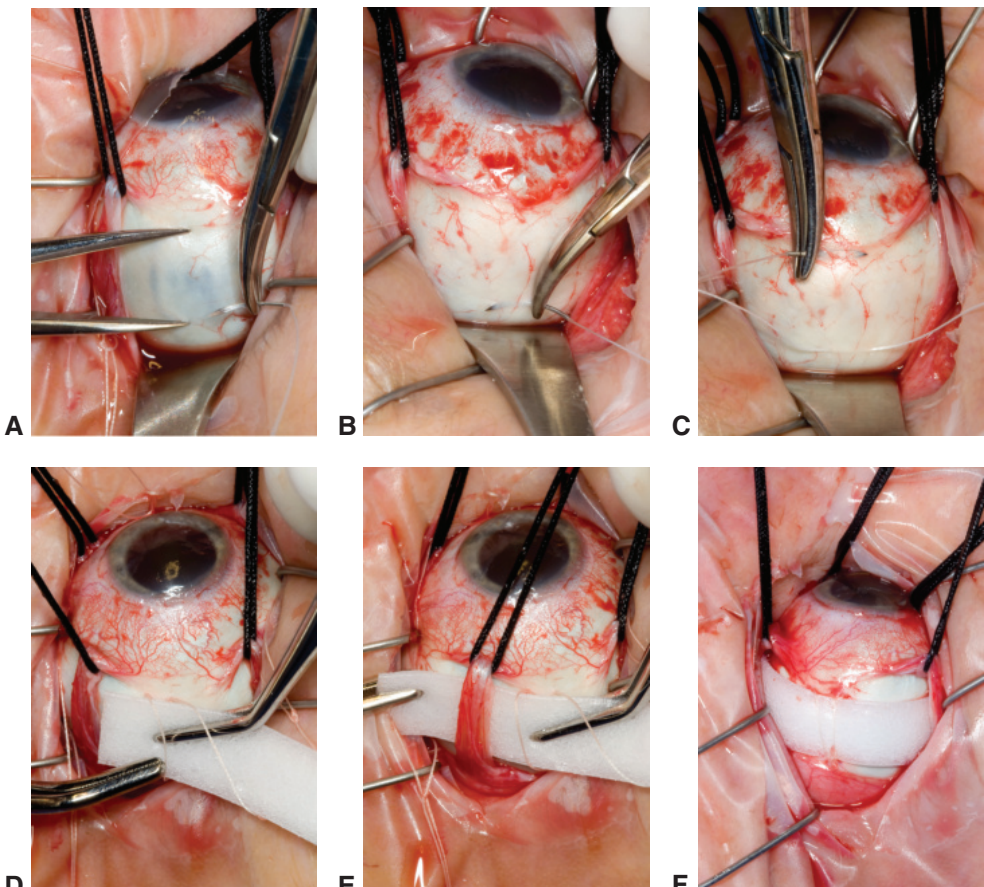


Figure 20-15 Scleral buckle procedure. The conjunctiva is opened; the rectus muscles are isolated and tagged with a "0" silk suture. **A**, The eye is rotated so the sclera is exposed. Using calipers, the surgeon measures and marks the location for the anterior and posterior scleral pass for the radial mattress suture. **B, C**, The posterior scleral suture pass is accomplished. **D, E**, The encircling element, a 506 sponge, is passed, using forceps, under the suture and rectus muscle. **F**, The scleral buckle is fully installed; the tied-up radial mattress suture is shown with the knot rotated posteriorly. (*Courtesy of Colin A. McCannel, MD.*)

or both. Chronic viscous subretinal fluid, “fish-mouthing” of large retinal breaks, and bullous retinal detachments may necessitate treatment with intraocular gas tamponade, drainage, or both. Complications of scleral buckling include induced myopia, anterior ocular ischemia, diplopia, ptosis, orbital cellulitis, subretinal hemorrhage from drainage, and retinal incarceration at the drainage site.

Primary vitrectomy

Traction on focal areas of adhesion of the vitreous to the peripheral retina (frequently at the posterior vitreous base insertion) may cause retinal breaks, allowing intraocular fluid to migrate into the subretinal space, which leads to retinal detachment. Consequently, the goals of primary vitrectomy are to remove cortical vitreous adherent to retinal breaks, directly drain the subretinal fluid, tamponade the breaks (using air, gas, or silicone oil), and create chorioretinal adhesions around each retinal break with endolaser photocoagulation or cryopexy.

In general, the 3-port vitrectomy technique is used, employing 20-gauge, 23-gauge, 25-gauge, or 27-gauge instruments. At the surgeon’s discretion, vitrectomy can be combined with a scleral buckle procedure. During vitrectomy, a complete posterior vitreous separation is ensured, and the peripheral cortical vitreous is carefully shaved toward the vitreous base to relieve traction on the retinal breaks (Video 20-9, Fig 20-16). To drain the subretinal fluid and achieve intraoperative retinal reattachment, the surgeon can use either an intentional drainage retinotomy or perfluorocarbon liquid technique. If PVR is present, it may be necessary to peel the epiretinal (and, less commonly, subretinal) membranes to facilitate the retinal reattachment. For extensive PVR, a relaxing retinotomy or retinectomy may be required. Once the retina is flattened, chorioretinal laser photocoagulation or cryopexy can be applied. Postoperative tamponade is generally provided by intraocular air or nonexpansile concentrations of SF₆ or C₃F₈ gas, although in complex cases the use of silicone oil may be required. Complications of vitrectomy for retinal detachment include postvitrectomy nuclear sclerosis (in phakic eyes), glaucoma, PVR, and retinal redetachment.



VIDEO 20-9 Vitrectomy for rhegmatogenous retinal detachment.

Courtesy of Colin A. McCannel, MD.

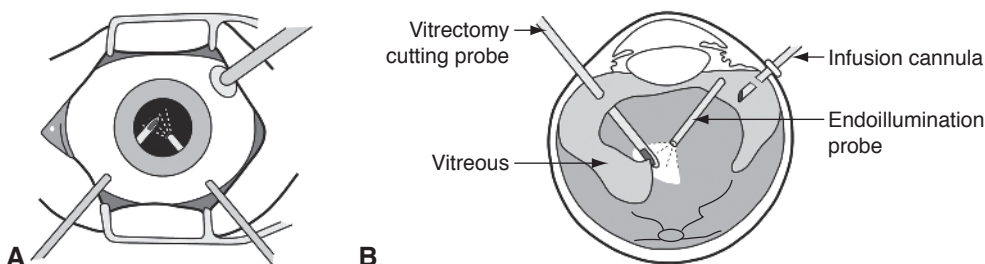


Figure 20-16 Vitrectomy schematic. **A**, Surgeon’s view of a 20-gauge, 3-port pars plana vitrectomy. **B**, A cross-sectional view shows an infusion cannula, endoillumination probe, and vitrectomy cutting probe. (Illustration by Dave Yates.)

Complex retinal detachment includes giant retinal tears, recurrent retinal detachment, vitreous hemorrhage, and PVR. The surgeon must use pars plana vitrectomy techniques in order to address the common features of PVR, including proliferative membranes, retinal folds, and media opacities (see Chapter 16). In the past, controversy surrounded the use of long-acting gas versus silicone oil in retinal tamponade for eyes with complex retinal detachment caused by advanced grades of PVR. This issue was addressed in the Silicone Study, a prospective, multicenter, randomized study, which concluded that tamponade with SF₆ was inferior to long-term tamponade with either C₃F₈ or silicone oil. Differences in outcomes from the use of C₃F₈ and silicone oil were statistically insignificant; however, patients treated with silicone oil experienced a lower rate of hypotony than those treated with C₃F₈.

Vitrectomy with silicone oil or sulfur hexafluoride gas in eyes with severe proliferative vitreoretinopathy: results of a randomized clinical trial. Silicone Study report 1. *Arch Ophthalmol.* 1992;110(6):770–779.

Vitrectomy with silicone oil or perfluoropropane gas in eyes with severe proliferative vitreoretinopathy: results of a randomized clinical trial. Silicone Study report 2. *Arch Ophthalmol.* 1992;110(6):780–792.

Outcomes Following Retinal Reattachment Surgery

Anatomical reattachment

In the absence of PVR, the overall rate of primary anatomical reattachment with current techniques is 80%–90% for the primary surgery. The exact rate depends on technique and preoperative ocular findings. In patients with PVR or who have had previous reattachment surgeries, success rates are in the 70% range. However, rates for final reattachment, even if multiple procedures are required, are in the 90%–100% range. Retinal detachments caused by dialyses or small holes or that are associated with demarcation lines have a better prognosis. Aphakic and pseudophakic eyes have a slightly less favorable prognosis. Detachments caused by giant tears or that are associated with PVR, uveitis, choroidal detachments, or posterior breaks secondary to trauma have the worst prognosis for anatomical reattachment.

Sullivan P. Techniques of scleral buckling. In: Schachat AP, Wilkinson CP, Hinton DR, Sadda SR, Wiedemann P, eds. *Ryan's Retina*. Vol 3. 6th ed. Philadelphia: Elsevier/Saunders; 2018.

Postoperative visual acuity

The status of the macula—whether it was detached and for how long—is the primary presurgical determinant of postoperative visual acuity. If the macula was not detached (“macula-on” retinal detachment) and the retinal detachment is successfully repaired, restoration of preoperative visual acuity is usually expected. However, 10%–15% of these eyes do not return to preoperative visual acuity.

If the macula was detached preoperatively (“macula-off” retinal detachment), damage to—or degeneration of—photoreceptors may prevent good postoperative visual acuity. Only approximately one-third to one-half of eyes with a detached macula recover visual acuity to the level of 20/50 or better. Among patients with a macular detachment of

less than 1 week's duration, 75% will obtain a final visual acuity of 20/70 or better, as opposed to 50% with a macular detachment of a duration exceeding 7–10 days but shorter than 8 weeks.

In addition to photoreceptor damage from the detachment, factors associated with visual acuity deterioration or incomplete recovery following successful retinal reattachment surgery include irregular astigmatism, cataract progression, persistent subfoveal fluid, macular edema, or macular pucker. Intraoperative complications such as hemorrhage and preexisting ocular pathology may also limit visual recovery.

Complications of Pars Plana Vitrectomy

Nuclear sclerotic cataract is the most common complication of vitrectomy. Within 3–6 months following vitrectomy, as many as 90% of phakic eyes in patients older than 50 years may develop visually significant nuclear sclerotic cataract. Vitrectomy may also increase the long-term risk of open-angle glaucoma. Both cataract progression and glaucoma are speculated to be the result of increased oxygen tension in the eye after vitrectomy, which in turn results in oxidative damage to the lens and trabecular meshwork, respectively.

Other complications of pars plana vitrectomy include intraoperative retinal tears (approximately 1%–5%), postoperative detachment (approximately 1%–2%), retention of subretinal perfluorocarbon liquid (when used), retinal and vitreous incarceration, endophthalmitis (approximately 0.05%), suprachoroidal hemorrhage and recurrent vitreous hemorrhage (approximately less than 1%; up to 5% and higher in diabetics). Endophthalmitis after vitrectomy is more common in patients with diabetes mellitus and in eyes with retained intraocular foreign bodies. Table 20-2 lists the most common complications of pars plana vitrectomy.

Banker AS, Freeman WR, Kim JW, Munguia D, Azen SP; Vitrectomy for Macular Hole Study Group. Vision-threatening complications of surgery for full-thickness macular holes. *Ophthalmology*. 1997;104(9):1442–1453.

Table 20-2 Complications of Pars Plana Vitrectomy

Complications commonly associated with pars plana vitrectomy

- Postoperative nuclear sclerotic cataract
- Long-term risk of open-angle glaucoma
- Intraoperative or postoperative retinal break
- Intraoperative or postoperative retinal detachment
- Intraoperative cataract
- Postoperative vitreous hemorrhage
- Postoperative massive fibrin exudation
- Postoperative anterior segment neovascularization
- Endophthalmitis
- Retinal phototoxicity

Complications associated with silicone oil

- Glaucoma
 - Band keratopathy
 - Corneal decompensation
-

Chang S. LXII Edward Jackson lecture: open angle glaucoma after vitrectomy. *Am J Ophthalmol.* 2006;141(6):1033–1043.

Thompson JT. The role of patient age and intraocular gases in cataract progression following vitrectomy for macular holes and epiretinal membranes. *Trans Am Ophthalmol Soc.* 2003; 101:485–498.

Intravitreal Injections

Intravitreal injections are the fastest-growing procedure in ophthalmology and in medicine in general (Video 20-10, Fig 20-17). The most common indications for injections include AMD, diabetic retinopathy, and venous occlusive disease-associated macular edema. The most common injections are anti-angiogenic agents (eg, aflibercept, bevacizumab, and ranibizumab). Other intravitreal injections include steroid preparations, including sustained delivery devices, antimicrobial medications, and many medications used in clinical trials that will likely be approved in the coming years. The number of injections performed in the United States, estimated from Medicare procedure codes, increased from fewer than 3000 per year in 1999 to an estimated 6.5 million in 2016. This number continues to increase as a result of the aging population, new medications becoming available, and an expanding list of indications.



VIDEO 20-10 Intravitreal injection of pharmacologic agent.

Courtesy of Stephen J. Kim, MD.



Injections can be accomplished safely 3–4 mm posterior to the limbus. Commonly used methods for anesthesia administration before intravitreal injections include pledges or cotton-tip applicators soaked with anesthetic and held against the site of injection, application of topical (including viscous) formulations of anesthetic, and subconjunctival lidocaine injection. There is no consensus regarding the optimal method of anesthesia for patient comfort and reduced risk of infection.

Strict aseptic technique, including managing the eyelid to prevent contamination from the margin and lashes, is recommended. The application of povidone-iodine, 5%, to the ocular surface for at least 60–90 seconds prior to injection is widely considered



Figure 20-17 Intravitreal injection. The ocular surface was anesthetized with subconjunctival injection of lidocaine, 2%, in the inferotemporal quadrant. An eyelid speculum was inserted, and povidone-iodine, 5%, applied to the ocular surface. After 2 minutes, povidone-iodine was reapplied over the injection site and—after proper hand placement and no talking—the injection was made approximately 4 mm from the limbus. (Courtesy of Stephen J. Kim, MD.)

beneficial. Antibiotic eyedrop use before or after injections is controversial and is not recommended in routine procedures, particularly given that repeat topical antibiotic application results in the development of resistant ocular flora.

Endophthalmitis remains the most feared complication resulting from an intravitreal injection; the reported incidence ranges from 0.02% to 0.2%. Although respiratory organisms could cause endophthalmitis (via contamination from respiratory droplets), the most common source of infection is presumed to be the patient's own conjunctiva or eyelids. Therefore, potential mechanisms of infection include direct inoculation of ocular surface bacteria into the vitreous or subsequent entry through a wound track. Multiple studies have reported that *Streptococcus viridans*, a common component of oral flora, is a more frequent cause of endophthalmitis following intravitreal injections than after other intraocular procedures, presumably from contamination by respiratory droplets. Consequently, attention should be paid to efforts that reduce the risk of respiratory-droplet contamination such as minimizing talking of both the patient and provider and the use of face masks during the procedure. In addition, excessive manipulation of the eyelid margin should be avoided to limit expression of bacteria-laden secretions from the meibomian glands, and aggressive treatment of blepharitis prior to intravitreal injection should be considered for patients with severe disease.

Outbreaks of endophthalmitis from contaminated bevacizumab in the past have prompted periodic review of compounding pharmacy practices and accreditation status to reduce the risk of future outbreaks. To minimize patient risk when bilateral injections are performed, many practitioners have adopted a workflow in which different lot numbers of compounded medications are used for each eye.

Other complications include the development of elevated intraocular pressure following intravitreal injections of anti-VEGF agents, or as a common adverse effect of steroid injections. A complication unique to the dexamethasone sustained-release implant is severe corneal endothelial toxicity if the implant migrates into the anterior chamber. Such migration has been reported to be common in aphakic eyes, but it can also occur in pseudophakic eyes.

Khurana RN, Appa SN, McCannel CA, et al. Dexamethasone implant anterior chamber migration: risk factors, complications, and management strategies. *Ophthalmology*. 2014;121(1):67–71.

Kim SJ, Chomsky AS, Sternberg P Jr. Reducing the risk of endophthalmitis after intravitreous injection. *JAMA Ophthalmol*. 2013;131(5):674–675.

Kim SJ, Toma HS. Antimicrobial resistance and ophthalmic antibiotics: 1-year results of a longitudinal controlled study of patients undergoing intravitreal injections. *Arch Ophthalmol*. 2011;129(9):1180–1188.

McCannel CA. Meta-analysis of endophthalmitis after intravitreal injection of anti-vascular endothelial growth factor agents: causative organisms and possible prevention strategies. *Retina*. 2011;31(4):654–661.

Basic Texts

Retina and Vitreous

- Agarwal A. *Gass' Atlas of Macular Diseases*. 5th ed. Philadelphia: Elsevier/Saunders; 2012.
- Chow D, Chaves de Olivera PR. *OCT Angiography*. Stuttgart, Germany: Thieme; 2017.
- Duker JS, Waheed NK, Goldman DR, eds. *Handbook of Retinal OCT*. Philadelphia: Elsevier/ Saunders; 2014.
- Freund KB, Sarraf D, Mieler WF, Yannuzzi LA. *The Retinal Atlas*. 2nd ed. Philadelphia: Elsevier; 2017.
- Gupta AK, Aggarwal VK, Goel N, Nayak BK. *Handbook of Clinical Trials in Ophthalmology*. New Delhi, India: Jaypee Brothers Medical Publishers; 2014.
- Hartnett ME. *Pediatric Retina*. 2nd ed. Philadelphia: Lippincott Williams & Wilkins; 2014.
- Ho AC, Regillo CD, eds. *Age-related Macular Degeneration Diagnosis and Treatment*. New York: Springer; 2011.
- Landry DA, Kashani AH. *Optical Coherence Tomography and OCT Angiography: Clinical Reference and Case Studies*. Saco, Maine: Bryson Taylor Publishing; 2016.
- Rizzo S, Patelli F, Chow DR, eds. *Vitreo-retinal Surgery: Progress III*. New York: Springer-Verlag; 2009. *Essentials in Ophthalmology*.
- Saxena S, Meyer CH, Ohji M, Akduman L, eds. *Vitreoretinal Surgery*. New Delhi, India: Jaypee Brothers Medical Publishers; 2012.
- Schachat AP, Wilkinson CP, Hinton DR, Sadda SR, Wiedemann P, eds. *Ryan's Retina*. 6th ed. Philadelphia: Elsevier; 2018.
- Sebag J, ed. *Vitreous: in Health and Disease*. New York: Springer-Verlag; 2014.
- Tabandeh H, Goldberg MF. *The Retina in Systemic Disease: A Color Manual of Ophthalmoscopy*. New York: Thieme; 2009.
- Tasman WS, Jaeger EA, eds. *Duane's Ophthalmology on DVD-ROM*. Philadelphia: Lippincott Williams & Wilkins; 2013.
- Wilkinson CP, Rice TA. *Michels Retinal Detachment*. 2nd ed. St Louis: Mosby–Mosby Year Book; 1997.

Related Academy Materials

The American Academy of Ophthalmology is dedicated to providing a wealth of high-quality clinical education resources for ophthalmologists.

Print Publications and Electronic Products

For a complete listing of Academy products related to topics covered in this BCSC Section, visit our online store at <https://store.aao.org/clinical-education/topic/retina-vitreous.html>. Or call Customer Service at 866-561-8558 (toll free, US only) or +1 415-561-8540, Monday through Friday, between 8:00 AM and 5:00 PM (PST).

Online Resources

Visit the Ophthalmic News and Education (ONE[®]) Network at aao.org/onenetwork to find relevant videos, online courses, journal articles, practice guidelines, self-assessment quizzes, images, and more. The ONE Network is a free Academy-member benefit.

Access free, trusted articles and content with the Academy's collaborative online encyclopedia, EyeWiki, at aao.org/eyewiki.

Get mobile access to the *Wills Eye Manual*, watch the latest 1-minute videos, and set up alerts for clinical updates relevant to you with the AAO Ophthalmic Education App. Download today: Search for "AAO Ophthalmic Education" in the Apple app store or in Google Play.

Requesting Continuing Medical Education Credit

The American Academy of Ophthalmology is accredited by the Accreditation Council for Continuing Medical Education (ACCME) to provide continuing medical education for physicians.

The American Academy of Ophthalmology designates this enduring material for a maximum of 15 *AMA PRA Category 1 Credits™*. Physicians should claim only the credit commensurate with the extent of their participation in the activity.

To claim *AMA PRA Category 1 Credits™* upon completion of this activity, learners must demonstrate appropriate knowledge and participation in the activity by taking the post-test for Section 12 and achieving a score of 80% or higher.

This activity meets the Self-Assessment CME requirements defined by the American Board of Ophthalmology (ABO). Please be advised that the ABO is not an accrediting body for purposes of any CME program. ABO does not sponsor this or any outside activity, and ABO does not endorse any particular CME activity. Complete information regarding the ABO Self-Assessment CME Maintenance of Certification requirements is available at <https://abop.org/maintain-certification/cme-self-assessment/>.

To take the posttest and request CME credit online:

1. Go to www.aao.org/cme-central and log in.
2. Click on “Claim CME Credit and View My CME Transcript” and then “Report AAO Credits.”
3. Select the appropriate media type and then the Academy activity. You will be directed to the posttest.
4. Once you have passed the test with a score of 80% or higher, you will be directed to your transcript. *If you are not an Academy member, you will be able to print out a certificate of participation once you have passed the test.*

CME expiration date: June 1, 2022. *AMA PRA Category 1 Credits™* may be claimed only once between June 1, 2018, and the expiration date.

For assistance, contact the Academy’s Customer Service department at 866-561-8558 (US only) or +1 415-561-8540 between 8:00 AM and 5:00 PM (PST), Monday through Friday, or send an e-mail to customer_service@ao.org.

Study Questions

Please note that these questions are not part of your CME reporting process. They are provided here for your own educational use and identification of any professional practice gaps. The required CME posttest is available online (see “Requesting Continuing Medical Education Credit”). Following the questions are a blank answer sheet and answers with discussions. Although a concerted effort has been made to avoid ambiguity and redundancy in these questions, the authors recognize that differences of opinion may occur regarding the “best” answer. The discussions are provided to demonstrate the rationale used to derive the answer. They may also be helpful in confirming that your approach to the problem was correct or, if necessary, in fixing the principle in your memory. The Section 12 faculty thanks the Self-Assessment Committee for reviewing the self-assessment questions.

1. Vitreous attaches to the internal limiting membrane (ILM) of the retinal surface via what 2 primary adhesion molecules?
 - a. fibronectin and laminin
 - b. fibronectin and integrin
 - c. fibronectin and connectin
 - d. laminin and connectin
2. What percentage of cones overall reside outside the foveal region?
 - a. 30%
 - b. 50%
 - c. 70%
 - d. 90%
3. What noninvasive diagnostic test is most specific for detecting retinal pigment epithelial (RPE) cell death?
 - a. fundus autofluorescence (FAF)
 - b. fluorescein angiography
 - c. fundus photography
 - d. optical coherence tomography angiography (OCTA)
4. What electrophysiologic diagnostic study serves as a direct measure of central retinal ganglion cell function?
 - a. pattern electroretinogram (PERG)
 - b. electro-oculogram (EOG)
 - c. multifocal electroretinogram (mfERG)
 - d. visual evoked potential (VEP)

412 • Study Questions

5. What is a defining feature of a stage 2 macular hole?
 - a. spontaneous closure that occurs in 50% of cases
 - b. visible operculum
 - c. full-thickness defect less than 400 µm in diameter
 - d. posterior hyaloid that is detached from the macula and nerve
6. What diagnostic device is used for the evaluation of contrast sensitivity?
 - a. Pelli-Robson test
 - b. anomaloscope
 - c. Farnsworth-Munsell 100-hue test
 - d. Ishihara plates
7. What electrophysiologic diagnostic study serves as a direct measure of macular function?
 - a. mfERG
 - b. EOG
 - c. PERG
 - d. full-field (Ganzfeld) electroretinogram (ERG)
8. Verteporfin is approved by the US Food and Drug Administration (FDA) for what indication?
 - a. central serous chorioretinopathy (CSC)
 - b. subfoveal choroidal neovascularization (CNV) secondary to posterior uveitis
 - c. subfoveal CNV secondary to myopia
 - d. choroidal hemangioma
9. What are the 2 known major susceptibility genes for age-related macular degeneration (AMD)?
 - a. ARMS2 and *CFH*
 - b. *CFI* and ARMS2
 - c. *CFI* and *CFH*
 - d. *APOE* and ARMS2
10. In patients with intermediate or advanced AMD, to what degree did the nutritional supplementation used in the AREDS (Age-Related Eye Disease Study) reduce the risk for progression to more-advanced stages of AMD?
 - a. 45%
 - b. 25%
 - c. 35%
 - d. 55%

11. A patient develops branch retinal vein occlusion (BRVO) at a site other than an arteriovenous crossing. What underlying etiology should be considered?
 - a. hypertension
 - b. embolus
 - c. vasculitis
 - d. glaucoma
12. A 35-year-old, otherwise healthy man presents with recent-onset blurred vision. An examination reveals 20/400 visual acuity in the right eye and 20/20 visual acuity in the left eye, and dilated, tortuous veins with retinal hemorrhages in all quadrants in the right eye. The left eye is normal. The intraocular pressure (IOP) is normal in both eyes, and the patient is not taking any medications. Blood pressure (BP) measured in office is 122/76. For what possible underlying etiology could the patient be evaluated?
 - a. hypercoagulable condition
 - b. infectious etiology
 - c. giant cell arteritis
 - d. thromboembolic disease
13. What is the most important management consideration in a patient who presents with a branch retinal artery occlusion?
 - a. checking erythrocyte sedimentation rate (ESR), C-reactive protein (CRP), and platelets
 - b. lowering the IOP
 - c. emergent embolic workup
 - d. ocular massage
14. A 60-year-old patient reports gradual vision loss in the left eye, washed out vision after exposure to bright light, and aching pain localized to the left orbital area. Examination reveals iris neovascularization with an IOP of 11 mm Hg, anterior chamber flare, scattered retinal blot hemorrhages, and dilated veins. The retinal artery collapses with gentle scleral depression. What is the most likely underlying etiology for this presentation?
 - a. carotid occlusive disease
 - b. proliferative diabetic retinopathy
 - c. retinal vein occlusion
 - d. radiation retinopathy
15. What sickle cell hemoglobinopathy is most commonly associated with proliferative sickle cell retinopathy?
 - a. sickle cell trait (AS)
 - b. sickle cell homozygote (SS)
 - c. sickle cell hemoglobin C (SC)
 - d. sickle cell thalassemia (SThal)

414 • Study Questions

16. What is the most characteristic abnormality that can be seen on fluorescein angiography (FA) in a patient with CSC?
 - a. smokestack pattern
 - b. multifocal hyperfluorescence
 - c. hyperfluorescent dot
 - d. lacy hyperfluorescence
17. What complication is seen more often after laser photocoagulation for proliferative sickle cell retinopathy than for other proliferative retinopathies?
 - a. retinal tear
 - b. reduced peripheral vision
 - c. choroidal detachment
 - d. vitreous hemorrhage
18. What is the mode of inheritance for von Hippel–Lindau syndrome?
 - a. autosomal recessive
 - b. autosomal dominant
 - c. X-linked
 - d. sporadic
19. Retinal cavernous hemangiomas are usually asymptomatic and can be monitored. What complication can develop that requires treatment of retinal cavernous hemangiomas?
 - a. lipid exudation
 - b. retinal neovascularization
 - c. vitreous hemorrhage
 - d. progressive enlargement
20. In a premature infant born at 29 weeks' gestation, what is the appropriate time for the initial screening examination for retinopathy of prematurity (ROP)?
 - a. at birth
 - b. 1–3 weeks after birth
 - c. 4–6 weeks after birth
 - d. no examination indicated

21. A 24-year-old woman presents with acute onset, paracentral “flashing lights” in 1 eye, nasal visual field loss by confrontation in both eyes, and normal visual acuity in both eyes. Vitreous cells are present posteriorly in both eyes. The fundus is otherwise unremarkable. Visual field, mfERG, and optical coherence tomography (OCT) testing reveal scotomas corresponding to focally decreased mfERG responses and outer retinal layer disruption in both eyes. What is this patient’s most likely diagnosis?
- multiple evanescent white dot syndrome
 - acute zonal occult outer retinopathy
 - acute macular neuroretinopathy
 - intermediate uveitis (pars planitis)
22. A premature infant has immature vascularization in zone I but no evidence of ROP on initial screening examination. What is the appropriate interval for the next screening examination?
- 1 week
 - 2 weeks
 - 3 weeks
 - 4 weeks
23. A 45-year-old man presents with recent left-eye decreased vision, vitreous cells, optic pallor, retinal arteriolar narrowing, and diffuse RPE pigment loss and clumping. The ERG demonstrates normal responses in the right eye and severely subnormal a- and b-wave amplitudes with delayed latencies in the left eye. What is the most likely cause?
- P23H mutation in the rhodopsin gene
 - virus
 - fungus
 - nematode
24. A premature infant has zone II threshold ROP without plus disease. What is the most appropriate treatment?
- laser surgery
 - cryoablation surgery
 - anti-vascular endothelial growth factor (anti-VEGF) monotherapy
 - no intervention indicated
25. A 28-year-old otherwise healthy man presents with recent onset of unilateral slightly blurred vision. On evaluation, the right eye has a visual acuity of 20/25, there is serous subretinal fluid in the macula, and the choroid is thickened. The patient is minimally symptomatic. What is the most appropriate initial management?
- observation
 - topical steroids
 - photodynamic therapy
 - argon laser treatment

26. For what white dot syndrome is profound vision loss typically followed by full or near-full vision recovery?
 - a. acute posterior multifocal placoid pigment epitheliopathy (APMPPE)
 - b. birdshot uveitis or vitiliginous chorioretinitis
 - c. multifocal choroiditis
 - d. serpiginous chorioretinopathy
27. A 7-year-old boy presents with photophobia, a visual acuity of 20/80, and congenital nystagmus. What additional information would aid a clinician in making a diagnosis?
 - a. absent iris transillumination
 - b. learning that the boy's brother was similarly affected
 - c. ERG test results
 - d. learning that the boy's father has deuteranomaly
28. What is the reason that enucleation is recommended in NLP (no light perception) eyes within 14 days of penetrating injury?
 - a. sympathetic ophthalmia
 - b. chronic pain
 - c. bacterial endophthalmitis
 - d. lens-associated uveitis
29. A 20-year-old man reports lifelong night blindness. Fundus examination is normal, and ERG testing shows a negative pattern. What information can the ophthalmologist provide to the patient about his condition?
 - a. His peripheral vision will become progressively constricted.
 - b. He needs to be screened for malignancies.
 - c. There is no risk of passing his condition to future generations.
 - d. His pupils may respond abnormally to light.
30. In the context of ocular genetic disorders, what is the definition of pleiotropy?
 - a. Multiple genes give rise to the same phenotype.
 - b. Diverse phenotypes share mutations in a common causative gene.
 - c. Mutations in a single allele cause a disease phenotype.
 - d. Mutations in both alleles cause a disease phenotype.
31. Mutation in the *TIMP3* gene may cause early-onset drusen, which may be associated with CNV in young adulthood. What is the clinical name for this disorder?
 - a. Malattia Leventinese
 - b. Doyne honeycomb dystrophy
 - c. cuticular drusen
 - d. Sorsby macular dystrophy

32. Mutations in the *CYP4V2* gene may lead to characteristic crystalline deposits in the retina with initially normal visual function, but with enlarging regions of geographic-like para-central atrophy. What disorder does this mutation cause?
- cystinosis
 - oxalosis
 - Bietti crystalline dystrophy
 - tamoxifen retinopathy
33. Supplementation with vitamins A and E is recommended for patients with what condition?
- abetalipoproteinemia
 - Refsum disease
 - neuronal ceroid lipofuscinosis
 - Zellweger syndrome
34. What is a ciliopathy associated with pigmentary retinopathy and hearing loss?
- Usher syndrome
 - maternally inherited diabetes and deafness
 - Bardet-Biedl syndrome
 - Joubert syndrome
35. A bull's-eye maculopathy can be present in what disease?
- Tay-Sachs disease
 - cystinosis
 - Fabry disease
 - Batten disease
36. What drug can characteristically cause cystoid macular edema that does not leak or stain on fundus fluorescein angiogram?
- fingolimod
 - rosiglitazone
 - paclitaxel
 - nicotinic acid
37. A 19-year-old man developed an acute reduction in central vision, a central scotoma, and a yellow spot in his central macula. What drug may lead to this presentation?
- alkyl nitrites
 - MEK inhibitors
 - sildenafil
 - corticosteroids

418 • Study Questions

38. For what retinal break would laser demarcation be controversial?
 - a. retinal dialysis
 - b. round hole
 - c. horseshoe tear
 - d. tear at edge of lattice degeneration
39. What type of retinal detachment is most likely to be asymptomatic?
 - a. rhegmatogenous
 - b. tractional
 - c. exudative
 - d. retinoschisis-associated
40. A 60-year-old woman with unexplained peripheral neuropathy but no additional ophthalmic or medical history reports bilateral visually significant floaters. What is the most likely diagnosis?
 - a. asteroid hyalosis
 - b. cholesterolosis
 - c. amyloidosis
 - d. chronic vitreous hemorrhage
41. Angle-closure glaucoma is associated with what condition?
 - a. anterior persistent fetal vasculature (PFV)
 - b. posterior persistent fetal vasculature
 - c. Stickler syndrome
 - d. remnant tunica vasculosa lentis
42. What finding is most consistent with siderosis bulbi?
 - a. dense vitritis
 - b. sunflower cataract
 - c. deposits in Descemet membrane
 - d. peripheral retinal pigmentation
43. What is the most important predictor of final visual outcome after globe trauma?
 - a. presence of endophthalmitis
 - b. presence of a retinal detachment
 - c. initial visual acuity
 - d. presence of an afferent pupillary defect

44. What is an advantage of subthreshold laser treatment in comparison to conventional laser treatment?
- Heat conduction is confined to the RPE.
 - Treatment does not require pupillary dilation.
 - Visual cues allow more precise titration of the laser as it is applied.
 - The effect lasts longer.
45. A 27-year-old woman developed posterior subcapsular cataracts from exposure to oral steroid treatment for systemic lupus erythematosus and underwent cataract surgery. Nine weeks after surgery, she developed a steroid-responsive granulomatous uveitis/endophthalmitis, with a white plaque on her intraocular lens. What would be the most appropriate management of this condition?
- injection of vitreous antibiotics
 - sampling of the anterior chamber
 - pars plana vitrectomy (PPV) and partial capsulectomy with intravitreal antibiotic injection
 - topical antibiotics and steroids
46. What identifiable preoperative feature is a contraindication to retrobulbar anesthesia?
- axial high myopia
 - older age
 - use of continuous positive airway pressure (CPAP) at night
 - obesity
47. Vitrectomy is a required procedural component of surgery when treating what vision-compromising condition?
- multiple horseshoe tears
 - vitreous hemorrhage obscuring the inferior retina
 - proliferative vitreoretinopathy (grade C or above)
 - retinal dialysis (2 clock-hours)
48. What symptom following intravitreous injection would be unexpected and warrant immediate evaluation?
- progressive floaters with progressive blurring of vision
 - sharp pain following the injection
 - foreign body sensation
 - small floaters that are noticed immediately following injection

Answer Sheet for Section 12

Study Questions

Question	Answer	Question	Answer
1	a b c d	25	a b c d
2	a b c d	26	a b c d
3	a b c d	27	a b c d
4	a b c d	28	a b c d
5	a b c d	29	a b c d
6	a b c d	30	a b c d
7	a b c d	31	a b c d
8	a b c d	32	a b c d
9	a b c d	33	a b c d
10	a b c d	34	a b c d
11	a b c d	35	a b c d
12	a b c d	36	a b c d
13	a b c d	37	a b c d
14	a b c d	38	a b c d
15	a b c d	39	a b c d
16	a b c d	40	a b c d
17	a b c d	41	a b c d
18	a b c d	42	a b c d
19	a b c d	43	a b c d
20	a b c d	44	a b c d
21	a b c d	45	a b c d
22	a b c d	46	a b c d
23	a b c d	47	a b c d
24	a b c d	48	a b c d

Answers

1. **a.** The vitreous attaches to the internal limiting membrane (ILM) of the retinal surface primarily via fibronectin and laminin. The integrin molecule has been shown to induce posterior vitreous detachment, not facilitate attachment. The connectin molecule does not appear to play a significant role in vitreoretinal adhesion.
2. **d.** The density and distribution of photoreceptors vary with topographic location. In the fovea, cones are predominantly red- and green-sensitive, with a density exceeding 140,000 cones/mm². The foveola has no rods. The fovea contains only photoreceptors, rods and cones, and processes of Müller cells. The number of cone photoreceptors decreases rapidly away from the fovea, even though 90% of cones overall reside outside the foveal region. The density of rods also decreases toward the periphery.
3. **a.** Fundus autofluorescence (FAF) is a rapid, noncontact, noninvasive way to image fluorophores in the ocular fundus. Excitation light is introduced to the eye, and fluorescence from intrinsic fluorophores is detected by excluding the imaging of that excitation light via the use of a barrier filter. The main source of autofluorescence from the fundus is lipofuscin in the retinal pigment epithelium (RPE). If an RPE cell dies, its contained lipofuscin goes away, resulting in a loss of autofluorescence. These areas appear dark in auto-fluorescence images. This principle can be used to monitor the absence of RPE cells in geographic atrophy, a manifestation of nonexudative age-related macular degeneration (AMD). Fundus photography is not specific for detecting RPE cell death. Optical coherence tomography angiography (OCTA) is a noninvasive technique that acquires volumetric angiographic information without the use of a dye, and images the individual vascular plexuses of the inner retina, outer retina, and choriocapillaris. Fluorescein angiography is an invasive diagnostic test, primarily used for imaging the retinal vasculature.
4. **a.** The pattern electroretinogram (PERG) is the retinal response to an isoluminant alternating checkerboard stimulus presented to the macula. The stimulus is primarily alternating contrast stimulus. The responses are small, and signal averaging is needed. There are 2 main components, P50 and N95, with most subjects showing an earlier negative component, N35. N95 arises in the retinal ganglion cells (RGCs) and thus acts as a direct measure of central RGC function. The electro-oculogram (EOG) assesses the health of the RPE by measuring the changes in the corneo-retinal standing potential during light adaptation. The multifocal electroretinogram (mfERG) can be of use in the diagnosis of macular dysfunction and in assessing the extent of central retinal involvement in generalized retinal disease by producing a topographic electroretinogram (ERG) map of central retinal cone-system function. The visual evoked potential (VEP), or visual evoked response (VER), is a measurement of the electrical signals produced in the brain in response to light stimulus, recorded at the scalp over the occipital cortex; it is a measure of the integrity of the afferent visual pathway.
5. **b.** A stage 2 macular hole is a full-thickness defect measuring less than 400 µm in diameter, without a visible operculum, and a persistent posterior hyaloid attachment at the optic nerve head. Although approximately 50% of stage 1 macular holes close spontaneously, pars plana vitrectomy with gas tamponade is recommended for stage 2 or greater macular holes and has a success rate of approximately 90% or greater for a recent-onset hole.

6. **a.** The Pelli-Robson test measures contrast sensitivity using a single, large letter size (20/60 optotype), with contrast varying across groups of letters. Patients read the letters, starting with the highest contrast and continue until they are unable to read 2 or 3 letters in a single group. The subject is assigned a score based on the contrast of the last group in which 2 or 3 letters were correctly read. The Pelli-Robson score is a logarithmic measure of the subject's contrast sensitivity. The anomaloscope, Farnsworth-Munsell 100-hue test, and Ishihara plates are all used to evaluate color vision, not contrast sensitivity.
7. **a.** The mfERG is useful in the diagnosis of macular dysfunction and in assessing the extent of central retinal involvement in generalized retinal disease by producing a topographic ERG map of the central retinal cone-system function. The stimulus consists of multiple hexagons, smaller in the center than the periphery, to reflect cone photoreceptor density, each of which flashes with a pseudorandom sequence. Cross-correlation techniques are used to calculate the small ERGs corresponding to each hexagon. Overall stimulus field size is approximately 50°. The EOG assesses the health of the RPE by measuring the changes in the corneo-retinal standing during light adaptation. The VEP, or VER, is a measurement of the electrical signal in the brain in response to light stimulus, recorded at the scalp over the occipital cortex; it is a measure of the integrity of the afferent visual pathway. The PERG is a measure of central RGC function and is a less-direct objective index of macular function than the mfERG.
8. **c.** Verteporfin is a photosensitizing drug that is locally activated by laser during photodynamic therapy (PDT). PDT is approved by the US Food and Drug Administration (FDA) for use in the treatment of subfoveal choroidal neovascularizations (CNVs) associated with AMD, myopia, and presumed ocular histoplasmosis syndrome (POHS). The use of PDT for managing CNV has declined dramatically, given the better success of anti-VEGF agents, but it remains an adjunctive therapy for CNV in some scenarios. PDT is used off-label to treat CSC and circumscribed choroidal hemangiomas.
9. **a.** A genome-wide association study of 43,000 people has identified 52 common and rare genetic variants located on 34 loci associated with AMD. The 2 major susceptibility genes for AMD are *CFH* (1q31), which codes for complement factor H, and *ARMS2* (10q26), for which the gene product and function are poorly understood. The *CFH* Y402H mutation confers a 4.6-fold increased risk for AMD when heterozygous and a 7.4-fold increased risk when homozygous. The *ARMS2* A69S mutation confers a 2.7-fold increased risk for AMD when heterozygous and an 8.2-fold increased risk when homozygous. When both of these genes are homozygous for the aforementioned mutations in an individual, the risk for AMD is increased to 50-fold. Although mutations involving *CFI* and *APOE* have been associated with AMD, they are not the 2 major susceptibility genes.
10. **b.** In the AREDS (Age-Related Eye Disease Study), nutritional supplementation with the antioxidant vitamins C (500 mg) and E (400 IU), beta carotene (15 mg), and the micro-nutrient zinc (80 mg zinc oxide and 2 mg cupric oxide to prevent zinc-induced anemia) in patients with intermediate or advanced AMD showed a 25% risk reduction for progression to more-advanced stages of AMD and a 19% risk reduction in rates of moderate vision loss (≥ 3 lines of visual acuity) at 5 years. In the AREDS 2 Study, replacing beta carotene with lutein and zeaxanthin yielded very similar results.
11. **c.** In branch retinal vein occlusion (BRVO), obstruction of the vein occurs most commonly at an arteriovenous crossing, where thickening of the arterial wall compresses the adjacent vein within a common adventitial sheath. When the occlusion does not occur

at an arteriovenous crossing, the possibility of an underlying retinochoroiditis or retinal vasculitis should be considered. Hypertension and glaucoma are risk factors for BRVO but not implicated in occlusion at sites other than arteriovenous crossings. An embolus may cause a retinal artery occlusion but not a retinal vein occlusion.

12. **a.** The patient has a central retinal vein occlusion (CRVO). When CRVO occurs in patients more than 50 years of age with typical risk factors, it is generally considered unnecessary to pursue an elaborate systemic workup. However, in patients younger than 50 years and in absence of common risk factors, workup for hypercoagulable conditions should be considered. Infectious etiologies are unlikely to cause a CRVO. Giant cell arteritis is uncommon at a young age and primarily affects arteries. Risk factor evaluation for thromboembolic disease would be relevant in a patient with a retinal artery occlusion.
13. **c.** Branch retinal artery occlusions are considered embolic events. Retinal arterial emboli have been associated with an increased risk of cardiovascular mortality; therefore, emergent referral for embolic workup that includes brain imaging, evaluation of carotid arteries, and transesophageal echocardiography should be considered. Checking erythrocyte sedimentation rate (ESR), C-reactive protein (CRP), and platelets would be relevant if giant cell arteritis is suspected, but that would be less likely with a branch retinal artery occlusion. Lowering intraocular pressure (IOP) and applying intermittent pressure on the globe (“ocular massage”) have been suggested but have not been found to be consistently effective in improving the patient’s visual prognosis.
14. **a.** The patient’s presentation is consistent with ocular ischemic syndrome (OIS), which is most commonly due to carotid occlusive disease. Proliferative diabetic retinopathy, retinal vein occlusion, and radiation retinopathy can all cause retinal hemorrhages and iris neovascularization, but the retinal artery pressure is normal in all of those conditions. An eye with carotid occlusive disease will have low artery pressure, and the artery will therefore collapse easily with pressure on the globe. Symptoms of delayed dark adaptation and aching pain present for months with a normal IOP are also more consistent with OIS and would be less likely in the other conditions.
15. **c.** Proliferative sickle cell retinopathy occurs most commonly with sickle cell hemoglobin C (SC), at a rate of approximately 33%. It occurs less commonly with sickle cell thalassemia (SThal), at a rate of approximately 14%. Sick cell homozygote (SS) disease results in more systemic complications but has a very low incidence of proliferative retinopathy, approximately 3%. Proliferative retinopathy is rare with sickle cell trait (AS).
16. **a.** FA imaging of an eye with central serous chorioretinopathy (CSC) may show fluorescein leakage in a pattern that resembles a smokestack. This pattern of fluorescein leakage is unique to CSC. Irregular window defects from RPE abnormalities are commonly seen, but similar appearing changes can occur from other conditions, such as AMD. In some cases, the FA appears normal. Multifocal hyperfluorescence is not seen commonly in eyes with CSC. Lacy hyperfluorescence may be seen in rare instances, if the CSC is complicated by a choroidal neovascular membrane.
17. **a.** Retinal tears and subsequent rhegmatogenous retinal detachment can occur after peripheral laser photocoagulation to treat proliferative sickle cell retinopathy. Retinal tears occur more commonly after laser treatment in proliferative sickle cell retinopathy than in other proliferative retinopathies. Reduced peripheral vision, choroidal detachments, and vitreous hemorrhage may occur after laser photocoagulation but do not have a specific predilection for sickle cell retinopathy.

18. **b.** Von Hippel–Lindau syndrome is caused by a tumor suppressor gene mutation on the short arm of chromosome 3 (3p26–p25), the inheritance of which is autosomal dominant with incomplete penetrance and variable expression.
19. **c.** Retinal cavernous hemangiomas may bleed into the vitreous in rare instances. Treatment of retinal cavernous hemangiomas is indicated in cases with recurrent vitreous hemorrhage. Laser photocoagulation or cryotherapy may be used. Lipid exudation and retinal neovascularization do not typically occur from retinal cavernous hemangiomas. The lesions are static, so progressive enlargement is not expected or seen.
20. **c.** Screening should be done on all infants with a birth weight of less than 1500 g or a gestational age of 30 weeks or less. The first examination should generally be performed between 4 and 6 weeks of postnatal age or, alternatively, between 31 and 33 weeks' postconceptional or postmenstrual age, whichever is later. In this case the infant is born at 29 weeks, hence the first examination should be done 4 to 6 weeks after birth.
21. **b.** The findings are most consistent with acute zonal occult outer retinopathy (AZOOR). This idiopathic condition typically affects young women with myopia. The acute onset of posterior photopsias is common to many posterior inflammatory conditions, including multiple evanescent white dot syndrome (MEWDS) and multifocal choroiditis; however, the early disruption of outer retina on optical coherence tomography (OCT) differentiates AZOOR from both MEWDS or multifocal choroiditis. Acute macular neuroretinopathy is characterized by 1 or multiple brick-colored wedge-shaped or slightly elevated lesions adjacent to or near the fovea, as well as transitory reduction of the visual acuity in affected eyes. Intermediate uveitis is characterized by anterior vitreous cells. Further, MEWDS is characterized by multiple small gray, white, or yellow-white dots at the level of the outer retina and typically presents unilaterally.
22. **a.** The follow-up interval for retinopathy of prematurity (ROP) screening is determined based on the disease features; more severe disease indicates a need for shorter follow-up intervals. A premature infant with immature vascularization in zone I should be reevaluated in 1 week or less, even in the absence of ROP.
23. **d.** The patient in this clinical scenario has diffuse unilateral subacute neuroretinitis (DUSN), in the chronic stage. Vitreous cells are commonly observed in retinitis pigmentosa; this condition mimics retinitis pigmentosa (which can be caused by a P23H mutation). Retinitis pigmentosa (RP) is almost always bilateral, usually symmetric, and follows a course of chronic deterioration. Viral and fungal infections of the retina and choroid result in active retinitis or chorioretinitis, as well as later chorioretinal changes or scarring that is usually patchy and not as extensive as those seen in DUSN.
24. **a.** Ablation treatment of threshold or prethreshold type 1 ROP should be accomplished whenever possible with laser surgery rather than cryoablation surgery, because laser photocoagulation is associated with less treatment-related morbidity. Anti-vascular endothelial growth factor (anti-VEGF) monotherapy may have similar outcomes to laser treatment for zone II disease; however, at this time further studies are needed to sufficiently assess the long-term safety of using anti-VEGF drugs to treat ROP.
25. **a.** The patient almost certainly has CSC. In most cases, initial observation, with the expectation of spontaneous resolution of the subretinal fluid, is the appropriate management. Focal argon laser or photodynamic therapy can be considered for the treatment of CSC if the patient is symptomatic or if the subretinal fluid does not resolve after a period of observation. Steroids are contraindicated in a patient with CSC.

26. **a.** Acute posterior multifocal placoid pigment epitheliopathy (APMPPE) is an uncommon, usually bilateral inflammatory disorder characterized by acute onset visual loss, usually followed weeks to months later by substantial or near-complete improvement. On FA, APMPPE (also known as AMPPE or AMPPPE) in the acute phase demonstrates a characteristic fundus pattern of early lesion blockage, followed by lesion staining in the middle and late phases. No treatment has been demonstrated to affect the time or final outcome of recovery. Birdshot uveitis is characterized by insidious onset and chronic progression. Multifocal choroiditis is often asymptomatic unless complicated by acute visual deterioration from CNV involving the central macula. Vision recovery, if it occurs, is typically slow and incomplete following intervention. Serpiginous chorioretinopathy is typically relentlessly progressive, and destroys the RPE on photoreceptors. Thus, recovery of vision, even following immunosuppression, is atypical.
27. **c.** Individuals with achromatopsia (rod monochromatism and S-cone monochromatism) and albinism (ocular and oculocutaneous) share the features of photophobia, decreased visual acuity, and nystagmus. The absence of iris transillumination would eliminate either type of albinism but would not indicate which type of achromatopsia was present. Similarly, although all 4 conditions have a genetic basis, the presence of an affected brother would not indicate whether inheritance is autosomal recessive, as in rod monochromatism and oculocutaneous albinism, or X-linked, as in S-cone monochromatism and ocular albinism. Red-green color deficits such as deuteranomaly are common, are not accompanied by the additional findings above, and are most often X-linked. Because ERG testing can be used to assess cone function (including whether any S-cone function remains), it can thus help the clinician establish a diagnosis in this scenario.
28. **a.** Immune system sensitization to choroidal antigens is much less likely if the inciting tissues are removed within 14 days of exposure. Therefore, prevention of sympathetic ophthalmia is the primary reason for the early enucleation. Enucleation should be contemplated within 2 weeks following visually nonrecoverable penetrating ocular injury. Chronic pain may result from penetrating injury, but its management with enucleation is not time-dependent. Similarly, bacterial endophthalmitis and/or lens-associated uveitis can be managed medically or by enucleation, and if surgical removal is necessary, it can be performed when required for medical management or cosmesis.
29. **d.** A negative ERG describes a bright-flash, dark-adapted ERG with a normal or near-normal a-wave but a b-wave with markedly decreased amplitude. This pattern can be associated with some forms of congenital stationary night blindness (CSNB), as well as with melanoma-associated retinopathy (MAR), which may be accompanied by acquired nyctalopia. The electronegative ERG is also a feature of juvenile X-linked retinitis pigmentosa and central retinal artery occlusions. Unlike retinitis pigmentosa, in which the ERG a-wave is also abnormal and progressive visual field loss occurs, CSNB is nonprogressive. CSNB is a hereditary and most-often X-linked condition in which individuals may have variable degrees of nystagmus and decreased visual acuity. Some individuals with CSNB have a paradoxical pupillary response in which the pupil constricts in response to decreased light.
30. **b.** Pleiotropy is the term for mutations in a single gene that may lead to multiple phenotypes. An excellent example of this is the *ABCA4* gene, which has differing phenotypes for different mutations within the gene. The most common phenotype caused by mutation of *ABCA4* is Stargardt disease (autosomal recessive, requires both alleles to harbor disease-causing mutations), but other mutations may cause pattern dystrophy, cone–rod dystrophy, or autosomal-recessive retinitis pigmentosa. Genetic heterogeneity is the term

that describes multiple genes that give rise to an indistinguishable phenotype. For instance, mutations in at least 17 different genes may lead to Leber congenital amaurosis (LCA). Disorders caused by a mutation in a single allele arise from dominant inheritance. If mutations in both alleles are necessary to cause disease, then the inheritance is recessive.

31. **d.** When early-onset drusen are associated with CNV in young adulthood, the diagnosis of Sorsby macular dystrophy should be considered. The diagnosis can be confirmed by demonstrating a disease-causing mutation in the *TIMP3* gene. Doyne honeycomb dystrophy, Malattia Leventinese, and radial drusen are the same disorder, and are caused by mutation in the *EFEMP1* gene. Cuticular drusen is a clinical syndrome of small clustered drusen in young adults. Although associated with mutation in complement factor H, in contrast to the other choices, cuticular drusen is not a monogenic disorder.
32. **c.** The clinical description is most consistent with Bietti crystalline dystrophy, which is associated with mutations in the *CYP4Y2* gene. Oxalosis is a rare inherited disorder of primary hyperoxaluria, which has been associated with mutations in 3 genes (*AGXT*, *GRHPR*, *DHDPSL*). Cystinosis is an abnormality of cystine accumulation that may result from genetic causes (mutation in the *CTNS* gene) or exposure to some anesthetics. Typically, patients with oxalosis and cystinosis have renal insufficiency or failure resulting from amino acid crystallization in the kidneys. Tamoxifen retinopathy is a perifoveal crystalline retinopathy resulting from retinal toxicity to tamoxifen, an antiestrogen drug used as adjuvant treatment for estrogen-responsive breast cancer.
33. **a.** All of the answer options are systemic metabolic disorders with associated retinal degenerations. In abetalipoproteinemia, the failure to synthesize apolipoprotein B results in abnormal absorption of fat and fat-soluble vitamins, leading to problems including retinal and spinocerebellar degeneration. Treatment with vitamins A and E is advised. Refsum disease results from elevated plasma levels of phytanic acid, for which dietary restriction of phytanic acid precursors such as dairy products and some meats is advised. Zellweger syndrome is a peroxisomal disease resulting from defective oxidation and accumulation of very-long-chain fatty acids. Neuronal ceroid lipofuscinosis (NCL) results from the lysosomal accumulation of lipopigments, and some forms may first present with visual symptoms. No interventions are currently available for NCL or Zellweger syndrome.
34. **a.** Ciliopathies are diseases or syndromes in which a mutation in a gene needed for ciliary function affects multiple organ systems. Usher syndrome is a ciliopathy defined by the association of retinitis pigmentosa with congenital sensorineural hearing loss. In contrast, maternally inherited diabetes and deafness is a mitochondrial disease. Bardet-Biedl syndrome is a ciliopathy with findings that include pigmentary retinopathy and bull's-eye maculopathy, obesity, polydactyly, hypogonadism, renal disease, and cognitive disability. Joubert syndrome is a ciliopathy characterized by cerebellar malformation ("molar tooth" sign) and hypotonia, with additional features that include retinal dystrophy and renal disease.
35. **d.** Batten disease, which is an example of a neuronal ceroid lipofuscinosis, can have retinal findings including an atrophic bull's-eye maculopathy, optic nerve pallor, and attenuation of retinal vessels. The ophthalmic symptoms and signs may be the first, earliest manifestations of this disorder. Pigmentary abnormalities and fine retinal crystals are present in cystinosis. The cherry-red spots seen in Tay-Sachs result from ganglioside accumulation within ganglion cells. Tortuous and dilated retinal vessels, as well as corneal verticillata and tortuous conjunctival vessels, are present in Fabry disease.

36. **d.** Nicotinic acid, a treatment for elevated cholesterol and triglycerides, in rare cases characteristically causes a cystoid macular edema that demonstrates no leakage or staining on fundus fluorescein angiography. Fingolimod, a drug used to treat multiple sclerosis, can cause conventional cystoid macular edema with typical late leakage in a “petaloid,” or flower-shaped, pattern. Similarly, rosiglitazone, a newer oral hypoglycemic agent, may cause conventional cystoid macular edema that may be confused with diabetic macular edema. Paclitaxel, a chemotherapeutic agent, may also cause a reversible, angiographically silent cystoid macular edema, but this is rare.
37. **a.** “Poppers” is a slang term for alkyl nitrites, which are a class of chemicals used as recreational drugs. The chemicals are inhaled to induce euphoria and relax smooth muscles, usually in preparation for sexual activity. In rare cases, use can lead to acute central scotoma and vision reduction associated with a yellow, “vitelliform”-like macular lesion. In rare cases, MEK inhibitors, which are a class of chemotherapeutic agents, and sildenafil have been associated with serous macular fluid, which may simulate central serous choroidopathy. Corticosteroids may precipitate serous exudation from central serous retinopathy.
38. **b.** Round holes rarely lead to retinal detachment, but may complicate repair if the retina is detached due to other, higher-risk breaks. Retinal dialyses, horseshoe or flap tears, and slit tears at the edge of lattice degeneration are higher-risk tears and are typically treated with demarcation laser, even if asymptomatic.
39. **b.** Many, if not most, tractional retinal detachments begin distant from the fovea and are typically asymptomatic unless they have recently converted to a combined rhegmatogenous-tractional retinal detachment. Similarly, retinoschisis is usually asymptomatic, but if an outer layer break develops and causes an associated rhegmatogenous component, the detachment becomes symptomatic. Exudative retinal detachments (in particular, macular detachments associated with CNV) and rhegmatogenous retinal detachments are usually symptomatic.
40. **c.** Vitreous opacities can be one of the initial signs of familial amyloidosis. Amyloid material can also be deposited elsewhere in ocular structures, and early nonocular complaints may include peripheral neuropathies. Congo red staining of vitreous samples can confirm the diagnosis. Asteroid hyalosis is typically unilateral and is rarely visually significant. Cholesterolosis, or synchysis scintillans, occurs in eyes with a history of intravitreal hemorrhage usually related to prior accidental or surgical ocular trauma. Although prior ophthalmic pathology leading to dehemoglobinized vitreous hemorrhage should always be considered, it is less likely in this scenario.
41. **a.** Anterior persistent fetal vasculature is characterized by a retrolental fibrovascular membrane. Angle-closure glaucoma can result from the lenticular abnormalities associated with this membrane, and incomplete development of the angle can also contribute to glaucoma. Posterior persistent fetal vasculature does not involve the anterior segment structures, and therefore is not associated with angle-closure glaucoma. Open-angle glaucoma can be present in Stickler syndrome. Remnants of the tunica vasculosa lentis, including Mittendorf dots, are common and visually insignificant.
42. **d.** The chalcosis and siderosis bulbi that result from retaining intraocular copper and iron, respectively, have distinct manifestations. Pure copper can cause an intense inflammatory response, whereas a copper content of less than 85% can result in chronic chalcosis, with findings that include sunflower cataract and a Kayser-Fleischer-like ring of deposits in Descemet membrane. Intraocular iron deposits in neuroepithelial tissues produce

- findings that include retinal pigmentation. ERG can be used to assess retinal toxicity in siderosis bulbi.
43. c. A complex interplay of all of these factors influences the visual prognosis after globe trauma, but as a general guide and as represented by The Ocular Trauma Score, initial visual acuity is the most important predictor of final visual outcome.
44. a. The goal of subthreshold laser is to achieve the therapeutic benefits of laser while minimizing secondary retinal damage. The micropulse doses limit heat conduction from the RPE to photoreceptors and thus minimize neuroretinal damage and the size and number of scotomas. Computer software is critical in planning and applying treatment, because the laser spots cannot be directly visualized.
45. c. The clinical history is characteristic of *Propionibacterium acnes* endophthalmitis. Although injection of intravitreous antibiotics may clear the infection in up to 50% of cases, an appropriate management is pars plana vitrectomy (PPV) with partial capsulectomy and antibiotic injection. Occasionally, removal of the intraocular lens and the entire capsular bag is required to definitively treat the condition. Sampling the anterior chamber, especially the vitreous, is the usual approach for identification of the causative microbe, not for management of the condition. However, because *P acnes* is an obligate microaerophilic bacterium, it may not survive in a culture unless that culture is maintained in a low-oxygen environment. Thus, the culture positivity rate is low. Topical antibiotics and steroids will treat the symptoms, but will not eradicate the infection.
46. a. Axial high myopia is a risk factor for ocular perforation with a retrobulbar injection. It is a relative, not an absolute, contraindication. Older age is not a contraindication to retrobulbar anesthesia injection. Use of continuous positive airway pressure (CPAP) is a relative contraindication to general anesthesia, not retrobulbar anesthesia, because laryngeal swelling following intubation may necessitate hospitalization for postanesthesia observation. Because obesity may make endotracheal intubation more difficult, the use of retrobulbar anesthesia would be favored.
47. c. Proliferative vitreoretinopathy is defined as membrane proliferation associated with retinal detachment. This condition necessarily results in retinal traction (especially grade C or higher) that requires vitrectomy to achieve retinal reattachment. Multiple retinal tears and retinal dialysis (especially without an associated retinal detachment) are typically treated with laser or cryopexy demarcation. Vitreous hemorrhage that spares the visual axis may only require observation or treatment of the underlying condition (such as proliferative diabetic retinopathy), depending upon the setting and any associated disorders.
48. a. Vitritis, or inflammation of the vitreous, is the first presenting feature of injection-related endophthalmitis. It is perceived by patients as progressive floaters and blurring of vision, often culminating in essentially no formed vision (eg, light perception only). Immediate evaluation is necessary to determine whether endophthalmitis is present. Sharp pain following the injection or foreign body sensation are likely caused by surface irritation or damage from the povidone iodine solution, the manipulation of the conjunctiva, or from the needle stick. Occasionally, patients may suffer severe pain that starts some time following the injection, which may be caused by corneal abrasions. Small floaters that are noticed immediately following injection are usually caused by small air bubbles, and less commonly by silicone oil bubbles from the syringe lubricant, in the injected liquid, a common occurrence. Air bubbles usually disappear after a few hours, while the silicone oil bubbles persist, but usually float out of view.

Index

(*f*=figure; *t*=table)

- ABCA4* gene
retinopathy caused by, 31
Stargardt disease caused by, 271
- ABCC6* gene, 87
- Abetalipoproteinemia, 289–290
- Absolute scotomas, 327
- Abusive head trauma, 365–366, 366*f*
- ACCORD trial, 98
- Acetazolamide, 305, 393
- Achromatopsia, 250, 250*t*
- Acquired vasoproliferative lesions, 168
- Acute exudative polymorphous vitelliform maculopathy, 287
- Acute idiopathic maculopathy (AIM), 228–229
- Acute macular neuroretinopathy (AMN), 228, 229*f*, 277
- Acute posterior multifocal placoid pigment epitheliopathy (APMPPE), 220*t*, 221*f*, 221–222
- Acute retinal necrosis (ARN), 236, 236*f*
- Acute syphilitic posterior placoid chorioretinitis (ASPPC), 241
- Acute zonal occult outer retinopathy (AZOOR)
description of, 226–228, 227*f*
electro-oculography of, 51
- Acyclovir
acute retinal necrosis treated with, 236
herpetic retinitis treated with, 238*t*
progressive outer retinal necrosis syndrome treated with, 236
- Adaptation
dark
in electro-oculography, 50
in full-field (Ganzfeld) electroretinography, 42
- light
in electro-oculography, 50
in full-field (Ganzfeld) electroretinography, 42
- Adaptive optics imaging, 33
- Adaptive optics scanning laser ophthalmoscope, of macula, 13*f*
- Adult-onset foveomacular vitelliform dystrophy, 272, 276
- Adult-onset vitelliform lesions, 272, 273*f*
- Adult-onset vitelliform maculopathy
fluorescein angiography of, 68
spectral-domain optical coherence tomography of, 67–68, 68*f*
- A2E, 31
- Aedes aegypti* mosquito, 247
- Afferent pupillary defect, 352
- Aflibercept
branch retinal vein occlusion treated with, 135
central retinal vein occlusion treated with, 135
diabetic macular edema treated with, 113
macular telangiectasia type 1 treated with, 161
neovascular age-related macular degeneration treated with, 82–83
retinal vein occlusion treated with, 135
- African Americans. *See also* Race
sickle cell hemoglobinopathies and, 149, 154
systemic lupus erythematosus in, 230
- Age
central retinal vein occlusion and, 133
central serous chorioretinopathy and, 189
choroidal thickness affected by, 19, 212
posterior vitreous detachment associated with, 307–308
- Age-Related Eye Disease Study (AREDS), 64, 69–71, 70*t*
- Age-related macular degeneration (AMD)
adult-onset foveomacular vitelliform dystrophy versus, 272, 273*f*
aging as cause of, 61
blindness caused by, 61
Bruch membrane calcification in, 19
cataract surgery effects on, 71
central blindness progression of, 86
central serous chorioretinopathy versus, 67, 76, 79
choroidal neovascularization progression of, 64
cigarette smoking and, 62
exudative, 79
genetics of, 62–63
genetic testing for, 63
low vision therapies and rehabilitation, 86
management of, 68–71, 79–86, 81*f*, 82*t*, 84*t*
neovascular (“wet”)
aflibercept for, 82–83
Amsler grid testing of, 71
antiangiogenic therapies for, 79–80
bevacizumab for, 83–85, 84*t*
choroidal neovascularization associated with, 71–79. *See also* Choroidal neovascularization
combination treatment for, 85
differential diagnosis of, 76, 79
intravitreal injections, 85
laser photocoagulation for, 79
low vision therapies for, 86
macular translocation surgery for, 85
management of, 79–86, 81*f*, 82*t*, 84*t*
pegaptanib for, 80
photodynamic therapy for, 79
polypoidal choroidal vasculopathy, 75
prevalence of, 61
ranibizumab for, 80–82, 82*t*
signs and symptoms of, 71
submacular hemorrhage in, 85, 385
surgical treatment for, 85–86
treatment effect modifiers, 85
verteporfin for, 79
nonneovascular (“dry”)
Amsler grid testing for, 68–69
differential diagnosis of, 67–68
disproven treatment approaches for, 71
drusen associated with. *See* Drusen
education regarding, 68
focal atrophy in, 66
follow-up for, 68

- geographic atrophy in, 64, 66, 67f, 68
 hydrochloroquine toxicity versus, 68
 hyperacuity testing for, 69
 lifestyle changes for, 71
 management of, 68–71
 micronutrients for, 69–71
 preferential hyperacuity perimetry for, 69
 prevalence of, 61
 retinal pigment epithelium abnormalities in, 66–67
 shape-discrimination hyperacuity for, 69
 nonsubfoveal, 69
 pharmacogenomic testing for, 63
 prevalence of, 61
 race and, 62
 risk factors for, 62, 70t
 susceptibility genes for, 63
- Aggressive posterior retinopathy of prematurity, 177, 178t
- AIDS. *See also* HIV
Cytomegalovirus retinitis associated with, 235–236
progressive outer retinal necrosis syndrome associated with, 236–237, 237f
- AIM. *See* Acute idiopathic maculopathy
- Alagille syndrome, 282t, 285
- Albinism, 288
- Albinoidism, 288
- Alkyl nitrates, 300, 300f
- Alphavirus*, 247
- Alström syndrome, 285
- Aluminum, in intraocular foreign body, 362
- Amacrine cells
 description of, 15
 illustration of, 15f
- Amalric triangles, 198
- AMD. *See* Age-related macular degeneration
- Amelogenesis imperfecta, 286
- Amikacin, 300
- Amino acid disorders, 293
- Aminoglycosides, 300
- AMN. *See* Acute macular neuroretinopathy
- Amphotericin B, for fungal endophthalmitis, 239
- Amsler grid testing, in age-related macular degeneration, 68–69, 71
- Amyloidosis, 348, 349f
- ANCHOR study, 80–81
- Ancylostoma caninum*, 246
- Anemia, diabetic retinopathy and, 98
- Anesthesia
 for intravitreal injections, 403
 for photocoagulation, 375
- Aneurysmal telangiectasia, 161
- Aneurysms, retinal arterial, 147–148, 148f
- Angiogenesis
 activators of, 80
 definition of, 79
 endothelial cells in, 79
 inhibitors of, 80
- Angiography
 dye injection in, 24
fluorescein. See Fluorescein angiography (FA)
indocyanine green. See Indocyanine green angiography (IGA)
- optical coherence tomographic artifacts in, 29, 30f
 choroidal circulation abnormalities, 198
 choroidal neovascularization on, 75–76, 76–78f, 192
 depth resolution using, 29
 diabetic retinopathy on, 93, 94f
 fluorescein angiography versus, 29
 macular telangiectasia type 2 on, 163, 164f
 motion artifacts in, 29
 projection artifacts in, 29, 30f
pseudoxanthoma elasticum on, 199f
 retinal capillary layers on, 16
 retinal disease evaluations using, 28–29
 retinal vasculature on, 29, 30f
 severity of, 93, 94f
 scanning laser ophthalmoscopy versus, 24
- Angiod streaks
 choroidal neovascularization caused by, 87–89, 89f
 definition of, 87
 description of, 19
 fluorescein angiography of, 87, 89f
pseudoxanthoma elasticum and, 87, 89f
 safety glasses for patients with, 88
 in sickle cell disease, 154
 visual disturbances caused by, 88
- Angiokeratoma corporis diffusum. *See* Fabry disease
- Angiomas, retinal, 168
- Angle-closure glaucoma, in retinopathy of prematurity, 181. *See also* Glaucoma
- Annular gap, 7
- Anomaloscope, 54
- Anomalous trichromatism, 249
- Anterior capsular phimosis, 116
- Anterior chamber
 paracentesis of, for central retinal artery occlusion, 146
 ultrasound biomicroscopy of, 40
- Anterior chamber angle neovascularization, in diabetes mellitus, 107
- Anterior cortical gel, 7
- Anterior hyaloid, 8f
- Anterior persistent fetal vasculature, 341–342
- Anterior segment
 blunt trauma to, 353
 neovascularization in, in central retinal vein occlusion, 125
 surgery of
cystoid macular edema after, 393, 394f
endophthalmitis after. See Endophthalmitis, postoperative
posteriorly dislocated intraocular lenses after, 393
suprachoroidal hemorrhage after, 394–395, 395f
vitrectomy for posterior segment complications of, 388–396
- Anterior vitreous, patellar fossa of, 7
- Antiangiogenic therapies
 complications of, 85
 neovascular age-related macular degeneration treated with, 79–80
- Antibiotics, for toxoplasmic retinochoroiditis, 243
- Anticoagulants, 346
- Antioxidants, for age-related macular degeneration, 69

- Anti-VEGF therapy
 adverse effects of, 113
 bevacizumab, 83–85, 84*f*
 central retinal artery occlusion treated with, 146
 choroidal neovascularization treated with, 87–88, 212, 355
 clinical trials of, 81
 Coats disease treated with, 161
 complications of, 104
 diabetic macular edema treated with, 101, 110–113, 112*f*
 diabetic retinopathy treated with
 description of, 101–102
 nonproliferative, 101–102
 proliferative, 103–104, 386
 follow-up after, 134
 intravitreal injections, 404
 low vision and, 86
 myopic choroidal neovascularization treated with, 212
 neovascular age-related macular degeneration treated with, 80–81
 nonproliferative diabetic retinopathy treated with, 101–102
 pathologic myopia treated with, 89
 polypoidal choroidal vasculopathy treated with, 76
 proliferative diabetic retinopathy treated with, 103–104
 radiation retinopathy treated with, 171
 retinal arterial macroaneurysms treated with, 148
 retinal vein occlusion treated with, 126
 retinopathy of prematurity treated with, 186–187
 subretinal neovascularization treated with, 164
- Antiviral therapy
 acute retinal necrosis treated with, 236
 progressive outer retinal necrosis syndrome treated with, 236
- APC gene, 286
- Aphakia, retinal detachment risks, 319
- APMPPE. *See* Acute posterior multifocal placoid pigment epitheliopathy
- Appositional suprachoroidal hemorrhage, 394–395
- ARB. *See* Autosomal recessive bestrophinopathy
- Arden index/ratio, 50
- Area centralis, 9, 9*f*
- Area of Martegiani, 7, 8*f*, 307
- AREDS. *See* Age-Related Eye Disease Study
- Argus II Retinal Prosthesis System, 264
- Argyria, 306
- Argyrosis, ocular, 306
- ARMS2 gene, 63
- ARN. *See* Acute retinal necrosis
- Arrestin, 253
- Arterial macroaneurysms, retinal, 147–148, 148*f*
- Arteriohepatic dysplasia, 282*t*
- Arteriosclerotic retinopathy, 122
- Arthro-ophthalmopathy, 282*t*
- Artifacts
 in optical coherence tomography angiography, 29, 30*f*
 projection, 29, 30*f*
- Ascorbate, vitreous levels of, 9
- Aspergillus fungal endophthalmitis, 239
- Aspirin, diabetic retinopathy and, 100
- ASPPC. *See* Acute syphilitic posterior placoid chorioretinitis
- Asteroid hyalosis, 346*f*, 346–347
- Asymptomatic retinal breaks, 318
- ATOH7 gene, 341
- Atrophic retinal holes
 definition of, 315
 lattice degeneration with, 310, 311*f*, 316*f*
 retinal detachment secondary to, 310
- Atrophy
 chorioretinal
 genes and loci associated with, 256*t*
 in pathologic myopia, 214*f*
 choroid, age-related, 200, 212
 geographic
 in Best vitelliform dystrophy, 271
 description of, 64, 66, 67*f*, 68
 in drusenoid retinal pigment epithelium detachment, 272
 gyrate, 268–269, 269*f*
 macula, 265, 265*f*
 retinal pigment epithelium, 106*f*, 294*f*
- Atrophy creep, 89
- Autofluorescence
 central serous chorioretinopathy findings, 192*f*
 enhanced depth imaging optical coherence tomography and, 39
 fluorescein angiography, 35
 retinitis pigmentosa findings, 261
 serpiginous choroidopathy findings, 223*f*
- Autoimmune retinopathy, 286
- Autosomal recessive bestrophinopathy (ARB)
 description of, 271
 electro-oculography of, 51
 a-waves
 electroretinography, 46, 251
 in rod-cone dystrophies, 261
- Axial resolution, of contact B-scan ultrasonography, 39
- Azathioprine, for Behçet disease, 230
- AZOOR. *See* Acute zonal occult outer retinopathy
- Bacillus cereus endophthalmitis, 363
- Bacterial endophthalmitis, endogenous, 237–239, 238*f*
- Bardet-Biedl syndrome
 clinical features of, 282*t*
 genes and loci associated with, 256*t*
 renal abnormalities associated with, 285
 retinal degeneration associated with, 281, 284, 284*f*
- Bartonella henselae, 243*f*
- Basilar laminar deposits
 age-related changes in, 61
 definition of, 64
 illustration of, 62*f*
- Basilar linear deposits
 definition of, 64
 illustration of, 62*f*
- Batten disease, 283*t*, 290*f*
- Baylisascaris procyonis, 246
- BDUMP. *See* Bilateral diffuse uveal melanocytic proliferation
- BEAT-ROP Cooperative Group study, 186–187
- Behçet disease, 230, 230*t*
- Berger space, 7, 8*f*
- Bergmeister papilla, 341

- Best disease
 characteristics of, 271, 272*f*
 definition of, 51
 electro-oculography of, 51, 271
- BEST1* gene, 271
- Bestrophin, 50
- Best vitelliform dystrophy, 271, 272*f*
- Bevacizumab
 adverse effects of, 85
 branch retinal vein occlusion treated with, 135
 central retinal vein occlusion treated with, 135
 choroidal neovascularization treated with, 73*f*, 213*f*
 diabetic macular edema treated with, 113
 endophthalmitis caused by, 404
 neovascular age-related macular degeneration treated with, 83–85, 84*t*
 off-label uses of, 85
 ranibizumab and, comparison between, 83, 84*t*
 retinal vein occlusion treated with, 135
 retinopathy of prematurity treated with, 186–187
- Bietti crystalline dystrophy, 258, 269, 282*t*
- Bilateral diffuse uveal melanocytic proliferation (BDUMP), 204–205, 205*f*, 287
- Binocular indirect ophthalmoscopes/ophthalmoscopy
 disadvantages of, 22
 retinal disease evaluations using, 21–22
- Bipolar cells
 ganglion cells and, 13
 illustration of, 15*f*
 midget, 13
- Birdshot chorioretinopathy, 49
- Birdshot uveitis
 characteristics of, 220*t*, 224–225, 225*f*
 uveal lymphoma and, 234
- Bis-retinoids, 31
- Bleb-associated endophthalmitis, 390–391, 391*f*
- Blebitis, 390–391
- Blind loop syndrome, 290
- Blindness
 central, age-related macular degeneration progression to, 86
 methanol toxicity as cause of, 301
 night. *See* Night blindness
 retinopathy of prematurity as cause of, 182
- Bloch-Sulzberger syndrome, 283*t*, 286
- Blocked fluorescence, in fluorescein angiography, 35
- Blood-brain barrier, 16
- Blood-ocular barrier, fluorescein passage affected by, 33
- Blood-retina barrier
 fluorescein passage affected by, 33
 hyperglycemia-induced breakdown of, 108
- Blue-cone monochromatism
 description of, 250, 250*t*
 electroretinography findings in, 46, 47*f*
- Blue-yellow color deficiency, 54
- Blunt trauma, 315, 353–358, 354–357*f*
- Bone marrow derived stem cells, hyalocytes from, 7
- Borrelia burgdorferi*, 245
- Bradyopsia, electroretinography findings in, 49
- Branch retinal artery occlusion (BRAO)
 emboli that cause, 141, 142*f*
 hypertensive retinopathy and, 122
 imaging of, 141*f*
- management of, 142
 multiple, 152*f*
 in nonproliferative sickle cell retinopathy, 152*f*
 retinal infarction caused by, 141
 in Susac syndrome, 156
- Branch retinal vein occlusion (BRVO)
 afibercept for, 135
 at arteriovenous crossing, 126
 bevacizumab for, 135
 clinical findings of, 125–127, 126*f*
 corticosteroids for, 137–138
 diabetes mellitus and, 128
 fluorescein angiography of, 129*f*
 glaucoma as risk factor for, 125
 hypertensive retinopathy and, 122
 intraretinal hemorrhages associated with, 125, 126*f*
 macular laser surgery for, 128
 neovascularization in, 125, 128, 129*f*
 pars plana vitrectomy for, 130
 pharmacologic management of, 135–138
 prognosis for, 128
 ranibizumab for, 135
 risk factors for, 127–128
 scatter photocoagulation for, 128–130
 spontaneous resolution of, 125
 surgical management of, 128–130
 treatment of, 128–130
 triamcinolone for, 137
 vision loss caused by, 128
- BRAO. *See* Branch retinal artery occlusion
- Bruch membrane
 anatomy of, 210–211
 argyrosis effects on, 306
 basilar laminar deposits effect on, 62*f*, 64
 choroidal neovascularization after damage to, 355, 355*f*
 degeneration of, 19, 71
 disorders that affect, 89
 embryologic development of, 210
 histology of, 18*f*
 layers of, 18*f*, 19
 ocular expansion effects on, 211
 outer lamella of, 211
 photocoagulation-related rupture of, 378
 remodeling of, 210
 rupture of, 378
 supertraction crescent, 210
 tears in, 354
 type 1 choroidal neovascularization in, 72*f*
- BRVO. *See* Branch retinal vein occlusion
- B-scan optical coherence tomography
 definition of, 26
 retinal pigment epithelium subretinal fluid on, 77*f*
 volume rendering versus, 27
- B-scan ultrasonography, intraocular foreign body evaluations using, 352. *See also* Contact B-scan ultrasonography
- Bullous retinoschisis, 326
- Bull's-eye maculopathy
 chloroquine toxicity as cause of, 295, 296*f*
 clofazimine as cause of, 298
 in neuronal ceroid lipofuscinoses, 289
- Bull's-eye pattern
 in acute idiopathic maculopathy, 229

- in Bardet-Biedl syndrome, 284
 in Lyme disease, 245
 in macular atrophy, 265
 in Stargardt disease, 270
 Bull's-eye rash, 245, 265f
 Bupropion, 306
 Butterfly-type pattern dystrophy, 276, 276f
 b-waves, 42–44, 43f, 46, 47f, 50, 261
- Calcific drusen, 66
 Canals, in vitreous, 7
 Cancer-associated retinopathy (CAR), 286, 287f
Candida endophthalmitis, 239–240, 240f
 Canthaxanthine, 303
 Capillary plexus
 deep, 16
 intermediate, 16
 CAR. *See* Cancer-associated retinopathy
 Carbogen, for central retinal artery occlusion, 146
 Carbonic anhydrase inhibitors, in sickle cell patients, 154–155
 Carotid-cavernous fistulas, 198
 Carotid occlusive disease
 retinal hemorrhages in, 138
 retinopathy of, 138
 Cataract, nuclear sclerotic, 402, 402f
 Cataractous lens, B-scan ultrasonography of, 40f
 Cataract surgery
 age-related macular degeneration progression
 affected by, 71
 cystoid macular edema after, 157, 159, 260
 photic retinopathy after, 368
 posterior capsular opacification after, 260
 retinal detachment after, 319
 vitreous abnormalities secondary to, 349
 vitreous loss during, 349
 wound management in, 349
 Cat-scratch disease, 242–243, 243f
 CATT clinical trial, 83, 84t
 Cavernous hemangioma, retinal, 168, 169f
 CD4+ T cells, in cytomegalovirus retinitis, 235
 Ceftazidime, for postoperative endophthalmitis, 389
 Cellophane maculopathy, 335
 Center-involved diabetic macular edema
 description of, 92
 imaging of, 109, 110f
 Central areolar choroidal dystrophy, 277
 Central blindness, age-related macular degeneration
 progression to, 86
 Central macular atrophic lesions, 266
 Central nervous system
 Behçet disease involvement of, 230
 incontinentia pigmenti involvement of, 286
 metabolic abnormalities of
 abetalipoproteinemia, 289–290
 lysosomal, 291–292, 292f
 mucopolysaccharidoses, 290–291
 neuronoid ceroid lipofuscinoses, 289, 290f
 peroxisomal disorders, 290
 Refsum disease, 290
 retinal degeneration caused by, 288–292
 vitamin A deficiency, 289–290
 primary vitreoretinal lymphoma involvement of, 234
- Central retinal artery
 anatomy of, 16
 retinal inner layers supplied by, 140
 Central retinal artery occlusion (CRAO)
 anti-VEGF therapy for, 146
 causes of, 144
 ciliary artery occlusion with, 144, 145f
 electroretinography findings in, 50
 emboli as cause of, 144
 giant cell arteritis as cause of, 145
 illustration of, 16f, 144f
 iris neovascularization in, 146
 management of, 146
 retinal infarction caused by, 143
 spectral-domain optical coherence tomography
 of, 144f
 symptoms and signs of, 143
 vision loss caused by, 143–144
 Central retinal vein occlusion (CRVO)
 aflibercept for, 135
 age and, 133
 bevacizumab for, 135
 causes of, 133–134
 chronic changes caused by, 127f
 cilioretinal artery occlusion caused by, 143
 clinical findings of, 127f, 130
 complications of, 135
 corticosteroids for, 137–138
 cystoid macular edema caused by, 136f
 differential diagnosis of, 134
 diuretic and, 134
 electroretinography findings in, 50
 evaluation of, 134–135
 follow-up for, 134
 hypercoagulable conditions presenting with, 134
 hypertensive retinopathy and, 122
 hyperviscosity retinopathy versus, 134
 intraocular pressure in, 133
 iris neovascularization in, 133, 135
 ischemic, 132f
 macular laser surgery for, 135
 management of, 134–135
 neovascularization in, 125
 nonischemic, 130, 131f
 ocular ischemic syndrome versus, 134
 open-angle glaucoma in, 133
 oral contraceptives and, 134
 panretinal photocoagulation for, 135
 pars plana vitrectomy for, 135
 pharmacologic management of, 135–138
 progression of, follow-up for, 134
 ranibizumab for, 135
 retinal microvascular changes in, 125, 127f
 risk factors for, 133–134
 spontaneous resolution of, 125
 treatment of, 135
 vision loss caused by, 130
 Vitreous hemorrhage secondary to, 135
- Central scotomas, 86, 265
 Central serous chorioretinopathy (CSC)
 age and, 189
 age-related macular degeneration versus, 67, 76, 79
 autofluorescence abnormalities in, 192f

- choroidal thickening in, 191
 corticosteroids as cause of, 300
 demographics of, 189–191, 190/
 differential diagnosis of, 193–194
 discovery of, 189
 enhanced depth imaging optical coherence
 tomography findings, 67, 191, 193/
 fluorescein angiography findings in, 190, 191/
 fundus autofluorescence of, 32
 historical descriptions of, 189
 imaging of, 190–192, 191–193/
 indocyanine green angiography of, 38, 192, 194/
 neovascularization associated with, 194
 nonneovascular age-related macular degeneration
 versus, 67, 76
 optical coherence tomography of, 32
 photodynamic therapy for, 194
 polypoidal choroidal vasculopathy versus, 193
 retinal detachment caused by, 189, 191
 retinal pigment epithelium pigmentation in, 190, 190/
 sildenafil as cause of, 299
 stress and, 191
 symptoms and signs of, 189–190
 systemic conditions associated with, 191
 systemic corticosteroids as risk factor for, 191
 treatment of, 194
 visual acuity in, 190
 white dots with, 191, 191/
 Central vitreous, 7
 Ceramide trihexoside, 291
 Cerebral vasculitis, 222
 C_3F_8 . *See* Perfluoropropane
CFH gene, 63
 Chalcosis, 362
 Charcot-Marie-Tooth disease, 282/
 Charles Bonnet syndrome, 86
 Chédiak-Higashi syndrome, 288
 Chemotherapy
 MEK inhibitors, 299
 primary vitreoretinal lymphoma treated with, 234
 Cherry-red spot
 in central retinal artery occlusion, 143
 in commotio retinae, 353
 ophthalmic artery occlusion and, 146
 in Tay-Sachs disease, 291, 292/
 Chikungunya virus retinitis, 247
 Children. *See also* Infants
 Coats disease in, 159
 congenital toxoplasmosis in, 243
 electroretinography applications in, 50
 trauma in, 316–317, 365–366, 366/
 visual evoked potentials application in, 53
 Chloroquine
 bull's-eye maculopathy caused by, 295, 296/
 indications for, 295
 retinal pigment epithelium abnormalities caused by,
 295–297, 296/
 Chlorpromazine, 297
 CHM gene, 268
 Cholesterolosis, 348
 Choriocapillaris
 age-related changes in, 61
 anatomy of, 17, 19, 20/
 atrophy of, in choroideremia, 258
 blood flow abnormalities in, 198
 ghost vessels in, 198
 hypertensive choroidopathy findings, 123
 optical coherence tomography angiography of, 30/
 in pseudoxanthoma elasticum, 199/
 in type 1 choroidal neovascularization, 71
 Chorioretinal atrophy
 genes and loci associated with, 256/
 in pathologic myopia, 214/
 Chorioretinal disruption, traumatic, 357/
 Chorioretinal edema, 379
 Chorioretinal folds, 200–201, 201/
 Chorioretinal scars
 in congenital toxoplasmosis, 243
 in ocular histoplasmosis syndrome, 87
 Chorioretinitis
 acute syphilitic posterior placoid, 241
 focal, 238, 238/
 in neuroretinitis, 242
 syphilitic, 241–242, 242/
 vitiliginous. *See* Birdshot uveitis
 West Nile virus, 246, 247/
 Zika virus, 247
 Chorioretinopathy
 birdshot, 49
 central serous
 age and, 189
 age-related macular degeneration versus, 67, 76, 79
 autofluorescence abnormalities in, 192/
 choroidal thickening in, 191
 corticosteroids as cause of, 300
 demographics of, 189–191, 190/
 differential diagnosis of, 193–194
 discovery of, 189
 enhanced depth imaging optical coherence
 tomography findings, 67, 191, 193/
 fluorescein angiography findings in, 190, 191/
 fundus autofluorescence of, 32
 historical descriptions of, 189
 imaging of, 190–192, 191–193/
 indocyanine green angiography of, 38, 192, 194/
 neovascularization associated with, 194
 nonneovascular age-related macular degeneration
 versus, 67, 76
 optical coherence tomography of, 32
 photodynamic therapy for, 194
 polypoidal choroidal vasculopathy versus, 193
 retinal detachment caused by, 189, 191
 retinal pigment epithelium pigmentation in, 190,
 190/
 sildenafil as cause of, 299
 stress and, 191
 symptoms and signs of, 189–190
 systemic conditions associated with, 191
 systemic corticosteroids as risk factor for, 191
 treatment of, 194
 visual acuity in, 190
 white dots with, 191, 191/
 Choroid
 age-related atrophy of, 200, 212
 anatomy of, 19–20, 20/
 arterial supply to, 194, 195/

- autoimmune conditions of
 Behçet disease, 230, 230*t*
 inflammatory vasculitis, 230–231
 intermediate uveitis, 231–232
 intraocular lymphoma, 233–234, 234*f*
 lupus vasculitis, 230–231, 231*f*
 overview of, 229
 sympathetic ophthalmia, 233
 Vogt-Koyanagi-Harada disease, 232*f*, 232–233
- bilateral diffuse uveal melanocytic proliferation
 effects on, 204
 blood circulation in, 19–20, 20*f*, 194, 195*f*
 blood flow abnormalities in, 198
 capillary arrangement in, 19
 in choroidal neovascularization, 36, 37*f*
 detachment of, 379, 379*f*
 enhanced depth imaging optical coherence
 tomography of, 25, 193*f*
 filling defects in, 198
 folds in, 200–201, 201*f*
 functions of, 212
 Haller layer, 19
 as heat sink, 20
 inflammation of
 infectious causes, 235–247
 noninfectious causes, 219–234
 white dot syndromes as cause of. *See* White dot
 syndromes
 inner structure of, 193*f*
 in pathologic myopia, 212–216, 214–215*f*
 retinal metabolic needs supplied by, 20
 rupture of, 88, 354–355, 354–356*f*
 Sattler layer, 19
 subfoveal thickness of, 19
 thickness of
 description of, 19
 measurement of, 212
 subfoveal, 212, 214*f*
 thinning of, 214
 trauma-related rupture of, 354–355, 354–356*f*
 venous pressure increases in, 198
 vortex veins in, 19
- Choroidal detachment, 379, 379*f*
- Choroidal diseases
- bilateral diffuse uveal melanocytic proliferation, 204–205, 205*f*
 - central serous chorioretinopathy. *See* Central serous chorioretinopathy (CSC)
 - hemangiomas, 202*f*, 202–203
 - nonarteritic, 195–196, 197*f*
 - perfusion abnormalities, 194, 195–197*f*, 199–200*f*
 - uveal effusion syndrome, 203, 204*f*
- Choroidal dystrophies
- Bietti crystalline dystrophy, 258, 269, 282*f*
 - central areolar, 277
 - choroideremia, 267–268, 268*f*
 - classification of, 255
 - gyrate atrophy, 268–269, 269*f*
- Choroidal effusions
- bupropion as cause of, 306
 - contact B-scan ultrasonography of, 39*f*
- Choroidal granuloma, 241*f*
- Choroidal neovascularization (CNV)
- in acute posterior multifocal placoid pigment epitheliopathy, 222
 - age-related macular degeneration progression to, 64
 - anatomical classification of, 71–75
 - angioid streaks as cause of, 87–89, 89*f*
 - anti-VEGF therapy for, 87–88, 212, 355
 - bevacizumab for, 73*f*, 213*f*
 - after Bruch membrane damage, 355, 355*f*
 - classic, 72, 73*f*
 - conditions associated with, 90*t*
 - fluorescein angiography of, 36, 37*f*, 72–73, 73–74*f*
 - green laser for, 373
 - idiopathic, 89–90
 - indocyanine green angiography of, 73
 - laser photocoagulation for, 376
 - late leakage from an undetermined source, 72
 - miscellaneous causes of, 89–90
 - multifocal choroiditis in, 226, 226*f*
 - occult, 72–73
 - ocular histoplasmosis syndrome as cause of, 86–87, 88*f*
 - optical coherence tomographic angiography of, 75–76, 76–78*f*, 192
 - optical coherence tomography of, 192, 194
 - in pathologic myopia, 89, 211*f*, 211–212
 - photocoagulation for, 376
 - photodynamic therapy for, 212, 213*f*, 380
 - retinal pigment epithelium tears in, 31
 - scar tissue versus, 73
 - signs and symptoms of, 71
 - spectral-domain optical coherence tomography of, 73–75, 75*f*
 - subfoveal, 355, 380
 - subretinal hemorrhages versus, 211
 - susceptibility genes for, 63
 - type 1, 71–72, 72*f*, 76*f*
 - type 2, 72, 75, 77*f*
 - type 3, 72–73, 75, 78*f*
 - vascular endothelial growth factor concentrations in, 80
 - vitelliform exudative macular detachment versus, 272
 - vitreous hemorrhage secondary to, 231*f*
- Choroidal nevi, scanning laser ophthalmoscopy of, 24
- Choroidehemia, 267–268, 268*f*
- choriocapillaris atrophy in, 258
 - electroretinography findings in, 50
- Choroiditis
- birdshot uveitis on, 225, 225*f*
 - multifocal, 220*t*, 225–226, 226*f*
- Choroidopathy, hypertension, 123, 123–124*f*
- Chronic progressive external ophthalmoplegia (CPEO), 293–294
- Cicatricial retinal detachment, 286
- Cigarette smoking, age-related macular degeneration risks, 62
- Ciliary artery occlusion, 144, 145*f*
- Ciliary body, 40
- Cilioretinal artery
- anatomy of, 16, 16*f*
 - occlusion of, 143
- Circle of Zinn-Haller, 217

- Circulation
 choroid, 19–20
 retinal, 16*f*, 16–17
11-cis-retinaldehyde, 17
11-cis-retinol dehydrogenase, 252
 Cisterns, in vitreous, 7
 Clindamycin, for toxoplasmic retinochoroiditis, 243
 Clinically significant diabetic macular edema (CSME), 92, 110, 114. *See also* Diabetic macular edema
 Clinically significant retinopathy of prematurity (CSROP), 184*t*. *See also* Retinopathy of prematurity
 Clofazimine, 298
 Cloquet canal
 anatomy of, 7, 8*f*
 formation of, 341
 CME. *See* Cystoid macular edema
 CMV. *See* Cytomegalovirus (CMV) retinitis
 CNV. *See* Choroidal neovascularization
 Coats disease, 159–161, 160*f*, 326
 Coats reaction, 260
 Cobblestone degeneration, 313, 314*f*
 COL2A1 gene, 343
 Collagen fibers, in vitreous, 7, 344
 Color vision
 abnormalities of
 —achromatopsia, 250, 250*t*
 —acquired, 249, 250*t*
 —congenital, 249–251, 250*t*
 —description of, 249
 —drugs that cause, 304–305
 —blue-yellow deficiency, 54
 —description of, 54
 —red-green deficiency, 54
 Color vision tests
 Farnsworth–Munsell 100-hue test, 55
 Farnsworth Panel D-15 test, 55*f*, 55–56
 Hardy–Rand–Rittler plates, 54
 Ishihara plates, 54, 55*f*
 panel tests, 55
 pseudoisochromatic plates, 54, 55*f*
 Comma sign, 154
 Commotio retinae, 353, 354*f*
 Computed tomography
 intraocular foreign body evaluations, 352
 uveal lymphoma evaluations, 234
 Cone(s)
 bipolar cells synapsing with, 13
 in fovea, 11
 inner segments of, 11–12, 12*f*
 L, 54
 light-sensitive molecules in, 12
 M, 54
 outer segments of, 11, 12*f*
 photoreceptors in, 13
 S, 54
 schematic diagram of, 14*f*
 types of, 54
 Cone dystrophies
 bull's-eye pattern associated with, 265, 265*f*
 description of, 264–265
 electroretinography findings in, 46, 47*f*, 265
 genes and loci associated with, 256*t*
 with supernormal rod ERG, 49
 Cone–rod dystrophies
 genes and loci associated with, 256*t*
 Jalili syndrome, 286
 retinitis punctata albescens, 258, 258*f*
 Confluent drusen, 65
 Confocal scanning laser ophthalmoscopy (SLO), for
 retinal disease evaluations, 24
 Congenital stationary night blindness (CSNB)
 Duchenne muscular dystrophy and, 285
 electroretinography findings in, 46, 47*f*, 251, 252*f*
 genes and loci associated with, 256*t*
 retinitis pigmentosa versus, 251
 subtypes of, 251
 X-linked, 252
 Congenital toxoplasmosis, 243
 Conjunctival filtering blebs, endophthalmitis associated with, 390–391, 391*f*
 Contact B-scan ultrasonography, 39, 39*f*
 Contact lenses
 fundus on, 22
 in photocoagulation delivery, 375
 Contraceptives (oral), central retinal vein occlusion risks, 134
 Contrast sensitivity, 56–57, 57*f*
 Contrecoup, 315
 Copper, 362
 Corneal lacerations, 359
 Corneal verticillata, 295
 Corticosteroids
 acute posterior multifocal placoid pigment epitheliopathy treated with, 222
 acute retinal necrosis treated with, 236
 branch retinal vein occlusion treated with, 137–138
 central retinal vein occlusion treated with, 137–138
 central serous chorioretinopathy caused by, 300
 cytomegalovirus retinitis and, 236
 diabetic macular edema treated with, 113–114
 giant cell arteritis treated with, 145
 progressive outer retinal necrosis syndrome treated with, 237
 retinal vein occlusion treated with, 137–138
 toxoplasmic retinochoroiditis treated with, 244
 Cotton–wool spots
 cytomegalovirus retinitis and, 235
 in diabetic retinopathy, 140–141
 in hypertensive retinopathy, 122, 122*f*
 in Purtscher retinopathy, 171
 in systemic lupus erythematosus, 230
 Coup, 315
 CPEO. *See* Chronic progressive external ophthalmoplegia
 CRAO. *See* Central retinal artery occlusion
 CRAVE study, 135
 CRB1 mutations, 258
 CRVO. *See* Central retinal vein occlusion
 Cryoablation, for retinopathy of prematurity, 185–186
 Cryopexy
 transconjunctival, 398
 transscleral, 398
 Cryotherapy
 retinal cavernous hemangioma treated with, 168
 von Hippel–Lindau syndrome treated with, 167

- Crystalline retinopathy**
 cause of, 302–304, 303*t*
 drugs that cause, 302–304
 tamoxifen as cause of, 303, 304*f*
 West African, 303–304, 305*f*
- CSC.** *See* Central serous chorioretinopathy
- C-scan,** 26
- CSME.** *See* Clinically significant diabetic macular edema
- CSNB.** *See* Congenital stationary night blindness
- CSROP.** *See* Clinically significant retinopathy of prematurity
- Culex** mosquitoes, 246
- Cuticular drusen,** 274, 275*f*
- Cyclosporine,** for Behçet disease, 230
- CYP4V2,** 257*t*, 258, 269
- Cysteamine,** 293
- Cystinosis,** 293
- Cystoid macular edema (CME)**
 birdshot uveitis in, 224
 cataract surgery as cause of, 157, 159, 260
 central retinal vein occlusion as cause of, 136*f*
 characteristics of, 156–157
 corticosteroids for, 159, 393
 in cytomegalovirus retinitis, 235
 differential diagnosis of, 157
 drugs that cause, 301
 edema sources in, 156–157
 etiologies of, 157
 fingolimod as cause of, 302
 fluorescein angiography of, 36*f*, 157
 incidence of, 157, 159
 in Irvine-Gass syndrome, 157
 nicotinic acid as cause of, 301
 optical coherence tomography of, 132*f*, 157, 158*f*
 petaloid, 157
 predisposing factors for, 157, 159
 pseudophakic
 definition of, 157
 imaging of, 394*f*
 optical coherence tomography of, 158*f*
 pars plana vitrectomy for, 394*f*
 in retinal dystrophies, 260, 260*f*
 retinal vein occlusion as cause of, 135. *See also* Retinal vein occlusion (RVO)
 retinitis pigmentosa and, 260
 spontaneous resolution of, 159
 subretinal diseases that cause, 157
 taxanes as cause of, 301
 treatment of, 159
 vision loss caused by, 225
 vitrectomy for, 159, 393, 394*f*
- Cytomegalovirus (CMV) retinitis,** 235–236, 238*t*
- Dark adaptation**
 in electro-oculography, 50
 in full-field (Ganzfeld) electroretinography, 42
 in Oguchi disease, 253
- Dark adaptometry,** 57–58
- DCCT.** *See* Diabetes Control and Complications Trial
- Deep capillary plexus,** 16
- Deferoxamine,** 298–299
- Dehiscescences,** in lamina cribrosa, 218, 218*f*
- Demarcation lines**
 pigmented, in rhegmatogenous retinal detachment, 324
 in retinoschisis, 328
- Demyelinating optic neuritis, visual evoked potentials in,** 52
- Dental diseases, retinal degeneration associated with,** 286
- Dentate processes**
 definition of, 10
 illustration of, 11*f*
- Dermatologic diseases, retinal degeneration associated with,** 286
- Descemet membrane, chalcosis findings in,** 362
- Deutan red-green color deficiency,** 54
- Deuteranomalous dichromatism,** 250*t*
- Deuteranomalous trichromatism,** 250*t*
- Dexamethasone implant**
 complications of, 404
 retinal vein occlusion treated with, 137
- DHA.** *See* Docosahexaenoic acid
- Diabetes Control and Complications Trial (DCCT),** 96
- Diabetes mellitus**
 asteroid hyalosis and, 346
 cataract surgery in, 116, 117–120*t*
 Diabetes Control and Complications Trial, 96
 insulin-dependent, 91
 non-insulin-dependent, 91
 ophthalmic examinations for, 93–94, 95*t*
 retinal vein occlusion risks, 128
 type 1, 91
 type 2, 91
 United Kingdom Prospective Diabetes Study, 96–97
- Diabetic macular edema (DME)**
 cataract surgery effects on, 116
 center-involved, 92, 109, 110*f*
 classification of, 109–110, 110*f*
 clinically significant (CSME), 92, 110, 114
 contrast sensitivity issues in, 56
 definition of, 92
 focal, 110
 mechanism of, 108, 109*f*
 non-center-involved, 109, 111*f*
 optical coherence tomography of, 111*f*
 spectral-domain optical coherence tomography of, 109*f*, 125
 treatment of
 aflibercept, 113
 anti-VEGF therapy, 101, 110–113
 bevacizumab, 113
 corticosteroids, 113–114
 Diabetic Retinopathy Clinical Research Network findings, 112*f*, 113
 intravitreal steroids, 101
 laser surgery, 114–115, 376
 overview of, 110–111
 pars plana vitrectomy, 115
 ranibizumab, 111–112, 112*f*
 surgery, 114–115, 388
 vitrectomy, 388
 vision loss caused by, 94
- Diabetic nephropathy,** 98
- Diabetic retinopathy**
 anemia and, 98
 aspirin and, 100

- cotton-wool spots associated with, 140–141
 description of, 91
 diabetic nephropathy associated with, 98
 epidemiology of, 92–93
 4:2:1 rule for, 99
 glycemic control for, 96–98
 hemoglobin A_{1c} levels in, 96, 98
 medical management of, 96–98
 nonproliferative (NPDR)
 anti-VEGF therapy for, 101–102
 clinical findings in, 99
 definition of, 91
 intraretinal hemorrhages associated with, 100f
 intraretinal microvascular abnormalities in, 100f
 microaneurysms associated with, 100f
 optical coherence tomography angiography of, 94f
 panretinal photocoagulation for, 101
 posterior vitreous detachment creation for, 102
 progression of, to proliferative diabetic retinopathy, 101
 ranibizumab for, 102
 scatter photocoagulation for, 116
 severity of, 95t, 99
 treatment of, 101–102
 venous beading associated with, 100f
 vision loss in, 101
 ophthalmic examinations for, 93–94, 95t
 pathogenesis of, 93
 pregnancy-related progression of, 93–94
 progression of
 fenofibrate effects on, 102
 hypertension as risk factor for, 98
 pregnancy-related, 93–94
 proliferative (PDR)
 anti-VEGF therapy for, 103–104, 386
 complications of, 103–108
 definition of, 91–92
 extraretinal fibrovascular proliferation associated with, 102
 high-risk characteristics of, 103
 laser surgery for, 104–107
 management of, 103–108
 neovascular proliferation associated with, 102
 neovascularization in, 151
 nonproliferative diabetic retinopathy progression to, 101
 nonsurgical management of, 103–104
 optical coherence tomography angiography of, 94f
 panretinal photocoagulation for, 104, 106, 106f
 photocoagulation for, 94
 in pregnancy, 94
 proangiogenic factors in, 102
 proliferative sickle cell retinopathy versus, 151
 ranibizumab for, 104
 scatter photocoagulation for, 116
 severe carotid artery occlusive disease associated with, 98
 severity of, 95t
 stages of, 102
 steroids for, 103–104
 surgical management of, 104–107
 tractional retinal detachment caused by, 103, 108, 387–388
 vitreous hemorrhage caused by, 103, 103f, 107–108, 386–387
 retinal capillary nonperfusion associated with, 101
 severity of, 95t, 101
 studies of
 Diabetes Control and Complications Trial, 96
 Early Treatment Diabetic Retinopathy Study, 99–101
 United Kingdom Prospective Diabetes Study, 96–97
 systemic medical management of, 96–98
 terminology associated with, 91–92
 vision loss from
 abnormalities associated with, 98
 lipid levels and, 98
 mechanisms of, 101
 Diabetic Retinopathy Clinical Research Network
 cataract surgery in diabetes mellitus studies, 116, 117–120t
 diabetic macular edema treatment, 112f, 113
 Diabetic Retinopathy Study (DRS), 104–105
 Dichromacy, 250
 Dideoxyinosine, 299
 Diet, retinopathy of prematurity and, 184–185
 Diffuse macular edema, 110, 111f
 Diffuse unilateral subacute neuroretinitis (DUSN), 246
 Digitalis, 305
 Digital resolution, of scanning laser ophthalmoscopy, 24
 Direct ophthalmoscope/ophthalmoscopy. *See also Ophthalmoscopy*
 limitations of, 21
 retinal disease evaluations using, 21
 Disseminated intravascular coagulation, 196
 Diuretics, 134
 DME. *See Diabetic macular edema*
 Docetaxel, 301
 Docosahexaenoic acid (DHA), 70
 Doxycycline, for cat-scratch disease, 242–243
 Doyne honeycomb dystrophy, 275
 DRS. *See Diabetic Retinopathy Study*
 Drugs. *See also specific drug*
 color-vision abnormalities caused by, 304–305
 crystalline retinopathy caused by, 302–304, 304t
 ganglion cell toxicity caused by, 301
 hyaloidal separation effects on, 85
 macular edema caused by, 301–302, 302f
 microvasculopathy caused by, 300–301
 occlusive retinopathy caused by, 300–301
 ocular toxicities caused by, 305–306
 optic nerve toxicity caused by, 301
 retinal toxicity caused by
 alkyl nitrates, 300, 300f
 chloroquine derivatives, 295–297, 296f
 clofazimine, 298
 deferoxamine, 298–299
 dideoxyinosine, 299
 hydroxychloroquine, 295–297, 296f
 MEK inhibitors, 299, 299f
 nucleoside reverse transcriptase inhibitors, 299
 pentosan polysulfate, 300
 phenothiazines, 297–298, 298f
 scleral delivery of, 20
 toxicity caused by, retinal signs of, 68

- Drusen
 boundaries of, 65
 calcific, 66
 categorization of, 64–65
 confluent, 65
 cuticular, 274, 275f
 definition of, 63
 early-onset, 273, 274f
 fluorescein angiography of, 65
 fundus camera imaging of, 23, 23f
 geographic atrophy and, 66
 hard, 65
 histologic appearance of, 63, 64f
 large colloid, 274
 optical coherence tomography of, 65–66
 photoreceptors affected by, 64
 pigment epithelial detachment associated with, 64
 refractive, 23f
 soft, 65, 68, 75, 200f, 272
 spectral-domain optical coherence tomography of, 64f
 subretinal deposits, 200
- Drusenoid pigment epithelial detachment, 64, 272, 274f
- “Dry” age-related macular degeneration. *See*
 Nonneovascular (“dry”) age-related macular degeneration
- Duchenne muscular dystrophy, 285
- Dural arteriovenous malformations, 198, 199f
- DUSN. *See* Diffuse unilateral subacute neuroretinitis
- Dyschromatopsia, 249, 265
- Dystrophic lipidization, 66
- Dystrophies
 adult-onset foveomacular vitelliform, 272, 276
 butterfly-type pattern, 276, 276f
 choroidal
 Bietti crystalline dystrophy, 258, 269, 282t
 central areolar, 277
 choroideremia, 267–268, 268f
 classification of, 255
 gyrate atrophy, 268–269, 269f
 cone
 bull’s-eye pattern associated with, 265, 265f
 description of, 264–265
 electroretinography findings in, 46, 47f, 265
 genes and loci associated with, 256t
 with supernormal rod ERG, 49
 cone-rod
 genes and loci associated with, 256t
 Jalili syndrome, 286
 retinitis punctata albescens, 258, 258f
- macular
 adult-onset vitelliform lesions, 272, 273f
 atypical, 277
 Best disease, 271, 272f
 early-onset “drusenoid,” 273–276, 274–275f
 electroretinography findings in, 46, 47f
 North Carolina, 277, 278f
 occult, 277
 pattern dystrophies, 276f, 276–277
 Sorsby, 275f, 275–276
 Stargardt disease. *See* Macular dystrophies
- panretinal
 clinical findings of, 261, 263f
- Coats reaction associated with, 260
 nonsyndromic, 258–259
 syndromic, 259
 pattern, 67, 272, 276f, 276–277
 rod-cone. *See also* Retinitis pigmentosa
 in Bardet-Biedl syndrome, 284
 characteristics of, 261–264, 262–264f
 conventional testing of, 261
 electroretinography evaluations, 46, 47f, 261
 imaging of, 262–264f
 macula-spared, 46, 47f
- Dystrophin, 285
- Eales disease, 156, 241
- Early macular telangiectasia, 277
- Early-onset “drusenoid” macular dystrophies, 273–276, 274–275f
- Early Treatment Diabetic Retinopathy Study (ETDRS), 99–101, 110
- Early Treatment of Retinopathy of Prematurity (ETROP), 179, 185
- Ebola virus (EBOV) panuveitis, 247
- Echography, for vitreous hemorrhage, 347
- Eclampsia, 196
- Eclipse retinopathy. *See* Solar retinopathy
- EDI-OCT. *See* Enhanced depth imaging optical coherence tomography
- EFEMP1 gene, 275
- Eicosapentaenoic acid (EPA), 70
- Electrical injuries, 357
- Electro-oculography/electro-oculogram (EOG)
 acute zonal occult outer retinopathy evaluations, 51
 autosomal recessive bestrophinopathy evaluations, 51
- Best disease evaluations, 51, 271
- bestrophin mutation evaluations, 51
- illustration of, 52f
 purpose of, 50
 technique of, 50
- vitelliform macular dystrophy evaluations, 51
- Electrophysiologic testing
 International Society for Clinical Electrophysiology of Vision standards for, 41
 purpose of, 41
 retinal, 41–42
- Electroretinography (ERG)
 ABCA4 retinopathy findings, 48f
 achromatopsia, 250
 acute zonal occult outer retinopathy findings, 227
 a-waves, 46, 251, 261
 Best disease findings, 271
 birdshot chorioretinopathy findings, 49
 bradyopsia findings, 49
 b-waves, 42–44, 43f, 46, 47f, 50, 261
 central retinal artery occlusion findings, 50
 central retinal vein occlusion findings, 50
 in children, 50
 choroideremia findings, 50
 clinical considerations for, 46, 49–50
 cone dystrophies
 findings associated with, 46, 47f, 265
 with supernormal rod ERG findings, 49
- cone-rod dystrophy phenotype in, 44

- congenital stationary night blindness findings, 46, 47f, 251, 252f
 dark adaptometry and, 58
 drugs that cause abnormalities in, 304–305
 electrodes used in, 42
 enhanced S-cone disease/syndrome findings, 49, 266, 267f
 full-field (Ganzfield). *See* Full-field (Ganzfield)
 electroretinography
 functions of, 42
 fundus albipunctatus findings, 252
 hydrochloroquine toxicity findings, 45, 49f
 inherent noise in, 44
 Leber congenital amaurosis findings, 266
 macular dystrophy findings, 44, 46, 47f
 melanoma-associated retinopathy findings, 286
 multifocal, 45, 48–49f
 multiple evanescent white dot syndrome on, 224
 in newborn, 44
 night blindness findings, 46
 ocular ischemic syndrome findings, 138, 139f
 pattern, 45–46, 46–49f
 peak-time shift in, 44
 photophobia findings, 46
 rod monochromatism findings, 250
 S-cone monochromatism findings, 250
 siderosis bulbi findings, 362
 vigabatrin-related abnormalities of, 305
 X-linked retinitis pigmentosa findings, 50
- Elevated intraocular pressure
 in central retinal artery occlusion, 146
 in central retinal vein occlusion, 133
 after intravitreal injection of anti-VEGF drugs, 404
- ELISA. *See* Enzyme-linked immunosorbent assay
- Ellipsoid, 12
- Ellipsoidal mirror, scanning laser ophthalmoscopy use of, 24
- ELM. *See* External limiting membrane
- Elschnig spots, 123, 123f, 196
- Embolism, retinal vasculitis versus, 156
- Endogenous bacterial endophthalmitis, 237–239, 238f
- Endophthalmitis
Bacillus cereus, 363
 bevacizumab and, 85
 bleb-associated, 390–391, 391f
 endogenous
 bacterial, 237–239, 238f
 fungal, 239–240, 240f
 exogenous fungal, 239–240
 fungal, 239, 239f
 after intravitreal injections, 404
 postoperative
 acute-onset, 388–390, 390f
 bleb-associated, 390–391, 391f
 chronic (delayed-onset), 390, 391f
 posttraumatic, 362–363
Streptococcus viridans as cause of, 404
 yeast, 239–240, 240f
- Endophthalmitis Vitrectomy Study (EVS), 389–390
- Endothelial cells, in angiogenesis, 79
- En face scan
 definition of, 26
 retinal disease evaluations, 26, 29
- Enhanced depth imaging optical coherence tomography (EDI-OCT)
- autofluorescence imaging and, 39
 central serous chorioretinopathy findings, 67, 191, 193f
 choroidal layer on, 79, 193f
 choroidal-scleral interface on, 66
 description of, 25
 pachychoroid on, 76
- Enhanced S-cone disease (ESCD), 266, 267f
- Enhanced S-cone syndrome, 49
- Enucleation, for penetrating ocular injury, 233
- Enzyme-linked immunosorbent assay (ELISA)
 in Lyme disease, 246
 in toxocariasis, 245
- EOG. *See* Electro-oculography/electro-oculogram
- EPA. *See* Eicosapentaenoic acid
- Epiretinal membranes (ERMs)
 asymptomatic, 336
 causes of, 332
 contracture of, 335
 definition of, 332
 fluorescein angiography findings, 335
 incidence of, 333
 optical coherence tomography of, 335, 383f
 prevalence of, 333
 “pseudohole” appearance with, 334
 scanning laser ophthalmoscopy of, 334f
 secondary, 333
 signs and symptoms of, 334–335f, 334–336
 spectral-domain optical coherence tomography of, 335f
 treatment of, 336, 382, 383f
 vitrectomy for, 382, 383f
 vitreomacular traction syndrome versus, 382–383
- Equatorial retina, 9–10
- ERG. *See* Electrotretinography
- Ergot alkaloids, 300
- ERMs. *See* Epiretinal membranes
- Erythema migrans, 245
- ESCD. *See* Enhanced S-cone disease
- Escherichia coli*, urinary tract infections caused by, 238
- ETDRS. *See* Early Treatment Diabetic Retinopathy Study
- Ethylene glycol, 303
- ETROP. *See* Early Treatment of Retinopathy of Prematurity
- Evisceration, for penetrating ocular injury, 233
- EVRI gene, 346t
- EVR2 gene, 346t
- EVR3 gene, 346t
- EVR4 gene, 346t
- EVR5 gene, 346t
- EVS. *See* Endophthalmitis Vitrectomy Study
- External limiting membrane (ELM)
 anatomy of, 15
 histology of, 11, 12f
- Extra-areal periphery, 9
- Extracranial to intracranial bypass surgery, for ocular ischemic syndrome, 140

- Exudates
 hard, 122, 160
 macular, 124f
 soft, 122
- Exudative retinal detachment
 causes of, 320
 diagnostic features of, 321t
 in familial exudative vitreoretinopathy, 343
 imaging of, 325f
 management of, 325–326
 photocoagulation as cause of, 379
 retinal surface in, 326
 subretinal fluid findings in, 326
- Eye movement tracking, optical coherence tomography with, 27
- FA. *See* Fluorescein angiography
- Fabry disease, 291–292
- Familial adenomatous polyposis (FAP), 285–286
- Familial cerebello retinal angiomas. *See* von Hippel-Lindau (VHL) syndrome
- Familial exudative vitreoretinopathy (FEVR), 343–344, 345f
- Familial juvenile nephronophthisis, 285
- FAP. *See* Familial adenomatous polyposis
- Farnsworth-Munsell 100-hue test, 55
- Farnsworth Panel D-15 test, 55f, 55–56
- Fat emboli/embolism, 141, 173
- FAZ. *See* Foveal avascular zone
- Fellow eye
 macular hole risks, 339
 retinal detachment in, 319
- Fenofibrate, diabetic retinopathy progression affected by, 102
- FEVR. *See* Familial exudative vitreoretinopathy
- Fibronectin, 7
- Fibrovascular pigment epithelial detachment, 72–73
- Fingolimod, 301
- FIPTs. *See* Focal intraretinal periorteriolar transudates
- Flap tears, of retina, 315, 318–319
- Flaviviridae*, 247
- Floatters
 description of, 344
 in posterior vitreous detachment, 308–309
 in rhegmatogenous retinal detachment, 320
 in toxocariasis, 244
 in toxoplasmic retinochoroiditis, 243
 vitrectomy for, 386
- Fluconazole, for yeast endophthalmitis, 240
- Fluorescein
 characteristics of, 33
 leakage of, 35
 pooling of, 35, 36f
- Fluorescein angiography (FA)
 acute idiopathic maculopathy on, 228
 acute posterior multifocal placoid pigment epitheliopathy on, 221f, 222
 acute zonal occult outer retinopathy on, 227
 adult-onset vitelliform maculopathy on, 68
 adverse effects of, 36
 angioid streaks on, 87, 89f
 asteroid hyalosis on, 347
 autofluorescence, 35
- bilateral diffuse uveal melanocytic proliferation on, 205f
- birdshot uveitis on, 224–225, 225f
- blocked fluorescence in, 35
- branch retinal artery occlusions on, 152f
- central retinal artery occlusion on, 144f
- central retinal vein occlusion on, 130, 131f
- central serous chorioretinopathy on, 190, 191f
- choroidal neovascularization on, 36, 37f, 72–73, 73–74f
- choroideremia on, 268
- Coats disease on, 160f
- cystoid macular edema on, 36f, 157
- drusen on, 65
- epiretinal membranes on, 335
- familial exudative vitreoretinopathy on, 345f
- fluorescein dye used in, 33
- fovea in, 34
- foveal avascular zone in, 9
- fundus camera for, 23, 36
- hyperfluorescence in, 35
- hypertensive choroidopathy findings, 123, 124f
- illustration of, 34f
- ischemic central retinal vein occlusion on, 132f
- laser therapy for diabetic macular edema guided using, 115
- lupus vasculitis on, 231f
- macular telangiectasia type 2 on, 163, 163f
- multiple evanescent white dot syndrome on, 223–224
- nonischemic central retinal vein occlusion on, 130, 131f
- ocular ischemic syndrome findings, 138, 139f
- optical coherence tomography angiography versus, 29
- in pregnancy, 36
- pre papillary vascular loops on, 341
- radiation retinopathy on, 170, 170f
- recirculation phase of, 34
- retinal cavernous hemangioma on, 169f
- retinal disease evaluations using, 33–38, 34f, 36–37f
- retinal pigment epithelium cells on, 34
- skin yellowing caused by, 36
- Stargardt disease on, 269–270, 270f
- technique for, 33–34, 34f
- uveal effusion syndrome on, 204f
- vascular filling defects in, 35
- vitreoretinal traction syndrome on, 337
- Vogt-Koyanagi-Harada disease findings, 232
- wide-angle, 36, 37f
- Fluorescent treponemal antibody absorption (FTA-ABS) test, 241
- Fluorophores, in fundus autofluorescence, 29
- Focal chorioretinitis, 238, 238f
- Focal intraretinal periorteriolar transudates (FIPTs), 121–122, 122f
- Focal macular edema, 110, 111f
- Footplates of Müller cells, 15, 15f
- Foreign bodies, intraocular
 aluminum, 362
 chalcosis secondary to, 362
 composition of, 362
 copper, 362
 evaluation of, 351
 imaging of, 352–353, 360, 361f

- iron, 362
 magnetic resonance imaging of, 353
 migration of, 362
 ocular reaction to, 362
 plain-film x-ray studies of, 352–353
 retained, 362
 siderosis bulbi secondary to, 362, 363*t*
 surgical removal of, 360–362
 zinc as, 362
- Form-deprivation errors, 216
- Foscarnet
 acute retinal necrosis treated with, 236
 cytomegalovirus retinitis treated with, 235, 238*t*
 progressive outer retinal necrosis syndrome treated with, 236
- 4:2:1 rule, for diabetic retinopathy, 99
- Fovea
 anatomy of, 9, 9*f*
 characteristics of, 10*t*
 cones in, 11
 fluorescein angiography of, 34
 inner cellular layers in, 12*f*
 photocoagulation-related burns of, 378
- Fovea centralis, 9, 9*f*
- Foveal avascular zone (FAZ)
 definition of, 9
 optical coherence tomography angiography of, 77*f*
- Foveal center, rods in, 11
- Foveola
 anatomy of, 9, 9*f*, 11
 characteristics of, 10*t*
- Foveomacular retinitis. *See* Solar retinopathy
- FTA-ABS. *See* Fluorescent treponemal antibody absorption (FTA-ABS) test
- Full-field (Ganzfeld) electroretinography
ABCA4 retinopathy findings, 48*f*
 cone dystrophies, 265
 cone-rod dystrophies, 265
 description of, 42–45, 43*f*
 mixed rod-cone, 43
 normal response in, 43*f*, 44
 photopic flicker, 44
 photopic single-flash, 44
 quinine toxicity on, 302*f*
 rod-specific, 42
- Fundus
 arteriolar narrowing of, 261
 autofluorescence imaging of, 23*f*
 color photograph of, 23, 23*f*
 retinitis pigmentosa findings, 261, 262*f*
 “sunset glow” appearance of, 232*f*, 232–233
- Fundus albipunctatus, 252, 253*f*
- Fundus autofluorescence
 definition of, 29
 fluorophores, 29
 hyperspectral, 33
 near-infrared, 32–33
 retinal disease evaluations, 29, 31–33
 retinal pigment epithelium tears on, 31, 32*f*
 Stargardt disease on, 270
- Fundus camera
 disadvantages of, 23
 flash illumination used by, 23
- for fluorescein angiography, 23, 36
 for indocyanine green angiography, 23
 operating principles of, 22–23
 retinal disease evaluations using, 22–23, 23*f*
- Fundus flavimaculatus, 269
 description of, 44
 electroretinography findings in, 48*f*
- Fundus photography
 exudative retinal detachment on, 325*f*
 lattice degeneration on, 310–311*f*
 retinopathy of prematurity screening uses of, 184
- Fundus pulvérulentus, 276–277
- Fungal endophthalmitis, 239, 239*f*
- Fungemia, 239
Fusarium endophthalmitis, 239
- Ganciclovir
 acute retinal necrosis treated with, 236
 cytomegalovirus retinitis treated with, 235, 238*t*
 progressive outer retinal necrosis syndrome treated with, 236
- Ganglion cell(s)
 bipolar cells and, 13
 drug toxicity affecting, 301
- Ganglion cell layer (GCL)
 anatomy of, 15
 histology of, 11, 12*f*
 quinine effects on, 301
 superficial vascular plexus in, 16
- Ganzfeld bowl, 42
- Ganzfeld ERG. *See* Full-field (Ganzfeld) electroretinography
- Gardner syndrome. *See* Familial adenomatous polyposis (FAP)
- Gastrointestinal diseases, retinal degeneration associated with, 285–286
- Gaucher disease, 291
- GCA. *See* Giant cell arteritis
- GCL. *See* Ganglion cell layer
- General anesthesia, 50
- Gene therapy
 for choroideremia, 268
 for Leber congenital amaurosis, 266
 for retinal dystrophies, 260, 266
- Genetic heterogeneity, 255
- Genetic testing, for age-related macular degeneration, 63
- Gentamicin, 300
- Geographic atrophy, of retinal pigment epithelium
 in Best vitelliform dystrophy, 271
 description of, 64, 66, 67*f*, 68
 in drusenoid retinal pigment epithelium detachment, 272
- Ghost cell glaucoma, 347
- Giant cell arteritis (GCA)
 central retinal artery occlusion caused by, 145
 description of, 195
 indocyanine green angiography of, 196*f*
- Giant tears, of retina, 315
- Glaucoma
 angle-closure, in retinopathy of prematurity, 181
 ghost cell, 347
 nerve damage caused by, 328

- open-angle
 in central retinal vein occlusion, 133
 vitrectomy as risk factor for, 402
- in pathologic myopia, 218, 218f
- pupillary-block, in retinopathy of prematurity, 181
- retinal vein occlusion risks secondary to, 125
- Globe injuries
 lacerating injuries, 358
 needle perforation/penetration of, 358, 395f, 395–396
- penetrating, 358
- perforating, 358
- primary repair of, 359
- scleral rupture, 352, 358
- surgical management of, 359–360
- vitrectomy for, 359–360
- wound closure of, 359
- Glycemic control, for diabetic retinopathy, 96–98
- GM₂ gangliosidosis type I, 291
- Goldmann-Favre syndrome. *See* Enhanced S-cone disease (ESCD)
- Goldmann-Weekers (G-W) adaptometer, 57–58
- Granulomas
 choroidal, 241f
 posterior pole, 245
 in toxocariasis, 244, 245f
- Granulomatosis with polyangiitis, 195, 196f
- Green laser, 373
- GRK1 gene, 253
- Grönblad-Strandberg syndrome, 87
- “Guttering,” 79
- Gyrate atrophy, 268–269, 269f
- Haemophilus* spp, bleb-associated endophthalmitis caused by, 391
- Haller layer, 19
- Handheld laser-pointer injury, 369
- HARBOR study, 82
- Hard drusen, 65
- Hard exudates, 122, 160
- Hardy-Rand-Rittler plates, for color vision testing, 54
- Hearing loss
 pigmentary retinopathy and, 284
 retinitis pigmentosa and, 284
- Helicoid peripapillary choroidopathy. *See* Serpiginous choroidopathy
- HELLP (hemolysis, elevated liver enzymes, and low platelet count) syndrome, 197f
- Hemangioblastomas, in von Hippel-Lindau syndrome, 165–166, 166f, 168
- Hemangiomas
 cavernous, 168, 169f
 choroidal, 202f, 202–203
- Hemeralopia, 264
- Hemiretinal vein occlusion (HRVO), 130, 133f
- Hemoglobin, 373, 374f
- Hemoglobin A_{1c}, diabetic retinopathy and, 96, 98
- Hemoglobin S, 149
- Hemorrhage
 retinal
 in abusive head trauma, 366, 366f
 in carotid occlusive disease, 138
- salmon-patch, 150, 150f
- submacular
 in neovascular age-related macular degeneration, 85, 385
- posttraumatic, 354f
- vitrectomy for, 385, 386f
- subretinal
 choroidal neovascularization versus, 211
 in polypoidal choroidal vasculopathy, 76
- suprachoroidal, 394–395, 395f
- vitreous
 in central retinal vein occlusion, 135
 echography for, 347
 peripheral neovascularization, 232
 photocoagulation as cause of, 379
 in polypoidal choroidal vasculopathy, 75
 posterior vitreous detachment and, 309
 in proliferative diabetic retinopathy, 103, 103f, 107–108
 trauma-related, 357
 treatment of, 309
 in Valsalva retinopathy, 171
 vision loss caused by, 346
- Hemorrhagic occlusive retinal vasculitis (HORV), 300–301
- Henle fiber layer (HFL)
 definition of, 9
 histology of, 11, 12f
 myopia macular schisis of, 209
- Heredity dystrophies
 choroidal
 Bietti crystalline dystrophy, 258, 269, 282f
 choroidema, 267–268, 268f
 classification of, 255
 gyrate atrophy, 268–269, 269f
 retinal
 bilateral symmetric involvement of, 258
 blindness concerns of patients with, 260
 cystoid macular edema in, 260, 260f
 diagnostic considerations for, 258–259
 enhanced S-cone disease, 266, 267f
 genes and loci associated with, 256–257t
 gene therapy for, 260, 266
 genetic considerations for, 259
 inheritance patterns for, 259
 Leber congenital amaurosis, 265–266
 management of, 259–260, 260f
 molecular genetic testing for, 259
 rod-cone dystrophies, 261–264, 262–264f
 stem cell therapy for, 260
- Heredity hyaloideoretinopathies with optically empty vitreous, 342–343, 343f
- Hermansky-Pudlak syndrome, 288
- Herpes simplex virus (HSV), necrotizing retinitis caused by, 236–237, 236–237f, 238f
- HFL. *See* Henle fiber layer
- High myopia. *See* Pathologic myopia
- High-plus-power lenses, 375
- Histiocytic lymphoma. *See* Primary vitreoretinal lymphoma
- Histoplasma capsulatum*, 86–87
- Histoplasmosis, 86–87
- HIV. *See also* AIDS
 cytomegalovirus retinitis and, 235

- intraocular lymphoma risks, 234
toxoplasmic retinochoroiditis and, 243
- Hives, fluorescein angiography as cause of, 36
- HLA-B5, 230
- Holes
- macular
 - contusion injury as cause of, 315
 - fellow-eye risk for development of, 339
 - formation of, 339, 340*f*
 - idiopathic
 - description of, 337–339, 338*f*
 - vitrectomy for, 384–385, 385*f*
 - International Vitreomacular Traction Study Classification System for, 336*t*
 - lamellar, 28*f*
 - management of, 339–340
 - optical coherence tomography of, 27*f*
 - in pathologic myopia, 209
 - posttraumatic, 355–357, 356*f*
 - rhegmatogenous retinal detachment caused by, 330, 330*f*
 - spontaneous resolution of, 340
 - stage 0, 339
 - stage 1, 339–340
 - stage 2, 339
 - stage 3, 339
 - stage 4, 339
 - surgical management of, 339–340
 - outer-schisis-layer, 327, 327*f*
 - retinal
 - atrophic
 - definition of, 315
 - lattice degeneration with, 310, 311*f*, 316*f*
 - retinal detachment secondary to, 310
 - description of, 378
 - operculated, 315–316
 - Hollenhorst plaques, 141, 142*f*, 144
 - Homocystinuria, 282*t*
 - HORIZON study, 81–82
 - Horseshoe-shaped retinal tears, 316, 323*f*
 - HORV. *See* Hemorrhagic occlusive retinal vasculitis
 - HRVO. *See* Hemiretinal vein occlusion
 - HSV. *See* Herpes simplex virus
 - Hunter syndrome, 283*t*, 291
 - Hurler syndrome, 282*t*, 290
 - Hyalocytes
 - oxygen consumption by, 7
 - in vitreous, 7
 - Hyaloid artery, 340–341
 - Hyaluronan, 331
 - Hydroxychloroquine toxicity
 - description of, 295–297
 - multifocal electroretinography findings in, 45, 49*f*
 - nonneovascular age-related macular degeneration versus, 68
 - Hyperacuity testing, in age-related macular degeneration, 69
 - Hyperautofluorescence, in chloroquine toxicity, 297
 - Hyperfluorescence, in fluorescein angiography, 35
 - Hyperglycemia, blood–retina barrier breakdown caused by, 108
 - Hyperhomocysteinemia, 134
 - Hyperopia, 201
- Hypertension
 - arteriosclerotic vascular disease and, 122
 - asteroid hyalosis and, 346
 - choroidopathy caused by, 123, 123–124*f*
 - classification of, 121
 - diabetic retinopathy progression associated with, 98
 - focal intraretinal peripapillary transudates caused by, 121–122, 122*f*
 - malignant, 196
 - optic neuropathy caused by, 123, 125
 - prevalence of, 121
 - retinal vascular diseases associated with, 121–125, 122–124*f*
 - retinopathy caused by, 121–123, 122*f*, 124*f*
- Hyperviscosity retinopathy, central retinal vein occlusion versus, 134
- HypHEMA, traumatic, 154
- Hypoautofluorescence, in chloroquine toxicity, 297
- Hypopyon, 390
- Hypotony maculopathy, 201
- Idiopathic macular holes
 - description of, 337–339, 338*f*
 - vitrectomy for, 384–385, 385*f*
- Idiopathic retinal vasculitis, aneurysms, and neuroretinitis (IRVAN), 156
- IGA. *See* Indocyanine green angiography
- IGF-1. *See* Insulin growth factor-1
- Illumination, in indirect ophthalmoscope/ophthalmoscopy, 21
- ILM. *See* Internal limiting membrane
- Incontinentia pigmenti, 283*t*, 286
- Indirect ophthalmoscope/ophthalmoscopy
 - illumination in, 21
 - posterior vitreous detachment diagnosed using, 309, 331
 - retinal disease evaluations using, 21–22
- Indocyanine green angiography (IGA)
 - acute idiopathic maculopathy on, 228
 - acute posterior multifocal placoid pigment epitheliopathy on, 222
 - acute zonal occult outer retinopathy on, 227
 - adverse effects of, 39
 - applications of, 38–39
 - central serous chorioretinopathy on, 38, 192, 194*f*
 - choroidal hemangiomas on, 202*f*
 - choroidal neovascularization on, 73
 - definition of, 38
 - fundus camera for, 23
 - giant cell arteritis findings, 196*f*
 - multiple evanescent white dot syndrome on, 223–224
 - polypoidal choroidal vasculopathy on, 38, 38*f*
- Infants. *See also* Children
 - abusive head trauma in, 365–366, 366*f*
 - congenital toxoplasmosis in, 243
 - Leber congenital amaurosis in, 265–266
 - neuronoid ceroid lipofuscinoses in, 289
 - Refsum disease in, 290
 - retinopathy of prematurity in, 175
 - trauma in, 316–317, 365–366, 366*f*
 - visual evoked potentials application in, 53
- Inferior staphyloma syndrome, 217, 217*f*

- Inflammatory vasculitis, 230, 230t
 Infrared laser, 374
 Inner nuclear layer (INL)
 histology of, 11, 12f, 15f
 paracentral acute middle maculopathy of, 143
 Inner-outer segment junction, 12
 Inner plexiform layer (IPL), 11, 12f
 Inner segments
 of cones, 11, 12f
 ellipsoid, 12
 of rods, 11, 12f
 Insulin-dependent diabetes mellitus, 91
 Insulin growth factor-1 (IGF-1), retinopathy of
 prematurity screening and, 182
 Interferogram, 25
 Interferon alfa-2a, 300
 Intermediate capillary plexus, 16
 Intermediate uveitis, 231–232
 Internal limiting membrane (ILM)
 amacrine cells in, 15
 anatomy of, 15
 epiretinal membranes, 332
 hemorrhagic detachment of, 171
 histology of, 11, 12f
 nonproliferative sickle cell retinopathy findings, 150
 peeling of, 209
 vitreous remnants on, 332
 International Federation for Clinical Neurophysiology
 electrophysiologic testing standards, 41
 International Society for Clinical Electrophysiology of
 Vision (ISCEV)
 electrophysiologic testing standards of, 41
 full-field electroretinography standards, 42, 43f
 International Vitreomacular Traction Study
 Classification System, 336t
 Intraocular foreign bodies (IOFBs)
 aluminum, 362
 chalcosis secondary to, 362
 composition of, 362
 copper, 362
 evaluation of, 351
 imaging of, 352–353, 360, 361f
 iron, 362
 magnetic resonance imaging of, 353
 migration of, 362
 ocular reaction to, 362
 plain-film x-ray studies of, 352–353
 retained, 362
 siderosis bulbi secondary to, 362, 363t
 surgical removal of, 360–362
 zinc as, 362
 Intraocular lenses (IOLs), posteriorly dislocated, 393
 Intraocular lymphoma, 233–234, 234f
 Intraocular pressure (IOP)
 elevated
 in central retinal artery occlusion, 146
 in central retinal vein occlusion, 133
 after intravitreal injection of anti-VEGF drugs, 404
 in rhegmatogenous retinal detachment, 320
 scleral buckling effects on, 399
 in sickle cell retinopathy, 154
 in trauma patients, 352
 Intraretinal hemorrhage
 in branch retinal vein occlusion, 125, 126f
 in nonproliferative diabetic retinopathy, 100f
 in systemic lupus erythematosus, 230–231
 Intraretinal microvascular abnormalities (IRMAs), in
 nonproliferative diabetic retinopathy, 100f
 Intrascleral fixation, 393
 Intravitreal injections
 anesthesia for, 403
 anti-VEGF drugs, 404
 aseptic technique for, 403–404
 complications of, 404
 corticosteroids
 diabetic macular edema treated with, 101
 proliferative diabetic retinopathy treated with, 104
 retinopathy of prematurity treated with, 187
 endophthalmitis after, 404
 indications for, 403
 prevalence of, 403
 technique for, 403, 403f
 Ionizing radiation, retinopathy caused by exposure to,
 170f, 170–171
 IOFBs. *See* Intraocular foreign bodies.
 IOLs. *See* Intraocular lenses.
 IOP. *See* intraocular pressure
 IPL. *See* Inner plexiform layer
 Iris
 neovascularization of
 in branch retinal vein occlusion, 128–129, 129f
 in central retinal artery occlusion, 146
 in central retinal vein occlusion, 133, 135
 in diabetes mellitus, 107
 in radiation retinopathy, 170
 vitreous adhesions to, 159
 Iris fixation, 393
 IRMAs. *See* Intraretinal microvascular abnormalities
 IRVAN. *See* Idiopathic retinal vasculitis, aneurysms, and neuroretinitis
 Irvine-Gass syndrome, 157, 349
 ISCEV. *See* International Society for Clinical
 Electrophysiology of Vision
 Ischemia
 choroidal, 196, 196f
 macular, 98, 101, 115
 ocular. *See* Ocular ischemic syndrome
 Ishihara plates, for color vision testing, 54, 55f
 Isotretinoin, 305
 Jalili syndrome, 286
 Joubert syndrome, 285
 Juxtafoveal telangiectasia, 161
 Kayser-Fleischer ring, 362
 Kearns-Sayre syndrome, 283t, 294
 Keratitis, fungal, 239
Klebsiella pneumoniae endophthalmitis, 238
 Kyrieleis plaques, 244f
 Lacerations
 corneal, 359
 globe, 358
 scleral, 359
 Lacquer cracks, 211, 211f

- Lamellar macular hole, 28*f*
- Lamina cribrosa, dehiscences in, 218, 218*f*
- Laminin, 7
- Lampalizumab, 71
- Large colloid drusen, 274
- Laser(s)
- green, 373
 - infrared, 374
 - photochemical effect caused by, 374
 - photocoagulation using. *See* Photocoagulation
 - red, 374
 - transpupillary thermotherapy using, 380
 - vaporization caused by, 374–375
 - wavelength of, for photocoagulation, 373–375
 - yellow, 374
- Laser-pointer injury, 369
- Laser retinopexy, 376–377
- Laser surgery
- adverse effects of, 114
 - branch retinal vein occlusion treated with, 128
 - central retinal vein occlusion treated with, 135
 - diabetic macular edema treated with, 114–115
 - proliferative diabetic retinopathy treated with, 104–107
 - retinopathy of prematurity treated with, 185–186
- Lattice degeneration
- prophylactic treatment of, 319
 - retinal detachment and, 309–311, 310–311*f*, 316*f*, 319
- LCA. *See* Leber congenital amaurosis
- L cone, 54
- LCPUFAs. *See* Long-chain polyunsaturated fatty acids
- Leakage, hyperfluorescence and, 35
- Leber congenital amaurosis (LCA)
- characteristics of, 265–266
 - genes and loci associated with, 256*t*
 - retinal degeneration associated with, 281
- Leber stellate neuroretinitis, 242
- Lenses
- contact. *See* Contact lenses
 - high-plus-power, 375
 - for photocoagulation, 375, 376*f*
- Leptochoroid, 19
- Leukocoria, 342
- Lifestyle changes, for age-related macular degeneration, 71
- Ligament of Wieger, 7, 8*f*
- Light adaptation
- in electro-oculography, 50
 - in full-field (Ganzfeld) electroretinography, 42
- Lightning injuries, 357
- Limiting membrane
- external
 - anatomy of, 15
 - histology of, 11, 12*f* - internal
 - amacrine cells in, 15
 - anatomy of, 15
 - epiretinal membranes, 332
 - hemorrhagic detachment of, 171
 - histology of, 11, 12*f*
 - nonproliferative sickle cell retinopathy findings, 150
 - peeling of, 209
 - vitreous remnants on, 332
- middle
- anatomy of, 15
 - definition of, 16
 - histology of, 11, 12*f*
- Lincoff rules, 320, 322*f*
- Lipofuscin
- in lysosomes, 31
 - in retinal pigment epithelium, 32
- Liver abscesses, endogenous bacterial endophthalmitis and, 238
- Liver diseases, retinal degeneration associated with, 285
- Long-chain polyunsaturated fatty acids (LCPUFAs), 70
- Low-coherence light, in optical coherence tomography, 25
- Low vision
- rehabilitation for, 86, 260
 - therapies for, 86
- LRP5* gene, 345*f*
- Lupus vasculitis, 230–231, 231*f*
- Lutein
- age-related macular degeneration managed with, 70*t*
 - description of, 367
- Lyme disease, 245–246
- Lymphoma
- intracocular, 233–234, 234*f*
 - primary vitreoretinal, 233–234
 - veal, 234, 235*f*
- Lysosomal metabolic diseases, 291–292, 292*f*
- Lysosomes
- lipofuscin in, 31
 - outer segment digestion by, 17
- Macroaneurysms, retinal arterial, 147–148, 148*f*
- Macula
- adaptive optics scanning laser ophthalmoscope of, 13*f*
 - aminoglycoside effects on, 300
 - anatomy of, 9
 - atrophy of, 265, 265*f*
 - characteristics of, 10*t*
 - length of, 9
 - photic lesions of, 369
 - photocoagulation applications, 375–376
 - puckering of, 335
 - schisis of, 328
 - superior, rods in, 12
- Macular colobomas, 266
- Macular degeneration
- age-related. *See* Age-related macular degeneration (AMD)
 - exudative, 68
 - genes and loci associated with, 256*t*
- Macular detachment
- optic nerve pit with, 329*f*
 - vitelliform exudative, 272, 274*f*
- Macular dystrophies
- adult-onset vitelliform lesions, 272, 273*f*
 - atypical, 277
 - Best disease, 271, 272*f*
 - early-onset "drusenoid," 273–276, 274–275*f*
 - electroretinography findings in, 46, 47*f*
 - North Carolina, 277, 278*f*
 - occult, 277
 - pattern dystrophies, 276*f*, 276–277

- Sorsby, 275*f*, 275–276
 Stargardt disease. *See* Stargardt disease
 Macular edema
 cystoid (CME)
 birdshot uveitis in, 224
 cataract surgery as cause of, 157, 159, 260
 central retinal vein occlusion as cause of, 136*f*
 characteristics of, 156–157
 corticosteroids for, 159, 393
 in cytomegalovirus retinitis, 235
 differential diagnosis of, 157
 drugs that cause, 301
 edema sources in, 156–157
 etiologies of, 157
 fingolimod as cause of, 302
 fluorescein angiography of, 36*f*, 157
 incidence of, 157, 159
 in Irvine-Gass syndrome, 157
 nicotinic acid as cause of, 301
 optical coherence tomography of, 132*f*, 157, 158*f*
 petaloid, 157
 predisposing factors for, 157, 159
 pseudophakic
 definition of, 157
 imaging of, 394*f*
 optical coherence tomography of, 158*f*
 pars plana vitrectomy for, 394*f*
 in retinal dystrophies, 260, 260*f*
 retinal vein occlusion as cause of, 135. *See also*
 Retinal vein occlusion (RVO)
 retinitis pigmentosa and, 260
 spontaneous resolution of, 159
 subretinal diseases that cause, 157
 taxanes as cause of, 301
 treatment of, 159
 vision loss caused by, 225
 vitrectomy for, 159, 393, 394*f*
 diabetic (DME)
 cataract surgery effects on, 116
 center-involved, 92, 109, 110*f*
 classification of, 109–110, 110*f*
 clinically significant, 92, 110, 114
 contrast sensitivity issues in, 56
 definition of, 92
 focal, 110
 mechanism of, 108, 109*f*
 non-center-involved, 109, 111*f*
 optical coherence tomography of, 111*f*
 spectral-domain optical coherence tomography of, 109*f*, 125
 treatment of
 afibercept, 113
 anti-VEGF therapy, 101, 110–113
 bevacizumab, 113
 corticosteroids, 113–114
 Diabetic Retinopathy Clinical Research Network findings, 112*f*, 113
 intravitreal steroids, 101
 laser surgery, 114–115, 376
 overview of, 110–111
 pars plana vitrectomy, 115
 ranibizumab, 111–112, 112*f*
 surgery, 114–115, 388
 vitrectomy, 388
 vision loss caused by, 94
 diffuse, 110, 111*f*
 drugs that cause, 301–302, 302*f*
 Early Treatment Diabetic Retinopathy Study
 findings for, 99–100
 focal, 110, 111*f*
 in gyrate atrophy, 268
 panretinal photocoagulation effects on, 106, 379
 Macular exudates, 124*f*
 Macular halo, 292*f*
 Macular holes
 contusion injury as cause of, 315
 fellow-eye risk for development of, 339
 formation of, 339, 340*f*
 idiopathic
 description of, 337–339, 338*f*
 vitrectomy for, 384–385, 385*f*
 International Vitreomacular Traction Study
 Classification System for, 336*t*
 lamellar, 28*f*
 management of, 339–340
 optical coherence tomography of, 27*f*
 in pathologic myopia, 209
 posttraumatic, 355–357, 356*f*
 rhegmatogenous retinal detachment caused by, 330, 330*f*
 spontaneous resolution of, 340
 stage 0, 339
 stage 1, 339–340
 stage 2, 339
 stage 3, 339
 stage 4, 339
 surgical management of, 339–340
 Macular pits, 356
 Macular telangiectasia
 early, 277
 type 1, 161
 type 2, 161–164, 162–164*f*
 type 3, 164–165
 volume rendering of, 31
 Macular translocation surgery, 85
 Maculopathy
 acute exudative polymorphous vitelliform, 287
 acute idiopathic (AIM), 228–229
 adult-onset vitelliform
 fluorescein angiography of, 68
 spectral-domain optical coherence tomography of, 67–68, 68*f*
 bull's-eye
 chloroquine toxicity as cause of, 295, 296*f*
 clofazimine as cause of, 298
 in neuronal ceroid lipofuscinoses, 289
 cellophane, 335
 hypotony, 201
 optic pit, 328–329, 329*f*
 paracentral acute middle (PAMM), 143
 Magnetic resonance imaging (MRI)
 intraocular foreign body evaluations, 353
 primary vitreoretinal lymphoma evaluations, 234
 Magnification, in indirect ophthalmoscope/ophthalmoscopy, 21

- Malattia Leventinese, 274–275
 Malignant hypertension, 196
 Mannosidosis, 282t
 MAR. *See* Melanoma-associated retinopathy
 MARINA study, 80–81
 Maternally inherited diabetes and deafness (MIDD), 283t, 294, 294f
 M cone, 54
 MEK inhibitors, 299, 299f
 Melanin, 32–33, 367, 373, 374f
 Melanolipofuscin, 33
 Melanolysosomes, 32
 Melanoma-associated retinopathy (MAR), 286
 MELAS. *See* Mitochondrial encephalopathy, lactic acidosis, strokelike episodes
 Meridional complex
 definition of, 10
 illustration of, 10f
 Meridional folds
 definition of, 10, 312
 retinal detachment and, 312
 Methanol toxicity, 301
 Methotrexate, for primary vitreoretinal lymphoma, 234
 Methoxyflurane, 303
 MEWDS. *See* Multiple evanescent white dot syndrome
 mfERG. *See* Multifocal electroretinography
 MHA-TP. *See* Microhemagglutination assay for *T pallidum* antibodies
 Microaneurysms, in nonproliferative diabetic retinopathy, 100f
 Microelectromechanical systems, in swept-source optical coherence tomography, 25–26
 Microexplosions, 375
 Microhemagglutination assay for *T pallidum* antibodies (MHA-TP), 241
 Micronutrients, for age-related macular degeneration, 69–71
 MIDD. *See* Maternally inherited diabetes and deafness
 Middle limiting membrane (MLM)
 anatomy of, 15
 definition of, 16
 histology of, 11, 12f
 Midget bipolar cell, 13
 “Milky Way” sign, in Vogt-Koyanagi-Harada disease, 232
 Mitochondrial disorders, 293–294
 Mitochondrial encephalopathy, lactic acidosis, strokelike episodes (MELAS), 283t, 294
 Mitochondrial myopathies, 293f, 293–294
 Mittendorf dot, 340
 Mizuo-Nakamura phenomenon, 253, 253f
 MLM. *See* Middle limiting membrane
 Monochromatism, 250t
 Mosquito-borne diseases, 246–247
 Motion artifacts, in optical coherence tomography angiography, 29
 Motion contrast, 28
 MRI. *See* Magnetic resonance imaging
 Mucopolysaccharidoses, 282–283t, 290–291
 Müller cells
 defect of, 162
 footplates of, 15, 15f, 326
 outer extent of, 15
 retinoschisin and, 279
 Multi-Ethnic Study of Atherosclerosis (MESA), 62
 Multifocal choroiditis, 220t, 225–226, 226f
 Multifocal electroretinography (mfERG), 45, 48–49f
 Multiple evanescent white dot syndrome (MEWDS), 220t, 223–224, 224f
 Multiple sclerosis
 intermediate uveitis associated with, 231
 optic nerve conduction delay in, 52
Mycobacterium tuberculosis, 240
 Myoid, 12
 Myopia
 historical treatments for, 208
 pathologic
 chorioretinal atrophy in, 214f
 choroidal neovascularization caused by, 89, 90f, 211f, 211–212
 choroid in, 212–216, 214–215f
 definition of, 207
 factors associated with, 207
 glaucoma in, 218, 218f
 global prevalence of, 207
 macular holes in, 209
 ocular expansion related to, 216
 optic nerve in, 217–218, 218f
 prevalence of, 207
 prevention of, 207–208
 retina in, 207–216, 209–215
 sclera in, 216–217, 217f
 swept-source optical coherence tomography of, 209f
 traction effects on retinal vessels in, 209
 topiramate as cause of, 305
 Myopic macular schisis, 209, 210f
 Myotonic dystrophy, 282t
 N95, 45
 NARP. *See* Neurogenic muscle weakness, ataxia, and retinitis pigmentosa
 Nausea and vomiting, fluorescein angiography as cause of, 36
 NCLs. *See* Neuronal ceroid lipofuscinoses
 Nd:YAG laser
 cystoid macular edema treated with, 159
 mechanism of, 367
 ocular injury caused by, 367
 Near-infrared fundus autofluorescence, 32–33
 Near periphery, 9
 Necrotizing herpetic retinitis, 236–237, 236–237f, 238t
 Necrotizing retinochoroiditis, 243
 Needle perforation/penetration injuries, of globe, 358, 395f, 395–396
 Neonatal adrenoleukodystrophy, 283t, 290, 291f
 Neovascularization
 in branch retinal vein occlusion, 125, 128, 129f
 in central retinal vein occlusion, 125
 in central serous chorioretinopathy, 194
 choroidal. *See* Choroidal neovascularization
 iris
 in branch retinal vein occlusion, 128–129, 129f
 in central retinal artery occlusion, 146
 in central retinal vein occlusion, 133, 135
 in diabetes mellitus, 107
 in radiation retinopathy, 170
 optic nerve head, 128, 129f

- peripheral, 232
 peripheral retinal, 154*t*
 in proliferative sickle cell retinopathy, 151, 153*f*
 in retinopathy of prematurity, 180–181
 sea fan, 151, 153*f*
 subretinal, 162
- Neovascular proliferation, in proliferative diabetic retinopathy, 102
- Neovascular (“wet”) age-related macular degeneration
 aflibercept for, 82–83
 Amsler grid testing of, 71
 antiangiogenic therapies for, 79–80
 bevacizumab for, 83–85, 84*t*
 choroidal neovascularization associated with, 71–79.
See also Choroidal neovascularization
 combination treatment for, 85
 differential diagnosis of, 76, 79
 intravitreal injections, 85
 laser photocoagulation for, 79
 low vision therapies for, 86
 macular translocation surgery for, 85
 management of, 79–86, 81*f*, 82*t*, 84*t*
 pegaptanib for, 80
 photodynamic therapy for, 79
 polypoidal choroidal vasculopathy, 75
 prevalence of, 61
 ranibizumab for, 80–82, 82*t*
 signs and symptoms of, 71
 submacular hemorrhage in, 85, 385
 surgical treatment for, 85–86
 treatment effect modifiers, 85
 verteporfin for, 79
- Nerve fiber layer (NFL)
 anatomy of, 15
 cotton-wool spots, 122, 122*f*, 140, 140*f*
 histology of, 11, 12*f*
 infarction of, 140
 measurement of, 26
 optical coherence tomography measurement of, 218
- Nerve head sign of sickling, 154
- Neurogenic muscle weakness, ataxia, and retinitis pigmentosa (NARP), 294
- Neuromuscular disorders, retinal degeneration associated with, 285
- Neuronal ceroid lipofuscinoses (NCLs), 283*t*, 289, 290*f*
- NFL. *See* Nerve fiber layer
- Nicotinic acid, 301
- Niemann-Pick disease, 291
- Night blindness
 in choroioderemia, 267
 congenital stationary
 electroretinography findings in, 46, 47*f*, 251, 252*f*
 retinitis pigmentosa versus, 251
 subtypes of, 251
 dark adaptometry evaluations, 58
 electroretinography evaluations, 46
 fundus albipunctatus, 252, 253*f*
 in gyrate atrophy, 268
- Night vision abnormalities, 251–253, 251–253*f*
- Nonarteritic anterior ischemic optic neuropathy, visual evoked potentials in, 52
- Non-center-involved diabetic macular edema, 109, 111*f*
- Noncontact indirect biomicroscopy, 22
 Non-contact lens, indirect ophthalmoscopy using, 22
- Nonexudative macular degeneration, contrast sensitivity issues in, 56
- Non-Hodgkin lymphoma of the central nervous system.
See Primary vitreoretinal lymphoma
- Non-insulin-dependent diabetes mellitus, 91
- Nonneovascular (“dry”) age-related macular degeneration
 Amsler grid testing for, 68–69
 differential diagnosis of, 67–68
 disproven treatment approaches for, 71
 drusen associated with. *See* Drusen
 education regarding, 68
 focal atrophy in, 66
 follow-up for, 68
 geographic atrophy in, 64, 66, 67*f*, 68
 hydrochloroquine toxicity versus, 68
 hyperacuity testing for, 69
 lifestyle changes for, 71
 management of, 68–71
 micronutrients for, 69–71
 preferential hyperacuity perimetry for, 69
 prevalence of, 61
 retinal pigment epithelium abnormalities in, 66–67
 shape-discrimination hyperacuity for, 69
- Nonproliferative diabetic retinopathy (NPDR)
 anti-VEGF therapy for, 101–102
 clinical findings in, 99
 definition of, 91
 intraretinal hemorrhages associated with, 100*f*
 intraretinal microvascular abnormalities in, 100*f*
 microaneurysms associated with, 100*f*
 optical coherence tomography angiography of, 94*f*
 panretinal photocoagulation for, 101
 posterior vitreous detachment creation for, 102
 progression of, to proliferative diabetic retinopathy, 101
 ranibizumab for, 102
 scatter photocoagulation for, 116
 severity of, 95*t*, 99
 treatment of, 101–102
 venous beading associated with, 100*f*
 vision loss in, 101
- Nonproliferative sickle cell retinopathy (NPSR)
 branch retinal artery occlusions in, 152*f*
 characteristics of, 149–150
 imaging of, 150–152*f*
 retinal arteriolar occlusions in, 151*f*
 salmon-patch hemorrhage in, 150*f*
- Nonsyndromic panretinal dystrophies, 258–259
- North Carolina macular dystrophy, 277, 278*f*
- NPDR. *See* Nonproliferative diabetic retinopathy
- NPSR. *See* Nonproliferative sickle cell retinopathy
- NR2E3 gene, 49, 266
- NRTIs. *See* Nucleoside reverse transcriptase inhibitors
- Nuclear sclerotic cataract, 402, 402*t*
- Nucleoside reverse transcriptase inhibitors (NRTIs), 299
- Nystagmus
 visual evoked potentials in, 53
 wandering, 266

- OAT gene, 269
- Occclusive arterial disease
- branch retinal artery
 - emboli that cause, 141, 142^f
 - hypertensive retinopathy and, 122
 - imaging of, 141^f
 - management of, 142
 - multiple, 152^f
 - in nonproliferative sickle cell retinopathy, 152^f
 - retinal infarction caused by, 141
 - in Susac syndrome, 156
 - branch retinal vein
 - aflibercept for, 135
 - at arteriovenous crossing, 126
 - bevacizumab for, 135
 - clinical findings of, 125–127, 126^f
 - corticosteroids for, 137–138
 - diabetes mellitus and, 128
 - fluorescein angiography of, 129^f
 - glaucoma as risk factor for, 125
 - hypertensive retinopathy and, 122
 - intraretinal hemorrhages associated with, 125, 126^f
 - macular laser surgery for, 128
 - neovascularization in, 125, 128, 129^f
 - pars plana vitrectomy for, 130
 - pharmacologic management of, 135–138
 - prognosis for, 128
 - ramibizumab for, 135
 - risk factors for, 127–128
 - scatter photocoagulation for, 128–130
 - spontaneous resolution of, 125
 - surgical management of, 128–130
 - treatment of, 128–130
 - triamcinolone for, 137
 - vision loss caused by, 128
 - central retinal artery
 - anti-VEGF therapy for, 146
 - causes of, 144
 - ciliary artery occlusion with, 144, 145^f
 - electroretinography findings in, 50
 - emboli as cause of, 144
 - giant cell arteritis as cause of, 145
 - illustration of, 16^f, 144^f
 - iris neovascularization in, 146
 - management of, 146
 - retinal infarction caused by, 143
 - spectral-domain optical coherence tomography of, 144^f
 - symptoms and signs of, 143
 - vision loss caused by, 143–144
 - central retinal vein occlusion. *See* Central retinal vein occlusion (CRVO)
 - Occulsive retinopathy, 300–301
 - Occult choroidal neovascularization, 72–73
 - Occult macular dystrophies, 277
 - Occupational light toxicity, 369
 - Ocriplasmin, 337, 340
 - OCT. *See* Optical coherence tomography
 - OCTA. *See* Optical coherence tomographic angiography
 - Ocular albinism
 - characteristics of, 288
 - pattern-appearance visual evoked potentials in, 53
 - Ocular argyrosis, 306
 - Ocular expansion, pathologic myopia as cause of, 216
 - Ocular histoplasmosis syndrome (OHS), choroidal neovascularization caused by, 86–87, 88^f
 - Ocular ischemic syndrome (OIS)
 - central retinal vein occlusion versus, 134
 - course of, 139
 - definition of, 138
 - etiology of, 139
 - ischemic cardiovascular disease associated with, 139
 - retinopathy caused by, 138
 - stroke rate in, 139
 - symptoms and signs of, 138–139
 - treatment of, 140
 - Ocular-retinal developmental disease, genes and loci associated with, 256^t
 - Ocular surgery, sympathetic ophthalmia secondary to, 233. *See also* Surgery
 - Ocular trauma. *See* Trauma
 - Ocular Trauma Score, 364, 364^t
 - Oculocutaneous albinism
 - description of, 288
 - pattern-appearance visual evoked potentials in, 53
 - Oculodentodigital dysplasia syndrome, 282^t
 - Oculodigital reflex, 266
 - Oguchi disease, 253
 - “Ohno” sign, 233
 - OHS. *See* Ocular histoplasmosis syndrome
 - OIS. *See* Ocular ischemic syndrome
 - Olivopontocerebellar atrophy, 282^t
 - Omega-3 long-chain polyunsaturated fatty acids, 70
 - OMIM. *See* Online Mendelian Inheritance in Man (OMIM) website
 - ONL. *See* Outer nuclear layer
 - Online Mendelian Inheritance in Man (OMIM) website, 255
 - Opacities, vitreous
 - amyloidosis, 348, 349^f
 - asteroid hyalosis, 346^f, 346–347
 - bilateral, 348
 - cholesterolosis, 348
 - pigment granules, 348
 - vitrectomy for, 386
 - vitreous degeneration and detachment associated, 344
 - vitreous hemorrhage, 347
 - Open-angle glaucoma. *See also* Glaucoma
 - in central retinal vein occlusion, 133
 - vitrectomy as risk factor for, 402
 - Operculated retinal holes, 315–316
 - Ophthalmic artery occlusion, 146, 147^f
 - Ophthalmic examinations, diabetes mellitus-related, 93–94, 95^t
 - Ophthalmic instrumentation, phototoxicity from, 368–369
 - Ophthalmoscopy
 - direct
 - limitations of, 21
 - retinal disease evaluations using, 21
 - indirect
 - illumination in, 21
 - posterior vitreous detachment diagnosed using, 309, 331
 - retinal disease evaluations using, 21–22
 - retinal disease evaluations using, 21–22
 - scanning laser. *See* Scanning laser ophthalmoscopy

- OPL. *See* Outer plexiform layer
- Opportunistic infections, 235–236
- Optical coherence tomographic angiography (OCTA)
- artifacts in, 29, 30*f*
 - choroidal circulation abnormalities, 198
 - choroidal neovascularization on, 75–76, 76–78*f*, 192
 - depth resolution using, 29
 - diabetic retinopathy on, 93, 94*f*
 - fluorescein angiography versus, 29
 - macular telangiectasia type 2 on, 163, 164*f*
 - motion artifacts in, 29
 - projection artifacts in, 29, 30*f*
 - pseudoxanthoma elasticum on, 199*f*
 - retinal capillary layers on, 16
 - retinal disease evaluations using, 28–29
 - retinal vasculature on, 29, 30*f*
 - severity of, 93, 94*f*
- Optical coherence tomography (OCT)
- acute idiopathic maculopathy on, 228
 - acute macular neuroretinopathy on, 228
 - acute posterior multifocal placoid pigment epitheliopathy on, 221*f*, 222
 - acute zonal occult outer retinopathy on, 227, 227*f*
 - cancer-associated retinopathy on, 287*f*
 - central serous chorioretinopathy evaluations, 32
 - choroidal neovascularization on, 192, 194
 - cystoid macular edema on, 132*f*, 157, 158*f*
 - definition of, 25
 - diabetic macular edema on, 111*f*
 - drusen on, 65–66
 - enhanced depth imaging, 25
 - epiretinal membranes on, 335, 383*f*
 - eye movement tracking with, 27
 - low-coherence light in, 25
 - macular hole on, 27*f*
 - myopic macular schisis on, 210*f*
 - nerve fiber layer measurement using, 218
 - nomenclature terminology for, 26–27
 - peripapillary intrachoroidal cavitations on, 215, 215*f*
 - pigment epithelial detachment on, 74*f*
 - posterior vitreous detachment on, 309, 332
 - retinal disease evaluations using, 25–27, 27*f*
 - solar retinopathy on, 368*f*
 - spectral-domain
 - adult-onset vitelliform maculopathy on, 67–68, 68*f*
 - alkyl nitrite findings, 300, 300*f*
 - chloroquine toxicity monitoring uses of, 297
 - choroidal neovascularization on, 73–75, 75*f*
 - diabetic macular edema on, 109*f*, 125
 - drusen on, 64*f*, 65
 - epiretinal membranes on, 335*f*
 - Gaucher disease on, 291
 - pathologic myopia on, 90*f*
 - reticular pseudodrusen on, 65*f*
 - retinal layers on, 10–11, 12*f*
 - retinitis pigmentosa findings, 263*f*
 - sensitivity of, 26
 - swept-source optical coherence tomography
 - versus, 25–26
- swept-source
- pathologic myopia findings, 209*f*
 - sensitivity of, 26
- spectral-domain optical coherence tomography
- versus, 25–26
- time-domain, 25
- vitreoretinal traction syndrome on, 337, 337*f*
- volume rendering, 27, 28*f*
- X-linked retinoschisis on, 278, 278*f*
- Optically empty vitreous, hereditary
- haloideoretinopathies with, 342–343, 343*f*
- Optic atrophy, genes and loci associated with, 256*t*
- Optic nerve
- conduction delay, visual evoked potentials of, 52
 - in pathologic myopia, 217–218, 218*f*
 - peripapillary intrachoroidal cavitations, 215, 215*f*
- Optic nerve head (optic disc)
- angiomaticous lesion of, 242
 - avulsion of, 365, 365*f*
 - drusen of, 260
 - edema of, 234, 349
 - hyperemia of, 232
 - neovascularization of, 128, 129*f*, 170
 - in pathologic myopia, 217–218, 218*f*
 - subretinal hemorrhage, 355*f*
- Optic neuropathy, hypertensive, 123, 125
- Optic pit(s), 328–329, 329*f*
- Optic pit maculopathy, 328–329, 329*f*
- Ora bays
- definition of, 10
 - illustration of, 11*f*
 - retinal tears near, 312
- Oral contraceptives, central retinal vein occlusion risks, 134
- Ora serrata
- anatomy of, 7, 11*f*
 - binocular indirect ophthalmoscopy of, 22
 - definition of, 10
- Oscillary potentials, 43*f*, 43–44
- Outer nuclear layer (ONL), 11, 12*f*
- Outer plexiform layer (OPL)
- histology of, 11, 12*f*
 - oxygen supply to, 16
 - paracentral acute middle maculopathy of, 143
 - typical degenerative retinoschisis findings, 326
- Outer-schisis-layer holes, 327, 327*f*
- Outer segments
- of cones, 11, 12*f*
 - phagocytosis of, 17
 - of rods, 11, 12*f*
- Oxalate, 303
- Oxygen
- hyalocyte consumption of, 7
 - retinal supply of, 16*f*, 16–17
 - supplementation of, retinopathy of prematurity and, 184
- P50, 45, 47*f*
- Pachychoroid, 19, 76
- Paclitaxel, 301
- PAMM. *See* Paracentral acute middle maculopathy
- Panel D-15 test (Farnsworth), 55*f*, 55–56
- Panretinal dystrophies
- clinical findings of, 261, 263*f*
 - Coats reaction associated with, 260
 - nonsyndromic, 258–259
 - syndromic, 259

- Panretinal photocoagulation (PRP)
 adverse effects of, 106
 applications of, 376–377, 377f
 central retinal vein occlusion treated with, 135
 idiopathic retinal vasculitis, aneurysms, and
 neuroretinitis treated with, 156
 iris neovascularization and, 135
 macular edema exacerbation by, 379
 nonproliferative diabetic retinopathy treated
 with, 101
 oxygen tension affected by, 104
 proliferative diabetic retinopathy treated with, 104,
 106, 106f
 retinal vein occlusion treated with, 126
- Panuveitis. *See also* Uveitis
 Ebola virus, 247
 multifocal choroiditis with, 226f
 in syphilitic uveitis, 241
 in toxocariasis, 245
 in Vogt-Koyanagi-Harada disease, 233
- Paracentral acute middle maculopathy (PAMM), 143
- Paracentral scotomas, 228, 367
- Parafovea
 characteristics of, 10t
 definition of, 9
- Parafoveal macula, 9f
- Paraneoplastic retinopathies, 286–287
- Parasitic infections, 244
- Parinaud oculoglandular syndrome, 242
- Pars plana, 10
- Pars plana vitrectomy. *See also* Vitrectomy
 branch retinal vein occlusion treated with, 130
 central retinal vein occlusion treated with, 135
 complications of, 402t, 402–403
 cystoid macular edema treated with, 393, 394f
 diabetic macular edema treated with, 115, 388
 diabetic retinopathy complications treated
 with, 107
 epiretinal membranes treated with, 382–383
 idiopathic macular holes treated with,
 384–385, 385f
 indications for, 381
 intraocular foreign body removed with, 361
 needle perforation/penetration of globe treated
 with, 396
 posteriorly dislocated intraocular lenses treated
 with, 393
 postoperative endophthalmitis treated with
 acute-onset, 388–390, 390f
 bleb-associated, 390–391, 391f
 chronic (delayed-onset), 390, 391f
 retained lens fragments after phacoemulsification
 treated with, 391–393, 392f
 rhegmatogenous retinal detachment treated with,
 400f, 400–401
 submacular hemorrhage treated with, 385, 386f
 suprachoroidal hemorrhage treated with, 394–395,
 395f
 technique for, 381
 tractional retinal detachment treated with, 387–388
 vitreous opacities treated with, 386
- Pars planitis, 231
- Patellar fossa, 7
- Pathologic (high) myopia
 chorioretinal atrophy in, 214f
 choroidal neovascularization in, 89, 90f, 211f, 211–212
 choroid in, 212–216, 214–215f
 definition of, 207
 factors associated with, 207
 glaucoma in, 218, 218f
 global prevalence of, 207
 macular holes in, 209
 ocular expansion related to, 216
 optic nerve in, 217–218, 218f
 prevalence of, 207
 prevention of, 207–208
 retina in, 207–216, 209–215
 sclera in, 216–217, 217f
 swept-source optical coherence tomography of, 209f
 traction effects on retinal vessels in, 209
- Pattern-appearance stimulation, of visual evoked
 potentials, 53
- Pattern dystrophies, 67, 272, 276f, 276–277
- Pattern electroretinography (PERG), 45–46, 46–49f
- Pattern-reversal visual evoked potential, 52, 53f
- Patton lines, 201
- Paving-stone degeneration, 313, 314f
- PCIOLs. *See* Posteriorly dislocated intraocular lenses
- PCV. *See* Polypoidal choroidal vasculopathy
- PDR. *See* Proliferative diabetic retinopathy
- PDT. *See* Photodynamic therapy
- Peau d'orange, 87, 89f
- PED. *See* Pigment epithelial detachments
- Pegaptanib, for neovascular age-related macular
 degeneration, 80
- Pelizaeus-Merzbacher disease, 283t
- Pelli-Robson test, 56–57, 57f
- Penetrating ocular injury, sympathetic ophthalmia
 secondary to, 233. *See also* Trauma
- Pentosan polysulfate, 300
- Perfluorocarbon (C_3F_8), 382
- Perfluoropropane, 382, 401
- PERG. *See* Pattern electroretinography
- Pericytes, 93
- Perifovea
 characteristics of, 10t
 definition of, 9
- Perifoveal macula, 9f
- Peripapillary intrachoroidal cavitations, 215, 215f
- Peripheral cystoid degeneration
 description of, 314
 reticular, 326
 typical, 326
- Peripheral granuloma, in toxocariasis, 244, 245f
- Peripheral neovascularization, vitreous hemorrhage
 associated with, 232
- Peripheral retina
 definition of, 10
 excavations, 312–313
- Peripheral retinal neovascularization, 154t
- Peripheral vitreous, 7
- Periphlebitis, in cytomegalovirus retinitis, 235
- Peroxisomal disorders, 290
- Persistent fetal vasculature (PFV), 341–342
- Phacoemulsification, vitrectomy for retained lens
 fragments after, 391–393, 392f

- Phagocytosis
of outer segments, 17
pathologic changes that affect, 17
retinal pigment epithelium cell, 17
- Phakomatoses
definition of, 165
retinal cavernous hemangioma, 168, 169*f*
von Hippel–Lindau syndrome, 165–168, 166–167*f*
Wyburn–Mason syndrome, 168
- Pharmacogenomic testing, for age-related macular degeneration, 63
- Phenothiazines, 297–298, 298*f*
- Phosphodiesterase-5 inhibitors, 304
- Photic damage, 367–369, 368*f*
- Photochemical injury, 367
- Photocoagulation
anesthesia for, 375
Bruch membrane rupture caused by, 378
choroidal detachment caused by, 379, 379*f*
clinically significant diabetic macular edema treated with, 110
Coats disease treated with, 161
complications of, 378–379
diabetic macular edema treated with, 376
- Early Treatment Diabetic Retinopathy Study findings
for, 100
exudative retinal detachment caused by, 379
factors that affect, 373
foveal burns caused by, 378
indications for, 375–377
lasers used in
alternative systems, 377–378
wavelength of, 373–375
lenses for, 375, 376*f*
macular applications of, 375–376
neovascular age-related macular degeneration treated with, 79
parameters for, 375–377
principles of, 373–379
proliferative diabetic retinopathy treated with
description of, 104
in pregnancy, 94
retinal arterial macroaneurysms treated with, 147
retinal cavernous hemangioma treated with, 168
retinal holes caused by, 378
retinal lesions caused by, 378–379
retinal vascular lesions treated with, 377
retinopathy of prematurity treated with, 186*f*
slit-lamp delivery systems, 377
vitreous hemorrhage caused by, 379
von Hippel–Lindau syndrome treated with, 167
- Photodynamic therapy (PDT). *See also* Verteporfin
applications of, 380
central serous chorioretinopathy treated with, 194
choroidal neovascularization treated with, 212, 213*f*
380
complications of, 380
half-fluence, 380
neovascular age-related macular degeneration treated with, 79
photosensitivity reactions caused by, 380
polypoidal choroidal vasculopathy treated with, 76
ranibizumab added to, 85
- steps involved in, 380
von Hippel–Lindau syndrome treated with, 167
- Photophobia, 46, 264
- Photopsias. *See also* Floaters
electroretinography findings in, 46
in posterior vitreous detachment, 308
in rhegmatogenous retinal detachment, 320
- Photoreceptor(s)
age-related changes in, 61
cone. *See* Cone(s)
density of, 11
distribution of, 11
drusen effects on, 64
iron damage to, 362
rod. *See* Rod(s)
as waveguides, 33
- Photoreceptor dystrophies
cone, 264–265
cone–rod, 264–265
rod–cone, 261–264, 262–264*f*
- Phototoxicity from ophthalmic instrumentation, 368–369
- PHP. *See* Preferential hyperacuity perimetry
- PIC. *See* Punctate inner choroiditis
- PIER study, 80
- Pigmented paravenous retinopathy, 263
- Pigment epithelial detachments (PEDs)
definition of, 64
drusenoid, 64, 272, 274*f*
fibrovascular
anti-VEGF therapy for, 201*f*
description of, 72–73
retinal pigment epithelial tear risks, 82
in hypertensive choroidopathy, 123
optical coherence tomography of, 74*f*
serous, 72–73, 74*f*
subfoveal, 74–75*f*
- Pigment granules, 348
- Pigments, in retinal pigment epithelium, 12*f*, 17
- Pioglitazone, 301
- Planoconcave lenses, 375
- Plus disease, 176–177, 176*t*, 178*f*, 178*t*, 179, 179*f*, 184*t*, 186, 186*f*
- Pneumatic displacement, 85
- Pneumatic retinopexy, for rhegmatogenous retinal detachment, 324, 397–398, 398*f*
- POHS. *See* Presumed ocular histoplasmosis syndrome
- Polyoidal choroidal vasculopathy (PCV)
central serous chorioretinopathy versus, 193
clinical presentation of, 75
definition of, 75
indocyanine green angiography for, 38, 38*f*
subretinal hemorrhage associated with, 76
verteporfin for, 76
- Pooling, fluorescein, 35, 36*f*
- PORN. *See* Progressive outer retinal necrosis
- Positron emission tomography, of uveal lymphoma, 234
- Posterior capsular opacification, 260
- Posterior chamber intraocular lenses (PCIOLs), 393
- Posterior ciliary arteries
anatomy of, 195*f*
choroid blood supply from, 19, 20*f*, 195*f*
- Posterior persistent fetal vasculature, 342
- Posterior pole granuloma, 245

- Posterior segment
anterior segment surgery complications of,
vitrectomy for, 388–396
- Behcet disease involvement of, 230
- blunt trauma to, 353
- laser effects on, 374
- Posterior uveal bleeding syndrome, 75
- Posterior uveitis
electroretinography findings in, 44
- intermediate uveitis, 231
- Posterior vitreoschisis, 332–333
- Posterior vitreous detachment (PVD)
age-related, 307–308
- anatomy of, 331
- atrophic holes presenting with, 318
- cholesterolosis and, 348
- conditions associated with, 307
- definition of, 331
- diagnosis of, 331
- epiretinal membranes. *See* Epiretinal membranes (ERM)
- examination of, 309
- fibroglial tissue in, 331
- floaters associated with, 308–309
- idiopathic macular holes, 337–339, 338f
- imaging of, 308f
- indirect ophthalmoscopy of, 309, 331
- management of, 309
- myopia macular retinoschisis in, 209
- nonproliferative diabetic retinopathy progression
affected by, 102
- optical coherence tomography of, 309, 332
- in pars plana vitrectomy for diabetic macular edema, 115
- pathologic conditions caused by, 332
- photopsias associated with, 308
- prevalence of, 331
- retinal breaks associated with, 309
- retinal tears caused by, 307, 308f,
309
- risk factors for, 309
- signs and symptoms of, 308
- slit-lamp biomicroscopy of, 331
- vitrectomy for, 333f, 359
- vitreomacular adhesions, 336, 336t
- vitreomacular traction syndrome, 332, 332f, 336t,
336–337, 337f
- vitreous hemorrhage associated with, 309
- Postoperative endophthalmitis, 388–391, 390–391f
- Posttraumatic endophthalmitis, 362–363
- Precortical vitreous pocket, 7, 8f
- Prednisone, for herpetic retinitis, 238t
- Preeclampsia, 197f
- Preferential hyperacuity perimetry (PHP), 69
- Pregnancy
diabetic retinopathy in
progression of, 93–94
proliferative, 94
- fluorescein angiography in, 36
- Toxoplasma gondii* exposure, 243
- Zika virus exposure during, 247
- Premacular bursa, 7, 8f
- Pre papillary vascular loops, 341, 341f
- Preretinal macular fibrosis, 335
- Preretinal tract, 7
- Presumed ocular histoplasmosis syndrome (POHS), 87
- Prethreshold disease (retinopathy of prematurity), 178t,
179, 185
- Primary vitreoretinal lymphoma, 233–234
- Procainamide, 300
- Progressive outer retinal necrosis (PORN) syndrome,
236–237, 237f
- Projection artifact, 29, 30f
- Proliferative diabetic retinopathy (PDR)
anti-VEGF therapy for, 103–104, 386
- complications of, 103–108
- definition of, 91–92
- description of, 91–92
- extraretinal fibrovascular proliferation associated
with, 102
- high-risk characteristics of, 103
- laser surgery for, 104–107
- management of, 103–108
- neovascular proliferation associated with, 102
- neovascularization in, 151
- nonproliferative diabetic retinopathy progression
to, 101
- nonsurgical management of, 103–104
- optical coherence tomography angiography of, 94f
- panretinal photocoagulation for, 104, 106, 106f
- photocoagulation for, 94
- in pregnancy, 94
- proangiogenic factors in, 102
- proliferative sickle cell retinopathy versus, 151
- ranibizumab for, 104
- scatter photocoagulation for, 116
- severe carotid artery occlusive disease associated
with, 98
- severity of, 95t
- stages of, 102
- steroids for, 103–104
- surgical management of, 104–107
- tractional retinal detachment caused by, 103, 108,
387–388
- vitreous hemorrhage caused by, 103, 103f, 107–108,
386–387
- Proliferative vitreoretinopathy (PVR), 320, 323f, 323t,
323–324
- Propionibacterium acnes*, 390
- Protanomalous dichromatism, 250t
- Protanomalous trichromatism, 250t
- Protan red-green color deficiency, 54
- Protein C deficiency, 134
- Protein S deficiency, 134
- PRP. *See* Panretinal photocoagulation
- PRPH2* gene, 272, 273f
- Pseudodrusen
characteristics of, 200, 200f
- imaging of, 200
- in pseudoxanthoma elasticum, 198
- reticular, 65f, 65–66
- scanning laser ophthalmoscopy of, 24
- Pseudoisochromatic plates, for color vision testing,
54, 55f
- Pseudophakia, retinal detachment risks associated with,
319

- Pseudophakic cystoid macular edema
definition of, 157
imaging of, 394f
optical coherence tomography of, 158f
pars plana vitrectomy for, 394f
- Pseudo-POHS. *See* Pseudo-presumed ocular histoplasmosis syndrome
- Pseudo-presumed ocular histoplasmosis syndrome (pseudo-POHS), 225
- Pseudoxanthoma elasticum (PXE)
angiod streaks and, 87, 89f
Bruch membrane calcification in, 19
optical coherence tomographic angiography of, 199f
pseudodrusen in, 198
- Psychophysical testing
color vision, 54–56, 55f
contrast sensitivity, 56–57, 57f
dark adaptometry, 57–58
tests used in, 53–54
- Punctate inner choroiditis (PIC), 225
- Pupillary-block glaucoma, in retinopathy of prematurity, 181
- Puttscher flecken, 171
- Puttscherlike retinopathy, 171–173, 172f, 173t
- Puttscher retinopathy, 171–173, 173t
- PVD. *See* Posterior vitreous detachment
- PVR. *See* Proliferative vitreoretinopathy
- PXE. *See* Pseudoxanthoma elasticum
- Quadruple therapy, for toxoplasmic retinochoroiditis, 243
- Quinine, 301
- Raccoons, 246
- Race
age-related macular degeneration and, 62
polypoidal choroidal vasculopathy and, 75
sickle cell hemoglobinopathies and, 149, 154
systemic lupus erythematosus and, 230
Vogt-Koyanagi-Harada disease and, 232
- Radial peripapillary capillary network, 16
- Radiation
ionizing, retinopathy caused by exposure to, 170f, 170–171
primary vitreoretinal lymphoma treated with, 234
- Radiation retinopathy, 170f, 170–171
- RAINBOW study, 187
- Ranibizumab
bevacizumab and, comparison between, 83, 84t
branch retinal vein occlusion treated with, 135
central retinal vein occlusion treated with, 135
clinical trials of, 82t
diabetic macular edema treated with, 111–112, 112f
diabetic retinopathy treated with, 102
neovascular age-related macular degeneration treated with, 80–82, 82t
- photodynamic therapy and, 85
- proliferative diabetic retinopathy treated with, 104
- retinal vein occlusion treated with, 135
- R9AP gene, 49
- Rapid plasma reagin (RPR) test, 241
- RAPs. *See* Retinal angiomatic proliferations
- RDH5* gene, 252
- Red-green color deficiency
anomaloscope of, 54
types of, 54
- Red laser, 374
- Retsum disease, 283t, 286, 290
- Renal diseases, retinal degeneration associated with, 285
- Retained lens fragments after phacoemulsification, 391–393, 392f
- Reticular degenerative retinoschisis, 326–327
- Reticular peripheral cystoid degeneration, 326
- Reticular pseudodrusen, 65f, 65–66
- Reticular-type pattern dystrophy, 276, 276f
- Reticulum cell sarcoma. *See* Primary vitreoretinal lymphoma
- Retina
angiomas of, 168
blood supply to, 140
circulation of, 16f, 16–17
drug-induced toxicity of
alkyl nitrates, 300, 300f
chloroquine derivatives, 295–297, 296f
clofazimine, 298
deferoxamine, 298–299
dideoxyinosine, 299
hydroxychloroquine, 295–297, 296f
MEK inhibitors, 299, 299f
nucleoside reverse transcriptase inhibitors, 299
pentosan polysulfate, 300
phenothiazines, 297–298, 298f
electro-oculography of, 50–51, 51–52f
electrophysiologic testing of, 41–42
electroretinography of. *See* Electroretinography (ERG)
- equatorial, 9–10
- hemangioblastomas of, in von Hippel–Lindau syndrome, 165–166, 166f, 168
- inflammation of
acute retinal necrosis, 236, 236f
cat-scratch disease, 242–243, 243f
cytomegalovirus retinitis, 235–236
diffuse unilateral subacute neuroretinitis, 246
endogenous bacterial endophthalmitis, 237–239, 238f
fungal endophthalmitis, 239, 239f
infectious causes, 235–247
Lyme disease, 245–246
necrotizing herpetic retinitis, 236–237, 236–237f, 238t
noninfectious causes, 219–234
progressive outer retinal necrosis syndrome, 236–237, 237f
- syphilitic chorioretinitis, 241–242, 242f
toxocariasis, 244–245, 245f
toxoplasmic retinochoroiditis, 243–244, 244f
tuberculosis, 240–241, 241f
West Nile virus chorioretinitis, 246, 247f
- white dot syndromes as cause of. *See* White dot syndromes
- yeast endophthalmitis, 239–240, 240f
- layers of
blood supply to, 140
external limiting membrane, 11, 12f
ganglion cell layer, 11, 12f
Henle fiber layer, 11, 12f
imaging of, 10–11, 12f

- inner nuclear layer, 11, 12*f*
- inner plexiform layer, 11, 12*f*
- internal limiting membrane, 11, 12*f*
- middle limiting membrane, 11, 12*f*
- nerve fiber layer, 11, 12*f*
- optical coherence tomography angiography of, 29
- outer nuclear layer, 11, 12*f*
- outer plexiform layer, 11, 12*f*, 16
- oxygen supply to, 16
- lesions of, 378–379
- light-related injury to, 367
- metabolic needs of, 20
- neurosensory, 9–17
- noninfectious inflammation of
 - acute idiopathic maculopathy, 228–229
 - acute macular neuroretinopathy, 228, 229*f*
 - acute zonal occult outer retinopathy, 226–228, 227*f*
- white dot syndromes. *See* White dot syndromes
- oxygen supply to, 16*f*, 16–17
- in pathologic myopia, 207–216, 209–215*f*
- peripheral, 10
- psychophysical testing of. *See* Psychophysical testing
- retinal pigment epithelium separation of, 17
- surface of, in exudative retinal detachment, 326
- thickness of, in pathologic myopia, 208
- topography of, 9*f*, 9–10
- vascularization of, 180
- vascular occlusion of, 231
- vasculature of, 16*f*, 16–17
- vasculature of, optical coherence tomography
 - angiography of, 29, 30*f*
- venous pressure in, 125
- visual evoked cortical potentials of, 52–53
- Retinal angiomatic proliferations (RAPs), 72, 78*f*
- Retinal arterial macroaneurysms, 147–148, 148*f*
- Retinal artery occlusion
 - branch. *See* Branch retinal artery occlusion (BRAO)
 - capillary retinal arteriole obstruction, 140*f*, 140–141
 - central. *See* Central retinal artery occlusion (CRAO)
 - cilioretinal artery occlusion, 143
 - ophthalmic artery occlusion, 146, 147*f*
 - paracentral acute middle maculopathy, 143
- Retinal breaks
 - aphakia and, 319
 - asymptomatic, 318
 - classification of, 315
 - cryotherapy of, as prophylactic treatment, 317
 - definition of, 314
 - description of, 396
 - lattice degeneration and, 310
 - Lincoff rules for finding, 320, 322*f*
 - posterior vitreous detachment and, 309
 - prophylactic treatment of, 317*t*, 317–320
 - pseudophakia and, 319
 - retinal detachment caused by
 - illustration of, 318*f*
 - prophylactic treatment to prevent, 317*t*, 317–320
 - rhegmatogenous, 314–315, 320, 322*f*, 324
 - significance of, 314
 - symptomatic, 318
 - traumatic, 315–316, 316*f*
 - vitreoretinal traction as cause of, 315
- Retinal capillaries
 - nonperfusion of, in diabetic retinopathy, 101
 - perifoveal, 157
- Retinal degeneration
 - amino acid disorders that cause, 293
 - autoimmune causes of, 286–287
 - cancer-associated retinopathy as cause of, 286, 287*f*
 - dental diseases associated with, 286
 - dermatologic diseases associated with, 286
 - gastrointestinal diseases associated with, 285–286
 - liver diseases associated with, 285
 - melanoma-associated retinopathy as cause of, 286
 - metabolic diseases that cause
 - abetalipoproteinemia, 289–290
 - albinism, 288
 - central nervous system, 288–292
 - lysosomal, 291–292, 292*f*
 - mucopolysaccharidoses, 290–291
 - neuronoid ceroid lipofuscinoses, 289, 290*f*
 - Niemann-Pick disease, 291
 - peroxisomal disorders, 290
 - Refsum disease, 290
 - Tay-Sachs disease, 291, 292*f*
 - vitamin A deficiency, 289–290
 - Zellweger syndrome, 290
 - mitochondrial disorders that cause, 293–294
 - neuromuscular disorders associated with, 285
 - paraneoplastic retinopathies that cause, 286–287
 - renal diseases associated with, 285
 - systemic disorders associated with
 - Bardet-Biedl syndrome, 281, 282*t*, 284, 284*f*
 - Leber congenital amaurosis, 281
 - list of, 282–283*t*
 - overview of, 281
 - Usher syndrome, 284
- Retinal detachment
 - after cataract surgery, 319
 - central serous chorioretinopathy as cause of, 189, 191
 - chronic, 324*f*
 - classification of, 320
 - cobblestone degeneration and, 313, 314*f*
 - diagnostic features of, 320, 321*t*
 - differential diagnosis of
 - description of, 320
 - retinoschisis, 326–328
 - exudative
 - causes of, 320
 - diagnostic features of, 321*t*
 - in familial exudative vitreoretinopathy, 343
 - imaging of, 325*f*
 - management of, 325–326
 - photocoagulation as cause of, 379
 - retinal surface in, 326
 - subretinal fluid findings in, 326
 - in fellow eye, 319
 - lattice degeneration and, 309–311, 310–311*f*, 316*f*, 319
 - lesions not predisposing to, 313–314
 - lesions predisposing to, 309–312, 310–313*f*
 - macular hole as cause of, 330, 330*f*
 - macular lesions associated with, 328–329
 - management of, 324, 324*f*
 - meridional folds and, 312, 313*f*

- optic pit maculopathy and, 328–329, 329*f*
 paving-stone degeneration and, 313, 314*f*
 peripheral cystoid degeneration and, 314
 retinal pigment epithelial hyperplasia and,
 313–314
 retinal pigment epithelial hypertrophy and, 314
 retinal tear progression to, 347
 in retinoschisis, 328
 rhegmatogenous (RRD)
 chronic, 324*f*
 complex, 401
 definition of, 396
 diagnostic features of, 320, 321*t*
 floaters associated with, 320
 incidence of, 320
 intraocular pressure in, 320
 lattice degeneration associated with, 310
 “macula-off,” 401
 macular hole as cause of, 330, 330*f*
 management of, 324, 324*f*, 397
 pigmented demarcation lines with, 324
 pneumatic retinopexy for, 324, 397–398, 398*f*
 proliferative vitreoretinopathy associated with, 320,
 323*f*, 323*t*, 323–324
 reattachment surgery for, 401–402
 retinal breaks as cause of, 314–315, 396
 retinoschisis versus, 327*t*, 320, 322*f*, 327–328
 risk factors for, 396
 scatter photocoagulation as cause of, 155
 scleral buckling for, 324, 398–400, 399*f*
 Shafer sign, 320
 surgical repair of, 397–401, 398–400*f*
 tractional retinal detachment versus, 325
 vision loss caused by, 128
 vitrectomy for, 324, 400*f*, 400–401
 word origin of, 320
 serous
 in intraocular lymphoma, 234
 MEK inhibitors as cause of, 299
 in sickle cell retinopathy, 155
 subclinical, 319–320
 tractional
 causes of, 320
 description of, 286
 diagnostic features of, 321*t*, 325
 in familial exudative vitreoretinopathy, 343
 imaging of, 387*f*
 management of, 325
 pathophysiology of, 387
 in proliferative diabetic retinopathy, 103, 108,
 387–388
 rhegmatogenous retinal detachment versus, 325
 vitrectomy for, 325, 387–388
 trauma-induced, 317
 vitreoretinal tufts and, 311–312, 312*f*
 vitreous contraction as cause of, 349
 Retinal dialyses, 315
 Retinal disease
 arterial macroaneurysms, 147–148, 148*f*
 arterial occlusive
 branch retinal artery occlusion. *See Branch retinal artery occlusion (BRAO)*
 capillary retinal arteriole obstruction, 140*f*, 140–141
 central retinal artery occlusion. *See Central retinal artery occlusion (CRAO)*
 cilioretinal artery occlusion, 143
 ophthalmic artery occlusion, 146, 147*f*
 paracentral acute middle maculopathy, 143
 imaging modalities for
 adaptive optics imaging, 33
 fluorescein angiography, 33–38, 34*f*, 36–37*f*
 fundus autofluorescence, 29, 31–33
 fundus camera imaging, 22–23, 23*f*
 indirect ophthalmoscopy, 21–22
 indocyanine green angiography, 38–39
 ophthalmoscopy, 21–22
 optical coherence tomography, 25–27, 27*f*. *See also Optical coherence tomography*
 optical coherence tomography angiography, 28–29
 scanning laser ophthalmoscopy, 24
 ultrasonography, 39–40
 vascular
 branch retinal vein occlusion. *See Branch retinal vein occlusion (BRVO)*
 cavernous hemangioma, 168, 169*f*
 central retinal vein occlusion. *See Central retinal vein occlusion (CRVO)*
 Coats disease, 159–161, 160*f*, 326
 cystoid macular edema. *See Cystoid macular edema (CME)*
 hypertension, 121–125, 122–124*f*
 macular telangiectasia. *See Macular telangiectasia*
 ocular ischemic syndrome, 138–140, 139*f*
 Purtscherlike retinopathy, 171–173, 172*f*, 173*t*
 Purtscher retinopathy, 171–173, 173*t*
 radiation retinopathy, 170*f*, 170–171
 retinal vein occlusion. *See Retinal vein occlusion (RVO)*
 sickle cell retinopathy. *See Sickle cell retinopathy*
 systemic arterial hypertension, 121–125, 122–124*f*
 Terson syndrome, 173
 Valsalva retinopathy, 171
 vasculitis, 155*f*, 155–156
 von Hippel–Lindau syndrome, 165–168,
 166–167*f*
 Wyburn–Mason syndrome, 168
 Retinal dystrophies
 classification of, 255
 hereditary
 bilateral symmetric involvement of, 258
 blindness concerns of patients with, 260
 cystoid macular edema in, 260, 260*f*
 diagnostic considerations for, 258–259
 enhanced S-cone disease, 266, 267*f*
 genes and loci associated with, 256–257*t*
 gene therapy for, 260, 266
 genetic considerations for, 259
 inheritance patterns for, 259
 Leber congenital amaurosis, 265–266
 management of, 259–260, 260*f*
 molecular genetic testing for, 259
 rod–cone dystrophies, 261–264, 262–264*f*
 stem cell therapy for, 260
 inner, 278–279
 sporadic, 263
 X-linked retinoschisis, 278*f*, 278–279

- Retinal edema, myopia choroidal neovascularization as cause of, 212
- Retinal folds
in familial exudative vitreoretinopathy, 343, 345*f*
fixed, 326
- Retinal ganglion cells, 45
- Retinal grafts, 340
- Retinal hemorrhages
in abusive head trauma, 366, 366*f*
in carotid occlusive disease, 138
- Retinal holes
atrophic
definition of, 315
lattice degeneration with, 310, 311*f*, 316*f*
retinal detachment secondary to, 310
- description of, 378
operculated, 315–316
- Retinal ischemia, 140
- Retinal pigment epithelium (RPE)
abnormalities of
in age-related macular degeneration, 66–67
central serous chorioretinopathy as cause of, 67
focal atrophy, 66
geographic atrophy, 64, 66, 67*f*, 68
hyperpigmentation, 68
pattern dystrophies, 67
age-related changes in, 62
anatomy of, 17–19, 18*f*
atrophy of, 106*f*, 294*f*
barrier functions of, 18
cells of
bis-retinoid accumulation in, 31
description of, 17, 20
in epiretinal membranes, 334
fluorescein angiography of, 34
pigment-laden, 66
degeneration of, 258
depigmentation of, 227, 293
detachment of. *See Pigment epithelial detachments (PEDs)*
- drugs that affect
alkyl nitrates, 300, 300*f*
chloroquine derivatives, 295–297, 296*f*
chlorpromazine, 297
clofazimine, 298
deferoxamine, 298–299
dideoxynucleoside, 299
MEK inhibitors, 299, 299*f*
nucleoside reverse transcriptase inhibitors, 299
pentoxifylline, 300
phenothiazines, 297–298
thioridazine, 297
- electro-oculography of, 50
- functions of, 17–18
- hyperpigmentation of, 106*f*
- hyperplasia of
around retinal tuft, 312
retinal detachment and, 313–314
- hypertrophy of, 314
- leaks from, 190, 190*f*
- lipofuscin in, 32
- lipofuscin-like material, 270, 270*f*
- nummular loss of, 204
- pigmentation of, 214, 277
- pigments in
description of, 12*f*, 17
mottling of, 79, 87, 90*f*
- progressive atrophy of, 66
- retinal separation from, 17
- siderosis bulbi effects on, 362
- standing potential, 50, 51*f*
- Stargardt disease findings, 270, 270*f*
- tears of
autofluorescence of, 31, 32*f*
in choroidal neovascularization, 31
- fibrovascular pigment epithelial detachment
as risk for, 82
- thermal injury to, 367
- water transport in, 18
- Retinal precipitates, 241
- Retinal scleropapilla, 356–358, 357*f*
- Retinal tears. *See also Retinal breaks*
chorioretinal adhesions around, using laser
retinopexy, 377
classification of, 315
flap, 315, 318–319
giant, 315
horseshoe-shaped, 316, 323*f*
mechanisms of, 308*f*
ora bays and, 312
peripheral retinal excavations and, 312–313
posterior vitreous detachment as cause of, 307, 308*f*, 309
- retinal detachment progression of, 347
- ultrasonography of, 39
in vitreous hemorrhage, 347
- Retinal tufts, 311–312, 312*f*
- Retinal vascular sheathing, 231*f*
- Retinal vasculitis, 155*f*, 155–156
- Retinal vein occlusion (RVO)
afibbercept for, 135
anti-VEGF drugs for, 126, 136–137
bevacizumab for, 135
branch (BRVO)
afibbercept for, 135
at arteriovenous crossing, 126
bevacizumab for, 135
clinical findings of, 125–127, 126*f*
corticosteroids for, 137–138
diabetes mellitus and, 128
fluorescein angiography of, 129*f*
glaucoma as risk factor for, 125
hypertensive retinopathy and, 122
intraretinal hemorrhages associated with, 125, 126*f*
macular laser surgery for, 128
neovascularization in, 125, 128, 129*f*
pars plana vitrectomy for, 130
pharmacologic management of, 135–138
prognosis for, 128
ranibizumab for, 135
risk factors for, 127–128
scatter photocoagulation for, 128–130
spontaneous resolution of, 125
surgical management of, 128–130
treatment of, 128–130
triamcinolone for, 137
vision loss caused by, 128

- central (CRVO)
 afibbercept for, 135
 age and, 133
 bevacizumab for, 135
 causes of, 133–134
 chronic changes caused by, 127f
 cilioretinal artery occlusion caused by, 143
 clinical findings of, 127f, 130
 complications of, 135
 corticosteroids for, 137–138
 cystoid macular edema caused by, 136f
 differential diagnosis of, 134
 diuretic and, 134
 electroretinography findings in, 50
 evaluation of, 134–135
 follow-up for, 134
 hypercoagulable conditions presenting with, 134
 hypertensive retinopathy and, 122
 hyperviscosity retinopathy versus, 134
 intraocular pressure in, 133
 iris neovascularization in, 133, 135
 ischemic, 132f
 macular laser surgery for, 135
 management of, 134–135
 neovascularization in, 125
 nonischemic, 130, 131f
 ocular ischemic syndrome versus, 134
 open-angle glaucoma in, 133
 oral contraceptives and, 134
 panretinal photocoagulation for, 135
 pars plana vitrectomy for, 135
 pharmacologic management of, 135–138
 progression of, follow-up for, 134
 ranibizumab for, 135
 retinal microvascular changes in, 125, 127f
 risk factors for, 133–134
 spontaneous resolution of, 125
 treatment of, 135
 vision loss caused by, 130
 vitreous hemorrhage secondary to, 135
 cystoid macular edema caused by, 135, 136f
 dexamethasone implant for, 137
 glaucoma as risk factor for, 125
 improvements in, 125
 intravitreal corticosteroids for, 137–138
 ocular examination for, 125
 panretinal photocoagulation for, 126
 pharmacologic management of, 135–138
 ranibizumab for, 135
 spontaneous resolution of, 125
 triamcinolone for, 137
- Retinitis**
 Chikungunya virus, 247
 cytomegalovirus, 235–236, 238t
 foveomacular. *See Solar retinopathy*
 necrotizing herpetic, 236–237, 236–237f, 238t
 in neuroretinitis, 242
 solar. *See Solar retinopathy*
- Retinitis pigmentosa (RP). *See also* Rod-cone dystrophies**
 autofluorescence imaging of, 261
 clinical presentation of, 261
 congenital stationary night blindness versus, 251
 cystoid macular edema associated with, 260
- electroretinography findings in, 44, 261
 fundal findings in, 261, 262f
 genes and loci associated with, 257t
 hearing loss and, 284
 management of, 264
 nutritional supplements for, 264
 sectorial, 263, 264f
sine pigmento, 261
 spectral-domain optical coherence tomography findings, 263f
 unilateral, 263
 visual fields in, 263f
 X-linked, 50
- Retinitis punctata albescens**, 258, 258f
- Retinochoroiditis**
 necrotizing, 243
 in syphilitic uveitis, 241
 toxoplasmic, 243–244, 244f
- Retinopathy**
 acute zonal occult outer, 226–228, 227f
 arteriosclerotic, 122
 autoimmune, 286
 cancer-associated, 286, 287f
CRB1-related, 258
 crystalline
 cause of, 302–304, 303t
 drugs that cause, 302–304
 tamoxifen as cause of, 303, 304f
 West African, 303–304, 305f
 diabetic. *See Diabetic retinopathy*
 hypertensive, 121–123, 122f, 124f
 hyperviscosity, 134
 melanoma-associated, 286
 occlusive, 300–301
 ocular ischemic syndrome as cause of, 138
 pigmentary, 282–283t
 pigmented paravenous, 263
 Purtscher, 171–173, 173t
 Purtscherlike, 171–173, 172f, 173t
 radiation, 170f, 170–171
 sickle cell. *See Sickle cell retinopathy*
 solar, 277, 367, 368f
 syndromic/systemic diseases associated with, 257t
 thioridazine as cause of, 297
 Valsalva, 171
- Retinopathy of prematurity (ROP)**
 aggressive posterior, 177
 angle-closure glaucoma in, 181
 birth weight and, 182
 blindness caused by, 182
 cicatricial, 181
 classification of, 175–179, 176t, 178t
 clinically significant, 184t
 conditions associated with, 181–182
 definition of, 175
 diet and, 184–185
 end stage of, 175
 epidemiology of, 175
 familial exudative vitreoretinopathy versus, 344
 incidence of, in premature infants, 182
 in infants, 175
 insulin growth factor-1 levels and, 182
 late sequelae of, 181–182

- natural course of, 181
 neovascularization in, 180–181
 oxygen supplementation and, 184
 pathophysiology of, 180–182
 posterior persistent fetal vasculature versus, 342
 prethreshold disease, 178*t*, 179, 185
 prevention of, 184–185
 pupillary-block glaucoma in, 181
 risk factors for, 184–185
 screening of
 birth weight–based criteria for, 182
 criteria for, 182–183
 discontinuation of, criteria for, 183
 fundus photographic, 184
 intervals for, 183
 sequelae of, 181–182
 severity of, 176*t*
 spontaneous regression of, 181
 stage 1, 176, 176*f*, 180
 stage 2, 176, 176*f*, 180
 stage 3, 176, 177*f*, 180
 stage 4, 176, 177*f*, 180, 187–188
 stage 5, 188
 terminology for, 175–176, 176*f*
 threshold disease, 177, 178*t*, 179, 180*f*, 181, 185
 treatment of
 anti-VEGF drugs, 186–187
 bevacizumab, 186–187
 cryoablation, 185–186
 intravitreal injections, 187
 laser surgery, 185–186
 overview of, 185
 photocoagulation, 186*f*
 scleral buckling surgery, 187–188
 vitrectomy, 187–188
 weight, IGF-1, neonatal ROP algorithm for, 182
- Retinopexy**
 laser, 376–377
 pneumatic, for rhegmatogenous retinal detachment, 397–398, 398*f*
- Retinoschisin**, 279
- Retinoschisis**
 bullous, 326
 demarcation lines in, 328
 imaging of, 327*f*
 outer-schisis-layer holes associated with, 327, 327*f*
 reticular degenerative, 326–327
 retinal detachments and, 326–328
 rhegmatogenous retinal detachment versus, 327*t*, 327–328
 typical degenerative, 326
- Retrolental fibroplasia.** *See Retinopathy of prematurity (ROP)*
- RGS9 gene**, 49
- Rhegmatogenous retinal detachment (RRD)**
 chronic, 324*f*
 complex, 401
 definition of, 396
 diagnostic features of, 320, 321*t*
 floaters associated with, 320
 incidence of, 320
 intraocular pressure in, 320
 lattice degeneration associated with, 310
 “macula-off,” 401
 macular hole as cause of, 330, 330*f*
 management of, 324, 324*f*, 397
 pigmented demarcation lines with, 324
 pneumatic retinopexy for, 324, 397–398, 398*f*
 proliferative vitreoretinopathy associated with, 320, 323*f*, 323*t*, 323–324
 reattachment surgery for, 401–402
 retinal breaks as cause of, 314–315, 320, 322*f*, 396
 retinoschisis versus, 327*t*, 327–328
 risk factors for, 396
 scatter photocoagulation as cause of, 155
 scleral buckling for, 324, 398–400, 399*f*
 Shafer sign, 320
 surgical repair of, 397–401, 398–400*f*
 tractional retinal detachment versus, 325
 vision loss caused by, 128
 vitrectomy for, 324, 400*f*, 400–401
 word origin of, 320
- Rheophoresis**, 71
- Rhodopsin**, 252, 264
- Rifabutin**, 305
- Rifampin**, for cat-scratch disease, 243
- Rituximab**, for primary vitreoretinal lymphoma, 234
- RLBP1 gene**, 252
- Rod(s)**
 density of, 11–12
 in foveal center, 11
 inner segments of, 11–12, 12*f*
 light-sensitive molecules in, 12
 outer segments of, 11, 12*f*
 schematic diagram of, 14*f*
Rod-cone dystrophies. *See also Retinitis pigmentosa*
 in Bardet-Biedl syndrome, 284
 characteristics of, 261–264, 262–264*f*
 conventional testing of, 261
 electroretinography evaluations, 46, 47*f*, 261
 imaging of, 262–264*f*
 macula-spared, 46, 47*f*
Rod monochromatism, 250, 250*t*
- ROP.** *See Retinopathy of prematurity*
- Rosiglitazone**, 301
- RP.** *See Retinitis pigmentosa*
- RPE.** *See Retinal pigment epithelium*
- RPE65 gene**, 266
- RPR.** *See Rapid plasma reagin (RPR) test*
- RRD.** *See Rhegmatogenous retinal detachment*
- RS1 gene**, 279
- Rush disease**, 177, 178*t*
- RVO.** *See Retinal vein occlusion*
- SAG gene**, 253
- SAILOR study**, 81
- Salmon-patch hemorrhage**, 150, 150*f*
- Sanfilippo syndrome**, 282*t*, 291
- Sarcoidosis**, 134, 231, 231*f*
- Sattler layer**, 19
- Scanning laser ophthalmoscopy (SLO)**
 angiography versus, 24
 blue excitation light used by, 31
 choroidal nevi on, 24
 digital resolution of, 24
 ellipsoidal mirror in, 24

- epiretinal membrane on, 334f
- pseudodrusen on, 24
- resolution of, 24
- retinal disease evaluations, 24
- wavelengths in, 24
- Scatter photocoagulation.** *See also* Photocoagulation
 - branch retinal vein occlusion treated with, 128–130
 - sickle cell retinopathy treated with, 155
 - vitreoretinal surgery for, 155
- Scheie syndrome,** 282*t*, 290–291
- Schisis,** macular, 328
- Schlaegel lines,** 225
- Sclera**
 - anatomy of, 20
 - indentation of, 310*f*
 - laceration of, 359
 - in pathologic myopia, 216–217, 217*f*
 - permeability of, 20
 - rupture of, 352, 358
 - thickness of, 20, 216
 - traumatic injuries to, 352, 358
- Scleral buckles,** 201
- Scleral buckling**
 - complications of, 400
 - intraocular pressure affected by, 399
 - retinopathy of prematurity treated with, 187–188
 - rhegmatogenous retinal detachment treated with, 324, 398–400, 399*f*
- Scleral fixation,** 393
- S cone,** 54
- S-cone monochromatism,** 250
- Scotomas**
 - absolute, 327
 - central, 86, 265
 - paracentral, 228, 367
 - retinoschisis as cause of, 327
- SDH.** *See* Shape-discrimination hyperacuity
- SD-OCT.** *See* Spectral-domain optical coherence tomography
- Sea-blue histiocyte syndrome,** 291
- Sea fan neovascularization,** 151, 153*f*
- Sectorial retinitis pigmentosa,** 263, 264*f*
- Segmental phlebitis,** 232
- Septic emboli,** 141
- Serous pigment epithelial detachment,** 72–73, 74*f*
- Serous retinal detachment**
 - in intraocular lymphoma, 234
 - MEK inhibitors as cause of, 299
- Serpiginous choroidopathy,** 220*t*, 222–223, 223*f*
- SF₆.** *See* Sulfur hexafluoride
- Shafer sign,** 320, 348
- Shaken baby syndrome,** 365–366, 366*f*
- Shape-discrimination hyperacuity (SDH),** 69
- Shimmering, electroretinography findings in,** 46
- Sickle cell disease, proliferative sickle cell retinopathy**
 - complications in, 150
- Sickle cell hemoglobin C disease (SC)**
 - ocular findings in, 153*f*
 - proliferative sickle cell retinopathy complications in, 150
- Sickle cell hemoglobinopathies**
 - description of, 149
- incidence of, 149*t*
- ocular abnormalities in, 154
- racial predilection of, 149, 154
- Sickle cell retinopathy**
 - management of, 154–155
 - nonproliferative
 - branch retinal artery occlusions in, 152*f*
 - characteristics of, 149–150
 - imaging of, 150–152*f*
 - retinal arteriolar occlusions in, 151*f*
 - salmon-patch hemorrhage in, 150*f*
 - proliferative
 - complications of, 150
 - proliferative diabetic retinopathy versus, 151
 - scatter photocoagulation for, 155
 - sea fan neovascularization associated with, 151, 153*f*
 - stages of, 150–151
 - retinal detachment secondary to, 155
 - scatter photocoagulation for, 155
 - thalassemia as cause of, 149
- Siderosis bulbi,** 362, 363*t*
- Siegrist streaks,** 123, 198
- Sildenafil,** 299, 304
- Silicone oil,** 401
- Silver,** 306
- Skin, fluorescein angiography effects on,** 36
- Slit-lamp biomicroscopy**
 - operculated holes on, 318
 - posterior vitreous detachment diagnosis using, 331
- SLO.** *See* Scanning laser ophthalmoscopy
- Snowballs,** in intermediate uveitis, 231
- Snowbanks,** in intermediate uveitis, 231–232, 245
- “Snowflakes,” 326
- Soft drusen,** 65, 68, 75, 200*f*, 272
- Soft exudates,** 122
- Solar retinitis.** *See* Solar retinopathy
- Solar retinopathy,** 277, 367, 368*f*
- Sorsby macular dystrophy,** 275*f*, 275–276
- Spatial frequency,** 56, 57*f*
- Spectral-domain optical coherence tomography (SD-OCT)**
 - adult-onset vitelliform maculopathy on, 67–68, 68*f*
 - alkyl nitrite findings, 300, 300*f*
 - central retinal artery occlusion on, 144*f*
 - chloroquine toxicity monitoring uses of, 297
 - choroidal neovascularization on, 73–75, 75*f*
 - commotio retinae on, 353
 - diabetic macular edema on, 109*f*, 125
 - drusen on, 64*f*, 65
 - epiretinal membranes on, 335*f*
 - Gaucher disease on, 291
 - pathologic myopia on, 90*f*
 - reticular pseudodrusen on, 65*f*
 - retinal layers on, 10–11, 12*f*
 - retinitis pigmentosa findings, 263*f*
 - sensitivity of, 26
 - swept-source optical coherence tomography versus, 25–26
 - vitreomacular traction on, 332*f*
- Spinocerebellar degeneration,** 282*t*
- Staining, hyperfluorescence and,** 35
- Standing potential,** 50, 51*f*

- Staphylococcus* spp
 endogenous bacterial endophthalmitis caused by, 238
 postoperative endophthalmitis caused by, 389
Staphyloma, 209, 216, 217f, 330
Stargardt disease
ABCA4 gene mutations as cause of, 271
 clinical findings of, 269–270, 270f
 description of, 31, 44
 electroretinography findings in, 48f
 fluorescein angiography findings, 269–270, 270f
 fundus autofluorescence findings, 270
 phenotype of, 269
 retinal pigment epithelium findings in, 270, 270f
 visual acuity in, 269
 “Starry night” sign, in Vogt-Koyanagi-Harada disease, 232
Static dyschromatopsia, 249
Steinert disease, 282f
Stereopsis, binocular indirect ophthalmoscopes for, 22
Stickler syndrome, 282t, 309, 342–343, 343f
Streptococcus spp
 endophthalmitis caused by
 bleb-associated, 391
 endogenous bacterial, 238
 postoperative, 389
S viridans, 404
Stroke, in ocular ischemic syndrome patients, 139
Sturge-Weber syndrome, 202
Subarachnoid hemorrhage, 173
Subclinical retinal detachment, 319–320
Subfoveal pigment epithelial detachment, 74–75f
Subhyaloid hemorrhage, 173
Submacular hemorrhage
 in neovascular age-related macular degeneration, 85, 385
 posttraumatic, 354f
 vitrectomy for, 385, 386f
Subretinal drusenoid deposits, 65, 65f, 200
Subretinal fibrosis, in multifocal choroiditis, 226, 226f
Subretinal fluid
 in central serous chorioretinopathy, 76
 in choroidal neovascularization, 71
 in exudative retinal detachment, 326
 optic pit and, 329f
Subretinal hemorrhage
 choroidal neovascularization versus, 211
 in polypoidal choroidal vasculopathy, 76
Subretinal hyperreflective material (SHRM), 75
Subretinal neovascularization, 162, 164
Subretinal space
 fluorophore accumulation in, 32
 retinal pigment epithelium-mediated dehydration of, 18
Sub-Tenon space, 20
 “Sugiura” sign, 233
Sulfadiazine, for toxoplasmic retinochoroiditis, 243
Sulfur hexafluoride (SF₆), 382
 “Sunset glow” sign, 232f, 232–233
Superficial vascular plexus, 16
Supertraction crescent, 210
Suprachoroidal hemorrhage, 394–395, 395f
Surgery. *See also* Cataract surgery; Laser surgery
 diabetic macular edema treated with, 114–115
 endophthalmitis after, 388–391, 390–391f
 intraocular foreign bodies removed with, 360–362
 macular holes managed with, 339–340
 neovascular age-related macular degeneration treated with, 85–86
 open-globe injuries managed with, 359–360
 rhegmatogenous retinal detachment treated with, 397–401, 398–400f
 sympathetic ophthalmia secondary to, 233
 vitreous loss during, 349
Susac syndrome, 156
SUSTAIN study, 81
Swept-source optical coherence tomography (SS-OCT)
 pathologic myopia findings, 209f
 sensitivity of, 26
 spectral-domain optical coherence tomography versus, 25–26
Sympathetic ophthalmia
 characteristics of, 233
 trauma as cause of, 364–365
 Vogt-Koyanagi-Harada disease versus, 232
Symptomatic retinal breaks, 318
Synchysis scintillans, 348
Syndromic panretinal dystrophies, 259
Syneresis, vitreous, 307, 316
Syphilis
 acute syphilitic posterior placoid chorioretinitis caused by, 241
 uveitis caused by, 241
Syphilitic chorioretinitis, 241–242, 242f
Systemic lupus erythematosus
 description of, 134
 procainamide as cause of, 300
 vasculitis associated with, 230–231, 231f
Tadalafil, 304
Talc emboli, 141, 303
Tamoxifen, 302–303, 304f
Taxanes, 301
Tay-Sachs disease, 291, 292f
T cells, CD4+, 235
Telangiectasia. *See also* Macular telangiectasia
 aneurysmal, 161
 juxtafoveal, 161
Terson syndrome, 366
Tessellation, 214
Thalassemia, 149, 149t
Thermal laser, for neovascular age-related macular degeneration, 79
Thioridazine, 297
3-mirror lens, 22
Threshold disease (retinopathy of prematurity), 177, 178t, 179, 180f, 181, 185
Thrombi, comma-shaped, 154
Thrombosis, retinal vasculitis versus, 156
Thrombotic thrombocytopenic purpura, 195
Tick-borne diseases, 245–246
Tilted disc syndrome, 217
TIMP3 gene, 275–276
Topiramate
 choroidal swelling caused by, 201
 myopia caused by, 305
Topography, retinal, 9f, 9–10

- Toxocara canis*, 244, 246
Toxocara catti, 244, 246
 Toxocariasis, 244–245, 245f
Toxoplasma gondii
 definition of, 243
 retinchoroiditis caused by, 243–244, 244f
 TP-PA. *See Treponema pallidum* particle agglutination assay
 Tractional retinal detachment. *See also* Retinal detachment
 description of, 286
 diagnostic features of, 321t, 325
 in familial exudative vitreoretinopathy, 343
 imaging of, 387f
 management of, 325
 pathophysiology of, 387
 in proliferative diabetic retinopathy, 103, 108, 387–388
 rhegmatogenous retinal detachment versus, 325
 vitrectomy for, 325, 387–388
 Transconjunctival cryopexy, 398
 Transmission defect, hyperfluorescence in, 36
 Transpupillary thermotherapy (TTT), 380
 11-trans-retinal, 31
 11-trans-retinaldehyde, 17
 Transscleral cryopexy, 398
 Trauma
 abusive head, 365–366, 366f
 blunt, 315, 353–358, 354–357f
 in children, 316–317
 choroidal rupture, 354–355, 354–356f
 classification of, 351
 closed-globe, 351–352
 commotio retinae, 353, 354f
 endophthalmitis after, 362–363
 evaluation of patient after, 351–353, 352t
 fibrocellular proliferation secondary to, 315
 handheld laser-pointer injury, 369
 in infants, 316–317
 intraocular pressure evaluations, 352
 laser-pointer injury, 369
 macular hole caused by, 355–357, 356f
 microsurgery for, 351
 occupational light toxicity, 369
 Ocular Trauma Score, 364, 364t
 open-globe
 description of, 351–352
 intraocular foreign bodies, 351–352, 360–362, 361f
 lacerating injuries, 358
 needle perforation/penetration, 358, 395f, 395–396
 penetrating injuries, 358
 prognosis for, 363–364
 scleral rupture, 358
 optic nerve head avulsion caused by, 365, 365f
 photic damage, 367–369, 368f
 phototoxicity from ophthalmic instrumentation, 368–369
 prognosis after, 363–364
 retinal breaks caused by, 315–316, 316f
 retinal detachments caused by, 317
 retinal scleropatia, 356–358, 357f
 scleral rupture, 352
 submacular hemorrhage secondary to, 354f
 sympathetic ophthalmia secondary to, 364–365
 vitreous hemorrhage secondary to, 357
 whiplash, 356–357
 in young patients, 316–317
Treponema pallidum particle agglutination assay (TP-PA), 241
 Triamcinolone acetonide
 branch retinal vein occlusion treated with, 137
 diabetic macular edema treated with, 113
 uveal effusion syndrome treated with, 203
 Trichromatism, 249
 Trimethoprim-sulfamethoxazole, for toxoplasmic retinchoroiditis, 243–244
 Tritanomalous dichromatism, 250t
 Tritanomalous trichromatism, 250t
 TTT. *See* Transpupillary thermotherapy
 Tubercular serpiginous-like choroiditis, 222
 Tuberculosis, ocular, 240–241, 241f
 Tunica vasculosa lentis, 186, 340–341
 Typical degenerative retinoschisis, 326
 Typical peripheral cystoid degeneration, 326
 UKPDS. *See* United Kingdom Prospective Diabetes Study
 Ultrasonography
 applications of, 40
 contact B-scan, 39, 39f
 intraocular foreign body evaluations, 352
 retinal disease evaluations using, 39–40
 Ultrasound biomicroscopy
 anterior chamber evaluations, 40
 ciliary body evaluations, 40
 Umbo
 anatomy of, 9, 9f
 characteristics of, 10t
 United Kingdom Prospective Diabetes Study (UKPDS), 96–97
 Urinary tract infections, *Escherichia coli* as cause of, 238
 Usher syndrome
 clinical features of, 283t, 284
 description of, 259
 genes and loci associated with, 257t
 types of, 284
 Uveal effusion syndrome, 203, 204f
 Uveal lymphoma, 234, 235f
 Uveal thickening, 234, 235f
 Uveitis
 in Behçet disease, 230
 birdshot
 characteristics of, 220t, 224–225, 225f
 uveal lymphoma and, 234
 immune recovery, 235
 indocyanine green angiography of, 38–39
 intermediate, 231–232
 intraocular lymphoma and, 233–234
 in Lyme disease, 245
Mycobacterium tuberculosis, 240
 syphilitic, 241
 in toxocariasis, 245
 Valacyclovir, for herpetic retinitis, 238t
 Valsalva retinopathy, 171
 Vancomycin, 300

- Variable expressivity, 255
- Varicella-zoster virus (VZV), necrotizing retinitis caused by, 236–237, 236–237*f*, 238*f*
- Vascular endothelial growth factor (VEGF) choroidal neovascularization concentrations of, 80 isoforms of, 80 therapy inhibiting. *See* Anti-VEGF therapy
- Vascular filling defects, in fluorescein angiography, 35
- Vasculation, retinal, 16*f*, 16–17
- Vasculitis inflammatory, 230*t*, 230–231, 231*f* lupus, 230–231, 231*f* retinal, 155*f*, 155–156
- VECP. *See* Visual evoked cortical potential
- VEGF. *See* Vascular endothelial growth factor
- VEGFR1 gene, 82
- VEGFR2 gene, 82
- VEGF Trap, 82. *See also* Aflibercept
- Venous beading, in nonproliferative diabetic retinopathy, 100*f*
- VEPs. *See* Visual evoked potentials
- Verteporfin. *See also* Photodynamic therapy (PDT) central serous chorioretinopathy treated with, 194 complications of, 388 neovascular age-related macular degeneration treated with, 79 polypoidal choroidal vasculopathy treated with, 76 von Hippel-Lindau syndrome treated with, 167
- VIEW 1 study, 83
- VIEW 2 study, 83
- Vigabatrin, 305
- Visceral larval migrans, 244
- Vision loss arteritic causes of, 195 branch retinal vein occlusion as cause of, 128 causes of, 346 central retinal artery occlusion as cause of, 143–144 in diffuse unilateral subacute neuroretinitis, 246 fungal endophthalmitis as cause of, 239 rhegmatogenous retinal detachment as cause of, 128 in toxocariasis, 245 vitreous hemorrhage as cause of, 346
- Visual acuity in central serous chorioretinopathy, 190 ranibizumab effects on, 80
- Visual evoked cortical potential (VECP), 52
- Visual evoked potentials (VEPs) albinism evaluations, 288 in children, 53 delayed, 52–53 demyelinating optic neuritis findings, 52 description of, 52 flash, 52 flash stimulation for, 53 in nystagmus, 53 optic nerve conduction delay diagnosis with, 52 pattern-appearance stimulation, 53 pattern electroretinography and, 45–46 pattern-reversal, 52, 53*f*
- Visual field defects, in acute zonal occult outer retinopathy, 227
- Vitamin A deficiency, 261, 289–290
- Vitamins, for age-related macular degeneration, 69, 70*t*
- Vitelliform exudative macular detachment, 272, 274*f*
- Vitelliform macular dystrophy description of, 32 electro-oculography findings in, 51
- Vitiliginous chorioretinitis. *See* Birdshot uveitis
- Vitrectomy. *See also* Pars plana vitrectomy complications of, 402*t*, 402–403 cystoid macular edema treated with, 159, 393, 394*f* delayed, 360 diabetic macular edema treated with, 388 diabetic retinopathy complications treated with, 107 epiretinal membranes treated with, 382–383 idiopathic macular holes treated with, 384–385, 385*f* immediate, 359 indications for, 359, 381 instrumentation used in, 381–382 needle perforation/penetration of globe treated with, 396 open-angle glaucoma risks secondary to, 402 open-globe injuries treated with, 359–360 posteriorly dislocated intraocular lenses treated with, 393
- posterior vitreous detachment treated with, 333*f*, 359
- postoperative endophthalmitis treated with acute-onset, 388–390, 390*f* bleb-associated, 390–391, 391*f* chronic (delayed-onset), 390, 391*f* retained lens fragments after phacoemulsification treated with, 391–393, 392*f*
- retinopathy of prematurity treated with, 187 rhegmatogenous retinal detachment treated with, 324, 400*f*, 400–401
- smaller-gauge instrumentation used in, 382
- submacular hemorrhage treated with, 385, 386*f*
- suprachoroidal hemorrhage treated with, 394–395, 395*f*
- technique for, 381
- tractional retinal detachment treated with, 325, 387–388
- visualization aids used in, 381–382
- vitreous hemorrhage treated with, 366, 386–387
- vitreous opacities treated with, 348, 386
- Vitreomacular adhesions, 336, 336*t*
- Vitreomacular traction (VMT) syndrome description of, 332, 332*f*, 336*t*, 336–337, 337*f* epiretinal membranes versus, 382–383 vitrectomy for, 382–384, 384*f*
- Vitreoretinal adhesions, 337
- Vitreoretinal lymphoma, primary, 233–234
- Vitreoretinal tufts, 311–312, 312*f*
- Vitreous anatomy of, 7–9, 8*f*, 331 ascorbate levels in, 9 attachments of, 7 canals in, 7 cisterns in, 7 collagen fibers in, 7, 344 composition of, 7, 331 cytomegalovirus retinitis findings, 235 definition of, 331 degeneration of, 344 developmental abnormalities of persistent fetal vasculature, 341–342

- prepapillary vascular loops, 341, 341f
 tunica vasculosa lentis, 340–341
 enhanced depth imaging optical coherence tomography of, 25
 familial exudative vitreoretinopathy of, 343–344, 345f
 hereditary hyaloideoretinopathies with optically empty vitreous, 342–343, 343f
 hyalocytes in, 7
 liquefaction of, 316–317, 344
 opacities of
 amyloidosis, 348, 349f
 asteroid hyalosis, 346f, 346–347
 bilateral, 348
 cholesterolosis, 348
 pigment granules, 348
 vitrectomy for, 386
 vitreous degeneration and detachment associated, 344
 vitreous hemorrhage, 347
 retinal cavernous hemangioma bleeding into, 168
 surgery-related abnormalities of, 349–350
 syneresis of, 307, 316
 traction, 208
 void of, 7
Vitreous base
 avulsion of, 315, 316f, 331
 posterior border of, 10
 retinal dialyses at, 315
 vitreous gel attachment to, 307
Vitreous body
 anatomy of, 8f
 anterior surface of, 7, 8f
 topographic areas of, 7
Vitreous detachment
 perifoveal, 337
 posterior
 age-related, 307–308
 anatomy of, 331
 atrophic holes presenting with, 318
 cholesterolosis and, 348
 conditions associated with, 307
 definition of, 331
 diagnosis of, 331
 epiretinal membranes. *See* Epiretinal membranes (ERM)
 examination of, 309
 fibroglial tissue in, 331
 floaters associated with, 308–309
 idiopathic macular holes, 337–339, 338f
 imaging of, 308f
 indirect ophthalmoscopy of, 309, 331
 management of, 309
 myopia macular retinoschisis in, 209
 nonproliferative diabetic retinopathy progression affected by, 102
 optical coherence tomography of, 309, 332
 in pars plana vitrectomy for diabetic macular edema, 115
 pathologic conditions caused by, 332
 photopsias associated with, 308
 prevalence of, 331
 retinal breaks associated with, 309
 retinal tears caused by, 307, 308f, 309
 risk factors for, 309
 signs and symptoms of, 308
 slit-lamp biomicroscopy of, 331
 vitrectomy for, 333f, 359
 vitreomacular adhesions, 336, 336t
 vitreomacular traction syndrome, 332, 332f, 336t, 336–337, 337f
 vitreous hemorrhage associated with, 309
Vitreous gel
 age-related changes in, 331
 attachment of, to vitreous base, 307
 composition of, 7
Vitreous hemorrhage
 in central retinal vein occlusion, 135
 echography for, 347
 peripheral neovascularization, 232
 photocoagulation as cause of, 379
 in polypoidal choroidal vasculopathy, 75
 posterior vitreous detachment and, 309
 in proliferative diabetic retinopathy, 103, 103f, 107–108, 386–387
 trauma-related, 357
 treatment of, 309
 in Valsalva retinopathy, 171
 vision loss caused by, 346
 vitrectomy for, 366, 386–387
VKH disease. *See* Vogt-Koyanagi-Harada (VKH) disease
VMT. *See* Vitreomacular traction (VMT) syndrome
Vogt-Koyanagi-Harada (VKH) disease, 232f, 232–233
Volume rendering
 B-scans versus, 27
 macular telangiectasia on, 31
von Hippel-Lindau (VHL) syndrome, 165–168, 166–167f
Voriconazole
 fungal endophthalmitis treated with, 239
 yeast endophthalmitis treated with, 240
Vortex veins, in choroid, 19
VZV. *See* Varicella-zoster virus
Waardenburg syndrome, 282t
Wagner disease, 342–343
Wagner hereditary vitreoretinal degeneration, 282t
Wandering nystagmus, 266
Watershed defects, 198
Water transport, in retinal pigment epithelium, 18
Wegener granulomatosis. *See* Granulomatosis with polyangiitis
Weight, IGF-1, neonatal ROP (WINROP) algorithm, 182
Weiss ring, 308f
WESDR. *See* Wisconsin Epidemiologic Study of Diabetic Retinopathy
West African crystalline retinopathy, 303–304, 305f
West Nile virus chorioretinitis, 246, 247f
“Wet” age-related macular degeneration. *See* Neovascular (“wet”) age-related macular degeneration
Whiplash injuries, 356–357
White dot syndromes
 acute posterior multifocal placoid pigment epitheliopathy, 220t, 221f, 221–222

- birdshot uveitis, 220*t*, 224–225, 225*f*
characteristics of, 220*t*
multifocal choroiditis, 220*t*, 225–226, 226*f*
multifocal choroiditis and panuveitis syndrome,
 220*t*
multiple evanescent, 220*t*, 223–224, 224*f*
punctate inner choroidopathy, 220*t*
 serpiginous choroidopathy, 220*t*, 222–223, 223*f*
Wide-angle fluorescein angiography
 description of, 36, 37*f*
 von Hippel-Lindau syndrome on, 167, 167*f*
Wilson disease, 362
Window defect, hyperfluorescence in, 36
Wisconsin Epidemiologic Study of Diabetic Retinopathy
 (WESDR), 92
Wyburn-Mason syndrome, 168
- Xanthophyll, 373, 374*f*
Xanthopsia, 305
X-linked cone dystrophy, 253*f*
X-linked congenital stationary night blindness, 252
- X-linked retinitis pigmentosa, electroretinography
 findings in, 50
X-linked retinoschisis (XLRS)
 characteristics of, 278*f*, 278–279
 electroretinography findings in, 46, 47*f*
XLRS. *See* X-linked retinoschisis
- Yeast endophthalmitis, 239–240, 240*f*
Yellow laser, 374
- Zeaxanthin
 age-related macular degeneration managed with, 70*t*
 description of, 367
- Zellweger syndrome, 283*t*, 290
- Zika virus chorioretinitis, 247
- Zinc
 age-related macular degeneration managed with,
 69, 70*t*
 in intraocular foreign body, 362
- Zonulae occludentes, 17
- Zonular traction retinal tufts, 311, 312*f*

